

University of Nottingham
UK | CHINA | MALAYSIA

Innovative Methodology for the Assessment of Thermal Comfort and Climate Resilience in Social Housing in Coahuila, Mexico

Ana Berenice Gómez de León

BArch, MSc

Thesis submitted to the University of Nottingham

for the degree of Doctor of Philosophy

2022

Abstract

Social housing in Mexico comprises of a repetitive design that does not respond to local climate. The scarce studies regarding thermal comfort combined with the use of accurate weather files represented a gap in knowledge that led to the development of the current research. Three locations for the state of Coahuila, a northeast state of the country, were considered for their analysis: Saltillo, Monclova and Torreón. These cities were selected because even if they are in the same state, have three different climates. Weather files for future climate scenarios are not available for the mentioned cities, as is also the case for many locations in the country.

The novelty of the research relies in the development of a new methodology for the generation of weather files used in dynamic simulation from diverse disposition of numerical data, for current and possible future climate scenarios. The applicability of these files was presented in dynamic thermal simulations in where results were shown in percentages of annual thermal comfort.

The mathematical procedures used for the methodology are based on the Least Squares Approximation technique to generate equations from current weather data, and further, interpolate using future weather data. With these, data needed for weather files can be obtained for specific points, and not only from weather stations. In addition, its application extends for purposes of energy studies and thermal comfort in the built environment. Data required for using the algorithms presented could be modified and adapted to analyse different scales and data disposition.

The climate scenarios from the International Panel on Climate Change adapted to the weather files were the Special Report on Emissions Scenarios A2 and B2, and the

Representative Concentration Pathway 4.5 for the near horizon (years 2015–2039), the medium horizon (years 2045–2069), and the far horizon (years 2075–2099).

These strategies were assessed in dynamic simulations, whose results showed that the weather files have a different impact depending on their location, even when the projects are placed in the same state, as was the case for Coahuila. Due to this, there is a necessity of using different characteristics in the thermal building envelope in order to offer best indoor qualities depending on the site. Through a parametric study, diverse thermal envelope characteristics were simulated, in envelope materials, glazing in windows, shading elements, different sizes and disposition of windows; no active heating or cooling systems were considered. The three chosen locations for each city shown different results, and improvements in annual thermal comfort for the city of Saltillo reach up to 36.93%, in Monclova of 22.52% and in Torreón of 29.69%.

These modifications in the building envelope benefit the users in terms of thermal comfort, bills savings, and facilitate the designers to propose better envelope characteristics adapted to the site of each project. Therefore, new designs can be considered by ends of having resilient and adaptable buildings to climate projections and possible weather changes in the near, medium and far futures.

Acknowledgments

I am extremely grateful to my first supervisor Prof. Lucelia Rodrigues for all the support and guidance received throughout this research work since its conception; thank you for pushing me to achieve the best and to helping me pursue my goals.

I want to thank my second supervisor Prof. Mark Gillot for the invaluable advice received, in particular, I appreciate the effort that you invested in this project since the very beginning, even if this was not part of your activities at the time.

Similarly, I want to thank my third supervisor Dr. John Calautit the in depth discussions about the multiple topics, processes, and updated research possibilities that gave me a great insight of new horizons for my professional life.

I would like to add in this section to my fellow PhD students and researchers for the support and experiences we shared in MGH and the SRB: Sean, Alan, Ken, Chris, Neil, Eldar, Jorge, Mariana and May.

There is not enough space to thank all the inspiring and wonderful people accompanying me on this path but I would still like to thank Lucía, Jesús, Karen, Maria Luigia, Nereyda and Angel for all the good times spent together, physically and on-line. Special thanks to Karina, who has been with me since I decided to study in the UK and helped me in every possible aspect without hesitation; also to her beautiful family Andrew and Andresito.

Likewise I want to thank my wonderful family, always cheering me up. To my father Daniel, my inspiration in life and my eternal partner in science. My mother Rebeca, also my teacher in life, art and constant source of joy. Rocío, for being my best friend

through life, along with Eduardo, and my new renovated inspiration, Ana Valeria.

To Dany and Maria José, María Inés and Daniela, for being there every time we go back home. Special thanks to Fernando, for his optimism and valuable support of my career, and to Liliana and Juan Antonio, for supporting me along this many years.

A special thanks for Génesis and Margarita, for their support, happiness and priceless treasures brought to my journey; and to Elda and Rogelio, for their support throughout these years.

I am particularly grateful to Alfonso for the constant support that I received during the past years. Thanks for all the unconditional help that you gave me in the course of this research project, and for being at my side through the tough and happy times that I encountered.

Finally, I wish to express my greatest gratitude to the National Council on Science and Technology, CONACyT, for having subsidized my doctoral studies through the scholarship CONACYT-SENER Energy Sustainability Sixth Period.

Authors Associated Publications to Date

- Ana Berenice Gómez de León, Lucelia Rodrigues, Mark Gillot and John Calautit. Resilience in Social Housing: Thermal Evaluation through a New Method to approach Climate Change Projections. In *International Academic Conference for Graduates NUAA. Nanjing, China*, 2019.
- Ana Berenice Gómez de León, Lucelia Rodrigues, Mark Gillot and John Calautit. An Innovative Method for the Assessment of Thermal Comfort and Resilience in Social Housing. In *International Academic Conference for Graduates NUAA. Nanjing, China*, 2018.

Contents

Abstract i

Acknowledgements iii

Authors Associated Publications to Date v

List of Figures xiv

List of Tables xxiii

List of Acronyms xxvii

Introduction 1

- **Aims and Objectives** 2
- **Methodology** 3
- **Research Structure and Key Outcomes** 5

I Literature Review 8

1 Energy and Social Housing in Mexico 9

1.1 National Energy Standards and Policies 11

1.1.1 Mexican Official Standards *NOM* 11

1.1.2 Mexican Standards *NMX* 13

1.1.3 Plans and Strategies 14

1.2 Housing in Mexico 17

1.2.1 Characteristics of Social Housing 19

1.2.2 Sustainable Housing 21

1.3 Housing Resilience and Adaptation 28

1.4 Conclusions 30

2 Weather, Climate and Thermal Comfort 32

2.1 Geographical Characteristics and Climates in Mexico 33

2.2 Climate Projections 35

2.2.1 Historical and Synthetic Weather Data 36

2.2.2 Weather Data-sets for Future Climate Scenarios 38

2.2.3 Climate Projections in Mexico and Coahuila 42

2.3 Thermal Comfort in Housing 48

2.3.1 Quantitative and Qualitative Approaches 51

2.3.2 Thermal Comfort Standards 52

2.3.3 Assessment Techniques and Housing Envelope 57

2.4 Conclusions 59

II Developed Methodology for Weather Files Generation for Building Simulation and Data Interpolation 62

3 Algorithm DGG1. Generation of Response Surface for a Rectangular Grid 63

3.1 Antecedents of Algorithm DGG1 66

3.2 Mathematical Development of Algorithm DGG1 68

3.2.1 Response Surface from a $\mathbf{3} \times \mathbf{3}$ Rectangular Mesh 68

3.2.2 Revision of some Adjustment Models 70

3.3 Programme Functioning 83

3.3.1 Input and Output Data 84

3.3.2 Running the Programme 86

3.3.3 Codification 98

3.4 Conclusions 98

4 Algorithm DGG2. Generation of Response Surface for an Irregular Mesh 101

4.1 Antecedents of Algorithm DGG2 102

4.1.1 Description of the Problem 104

4.1.2 Mathematical Development of Algorithm DGG2 106

4.2 Programme Functioning 107

4.2.1 Data Management 108

4.2.2 Input and Output Data in Programme *methodB.m* 108

4.2.3 Running the Programme 111

4.2.4 Codification 116

4.3 Conclusions 116

5 Algorithm DGG3. Generation of Weather Files for Climate Projections 119

5.1 Introduction 119

5.2 Antecedents of Algorithm DGG3 120

5.3 Mathematical Development of Algorithm DGG3 126

5.3.1 Fitting a Straight Line 126

5.3.2 Matrix Approach 128

5.3.3 Orthogonal Projection 129

5.3.4 Fitting by a Parabola 130

5.3.5 Using MATLAB 133

5.4 Programme Functioning 136

5.4.1 Required Historical Data 136

5.4.2 Required Climate Projections Data 138

5.4.3 Master Programmes and Subprogrammes 140

5.4.4 Master Programme for Saltillo 141

5.4.5 Programme *THR.m* 142

5.4.6 Programme *HR_T.m* 144

5.4.7 Programme *TempHorizontes.m* 146

5.4.8 Programme *HRh.m* 150

5.4.9 Master Programmes for Monclova y Torreón 153

5.5 Conclusions 153

III Social Housing Climate Resilience 156

6 Building Thermal Simulation 157

6.1 Dynamic Simulation Scope 159

6.2 Disposition of the Dwelling 165

6.2.1 Reference Dwelling 166

6.2.2 Base Case Dwelling 167

6.2.3 Compact Floor Plan Dwelling 170

6.3 Dynamic Thermal Simulation and Weather Files 173

6.3.1 Software for Dynamic Thermal Simulations 173

6.3.2 Assumptions for Dynamic Simulations 174

6.3.3 Solar Analysis 178

6.3.4 Weather files and Locations per City 180

6.4 Housing Envelope Simulation Parameters 181

6.4.1 Envelope Materials 183

6.4.2 Walls 185

6.4.3 Roofs 186

6.4.4 Windows and Frames 189

6.4.5 Floors 192

6.4.6 Disposition of Simulation Cases 192

6.5 Conclusions 197

7 Simulation Cases and Resilience 201

7.1 Simulation for Adapted Models, Saltillo 203

7.1.1 Current and Future Weather 203
7.1.2 Set 1 204
7.1.3 Set 2 209
7.1.4 Set 3 212
7.1.5 Results 214
7.2 Simulation for Adapted Models, Monclova 216
7.2.1 Current and Future Weather 216
7.2.2 Set 1 217
7.2.3 Set 2 221
7.2.4 Set 3 222
7.2.5 Results 223
7.3 Simulation for Adapted Models, Torreón 226
7.3.1 Current and Future Weather 226
7.3.2 Set 1 227
7.3.3 Set 2 231
7.3.4 Set 3 233
7.3.5 Results 234
7.4 Conclusions 236

IV Conclusions and Discussion 243

8 Conclusion and Discussion 244

8.1 Research Impact, Limitations, and Discussion 246

8.1.1 Literature Review 247

8.1.2 Algorithms 248

8.1.3 Dynamic Simulation of Cases 249

8.2 Recommendations for Further Work 250

8.2.1 For Algorithms 250

8.2.2 For Simulations and New Cases 252

8.3 Conclusions and Closing Comments 253

References **254**

V Appendices **274**

A Code of Algorithm DGG1 **275**

A.1 $\mathbf{3} \times \mathbf{3}$ Rectangular Mesh Code 275

A.1.1 Subroutine for Writing Quadratic Equations on the x-axis . . 295

A.1.2 Subroutine for Writing Quadratic Equations on the y-axis . . 297

A.1.3 Subroutine to Generate Titles 299

A.1.4 Subroutine to Convert Angles to Decimal Format 300

B Figures from Algorithm DGG1 **303**

B.1 Figures Obtained with grid9.m 303

C Code of Algorithm DGG2 **316**

C.1 Code *methodB.m* 316

C.1.1 Response Surface Interpolation 327

D 3D Figures from Algorithm DGG2 332

D.1 Response Surfaces obtained with Algorithm DGG2 332

E Fitting of Polynomials of Least Squares 345

E.1 Code *parabol.m*, Least Squares 345

F Temperature and Relative Humidity Estimates for Horizons in Saltillo from Algorithm DGG3 349

F.1 Code *SaltilloHorizontes.m* 349

F.1.1 Hourly Temperatures and Relative Humidity for Saltillo . . . 352

F.1.2 Other Subroutines 358

F.1.3 Summarized Results 358

G Temperature and Relative Humidity Estimates for Horizons in Monclova from Algorithm DGG3 362

G.1 Code *MonclovaHorizontes.m* 362

G.1.1 Hourly Temperatures and Relative Humidity for Monclova . . 365

G.1.2 Other Subroutines 370

G.1.3 Summarized Results 370

H Temperature and Relative Humidity Estimates for Horizons in Torreón from Algorithm DGG3 374

H.1 Code *TorreonHorizontes.m* 374

H.1.1 Hourly Temperatures and Relative Humidity for Torreón . . . 377

H.1.2 Other Subroutines 382

H.1.3 Summarized Results 382

I Extraction of Temperature and Relative Humidity Columns from Historical Weather Files **386**

I.1 Code *THR.m* for Algorithm DGG3 387

J Relative Humidity as a Function of Temperature **389**

J.1 Code *HR_T.m* for Algorithm DGG3 389

K Hourly Horizons Temperatures **392**

K.1 Coding of *TempHorizontes.m* for Algorithm DGG3 392

L Matrix of Simulation Cases **397**

L.1 Simulation Cases Saltillo, Monclova and Torreón 397

M Psychrometric Charts **407**

N Solar Analysis **420**

N.1 Sunny Periods 420

List of Figures

1.1 Urban Contained Perimeters in Coahuila 18

1.2 Global Performance Index Scale. 23

1.3 Mexican Climate Zones According to *NAMA* 27

2.1 Climates of Mexico, Coahuila and Saltillo 35

2.2 *SRES* Scenario Families 36

2.3 Douglas Regionalisation 43

2.4 *PRECIS* model projections for Coahuila 45

2.5 Atlas Climático 47

2.6 Operative Temperature Ranges for Naturally Conditioned Spaces . . . 54

2.7 Psychrometric Chart for Saltillo 56

3.1 Interaction Between the Three Algorithms. 65

3.2 Data of the 3×3 Rectangular Mesh 69

3.3 Linear Interpolation in 2D 70

3.4 Line in 3D 72

3.5 Quadratic Errors 74

3.6 Response Surface of Triangular Faces. 75

3.7 Vector Equation of the Plane. 76

3.8 Plane by Three Points. 77

3.9 Parabolas $z(x, w)$, $y =$constant. 79

3.10 Parabolas $z(y, w)$, $x =$constant. 80

3.11 Parabolic Scaffolding 80

3.12 Response Surface. 82

3.13 Contour Lines. 82

3.14 Flow Diagram of Algorithm 84

3.15 Nine Points Geographical Location. 87

3.16 Poles with Temperatures. 88

3.17 Parabolas Generated with Longitudes Direction. 88

3.18 Parabolas Generated with Latitudes Direction. 89

3.19 Parabolas Scaffolding. 90

3.20 Poles and Lattice with Generated Information. 91

3.21 Response Surface. 92

3.22 Temperature Colored Plan View. 93

3.23 Response Surface and Projected Contour Lines. 94

3.24 Contour Lines. 94

3.25 Points on Red Parabolas. 95

3.26 Equation of the Parabola Conformed by the Three Points. 96

3.27 Obtaining the Appropriate Height for Coordinates $(-102.9483, 25.4353)$. 96

3.28 Interpolation Point. 97

3.29 Poles from MATLAB 97

4.1 Weather Stations Locations. 104

4.2 Some Weather Stations in the Polygon. 106

4.3 Flow Diagram of Algorithm 107

4.4 Data Triangulation in 2D. 112

4.5 Triangles Colouring in 2D. 113

4.6 Truncated Prisms MATLAB 113

4.7 Coloured Upper Triangles MATLAB 114

4.8 Response Surface B MATLAB 114

4.9 Relative Errors B MATLAB 115

4.10 Contour Lines B MATLAB 115

5.1 Temperatures from Historical Weather Data. 121

5.2 Best Line of Least Squares 127

5.3 Projection of b on $col(A)$. 129

5.4 Best Parabola of Least Squares 132

5.5 Elements Tool Screen 137

5.6 Algorithm DGG3. 142

5.7 Adjustment Curve 144

5.8 Noise Diagram Relative Humidity 145

5.9 Saltillo: Near Horizon, Minimum Temperatures 149

5.10 Saltillo: Near Horizon, Average Temperatures 149

5.11 Saltillo: Near Horizon, Maximum Temperatures 149

6.1 Building Thermal Simulation Diagram. 158

6.2 First Part of Dynamic Simulation Diagram. 163

6.3 Second Part of Dynamic Simulation Diagram. 164

6.4 Third Part of Dynamic Simulation Diagram. 165

6.5 Detached House Typology 166

6.6 Base Case of Detached House Typology. 168

6.7 Base Case Floor Plan. 169

6.8 Base Case Perspective Section A-A'. 169

6.9 Base Case Perspective Section B-B'. 170

6.10 Case 36 Floor Plan with Site 171

6.11 Compact Case Floor Plan. 172

6.12 Compact Case Perspective Section A-A'. 172

6.13 Compact Case Perspective Section B-B'. 173

6.14 Projects Location. 181

6.15 Base Case Geometry. Simplified 3D model in SketchUp. 182

6.16 Compact Geometry. Simplified 3D model in SketchUp. 183

6.17 Details: Walls, not to scale. 186

6.18 Details: Roofs, not to scale. 188

6.19 Window Glass Materials. 189

6.20 Floor Slab Construction Detail, not to scale. 192

6.21 Geometry Modification. 196

7.1 Diagram of Simulations Results Arrangement. 202

7.2 Saltillo Cases 1 to 6. 206

7.3 Saltillo Cases 7 to 12. 206

7.4 Saltillo Cases 13 to 18. 207

7.5 Saltillo Cases 19 to 24. 208

7.6 Saltillo Cases 25 to 28. 210

7.7 Saltillo Cases 29 to 34. 211

7.8 Saltillo Cases 35 to 40. 213

7.9 Saltillo Best Case for current weather, Case 33. 215

7.10 Monclova Cases 1 to 6. 218

7.11 Monclova Cases 7 to 12. 219

7.12 Monclova Cases 13 to 18. 220

7.13 Monclova Cases 19 to 24. 220

7.14 Monclova Cases 25 to 28. 222

7.15 Monclova Cases 29 to 34. 222

7.16 Monclova Cases 35 to 40. 223

7.17 Monclova Best Case for future horizons, Case 16. 225

7.18 Torreón Cases 1 to 6. 228

7.19 Torreón Cases 7 to 12. 229

7.20 Torreón Cases 13 to 18. 230

7.21 Torreón Cases 19 to 24. 230

7.22 Torreón Cases 25 to 28. 232

7.23 Torreón Cases 29 to 34. 232

7.24 Torreón Cases 35 to 40. 234

7.25 Torreón Best Case for current weather, Case 29. 235

7.26 Compact model for Saltillo, Monclova and Torreón for current and future horizons. 238

B.1 Poles. 304

B.2 Coloured Response Mesh. 304

B.3 Black Response Mesh. 305

B.4 Response Mesh and Projected Contour Lines. 305

B.5 Lower Plane. 306

B.6 Response Surface. 306

B.7 Response Surface without Lines. 307

B.8 Soft Response Surface. 307

B.9 Response Surface in Waterfall. 308

B.10 Scaffolding to Interpolate One Point. 308

B.11 3 points in x. 309

B.12 Generation of Interpolation Parabola. 309

B.13 Height of the Parabola. 310

B.14 Interpolation Point. 310

B.15 Scaffolding to Interpolate One Point. 311

B.16 Generation of Interpolation Parabola. 311

B.17 Height of the Parabola. 312

B.18 Interpolation Point. 312

B.19 Scaffolding to Interpolate One Point. 313

B.20 3 points in x. 313

B.21 Generation of Interpolation Parabola. 314

B.22 Height of the Parabola. 314

B.23 Interpolation Point. 315

B.24 4 Interpolation Values. 315

D.1 Response Surfaces A2 2020, January - June 333

D.2 Response Surfaces A2 2020, July - December 334

D.3 Response Surfaces A2 2050, January - June 335

D.4 Response Surfaces A2 2050, July - December 336

D.5 Response Surfaces A2 2080, January - June 337

D.6 Response Surfaces A2 2080, July - December 338

D.7 Response Surfaces B2 2020, January - June 339

D.8 Response Surfaces B2 2020, July - December 340

D.9 Response Surfaces B2 2050, January - June 341

D.10 Response Surfaces B2 2050, July - December 342

D.11 Response Surfaces B2 2080, January - June 343

D.12 Response Surfaces B2 2080, July - December 344

M.1 Saltillo, Givoni Bioclimatic Chart for Current Weather. 408

M.2 Saltillo, ASHRAE 55-2017 for Current Weather. 408

M.3 Saltillo, Givoni Bioclimatic Chart for Near Horizon. 409

M.4 Saltillo, ASHRAE 55-2017 for Near Horizon. 409

M.5 Saltillo, Givoni Bioclimatic Chart for Medium Horizon. 410

M.6 Saltillo, ASHRAE 55-2017 for Medium Horizon. 410

M.7 Saltillo, Givoni Bioclimatic Chart for Far Horizon. 411

M.8 Saltillo, ASHRAE 55-2017 for Far Horizon. 411

M.9 Monclova, Givoni Bioclimatic Chart for Current Weather. 412

M.10 Monclova, ASHRAE 55-2017 for Current Weather. 412

M.11 Monclova, Givoni Bioclimatic Chart for Near Horizon. 413

M.12 Monclova, ASHRAE 55-2017 for Near Horizon. 413

M.13 Monclova, Givoni Bioclimatic Chart for Medium Horizon. 414

M.14 Monclova, ASHRAE 55-2017 for Medium Horizon. 414

M.15 Monclova, Givoni Bioclimatic Chart for Far Horizon. 415

M.16 Monclova, ASHRAE 55-2017 for Far Horizon. 415

M.17 Torreón, Givoni Bioclimatic Chart for Current Weather. 416

M.18 Torreón, ASHRAE 55-2017 for Current Weather. 416

M.19 Torreón, Givoni Bioclimatic Chart for Near Horizon. 417

M.20 Torreón, ASHRAE 55-2017 for Near Horizon. 417

M.21 Torreón, Givoni Bioclimatic Chart for Medium Horizon. 418

M.22 Torreón, ASHRAE 55-2017 for Medium Horizon. 418

M.23 Torreón, Givoni Bioclimatic Chart for Far Horizon. 419

M.24 Torreón, ASHRAE 55-2017 for Far Horizon. 419

N.1 Sunny Periods from January to April 421

N.2 Sunny Periods from May to August 422

N.3 Sunny Periods from September to December 423

N.4 Sunny Periods Annual and Annual Mean 424

N.5 Sunny Periods Floors, winter, summer, spring / autumn, annual 425

N.6 Sunny Periods Windows, winter, summer, spring, autumn 426

N.7 Sunny Periods Windows, annual 427

N.8 Sunny Periods Walls, annual 427

N.9 Sunny Periods Walls, winter, summer, spring, autumn 428

N.10 Stereographic Projections kitchen, bathroom, north and south bedrooms 429

N.11 Stereographic Projections living room 430

List of Tables

1.1 Mexican Official Standards for Energy, Water and Gas Efficiency . . . 12

1.2 Norms to Validate Thermal Insulators for Buildings 14

1.3 Housing Classification by Average Built Surface 20

1.4 Dwellings Inhabited by Material in Walls and Roofs 21

1.5 NAMA's Mitigation Actions on Building Sector 25

2.1 Bio-climated Elements 59

3.1 Algorithms Synopsis. 64

3.2 Geographic Coordinates from GCM. 67

4.1 Weather Stations 105

5.1 Annual Years Intervals by Horizon 121

5.2 Saltillo Monthly Temperatures for Future Horizons 123

5.3 Monclova Monthly Temperatures for Future Horizons 123

5.4 Torreón Monthly Temperatures for Future Horizons 124

5.5 Least Square Method 135

5.6 Annual Temperatures Data 139

5.7 Pairs of Temperatures and Relative Humidity 141

5.8 Horizons Temperatures for Saltillo 150

5.9 Fourth degree equations to calculate the relative humidity by month . 151

5.10 Temperatures and relative humidities for the near horizon, Saltillo . . 152

6.1 Key Codes for Envelope Components used in Dynamic Simulations. . 161

6.2 Reference House Characteristics 177

6.3 Chosen Locations for Each City 180

6.4 Design Strategies. 184

6.5 Window to Wall Ratio. 191

6.6 Zone Summary 191

6.7 Envelope Elements Set 1 193

6.8 Envelope Elements Set 2 194

6.9 Envelope Elements Set 3 197

7.1 Minimum and Maximum Temperatures and Relative Humidity from *.epw* files used in Saltillo simulations for future horizons. 204

7.2 Percentage of Annual Comfort Saltillo Set 1 204

7.3 Percentage of Annual Comfort Saltillo Set 2 209

7.4 Percentage of Annual Comfort Saltillo Set 3 212

7.5 Minimum and Maximum Temperatures and Relative Humidity from *.epw* files used in Monclova simulations for future horizons. 217

7.6 Percentage of Annual Comfort Monclova Set 1 217

7.7 Percentage of Annual Comfort Monclova Set 2 221

7.8 Percentage of Annual Comfort Monclova Set 3 223

7.9 Minimum and Maximum Temperatures and Relative Humidity from *.epw* files used in Torreón simulations for future horizons. 226

7.10 Percentage of Annual Comfort Torreón Set 1 227

7.11 Percentage of Annual Comfort Torreón Set 2 231

7.12 Percentage of Annual Comfort Torreón Set 3 233

7.13 Higher Values of Annual Comfort Percentage BC 239

7.14 Higher Values of Annual Comfort Percentage Compact 239

7.15 Final Best Cases. 240

F.1 Hourly Temperatures and Relative Humidity 353

F.2 Temperatures and relative humidities for the near horizon, Saltillo . . 358

F.3 Temperatures and relative humidities for the medium horizon, Saltillo 360

F.4 Temperatures and relative humidities for the far horizon, Saltillo . . . 361

G.1 Temperatures and relative humidities for the near horizon, Monclova . 371

G.2 Temperatures and relative humidities for the medium horizon, Monclova372

G.3 Temperatures and relative humidities for the far horizon, Monclova . . 373

H.1 Temperatures and relative humidities for the near horizon, Torreón . . 383

H.2 Temperatures and relative humidities for the medium horizon, Torreón 384

H.3 Temperatures and relative humidities for the far horizon, Torreón . . . 385

L.1 Simulation Cases Saltillo North-South 397

L.2 Simulation Cases Saltillo East-West 399

L.3 Simulation Cases Monclova North-South 400

L.4 Simulation Cases Monclova East-West 402

L.5 Simulation Cases Torreón North-South 403

L.6 Simulation Cases Torreón East-West 405

List of Acronyms

AACB Autoclaved Aerated Concrete Block 183

ACM Adaptive Comfort Model 53

AR4 Fourth Assessment Report, IPCC 35

AR5 Fifth Assessment Report, IPCC 36

AR6 Sixth Assessment Report, IPCC 36

ASHRAE American Society of Heating, Refrigerating and Air-Conditioning Engineers 37

BEM Building Energy Modeling 173

BMU Bundesministerium für Umwelt, Naturschutz und nukleare Sicherheit 22

CB Concrete Block 183

CEV Código de Edificación de Vivienda 14

CHB Clay Hollow Block 183

CMCC Centro Euro-Mediterraneo sui Cambiamenti Climatici 41

CNRM-CM5 Centre National de Recherches Meteorologiques Coupled Global Climate Model version 5 46

CONAFOVI Comisión Nacional de Fomento a la Vivienda 58

CONAGUA Comisión Nacional del Agua 22

CONAVI Comisión Nacional de Vivienda 10

CONUEE Comisión Nacional para el Uso Eficiente de la Energía 22

DSY Design Summer Year 41

EPW EnergyPlus Weather File 36

ESR Encuesta de Satisfacción Residencial 21

FONHAPO Fondo Nacional de Habitaciones Populares 18

FOVISSSTE Fondo de la Vivienda del Instituto de Seguridad y Servicios Sociales de los Trabajadores del Estado 18

GCM General Circulation Models 38

GDP Gross Domestic Product 16

GFDL-CM3 Geophysical Fluid Dynamics Laboratory Climate Model version 3 46

GIZ Deutsche Gesellschaft für Internationale Zusammenarbeit . . . 22

HadCM3 Hadley Centre Coupled Model Version 3 41

HadGEM2-ES Hadley Centre Global Environment Model version 2 Earth-System 46

HV Hipoteca Verde 19

IDG Índice de Desempeño Global 23

IEA International Energy Agency 125

IMSS Instituto Mexicano del Seguro Social 18

INECC Instituto Nacional de Ecología y Cambio Climático 66

INEGI Instituto Nacional de Geografía y Estadística 15

INFONAVIT Instituto del Fondo Nacional de la Vivienda para los Trabajadores 17

INMCM4.0 Institute of Numerical Mathematics Climate Model Version 4 . 41

IPCC Intergovernmental Panel on Climate Change 2

ISD Integrated Surface Database 138

ISSSTE Instituto de Seguridad y Servicios Sociales de los Trabajadores del Estado 18

IWEC International Weather for Energy Calculations 37

LGCC Ley General de Cambio Climático 32

MPI-ESM-LR Max Planck Institute Earth System Model, low resolution . . . 46

MRV Monitoreo, Reporte y Verificación 25

NAMA Nationally Appropriate Mitigation Action 17

NCDC National Climatic Data Center 40

NSRDB National Solar Radiation Data Base 40

NMX Normas Mexicanas 4

NOM Normas Oficiales Mexicanas 3

ONNCCE Organismo Nacional de Normalización y Certificación de la Construcción y Edificación 13

PCIC Pacific Climate Impacts Consortium 67

PHPP Passive House Planning Package 26

PRECIS Providing Regional Climates for Impact Studies 39

RCM Regional Climate Models 38

RCP Representative Concentration Pathways 36

RUV Registro Único de Vivienda 17

SEDATU Secretaría de Desarrollo Agrario, Territorial y Urbano 18

SEDESOL Secretaría de Desarrollo Social 18

SEMA Secretaría de Medio Ambiente 43

SHF Sociedad Hipotecaria Federal 21

SHGC Solar Heat Gain Coefficient 189

SISEVIVE Sistema de Evaluación de la Vivienda Verde 23

SMN Servicio Meteorológico Nacional 102

SRES Special Report on Emission Scenarios 35

TAR Third Assessment Report, IPCC 35

TMY Typical Meteorological Year 39

TRY Test Reference Year 41

UNAM Universidad Nacional Autónoma de México 46

Introduction

The development of social housing projects has a wide range of research aspects due to the complexity of its study in social, economic, physical and perceptual terms. The demand for social housing in Mexico results in large developments across the country with little consideration for specificity of the location.

Mexican social housing mostly comprises of a simple repetitive design that does not respond to local climate or users comfort requirements. The typical design also does not take into consideration the changes brought in by climate change, which even though approached for other disciplines in the country, has not been adapted to use data for energy simulations and the built environment.

The large scale of these projects means great environmental impact, but also an opportunity to cause a positive impact on many lives if the design is optimised to deliver better comfort in response to local climate today and in the future.

Mexico is a country of contrasts with varied climates due to the different geographical characteristics experienced from one place to another. By means of this, previous studies covered in the literature of this research regarding thermal comfort and energy savings have been carried out in different cities of the country. However, in these studies the state of Coahuila is considered under one type of climate, when there are three, and seven sub-types of climate.

For this research, the analysis of the thermal comfort that exists within the social housing in three cities of Coahuila: Saltillo, Monclova and Torreón, was proposed. For

the study, a base case is considered, and further modifications are made in the thermal envelope for their analysis through dynamic simulations.

The thermal comfort inside the simulated dwellings was studied with weather files for current weather based on historical data, and for weather files generated for future horizons. The latest were elaborated and adapted to the Intergovernmental Panel on Climate Change (IPCC[1]) future scenarios and horizons by developing new algorithms presented as an innovative methodology.

The analysis of the thermal behavior of the houses offers a perspective of the revision that can be made in the building envelope. The possible behavior of this over time is also considered to propose improvements in the short, medium and long terms, considering the location of the project with its corresponding weather files.

The novelty of this work lies on the combination of an innovative methodology generated for creating weather files specific for each site, considering historical and possible climate projections, and their applicability in social housing design, to improve the envelope characteristics in order to increase thermal comfort within them.

Aims and Objectives

The research aims to develop new algorithms to generate and provide the data needed to elaborate weather files in where weather projections for possible future scenarios can be implemented. This, applicable to specific locations, to consider better thermal envelope characteristics and architectural designs for social housing in the three climates of Coahuila.

The envelope of social housing is limited to buildings without active systems, as generally, this is an economic expense difficult to cover by users of these houses. The objectives proposed to achieve the research aim and to facilitate the improvement of the thermal performance along the years are mentioned below:

[1] Intergovernmental Panel on Climate Change

1. Investigation of the most relevant literature and its posterior analysis for the definition of the research importance and identification of the gap in knowledge.

2. Weather data gathering of General and Regional Climate Models from two reports of the IPCC: Special Report on Emission Scenarios, and Representative Concentration Pathways for Coahuila.

3. Development of new procedures to use the gathered weather data and interpolate the missing information in the studied surfaces.

4. Creation of new weather files for future horizons and scenarios adapted to the research proposed locations.

5. Definition of the housing typology and its typical parameters to study how they perform and analyse possible improvements.

6. Performing of dynamic simulations modifying individual parameters and further combination of them to find the best interaction between building elements.

7. Assessment and description of the best cases with their corresponding components for each city proposed in the study.

Methodology

The objectives proposed were approached with a methodology that will be explained in the following paragraphs.

To define the importance of the research and approach objective one, the making of an extensive literature review from the latest academic publications, journals and policies was performed to cover what has been done in the international panorama and in Mexico. Different methods and experimentation were studied to make improvements related to the thermal performance of the building envelopes in the built environment. Several gaps were found when comparing the regulations used in Mexico in terms of energy efficiency and thermal performance of the buildings. Official standards (NOM[2])

[2]Normas Oficiales Mexicanas

and the suggested regulations (NMX[3]) were reviewed and analysed in Chapter 1.

Covering objective two in Chapter 2, the collection of current weather data from Coahuila was gathered from the database of the National Meteorological Service. Complemented and more detailed information was obtained from the meteorological stations on the Wunderground website. This information is extensive and the process followed to collect it was explained. A deeper analysis of the impact of physiography in climate and thermal comfort was also explained in the Research Structure and Key Outcomes, in where a better description of chapters can be found.

The algorithms developed for the interpolation of data made use of mathematical procedures to obtain data response surfaces. They were created in order to suffice objective three; different dispositions of data are covered, as projections available for Mexico were assigned differently depending on the IPCC report. These are explained in Chapters 3 and 4.

Due to the large amount of scattered information contained in the weather files, the need to manage it mathematically in the form of equations arose. The review of assessment techniques highlighted the importance of the Least Squares Approximations method, which was used for being one of the most important assessment techniques to fit data in an equation form. Weather data management, and the generation of the algorithms were developed in MATLAB to obtain the stated on objective four; this development can be consulted in Chapter 5.

The housing typology was defined after the review of diverse typologies and materials used in construction for housing in Coahuila by obtaining data collected from the National Institute of Statistics and Geography in Mexico; after reviewing these official documents, the house characteristics were defined and objective five was explored in Chapter 6.

To approach the study of the building envelope thermal performance, a parametric study for the three predominant climates in the northeast of Mexico was performed; three different materials in envelopes were considered: concrete block, clay hollow block, and autoclaved aerated concrete block. Comparisons between them were per-

[3]Normas Mexicanas

formed through dynamic simulations in EnergyPlus in three different climate horizons for three different sets of years. Chapter 7 examined these cases, as proposed for objectives six and seven.

Research Structure and Key Outcomes

The research structure was divided into five parts containing eight chapters. The content of these are briefly described below.

Part I. Literature Review.

This part consists of two chapters and covers the literature review of Mexico's energy regulations, social housing, weather and thermal comfort.

Chapter 1. *Energy and Social Housing in Mexico*. Introduction to the characteristics of social housing in the country, current energy regulations and concepts of resilience and adaptation. Offers a description of the context in where the research is analysed and draws a descriptive problematic in social housing in Mexico.

Chapter 2. *Weather, Climate and Thermal Comfort*. The geographic characteristics of Mexico are shown along with current climatic and weather data. Regional weather projections are specified for possible future scenarios and horizons. Climate comfort qualities and adaptive comfort studies are described. The literature reviewed endows the need of covering some of the gaps found in the use of accurate weather files in most cities in the country, and the lack of them for specific sites.

Part II. Developed Methodology for Weather File Generation and Data Interpolation.

These chapters describe the creation of an innovative methodology, in where algorithms to obtain interpolated data, based on General and Regional Climate Models data, were developed. An algorithm to create new weather files for future horizons

under mathematical procedures is also shown.

Chapter 3. *Algorithm DGG1. Generation of Response Surface for a Rectangular Grid.* Mathematical concepts for the study of regular grids are described. It is based on data obtained from General Circulation Models. The development of algorithm DGG1 and its operation in MATLAB to obtain data in a response surface is shown. The results obtained from it are provided numerically and in different displays of graphics.

Chapter 4. *Algorithm DGG2. Generation of Response Surface for an Irregular Mesh.* The study of mathematical concepts for irregular meshes is described. It is based on data obtained from Regional Climate Models. The development of the DGG2 algorithm and its operation in MATLAB to obtain data on a response surface is shown along with the results obtained with said surface.

Chapter 5. *Algorithm DGG3. Generation of Weather Files for Climate Projections.* The mathematical foundation and the development of the DGG3 algorithm is presented. Data from the historical weather files are interpolated to consider the projections of future horizons and adapt the columns of temperatures and relative humidity in the new weather files. Its application for the creation of weather files used in dynamic simulation software is explained.

Part III. Social Housing Climate Resilience.

The parameters used to study thermal comfort within social housing in the cities and case studies proposed are shown. The results obtained with these simulations are discussed, so these chapters describe the proposed simulation cases, demonstrate the results in thermal comfort annual percentages, and analyse resilience in social housing from an envelope modification perspective.

Chapter 6. *Building Thermal Simulation.* The disposition of the case studies in the cities of Saltillo, Monclova, and Torreón is explained; this, for current weather and weather files of the near, medium and far horizons obtained with the algorithm of the previous chapter.

The architectural and spatial characteristics used in the dynamic simulations are spec-

ified. The parameters used in these are detailed individually, indicating the variations considered for each of them.

Chapter 7. *Simulation Cases and Resilience*. Simulations cases obtained with the parametric study are analysed. The results are shown based on percentages of thermal annual comfort and the best cases are chosen for each city. The cases with the highest number of comfort hours for current and future horizons are evaluated and compared between two adaptive comfort analyses.

Part IV. Conclusions and Discussion

The general conclusions and discussion of the research are presented in addition to suggestions for further work.

Chapter 8. *Conclusions and Discussion*. The conclusions from the results obtained are drawn, along with a discussion of the relevance of the research in terms of the algorithms created and the results of the simulations. Better design architectural practices are discussed. For this chapter, there are recommendations for further work to broaden the knowledge of comfort derived from good practices in architecture and the built environment. There is also proposed the use of the algorithms in different scales and disciplines.

Part V. Appendices

The appendices show codes, figures and tables relevant and extensive from the main chapters developed throughout the research. As the information is broad, it was provided in this part to facilitate the reading of the thesis. The MATLAB codes used for the algorithms of Part III, and the figures and graphs obtained with them, are shown. The complete simulations matrix and the graphs of the psychrometric charts from which the design strategies were derived are also displayed.

Part I

Literature Review

Chapter 1

Energy and Social Housing in Mexico

Energy is currently required for everyday activities, and it involves the use of renewable and non-renewable resources for its operation. The building sector is responsible for a large part of the global emissions of climate gases [20]; this represents 21.3% of the world total energy consumption [91], and relates to operational emissions such as heating, cooling and lighting, and to emissions related to production, maintenance and demolition, namely, the full life-cycle of buildings. In Mexico, the most recent national energy balance performed in 2018 [45], indicates the use of energy in the residential sector has increased by 1.20% compared to the previous year of the study. Its main use is for cooking food, heating, cooling, water heating, lighting and ironing.

Among the main aspects for energy efficiency in buildings are the strategies considered to save energy from early stages of design: the nearly zero energy passive building design approach; the use of low energy building materials, the use of low energy efficient equipment for low operational energy requirements; and the integration of renewable energies [28]. Once these procedures are analysed, electronic devices such as digital assistants (e.g. Amazon Echo, Google Home, Apple HomePod) can be implemented, and people can monitor and control the physical environment of their houses, and obtain information on energy consumption. Nonetheless, not all users can afford these technologies, therefore here relies the importance of providing passive strategies that allow energy savings without the use of devices that represent extra expense.

Occupant behaviour is a key issue for building design optimisation and depends on a

deeper understanding of physical phenomena, the analysis of energy consumption and the interaction between information blocks to provide architectural and building design improvements. For this research, direct interaction with occupants is not possible, but a previous study performed by the National Housing Commission (CONAVI[1]) [121], was used to consider occupancy for simulations; this is further explained in subsection 6.2. The same applies to the obtaining of data derived from measurements of physical parameters in buildings, and the analysis and interpretation of data for the benefit of users in terms of comfort and energy efficiency required for the operation of the building.

The awareness of the user and the desirable improvements accomplished by the designer, go beyond the energy savings obtained in buildings. From a global perspective, these enhancements represent the well being that can be shared on a small scale, creating systems that allow a better quality of life. Energy consumption in the domestic sector has been increasing over the last decades – the overall consumption is higher than in past years because the activities performed inside houses require the use of new appliances, in addition to the usual use of energy for lighting, cooling and heating. To regulate this, governments have introduced standards that require a minimum level of accepted quality or performance.

Mexican energy standards and current policies are discussed in this chapter along with plans and strategies to incentive and implement national housing policies that consider better energy practices, Section 1.1.

To delve into this, the characteristics of social housing are described in Section 1.2, in addition to how to obtain these dwellings, and the solutions that have been proposed to obtain sustainable housing. Finally, different approaches to resilience and adaptation are displayed in Section 1.3, as their applicability in the built environment.

[1]Comisión Nacional de Vivienda

1.1 National Energy Standards and Policies

In Mexican building regulations, two main ones stand out: the NOM and the NMX. The first one is mandatory, while the latter is suggested, based on international standardization where the efficiency of buildings' components is considered. These include physical elements, energy efficiency, material qualities, and systems used in the construction. Taking into account these regulations, different plans have been created to benefit the population in terms of housing, so they are generated for different purposes, from obtaining loans and subsidies, to developing tools that facilitate energy savings and comfort within households.

1.1.1 Mexican Official Standards *NOM*

The Official Mexican Standards, NOM, are Mexican regulations that combine information, specifications and requirements evaluated by the government and external professional experts. Their purpose is to establish metrics that avoid risks to the population and the environment; the ones focused on energy efficiency in buildings envelopes are divided in two, and encompass residential buildings and non-residential buildings. The *NOM-020-ENER-2011* [118] covers energy efficiency in residential buildings and determines the minimum standard of a building envelope in which one can live (houses and apartments). The *NOM-008-ENER-2001* [116] addresses energy efficiency in non-residential buildings, and the minimal thermal quantity that a non-residential property must adhere to, compared to a regulatory standard. These buildings include hospitals, hotels, schools, among others.

In both regulations is considered the building envelope study exclusively. This is made up of all the elements of the construction that divide the interior space of the building from the exterior – elements such as walls, doors, ceilings, windows and floors, which act as protection from the sun, rain, high or low temperatures from the outside and offer shelter, allowing people to benefit from a level of physical security and appropriate thermal comfort.

There are also other norms applied to construction elements in buildings, such as the

NOM-018-ENER-2011 in which characteristics, limits and testing methods for thermal insulators for buildings are stipulated, and the *NOM-024-ENER-2012* that provides labeling and testing methods for thermal and optical characteristics of glass and glazed systems for buildings. The *NOMs* related to energy and environmental efficiency in buildings are mentioned in Table 1.1.

Table 1.1: Mexican Official Standards for Energy, Water and Gas Efficiency. Modified and updated from *Fundación IDEA* [82]

Mexican Official Standard	**Description**
	Energy
NOM-009-ENER-1995	Energy Efficiency (EE) for thermal insulation in industrial use
NOM-006-ENER-1995	Electro mechanic EE in deep well water pumping systems
NOM-018-ENER-2011	Thermal insulation for buildings
NOM-001-ENER-2000	EE on vertical centrifugal pumps with external vertical electric motor
NOM-008-ENER-2001	EE in buildings, envelope of non residential buildings
NOM-015-ENER-2012	EE of household refrigerators and freezers
NOM-007-ENER-2004	EE for lighting systems in non-residential buildings
NOM-010-ENER-2004	EE of submersible deep well motor pumps
NOM-011-ENER-2006	EE in central, package and split type air conditioners
NOM-005-ENER-2012	EE of household washing machines
NOM-023-ENER-2010	EE in split type, free flow, ductless air conditioners
NOM-028-ENER-2010	EE for general use lamps
NOM-020-ENER-2011	EE in buildings. Envelope of residential buildings
NOM-017-ENER/SCFI-2012	EE and safety requirements of compact self-ballasted fluorescent lamps
NOM-021-ENER/SCFI-2008	EE and user safety requirements for room air-conditioners
NOM-003-SCFI-2000	Electrical products
	Water
NOM-008-CNA-1998	Showerheads used in personal hygiene
NOM-009-CNA-2001	Toilets for sanitary use
NOM-244-SSA1-2008	Equipment and germicides for domestic water treatment
NOM-127-SSA1-1994	Environmental health. Water for human use and consumption. Quality standards
NOM-230-SSA1-2002	Environmental health. Water for human use and consumption. Sanitary requirements
NOM-010-CONAGUA-2000	Specification and testing methods of admission and flush valves for toilet tanks
NOM-013-CONAGUA-2000	Specification for air-tightness/testing methods for drinking water distribution networks
NOM-007-CONAGUA-1997	Security requirements for construction and operation of water tanks
NOM-011-CONAGUA-2000	Conservation of water resources
	Gas
NOM-007-SECRE-2010	Natural gas transport through pipelines
NOM-002-SECRE-2010	Natural gas installations

For elements used in buildings, there is a Glass and Glazing Systems norm, the *NOM-*

024-ENER-2012, which specifies thermal and optical characteristics of glass and glazed systems for buildings. Regarding thermal efficiency, there are the *NOM-003-ENER-2011*, for domestic and commercial water heaters, and *NOM-025-ENER-2013*, for household LP gas or natural gas cooking appliances.

Barrios, Huelsz, & Rojas [14], consider there is inconsistency between objective and applicability in the official standards *NOM-008-ENER-2001* and *NOM-020-ENER-2011* nationwide as they are based on a time-independent heat transfer model – inadequate for climates of Mexico, since they present large external temperature variations throughout the day and have high solar radiation. The thermal storage capacity of a building's envelope is very relevant in these climates and a method based on a time-dependent heat transfer analysis should be used. Mexican norms and standardisation use methods based on a steady-state heat transfer analysis, thereby defining minimum values of the thermal resistance of the building envelope, but their thermal storage capacity is not taken into account. The aim is to rationalise the use of energy in the cooling systems, although the norms are not completely operational, because the construction execution is dependent on municipal competence.

1.1.2 Mexican Standards *NMX*

Mexican Standards, *NMX*, are designed specifically to ensure personal safety by reducing risk and damage to human, animal and plant health or the environment. Both the *NOM* and the *NMX* were created in 1993 in the prelude to the Free Trade Agreement signed by Mexico, the United States and Canada; the common goal was to guarantee the quality of products and different services.

The *NOM-018-ENER-2011* [117] is complemented by diverse *NMX* and documentation produced by the National Organization of Standardisation and Certification of Construction and Building, ONNCCE[2], which is a Mexican civil society dedicated to developing standardisation, certification, and verification for products, processes, systems and services. The validation of some thermal insulators for buildings are shown in Table 1.2.

[2]Organismo Nacional de Normalización y Certificación de la Construcción y Edificación

Table 1.2: Norms Used to Validate Thermal Insulators for Buildings.

Property	Testing Method
Apparent Density	NMX-C-125-ONNCCE-2010
	NMX-C-126-ONNCCE-2010
	NMX-C-213-ONNCCE-2010
	NMX-C-258-ONNCCE-2010
Thermal Conductivity	NMX-C-181-ONNCCE-2010
	NMX-C-189-ONNCCE-2010
Permeability to Water Vapour	NMX-C-210-ONNCCE-2010
Moisture Adsorption and Water Adsorption	NMX-C-228-ONNCCE-2010

NMX-C-460-ONNCCE-2009 [47] specifies the total thermal resistance (R-value) proposed in housing envelopes to improve conditions for habitability, and to decrease the energy demand caused by air conditioning. Thermal zones are assigned depending on the geographical location, and in general observations, the walls must have a minimum R-value of 1.0 m^2K/W, and roofs 1.4 m^2K/W. Sustainable building design criteria and minimum environmental requirements are covered in the *NMX-AA-164-SCFI-2013* [115]; the objective is to contribute to the mitigation of environmental impacts and the sustainable use of natural resources, without neglecting the socioeconomic aspects that ensure viability, habitability and integration to both urban and natural environments.

1.1.3 Plans and Strategies

The National Housing Commission *CONAVI* is a federal organisation; its purpose is to coordinate, promote and implement national housing policies. In 2010, this commission updated its Residential Building Code (CEV[3]), and established a system of subsidies for energy efficiency; developers can access and obtain incentives if they cover the code's guidelines. Although the *CEV* provides design and building recom-

[3]Código de Edificación de Vivienda

mendations for different climate zones in the country, according to Griego, Krarti, & Hernández-Guerrero [65], these do not correspond with the ones defined in the *NMX-C-460-ONNCCE-2009* and recommendations given for each climate zones are ambiguous and nonspecific. However, this is a solid starting point for the development of a building code.

The National Development Plan [41] is the governing document where strategies and priorities for the integral and sustainable development of the country are displayed. Under this scheme, the principal objective is to take Mexico to its maximum potential through five national goals: peace, inclusion, quality education, prosperity and global responsibility. Within the inclusion goal, topics such as access to decent housing, basic social infrastructure and territorial development are detailed. There are currently 2.8 million houses in Mexico that need to be replaced and 11.8 million that require some type of improvement or expansion. Likewise, in order to meet population growth, it is estimated that 10.8 million housing solutions will be required in the next 20 years.

According to the 2010 Population and Housing Census provided by the National Institute of Statistics and Geography (INEGI[4]) [85], the number of uninhabited houses was almost 5 million, while temporary homes stood at just over 2 million. Given this situation, it is necessary to promote the development of more compact cities with greater population density and economic activity. Alternatives such as the used and rental housing markets are still incipient, which makes it difficult to use the available offer to solve existing housing needs.

Within the aforementioned National Development Plan, in section Prosperous Mexico it is explained the importance of sustainable development; the effects of climate change and environmental degradation have intensified, so scientific and city solutions must be achieved. In the global scenario, the need to reduce our dependence on fossil fuels with encouragement to use alternative energy sources has fostered innovation in the technology market, both in the fields of energy and in the use of sustainable natural resources.

In the country, an agenda of participation is covered in more than 90 agreements and

[4]Instituto Nacional de Geografía y Estadística

current protocols, covering topics of climate change and biodiversity. However, economic growth is still closely linked to the emission of greenhouse compounds, the excessive generation of solid waste, pollutants released into the atmosphere, untreated waste-water and the loss of forests. The economic cost of depletion and environmental degradation in 2011 represented 6.9% of Mexico's Gross Domestic Product (GDP[5]) [84]. Regarding the use and supply of energy, half of the electricity was generated from natural gas because this fuel carries the lowest price per energy unit. In this context, generation technologies that use renewable energy sources should contribute to addressing the challenges of diversification and energy security. Despite the potential and rapid growth in the use of this type of energy, at present, its contribution to the national energy supply is only 2% of the total.

In the updated National Development Plan [42] social housing is considered as a priority, and improvement actions, expansions, and replacements will be carried out. In the Operation Rules of the Social Housing Programme 2020 published in the Official Federation Gazette [51], it is stated that in Mexico, the purchase of new housing is only accessible to those who receive more than five minimum wages, since public and private mortgage loans can be accessed from that income level. The credits generally last from 15 to 30 years [121]. Considering this situation, it is relevant to build or expand mechanisms to address housing-related deficiencies to serve those one lower-incomes.

In this context, the *CONAVI* promotes housing policies based on the principles of social inclusion, economic efficiency and environmental protection; this supports the effective use of public resources for affordable and sustainable housing through appropriate financial mechanisms aiding programme development. Within the Social Housing Programme, sustainable development for housing is structured on three main pillars: economic; social; and environmental.

Sustainable housing is defined as the living space that, from its architectural design, considers the fundamental needs of human beings and their urban, communal, cultural and natural contexts. It provides general well-being to its inhabitants with economic savings, mitigation of greenhouse gas emissions, and the efficient use of energy systems to reduce environmental impact. To adopt this, programmes such as the Na-

[5]Gross Domestic Product

tionally Appropriate Mitigation Action (NAMA[6]), Ecocasa, Laif, NAMA Facility programs, among others, are integrated. The baseline works with a system of points and the score cards are carried out in accordance with the applicable regulations aligned with the measures corresponding to INFONAVIT[7] programmes, which includes the location of the project, available equipment and services, and sustainability measures. The Institute of the National Housing Fund for Workers, INFONAVIT, offers this support for workers by allowing them to contribute a percentage of their salary, and the employer contributing another part, enabling access to credits and homes.

The Urban Contained Perimeters tool (*U1, U2, U3*) [40], was developed by the Unique Housing Registry (RUV[8]) from the Federal Government, and is used as a guide to obtain subsidies to the best located housing, close to employment sources and urban services in the cities. In Coahuila, the cities of Saltillo, Monclova and Torreón represent the main locations in terms of urban settlements, Figure 1.1. The locations in *U1* (*U1a* & *U1b*) contain the sources as the basic element to consolidate cities; the *U2* perimeter (*U2a* & *U2b*) is based on the existence of water and drainage services for housing, which contribute to the proliferation of nearby housing to the first perimeter. *U3* includes the adjacent growth areas to the consolidated urban areas, they are made up by a buffer that covers the *U1* and *U2* perimeters, depending on the city's population range.

As the Urban Development Plans officially define the regulations for city development, construction permits and licenses originate from land use authorisation. Houses are issued with the location score exclusively when they correspond with the geo-statistical model combined with the Urban Development Plan.

1.2 Housing in Mexico

From the most recent published national population census, a total of $28,607,568$ houses are registered for $112,336,538$ inhabitants in the country [85]. The Mexi-

[6]Nationally Appropriate Mitigation Action

[7]Instituto del Fondo Nacional de la Vivienda para los Trabajadores

[8]Registro Único de Vivienda

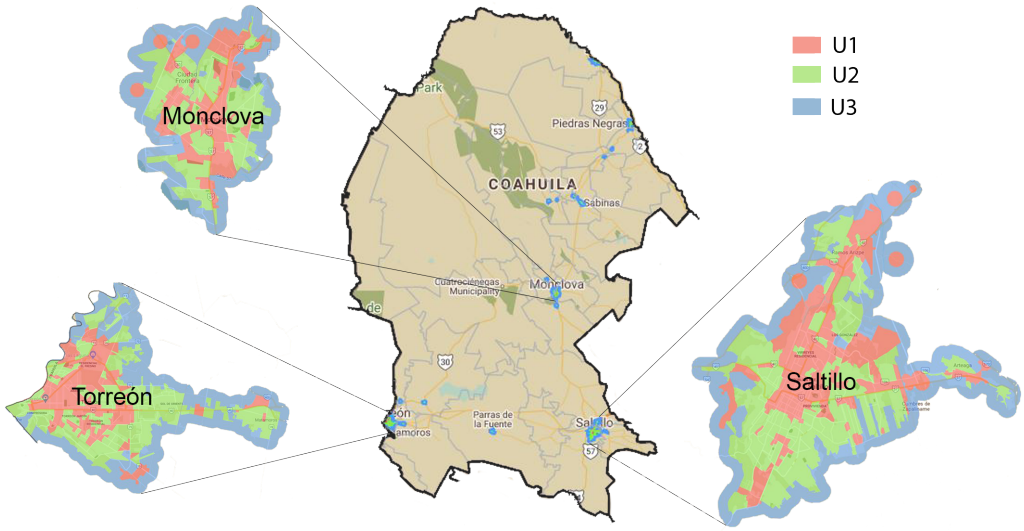


Figure 1.1: Urban Contained Perimeters, obtained with the Unique Housing Registry tool [40].

can Government offers diverse funding through its departments and commissions, and work together with the ones that offer funding to improve housing in terms of energy. Commissions and Ministries in charge of funding, loans for housing and urban developments regulation depend on the The Federal Mexican Government; these include public organisations, which contribute to employee housing costs, the CONAVI, the Ministry of Agrarian, Territorial and Urban Development (SEDATU[9]), and the Ministry of Social Development (SEDESOL[10]).

From entities such as SEDESOL, different public and private organisations subsidise or offer credits and funding for housing through institutions like the Mexican Social Security Institute and the Institute of the National Fund of Housing for Workers (IMSS[11]/INFONAVIT), the Institute of Security and Social Services of State Workers and its housing fund (ISSSTE[12]/FOVISSSTE[13]), and the National Fund of Popular Rooms (FONHAPO[14]).

SEDESOL evaluates the general social development policy such as human settlements,

[9]Secretaría de Desarrollo Agrario, Territorial y Urbano
[10]Secretaría de Desarrollo Social
[11]Instituto Mexicano del Seguro Social
[12]Instituto de Seguridad y Servicios Sociales de los Trabajadores del Estado
[13]Fondo de la Vivienda del Instituto de Seguridad y Servicios Sociales de los Trabajadores del Estado
[14]Fondo Nacional de Habitaciones Populares

urban development and housing, while the SEDATU is the entity in charge of agrarian, urban and housing development. These dependencies offer programmes for people interested in accessing finance to buy or refurbish social housing. These programmes are generally accessed by those on low-incomes who cannot afford housing on the open market, or access subsidised housing, which are savings programmes and subsidies for housing, community housing, improvements, and self-construction, etc.

The FONHAPO grants subsidies to families enduring patrimonial poverty to build, acquire or improve their housing, as the ISSSTE/FOVISSSTE establishes and operates the financing system for the granting of mortgages to the recognized workers of the ISSSTE. Under IMSS and INFONAVIT, companies and government sectors colaborate to grant credits for housing purposes. In the pursuit of energy savings, the latter handles different types of credit and loans like the Green Mortgage (HV[15]), where the use of household eco-technologies are considered, as well as accessories and products that are intended to contribute to environment care, and to help users save money on utilities like water, electricity and gas services.

In Coahuila, private houses are the predominant inhabited housing units. In the 2015 Intercensal Survey, the total was estimated at $809,275$ houses. In absolute terms, their number increased twice in the last quarter century. Until 2015, the highest number of inhabited private dwellings was Saltillo ($213,329$), then Torreón ($191,913$), Monclova ($65,951$) and Piedras Negras ($45,067$), with a total of $516,260$ dwellings, representing 63.8% of the total in the state [49].

1.2.1 Characteristics of Social Housing

Social Housing in Mexico has certain social, economic and physical characteristics that define it and encompass different natures. Through this project, the physical definition is the one characterising the main parameters considered to analyse thermal comfort. This does not mean that the components and problems inherent in this type of house are neglected, as these are mentioned in this section. Sánchez [35] specified that the term derives from the fact that, at the beginning of the 20th century, some companies

[15]Hipoteca Verde

were able to offer housing to their workers, so that later projects were generated by organisations that fulfilled the social function of providing these assets to workers; INFONAVIT established the institutionalised solidification of these efforts in the early 1970s.

In a physical environment, social housing is characterised by its area of construction. According to the INEGI [85], the typology of housing depends on the variation of the average built surface measured in square meters of construction, and this is accepted as a technical way to officially define it. Social housing is considered from 40 m^2 to 71 m^2; this includes the economic type, the popular type, and the traditional type of housing as shown in Table 1.3.

Table 1.3: Housing Classification by Average Built Surface [85].

Economic	**Popular**	**Traditional**	**Average**	**Residential**	**Residential Plus**
			Average Built Surface		
40 m^2	50 m^2	71 m^2	102 m^2	156 m^2	188 m^2
			House Areas		
1 Bathroom	1 Bathroom	1.5 Bathrooms	2 Bathrooms	3-4 Bathrooms	3-5 Bathrooms
Kitchen	Kitchen	Kitchen	Kitchen	Kitchen	Kitchen
Multiple Use Area	Living Room	Living Room	Living Room	Living Room	Living Room
	Dining Room	Dining Room	Dining Room	Dining Room	Dining Room
	1-2 Bedrooms	2-3 Bedrooms	2-3 Bedrooms	3-4 Bedrooms	3 or more Bedrooms
	1 Parking Spot	1 Parking Spot	Utility Room	Utility Room	1-2 Utility Rooms
			1-2 Parking S.	Family Room	Family Room
				2-3 Parking S.	3 or more Parking S.
					Gym
					Playing Room
					Garden

The minimum dimensions of housing are established in official regulations and published by INFONAVIT; each state has its own definitions. For Coahuila, the plot should have a surface of approximately 91.00 m^2, having a 7.00 m front, and 13.00 m depth. Measurements can vary but they have to adapt to the allowed site surface and to the permitted spaces. The boom in new developments of social housing has made the new developments increasingly remote from urban areas, implying higher costs of infrastructure, land, service provision and other factors that make buyers responsible

for absorbing the costs caused by having lower quality materials, finishes and house dimensions [35], although demand corresponds to the more affordable materials, as shown in Table 1.4. This data was published in the Statistical and Geographical Yearbook of Coahuila de Zaragoza by the INEGI [83]. In private dwellings the population census illustrates that there is a tendency to build with concrete blocks.

Table 1.4: Dwellings Inhabited by Material in Walls and Roofs [85].

		Roof Materiales (Percentage)									
Wall Materials	**Total**	Scrap	Cardboard sheet	Steel sheet	Asbestos sheet	Palm or palm strau	Wood	Clay with beams	Tile	Concrete	Not specified
Total	**736 427**	**0.1**	**0.6**	**6.2**	**0.3**	**0.2**	**5.8**	**7.8**	**0.8**	**77.8**	**0.6**
Scrap	**634**	42.4	3.9	22.2	0.0	0.0	7.9	0.5	4.9	18.1	0.0
Cardboard sheet	**2 023**	0.8	72.9	19.5	0.1	0.0	3.3	1.3	0.0	3.3	0.2
Asbestos or metallic sheet	**1 103**	4.7	9.2	49.2	3.5	0.0	5.3	0.1	2.5	25.7	0.0
Reed, bamboo or palm	**153**	0.0	0.0	28.1	3.9	52.3	0.0	9.8	0.0	5.9	0.0
Wattle and daub	**737**	0.0	0.0	34.2	0.0	10.2	33.4	6.0	0.8	11.1	4.3
Wood	**5 284**	0.2	10.7	45.4	0.7	0.1	24.1	2.2	2.7	13.4	0.5
Clay	**98 213**	0.1	0.2	9.8	0.4	1.0	23.4	48.7	2.3	13.7	0.2
Brick, concrete block, stone, quarry	**624 812**	0.0	0.3	5.1	0.3	0.0	2.8	1.5	0.5	89.4	0.1
Not specified	**3 468**	0.0	0.0	0.3	0.0	0.0	0.3	0.5	0.0	2.6	96.3

Since 2006, the Federal Mortgage Society (SHF[16]) introduced a Residential Satisfaction Survey (ESR[17]) in which variables are grouped by personal characteristics, economic dwelling elements, physical and social environments and location. These are analysed to obtain a resident satisfaction index. Among the main discoveries, it was observed that the sustainability of housing is coupled with residential satisfaction, the presence of energy saving elements also contributes to user satisfaction because of the savings they offer, and the value these add to their houses [110].

1.2.2 Sustainable Housing

Since 2009, the Federal Government has promoted various programmes to develop sustainable housing models, with the programme Green Mortgage, from INFONAVIT, being the precursor. This consists of equipping the house with a package that allows

[16]Sociedad Hipotecaria Federal

[17]Encuesta de Satisfacción Residencial

the sustainable use of water and energy savings corresponding to gas and electricity expenses. The payments are reduced as it is possible to obtain up to 48% of savings in energy consumption. This programme won the World Habitat Award 2012 awarded by the United Nations. The first step buyers need to take after deciding to purchase a house, is to submit a loan request to INFONAVIT and decide if the scheme will obtain a sustainable house with HV. This increases the available credit and eco-technologies are selected from public listings. After the house is bought, the buyer benefits from monthly savings due to the technologies and pays for the mortgage plus the HV credit; this extra credit is $151.54 MXN (£5.24) over 15 years.

An option for low-income families (less than 2.6 minimum wages) who cannot access HV, is This is Your House programme *Esta es tu casa*, which provides federal subsidies. To enhance efforts aimed at achieving sustainable housing, mechanisms derived from international agreements related to climate change have been implemented, such as the Clean Development Mechanism and the NAMA for Housing and Urban Development. Entities like the World Bank and the German Federal Ministry for the Environment, Nature Conservation and Nuclear Safety (BMU[18]) have participated, as well as the German Agency for International Cooperation (GIZ[19]).

Documentation regarding energy efficiency and sustainable housing is derived from the combined work of The British Embassy in Mexico, GIZ, CONAVI, INFONAVIT, SHF, the National Commission for the Efficient Use of Energy (CONUEE[20]), and the National Water Commission (CONAGUA[21]). The IDEA Foundation was responsible for the research, analysis process and publishing of the documents; this organisation is non-profit and independent, its mission being the designing and promoting of innovative public policies to produce tools and documentation for public servants and the general population, enabling well-informed decisions.

One organization is the National Strategy for Sustainable Housing [81], which divides activities into three categories: financing, housing evaluation and standards definition. There is an evaluation system promoted by INFONAVIT, Green Housing Evaluation

[18]Bundesministerium für Umwelt, Naturschutz und nukleare Sicherheit

[19]Deutsche Gesellschaft für Internationale Zusammenarbeit

[20]Comisión Nacional para el Uso Eficiente de la Energía

[21]Comisión Nacional del Agua

System - Eco house (SISEVIVE[22] - ECOCASA) [88], which was designed to complement efforts promoting housing sustainability in Mexico. A reference house is used as a standard and compared to the house to be evaluated, and the ones having lower energy demands are in a better position to obtain additional benefits from HV. The assessment is calculated considering the architectural design in regard to the orientation of the project, construction systems, materials and adapted-technologies.

These elements include shading, reflective painting, low thermal conductivity materials, building envelope thickness and components, double glazing, and eco-technologies such as the use of solar water heating. The energy and environmental impact is evaluated using a housing Global Performance Index (IDG[23]) obtained through a spreadsheet for energy efficient house design, and a water saving simulator. This index goes from A to G, A being the most efficient on the scale, Figure 1.2. The tools used to perform the simulations, different climate conditions and water availability are considered depending on the region, as well as whether detached, terraced, or in a block of flats.

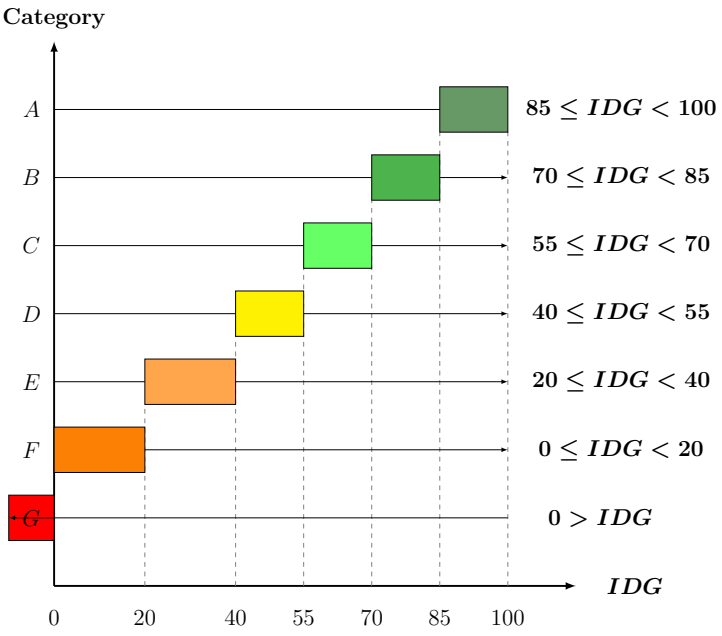


Figure 1.2: Global Performance Index *IDG* Scale. Retrieved and Modified from SISEVIVE Validation Manual [88].

The review of the housing energy efficiency in Mexico derived from practices and sur-

[22]Sistema de Evaluación de la Vivienda Verde

[23]Índice de Desempeño Global

veys carried out in different countries, and was condensed in the document Energy and Environmental Efficiency in Housing [82]. Evaluation systems were compared and adapted to identify common elements to design an Energy and Environmental Efficiency Evaluation System (EEEES). Both new housing and retrofit in existing housing can be evaluated considering energy demand, CO_2 emissions, days of the year the dwelling faces interior overheating, and potential primary consumption regarding the building envelope materials, electrical equipment, lighting, heating, cooling, hot water and household appliances.

These measurements are considered to be able to guarantee an acceptable level of comfort for the dwellings interior through appropriate thermal design, and thereby, obtaining a reduction in cooling and heating related costs. Materials are of great importance in house design, as well as the consideration of appropriate appliances for a large segment of the population with their income restrictions. Water consumption is determined by the occupancy level and water-saving devices are incorporated in the designs. The definition should also consider adaptation to the diverse bio-climates which have a direct impact in cooling and heating energy demands, and should suit to the existing regulations.

The analysis of national and international practices allowed also the implementation of adapted programmes for energy efficient housing in Mexico [81] like the Green Housing Assessment System from the programme SISEVIVE - ECOCASA [88], and the Supported NAMA for Sustainable Housing in Mexico. The latter was developed as a technical concept of the NAMA in the social housing sector and proposed standards of performance for the main bio-climatic zones of Mexico to reduce CO_2 emissions and to implement basic standards of efficiency. For the NAMA database, the distribution – by sector is 62% by energy supply; 18% by buildings; 10% by transport; 5% by waste; and 5% by industry. These are under development, except for one of the building sectors, the NAMA for Sustainable Housing in Mexico, that had already been implemented.

The mitigation actions regarding the building sector and their objectives are displayed in Table 1.5 [121]. As shown in this table, the NAMA for Sustainable Housing Retrofit

makes use of the Measurement, Reporting and Verification (MRV[24]) system, and its primary purpose is to measure the impact of the implemented actions through methodology to evaluate and contribute to future policies, in case these can be transformed into a credit programme with international collaboration. The Whole House Approach was used in the studies for housing retrofit, and consists of monitoring primary energy demand values from a building, instead of on individual energy-efficient technologies.

Table 1.5: Mitigation Actions Adapted from NAMA database in Mexico [121]

NAMA Building Sector Objectives
NAMA for Sustainable Housing in Mexico
Supplement on-going initiatives for energy-efficient housing as laid out in Mexico's Special Climate Change. Programme and as currently operated by INFONAVIT. Extend penetration of basic efficiency standards to the entire new housing market in Mexico, and upgrade efficiency standards to more ambitious levels.
NAMA for Sustainable Housing Retrofit
Maximize the efficiency of water, electricity and gas consumption in existing homes. Whole house approach with efficiency benchmarks set for total primary energy demand considering climatic variables. Cost-effective Measurement, Reporting and Verification system to allow a flexible range of interventions to achieve the performance standard desired.
Domestic Refrigerators NAMA
Decrease emissions from refrigeration through efficiency increase and phase-out of hydrofluorocarbons.
Low Emission Schools
Reduce CO_2 emissions in schools while students influence communities on climate change and sustainability.
NAMA for New Residential Buildings in Mexico
Mitigates emissions in residential sector by improving electrical, fossil fuel, and water efficiency. Develope eco-technologies, generation of design improvements, use of efficient building materials.
NAMA in the Urban Residential Sector
Achieve nation-wide emission reductions through deployment of sustainable houses, solid waste, water, sewage and public lighting infrastructure funded partly through the development of carbon credits.

These actions represent the many initiatives aimed at improving the sustainability of the country's construction environment. As a result of the participation of various agents, the methodology was developed under the Transversal Table of Sustainable Housing in Mexico [34] – the purpose being to develop a system that collected data and prepared reports. The certification process was divided into two phases: design and construction; and monitoring. In the first, the parameters of the housing are defined,

[24]Monitoreo, Reporte y Verificación

and results regarding the reductions in greenhouse gases are evaluated using a simulation tool. The emission reductions are the result of the difference between the project performance projections and the baseline. During construction, an auditor confirms that the building matches the characteristics of the simulated design, and subsequently, the house is entered into the NAMA database.

In the second phase, the project can be introduced into one of two systems, in the Monitoring of Greenhouse Gases system, the focus is on collecting the data necessary to calculate the impact of emissions; and in the Detailed Monitoring system, the focus is on collecting a broader range of indicators that can be used to calibrate emission models and track other variables. The performance is monitored and reports are evaluated to consider the more benign ones and possible improvements.

The study was developed using the Passivhaus Planning Package (PHPP[25]). The energy demand of a reference house was calculated for the four main bio-climatic regions of the country, see Figure 1.3, for three types of housing, and with three efficiency objectives called: *Eco Casa 1*; *Eco Casa 2*; and *Eco Casa Max*.

The *Eco Casa 1* represents the level of efficiency if all the technologies supported under the current Green Mortgage scheme are adopted (2.5 cm insulation on the ceiling and on a single wall, reflective painting, water solar heater, and efficient A/C unit if needed on the bio-climatic region). The *Eco Casa 2* represents a higher level of efficiency (all insulated walls, better windows, highly efficient appliances). While the *Eco Casa Max* standard foresees the optimisation of all the previous measures (passive elements, overhangs, extensive insulation, appropriate architectural design to achieve primary energy demand reductions) [121].

To establish the base line, the NOM 020 was considered and it was intended for further stages to perform the simulations in Mexico's seven climates according to the INEGI, not merely the initial four considered. These include the temperate semi-humid, temperate humid, dry and semi-dry, very dry, hot semi-humid, hot humid, and cold on high mountains. For the first stage, housing was chosen to be analysed in four cities representing different climates: Hermosillo (extremely hot dry), Guadalajara (temperate),

[25]Passive House Planning Package

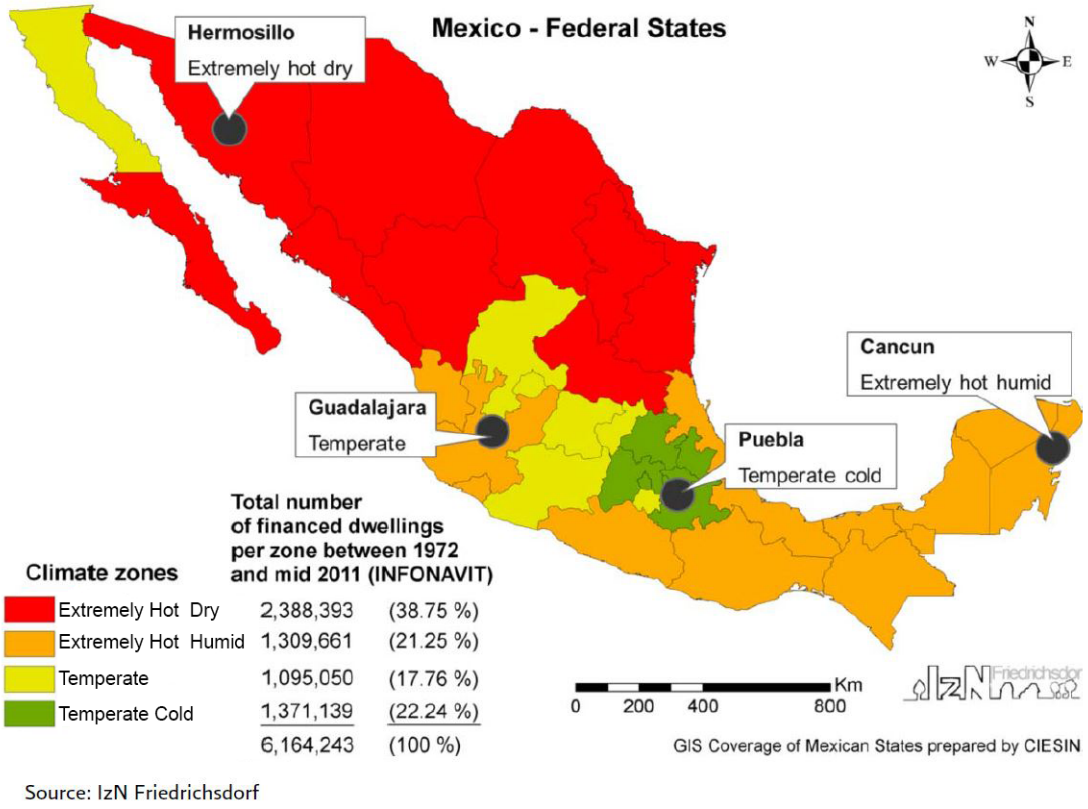


Figure 1.3: Mexican Climate Zones [121].

Puebla (temperate cold), and Cancún (extremely hot-humid). For a posterior stage, other cities with different climates were analysed apart from those already mentioned: Hidalgo (dry semi-cold), Monterrey (hot-dry) and Mérida (semi-humid).

Eligibility for financing is determined by the total energy demand of the home and not by the specific technologies used, so owners can use any combination of these elements, not necessarily all of them. A NAMA Fund was set up as a recipient of donor founds, as soft loans or subsidies. Donors could partner with CONAVI and, through the Transversal Table, the optimal allocation of resources was decided on. The goal was to establish an inter-institutional platform able to articulate the requirements for Sustainable Housing through a coordinating agent or an inter-sectoral commission, where the government, private industry and social organisations, collaborate to implement both new and existing programmes.

All building types were analysed as they were in the original projects without design changes other than insulation, air-tightness, improved U-values in windows and doors, and modified ventilation systems. Windows and the sizes of windows were left the

same without the addition of shading, overhangs or canopies, which resulted in high levels of insulation to improve the energy performance. Results showed that the additional costs to improve the baseline case to reach the different energy efficiency cases, are lower than the cost of the CO_2 emissions themselves. The average monthly savings obtained taking the proposed measures was of $229.00 MXN (£6.64) per household.

1.3 Housing Resilience and Adaptation

Buildings, in addition to representing a shelter for their inhabitants, are also elements that resist environmental external factors and, when properly designed, allow users to live comfortably. Many of these changes occur throughout the day (day-night variations), throughout seasons, when typical natural phenomena such as rain, blizzards, hail or snowfall occur, and changes that arise throughout the years like climate change. This is why the built environment must consider the possible changes in planning and design. This elasticity in buildings can be conceived as the adaptation and resilience of buildings, where adaptation refers to fitting different environments, while resilience represent the quality of being able to recover quickly or resist being affected by adversity.

To define resilience, there are a wide range of concepts from diverse fields, leading to a contrast with the traditional view of science and its precision and conceptual clarity, with empirical science aiming at generating valid and objective knowledge [144]. One definition from ecology is how fast the variables return to equilibrium after a disturbance, is not applicable for unstable systems and can be considered as a measure of stability [128]. Holling [76] as a descriptive concept conceived it as a measure of the persistence of systems and their ability to absorb change and disturbance, while maintaining the same relationships between variables.

Ecologists have developed resilience theories over the past three decades in an effort to explain surprising and nonlinear dynamics of complex adaptive systems. Resilience theory is especially important to environmental scientists for its role in underpinning adaptive management approaches to ecosystem and resource management [68], and these concepts can be adapted to other disciplines. In psychology for example, the term

was adapted considering similar factors, and refers to the process, capacity or outcome of successful adaptation despite challenging or threatening circumstances [111].

In the energy sector, the concept refers to the capacity of the energy system to cope with a hazardous event or trend, like extreme weather or unusual seasonal temperatures, and respond in ways that maintain their essential function, identity and structure while also maintaining the capacity for adaptation, learning and transformation [89]. In urban environments, green spaces are considered as helpful elements to mitigate the urban heat island effect, and green infrastructure is progressively being recognized as an important option to enhance resilience [133].

Some of these concepts were adapted for the built environment, being the resilience of a building something going beyond the safety of its structural elements to include the resilience of its supporting systems and the services they supply [146]. All these elements can be approached considering changes and the strategies to obtain a better performance of the variables – in this case, buildings. Within these system configurations, the possibility to adapt is linked with being resilient, and adaptability is at the same time considered as the capacity of actors in a system to influence resilience; it is mainly a function of the social component, where individuals and groups act to manage the system [149]. Buildings must be designed to withstand external nuisances that may arise over the building's lifetime for it to be sustainable; therefore, a resilient building should be able to adapt and remain functional while under pressure from more frequent and severe climatic events [27].

In the state of Coahuila, there is a vast amount of uninhabited housing – around $131,042$ units; this represents a problem within the category of housing backwardness. By the latter, it is understood the number of dwellings that, due to their occupation characteristics or the components and materials used in the building do not offer minimum well-being standards for their potential occupants [48].

When designing a house, all the energy and environmental components must be integrated to obtain benefits such as the creation of a healthy and comfortable indoor environment for users and optimal use of natural resources. Additional policies could be implemented to guarantee that new housing has a design that reduces energy consump-

tion, particularly in the northern part of the country where the climate is extreme [32]. The bio-climatic recommendations to achieve this and allow improved thermal conditions or reduced air conditioning requirements, include looking for the optimal orientation, the use of natural ventilation, suitable materials, and solar controls, etc.

1.4 Conclusions

For the analysis of energy and social housing in Mexico, the implementation of public policies has a primary role and goes beyond the publication of official standards such as the *NOM* and the *NXM*; in the preparation and analysis of these documents, is required an in-depth study that involves the participation of experts from different disciplines.

Mexico is a country with considerable contrasts – cultural, climatology, and physiography. This makes complex the assemble of documents that include all the possible cases and problems that must be addressed when designing and building social housing. When official regulations cannot be applied to all cases, municipal authorities have to take appropriate measures for their region, making it difficult to create standards applicable at a national level.

The social housing agents include the government entities that draw up these regulations. These include real estate developers, builders, academics, and buyers who represent a large portion of the population; because of this, the making of successful implementations becomes challenging. This is why the Mexican government has resorted to the revision of national and international policies and planning to create useful regulations and programmes for the development of social housing.

Programmes such as the Green Mortgage (HV) contributed to the obtaining of macroeconomic savings that benefit both developers and users; at the same time, programmes could be improved for better credit access, so benefits can reflect in, not only economic, but habitability advantages.

The SISEVIVE programme turns out to be a robust comprehensive system that represents a useful tool for developers and the public interested in these topics. Likewise, NAMA mitigation actions are very useful as they provide a basis form which to make

case comparison studies with well-founded information like the actual study of existing cases based on official standards. These contribute to the reduction of emissions in the residential sector by providing supplementary financing to improve the efficiency of homes in terms of electricity, gas and water consumption, and are accomplished with eco-technologies, improvements in architectural design, and the use of more efficient building materials.

These cover the analysis of energy expenditure and thermal comfort in homes of various bio-climates in the country, and in turn, can be improved by extending these to the entire national territory. In this sense, dwellings could be better adapted to the surrounding environment, allowing flexibility in the design and allowing users to experience improvements in comfort and energy savings.

Although in these studies an original attempt was made to undertake the possible solutions that could be adapted to different regions and climates of the country, not all of them are covered. A more comprehensive explanation of these characteristics and differences is addressed in the next chapter, with descriptions of climates, micro-climates, and assumed climate projections for years to come.

Likewise, the concepts and definitions of resilience and adaptation shown in this chapter are addressed in the next one through the changes that must be considered in the architectural design to propose this type of housing from a perspective of thermal comfort.

Chapter 2

Weather, Climate and Thermal Comfort

Amid environmental changes occurring over time, the economic and physical components of cities are directly impacted. From a general perspective, the impact is suffered in large masses of air and water, while in a more particular vision, the buildings and the environment of the users of these are affected. These changes have been addressed for the study and mitigation of energy crises and have taken on great importance in these last decades. Various entities have devoted their effort to the study of these transformations at a global level, and smaller entities use this information to create plans that benefit the regions at a more local level.

The system MRV, mentioned in 1.2.2, is considered as a useful element to generate reports related to the estimation of greenhouse gas emissions and mitigation goals at a national level, and afterwards, adapt these at a state level [43]. The Article 8 of the General Law on Climate Change (LGCC[1]) [50], specifies that mitigation criteria and adaptation to climate change should be incorporated into environmental policy instruments. Likewise, it is considered that scientific and technological research should be promoted to achieve these ends, and to develop state action programmes on climate change.

In Coahuila, these requests were considered and a state plan was developed by the Ministry of Environment. Possible mitigation actions and development of adaptive capacities to the adverse effects of global warming are specified. This documentation

[1] Ley General de Cambio Climático

mainly covers the impact on the agricultural sector, since it is one of the most important at an economic level, but also the one that will be most affected by this issue.

Within the physiographic characteristics in Mexico, there is a surface of 34.1 million hectares of forests, 31.6 million hectares of jungles, 59.05 million hectares of arid and semi-arid areas, 1.6 million hectares of hydrophilic vegetation, 6.11 million hectares of vegetation induced and 11.83 million hectares of grassland [87], so the criteria used in planning must consider the multiple micro climates generated by having such varied biodiversity and ecosystems.

The changes that occur over the years with the climate, influence the weather characteristics in cities, and in turn, the measures that must be taken in the design of buildings. This chapter offers a review of three key topics: weather, climate, and thermal comfort; these are explained as background to analyse their influence in buildings in subsequent chapters.

The geographical characteristics of Mexico are addressed in Section 2.1 to provide an overview of the complexity of the homogenization of actions taken at the national level. In Section 2.2 the projections that have been made for future years and in different climate scenarios are examined; a review of current and future weather data for dynamic building simulation is also analysed. This information was considered to develop the algorithms explained in Chapters 3, 4 and 5. Finally, Section 2.3 provides the definition of thermal comfort in housing, which is the basis on which comfort was approached for the simulations presented in Chapter 6.

2.1 Geographical Characteristics and Climates in Mexico

Mexico is located in the northern hemisphere of the American Continent. Its extension takes place between the parallels $14^\circ\,32'\,2''$ and $32^\circ\,43'\,06''$; likewise, its extreme coordinates range between the West Greenwich lengths of $118^\circ\,22'\,00''$ and $86^\circ\,42'\,36''$. Its surface is $1,964,375$ km^2 and the republic is comprised of 32 states. There are two main mountain ranges, the *Sierra Madre Oriental* and the *Sierra Madre Occidental*.

These traverse the country from north to south, and in the east and west respectively. Therefore, the cities near the mountains have dramatic variation in elevations within them, and as a consequence, of temperatures. Cities like Mexico City for example, have elevation differences of up to 1,470 m.

Coahuila is the third largest state in the country, made up of 38 municipalities, its surface is $151,563$ km^2 and its extreme geographic coordinates range from $29^\circ\, 52'\, 48''$ N to $24^\circ\, 32'\, 34''$ N; and west longitudes from $99^\circ\, 50'\, 35''$ to $103^\circ\, 57'\, 36''$ [83]. Its elevations vary from 150 m to $1,680$ m. There are three different climates and 11 subtypes of climates, 49% of land in Coahuila is arid and semi-arid; 46% very dry; 5% mild weather and sub-humid. Variations in temperature are frequent for its physiography. In December 2017 the lowest temperature registered in Coahuila was -18° C in Arteaga [110], and the highest temperature registered in the state was in Monclova on the same year with 46° C [21]. These municipalities are 200 km from each other. Precipitation registered over the last seven decades ranges from 5.5 mm to 2,834.8 mm [83].

Considering these variations, a city representative of each climate in the state was selected in order to examine how the different climate conditions affect the buildings. The three chosen cities are Saltillo, Monclova, and Torreón. These happen to be also the cities with most population in the state and represent the main locations for urban settlements, as stated on Chapter 1, p. 17.

In the official documents for the climatic classification of Mexico provided by INEGI [83], the Köeppen method of all stations was used according to the method modified by Enriqueta García [62]. In Figure 2.1 these modifications are shown, along with the state of Coahuila outlined in orange, and its capital city, Saltillo, outlined in purple.



Figure 2.1: Climates of Mexico, Coahuila and Saltillo. Adapted from INEGI [83].

2.2 Climate Projections

The Intergovernmental Panel on Climate Change (IPCC) is the United Nations body for the assessment of climate change from multiple disciplines; diverse sets of documents had been derived from these joint efforts. The first generation set of six scenarios, named IS92 (A, B, C, D, E, F) was published in the *1992 Supplementary Report to the IPCC Assessment* and was used to elaborate the IPCC Second Assessment Report. The second set, published in 2002, was the *Special Report on Emission Scenarios* (SRES[2]), and contemplated climate scenarios A1B, A1T, A1FI, A2, B1, B2. Scenarios A1 and A2 are predominantly focused on the economic topics, with B1 and B2 focusing on the environmental. In addition, A1 and B1 studies were made considering a more homogeneous globalised world, and scenarios A2 and B2 consider a more heterogeneous regionalised world (Figure 2.2). The outcomes were used to elaborate the IPCC Third Assessment Report (TAR[3]), and in the IPCC Fourth Assessment Report (AR4[4]).

[2]Special Report on Emission Scenarios
[3]Third Assessment Report, IPCC
[4]Fourth Assessment Report, IPCC

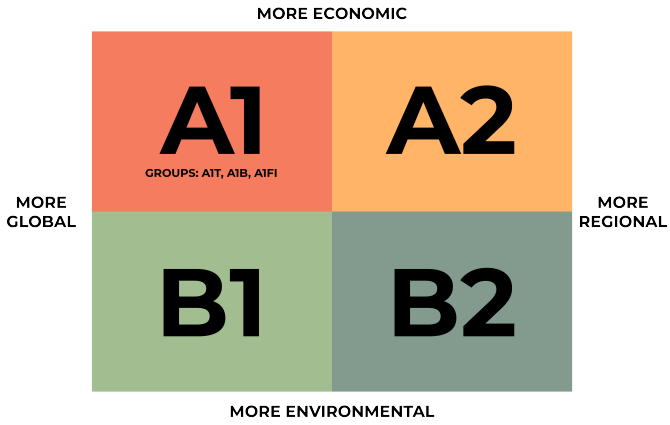


Figure 2.2: *SRES* Scenario Families. Adapted from TAR, IPCC [150].

The Representative Concentration Pathways (RCP[5]) of 2014 considered greenhouse gas concentration trajectories in four pathways, RCP2.6, RCP4.5, RCP6.0, and RCP8.5. These were used in the IPCC Fifth Assessment Report (AR5[6]). New RCPs (RCP1.9, RCP3.4, RCP7) emerged from the AR5 with the Shared Socioeconomic Pathways, and were used to elaborate the IPCC Sixth Assessment Report (AR6[7]) recently released on 2022.

2.2.1 Historical and Synthetic Weather Data

The use of software to evaluate energy performance in buildings has been adopted for its efficiency and the facility it provides when evaluating diverse parameters influenced by physical and meteorological phenomena. Information related to weather data to perform software simulations, are obtained from different sources depending on the country. One of the more robust software tools for the performance of energy simulations is EnergyPlus ™, and on its official web page a wide range of weather data files can be accessed through links to DDY (ASHRAE Design Conditions Design Day Data), EPW[8] (EnergyPlus Weather File), and STAT (system call) extension files. More than 2,100 locations are available and arranged by World Meteorological Organization

[5]Representative Concentration Pathways
[6]Fifth Assessment Report, IPCC
[7]Sixth Assessment Report, IPCC
[8]EnergyPlus Weather File

region and country.

The database provided by EnergyPlus for the region of North and Central America, includes three cities in Mexico: Acapulco, Mexico City, and Veracruz. There is a lack of information in this database considering that there are 2,464 municipalities in the country, according to legislation corresponding to each state up to 2017. The cities included are in the central strip of the country, and the climates are different from those of the cities in the northeast of the country, which are those studied in this research.

The weather data provided by EnergyPlus is derived from 20 sources; some of it was created in response to official commissions or building services (USA, Canada, UK, Poland, etc.), and others were developed by different authors. The one used for Mexico was developed by the International Weather for Energy Calculations (IWEC[9]), as a result of the Research Project 1015 by Numerical Logics and Bodycote Materials Testing Canada for the American Society of Heating, Refrigerating and Air-Conditioning Engineers (ASHRAE[10]), Technical Committee 4.2 Weather Information [3]. Although many cities are not considered in this database, if simulation weather data is missing, it is suggested to obtain weather files in EPW format purchasing them from Weather Analytics and Meteonorm when possible, or to generate this files by interpolation based on climate data statistics.

The structure of the weather format generated by EnergyPlus, the EPW file, was developed by the U. S. Department of Energy and is compatible with diverse building energy analysis software such as the EDSL-TAS, IES, and ESP-r. It can be modified depending on the needs of each research project. The IWEC files were developed to unify weather files on a global basis and have been used as a reference for many projects.

[9] International Weather for Energy Calculations

[10] American Society of Heating, Refrigerating and Air-Conditioning Engineers

2.2.2 Weather Data-sets for Future Climate Scenarios

From the socioeconomic storylines provided by the IPCC, the study of emission scenarios and concentration pathways gave rise to their impact through GCM[11] and RCM[12] models within some other studies. General Circulation Models (GCM) are climate models based on mathematical models of a general circulation of a planetary atmosphere or ocean. They are three-dimensional models that simulate atmospheric, oceanic, and continental components. Within atmospheres the elements that compose it are considered, such as winds, humidity, clouds, gases and the temporal variations that they suffer, as variations originated due to the height at which they are found.

The results of these models are obtained by solving physics equations in each of these three systems, and thus, the specific conditions are provided in a determined number of mesh points, defined by dividing the planet's surface into a series of rectangles. The size of these rectangles varies; among the most common, resolutions of 2 to 5 degrees latitude per longitude are considered, which represents approximately between 200 and 400 km. Being so broad, their spatial resolution does not allow them to be used directly in regional or local studies.

Due to this, the diverse Regional Climate Models (RCM) were created downscaling information from the GCMs to allow the generation of the same climate change scenarios at the regional level. RCM are numerical climate prediction models affected by specified ocean conditions from a GCM or observation-based data set, whereby atmospheric and land surface development are simulated considering high-resolution topographical data, land-sea contrasts, surface components, and other characteristics of the Earth-system.

From these models, climate projections can be conceived and downscaled through diverse techniques such as statistical or dynamical downscaling. The purpose of doing this is to use weather projections to obtain more appropriate information with spatial resolutions closer to the locations, and temporary results of future meteorological data. The result is the obtaining of meteorological files that can be useful for diverse

[11] General Circulation Models

[12] Regional Climate Models

disciplines. For this research, these files were useful to perform energy simulations and thermal evaluations in the buildings considering historical and future weather data from projected information in different possible future climate scenarios and future years.

A GCM developed at the Hadley Centre, in the United Kingdom, was used to generate future weather files. This model is a grid point model with large grid cells, has a high temperature sensitivity, vital for building energy performance, and has been used worldwide to study these phenomena. GCMs represent physical processes in the atmosphere, ocean, cryosphere and land surface, and are considered the most advanced tools for simulating the response of the global climate system to increasing greenhouse gas concentrations according to the Intergovernmental Panel of Climate Change (IPCC, 2007), and in conjunction with nested regional models, have the potential to estimate changes required in impact analysis.

At the Hadley Center a model named PRECIS[13] (Providing Regional Climates for Impact Studies) was also developed, which is a regional climate modelling system derived from the third generation GCM, HadRM3 model, and can be configured to cover any area of the globe. This model uses as conditions of borders the data provided by the GCM of the Hadley Center corresponding to a range of emission scenarios and produces substantial amounts of climate data including standard variables such as temperature and precipitation projections for future periods (2070-2100).

From GCM projections, data is statistically downscaled to the site scale for its use in building cooling and heating simulations, using typical year weather files [152]. These files are composed by hourly records of historical weather data including dry-bulb temperature, dew point temperature, atmospheric pressure and total horizontal solar radiation. Then, the data must be downscaled from the GCM projections to estimate future TMY[14] components. Results obtained from these tools are useful to decision makers responsible for long-term city planning and to the assessment of various adaptation approaches.

The use of a Typical Meteorological Year (TMY) has been used for different locations

[13]Providing Regional Climates for Impact Studies

[14]Typical Meteorological Year

and improvements over the years. The data of the TMY can be purchased from the National Climatic Data Centre. There were established 230 locations in the USA, Cuba, Marshall Islands, Palau, and Puerto Rico with data from 1948 to 1980 and information of solar radiation and meteorological elements of hourly values for a year period. The Typical Meteorological Year 2 (TMY2) has similar characteristics and the files are available for download from the National Renewable Energy Laboratory or on CD.

Wilcox & Marion [151] developed a Technical Report for the use of the Typical Meteorological Year 3 (TMY3). These Data Sets have data from 1,020 locations in the USA including Guam, Puerto Rico, and Virgin Islands derived from 1991 to 2005 National Solar Radiation Data Base (NSRDB[15]) and meteorological data from the National Climatic Data Center (NCDC[16]).

The assessment of climate change could be challenging because of the large data sets and can be based on synthesising several climate scenarios to generalise it despite the existence of climate uncertainties. Nik & Arfvidsson [123] created a one-year weather data, representing typical, extreme warm and cold conditions over 30 year periods, which results in decreasing the length of simulations.

In order to make use of the weather files that are required when running energy simulations in software like EnergyPlus, it is necessary to use those files that are appropriate to the place where these simulations are made. Weather files are generated with information from weather stations, generally, those located at airports, since they have robust historical weather information. Because of this, many times the results obtained in the simulations do not correspond precisely to those that would be obtained in a more realistic way in the projects.

Although some areas have similar weather characteristics to those observed in airports weather stations, many times they are far from being so because there are cities in which the altitudes and geographical environment vary greatly. An example of this is where natural sources of water are found, mountains, depressions on the earth's surface, or even in cities, where phenomena like heat island effect occurs. Therefore, there is a need of scaling this information to make it more location appropriate.

[15]National Solar Radiation Data Base

[16]National Climatic Data Center

To evaluate the climatic characteristics that are required to elaborate weather files useful in the simulations, historical weather data must be available, as data obtained in future climate projections scenarios, obtained from GCMs or RCMs. Using information provided by these models, coupled climate models are generated; these are computer-based models of the earth's climate, in where their components are coupled together and make an interaction through simulations. Historical weather files can be obtained through generation methods (TMY, TRY[17], DSY[18] formats, etc.), or through meteo-centres.

The weather files of future data can be obtained through coupled climate models (CMCC[19], HadCM3[20], INMCM4.0[21], etc.) and for different emission scenarios (SRES A1, A2, B1, B2, etc.) or concentration pathways (RCP 4.5, 8.5, etc.). To make use of these weather data sets, required to elaborate weather files in energy simulation software, the downscaling of historical weather data to projected data is necessary in order to create files with appropriate formats, such as the EPW of EnergyPlus. These downscaling techniques vary depending on the information that is kept in both historical and future weather files. Some relevant tools for the completion of these techniques are described below.

The Climate Change World Weather File Generator for World-Wide Weather Data *CCWorldWeatherGen* [94] is a tool generated in the University of Southampton, and can make calculations for HadCM3 A2 scenario in years 2020, 2050 and 2080. This tool does not provide with the required baseline weather files or climate change scenario data, and the proposed sources to obtain them mentioned in the manual [93], are not available for the studied cities of this research.

Because of the innovation of the morphing method to obtain data, the *CCWorldWeatherGen* has been a reference for the generation of future weather files with data of climate scenarios projections. One of these is the Weather Morph: Climate Change Weather File Generator *UNF tool* [95] of the University of Florida; it makes scenario

[17] Test Reference Year
[18] Design Summer Year
[19] Centro Euro-Mediterraneo sui Cambiamenti Climatici
[20] Hadley Centre Coupled Model Version 3
[21] Institute of Numerical Mathematics Climate Model Version 4

calculations and weather morphing calculations; its a modification of *CCWorldWeatherGen* with the addition of HadCM3 scenarios A1F1, B1, B2 for years 2020, 2050 and 2080. It also provides for a reduction in time calculations, and the weather files preloaded from the EPW weather morphing can be chosen from the EnergyPlus Weather Data platform online. This database was explained already on this section in p. 36, where it is explained that the information that can be obtained corresponds to three cities in the central strip of the country, so the cities in this study are not covered.

The *Weather-Shift*^{TM} application [8], produces EPW files (hourly values for a typical year) for three future time periods based on the RCP4.5 and RCP8.5 Representative Concentration Pathways. It was developed by a collaboration of Arup North America Ltd and Argos Analytics, and it must be purchased in order to be used. This site is preloaded with some EPW files provided to the public domain by the US Department of Energy. For all other shift locations an EPW file must be uploaded as the basis for shifting. EPW file near shift location must be uploaded or purchased from other sites.

In the University of Exeter, the Weather Generator *Prometheus* [52] was developed for UKCP09 calculations. The weather files are currently available for 45 locations in the UK, each for 3 time periods and 2 emissions scenarios for air temperature; weather files for other locations must be created if required.

The Advanced WEather GENerator is an hourly weather generator for 2-Dimensional grid *AWE-GEN* [57]. It generates gridded climate variables in a high spatial and temporal resolution and downscaling of GCM predictions. It works mainly for analysis of hydrological models, rainfall, cloud cover, radiation, atmospheric and vapour pressure, and near surface temperature, so it is more applicable to activities such as agriculture. Another generator used for different ends was developed in the Massachusetts Institute of Technology, the Urban Weather Generator 4.1 *UWG* [25]. It is a Urban Heat Island effect modelling software that uses CCWWG for years 2020 and 2050.

2.2.3 Climate Projections in Mexico and Coahuila

Climate Projections have been made in Mexico considering two sets of the IPCC Scenarios, initially the SRES, and more recently, the RCPs. Prior to the elaboration of the

SRES, studies of global (GCM) and regional (RCM) climate projections were developed.

In the study carried out by Magaña, Conde, Sánchez & Gay [107], regional climatic changes for Mexico were presented, considering 30 years of climate data (1951-1980) to represent the average conditions. For the study, 18 climatic regions defined by Arthur Douglas were used; those were derived from the use of data obtained from diverse climatic stations across the country (Figure 2.3). New data was obtained from the interpolation of GCM outputs from the atmospheric models *Geophysical Fluids Dynamics Laboratory* (GFDL-R30) and the *Canadian Climate Centre* (CCC). The first one showed an increase in the average temperature of 4°C, with a spatial resolution of $2.22°$ of latitude by $3.75°$ of longitude, defining a mesh of 96 x 80 points; the second showed an increase of 3.5°C, with a resolution of $3.75°$ latitude, $3.75°$ longitude, and a mesh of 96 x 48 points.

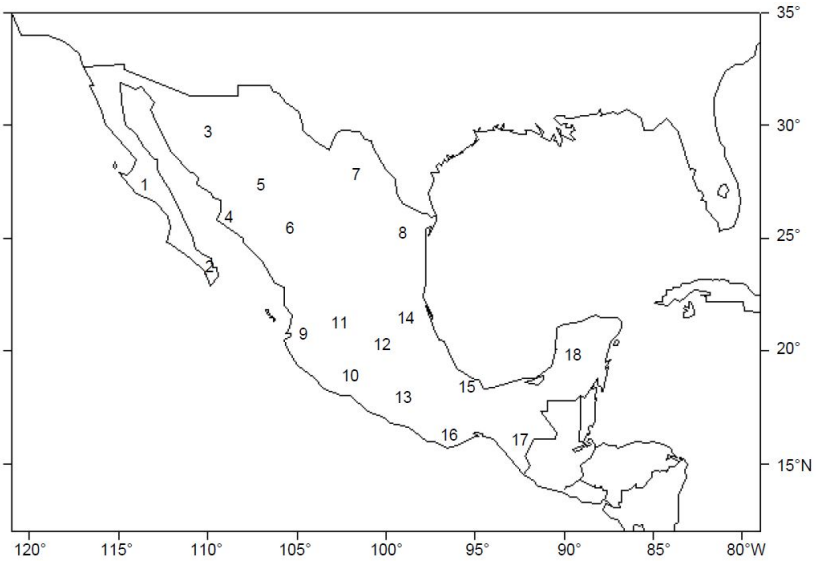


Figure 2.3: Douglas Regionalisation [107].

To contemplate emission scenarios, the data provided by the IPCC [16] was used, and different features were considered to study possible regional climate changes during the 21st century. The Ministry of Environment (SEMA[22]), developed a State Plan Against Climate Change in Coahuila, [46], in which it is explained how scenario families contain individual scenarios with common themes (A1Fl, A1B, A1T, A2, B1 and B2), and the ones chosen to be studied in the region. Given that scenarios A2 and B2

[22]Secretaría de Medio Ambiente

are focused on regional development, they considered the intermediate values in terms of the growth of greenhouse gas emissions, and population growth of between 100 and 160 million, respectively, for the year 2100; both were used to elaborate the projections of climate scenarios for the state. This data was included in the *Vulnerability and Threats Component of the State Climate Change Plan*.

The climate change scenarios are neither predictions of the future climate nor climate scenarios. They refer to the representation of the difference between possible and current future climate, usually presented by a climate model, and indicate the combination of both, the climate scenario and the current climate. Mendoza [72] worked with A2 and B1 scenarios using three of the twenty three models recognized by the IPCC at this time. The ECHAMPS, GCM developed in Germany by the Max Planck Society (2.81° x 2.81° resolution), the GFDRL, a GCM developed in the United States of America by the Geophysical Fluids Laboratory (4.4° x 7.5° resolution), and the RCM PRECIS, developed in the United Kingdom in the Hadley Center. As the latest, was established in a regional scale, downscaling was not required, and was suited for Latin American and Caribbean countries.

The world is considered as very heterogeneous in the A2 scenario. Local identities are preserved, and economic and technological developments are slow and local. A high population grow is contemplated along with an average growth of gross domestic product, a high use of fossil fuels, a change in land use from high to medium, a low oil reserve, a slow technological change and a regional change. Similarly, scenario B1 describes a convergent world that reaches its maximum population towards the halfway point of the 21st century, and then contracts. It anticipates rapid changes in the economic structures oriented to an information and service economy, less intensive use of materials and the introduction of clean technologies with an efficient use of resources. In it, a preeminence is given to world-class solutions aimed at delivering economic sustainability.

This study was used as the basis for the first algorithm developed for this research, as the most complete study for Coahuila before the last IPCC report was published. With ECHAMPS and GFDL models only four squares of the grid corresponding to the state were covered because of their resolution, so information was not precise enough.

The most detailed one was the PRECIS model; information from 41 weather stations was used to adapt weather data to a grid provided by the Pacific Climate Impacts Consortium (University of Victoria, Canada), generating a grid of nine points. Climate Change Projections for A2 and B2 scenarios were obtained, as rainfall and monthly mean temperatures for all those 41 points, for years the 2020, 2050, and 2080. Derived from this, a further study shows a comparison between scenarios A1 and B1 using the PRECIS model nested from HadCM3 model, and makes use of a $0.44°$ x $0.44°$ (latitude x longitude), getting a resolution of 50 km x 50 km [73]. The grid used for Coahuila is shown in Figure 2.4; similar figures were obtained for both scenarios, the reference period, and the three future years.

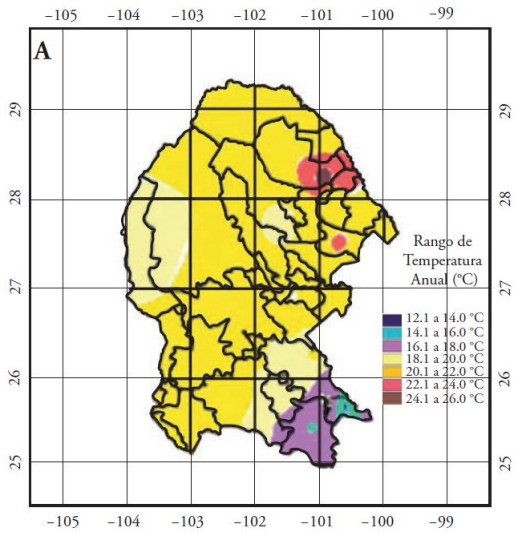


Figure 2.4: Grid used in Coahuila for projections performed with PRECIS model. Adapted from Mendoza-Hernández et al. [73].

The climate predictions for Coahuila, performed using the PRECIS model, showed that according to the A2 scenario, average temperatures increase of up to $4.4°$ C, and by 2080, minimum and maximum temperatures will be higher for each season. Even if control measures were established in scenario B1, by 2080 the temperature would rise by an average of $2.7°$ C. Total annual rainfall will be lower in the Lagunera (south-west) and South regions, and will increase in the North region. The climate formulas will change throughout the state. All the dry regions will continue to be dry, but with a higher degree of aridity. The Arteaga region (south-east), the only sub-humid region, will become semi-arid in both scenarios. However, this study must be actualised in order to compare the climate projections in the region. To work with this data, statisti-

cal regression methods have been used to generate future hourly weather data, which is based on the application of third-to-fifth order linear equations with coefficients trained using historical observations.

The second algorithm for this research was developed partly from information obtained by the National Autonomus University of Mexico (UNAM[23]) Atmospheric Science Centre [54]. The new projections for the country took into account the most recent IPCC report, so instead of using greenhouse gas emission scenarios SRES, RCP greenhouse gas concentration trajectories were used. Results obtained from these climate change projections are available on their website of the *Atlas Climático*. In here, the updated climate change scenarios for studies of impacts, vulnerability and adaptation are displayed. Data is derived from different GCMs through models CNRM-CM5[24], GFDL-CM3[25], HadGEM2-ES[26], and MPI-ESM-LR[27]. RCP4.5 and RCP8.5 are available for the near horizon (years 2015-2039), medium horizon (years 2045-2069) and far horizon (years 2075-2099).

Information is displayed for monthly periods for minimum, maximum and average temperatures, rainfall, and percentage of change in rainfall. The information is obtained after choosing the elements mentioned above, and clicking in the geographical coordinates for which the information is desired (Figure 2.5).

The RCP4.5 represents intermediate emissions, here it is considered that the radiative forcing is established shortly after year 2100, and it is consistent with a future of relatively ambitious emissions reductions. It is comparable with the B1 SRES scenario. This future is consistent with lower energy intensity, strong reforestation programmes, decreasing use of croplands and grasslands due to yield increases and dietary changes, stringent climate policies, stable methane emissions and CO_2 emissions increase only slightly before decline commences around 2040.

The RCP8.5 represents high emissions and it is consistent with a future with no policy changes to reduce emissions. It considers that incremental growth in greenhouse

[23]Universidad Nacional Autónoma de México

[24]Centre National de Recherches Meteorologiques Coupled Global Climate Model version 5

[25]Geophysical Fluid Dynamics Laboratory Climate Model version 3

[26]Hadley Centre Global Environment Model version 2 Earth-System

[27]Max Planck Institute Earth System Model, low resolution

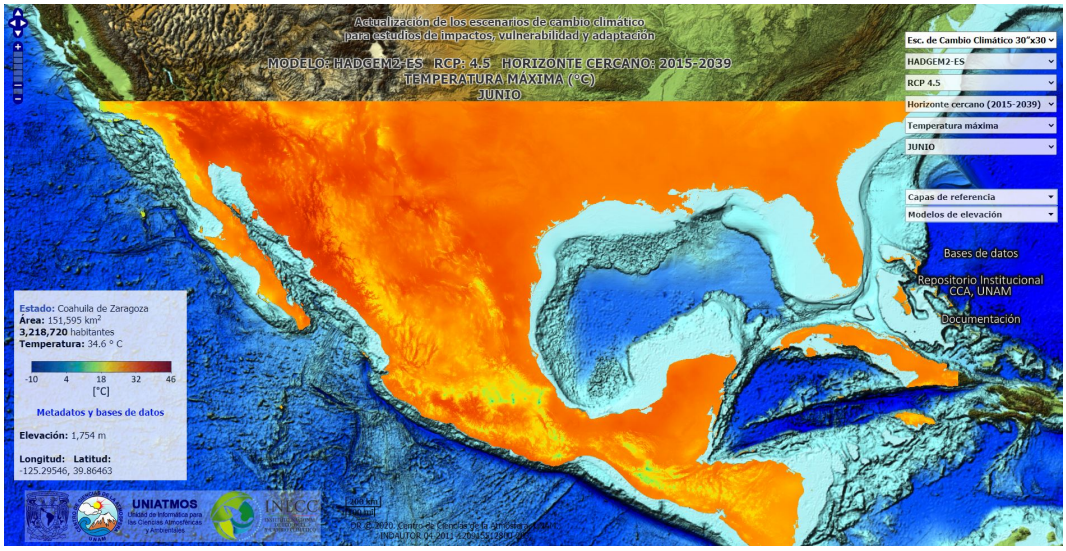


Figure 2.5: UNAM Climate Atlas [54].

gas emissions lead to high greenhouse gas concentrations over time. The comparable SRES scenario is A1F1. This future is consistent with three times today's CO_2 emissions by 2100, a rapid increase in methane emissions, an increased use of croplands and grasslands which is driven by an increase in world population (12 billion by 2100). It considers a lower rate of technology development, heavy reliance on fossil fuels, high energy intensity and no implementation of climate policies.

RCP4.5 was chosen for this research because it is deemed a more probable scenario compared with RCP8.5. According to the International Energy Agency [90], it is thought that global coal use peaked in 2013, and although increases are still possible, many energy forecasts expect it to flat line over the next few decades; besides, the falling cost of clean energy sources is a trend that is unlikely to reverse, even in the absence of new climate policies. Additionally, emission pathways to get to RCP8.5 generally require an unprecedented increase in coal use by the end of the century, that will require breakthroughs in coal recovery that greatly outpace technologies for other energy supply strategies [132].

2.3 Thermal Comfort in Housing

The main techniques used for improving thermal comfort in social housing in Mexico are related to thermal mass, protection from solar heat gain, and cross ventilation; some of which have been used in arid climates to improve the thermal performance of buildings. The assessment of performance risks for bioclimatic buildings can be made through experimental studies for thermal comfort based on meteorological data [145]. To consider climate data on thermal comfort in the buildings there are combined effects on dry weather, outdoor temperature measured in the shade, and relative humidity. Normal climatic averages are considered, including temperature, sunshine and relative humidity for all the months of the year. With this annual number of hours where occupants are comfortable inside the houses can be established. Comfort temperature inside a building is also considered by the adaptive approach to make use of natural ventilation, and is used in Bioclimatic design, which is considered important also in terms of economy for low-income populations [69].

Among the factors that affect the comfort conditions, some of the most significant are elements produced by nature and physical parameters, such as relative humidity, air velocity, the temperature of the building's outer shell and the air temperature. Having considered these factors, bio-environmental strategies can be used to minimise the impact of climatic corrections in buildings. For these matters, different solutions have been implemented, including the use of passive solar systems, appropriate ventilation, evaporative cooling and humidification of the environment, solar protection, thermal inertia and selective ventilation, among others, and the active and hybrid systems that make use of natural phenomena and technology to improve the comfort parameters inside buildings and, to make efficient energies.

The energy flow in a building is experienced when a different temperature exists inside and outside of it. The heat is transferred through the fabric or cavities, and these elements have different insulation values which determine the time used to carry out this transfer process. The measure, which describes the air-to-air behaviour [114], is called the overall thermal transmittance coefficient, or U-value. This value is a measure of the overall rate of heat transfer and its unit is W/m^2 K. All different mechanisms un-

der standard conditions are evaluated through a particular section of the construction. The coefficient is measured when there is a temperature difference across the structure of one degree, Kelvin or Celsius and the rate of heat flow in watts through 1 m^2 of a structure.

Thermal performance is considered as one of the most important factors to control in order to have an efficient energy behaviour in buildings, this is why solutions has been used in buildings to reduce peaks of temperature by taking advantage of the latent heat capacity [131]. The U-values are calculated from the thermal resistances of the different components of a structure, and these oppose the transmission of heat by the variation of the quantities. Thermal resistance, or R-value, with units given in m^2 K/W, describes the differences, where it is measured in opposition to heat transfer, offered by a particular element in the building.

To avoid the heating and cooling costs produced by the energy exchanged by the difference of temperatures, good thermal insulation must be implemented. This allows a better control of direct solar gaining, and ventilation when needed. The benefits obtained from good thermal insulation can be appreciated in both cold and hot variations of temperatures, alongside a decreased risk of surface condensation, because surfaces of the building can be kept at a temperature above the dew point of the air, as can be managed internally.

The main mechanisms considered when heat transfer is studied in buildings are conduction, convection and radiation, sometimes it is also important to consider condensation, since energy is released when exists the possibility of a change of water phase. In the building industry, there are used different materials that work as thermal insulators; they could be flexible, rigid, loose filled, reflective or materials formed on site. U-values and R-values are obtained to quantify the velocity of transmission of heat energy and how it goes through the fabrics and cavities of the construction. When this process occurs, insulation depends on thermal conductivity and thickness of the different layers and components of the building materials.

The thermal resistance of each layer of material in a structure depends on its thickness and the rate at which it conducts heat. If a material is homogeneous, the resistance

can be calculated with this formula: R = d/k, where R = thermal resistance (m^2 K/W); d = thickness (m); and k = thermal conductivity (W/m K). The thermal resistance of an open surface depends on the conduction, convection and radiation at that surface. Surface resistances are usually found by consulting standard values that have been found by measurement or by advanced calculations. Some of the factors affecting surface resistances are the direction of heat flow, the surface properties in terms of emissivity, and climatic effects.

There are various mechanisms and methods to estimate the buildings heat loss coefficient. One of which is the measurement of *in situ* U-values, heat flux plates in test cells are generally used as field measurements on the surface of the walls in a building. Heat measurements represent the heat flow through the section of wall covered by the sensor, but it is difficult to consider thermal bridges. Another method used to evaluate thermal behaviour is the Infrared Thermography. This technology allows visual checks across the building fabric and its heat loss. Visualisation applies only on the external surface and can hide thermal bypasses, gaps that allows ventilation, influence of the sun, precipitation, and long wave radiation losses. A limitation of this method is its accuracy in determining areas of heat loss against its inability to quantitatively estimate heat loss.

The co-heating test is a widely used method in the UK; it has provided significant evidence of a fabric performance gap and mechanisms that allow the heat to pass through the fabric and building elements. This test operates on the principle of setting up a constant internal temperature in a building and its energy balance, meaning the energy supplied towards heating is equal to the energy being lost from the building (Space Heating + Solar Gains = Fabric Heat Loss + Infiltration Losses) [130]. Some other available techniques that can be used to measure the performance of the building fabric are thermal imaging, post-construction audits, construction observations, leakage detection, pressurisation test, tracer gas measurement, heat flux measurement, partial deconstruction, cavity temperatures and airflow measurements [97].

This and a big spectrum of researches focus on the importance of heat loss measurements to study the energy performance gap, defined as the common discrepancy found between predicting building energy performance and actual energy performance, and

is considered to have negative impacts for the brand of ecological buildings, designers and operators [30].

For studies performed in Mexico, it was shown that when the oscillations of the external temperature and the value of the solar radiation are big, a wall or ceiling constructed with materials with a suitable combination of conductivity, density and specific heat values have a better performance, even if they have a low value of thermal resistance [78].

Solar radiation is significant in countries like Mexico; because of the oscillation of daily temperatures, there is an increased demand for energy in buildings for cooling. Hence, to estimate energy savings by the use of an appropriate envelope in these climates, a method based on a time-dependent heat transfer analysis should be used. This analysis can be done through programmes such as EnergyPlus and TRANSYS. According to the INEGI [83], most inhabited private dwellings are built with concrete blocks, therefore this material was used in base case simulations for the thermal comfort analysis.

2.3.1 Quantitative and Qualitative Approaches

There are different demand modelling methods and strategies used to to facilitate the analysis of certain thermal behaviour or phenomena in buildings. The relevance of the usage of these tools relies on the understanding of numerical procedures that can be used for its application in architecture. According to Parsons [126], modelling is an integral part of scientific activity and can not be a perfect representation. Thermal models incorporate concepts of heat transfer, heat balance, thermal physiology and thermoregulation along with anthropometry and anatomy into a mathematical representation of the human body. These models can simulate the thermal responses of a person and provide a prediction of the dynamic response of the body to any environment.

Methods for the creation of weather variables for use in building simulation have been created and analysed to address the fundamental limitations of each methodology, as robust information as weather files are key to design healthy, comfortable and sustainable buildings [75]. *Energy Signature* (ES) method of standard EN 15603:2008 is

a simplified method for building energy diagnosis, in which the heating and cooling energy use of a given building are correlated to climatic data over a suitable period. Plotting for several periods the average heating or cooling power versus the average external temperature provides useful information on building energy performance and allows a fast detection of malfunctions or changes in the building operation or features, as well as the verification of the efficacy of any retrofit intervention.

Although this method is preferably adopted in the case of constant internal temperature, and when the external temperature is the most influential parameter. It can also be applied to recording energy use for heating or cooling and accumulated temperature difference between indoor and outdoor, at average regular intervals. According to Pistore et al [129], the ES is the best fitting linear regression between these two quantities and, consequently, can be characterised by means of intercept and slope.

2.3.2 Thermal Comfort Standards

Seeking comfort is the result of a need for users to find better environmental conditions due to the large number of hours spent and activities that are undertaken within buildings. In recent decades, researchers have explored the best way to adapt comfort to the needs of the occupants. This is a complex task since it depends on many factors, both physical and physiological, as well as psychological and perception. The models that have been developed to explore responses include different variables. In respect of the personal variables, the thermal resistance of clothing and the metabolic rate are considered. The first is measured in units of clo. To determine the clo value, in the 1985 ASHRAE Handbook of Fundamentals [2] it is recommended to multiply the summation of the occupant clothing items by 0.82. The metabolic rate is a measure in W/h from the internal heat production of an occupant per unit of body surface area.

The environmental variables include dry bulb air temperature, mean radiant temperature, relative air velocity, and the water vapour pressure in ambient air. Within the physiological variables there are the skin temperature, the core or internal temperature, sweat rate, skin wetness, and the thermal conductance between the core and the skin. The first human comfort model was developed and published in the ISO 7730

by Fanger in 1967 [55], and then updated in 1970 [56]. He proposed a seven-point form to evaluate the condition of thermal comfort, involving human subjects in diverse environments. This standard presents the thermal sensation votes from these subjects, and the Predicted Mean Votes (PMV) thermal sensation scale, based on the relation between the energy loss and the metabolic rate. The Predicted Percent Dissatisfied (PPD) is obtained From the PMV, and is an index that predicts the percentage of thermally dissatisfied occupant.

In novel researches, authors [100] consider methodologies for indoor thermal comfort estimation that can be put into two broad categories. The first approach considers the human body heat balance, such as the ones from Fanger [56], and the Pierce Two-Node model [59]. The second approach considers thermal adaptation, like the Adaptive Comfort Model of the European Standard EN 15251 [33], and the Adaptive Comfort Model of the ASHRAE Standard 55-2010 [5] first developed by Nicole and Humphreys [122]. The first kind is used when buildings operate with mechanical heating, ventilation and air conditioning (HVAC) and the occupants are able to control the internal environment to desired levels of air temperature. The second kind is used when buildings are naturally-ventilated buildings.

The Adaptive Comfort Model (ACM[28]) is used for naturally ventilated buildings, and is used for this research as in all of the simulations considered buildings under these circumstances. In EnergyPlus, the ACM is based on the ASHRAE Standard 55-2010 and CEN 15251, and it determines the acceptability of indoor conditions given the monthly mean outdoor air temperature and the indoor operative temperature. With this information, it establishes an index for adaptation of occupants to outdoor, and the acceptability of indoor conditions. It is estimated that clothing is related to the acceptable range of indoor temperatures with the outdoor temperatures, and no humidity or air-speed limits are required when using this option (Figure 2.6).

With this, it is determined if the indoor conditions are considered comfortable. The operative temperature (T_{ot}) given in $^\circ$C, is calculated as the average of the indoor air dry-bulb temperature and the mean radiant temperature of the studied zone inside surfaces. It considers the monthly mean outdoor air dry-bulb temperature (T_o) also in

[28] Adaptive Comfort Model

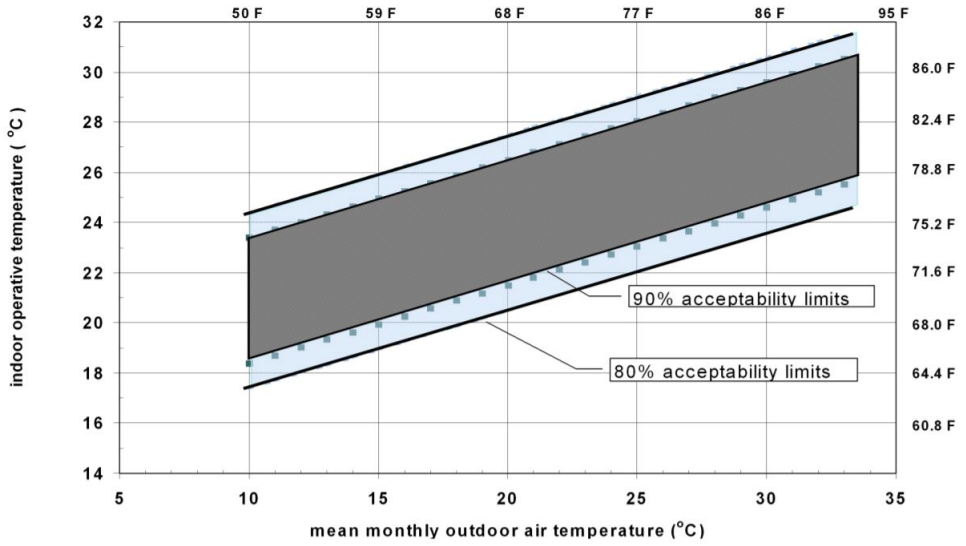


Figure 2.6: Acceptable Operative Temperature Ranges for Naturally Conditioned Spaces (ASHRAE Standard 55-2010).

° C, and is defined as

$$T_{ot} = 0.31T_o + 17.8 \tag{2.1}$$

The method only applies for activity levels between 1.0 and 1.3 met, for occupants with clothing whose insulation is between 0.5 and 1.0 clo. The average monthly temperature of the outdoor air should be between $10° C$ and $33.5° C$. The upper limit of comfort temperatures can be increased if air velocities are between $0.6\, m/s$ and $1.2\, m/s$.

Simulations were performed on EnergyPlus, and study subjects were considered like in the NAMAs, such as the number of users and occupancy values. From the weather files generated with the method, the .stat files are provided for the simulation, and EnergyPlus draws the (T_o) directly from the daily average temperatures. The ASHRAE standard was proposed because it is considered the most appropriate in the simulations, since is a well established model and comfort parameters have been widely studied for its making. When applying the method proposed in this research, an analysis of the differences and improvements that can be made considering external environmental factors. With the use and application of adaptive comfort methods specific for each place and with actual study subjects, the hours of thermal comfort can be increased, since the comfort spectrum is usually broader in those studies.

The study of adaptive comfort is complex to standardise in Mexico due to the great

variety of climates and micro climates within the country. Due to this, different related studies have been carried out to establish comfort ranges and rates by zones.

One of the first studies was made by Marincic et al [103] , which led to further studies regarding thermal comfort and the proposal of architectural design improvements in social housing for hot dry climate [104]. Derived from this previous research, the authors proposed acceptable comfort ranges for social housing users in the city of Hermosillo [105]. The study was placed in the northwest of the country, in which the predominant climate is hot dry, with maximum extreme temperatures of between $40°$ C - $45°$ C in summer and extreme minimums of $4°$ C and $7°$ C in winter.

Marincic study was done for nine social housing developments between $33.5\,m^2$ and $39\,m^2$, with at least one year of occupation. Comfort perception of inhabitants was registered in terms of comfort votes between -3 and +3 on the ASHRAE scale during the winter and summer. They are built with common characteristics for the building typology, with concrete blocks, flat roofs, without thermal insulation in the envelope, and with no solar protection on windows. The results showed that temperatures in degrees Celsius of the upper comfort limit, neutral, and lower comfort limit in summer are correspondingly $29.6°$ C, $32.2°$ C and $34.7°$ C, while for winter they are $23.5°$ C, $26.9°$ C and $31.3°$ C, taking into account that users have permanently lived in this city, and they are acclimatised to this weather variability. Further studies regarding thermal comfort and the possibility of architectural design improvements in social housing were performed by these authors.

Another adaptive comfort study was made for four main climatic regions in Mexico [125], considering regular conditions of predicted mean vote for the arid, dry tropic, temperate and humid tropic. The homes considered were in a range between $73.5\,m^2$ and $183.5\,m^2$, and the surveys were made for 74 students. The results for arid climate for the upper and lower heating limit medians were of $25°$ C and $22°$ C correspondingly, for cooling they were $34°$ C and $20.5°$ C, while the set point temperature for heating was $26°$ C, and for cooling $19.5°$ C.

Morgan & Gómez-Azpeitia [147] presented results for the first stage of a project to develop a Mexican Standard of Thermal Comfort for Natural Ventilated Buildings. A

mathematical model was developed using data from thirteen cities and based on the adaptive thermal comfort approach. The results were compared from international standards with differences of +0.73 and -2.07° C from ASHRAE55 and EN 15251 respectively, and in extreme dry warm climates with little more than 3° C, with respect to ASHRAE55. In the study there was found a greater amplitude of neutral temperatures: 28.78 K (12.75° C to 41.53° C) compared to 16 K (13° C to 33° C) presented in the findings by Nicol & Humphreys [122]; this indicates that people, particularly from extreme hot climates, felt comfortable at temperatures above 40° C.

A bio-climatic diagnosis suitable for the climates of Mexico can be made by calculating relative temperatures and humidity. Gómez-Azpeitia [11] generated a spreadsheet in which graphs and elements of comfort analysis can be obtained. The inputs include the city information, such as latitude, longitude, altitude, and the maximum, minimum, and the average relative humidity of each month throughout the year to be studied. Among the output data generated are graphs of monthly temperatures, hours, isotherms, a psychrometric chart (Victor Olgyay) like the one shown in Figure 2.7, a psychometric chart (Baruch Givoni), and comfort triangles (J. M. Evans).

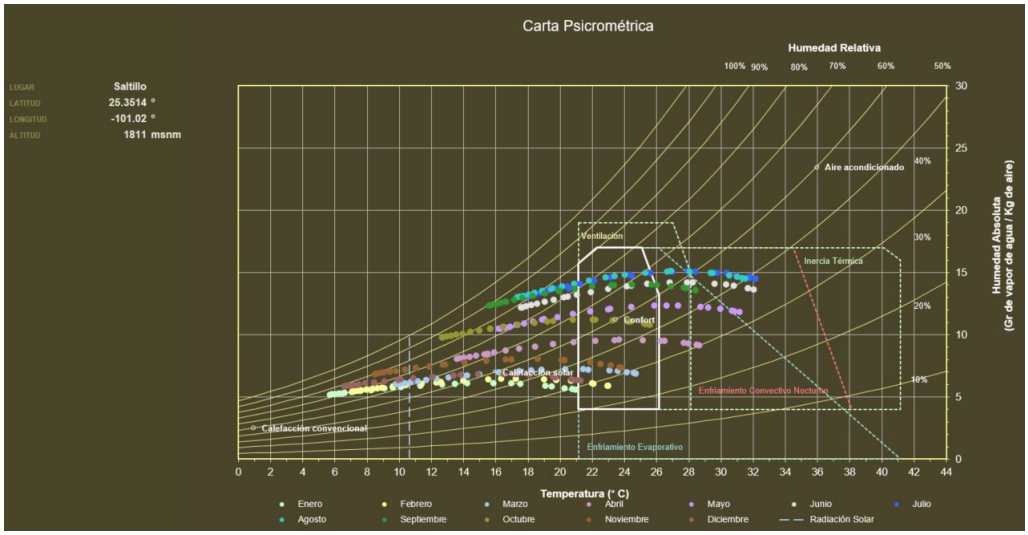


Figure 2.7: Psychrometric Chart for Saltillo [11].

2.3.3 Assessment Techniques and Housing Envelope

Of the 736,427 houses registered in the last census [85], 84% are made with concrete block, and 13.33% with clay, these are the two main materials used in the state. Efficiency of materials for envelopes in hot dry climates in Mexico were compared by Gutiérrez et al [69]. They evaluated a low-income housing prototype and results showed that concrete block walls were the ones with more hours of discomfort, along with shaded walls and concrete slab roof.

Medrano & Izquierdo [63] conclude that social housing in Mexico has been built without considering internal thermal comfort, and people live in adverse conditions because they can not afford air-conditioning systems, and nearly five million people have abandoned the houses because of this. These authors developed a project for hot dry climates, and the efficiency of materials for envelopes were evaluated for a housing prototype. Results showed the same as Gutierrez's analysis, that concrete block walls were the ones that resulted in more discomfort hours, along with shaded walls and concrete slab roof.

In developing countries, bio-climatic design is combined with new methodologies and it can be implemented to evaluate existing housing retrofits through the improvement of the overall heat transfer coefficient (U-value) of the envelope by incorporating layers of insulation and solar control films on windows.

A study was conducted to select envelope materials in non-air-conditioned buildings; the city of Torreón was chosen for the study completed in the month of May by Barrios et al [15]. Results showed that the thermal discomfort index (ID) is the most adequate to guide the selection of materials. This index is given by the sum of the index of warm (IDC) and cold discomforts (IDF). The IDF is the number of hours in which the temperature has a value greater than the maximum comfort range temperature multiplied by the difference in the average temperature during that time minus the maximum comfort range temperature. The IDC corresponds to the same IDF components evaluated for lower values than the minimum comfort range temperature.

Barrios et al analysed seven exterior surface configurations through numerical time-dependent heat transfer simulations. The best two were the roof consisting of 0.2cm of

waterproofing, 2.54 cm of sprayed polyurethane, and 10 cm of high-density concrete (R = 1,226 m^2 ° C / W), and consisting of 0.2 cm of waterproofing, 5 cm of vermiculite and 10 cm of high-density concrete (R = 0.582 m^2 ° C / W). According to the results obtained, it was deduced that when the building is not heated, using the R-value as a parameter for the selection of materials can give contrary results to what is desired. Likewise, it is shown that the colour of the outer surface is of utmost importance, with white greatly reducing the index of discomfort.

In the CONAFOVI[29] guide [32], design solutions are proposed to address passive climate control strategies for bio-climate. These consist of knowledge of the interaction of the climate with the human physiology and the forms of heat propagation to determine the thermal conditions or sensations for the human being. For the different ecological zones, three types of bio-climates were identified (semi-cold, warm-temperate, and warm), which derive in dry, semi-humid and humid depending on the humidity of the environment.

Within this classification, the climatic characteristics of Torreón and Monclova can be adapted to the dry warm bio-climate; these correspond to the deserts of North-America ecological region classification. Their daily temperature oscillation is between 10°C and 20°C, the relative humidity is low in spring and remains within the comfort ranges in the rainy season; the annual rainfall is less than 600 mm. The sensation of heat is present in the months from April to October and is concentrated from July to September. The humid heat for these months is observed in the early morning. The cold sensation appears in the months of December to March.

The city of Saltillo encompasses two ecological region classification: the deserts of North-America and tempered mountains, with dry temperate bio-climate and hot conditions occurring in the spring months. Minimum temperatures are below the comfort ranges at night and dawn throughout the year. The daily temperature fluctuation is between 13°C and 17°C. The rainfall is approximately 600 mm per year, and the maximum relative humidity is found above the comfort ranges from July to October; the minimum and averages are located within the comfort ranges. Bio-climatic elements that are suggested to consider are specified in the Table 2.1.

[29]Comisión Nacional de Fomento a la Vivienda

Table 2.1: Bio-climated Suggested Elements. Adapted from [32].

Torreón and Monclova	**Saltillo**
Cold Months December-March	**Moderate Cold Months** September, December and January
Direct heating in the morning and indirect in the afternoon	Direct heating in the early hours
Thermal inertia of the envelope	Indirect heating from the west, southeast, northwest façades
Minimal contact of the building with the environment	Control of humidity fluctuations
Avoid infiltration	Do not ventilate at night
Avoid cold winter winds	**Warm Months** March-June
Months in Transition April, May and November	Cooling w/ventilation and humidification in the afternoon
Adequate ventilation for hygrothermal control	Reduce temperature fluctuations
Humidification in the evenings	Thermal inertia in walls
Warm Months July-October	Ventilation in the afternoon
Avoid direct and indirect solar gains	
Buried, semi-buried spaces, slopes	
Compact and contiguous shapes	
Protected outdoor areas, micro-climates with patios	
Natural ventilation with pre-treatment	
Cooling and humidification	

These proposals and the design modifications were considered for the simulations shown in Chapter 6, and were adapted to the specific needs of the three studied cities and the location of the projects, making the pertinent adjustments for each case and their improvement.

2.4 Conclusions

The study of the geographical conditions leads to the possibility of considering suitable climatic parameters for the project site. Thermal comfort in the built environment is complex to achieve due to the multiple parameters that comprise it. From the particular to the general, comfort is the study of the user's well-being in buildings, and in turn, is influenced by the internal elements where there is an exchange of heat, and external elements that constitute the climate.

Various evaluations of thermal comfort were shown in previous studies carried out in Mexico, since the large fluctuations in temperature that are experienced in some cities represent a problem when trying to improve the thermal behavior of houses.

These studies are modifications of the Adaptive Comfort Model in ASHRAE 55-2010, nonetheless, they were suited and adapted to typical climate characteristics of cities in the north of the country.

Climate is defined by the physical and geographic parameters of the environment, the microclimate where the projects are placed, and the climate that makes up a larger region. The common way to determine the climate is by measuring its components in weather stations; some of these are dry and wet bulb temperatures, atmospheric pressure, winds, and solar incidence. As future climate can not be measured, it is studied through projections made under different greenhouse gas emissions or concentration scenarios, both adopted by the IPCC.

Physiography is varied both in Mexico and Coahuila. There are several climates within the states and the characteristics of social housing are the same regardless of where they are located. The first projections made for future climate scenarios in Mexico were prepared from GCM in 2009, considering the IPCC 4th Assessment Report *AR4* [140] for scenarios A2 and B2; they were mainly used by sectors such as agriculture, one of the most important economic activities in the country.

In Coahuila, this information was downscaled with RCM models, however, it was not adapted to the study of climate impact on buildings, so it was considered important to do so when this research was in its first stages, to assess the possible change that housing design must undergo to adapt to the climate throughout the years.

Subsequently, in 2012, the UNAM Atmosphere Science Centre developed the new projections issued by the IPCC in the 5th Assessment Report *AR5* [16] through RCM, and they were presented interactively as a result of methodologies carried out by Fernández Eguiarte, Romero Centeno, & Zavala Hidalgo (2014). They were recently updated on the website and have been available in an interactive map since 2020.

Climate generators use a large amount of information that must be stored in supercomputers that depend on the resources assigned to projects of this nature by the countries that develop them. In Mexico these data are not available all the time.

The weather generators analysed in this chapter are focused on SRES scenarios or RCP concentration pathways, not in both; this due to their own purposes and appropriate

attributes. It was specified in this chapter that each model or tool is suited to the needs of each investigation. For the present study, both are required, since the projections that were made for Mexico are initially focused on the SRES, and the most recent ones on the RCP. By having the opportunity of analysing both, the possibility of adapting the future projections made for the country is also expanded when having the new IPCC report available in RCMs for Mexico.

Some of the existing tools for data downscaling have a cost or only have adequate and complete information in respect to the countries where they were developed. This makes them unavailable for all countries or to researchers or projects that does not have the economic resources to buy sets of climate data and projections. They are also limited to specific cities estimations, and not for specific site locations.

In regions where there are big variations in elevations or with wide differences in physiographic characteristics, there are considerable differences in weather parameters even within the same cities. Thus, it is needed a tool in which, considering these projections, climate files are generated to be used in simulations and adapted to the characteristics of the weather corresponding to the specific geographic coordinates of the project site.

Therefore, in the search for the appropriate tool for this research, it was deduced that some of the existing ones are partially adapted to the needs of the project, but not in its entirely. Due to this, it is necessary to create a methodology assembled by tools that meet the characteristics needed for this research.

The proposed methodology to accomplish this is explained in the next part of this document, in Chapters 3, 4 and 5. It allows the analysis of the parameters considered in the weather files, and can be adapted to different scales or projections. This means that the SRES scenarios and the RCP emissions projected for Mexico, and specifically for Coahuila, can be considered. The projections data obtained from the AR4 and AR5 reports were used for the historical weather files adaptation in the studied region. With this, the gaps in knowledge covered in the literature are addressed from an innovative perspective and are explained in greater depth in the following chapters.

Part II

Developed Methodology for Weather Files Generation for Building Simulation and Data Interpolation

Chapter 3

Algorithm DGG1. Generation of Response Surface for a Rectangular Grid

In the analysis of the covered literature, it was identified the need to create tools that allow the use of data from climate projections in Coahuila, in order to apply them in building energy simulations. This chapter explains the first part of the methodology developed to adapt this information and make it appropriate for creating weather files of climate projections.

This first part consists of unifying the temperature information obtained for a wide grid that covers the state of Coahuila through a data response surface. With the obtained surface, the missing information of temperatures can be obtained. The methodology to achieve this interpolation of data is numerically explained.

An algorithm is defined as a procedure or set of rules used in calculation and problem-solving; a precisely defined set of mathematical or logical operations for the performance of a particular task [142]. The mathematical procedures described and developed for Chapters 3, 4 and 5 correspond to this definition.

Initially, the name of DGG was considered because it corresponded to the Design of a General Grid, which evolved throughout the investigation. These letters correspond in turn to the initials of the author's father, so they were preserved in his honor for the name of the three algorithms. To have continuity in the development of these, the use

of numbers from one to three was determined, having the algorithms DGG1, DGG2, and DGG3 constituting the proposed innovative methodology.

To describe the scopes of the algorithms developed, the basic questions related to them are answered in Table 3.1.

Table 3.1: Algorithms Synopsis.

Algorithm DGG1	**Algorithm DGG2**	**Algorithm DGG3**
What is it?		
Algorithm for obtaining interpolated data of temperatures from climate change projections on a response surface obtained from a regular grid.	Algorithm for obtaining interpolated data of temperatures from climate change projections on a response surface obtained from an irregular mesh.	Algorithm for creating columns of temperature and relative humidity in weather files for dynamic simulations from climate change projections.
Where does it start from?		
Temperature data provided by the *Pacific Climate Impacts Consortium*.	Temperatures obtained with *PRECIS model (SRES Climate Scenarios)*.	Historical Weather Data + temperatures obtained from *UNAM Climate Atlas (RCP Emission Trajectories)*.
What is its application?		
The temperatures obtained are used to generate weather files with *Algorithm DGG3*.	The temperatures obtained are used to generate weather files with *Algorithm DGG3*.	The generated *.epw* weather files are used to run energy simulations in EnergyPlus.

While Algorithms DGG1 and DGG2 are used to interpolate data and obtain temperature information from a response surface, Algorithm DGG3 can use information gen-

erated by these algorithms, or others sources of information, to produce weather files in *.epw* format. The interaction between them can be seen in Figure 3.1.

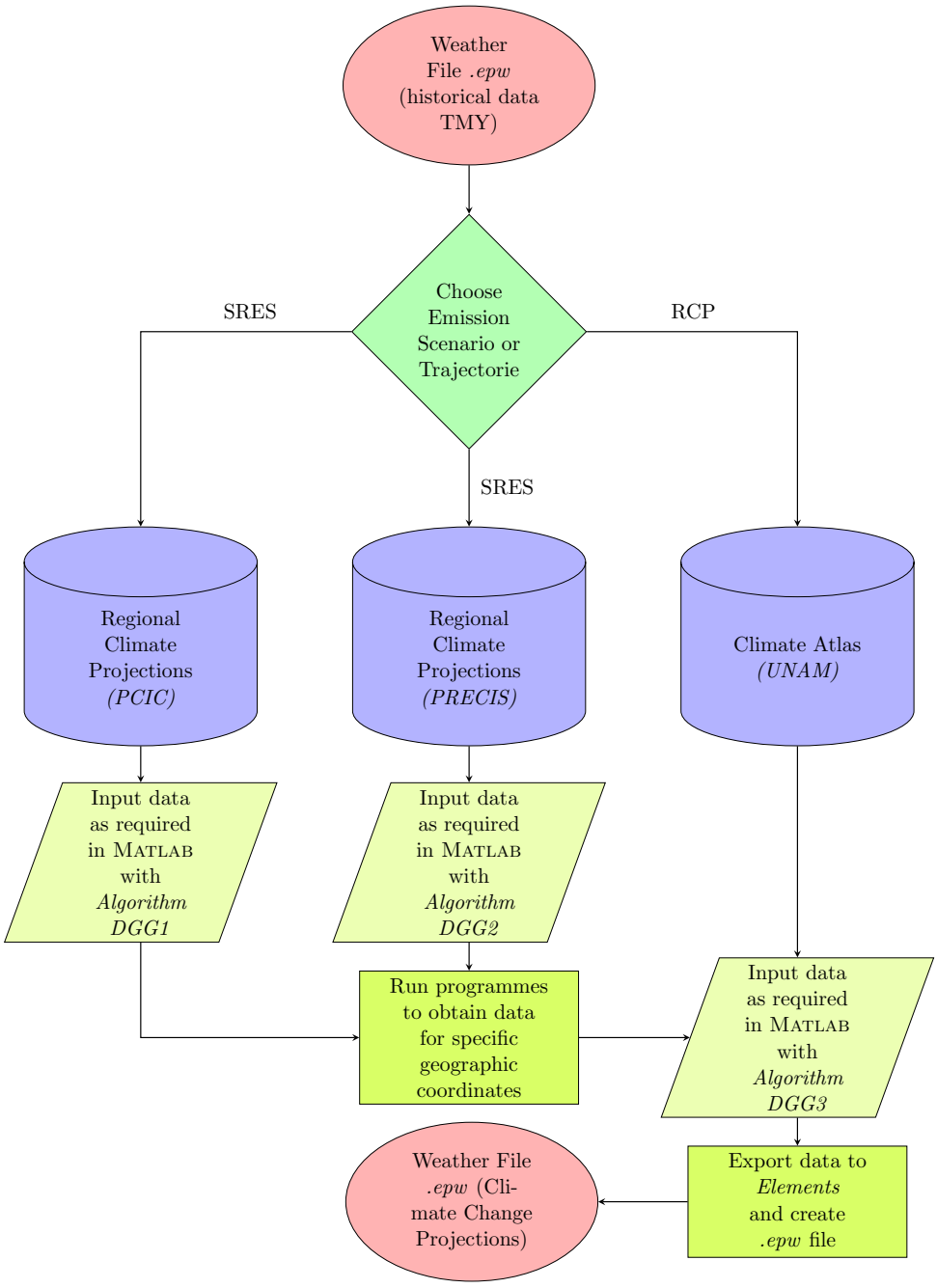


Figure 3.1: Interaction Between the Three Algorithms.

Once the weather files have been generated, they are ready to be input into EnergyPlus, so energy simulations can be carried out to evaluate the thermal performance of a house or building.

The use of numerical meshes obtained when using Algorithms DGG1 and DGG2 give a clear example of how the studied phenomena is behaving. And even if the data is scarce, the outcomes obtained when using the algorithms are enriched with the use of mathematical procedures.

The response surfaces obtained with Algorithms DGG1 and DGG2 allow qualitative visualisations of the phenomenon, and in turn, interpolations are obtained to estimate data at any point on the surface, meaning the quantitative estimates are objective and presented in numerical forms. The application of these developments is reduced to the introduction of data to obtain the results of the stages in graphical and numerical form.

From the temperatures provided by climate experts, equations are adjusted for each month of the studied year, type, horizon and location. This allowed the creation of weather files not only for the specific locations, but also for possible future weather scenarios. With this, a comparative of thermal behaviour could be studied, and a variety of architectural designs were analysed.

For the obtaining of missing information in weather files for climate change scenarios, the initial proposal for the generation of the algorithms was made for a rectangular grid of data. This disposition is due to data that were available at the beginning of this research and corresponds to the creation of algorithm DGG1 as the first part of the innovative methodology. Nine points or coordinates with their corresponding temperature data were assigned for the grid corresponding to Coahuila in the global models.

With these initial data, an interpolation was made to obtain a response surface in which the temperatures for any coordinate within this grid could be consulted. The development of the algorithm that allows this is extensively explained in this chapter.

3.1 Antecedents of Algorithm DGG1

In the official website of the National Institute of Ecology and Climate Change (INECC[1]), there is a platform with documentation of climate change derived from the collabora-

[1]Instituto Nacional de Ecología y Cambio Climático

tion between Mexico and Canada. The Pacific Climate Impacts Consortium (PCIC[2]) from the University of Victoria, is a regional climate service center that provides practical information on the physical impacts of climate variability and change in the Pacific and Yukon Region of Canada.

Data provided by them was used to create the outputs for weather stations in Coahuila. For each station, diverse GCM models were run to obtain temperatures and rainfall for the grid, as shown in Table 3.2. Data for year 2020, 2050 and 2080 were obtained with these nine points, as for A2 and B2 SRES climate change scenarios [72].

Table 3.2: Geographic Coordinates from GCM.

Longitude and Latitude of each Station		
$(-107.5,\ 32.5)$	$(-102.5,\ 32.5)$	$(-97.5,\ 32.5)$
$(-107.5,\ 27.5)$	$(-102.5,\ 27.5)$	$(-97.5,\ 27.5)$
$(-107.5,\ 22.5)$	$(-102.5,\ 22.5)$	$(-97.5,\ 22.5)$

The grid corresponds to a mesh used for the study of a rectangular grid explained in this Chapter. The study of rectangular meshes of 3×3 has diverse applications. They are presented in architecture and engineering in the study of physical or theoretical situations, with heights representing values of temperatures, atmospheric pressures, emissions of carbon dioxide, etc. As the outputs of the study mentioned above were temperatures and rainfall for the state in the selected weather stations, temperatures were the parameters aimed to obtain, for every specific point contained in the grid, as is one of the main components in the weather files used for running energy simulations, further explained in Chapter 6.

In the research applied to architecture, information required was not available for the state of Coahuila. Trying to take advantage of the global and broad results of the GCM and go from the general to the particular, a nine-point grid that includes the state was extracted. Although valuable, the information provided by the GCM was insufficient for this research, so the need to interpolate from these nine points arose.

For this purpose, several mathematical interpolation techniques were studied, which

[2]Pacific Climate Impacts Consortium

are detailed below. The original procedure to perform the interpolation from the nine-point mesh is also presented.

The very small information provided by the data from the nine points of the 3×3 grid, was a motivation to research various mathematical approaches that would allow the deduction of additional information to broaden the understanding of the behaviour of the mesh. Consequently, the focus of this part of the method is exclusively on establishing a mathematical model that enriches the original information provided by the nine data.

3.2 Mathematical Development of Algorithm DGG1

In this section, it is presented a way to obtain a response surface and its contour lines, from a 3×3 rectangular mesh. From the original information of the nine points of the mesh (x, y, z), it is offered the possibility to interpolate for the desired values (x_0, y_0) and to obtain their coordinates on the response surface (x_0, y_0, z_0).

3.2.1 Response Surface from a 3×3 Rectangular Mesh

The elements composing the points and coordinates will be managed with (x, y, z) variables to simplify information and work in a mathematical environment. The nine points correspond to the grid provided by the PCIC. For the weather stations where the most robust weather information was obtained, coordinates (x_0, y_0) are assigned. And finally, output data for any desired point in the response surface is shown with the form (x_0, y_0, z_0).

Proposal

A mathematical procedure is proposed to establish a response surface from a rectangular mesh of nine known points, of coordinates (x, y, z), as shown in Figure 3.2.

The points have coordinates with real values, $x, y, z \in \mathbb{R}$, contained in a three-dimensional

system of axes perpendicular to each other (axes of: abscissas, ordinates and heights).

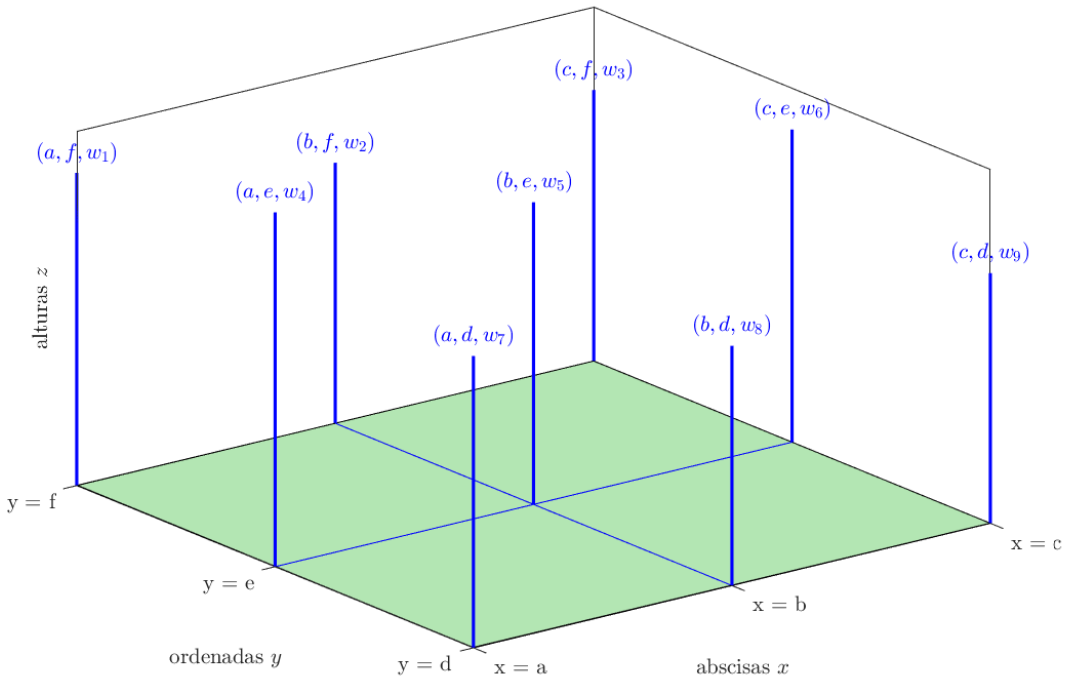


Figure 3.2: Data of the 3×3 Rectangular Mesh.

With the proposed response surface, the behaviour of the information is displayed in a broader form than the simple observation of the nine points. Additionally, contour lines can be obtained from it.

There is also a way of interpolating for values of interest (x_0, y_0) within the range of information. That is, for abscissas $a \leq x_0 \leq c$ and ordinates $d \leq y_0 \leq f$, the procedure obtains the heights z_0 that determine the points (x_0, y_0, z_0), on the response surface.

Coordinates of the base plane

As already mentioned, the coordinates (x, y, z) belong to the real numbers, or what is the same, x, y, z are on the so-called number line. Further:

$$\begin{aligned} a < b < c; \qquad & b - a = c - b = h \\ d < e < f; \qquad & e - d = f - e = v \end{aligned} \tag{3.1}$$

h can be less, or equal, o bigger than v. Although there are no specific restrictions, it is convenient that h and v are of the same order of magnitude to obtain more regular and reliable results.

3.2.2 Revision of some Adjustment Models

As it is of interest to have a set of points greater than the nine known to establish a response surface and its contour lines, the problem becomes the search for mathematical models that allow the plausible obtaining of additional information. The problem, therefore, leads to the revision of adjustment models.

Linear interpolation in 2D

The method of linear interpolation is used to calculate the value of y corresponding to a given x, using tabulated values (x_k, y_k) and (x_{k+1}, y_{k+1}). If x lies inside interval (x_k, x_{k+1}), then we interpolate for $y(x)$ [112]. To estimate values at points intermediate to those where its values are already known, interpolation is used.

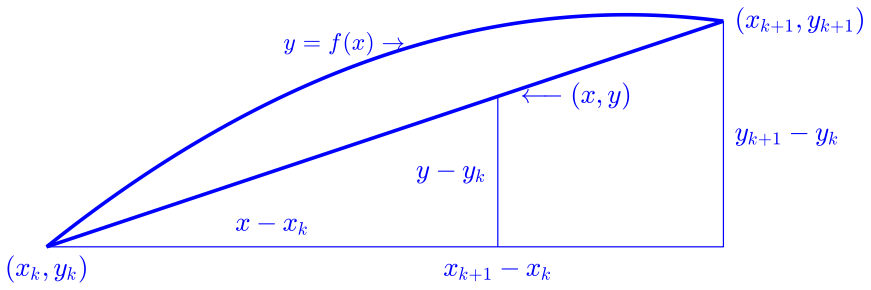


Figure 3.3: Linear Interpolation in 2D.

The formula for linear interpolation is obtained by simple constructing the straight line through points (x_k, y_k) and (x_{k+1}, y_{k+1}), and using the relations in the similar triangles in Figure 3.3, writing the two–point formula for this straight line:

$$\frac{y - y_k}{x - x_k} = \frac{y_k - y_{k+1}}{x_k - x_{k+1}}. \tag{3.2}$$

Equation (3.2) can be solved for y, and the result

$$y = y_k + \left(\frac{y_k - y_{k+1}}{x_k - x_{k+1}} \right) (x - x_k) \tag{3.3}$$

can be simplified and written in the form

$$y = \frac{y_k \left[x - x_{k+1} \right] - y_{k+1} \left[x - x_k \right]}{x_k - x_{k+1}}. \tag{3.4}$$

Equation (3.4) is one standard form of the linear interpolation formula for approximating y for a given x.

However, in this case, the above formulas have a very limited application because it is only possible to use them to interpolate between some values of x that are on a line, intermediate between two points of the 3×3 mesh.

Linear interpolation in 3D

A line L in the three–dimensional space is determined when we know a point $P_0(x_0, y_0, z_0)$ on L and the direction of L. A vector conveniently describes the direction of a line in three dimensions, so we let $\mathbf{v}$ be a vector parallel to L. Let $P(x, y, z)$ be an arbitrary point on L and let $\mathbf{r}_0$ and $\mathbf{r}$ the position vectors of P_0 and P, that is, they have representations $\overrightarrow{OP_0}$ and $\overrightarrow{OP}$ [143].

If $\mathbf{a}$ is the vector with representation $\overrightarrow{P_0P}$, as in Figure 3.4, then Triangle Law for vector addition gives $\mathbf{r} = \mathbf{r}_0 + \mathbf{a}$. But, since $\mathbf{a}$ and $\mathbf{v}$ are parallel vectors, there is a scalar t such that $\mathbf{a} = t\,\mathbf{v}$. Thus

$$\mathbf{r} = \mathbf{r}_0 + t\,\mathbf{v} \tag{3.5}$$

which is a *vector equation* of L. Each value of the *parameter* t gives the position vector $\mathbf{r}$ of a point on L.

If the vector $\mathbf{v}$ that gives the direction of L is written in component for as $\mathbf{v} = \langle a, b, c \rangle$, then $t\mathbf{v} = \langle ta, tb, tc \rangle$. It can also be written $\mathbf{r} = \langle x, y, z \rangle$ and $\mathbf{r}_0 = \langle x_0, y_0, z_0 \rangle$, the vector equation (3.5) becames

$$\langle x, y, z \rangle = \langle x_0 + ta, y_0 + tb, z_0 + tc \rangle.$$

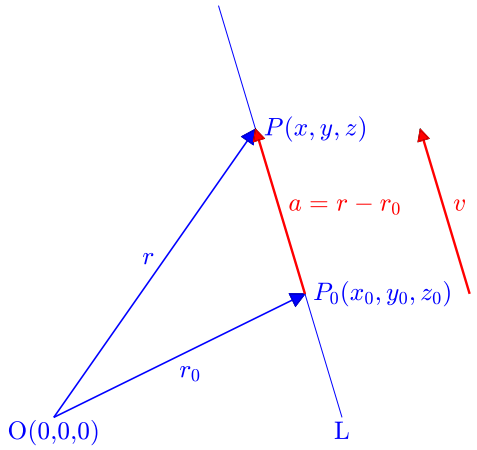


Figure 3.4: Line in 3D.

Two vectors are equal if and only if corresponding components are equal. Therefore, we have the three scalar equations:

$$x = x_0 + at, \quad y = y_0 + bt, \quad z = z_0 + ct \tag{3.6}$$

where $t \in \mathbb{R}$. These equations are called *parametric equations* of the line L through the point $P_0(x_0, y_0, z_0)$ and parallel to the vector $\mathbf{v} = \langle a, b, c \rangle$. Each value of the parameter t gives a point (x, y, z) on L.

Another way of describing a line L is to eliminate the parameter t from Equations (3.6). If none of a, b or c is 0, each of these equations for t can be solved, equal the results, and obtain

$$\frac{x - x_0}{a} = \frac{y - y_0}{b} = \frac{z - z_0}{c} \tag{3.7}$$

These equations are called *symmetric equations* of L. Notice that the numbers a, b and c that appear in the denominators of Equations (3.7) are *directions number* of L, that is, components of a vector parallel to L.

In general, the direction number of the line L through the points $P_0(x_0, y_0, z_0)$ and

$P_1(x_1, y_1, z_1)$ are $x_1 - x_0,\ y_1 - y_0,\ z_1 - z_0$ and so, symmetric equations of L are

$$\frac{x - x_0}{x_1 - x_0} = \frac{y - y_0}{y_1 - y_0} = \frac{z - z_0}{z_1 - z_0} \tag{3.8}$$

The observations of the previous point, in 2D, are the same for this interpolation in 3D. They are only applicable to the lines that join the 3×3 mesh heights, not to points placed out of them.

Multiple regression

When there are two independent variables, it is possible to use a multiple regression equation in the form

$$\hat{z} = a + b\,x + c\,y \tag{3.9}$$

and it is desirable to determine it with the method of least squares, that is, to select the values a, b and c in order to minimize the sum of the squares of the error $\sum(z - \hat{z})^2$, or sum of the n quadratic differences between the values of z known and the predicted $\hat{z}$. Following Chapter 13 of Snedecor and Cochran [139], with the sets of n data of x, y and z, it is needed to solve the *normal equations* associated with the problem:

$$\begin{array}{rcrcrcl} na & + & b\sum x & + & c\sum y & = & \sum z. \\ a\sum x & + & b\sum x^2 & + & c\sum xy & = & \sum xz. \\ a\sum y & + & b\sum yx & + & c\sum y^2 & = & \sum yz. \end{array} \tag{3.10}$$

The normal equations are easily remembered by observing that they can be obtained formally by multiplying the equation (3.9) by 1, x and y successively and adding. In a matrix format

$$\begin{bmatrix} n & \sum x & \sum y \\ \sum x & \sum x^2 & \sum xy \\ \sum y & \sum yx & \sum y^2 \end{bmatrix} \begin{bmatrix} a \\ b \\ c \end{bmatrix} = \begin{bmatrix} \sum z \\ \sum xz \\ \sum yz \end{bmatrix}. \tag{3.11}$$

To apply this procedure to the 3×3 mesh: if n is the number of elements of w or z, then n equidistant values must be set in the closed interval $[a \quad b]$ and $[d \quad f]$, in such a way that there are n elements of x, y and z

$$\begin{aligned} x &= [1.00 \quad 1.25 \quad 1.50 \quad 1.75 \quad 2.00 \quad 2.25 \quad 2.50 \quad 2.75 \quad 3.00] \\ y &= [2.00 \quad 2.50 \quad 3.00 \quad 3.50 \quad 4.00 \quad 4.50 \quad 5.00 \quad 5.50 \quad 6.00] \\ z &= [30 \quad 25 \quad 26 \quad 34 \quad 29 \quad 30 \quad 28 \quad 23 \quad 24]. \end{aligned}$$

With (3.10), the augmented matrix results $\left[\begin{array}{ccc|c} 9 & 18.00 & 36.0 & 249.0 \\ 19 & 39.75 & 79.5 & 490.5 \\ 36 & 79.50 & 159.0 & 981.0 \end{array}\right]$,

which has a solution $\begin{bmatrix} 31.6667 \\ 0.0000 \\ -1.0000 \end{bmatrix}$.

The least squares plane is thus obtained (3.9)

$$z(x, y) = 31.6667 + 0\,x - y.$$

The Figure 3.5 presents the plane edgewise, with points above and below it.

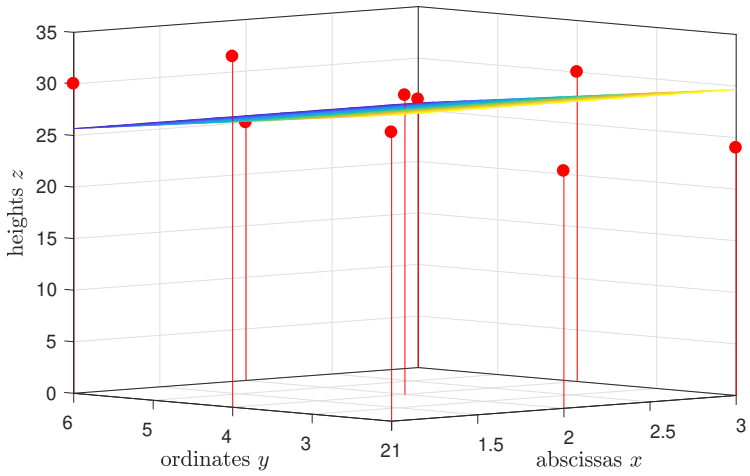


Figure 3.5: The sum of the quadratic deviations is kept at a minimum.

The previous equation is of the proposed type (3.9), which corresponds to a 3D plane. Their contour lines degenerate in straight lines, which do not represent a great contribution to the problem of the 3×3 rectangular mesh (Figure 3.2).

Response surface of triangular faces

To dissect the volume below the response surface, the formation of truncated triangular prisms of heights w is proposed, as in Figure 3.6. Some of the ways in which the equations of the planes are represented are explained below.

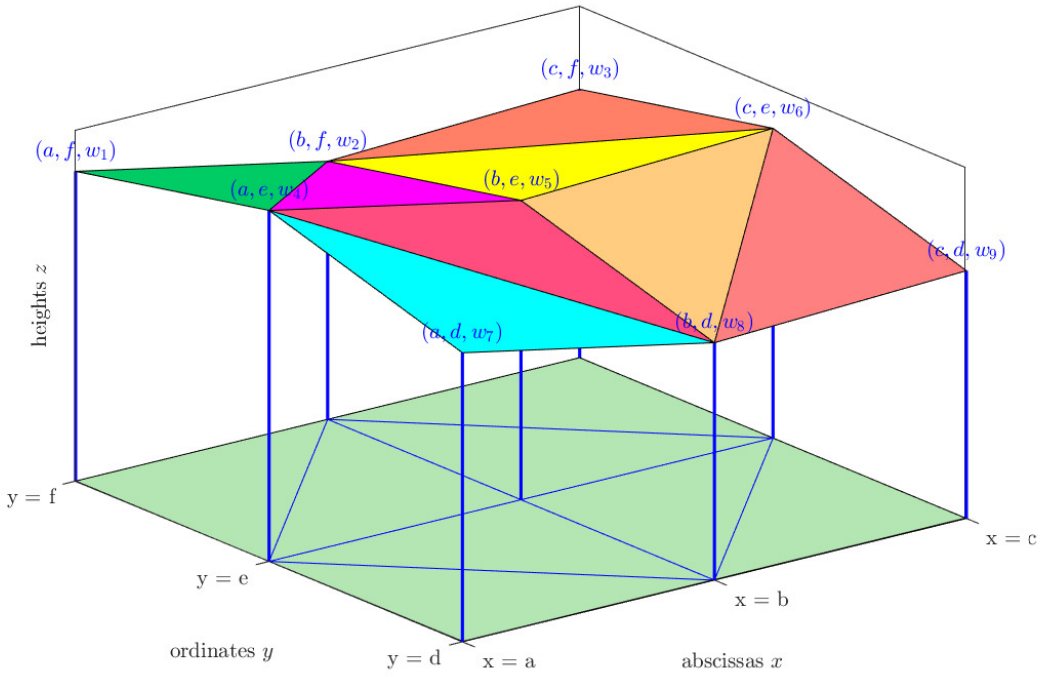


Figure 3.6: Response Surface of Triangular Faces.

Vector Equation of a Plane

Given a point ($\mathbf{R_0}$) on the plane, and a direction ($\mathbf{N}$) *normal or perpendicular* to it, it is possible to establish the plane equation without ambiguities.

The condition that $\mathbf{R}$ is the position vector with respect to a point in the plane, can be expressed by asserting that the *relative vector* $\mathbf{R} - \mathbf{R_0}$ found in the plane, is perpendicular to $\mathbf{N}$ (see Figure 3.7).

This means that the scalar product is zero

$$(\mathbf{R} - \mathbf{R_0}) \cdot \mathbf{N} = 0. \tag{3.12}$$

Therefore, the equation (3.12) is a vector equation that describes the plane. In terms of the components of $\mathbf{N} = a\,\mathbf{i} + b\,\mathbf{j} + c\,\mathbf{k}$, it becomes

$$a\,(x - x_0) + b\,(y - y_0) + c\,(z - z_0) = 0. \tag{3.13}$$

By grouping the constant terms, stems the expression

$$a\,x + b\,y + c\,z = d, \quad \text{where} \quad d = a\,x_0 + b\,y_0 + c\,z_0. \tag{3.14}$$

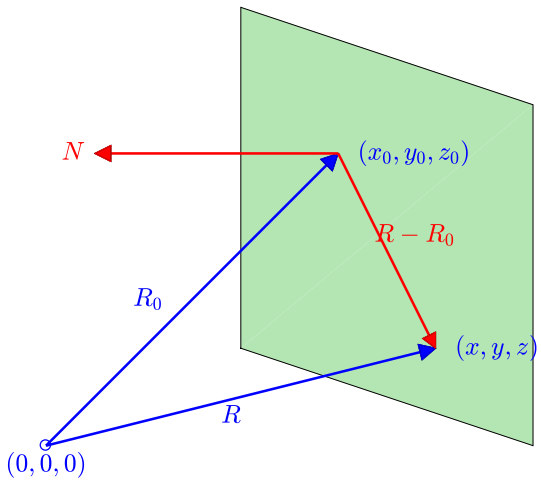


Figure 3.7: Vector Equation of the Plane.

Recall that the so-called **triple scalar product** of vectors $\mathbf{a}$, $\mathbf{b}$ and $\mathbf{c}$ is $\mathbf{a} \cdot (\mathbf{b} \times \mathbf{c})$. So

$$\begin{aligned}
\mathbf{a} \cdot (\mathbf{b} \times \mathbf{c}) =& (a_1\,\mathbf{i} + a_2\,\mathbf{j} + a_3\,\mathbf{k}) \cdot \begin{vmatrix} \mathbf{i} & \mathbf{j} & \mathbf{k} \\ b_1 & b_2 & b_3 \\ c_1 & c_2 & c_3 \end{vmatrix} \\
&= (a_1\,\mathbf{i} + a_2\,\mathbf{j} + a_3\,\mathbf{k}) \cdot \left(\begin{vmatrix} b_2 & b_3 \\ c_2 & c_3 \end{vmatrix} \mathbf{i} - \begin{vmatrix} b_1 & b_3 \\ c_1 & c_3 \end{vmatrix} \mathbf{j} + \begin{vmatrix} b_1 & b_2 \\ c_1 & c_2 \end{vmatrix} \mathbf{k} \right) \\
&= a_1 \begin{vmatrix} b_2 & b_3 \\ c_2 & c_3 \end{vmatrix} - a_2 \begin{vmatrix} b_1 & b_3 \\ c_1 & c_3 \end{vmatrix} + a_3 \begin{vmatrix} b_1 & b_2 \\ c_1 & c_2 \end{vmatrix}.
\end{aligned}$$

Like this, it is observed that

$$\mathbf{a} \cdot (\mathbf{b} \times \mathbf{c}) = \begin{vmatrix} a_1 & a_2 & a_3 \\ b_1 & b_2 & b_3 \\ c_1 & c_2 & c_3 \end{vmatrix}. \tag{3.15}$$

In addition we have, from the properties of the determinants, that

$$\mathbf{a} \cdot (\mathbf{b} \times \mathbf{c}) = (\mathbf{a} \times \mathbf{b}) \cdot \mathbf{c}.$$

Equation of a Plane Given Three Points

For obtaining the equation of a plane that passes through the non-collinear points, the following must be analysed.

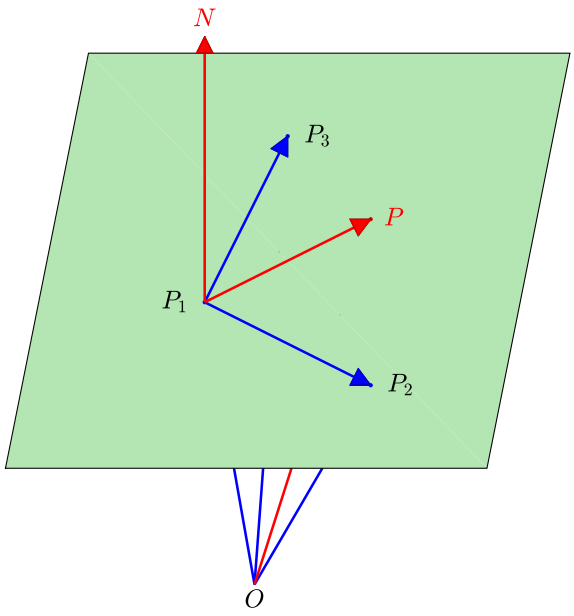


Figure 3.8: Plane by Three Points.

$P_1(x_1, y_1, z_1)$, $P_2(x_2, y_2, z_2)$ and $P_3(x_3, y_3, z_3)$. See Figure 3.8.

By definition, the vector product $\overrightarrow{P_1P_2} \times \overrightarrow{P_1P_3} = \mathbf{N}$ is a vector perpendicular to both vectors, that is, $\mathbf{N}$ is normal to the plane.

Since the vector $\overrightarrow{P_1P}$ is on the plane, its projection on $\mathbf{N}$ is equal to zero. Or in another way: $\overrightarrow{P_1P}$ is normal to $\mathbf{N}$, and the scalar product of the two vectors is zero.

$$\overrightarrow{P_1P} \cdot \left(\overrightarrow{P_1P_2} \times \overrightarrow{P_1P_3}\right) = 0.$$

This is, a triple scalar product, so by applying (3.15), depending on the components of the vectors, it takes the form

$$\begin{vmatrix} x - x_1 & y - y_1 & z - z_1 \\ x_2 - x_1 & y_2 - y_1 & z_2 - z_1 \\ x_3 - x_1 & y_3 - y_1 & z_3 - z_1 \end{vmatrix} = 0. \tag{3.16}$$

To interpolate with this procedure at a point in the base x_0, y_0 of Figure 3.6, its corresponding plane triangle is located on the superior face of the truncated triangular prism, to determine its equation with the expression (3.16). The values $x = x_0,\ y = y_0$ are substituted in it, to evaluate the height z_0.

Parabolic adjustment

From the analytic geometry is known that in the plane, two points are enough to determine the equation of a line, and that for three points it is possible to pass a parabola.

If it is necessary to determine the equation of a parabola containing in the Cartesian plane the known points $P_1\,(x_1, y_1)$, $P_2\,(x_2, y_2)$ and $P_3\,(x_3, y_3)$, the problem can be approached in several ways. Assuming that the equation of the parabola is

$$y(x) = a_1\,x^2 + a_2\,x + a_3 \tag{3.17}$$

then, it can be established a system of three equations substituting the coordinates of each point in the equation (3.17):

$$\begin{aligned} P_1: &\quad a_1\,x_1^2 + a_2\,x_1 + a_3 = y_1 \\ P_2: &\quad a_1\,x_2^2 + a_2\,x_2 + a_3 = y_2 \\ P_3: &\quad a_1\,x_3^2 + a_2\,x_3 + a_3 = y_3 \end{aligned}$$

Expressed in matrix form

$$\begin{bmatrix} x_1^2 & x_1 & 1 \\ x_2^2 & x_2 & 1 \\ x_3^2 & x_3 & 1 \end{bmatrix} \begin{bmatrix} a_1 \\ a_2 \\ a_3 \end{bmatrix} = \begin{bmatrix} y_1 \\ y_2 \\ y_3 \end{bmatrix}.$$

The solution of this system of equations provides the coefficients a_1, a_2 y a_3. Thus, the parabola (3.17) is determined.

It is possible to apply this equation to the 3×3 mesh of Figure 3.2, keeping certain constant values. In effect, the following two tables show how to obtain six parabolas in vertical planes from the original data (x, y, w).

1. With constant ordinates, there are parabolas in the plane xw.

Parabolas $z(x, w)$. Figure 3.9.

Constant Ordinates	Parabola	Obliged Points
$y = f$	$z_1(x, w)$	$(a, w_1),\ (b, w_2),\ (c, w_3)$
$y = e$	$z_2(x, w)$	$(a, w_4),\ (b, w_5),\ (c, w_6)$
$y = d$	$z_3(x, w)$	$(a, w_7),\ (b, w_8),\ (c, w_9)$

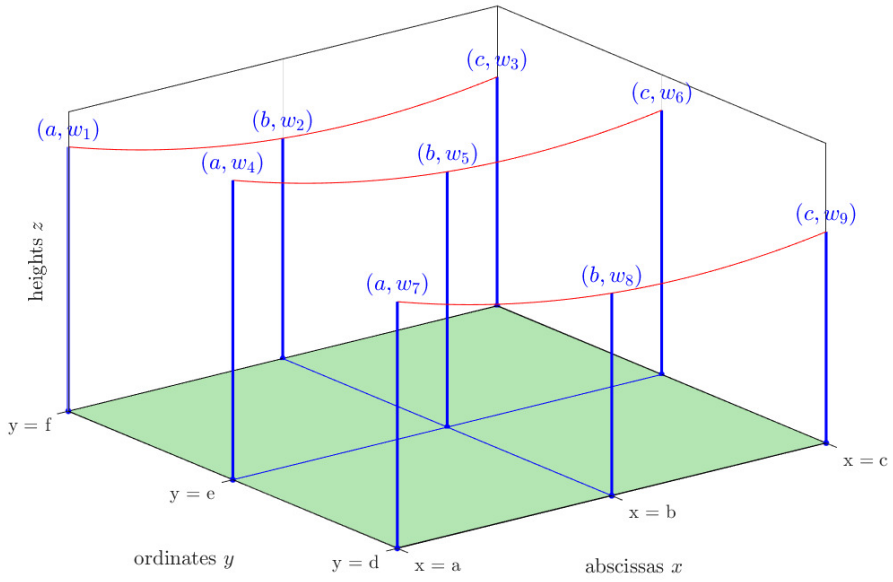


Figure 3.9: Parabolas $z(x, w)$, y =constant.

2. With constant abscissas, parabolas are generated in the plane yw

Parabolas $z(y, w)$. Figure 3.10.

Constant Abscissas	Parabola	Obliged Points
$x = a$	$z_4(y, w)$	$(f, w_1),\ (e, w_4),\ (d, w_7)$
$x = b$	$z_5(y, w)$	$(f, w_2),\ (e, w_5),\ (d, w_8)$
$x = c$	$z_6(y, w)$	$(f, w_3),\ (e, w_6),\ (d, w_9)$

Parabolic Interpolation

There are six parabolas that make up the *scaffolding or parabolic truss* of Figure 3.11, and its equations are known: $z_1(x),\ z_2(x),\ z_3(x),\ z_4(y),\ z_5(y),\ z_6(z)$. One of the procedures that can be used to interpolate in (x_0, y_0), considers values within the range of the mesh, $a < x_0 < c$ and $d < y_0 < f$.

It is recommended that when following the procedure outlined below, to refer the explanation to Figure 3.11; in particular, to the parts added to the scaffolding that appear in cyan color.

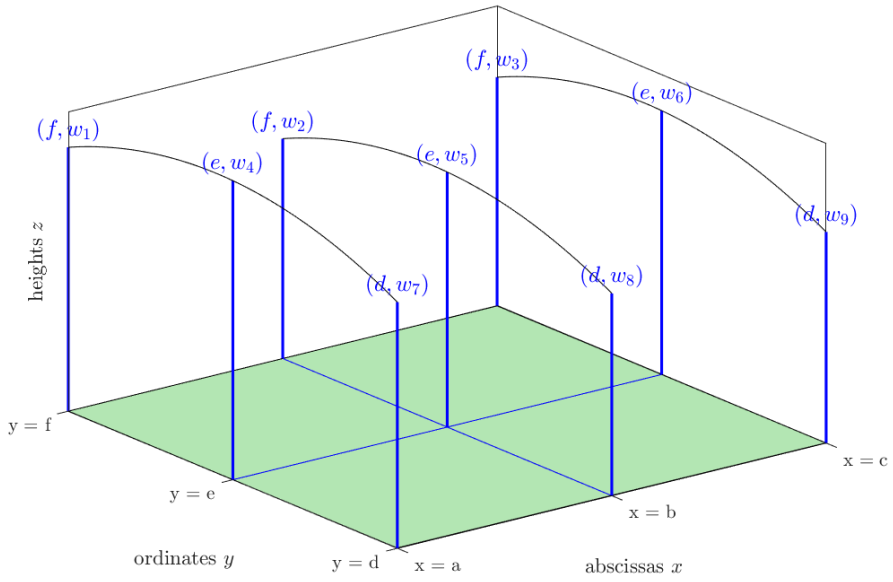


Figure 3.10: Parabolas $z(y, w)$, x =constant.

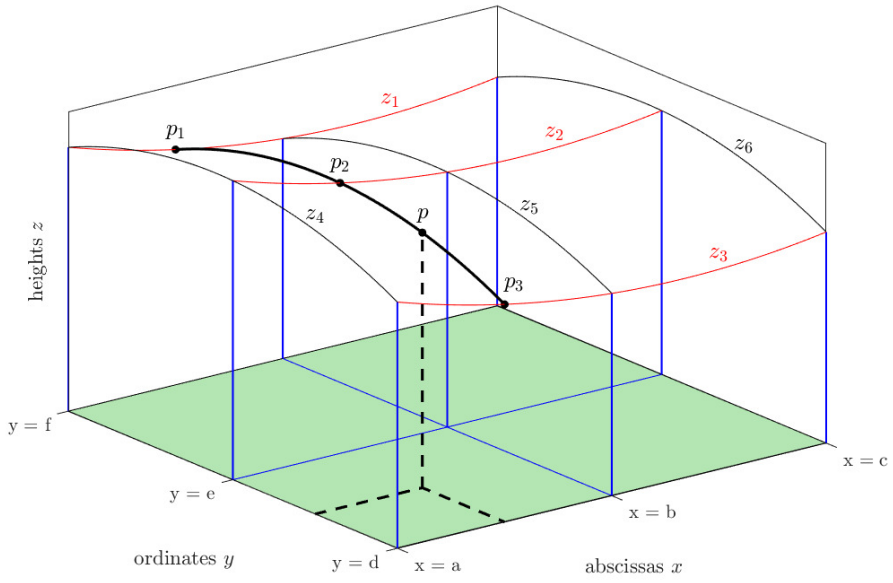


Figure 3.11: Parabolic Scaffolding. An Interpolation Point is Displayed.

1. Heights are located on $z_1(x)$, $z_2(x)$ and $z_3(x)$ to $x = x_0$, in the plane xz

$$z_{10} = z_1(x_0), \quad z_{20} = z_2(x_0), \quad z_{30} = z_3(x_0).$$

Establishing the points: $p_1(x_0, f, z_{10}), \quad p_2(x_0, e, z_{20}), \quad p_3(x_0, d, z_{30}).$

2. The coefficients of the parabola equation are determined in the plane yz

$$z_0(y) = A\,y^2 + B\,y + C$$

which pass through the points

$$(f, z_{10}), \quad (e, z_{20}), \quad (d, z_{30}).$$

3. With the equation of the parabola the height is evaluated in $y = y_0$

$$z_0 = z_0(y_0).$$

The interpolation point obtained

$$p(x_0, y_0, z_0)$$

is on the response surface, as will be seen later.

It is also possible to use the interpolation parabola in the other direction, supported by the three parabolas of the plane yz. For reasons of brevity in the document, it has been interpolated for one point. If interpolation is desired at several points, the procedure is similar to the already shown. Knowing the abscissas $x_0 = [u_1, u_2, \ldots, u_m]$ and the ordinates $y_0 = [v_1, v_2, \ldots, v_m]$, the interpolation heights are determined

$$z_0 = [w_1, w_2, \ldots, w_m]$$

which correspond to the points

$$(x_0, y_0, z_0) = [(u_1, v_1, w_1),\ (u_2, v_2, w_2),\ \ldots,\ (u_m, v_m, w_m)]\,.$$

Response surface

Proceeding to establishing sufficient parabolas resting on the scaffolding, as indicated in the previous point, a very smooth representation of the response surface is achieved.

For more clarity, it is convenient to have a lattice of parabolas in the perpendicular planes xz and yz. For example, the one in Figure 3.12. Since the interpolation parabolas are of the same type as those of the response surface, then the interpolation points belong to the response surface.

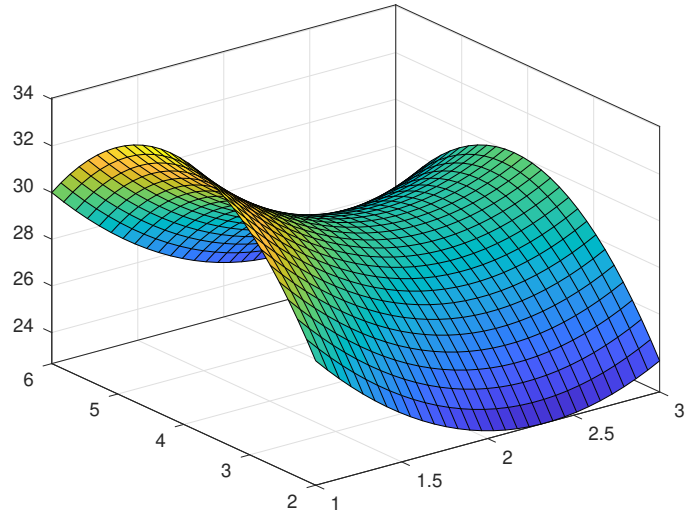


Figure 3.12: Response Surface.

Contour lines

Another possibility of studying the behaviour produced by the data in the 3×3 mesh, are constituted by the contour lines, as shown in Figure 3.13. The contour lines represent horizontal cuts on the response surface, with the characteristic of sharing the same height.

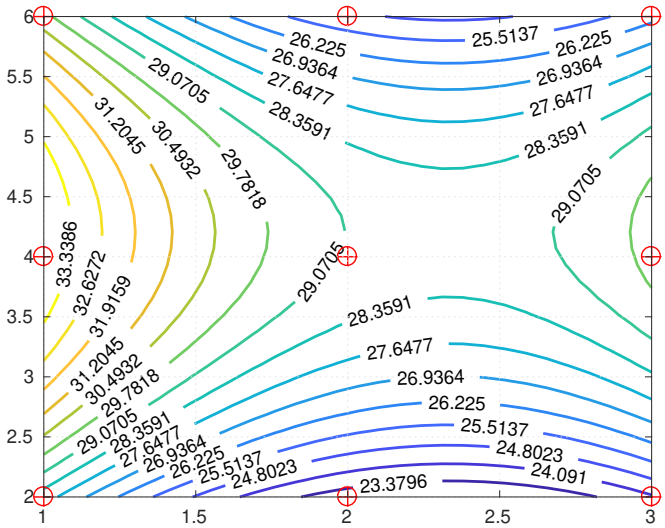


Figure 3.13: Contour Lines.

Some of the possibilities arising in the research are explained; the reaching of a surface

of response of the heights was generated with these procedures. Such surface presents desirable characteristics: it is smooth, continuous and without breaks. This characterization of the response surface allows the arrangement of contour lines, which provide information on the distribution of the values involved.

This is one of the many possibilities to address the problem, but this approach was made to support those interested in using it when analysing this type of rectangular meshes of 3×3.

3.3 Programme Functioning

In Section 3.2, beginning at p. 68, Algorithm DGG1 was mathematically justified.

Now it will be shown in research context, detailing the operation of the programme *grid9.m* developed in MATLAB; the code of this can be found in Appendix A.

An overview of the programme functioning can be appreciated in the flow diagram shown in Figure 3.14.

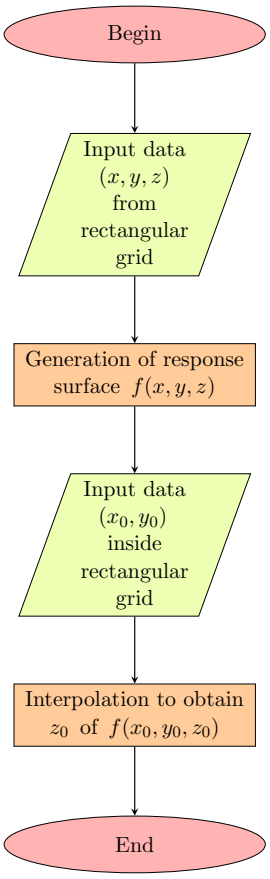


Figure 3.14: Flow Diagram of Algorithm DGG1 Functioning.

3.3.1 Input and Output Data

An example of the application of the programme is shown. To obtain an estimate of the temperatures in the municipalities of Coahuila: Ocampo, Parras de la Fuente, Carneros and Allende, the mesh under study is used for a certain data collection.

The programme requires the following information.

1. Data:

   - Abscissas of the stations.

     The variable x contains the abscissas of the Table 3.2, corresponding to the longitudes:

     $$x = [\ -107.5 \quad -102.5 \quad -97.5\ ]$$

They are values in degrees in decimal format, negative for being west longitudes. The variable x, is written in MATLAB as follows:

```
>>   x = [-107.5  -102.5  -97.5]
```

Symbols $>>$ is the prompt of MATLAB when they are in the *Command Window*, and from now on, it will be used to indicate that it is operating from it.

- Ordinates of stations.

  y are their latitudes:

  ```
  >>   y = [22.5  27.5  32.5]
  ```

  They are values in degrees in decimal format, positive for being north latitudes.

- Altitudes of the stations.

  They correspond to the observed temperatures in Celsius degrees:

  ```
  >>   w = [  30   27   30   34   30   29   30   24   23  ]
  ```

- Coordinates XY where its desired to perform the interpolation.

  The geographical coordinates of Ocampo, Parras de la Fuente, Carneros and Allende, belonging to the State of Coahuila are as follows.

Location	Latitude	Longitude
Ocampo	$28^\circ\ 05'\ 32''\ N$	$103^\circ\ 17'\ 14''\ W$
Parras	$25^\circ\ 26'\ 07''\ N$	$102^\circ\ 56'\ 54''\ W$
Carneros	$25^\circ\ 06'\ 00''\ N$	$101^\circ\ 06'\ 00''\ W$
Allende	$28^\circ\ 20'\ 40''\ N$	$100^\circ\ 51'\ 14''\ W$

  The matrix can be written in angular decimal format:

  ```
  >>   XY = [-103.2872  28.0922; -102.9483  25.4353; -101.1
  25.1; -100.8539  28.3444]
  ```

  When writing data, it can be separated with commas or spaces. The row change is denoted with a semicolon.

  The programme uses decimal format, but for convenience it also accepts data in DMS, Degree, Minute, Second format. For example, the above matrix could be written:

  ```
  >>   XY = [-103  17  14  28  05  32; -102  56  54  25  26  07;
  -101  06  00  25  06  00; -100  51  14  28  20  40]
  ```

- Optional additional data.

  The programme also accepts:

- fs: font size, default value is 18 points
- n: size of the mesh of order $n \times n$, default value is 30
- m: number of contour lines, default value is 12
- ex: x axis label, default value is *Abscissae*
- ey: y axis label, default value is *Ordinates*
- ez: z axis label, default value is *Heights*
- v: cantilevers, default value is null

2. Results.

   Temperatures of the mentioned cities, depending on the data entered. At the end, the programme provides the following information:

$$XYZ = \begin{bmatrix} -103.2872 & 28.0922 & 30.5122 \\ -102.9483 & 25.4353 & 28.9037 \\ -101.1000 & 25.1000 & 27.4872 \\ -100.8539 & 28.3444 & 29.5773 \end{bmatrix}$$

   Note that the program provides the coordinates of the cities and the estimated interpolation values in degrees Celsius, in the third column.

   The programme also presents the graphs developed during the calculation process.

3.3.2 Running the Programme

In this example, the abscissas correspond to the longitudes of the stations, the ordinates to the latitudes, and the heights to temperatures. It has been preferred not to resort to optional variables and the parameters take their default values indicated in p. 85.

With the command

`>>  XYZ = (x,y,w,XY)` The programme starts running.

Thereafter, results are displayed on the screen, and any key is pressed to advance to the next one.

1. The initial screen appears with the following message.

```
With the following coordinates:

x = Abscissas
-107.5000 -102.5000  -97.5000

y = Ordinates
 22.5000   27.5000   32.5000

w = heights of temperatures/atmospheric pressures, etc.
    in normal writing order of the nine given points,
    from left to right and from top to bottom.
  30    27    30    34    30    29    30    24    23

    A 3D response surface is generated

    Press Enter to continue...
```

2. Geographical Coordinates of the Stations, Fig. 3.15.

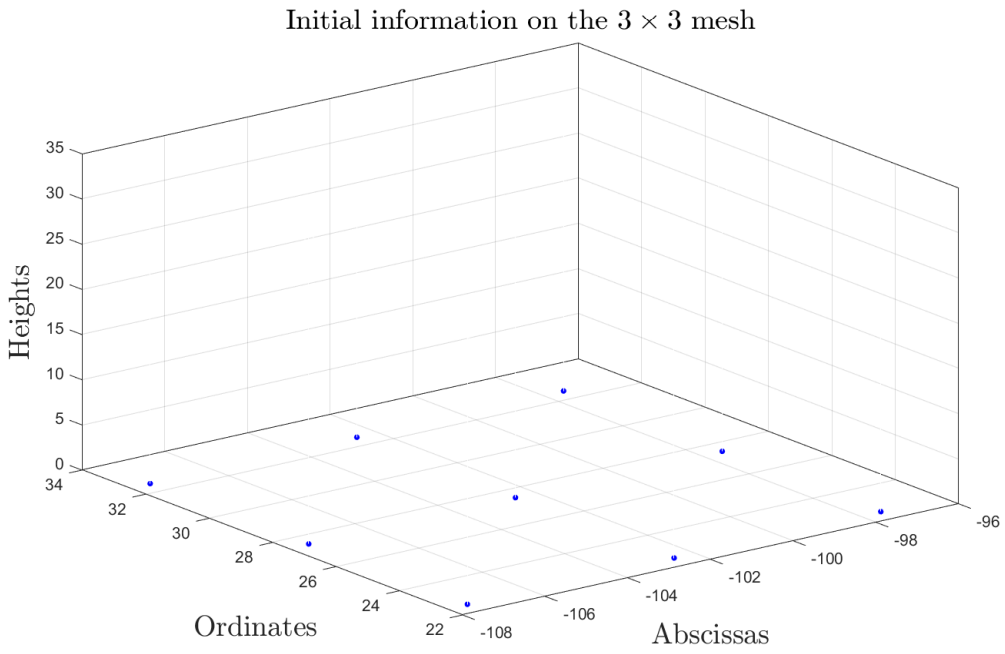


Figure 3.15: Nine Points Geographical Location.

3. Heights of the Stations, Fig. 3.16.

   These figures are used to verify the data. In this case, the heights represent the temperatures of the stations.

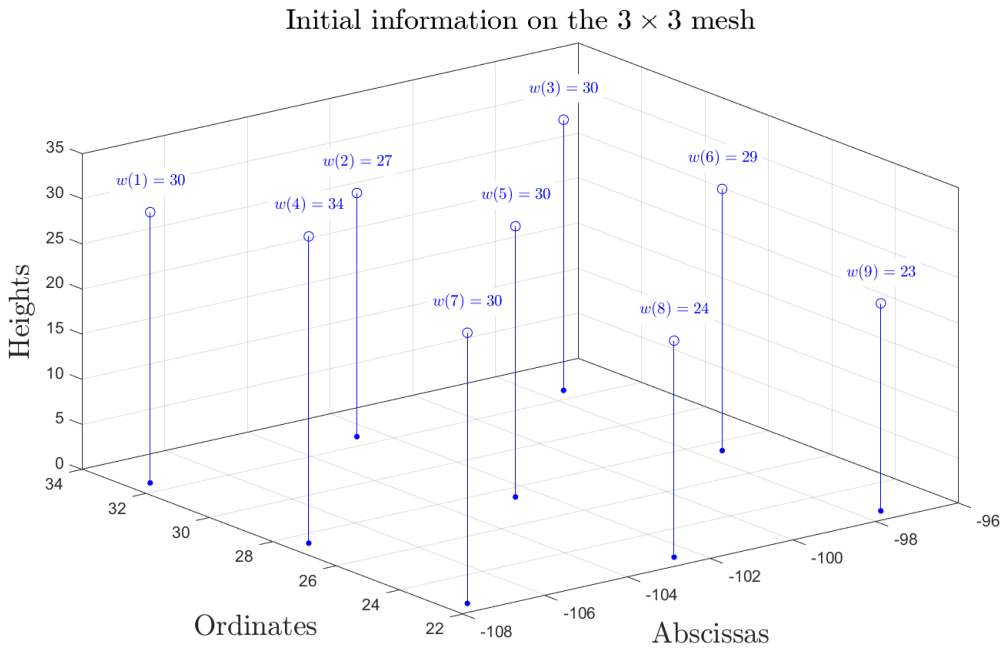


Figure 3.16: Poles with Temperatures.

4. Generation of parabolas in the direction of the abscissas, Fig. 3.17.

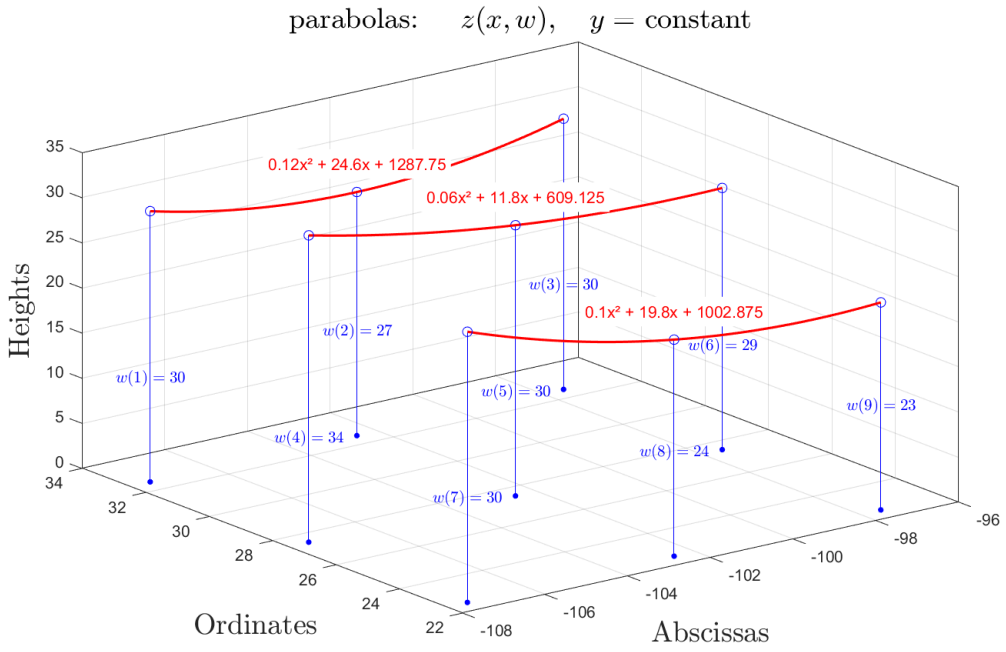


Figure 3.17: Parabolas Generated with Longitudes Direction.

From analytic geometry it is known that a line passes through two points. In the same way, three points determine exactly one parabola. The parabola is the only polynomial that meets this condition.

Parabolas generated are kept in planes parallel to the longitudes: the variables of length versus temperature of the stations, (1, 2, 3), (4, 5, 6), (7, 8, 9), respectively.

$$0.12x^2 + 24.6x + 1287.75 \tag{3.18a}$$

$$0.06x^2 + 11.8x + 609.125 \tag{3.18b}$$

$$0.1x^2 + 19.8x + 1002.875 \tag{3.18c}$$

In Fig. 3.17, the heights generated by each parabola are represented, as their corresponding graphs and equations.

5. Generation of parabolas in the direction of the ordinates, Fig. 3.18.

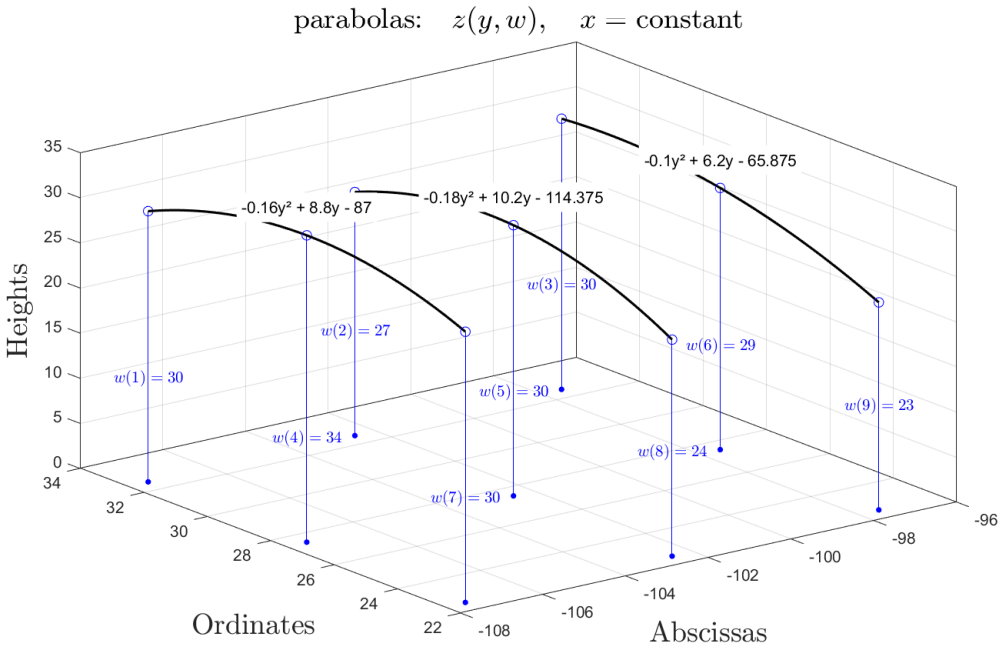


Figure 3.18: Parabolas Generated with Latitudes Direction.

Similarly, parabolas are generated in planes parallel to latitudes: the latitude versus temperature variables of the stations, (1, 4, 7), (2, 5, 8), (3, 6, 9), respectively. In Fig. 3.18, the heights generated by each parabola are also represented and their corresponding graphs and equations.

6. Integration of the two previous sets of parabolas.

Figure 3.19 highlights one of the fundamental ideas of Algorithm DGG1.

- The reports provided by the IPCC for the generation of GCM data were very important. For the first time, very reliable information was available for the Coahuila region in the form of the nine-point mesh already mentioned.
- However, it was insufficient for using it in field studies for locations outside the points for where it was produced, because they cover large areas of land and provide a very small amount of information.
- Ideally, users would like to have contour lines to properly study any locality within the mesh.
- Benefiting from this information, in a first instance, six equations of parabolas was obtained, as shown in previous figures.

7. Creation of a support scaffold.

   The integration of the six parabolas from the previous point, make up a kind of scaffolding to support any number of additional parabolas, Fig. 3.19. The scale of the heights was changed to make the scale of the temperatures more noticeable.

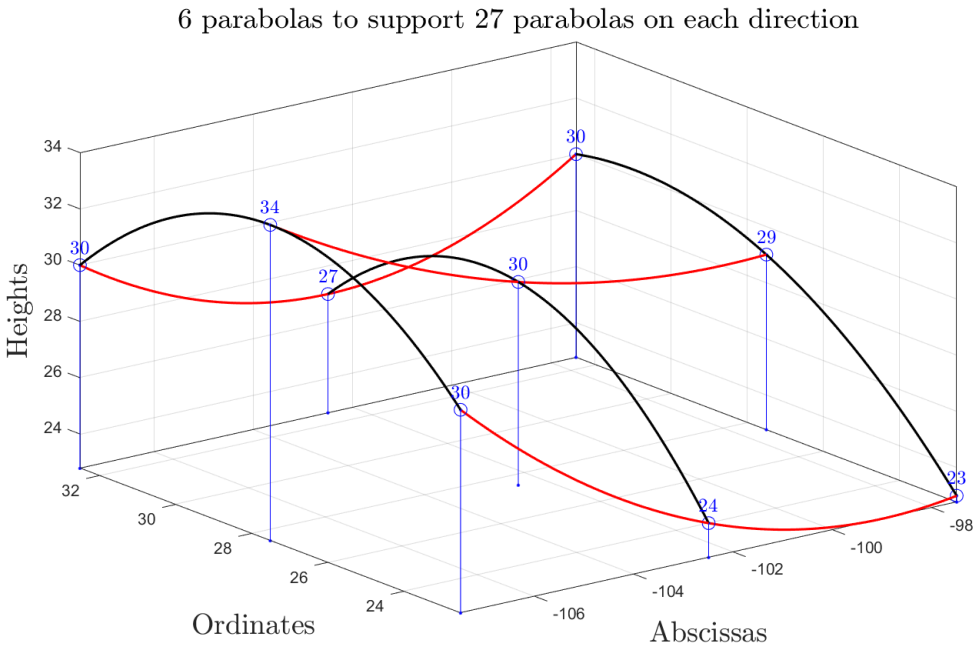


Figure 3.19: Parabolas Scaffolding.

8. Generation of a mesh $n \times n$.

   In this point, the information of the nine data is expanded.

   - Parabolas supported at three points of the scaffolding can always be determined on planes parallel to longitudes and latitudes.

- This way, $n-3$ parabolas equations are determined in the direction of longitudes, and another $n-3$ parabolas in the direction of the latitudes. The total number of parabolas, including the scaffolding is $n \times n = n^2$.

  This example uses the default value $n = 30$.

- This n^2 graphs of parabolas make up a lattice, as can be seen in Figure 3.20.

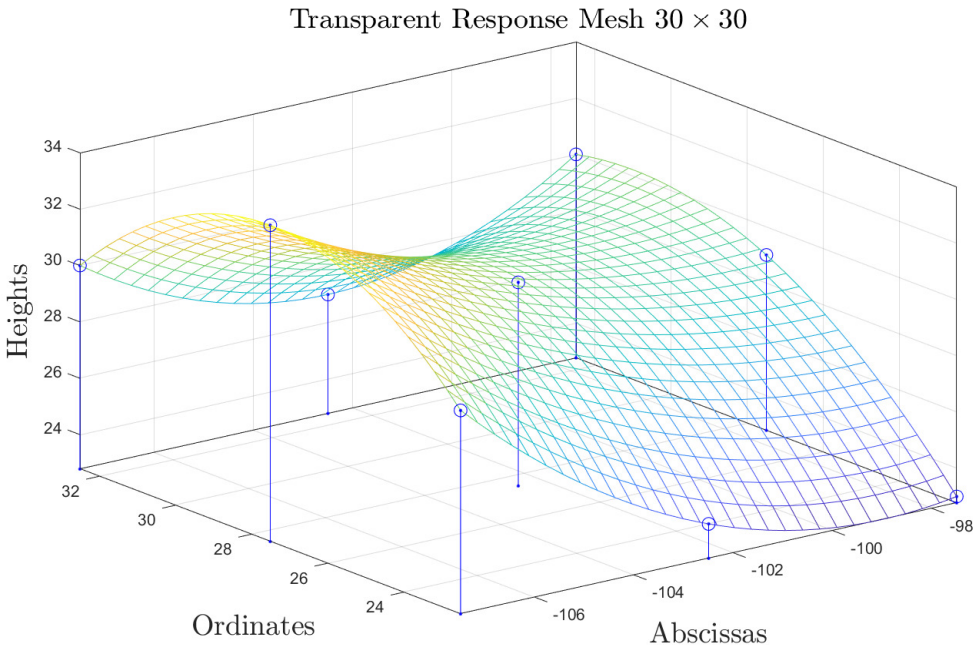


Figure 3.20: Poles and Lattice with Generated Information.

- Each of the intersections of two parabolas with perpendicular directions determines a new known point.
- Now it has $n \times n = n^2$ points, instead of just the initial nine.

In theory, it is possible to determine the n^2 parabolas, to obtain their graphs and their points of intersection. In practice, this would be very laborious and difficult, so this was made using a programme encoded in MATLAB that performs all the calculations and presents the corresponding graphs.

9. Generation of the Response Surface.

- The figure above can also take the form of a response surface, Fig. 3.21.
- The programme also provides other alternative forms of the response surface, presented in Appendix B of p. 303.

- The intention of transferring these figures to the Appendix is to shorten the chapter of Algorithm DGG1.
- Either way, the above graphs show the enormous potential of MATLAB graphing, as they show the multiple graphs and visual information regarding the generation of the response surface and the data forming it.

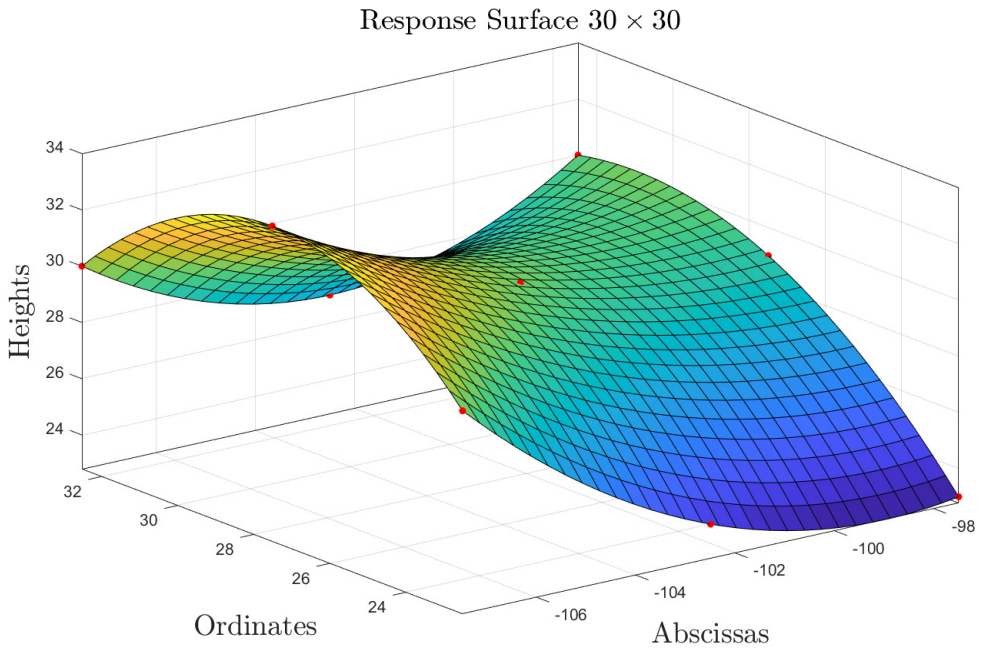


Figure 3.21: Response Surface.

10. Qualitative graph of temperatures.

    In Figure 3.22 it can be appreciated in a chromatic environment the distribution of temperatures in plan view. The cold temperatures also correspond to the colour palette's cold spectrum, and the warmer temperatures correspond to the warm colour's palette.

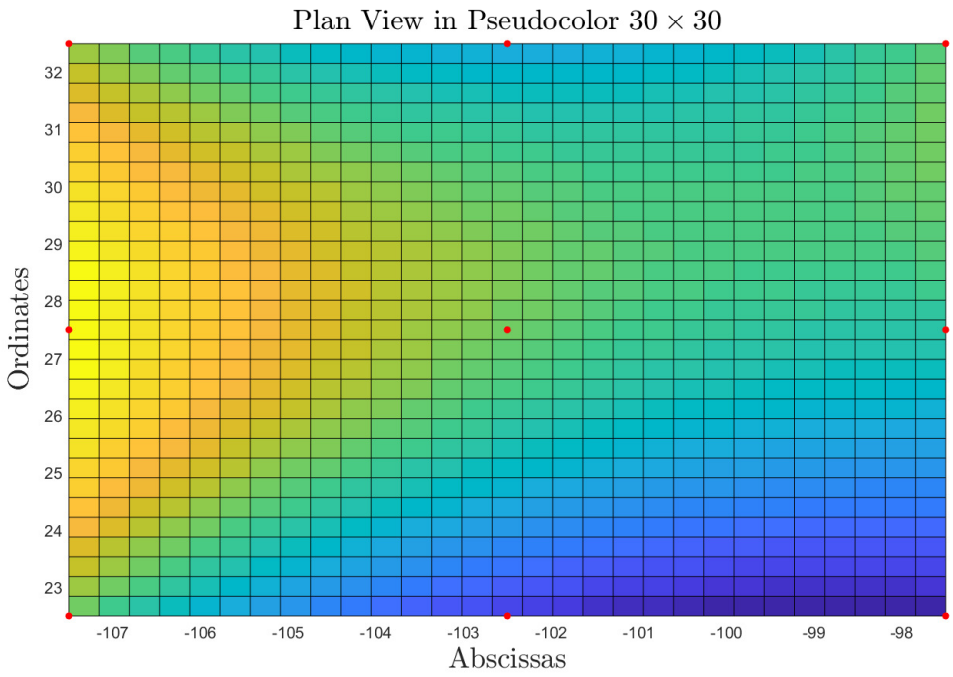


Figure 3.22: Temperature Colored Plan View.

11. Contour Lines.

    The programme also presents the information in the form of contour lines. Traditionally these representations are widely used to appreciate the distribution of a phenomenon. Figures 3.23 and 3.24 show the distribution of temperatures in the entire region belonging to the grid under study.

    This facilitates the obtaining of specific temperature data for any point within the mesh, since these are projected in plan and their behavior in neighboring places can be compared visually and numerically.

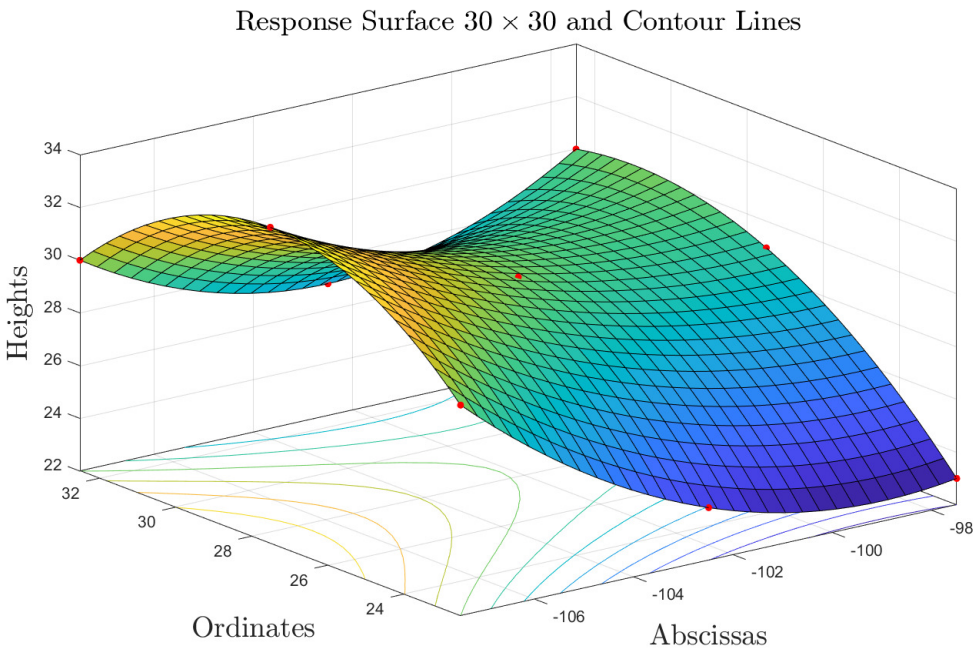


Figure 3.23: Response Surface and Projected Contour Lines.

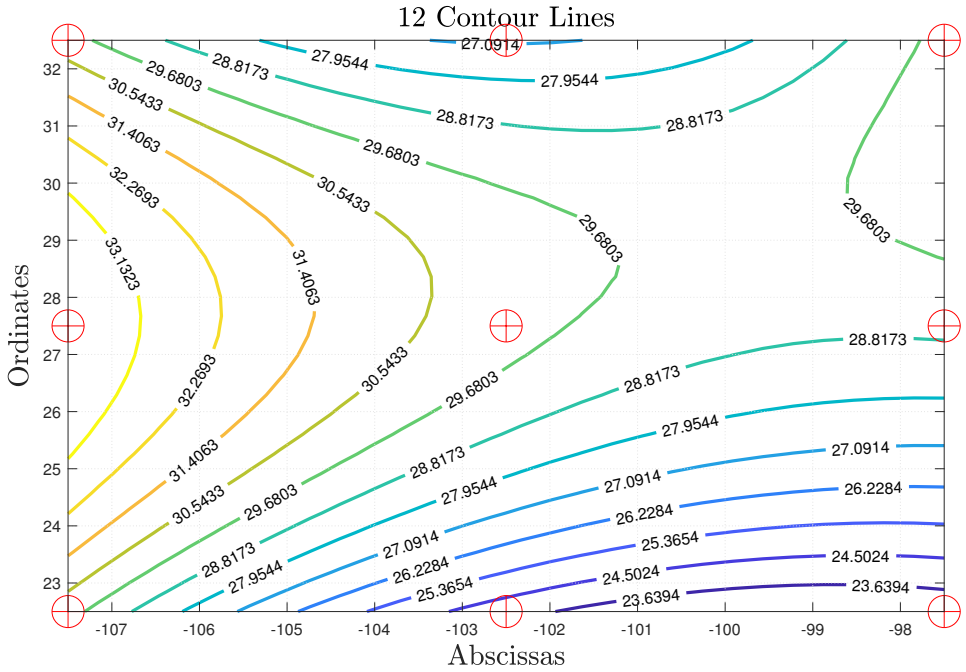


Figure 3.24: Contour Lines.

12. Interpolation.

So far, it has been seen how to develop a plausible response surface mathematically. One of the most important needs of Algorithm DGG1 is to be able to estimate the temperature at any location in that grid, and for this we will locate the temperature on the response

surface. For example, the following steps will be followed to estimate the temperature in Parras de la Fuente, whose geographic coordinates are $(102^\circ\ 56'\ 54''W,\ 25^\circ\ 26'\ 07''N)$.

- In $x = -102.9483$ three points are placed on the parabolas of Figure 3.19.

  Each equation of the red parabolas is of the type

  $$w = f(x)$$

  Evaluated in $x = -102.9483$, equations (3.18) produce the heights

  $$w_1 = f_1(-102.9483) = 27.0241$$
  $$w_2 = f_2(-102.9483) = 30.2362$$
  $$w_3 = f_3(-102.9483) = 24.3339$$

  See Figure 3.25.

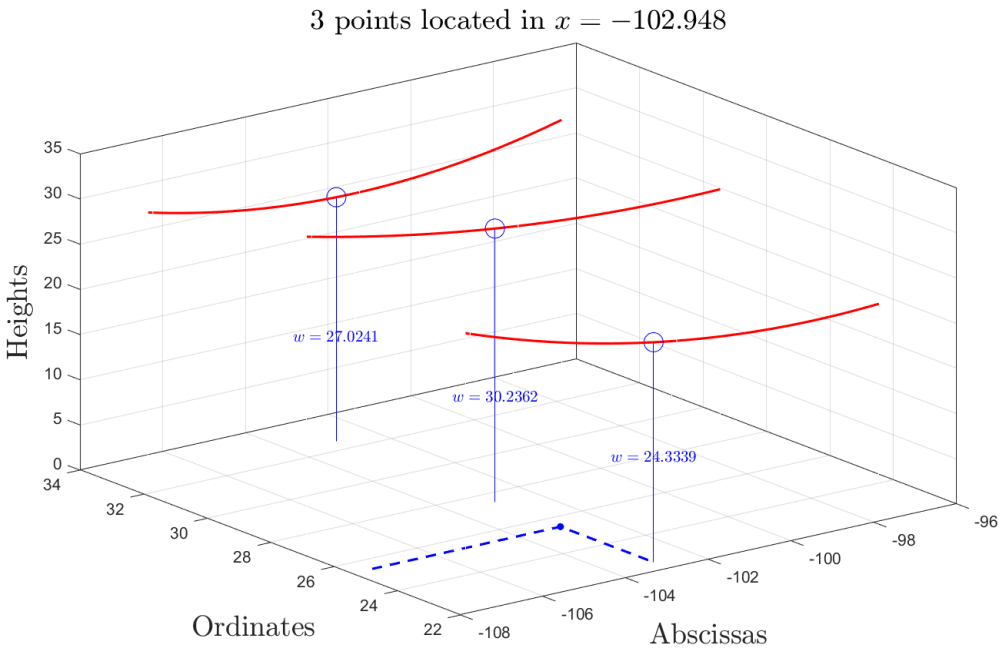


Figure 3.25: Points on Red Parabolas.

- Equation of the parabola.

  With the three previous points of the parabola in the direction of the latitudes:

  $$(22.5,\ 24.3339),\quad (27.5,\ 30.2362),\quad (32.5,\ 27.0241)$$

  The equation of the parabola that contains them is determined, Figure 3.26.

  $$w(y) = -0.18229y^2 + 10.2949y - 115.0171 \tag{3.19}$$

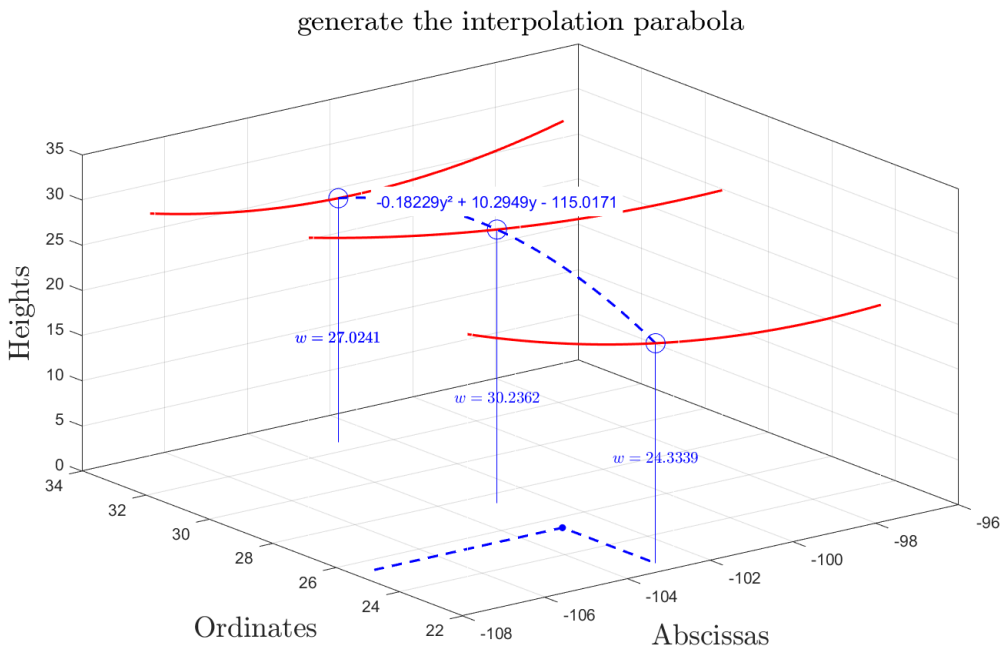


Figure 3.26: Equation of the Parabola Conformed by the Three Points.

- Height of the parabola in the coordinates $(-102.9483, 25.4353)$.

  Evaluating the dotted blue parabola in Fig. 3.26, with the equation (3.19)

$$w(25.4353) = 28.9037.$$

  Figure 3.27.

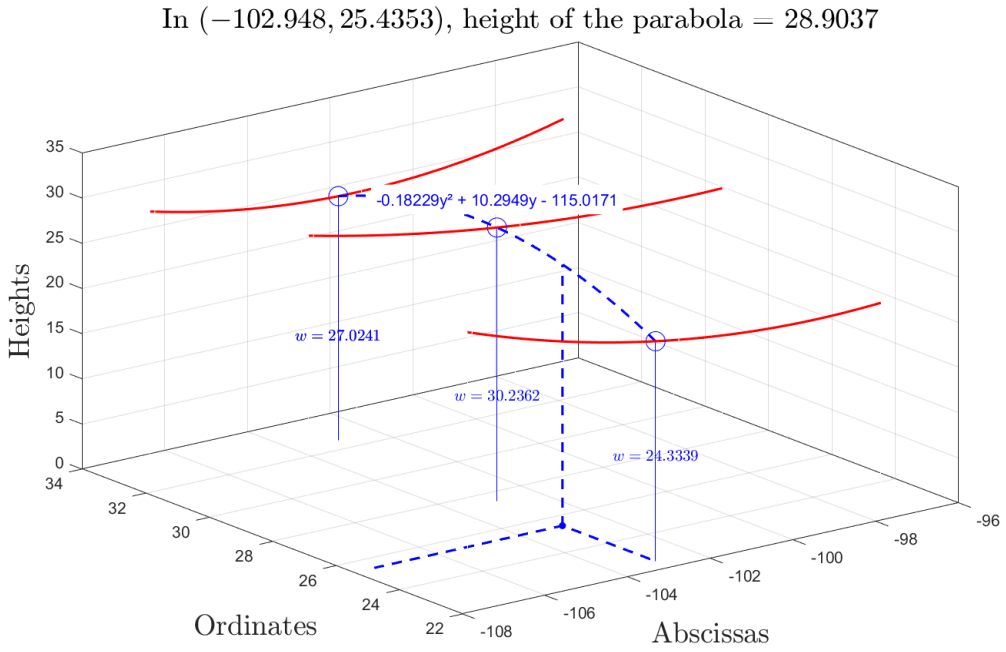


Figure 3.27: Obtaining the Appropriate Height for Coordinates $(-102.9483, 25.4353)$.

- Interpolation at the point with coordinates $(-102.9483, 25.4353)$.

  The problem has finally been solved: the interpolation point is

  $$(-102.9483,\ 25.4353,\ 28.9037)$$

  Figure 3.28.

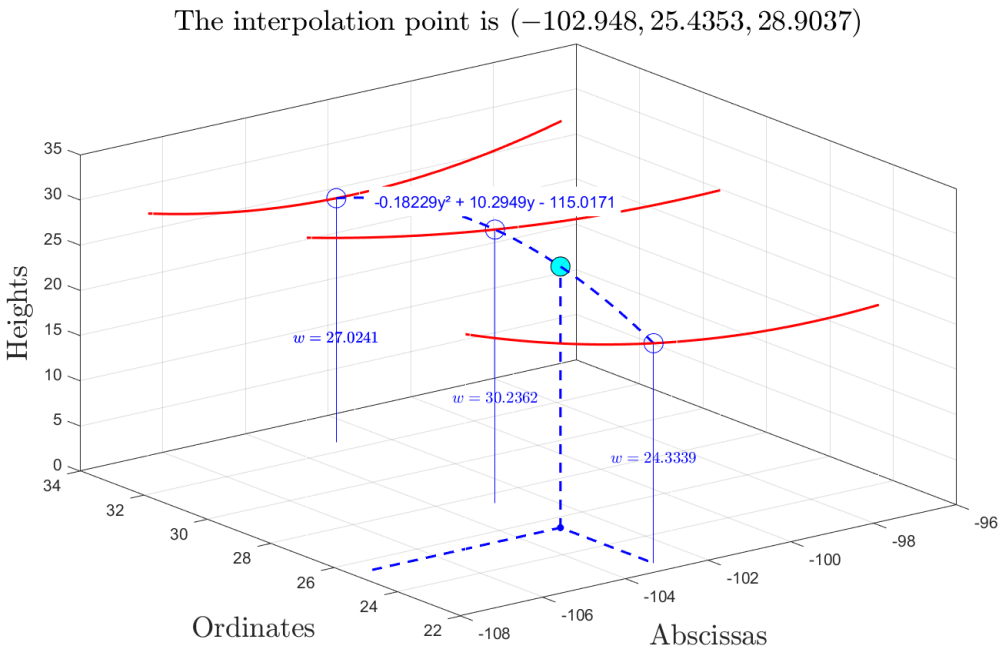


Figure 3.28: Interpolation Point.

This point belongs to the response surface, as can be seen in Figure 3.29.

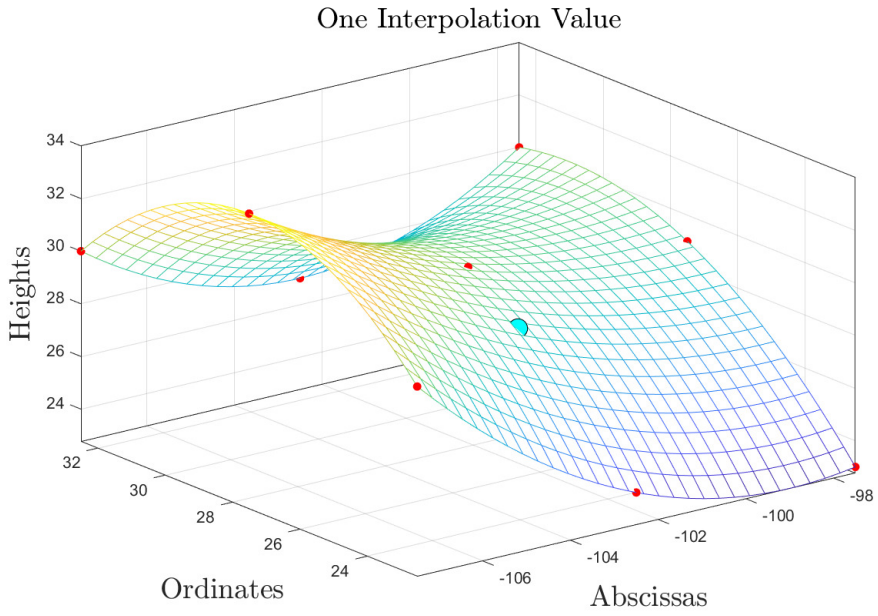


Figure 3.29: Poles.

The programme allows any number of points to be interpolated, and in this example it was interpolated for a single point, for the sake of brevity.

3.3.3 Codification

The encoding developed in MATLAB, which programme name is *grid9.m*, is shown in Appendix A.

3.4 Conclusions

In this chapter, the reasons why it is convenient to study rectangular meshes of 3×3 are mentioned. One of its applications is also explained, in particular, in the distribution of temperatures in the state of Coahuila. The conclusions derived from the creation of the DGG1 algorithm are shown below.

1. Additional applications may arise in architecture and engineering: in the study of physical or theoretical situations, with heights representing values of temperatures, or atmospheric pressures, or carbon dioxide emissions, etc.

2. The reduced information provided by the data of the nine points of the 3×3 mesh, led to the study of various mathematical approaches that enabled the deduction of additional information to broaden the understanding of the behavior of the mesh.

3. Consequently, this chapter focuses on the establishment and application of a mathematical model that enriches the original information provided by the nine data from the GCM.

4. Some of the possibilities that arose in the research are shown, until a response surface of the heights is achieved. Such a surface has desirable mathematical characteristics: it is smooth, continuous and without cracks, therefore it is very stable.

5. An additional advantage of the proposed algorithm DGG1 is derived from its mathematical nature, which bypasses the subjectivity of the researcher. In other words, it is a concrete and objective algorithm.

6. This goes beyond — at least in this type of documents in architecture — the very generalised position of resorting to subjective explanations that are conveniently based on the solvency of researchers.

7. This characterisation of the response surface allows the provision of contour lines, which provide information on the distribution of the values involved.

8. It is also proposed a procedure to interpolate and obtain the heights w_0 at the points (x_0, y_0), with the condition that they belong to the base plane of the mesh.

9. The response surface contains the original nine data and all the points belonging to the mesh.

10. The algorithm also establishes the possibility of extending the study rectangle with small overhangs. These have been added beyond the limits of the external poles.

11. In this most practical way, these poles can have information generated by system sensors, like thermometers or weather stations, which do not have to be placed on the limits.

12. When the boundaries of the mesh are the poles, the algorithm uses unobjectionable interpolation.

13. If there are small overhangs, interpolation is also used, which is justified by having the edges close to the poles considering that the overhangs represent a continuation of the response surface.

14. The algorithm meets one of the main objectives proposed for the methodology, to estimate the values of the heights for any number of locations. To do this, all the points are located on the generated response surface.

Since the algorithm allows to calculate any number of heights, it necessarily requires a huge amount of operations to obtain the equations and graphs required. Fortunately, the availability of technology makes it possible to carry out these tasks simply and efficiently. In this work, a programme coded in MATLAB language was developed, taking advantage of its enormous potential.

By just entering the minimum data, the programme performs all the actions of the algorithm, since it only requires the abscissas and ordinates of the nine points of the mesh, and of the locations where it is desired to interpolate. The algorithm is applicable to any nine-point mesh of the type considered here, or to any other phenomenon inscribed in this way.

The programme serves to obtain the interpolation of any number of points in the mesh, but it also serves as a presentation of the algorithm, since all the procedures and graphs necessary for its development appear.

In this chapter the first part of the methodology was shown, whose algorithm was derived from the need to study the generation of data when the available information is scarce and arranged in rectangular grids. These grids are used in GCMs and various ways of downscaling data from them have been proposed; for this research the way to do it was through the algorithm DGG1.

When the available information is arranged in an irregular way, another procedure must be followed; this is addressed in the next chapter with the temperature information obtained from meteorological stations located throughout Coahuila.

Chapter 4

Algorithm DGG2. Generation of Response Surface for an Irregular Mesh

The second part of the methodology is proposed in this chapter. Climate change projections were made for the first time in Coahuila taking into consideration various climate scenarios. The data provided was located in the meteorological stations, where the data was most reliable and robust. Consequently, the disposition of the data is described in an irregular way in the territory of Coahuila. Due to this, it was proposed to make a new procedure for the cases where the data had to be taken from this irregular mesh, being this the presented Algorithm DGG2.

Algorithms DGG1 and DGG2, can be used to tackle needs related with management of data for projections made for climate changes, and interpolation of missing data. The differences are in the way input data is presented and the IPCC report from which these data were obtained. For DGG2, the information of the SRES Climate Change Scenarios from RCMs was used. This can be adapted depending on the research needs, the ones regarding this project were explained in subsection 2.2.2.

From the information available, it was decided to generate a mathematical procedure to support the research. For reasons that will be detailed hereinafter, initially it was worked with the named Algorithm DGG2 presented in this chapter, and the information obtained with it was complemented with a subsequent part, Algorithm DGG3. In this and the next chapter, their development are detailed extensively.

4.1 Antecedents of Algorithm DGG2

The Intergovernmental Panel on Climate Change (IPCC) is an international body for assessing the science related to climate change, and according to Mendoza-Hernández [72] it recognises 23 climate models. In this research three models were compared to establish which one was more accurate for projecting future weather scenarios in Coahuila.

The ECHAMPS, the GSDL and the PRECIS models were compared and it was established that the last one was better for the case because is a regional model with great possibilities of downscaling. The PRECIS regional climate modelling system was developed at the Met Office Hadley Centre and do not require extensive IT infrastructure, it was created for allowing users in developing countries to easily produce detailed climate projections.

In the National Metereological Service (SMN[1]) website, weather information obtained by CONAGUA is available through tables, a map server and plug-in for Google Earth. There are 118 meteorological stations recognized by the SMN in Coahuila, but only 41 have been considered as they have more complete information. Mendoza-Hernández [72] obtained information of temperatures and precipitation from different regions in Coahuila, in the research, scenarios A2 and B2 were considered and data was created for years 2020, 2050 and 2080.

Actual data of these 41 stations has been gathered and a statistical regression method generated in MATLAB will be used to perform the downscaling of information. The important characteristic of the method is that is focused in the management of information obtained with the PRECIS Regional Climate Model for the zone, so the intention of using this data is not to perform a climate model, but a numerical one. Data will be used to study computerised mathematical procedures to simplify the process and obtain equations instead of obtaining the value of intermediate points by simple rule of three or similar triangles.

MATLAB (abbreviation of MATrix LABoratory) works with matrix data and information, for the development of the algorithm, information will be handled in matrix form

[1] Servicio Meteorológico Nacional

(three-dimensional matrix X, Y, Z, with numbers in three-dimensional space), and this is why the software is suitable for the kind of data used in the project. Information was adjusted in a grid with latitude and longitude in axis X and Y respectively, and temperatures in the axis Z. Data was placed in this order to obtain a response surface in where, further on, level curves and contour lines of temperatures are drawn. In each squared projected on the plane by information from the surface, temperature of different climate scenarios could be identify by coordinates.

Collection of weather data from Coahuila was gathered from the database of the SMN. Complemented and more detailed information was obtained from the meteorological stations on the wunderground website. Interpolation methods were used to obtain missing data, and PRECIS was used as a regional model to downscale information and work with climate scenarios A2 and B2.

Temperatures from specific points were considered, a mesh was established locating 34 weather stations in Coahuila in the form of a scatter diagram. Each weather station has a coordinate dictated by its longitude and latitude, and information was evaluated for these points. The algorithm was developed in MATLAB, in where information of coordinates was managed, as the temperatures provided by climate experts for years 2020, 2050 and 2080 for scenarios A2 and B2. The variation of data will be in terms of height only, as temperatures will be the ones varying along the years, seasons and climate scenarios. For every case (20a2ss, 20a2sw,20b2ss, 20b2sw, 50a2ss, etc.), the simulation can be run, and information can be obtained for a specific point just by inputting the desired coordinate.

The temperatures provided for climate experts in Coahuila and used for simulations, are average temperatures, as in their study they did not publish extreme temperatures on the reports. They are waiting for the new scenarios of the International Panel of Climate Change to be published with updated data, considering information of the new decade, and placing year 2020 as the current year. Future projections will contemplate years 2050, 2080 and 2110. This data along with extreme temperatures can be adapted easily to the algorithm and new data can be used in simulations. In addition, more weather stations from other states can be added in order to obtain a wider mesh, as information is managed in a matrix form.

4.1.1 Description of the Problem

To study the distribution of temperatures in the state of Coahuila, 34 weather stations were established in order to collect pertinent information. Figure 4.1 shows the geographical positions of the stations. Therefore, the mesh to be studied has an irregular configuration, so the treatment of the mesh under study posed a challenge with considerable difficulties.

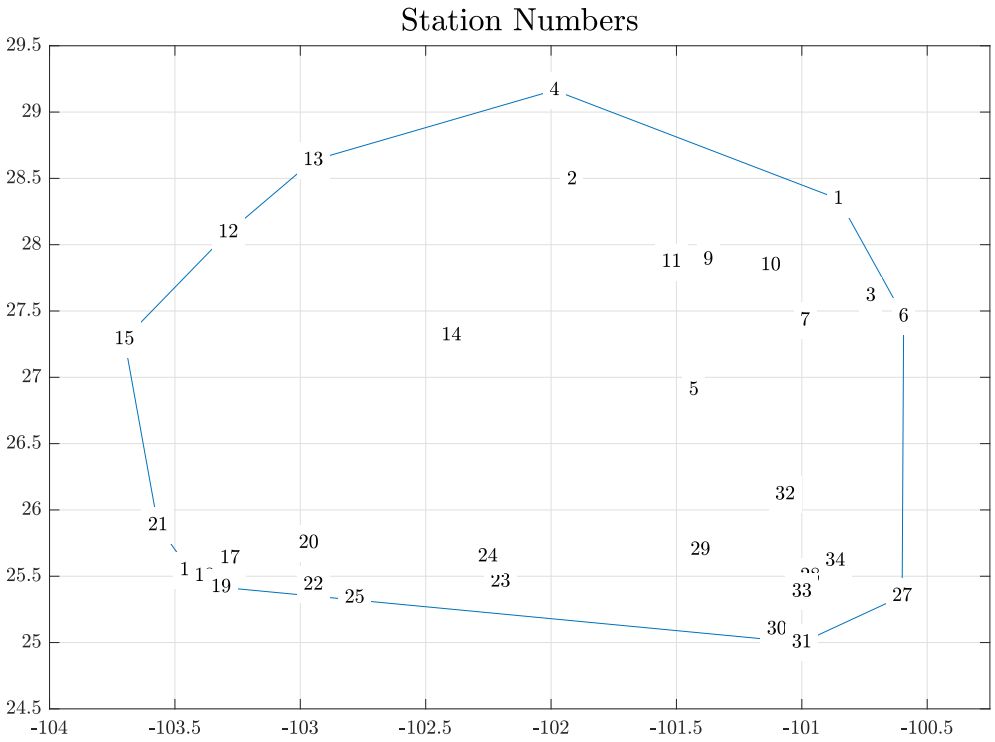


Figure 4.1: Weather Stations Locations.

The problem consists in establishing a two-dimensional interpolation in a mesh with these stations, from which it can be interpolated for any point inside it. When carrying out a bibliographic review of the subject, an example of a case of two-dimensional interpolation in a rectangular mesh was found [70].

Registered stations are displayed in Table 4.1. At each station there are two entries: the name of the town and the municipality. A municipality is a legal figure of political administration, which integrates several localities by region. This form of jurisdiction of a place is used throughout the country, and in practice when referring to a place, its name is enough.

Table 4.1: Weather Stations

	Stations	*Longitude*	*Latitude*
1	Allende, Allende	$-100.8539°$	$28.3444°$
2	Zaragoza, Zaragoza	$-101.9167°$	$28.4917°$
3	Villa Juárez, Juárez	$-100.7250°$	$27.6139°$
4	Palestina, Jiménez	$-101.9867°$	$29.1644°$
5	Monclova, Monclova	$-101.4308°$	$26.9047°$
6	Presa Venustiano Carranza, Juárez	$-100.5939°$	$27.4586°$
7	Progreso, Progreso	$-100.9872°$	$27.4283°$
8	Nueva Rosita, San Juan de Sabinas	$-101.1239°$	$27.8461°$
9	Conchos, Sabinas	$-101.3731°$	$27.8869°$
10	Sabinas, Sabinas	$-101.1239°$	$27.8444°$
11	Múzquiz, Múzquiz	$-101.5194°$	$27.8692°$
12	Ocampo, Ocampo	$-103.2872°$	$28.0922°$
13	Ejido San Miguel, Ocampo	$-102.9483°$	$28.6367°$
14	Eutimias, Ocampo	$-102.3975°$	$27.3156°$
15	Sierra Mojada, Sierra Mojada	$-103.7017°$	$27.2864°$
16	Torreón, Torreón	$-103.4414°$	$25.5442°$
17	Presa Coyote, Torreón	$-103.2806°$	$25.6353°$
18	Presa Guadalupe, Torreón	$-103.3819°$	$25.5006°$
19	El Cuije, Matamoros	$-103.3158°$	$25.4169°$
20	San Pedro de las Colonias, San Pedro	$-102.9667°$	$25.7500°$
21	Presa la Flor de Jimulco, Torreón	$-103.5678°$	$25.8833°$
22	Parras de la Fuente, Parras	$-102.9483°$	$25.4353°$
23	Las Nieves, Parras	$-102.2019°$	$25.4586°$
24	San Pedro, Parras	$-102.2525°$	$25.6483°$
25	Viesca, Viesca	$-102.7833°$	$25.3375°$
26	Saltillo, Saltillo	$-101.0000°$	$25.4167°$
27	General Cepeda, General Cepeda	$-100.6000°$	$25.3500°$
28	Ramos Arizpe, Ramos Arizpe	$-100.9667°$	$25.5000°$
29	Hipólito, Ramos Arizpe	$-101.4047°$	$25.6983°$
30	Carneros, Saltillo	$-101.1000°$	$25.1000°$
31	Gómez Farías, Saltillo	$-101.0000°$	$25.0000°$
32	Ejido Reata, Ramos Arizpe	$-101.0667°$	$26.1167°$
33	Buenavista (UAAAN), Saltillo	$-101.0000°$	$25.3833°$
34	Arteaga, Arteaga	$-100.8667°$	$25.6167°$

In Figure 4.2 a few stations appear with their names and locations, taken from Table 4.1 as an example, since all 34 stations appear in the programme.

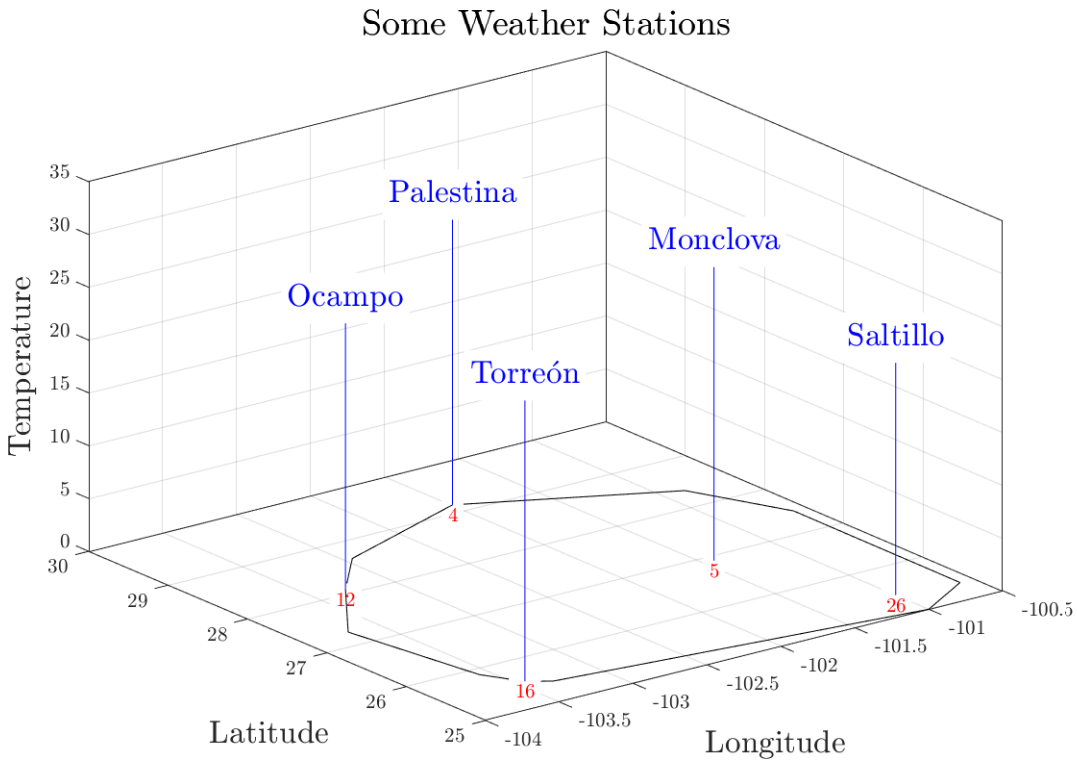


Figure 4.2: Some Weather Stations in the Polygon.

It can be seen that these locations coincide with those in Figure 4.1.

4.1.2 Mathematical Development of Algorithm DGG2

The development of this algorithm relies heavily on the mathematical aspects of Algorithm DGG1 established in Section 3.2.

Algorithm DGG2 deals with the temperatures of the mentioned locations. As in Algorithm DGG1, a mesh is established, but unlike it, this contains an additional difficulty because it is an irregular mesh. To develop the algorithm, it is proposed to generate a response surface from which contour lines can be obtained, and then estimate the heights at any point on the surface.

A procedure to interpolate is also proposed to obtain the heights z_0 at the points (x_0, y_0), with the condition that they belong to the plane of the base of the mesh.

The response surface contains the 34 original data and all the interpolation points. To carry out the large number of operations required, it was convenient to rely on technological resources. In this regard, codes in MATLAB language were developed to obtain all the necessary calculations and graphs. Its inclusion in this document is shown in Appendix C, in page 316.

4.2 Programme Functioning

An overview of the program functioning can be appreciated in the flow diagram shown in Figure 4.3.

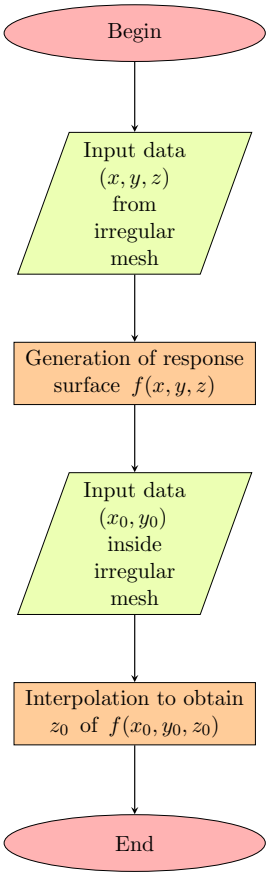


Figure 4.3: Flow Diagram of Algorithm Functioning.

The programme developed in MATLAB for the use of Algorithm DGG2, *methodB.m*, operates from certain input data that will be explained next.

4.2.1 Data Management

Because it is repetitive, the required information is saved only once, to be used later as many times as necessary.

Vectors x, y and z will be the same, so it is convenient to load them in a file *scenarios.mat* in the following way:

```
>>  save scenarios x y z
```

Every time this information is going to be used, it is simply downloaded from the *scenarios.mat* file:

```
>>  load scenarios
```

And in this way, data x, y and z is available.

4.2.2 Input and Output Data in Programme *methodB.m*

The program is a function called from the MATLAB prompt in the following way.

```
>>  [vert,XYZ,uvw] = methodB (x,y,z,cn,fs,u,v);
```

The names of the variables are arbitrary; the first three variables must be of the same order, 34 in this case, and the following two are integers; the last two are vectors of the same order between them. Take into account that it is essential to enter the data in the indicated order[2].

The following ellipsis denote that other data must be entered. In the examples in this Chapter, the column vectors involved have 34 elements, each one corresponding to a weather station. The data is entered from the *Command Window* of MATLAB.

1. **Longitudes.**

   ```
   >>  x = [-100.8539  -101.9167 ...  -100.8667];
   ```

[2]The final semicolon inhibits the presentation of the results, which would otherwise appear on the screen.

2. **Latitudes.**

   ```
   >>  y = [28.3444  28.4917 ...  25.6167];
   ```

3. **Temperatures.**

   ```
   >>  z = [28.9000  34.5000 ...  24.9000];
   ```

   The z corresponding to the temperatures can vary depending on the SRES and the year chosen, scenario A2 or B2, and years 2020, 2050 or 2080. The 72 column vectors of z are processed for the different temperatures (A2202001, A2202002, etc.).

4. **Number of Contour Lines.**

   ```
   >>  cn = 15;
   ```

   It can be any number of contour lines.

5. **Fonst Size in Points.**

   ```
   >>  fs = 12;
   ```

   Any reasonable Font Size can be chosen (1 inch = 72.27 pt = 2.54 cm = 25.4 mm).

6. **Abscissas where the interpolation is desired.**

   ```
   >>  u = [-100 59 58; -101 25 28; -103 19 46];
   ```

   These 3 abscissas are given in degrees, minutes and seconds. It can also be a column vector when the data are decimal degrees.

7. **Ordinates where interpolation is desired.**

   ```
   >>  v = [25 23 35; 26 50 40; 25 32 24];
   ```

   These three ordinates are given in degrees, minutes and seconds. It can also be a column vector when the data are decimal degrees.

The number of abscissas u must be equal to the number of ordinate v, and it can be any amount of data.

The programme *methodB.m* obtains:

1. **vert**

   number of vertices (stations) of the triangles in which the convex polygon of the data (x,y) has been dissected

$$vert = \begin{bmatrix} 20 & 25 & 24 \\ 20 & 22 & 25 \\ \vdots & \vdots & \vdots \\ 33 & 28 & 26 \end{bmatrix}, \quad (55 \times 3)$$

   that correspond to the 55 generated triangles.

2. **XYZ**

   (X, Y, Z) response surface values on a mesh, from the data (x, y, z).

   (x, y, z) are the coordinates of the 34 stations. (X, Y, Z) are the coordinates of any of the points on the response surface $Z = f(X, Y)$.

   XYZ is an array or matrix of (100×300), that is, they are the coordinates of 30000 points on the response surface. The program leaves this data available in the variable XYZ, although due to its magnitude it is not written here.

3. **uvw**

   coordinates of the interpolation belonging very approximately to the mesh

$$uvw = (u, v, w), \quad \text{where} \quad w = f(u, v).$$

   The estimate obtained with this interpolation is a very important aspect for the user.

To obtain these results, *methodB.m* does the following:

1. Determines interior triangles of a convex polygonal in the plane. It draws them and determines the indices of the coordinates (x, y) of the data (stations).

   Assuming that triangle number 1 is formed with the vertices (x_{20}, y_{20}), (x_{24}, y_{24}), (x_{25}, y_{25}), and the number 2 is formed with the vertices (x_{20}, y_{20}), (x_{22}, y_{22}), (x_{25}, y_{25}), and so on.

   The indices of the vertices, one line for each triangle, will be:

$$vert = [20\ 24\ 25\ ;\ 20\ 22\ 25; ...\ 33\ 28\ 26]$$

2. Colours the triangles of the previous convex polygonal.

3. Forms truncated triangular prisms by vertical projection, from the convex polygonal, to the heights

$$z_{20}, z_{24}, z_{25}, \quad z_{20}, z_{22}, z_{25}, \quad \dots \quad z_{26}, z_{28}, z_{33}$$

corresponding to the 55 prisms.

4. Colours the upper triangles of the truncated triangular prisms.

5. Forms a response surface with coordinates (X, Y, Z). To do this, it smooths the roofs of the prisms (x, y, z) by interpolation on a mesh (X, Y), obtaining the interpolation heights

$$Z = f(X, Y)$$

6. Presents relative errors of the response surface versus the values estimated by interpolation.

7. Draws the contour lines of the response surface. $Z = f(X, Y) = c$, being c a constant. Contour lines cut Z in horizontal planes of constant height c.

8. Interpolates to get the heights $w = f(u, v)$. If u and v are not given, x and y mean values are assigned.

$$uvw = [u\ v\ w] = \begin{bmatrix} -100.9994 & 25.3931 & 22.8639 \\ -101.4244 & 26.8444 & 30.1542 \\ -103.3294 & 25.5400 & 28.5618 \end{bmatrix}$$

Where column 1 are the abscissas, column 2 the ordinates, and column 3 the interpolation values for these coordinates, that is, the heights of the temperatures.

4.2.3 Running the Programme

The needed parameters will be described as they appear during the process. The programme starts running with command

```
>>  [vert,XYZ,uvw] = methodB (x,y,z,cn,fs,u,v);
```

The variables take the values established in the previous subsection.

Thereafter, results are displayed on the screen, and any key is pressed to advance to the next one.

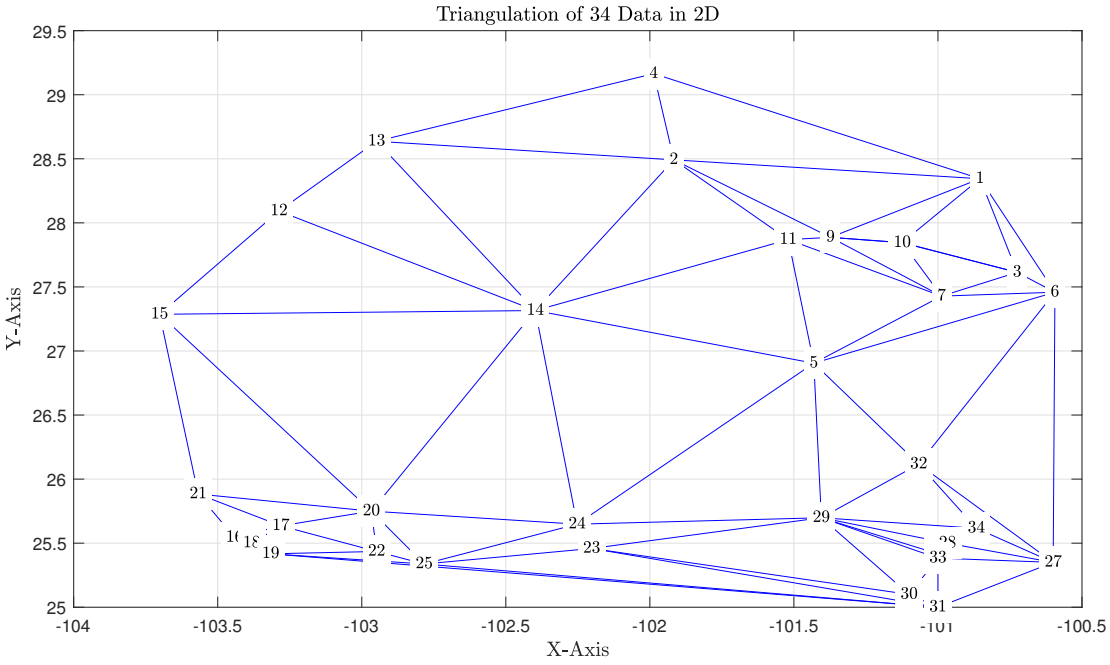


Figure 4.4: Data Triangulation in 2D.

In Figure 4.4, specific MATLAB functions were used.

Function *convhull* determines the boundary vertices k of the convex polygon and the surface it encloses, A.

```
>>  [k,A] = convhull (x,y);
```

$$k = [1, 4, 13, 12, 15, 21, 16, 19, 31, 27, 6, 1], \qquad A = 10.089$$

Delaunay was the function used to shape and determine the internal convex triangles.

```
>>  triang = delaunayTriangulation (x,y);
```

Produces three fields:

- `triang.Points` coordinates of the 34 vertices of the polygonal.
- `triang.ConnectivityList` vertices of each of the 55 triangles.

- `triang.Constraints` it was not used in this programme.

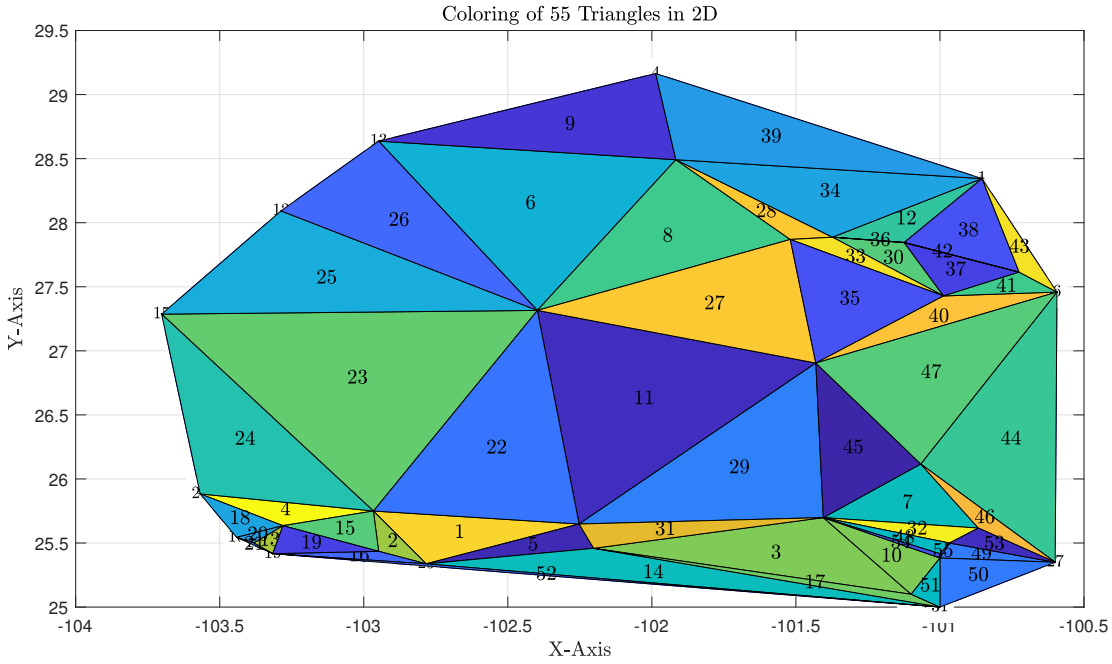


Figure 4.5: Triangles Colouring in 2D.

With function *triplot*, triangulation is drawn and triangles on the plane can be coloured, Fig. 4.5.

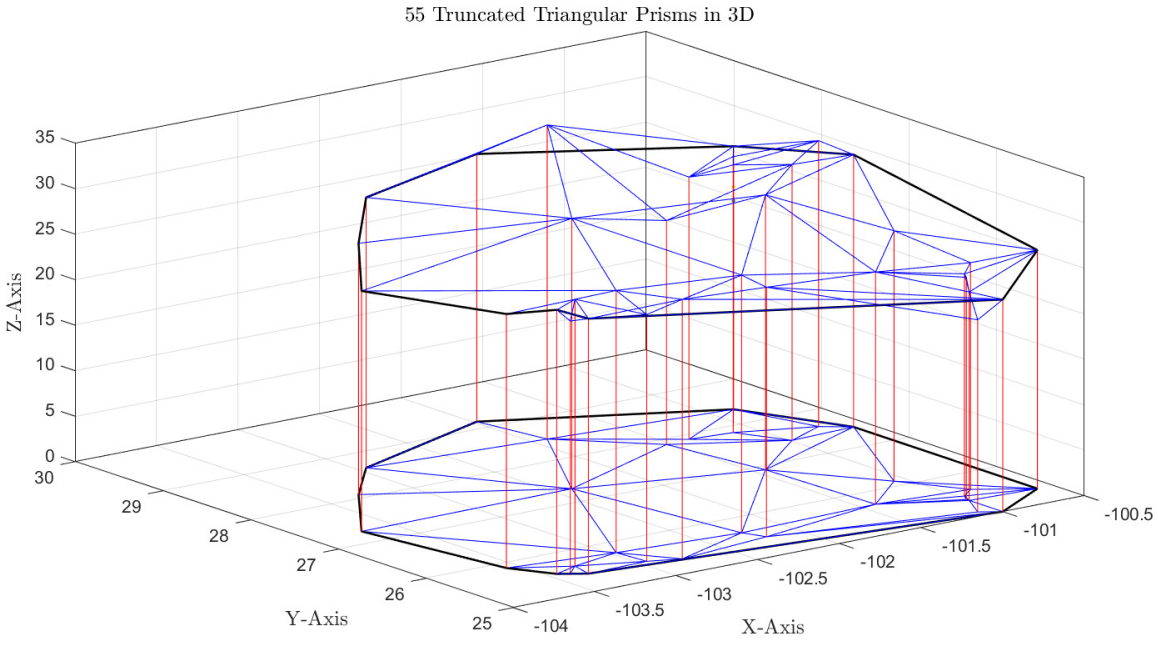


Figure 4.6: Truncated Triangular Prisms.

The vertices of each triangle extend vertically upwards, up to the heights of their temperatures, Fig. 4.6, thus generating flat roofs that when joined together form a mosaic, Fig. 4.7.

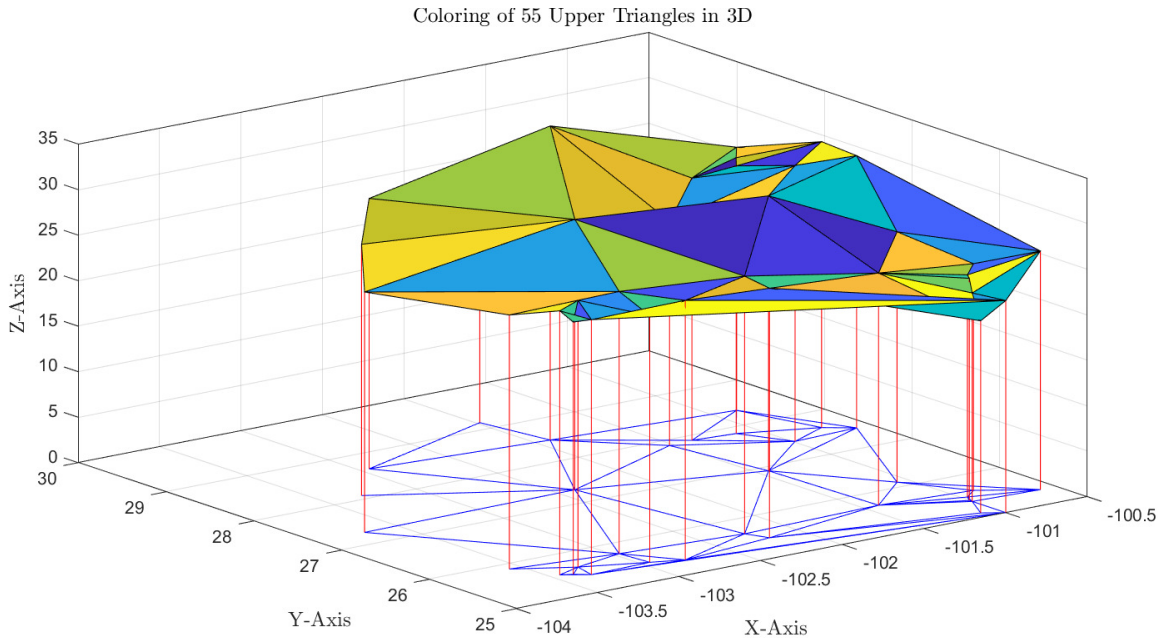


Figure 4.7: Coloured Upper Triangles.

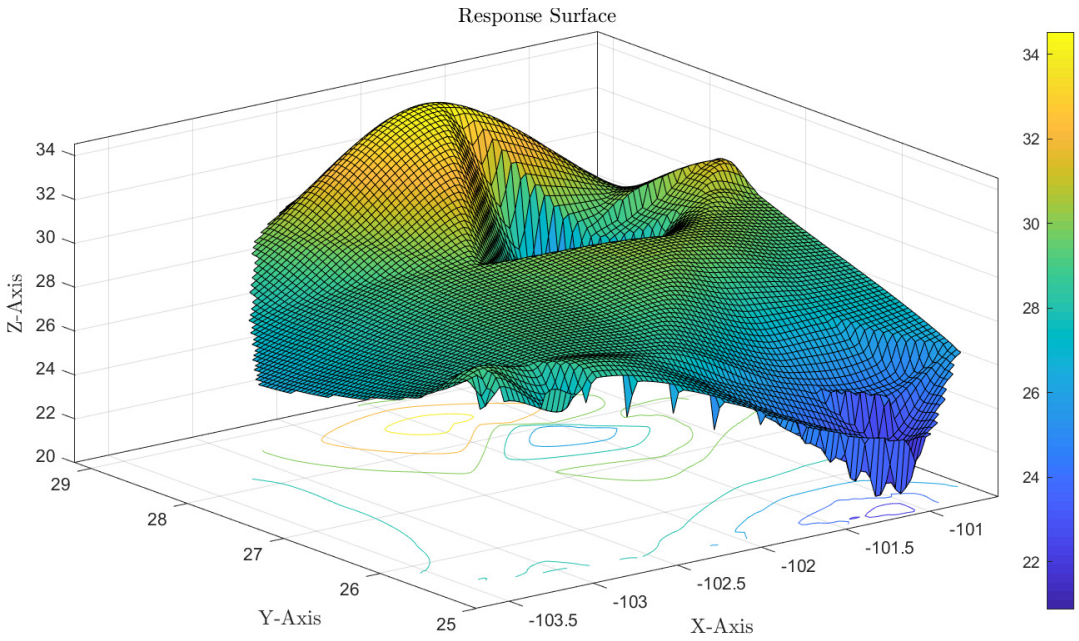


Figure 4.8: Response Surface.

Figure 4.8 shows the response surface of the temperatures, obtained with the smoothing of the roofs from the previous figure, as well as the temperatures bar. The slopes appear

pronounced due to the scale of the figure, because they do not start from zero, but from the minimum temperature.

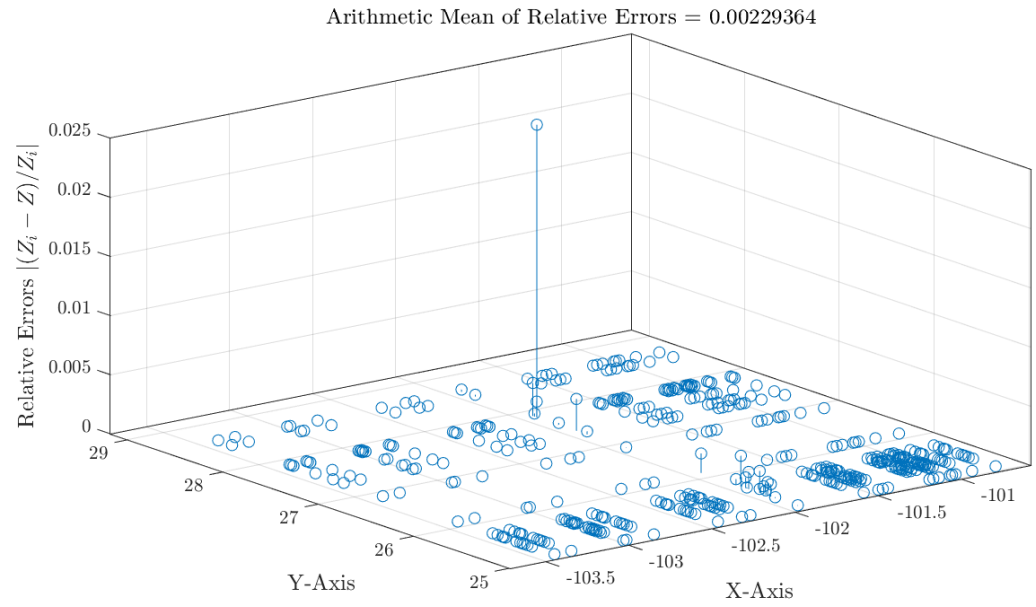


Figure 4.9: Relative Errors.

The relative errors of the interpolation are presented in Figure 4.9. Their description is shown on the z axis, where the values of Z are the estimates, and those of Z_i, are the data of the measurements.

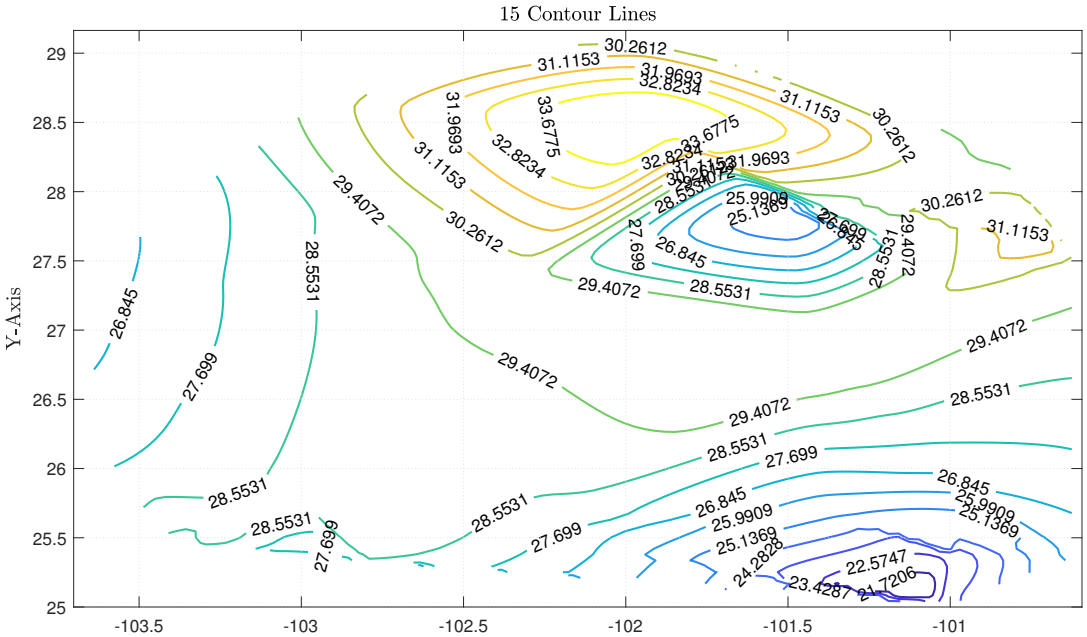


Figure 4.10: Contour Lines.

The projected contour lines of the response surface are shown in Figure 4.10, including their numerical values. These present lines of constant elevation or heights.

As the figures are presented, there is the possibility of appreciating the values of the coordinates, by placing the mouse cursor over the point of interest. When the figure is in 2D, it provides numerically the abscissa and ordinate of the point, and for a 3D figure, it provides abscissa, ordinate and height.

4.2.4 Codification

In Appendix C, the code listings in MATLAB of the programmes *methodB.m* and *enLaMalla.m* are included, specifically and respectively in Appendix C.1 and Appendix C.1.1.

4.3 Conclusions

To establish the characteristics of this procedure, a comparison will be made with Algorithm DGG1.

1. Similarities between Algorithms DGG1 and DGG2.
    - They arose as needs at different times in the investigation.
    - Both algorithms are original by the author.
    - They allow to approach the study of different phenomena.
    - The response surfaces obtained allow qualitative visualisations of the phenomenon.
    - Interpolations are obtained to estimate heights of the response surface at any point.
    - Quantitative estimates are objective. They do not depend on subjective criteria of the researcher, but are based on precise mathematical procedures.
    - They integrate their constitutive stages in computer programmes.

- The application of the algorithms is reduced to the introduction of the data to obtain the results of the stages in graphical and numerical form.

2. Differences between the rationale for Algorithms DGG1 and DGG2.

   - Algorithm DGG1 applies to a specific rectangular lattice, while Algorithm DGG2 has an application to an irregular mesh.
   - Algorithm DGG1 is based on the establishment of a succession of parabolas supported by 3 points.

     By the nature of the mesh irregularity, Algorithm DGG2 uses a diverse set of advanced mathematical techniques.

3. Strengths of Algorithm DGG2.

   - It is applicable to any phenomenon such as atmospheric pressure, temperatures, carbon dioxide emissions, heat islands effect in cities, etc.
   - It applies indistinctly to any source of information.

     For example, in this study, the information for the climate scenarios can come from the PRECIS, ECHAMPS, HADGEM, or any other model.
   - The stations or sources of information are not subject to any restrictions. It is applicable when conditions are not restricted, or when they are controlled, such as in the laboratory.
   - The stations can have any arrangement.
   - In all cases, the study of phenomena is covered by the same programme, Algorithm DGG2.
   - The programme can obtain multiple results of the same phenomenon. For example, in this research 72 different cases were studied for each city, which originated a set of graphs and results for each case.

     In Appendix D, 72 graphics belonging to the chosen location in the city of Saltillo can be appreciated.
   - The algorithm guarantees reliable, objective and irrefutable solutions for its conditions.

- The layout of the programme *methodB.m* provides very wide experimentation possibilities, of the type: *what would happen if...?*. In this way, not only the measured data can be used in the experimentation, but also values assumed by the researcher.

  For example, there are serious doubts about one of the common ways of dealing with the subject of temperatures in climate projections, which is to arbitrarily increase the temperature by a certain number of degrees. With the application of this algorithm, comparative experiments can be established between this practice and others, such as Algorithm DGG3, which will be explained in the next chapter.

Undoubtedly, there is massive information on climate change projections, but they are of limited application due to the large amount of technological and economic resources that the handling of this information requires.

It would be desirable to have regional procedures established with few resources and adapted to the circumstances of the study. In these cases, the programmes *methodA.m* and *methodB.m* can be applied, which is certainly an additional advantage of Algorithms DGG1 and DGG2. The results obtained with these two can be used to generate a weather file by using Algorithm DGG3 presented in the next chapter.

Chapter 5

Algorithm DGG3. Generation of Weather Files for Climate Projections

The Algorithm DGG3 presented in this chapter was created in order to generate weather files from future climate projections needed for dynamic building simulations. It considers historical weather data and climate projections like those presented in the two previous chapters. This is the third and last part of the proposed innovative methodology.

5.1 Introduction

The procedure followed for the development of this algorithm includes several stages, and to give greater clarity to the presentation, the subject is introduced through three fundamental questions: 1) what does the algorithm do?, 2) how does it do it?, 3) what does it do it for?

1. **What does Algorithm DGG3 do?**

   From the historical weather files, two columns corresponding to the temperature and relative humidity are extracted; each column has $8,760$ rows. The first column belongs to the temperatures of each hour of a year, and the second, to their corresponding relative humidities.

With Algorithm DGG3, these $17,520$ data are used as information to generate a total of $473,040$ values: $236,520$ values of temperatures and $236,520$ of relative humidity.

This information is presented in the forms of equations, tabular arrangements, and graphical presentations.

2. **How does it do it?**

   In Algorithm DGG3 robust mathematical tools are used (Least Squares Approximation being the main one), and to handle the enormous amount of information obtained in a matrix form, MATLAB was used.

3. **What for?**

   The $473,040$ estimated values (temperatures and their corresponding relative humidity) are processed to generate new *.epw* weather files:

   - For three proposed locations in the cities of Saltillo, Monclova and Torreón.
   - RCP studies are considered for the near horizon (years 2015–2039), medium horizon (years 2045–2069), and far horizon (years 2075–2099), for each of the three locations.
   - In each location and horizon, their average, minimum and maximum temperatures are determined.

   These weather files are used to perform energy simulations for case studies with EnergyPlus.

5.2 Antecedents of Algorithm DGG3

Posterior to the initial study explained in Algorithm DGG2, at the UNAM Atmospheric Science Centre [54] projections were performed from models CNRM-CM5, GFDL-CM3, HadGEM2-ES, and MPI-ESM-LR for the whole country. For Algorithm DGG3, RCP4.5 and RCP8.5 concentration trajectories were considered for the near horizon, medium horizon, and far horizon; years corresponding to each one of them can be seen in Table 5.1.

Table 5.1: Annual Years Intervals by Horizon

Horizon	**Years Interval**
Near	$2015 - 2039$
Medium	$2045 - 2069$
Far	$2075 - 2099$

A new code was also developed in MATLAB to obtain pertinent data, this, in order to generate weather files for future climate scenarios in any chosen location within the country.

In the study of the future housing behavior (Scenarios or Horizons), weather files are required. As future measured data obviously does not exist, we have to rely on the projections of temperatures provided by climate experts. Considering current information (hereinafter Historical Data), and projections, the Historical Data files were modified considering the projections to create new weather files and running energy simulations.

Starting from the historical data, differences in temperatures between cities, minimum, average and maximum temperatures, can be appreciated as shown in Figure 5.1.

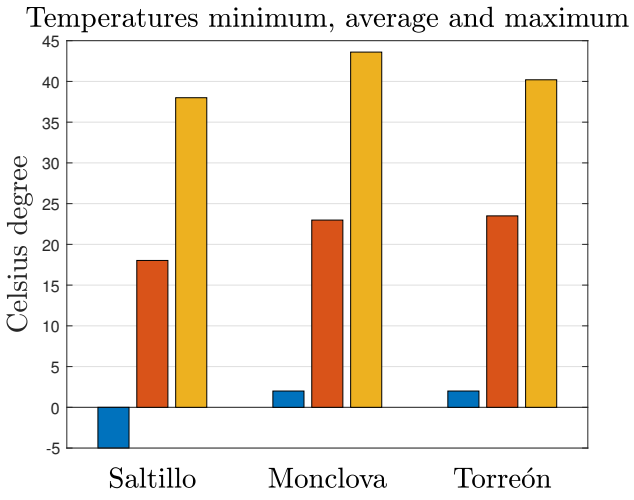


Figure 5.1: Temperatures from Historical Weather Data.

Considering that recently, energy performance evaluation has been a major topic in the building industry, building simulation is generally used as a helpful tool to study the

amount of energy consumption in buildings. These evaluations are approached differently in every country, although there are international standards that can be applied depending on the region.

In Mexico there are two official regulations for the building envelope evaluation for residence buildings, and non-residence buildings. These regulations used methods based on a steady-state heat transfer analysis and they define minimum values of the thermal resistance of the envelope, but the thermal storage capacity is not considered.

Mexico has an extensive range of climate variations so ideally a method based on time dependant heat transfer analysis should be used. When using software to make energy evaluations, the predicted performance outcome simulations are considerably different to the measured data, and this is generally for the uncertainty of the inputs.

EnergyPlus is considered by professionals as an accurate software to evaluate energy performance, and the provided weather data is derived from 20 sources worldwide. The International Weather for Energy Calculations (IWEC) developed the data for Mexico and include three cities in the central stripe of the country (Mexico City, Veracruz and Acapulco), so extreme climates from the north and south of the country are not documented.

In the UNAM Atmospheric Science Centre website, the most recent IPCC projections are considered, with this, the RCP greenhouse gas concentration trajectories for different scenarios in the country. To obtain data, it must be chosen the desired model, RCP, horizon, and the weather component. For this research the HadGEM2-ES model was selected, as is the most similar to the previous study made for Coahuila for finding it as the most suitable for the state.

The three horizons were studied for RCP4.5, and minimum, maximum and average temperatures for monthly periods were downloaded. This information was obtained by clicking on the desired location geographical coordinate in an interactive map of Mexico, under the different horizons and months. The collected data is shown in Table 5.2 for Saltillo, Table 5.3 for Monclova, and Table 5.4 for Torreón.

Table 5.2: Monthly Minimum, Average and Maximum temperatures for Saltillo future horizons according to the UNAM Digital Climate Atlas.

Month	Near Min	Near Ave	Near Max	Mid Min	Mid Ave	Mid Max	Far Min	Far Ave	Far Max
01	5.20	11.80	20.00	6.10	13.00	21.50	6.70	12.80	22.00
02	6.00	13.50	20.90	7.10	14.30	23.50	7.80	15.30	23.90
03	8.50	17.20	26.00	9.70	17.90	27.70	10.40	18.90	28.20
04	12.90	20.90	30.50	13.30	21.70	31.80	14.20	22.70	32.60
05	15.80	23.70	33.10	16.80	24.80	35.20	17.60	25.30	35.60
06	17.00	24.70	34.60	18.00	25.80	35.70	18.30	25.70	36.20
07	17.10	25.20	34.40	17.90	25.80	35.80	18.50	26.80	35.40
08	16.50	24.20	33.90	17.40	25.20	34.40	17.70	26.20	34.40
09	15.10	22.70	31.60	15.90	23.40	32.20	16.20	23.70	32.40
10	12.30	19.00	28.30	13.30	19.90	29.20	13.80	20.30	29.00
11	8.90	15.60	24.40	9.80	15.90	25.00	10.30	16.50	24.60
12	6.50	12.90	20.10	7.40	14.10	21.40	8.50	13.90	21.50

Table 5.3: Monthly Minimum, Average and Maximum temperatures for Monclova future horizons according to the UNAM Digital Climate Atlas.

Month	Near Min	Near Ave	Near Max	Mid Min	Mid Ave	Mid Max	Far Min	Far Ave	Far Max
01	5.50	13.60	22.00	6.40	14.80	23.80	7.10	14.40	23.70
02	6.00	15.10	21.90	7.30	15.70	25.00	7.80	16.80	25.20
03	10.60	19.70	28.20	11.60	20.60	30.40	12.30	21.60	30.80
04	15.80	23.90	32.10	16.10	24.30	34.00	16.80	25.60	34.00
05	19.40	27.30	34.70	20.80	28.10	37.40	21.20	28.10	37.40
06	21.60	28.60	36.80	22.40	29.70	39.10	22.70	29.60	38.70
07	21.70	29.10	37.20	23.30	29.90	39.40	23.40	30.40	38.30
08	21.40	28.20	37.00	23.30	29.10	37.90	23.10	29.60	37.60
09	19.70	26.30	34.60	20.70	27.00	35.50	20.90	27.20	35.50
10	15.90	22.10	30.90	17.10	22.90	32.20	17.50	23.20	31.30
11	10.40	17.90	26.90	11.60	18.10	27.80	11.90	18.70	27.20
12	6.90	14.30	21.80	7.50	15.60	23.70	8.90	15.40	23.60

Table 5.4: Monthly Minimum, Average and Maximum temperatures for Torreón future horizons according to the UNAM Digital Climate Atlas.

Month	Near Min	Near Ave	Near Max	Mid Min	Mid Ave	Mid Max	Far Min	Far Ave	Far Max
01	5.60	13.60	24.20	6.60	16.00	25.70	7.00	16.40	25.90
02	7.30	15.10	27.00	8.00	18.50	29.10	8.60	19.20	29.60
03	10.00	19.70	30.90	11.40	21.90	32.50	11.70	22.50	33.30
04	14.40	23.90	35.30	15.20	25.80	36.40	16.20	26.60	37.20
05	18.30	27.30	37.60	19.30	29.40	39.50	20.00	29.80	39.80
06	20.40	28.60	38.60	21.50	30.50	39.60	22.20	31.10	40.10
07	20.50	29.10	36.70	21.30	29.80	38.30	22.00	29.90	37.70
08	19.60	28.20	35.60	20.50	28.40	36.40	21.00	28.70	36.50
09	17.90	26.30	34.40	18.80	27.00	35.30	19.10	27.30	35.50
10	14.40	22.10	31.90	15.30	24.10	32.90	16.20	24.50	32.80
11	10.40	17.90	28.70	11.40	20.30	29.20	12.00	20.50	29.20
12	6.70	14.30	24.10	7.40	16.20	25.20	8.70	17.00	25.50

This is the third part of the methodology, in which obtaining interpolated data for specific locations should be approached differently, because it is more up-to-date and direct information than the one described in the previous part; likewise, it is presented differently. While in the first and second parts the information must be obtained from the proposed interpolation based on data from meteorological stations, here it is obtained directly from the UNAM Digital Climate Atlas website.

For any of all three parts, the next step after obtaining these data is to estimate the values of relative humidity and temperature for each case proposed. This to generate the appropriate weather files used in the energy simulations. An analysis of the best approach was performed and the least squares approximation was used to fit the sets of points to a curve which later, could be described in an equation and displayed per month. The scope was considered as the one provided by Meyer [119] and it is explained throughout the section.

A Representative Concentration Pathway (RCP) is a greenhouse gas concentration adopted by the IPCC on its 5th Assessment Report AR5 [16]. It supersedes the Special Report on Emissions Scenarios (SRES) projections previously published [150].

The RCP 4.5 contemplates the intermediate emissions, in where radiative forcing is

stabilised shortly after year 2100, consistent with a future with relatively ambitious emissions reductions. The comparable SRES scenario is B1, for a future consistent with lower energy intensity, strong reforestation programmes, a decrease of croplands and grasslands use due to yield increases and dietary changes. It considers also stringent climate policies, stable methane emissions. CO_2 emissions increase only slightly before their declining commencing around 2040.

The RCP 8.5 considers high emissions consistent with a future with no policy changes to reduce emissions. An increment in greenhouse gas emissions that leads to high greenhouse gas concentrations over time is foreseen. The comparable SRES scenario is A1 F1, for a future consistent with three times today's CO_2 emissions by 2100, rapid increase in methane emissions, increased use of croplands and grassland which is driven by an increase in population, with a world population of 12 billion by 2100. Lower rate of technology development is considered, with heavy reliance on fossil fuels, high energy intensity and no implementation of climate policies.

According to the International Energy Agency (IEA[1]) [90], it is thought that global coal use peaked in 2013, and although increases are still possible, many energy forecasts expect it to flat the line over the next few decades.

The falling cost of clean energy sources is a trend that is unlikely to reverse, even in the absence of new climate policies. Emission pathways to get to RCP 8.5 generally require an unprecedented fivefold increase in coal use by the end of the century, an amount larger than some estimates of recoverable coal reserves [132].

Due to this, RCP 4.5 was selected for the simulations study. A morphing method using curve fitting made use of the RCP 4.5 pathways data for Mexico to obtain the missing data needed for weather files.

The Algorithm DGG2 use data from 34 weather stations in Coahuila to obtain temperatures for years 2020, 2050, 2080 for A2 and B2 climate change scenarios for any point in the surface. As per Algorithm DGG3, the input data are the temperatures assigned for future horizons in the studied specific coordinates chosen for each city. Whit these, an interpolation of data from the historic weather files is made to create new weather

[1]International Energy Agency

files for simulation (.epw). Hourly data of temperature and relative humidity is generated.

5.3 Mathematical Development of Algorithm DGG3

Due to the large amount of scattered information contained in the weather files, the need to handle it mathematically in the form of equations arose.

The review of assessment techniques, in cases like this, highlighted the importance of the Least Squares Approximations technique, as it is one of the most important assessment techniques to fit data in an equation form. For research purposes, this technique was considered to be the most appropriate; in particular, in this chapter the least squares fitting of algebraic polynomials will be widely applied. The method is reviewed in the following cases.

5.3.1 Fitting a Straight Line

At discrete point t_i (often points in time), observations b_i of some phenomenon are made, and the results are recorded as a set of ordered pairs

$$D = \{(t_1, b_1),\ (t_2, b_2),\ \ldots,\ (t_m, b_m)\}.$$

On the basis of these observations, the problem is to make estimations or predictions at points (times) $\hat{t}$ that are between or beyond the observations points t_i. A standard approach is to find the equation of a curve $y = f(t)$ that closely fits the points in D so that the phenomenon can be estimated at any non-observations point $\hat{t}$ with the value $\hat{y} = f(\hat{t})$.

By initially fitting a straight line to the points in D, to fit the data with curved lines will be straightforward. The strategy is to determine the coefficients α y β in the equation of the line $f(t) = \alpha t + \beta$ that best fits the points (t_i, b_i) in the sense that the sum of the squares of the vertical[2] errors $\epsilon_1,\ \epsilon_2,\ \ldots,\ \epsilon_m$ indicated in Figure 5.2 is minimal.

[2]Only vertical errors are considered because there is a tacit assumption that only the observations b_i are subject to error or variation. The t_i's are assumed to be error-less constants —considering them as

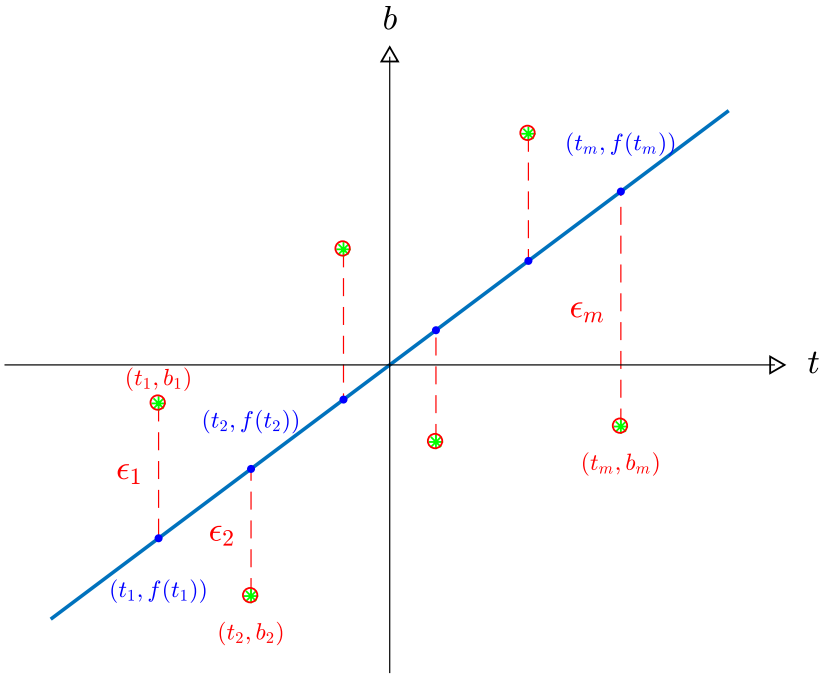


Figure 5.2: Line $f(t) = \alpha t + \beta$ that best fits in the sense of least square.

The distance from (t_i, b_i) to a line $f(t) = \alpha t + \beta$ is

$$e_i = |f(t_i) - b_i| = |\alpha t_i + \beta - b_i|,$$

so that the objective is to find values for α y β such that

$$\sum_{i=1}^{m} \epsilon_i^2 = \sum_{i=1}^{m} (\alpha t_i + \beta - b_i)^2 \quad \text{is minimal.}$$

In minimization techniques from calculus the minimum value must occur at a solution to the two equations

$$\frac{\partial \left(\sum_{i=1}^{m} (\alpha t_i + \beta - b_i)^2\right)}{\partial \alpha} = 2 \sum_{i=1}^{m} (\alpha t_i + \beta - b_i)\, t_i \quad = \quad 0,$$

$$\frac{\partial \left(\sum_{i=1}^{m} (\alpha t_i + \beta - b_i)^2\right)}{\partial \beta} = 2 \sum_{i=1}^{m} (\alpha t_i + \beta - b_i) \quad = \quad 0.$$

Rearranging terms produces two equations in the two unknowns α y β

Normal equations:

being exact points in time (as they often are). If the t_i's are also subject to variation, the horizontal as well as vertical errors have to be considered in Figure 5.2, and a more complicated theory known as total least squares (not considered in this document) emerges. The least squares line obtained by minimizing only vertical deviations will not be the closest of linear estimation.

$$\begin{aligned} \left(\sum_{i=1}^{m} t_i^2\right)\alpha + \left(\sum_{i=1}^{m} t_i\right)\beta &= \sum_{i=1}^{m} t_i b_i \\ \left(\sum_{i=1}^{m} t_i\right)\alpha + \left(\sum_{i=1}^{m} 1\right)\beta &= \sum_{i=1}^{m} b_i \end{aligned} \tag{5.1}$$

5.3.2 Matrix Approach

According to Meyer [119]: By setting

$$A = \begin{bmatrix} t_1 & 1 \\ t_2 & 1 \\ \vdots & \vdots \\ t_m & 1 \end{bmatrix}, \qquad b = \begin{bmatrix} b_1 \\ b_2 \\ \vdots \\ b_m \end{bmatrix}, \qquad \hat{x} = \begin{bmatrix} \alpha \\ \beta \end{bmatrix},$$

we see that the two equations (5.1) have the matrix form

$$A^T A\hat{x} = A^T b. \tag{5.2}$$

The t_i's are assumed to be distinct numbers, so $rank(A) = n$, and

$$\hat{x} = (A^T A)^{-1} A^T b. \tag{5.3}$$

insures that the normal equations have a unique solution[3].

In other words, (5.1) is the system of **normal equations** associated with the system

$$Ax = b$$

It often happens that $Ax = b$ has no solution. The usual reason is: *too many equations*. The matrix has more rows than columns. There are more equations than unknowns (m is greater than n). The n columns span a small part of m-dimensional space. Unless all measurements are perfect, b is outside that column space. Elimination reaches an impossible equation and stops. But these are real problems and they need an answer.

It is not possible to get the error $e = b - Ax$ down to zero every-time. When e is zero, x is an exact solution to $Ax = b$. When the length of e is as small as possible $\hat{x}$ is a least squares solution. The goal in this section is to compute $\hat{x}$ and use it:

[3] A $m \times n \quad (m > n)$, Rank $r(A) = n =$ number of pivots.

When the original $Ax = b$ has no solution, multiply by A^T and solve $A^T A\hat{x} = A^T b$.

Notice that the total sum of squares of the errors is given by

$$\sum_{i=1}^{m} \epsilon_i^2 = \sum_{i=1}^{m} (\alpha t_i + \beta - b_i)^2 = (A\hat{x} - b)^T (A\hat{x} - b).$$

5.3.3 Orthogonal Projection

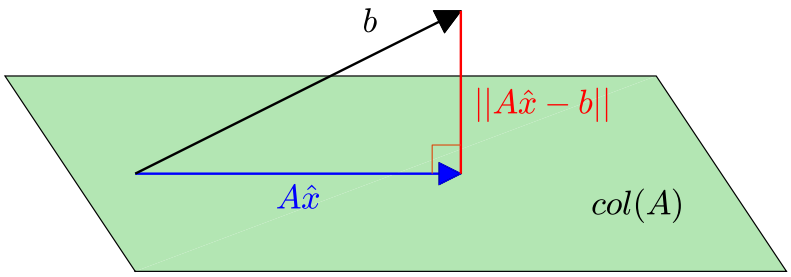


Figure 5.3: Projection of b on $col(A)$.

Non-rigorously, equations (5.2) can be seen as follows: the space column of A is a plane or hyperplane that contains all the linear combinations of the type Ay, (Figure 5.3), and if vector b is not included in the same plane, then it can be projected onto it, such that error vector $E = ||Ax - b||$ must be perpendicular to that space. To minimize error E, solution $\hat{x}$ must be looked for, localising point $p = A\hat{x}$ on the closest column space to b. Then:

$$Ay \perp (A\hat{x} - b) \quad \rightarrow \quad (Ay)^T (A\hat{x} - b) = 0$$

by the properties of the transposed matrix

$$\begin{aligned} (y^T A^T)(A\hat{x} - b) &= 0 \\ y^T (A^T A\hat{x} - A^T b) &= 0 \end{aligned}$$

which implies that the second factor is null

$$\begin{aligned} (A^T A\hat{x} - A^T b) &= 0 \\ A^T A\hat{x} &= A^T b. \end{aligned}$$

Normal equations (5.2). □

5.3.4 Fitting by a Parabola

If is desired to approximate by a quadratic polynomial of least squares

$$f(t) = \alpha\, t^2 + \beta\, t + \gamma \tag{5.4}$$

normal equations must be extended accordingly

Normal equations:

$$\begin{aligned}
\left(\sum_{i=1}^{m} t_i^4\right)\alpha + \left(\sum_{i=1}^{m} t_i^3\right)\beta + \left(\sum_{i=1}^{m} t_i^2\right)\gamma &= \sum_{i=1}^{m} t_i^2 b_i \\
\left(\sum_{i=1}^{m} t_i^3\right)\alpha + \left(\sum_{i=1}^{m} t_i^2\right)\beta + \left(\sum_{i=1}^{m} t_i\right)\gamma &= \sum_{i=1}^{m} t_i b_i \\
\left(\sum_{i=1}^{m} t_i^2\right)\alpha + \left(\sum_{i=1}^{m} t_i\right)\beta + \left(\sum_{i=1}^{m} 1\right)\gamma &= \sum_{i=1}^{m} b_i
\end{aligned} \tag{5.5}$$

Example

To find the parabola $Cx^2 + Dx + E$ that come closest (least squares error) to the values $b = (2,\ 3,\ 5,\ 8,\ 17)$ at the times $t = 1,\ 2,\ 3,\ 4,\ 5$, first the five equations $Ax = b$ in three unknowns $x = (C,\ D,\ E)$ for a parabola to go through the five points must be written. There is no solution because no such parabola exists. To solve $Ax = b$ by least squares (using $A^T A\hat{x} = A^T b$), assigned values must be managed as follows:

$$\begin{bmatrix} 1 & 2 \\ 2 & 3 \\ 3 & 5 \\ 4 & 8 \\ 5 & 17 \end{bmatrix}, \quad \begin{aligned} C(1)^2 + D(1) + E &= 2 \\ C(2)^2 + D(2) + E &= 3 \\ C(3)^2 + D(3) + E &= 5 \\ C(4)^2 + D(4) + E &= 8 \\ C(5)^2 + D(5) + E &= 17 \end{aligned}, \quad A = \begin{bmatrix} 1 & 1 & 1 \\ 4 & 2 & 1 \\ 9 & 3 & 1 \\ 16 & 4 & 1 \\ 25 & 5 & 1 \end{bmatrix}, \quad b = \begin{bmatrix} 2 \\ 3 \\ 5 \\ 8 \\ 17 \end{bmatrix}$$

$$A^T A = \begin{bmatrix} 979 & 225 & 55 \\ 225 & 55 & 15 \\ 55 & 15 & 5 \end{bmatrix}, \qquad A^T b = \begin{bmatrix} 612 \\ 140 \\ 35 \end{bmatrix}, \qquad A^T A\hat{x} = A^T b :$$

$$\begin{bmatrix} 979 & 225 & 55 \\ 225 & 55 & 15 \\ 55 & 15 & 5 \end{bmatrix} \begin{bmatrix} C \\ D \\ E \end{bmatrix} = \begin{bmatrix} 612 \\ 140 \\ 35 \end{bmatrix}, \qquad \hat{x} = \begin{bmatrix} C \\ D \\ E \end{bmatrix} = \begin{bmatrix} 1.2143 \\ -3.7857 \\ 5.0000 \end{bmatrix}$$

Solution

$$\begin{aligned} C(1)^2 + D(1) + E &= 2 \\ C(2)^2 + D(2) + E &= 3 \\ C(3)^2 + D(3) + E &= 5 \\ C(4)^2 + D(4) + E &= 8 \\ C(5)^2 + D(5) + E &= 17 \end{aligned}$$

$$A = \begin{bmatrix} 1 & 1 & 1 \\ 4 & 2 & 1 \\ 9 & 3 & 1 \\ 16 & 4 & 1 \\ 25 & 5 & 1 \end{bmatrix}, \; b = \begin{bmatrix} 2 \\ 3 \\ 5 \\ 8 \\ 17 \end{bmatrix} \begin{cases} A^T A = \begin{bmatrix} 979 & 225 & 55 \\ 225 & 55 & 15 \\ 55 & 15 & 5 \end{bmatrix} \\ A^T b = \begin{bmatrix} 612 \\ 140 \\ 35 \end{bmatrix} \end{cases}$$

$$A^T A\hat{x} = A^T b \; \rightarrow \; \begin{bmatrix} 979 & 225 & 55 \\ 225 & 55 & 15 \\ 55 & 15 & 5 \end{bmatrix} \begin{bmatrix} C \\ D \\ E \end{bmatrix} = \begin{bmatrix} 612 \\ 140 \\ 35 \end{bmatrix},$$

$$\hat{x} = \begin{bmatrix} C \\ D \\ E \end{bmatrix} = \begin{bmatrix} 1.2143 \\ -3.7857 \\ 5.0000 \end{bmatrix}$$

$$f(t) = 1.2143\,t^2 - 3.7857\,t + 5.0000. \qquad \text{(Figure 5.4).}$$

Now, with equations (5.5), a table with the summations is prepared and the normal

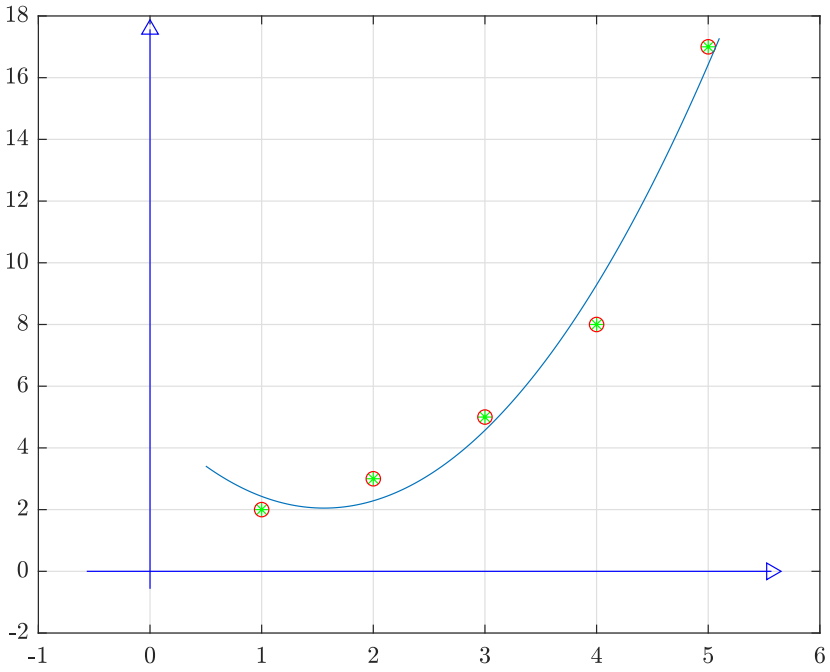


Figure 5.4: $f(t) = 1.2143\,t^2 - 3.7857\,t + 5.0000$

equations are presented

t	b	t^2	t^3	t^4	tb	t^2b
1	2	1	1	1	2	2
2	3	4	8	16	6	12
3	5	9	27	81	15	45
4	8	16	64	256	32	128
5	17	25	125	625	85	425
15	35	55	225	979	140	612

$$\begin{bmatrix} 979 & 225 & 55 \\ 225 & 55 & 15 \\ 55 & 15 & 5 \end{bmatrix} \begin{bmatrix} \alpha \\ \beta \\ \gamma \end{bmatrix} = \begin{bmatrix} 612 \\ 140 \\ 35 \end{bmatrix}$$

The same equations system as previously approached.

This process is useful to define en equation that follows the form of a certain parameter, for this case, temperatures, so the curve fitting more accurate to the temperatures behaviour can be described in an equation.

NOTE:

Similar to the previous equations, the process can be extended to fit with polynomials of degrees 3, 4, etc.

5.3.5 Using MATLAB

Calculations are greatly simplified using the programming platform MATLAB. The example mentioned above requires the following commands:

```
>> t = 1:5;  b = [2 3 5 8 17];  p = polyfit(t,b,2)
```

and produces the coefficients of the quadratic equation

```
>> p =  1.2143   -3.7857   5.0000
```

corresponding to the quadratic equation

$$y = f(t) = 1.2143\,t^2 - 3.7857\,t + 5.0000.$$

If the independent variable is x, then the equation is

$$y = f(x) = 1.2143\,x^2 - 3.7857\,x + 5.0000.$$

In the commands for this example *1:5* is the rank of t; *[2 3 5 8 17]* are the ordinates values, and the MATLAB function *polyfit* returns coefficients from polynomial curve fitting considering (t, b), and the value of the polynomial degree, which in this case is 2, because it is a quadratic equation[4].

Graphing is produced in a simple way. For instance, to obtain a graph from the above quadratic, including the points of the scatter diagram, and also the curve in the x interval $[0.5\ 5.2]$, in MATLAB would be stated the following:

to prepare 1000 equidistant points in the interval and evaluate $y = f(x)$

```
>> x = linspace(0.5,5.2,1000);  y = polyval(p,x);
```

it draws the points (t, b), with asterisks, on the Cartesian plane. The graphics window remains open with command *hold on*:

[4]To find the coefficients of a cubic polynomial, the following must be written from the command window:

```
f = polyfit(t,b,3)
```

```
>> plot(t,b,'*');  hold on;
```

it draws the curve $y = f(x)$ on the same graphical screen and makes it visible on the monitor:

```
>> plot(x,y);  shg
```

Figure 5.4 is done with the code in Appendix E.

For the research, quadratic, cubic, fourth and fifth degree polynomial were compared to find the most suitable.

When adjudicating an equation that describes the curve closest to the scattered points, the one with the smallest margin of error is estimated and is most attached to the behavior of the evaluated values, in this case, the temperatures.

In this document it was experimented with polynomials of degrees from $n = 1$ to $n = 5$ and the best of them is chosen as shown in Table 5.5.

Table 5.5: Least Square Method

1. **Data**

$$\left.\begin{matrix} x_i \\ y_i \end{matrix}\right\} i = 1,\, 2,\, \ldots,\, m$$

2. **Least Square Method**

   - for $n = 1 : 5$

     (a) Polynomial Coefficients p

$$\hat{y}_n = p_1\, x^n + p_2\, x^{n-1} + \cdots + p_n\, x + p_{n+1}$$

     (b) Graphics

     (c) Sum of Squared Deviations

$$SSD_n$$

   - end

3. **Optimum (minimum)**

$$SSD = \min(SSD_n) = SSD_k, \quad (1 \leq k \leq 5)$$
$$\hat{y} = \hat{y}_k$$

In step one, the m pairs of data from the problem are presented. In a generic form, this data is designated with (x, y).

In step two: (a) data is fitted to polynomials of degrees 1 to 5, (b) they are graphed, and (c) the sum of squared deviations are evaluated.

In step three the optimal curve is selected, which corresponds to the lowest value of the values between $SSD_1,\ SSD_2, \ldots, SSD_5$, that is, $SSD = SSD_k$, for some k between 1 and 5. The optimal curve is

$$\hat{y}_k = p_1\, x^k + p_2\, x^{k-1} + \cdots + p_k\, x + p_{k+1}$$

5.4 Programme Functioning

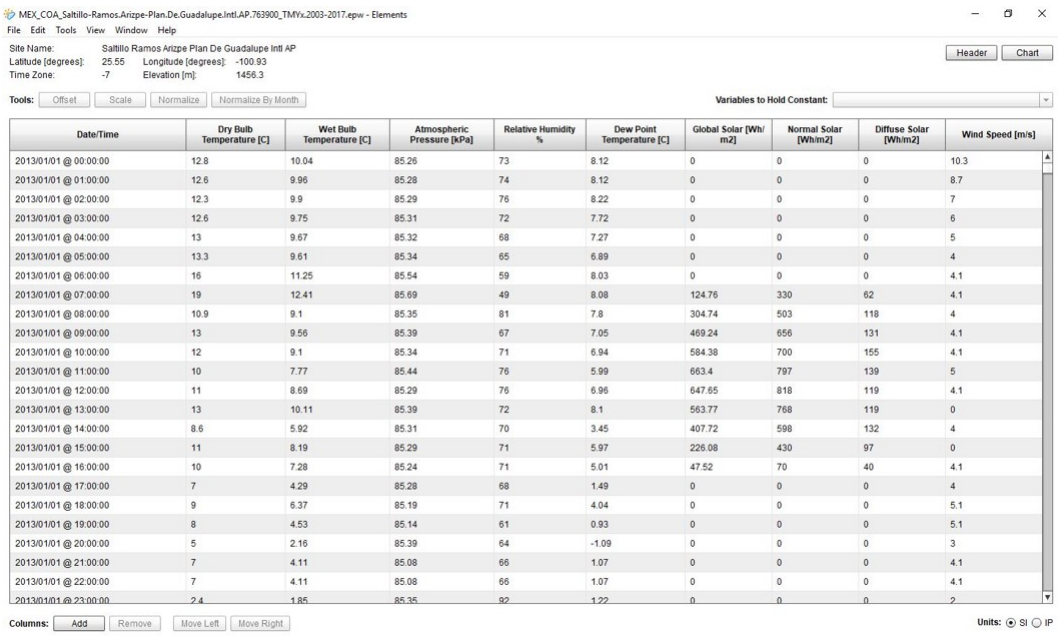
For using weather data projected in future climate change scenarios and using it in energy simulation software, diverse procedures of interpolation must be performed. To use EnergyPlus, *.epw* files need to be used. In this section, there is a detailed explanation of how this can be achieved using the programmes developed in MATLAB. The main ones (*SaltilloHorizontes.m*, *MonclovaHorizontes.m* and *TorreonHorizontes.m*) and further ones, used to run the main programmes, are detailed afterwards. Their codification is shown in Appendices from E to K.

5.4.1 Required Historical Data

The program uses historical weather information available in TMY files. To have the possibility of modifying this information, *Elements* software was used, since the columns that make up the weather files can be modified.

Elements is a free, open-source, cross-platform software tool used for creating or editing custom weather files and prepare them for building energy modeling. It was developed by Big Ladder, a company who provides software and services for the building energy modeling industry, mostly open-source software, specialised in the EnergyPlus simulation engine.

The interface allows to work with ten columns containing this information: date/time, dry bulb temperature ($^\circ C$), wet bulb temperature ($^\circ C$), atmospheric pressure (kPa), relative humidity ($\%$), dew point temperature ($^\circ C$), global solar (Wh/m^2), normal solar (Wh/m^2), diffuse solar (Wh/m^2) and wind speed (m/s), as shown in Figure 5.5.



Date/Time	Dry Bulb Temperature [C]	Wet Bulb Temperature [C]	Atmospheric Pressure [kPa]	Relative Humidity %	Dew Point Temperature [C]	Global Solar [Wh/m2]	Normal Solar [Wh/m2]	Diffuse Solar [Wh/m2]	Wind Speed [m/s]
2013/01/01 @ 00:00:00	12.8	10.04	85.26	73	8.12	0	0	0	10.3
2013/01/01 @ 01:00:00	12.6	9.96	85.28	74	8.12	0	0	0	8.7
2013/01/01 @ 02:00:00	12.3	9.9	85.29	76	8.22	0	0	0	7
2013/01/01 @ 03:00:00	12.6	9.75	85.31	72	7.72	0	0	0	6
2013/01/01 @ 04:00:00	13	9.67	85.32	68	7.27	0	0	0	5
2013/01/01 @ 05:00:00	13.3	9.61	85.34	65	6.89	0	0	0	4
2013/01/01 @ 06:00:00	16	11.25	85.54	59	8.03	0	0	0	4.1
2013/01/01 @ 07:00:00	19	12.41	85.69	49	8.08	124.76	330	62	4.1
2013/01/01 @ 08:00:00	10.9	9.1	85.35	81	7.8	304.74	503	118	4
2013/01/01 @ 09:00:00	13	9.56	85.39	67	7.05	469.24	656	131	4.1
2013/01/01 @ 10:00:00	12	9.1	85.34	71	6.94	584.38	700	155	4.1
2013/01/01 @ 11:00:00	10	7.77	85.44	76	5.99	663.4	797	139	5
2013/01/01 @ 12:00:00	11	8.69	85.29	76	6.96	647.65	818	119	4.1
2013/01/01 @ 13:00:00	13	10.11	85.39	72	8.1	563.77	768	119	0
2013/01/01 @ 14:00:00	8.6	5.92	85.31	70	3.45	407.72	598	132	4
2013/01/01 @ 15:00:00	11	8.19	85.29	71	5.97	226.08	430	97	0
2013/01/01 @ 16:00:00	10	7.28	85.24	71	5.01	47.52	70	40	4.1
2013/01/01 @ 17:00:00	7	4.29	85.28	68	1.49	0	0	0	4
2013/01/01 @ 18:00:00	9	6.37	85.19	71	4.04	0	0	0	5.1
2013/01/01 @ 19:00:00	8	4.53	85.14	61	0.93	0	0	0	5.1
2013/01/01 @ 20:00:00	5	2.16	85.39	64	-1.09	0	0	0	3
2013/01/01 @ 21:00:00	7	4.11	85.08	66	1.07	0	0	0	4.1
2013/01/01 @ 22:00:00	7	4.11	85.08	66	1.07	0	0	0	4.1
2013/01/01 @ 23:00:00	2.4	1.85	85.35	92	1.22	0	0	0	2

Figure 5.5: Weather File in *Elements*.

There is an interaction between the columns in this platform, so for example, when the dry bulb temperature is modified, also the wet bulb temperatures and the dew point temperatures are modified because they are directly affected. If the relative humidity is changed, also the wet bulb temperature and the dew point temperature change. The interaction between these values is managed internally by the software, and the ones that are not modified, remain the same as in the Historical Data weather file, as it is considered as the base for the modifications.

From the historical climate archive, the parameters of dry bulb temperature and relative humidity were extracted to establish a functional relationship between them; these data are hourly throughout a year, 8760 data for each one of the two columns. Given the complexity of the interaction of these parameters in energy simulations, generally only the temperature column is modified. In this research, the dry bulb temperature and relative humidity columns can be modified through mathematical procedures.

To enter this data and operate with the MATLAB codes prepared for Algorithm DGG3, the mentioned columns are extracted from the original *.epw* file from *Elements* to *Excel*, and from *Excel* to MATLAB, where the *.mat* files of both parameters are created.

Historical Data weather files displayed in *.epw* format, were obtained for Saltillo, Mon-

clova and Torreón from the repository of *Climate.OneBuilding.Org* [39], in which free climate data for building performance simulation can be downloaded. Data on this site are derived from public sources, typical meterological files (TMYx) are derived from ISD[5] (US National Oceanic and Atmospheric Administration's Integrated Surface Database) with hourly data through 2018 using the TMY/ISO 15927-4:2005 methodologies. ISD individual year files are created using the general principles from the IWEC (International Weather for Energy Calculations) Typical Meteorological Years that was published in 2001 [3].

The fields composing the Historical Data Files were extracted in *Excel*: *SaltilloWD.xls*. To operate the data management with MATLAB, the file *SaltilloWD.xls* became the *SaltilloWD.mat* permanent file.

Originally, the Historical Data of Saltillo is found in the *Excel* file *SaltilloWD.xls*, and is passed afterwards to the MATLAB table *SaltilloWD.mat*. This programme extracts the fields corresponding to temperature and relative humidity. Input data is downloaded inside the programme in MATLAB parting from data in *SaltilloWD.mat*.

5.4.2 Required Climate Projections Data

Temperatures

The temperatures of the horizons for RCP4.5 in Mexico were obtained from the UNAM Climatic Atlas for the localities considered for this study. These temperatures of the Representative Concentration Paths contemplate the minimum, average and maximum temperatures for the near, medium and far horizons.

Table 5.6 shows the amount of temperatures available on the UNAM website, as well as the amount of temperatures required for the simulations, and which can be obtained by Algorithm DGG3. It can be observed that 324 temperature data values are available and $236,520$ data values are required.

[5]Integrated Surface Database

Table 5.6: Annual Temperatures Data

		Available (*UNAM*)			Required (*Algorithm DGG3*)		
City	Horizon	Min	Ave	Max	Min	Ave	Max
	Near	12	12	12	8760	8760	8760
Saltillo	Medium	12	12	12	8760	8760	8760
	Far	12	12	12	8760	8760	8760
	Near	12	12	12	8760	8760	8760
Monclova	Medium	12	12	12	8760	8760	8760
	Far	12	12	12	8760	8760	8760
	Near	12	12	12	8760	8760	8760
Torreón	Medium	12	12	12	8760	8760	8760
	Far	12	12	12	8760	8760	8760
	Total	108	108	108	78840	78840	78840
	Total		**324**			**236520**	

Relative Humidity

With the hourly relative humidity and temperatures extracted from the historical data and contained in the corresponding *.mat* files, a functional relationship of relative humidity is obtained as a function of the temperatures.

These equations were obtained with the least squares procedure, and will be used in the determination of the relative humidity as a function of the temperatures for the weather projections of the horizons.

Relative humidity is typically measured in the field in real time. Obviously, the future relative humidities are not known; and although they depend on many factors, here the equations were obtained in terms of the temperature. In this way, there are $236,520$ temperature data *versus* $236,520$ relative humidity estimates.

Temperature plus Relative Humidity

For the three locations (Saltillo, Monclova, Torreón), the three horizons (near, medium,far), and the three types (minimum, average, maximum), there are:

$$\textbf{Total estimated data} = \mathbf{473040} \tag{5.6}$$

5.4.3 Master Programmes and Subprogrammes

The main objective of these master programmes, is to obtain temperature and relative humidity to create the *.epw* file needed for the energy simulation.

For Saltillo the master programme used is

$$\textit{SaltilloHorizontes.m} \tag{5.7a}$$

For Monclova the master programme used is

$$\textit{MonclovaHorizontes.m} \tag{5.7b}$$

For Torreón the master programme used is

$$\textit{TorreonHorizontes.m} \tag{5.7c}$$

The master programmes (5.7) delegate the calculations to the four programmes:

$$\textit{THR.m,} \qquad \textit{HR_T.m,} \qquad \textit{TempHorizontes.m,} \qquad \textit{HRh.m} \tag{5.8}$$

For the near, medium and far horizons of each city, with minimum, average and maximum temperatures, couples of temperature and relative humidity are estimated. Pairs of temperatures and relative humidity are estimated, so the total dimension of the results is 8760×3, giving a total of $157,680$ real values for each city. For the three cities a total of $473,040$ real values are given.

The master programmes (5.7), are used in similar ways. It will be exemplified with the city of Saltillo from the subsection 5.4.4, since the programmes for Monclova and Torreón operate the same way.

5.4.4 Master Programme for Saltillo

If it is only desired to obtain results from *Algorithm DGG3*, with the master programme (5.7a) for the specific location in Saltillo, it must be called in the following way:

```
>>  [C1,C2,C3,M1,M2,M3,L1,L2,L3] = SaltilloHorizontes;
```

Given that the weather file also resides in the folder where the programme is located

```
SaltilloWD.mat
```

For the three horizons of Saltillo: near, medium and far, with minimum, average and maximum temperatures, in each of them, hourly temperature and relative humidity pairs are estimated.

The explanation of the variables is presented in Table 5.7. Each one of the variables is of order (8760×2).

Table 5.7: Pairs of Temperatures and Relative Humidity

Horizon	Variables	Type
Near	(C1, C2, C3)	(Minimum, Average, Maximum)
Medium	(M1, M2, M3)	(Minimum, Average, Maximum)
Far	(L1, L2, L3)	(Minimum, Average, Maximum)

Important: At the end, it is suggested to generate *.mat* files for each variable to preserve the results. These results can be entered in *Elements*, in the two columns of dry bulb temperature and relative humidity. In this way, new climate files are created for the three horizons.

Figure 5.6 outlines the algorithm flow diagram.

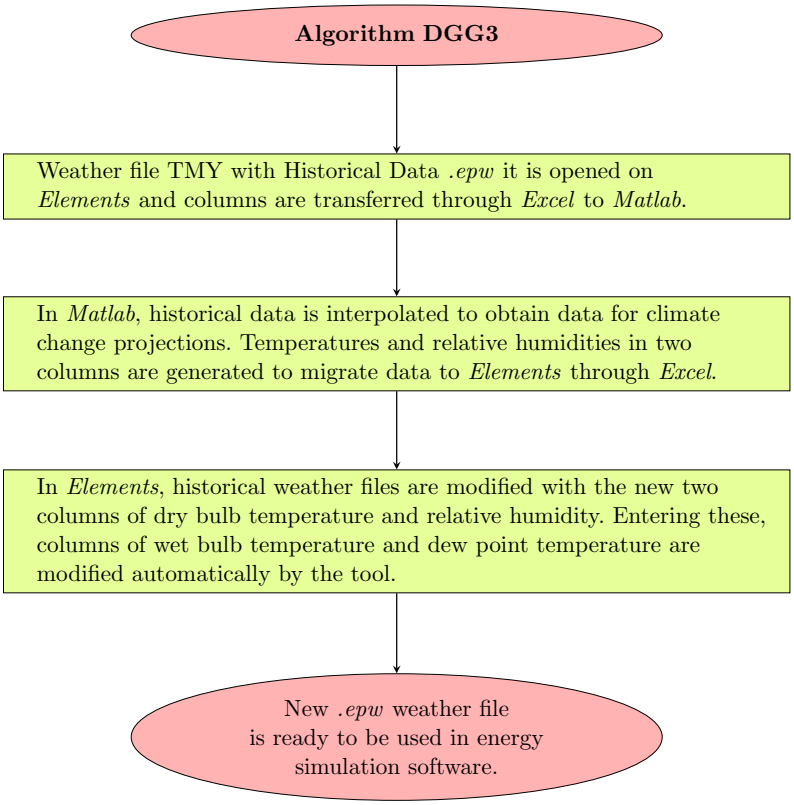


Figure 5.6: Algorithm DGG3.

SaltilloHorizontes.m Supporting Programmes

The master programme (5.7a), requires, for its operation, the programmes (5.8). Detailed information on these programmes is now provided. These can be found in the following subsections, 5.4.5, 5.4.6, 5.4.7 and 5.4.8.

5.4.5 Programme *THR.m*

This programme calls:

```
>>  [T,HR,hrMes] = THR;
```

Provides the results:

1. It converts the file *SaltilloWD.xls* (*Excel*) to the table *SaltilloWD.mat* (MATLAB)

of the annual historical files in their columns of temperature and relative humidity.

2. Shows the message

```
Annual Minimum, Average and Maximum Values in Saltillo
  Temperature in Celsius Degrees
   -5.0000   18.0265   38.0000
  Percentage of Relative Humidity in Saltillo
   12.0000   60.1990  100.0000
```

3. Gives temperature column vector.

$$T \quad (8760 \times 1)$$

4. Gives relative humidity column vector.

$$HR \quad (8760 \times 1)$$

5. Gives the interval in hours for each month, from January to December

```
hrMes = [1          744;          % January
         745        1416;         % February
        1417        2160;         % March
        2161        2880;         % April
        2881        3624;         % May
        3625        4344;         % June
        4345        5088;         % July
        5089        5832;         % August
        5833        6552;         % September
        6553        7296;         % October
        7297        8016;         % November
        8017        8760];        % December
```

Coding can be found in Appendix I.

5.4.6 Programme *HR_T.m*

Taking the results of the previous programme as data, this programme calls:

```
>> HRT = HR_T (T,HR,hrMes);
```

Obtains the least squares equations: relative humidity as a function of temperature, for each month of the year, according to the historical data in Saltillo, Coahuila, *(SaltilloWD.mat)* table.

Provides the results:

1. The graphs show the scatter diagrams and the corresponding fourth degree polynomials. Figure 5.7 presents the scatter diagram of the January temperatures and the least squares fit curve, which is, the best-fitting curve to the given set of points. Figure 5.8 is the relative humidity noise graph for this month.

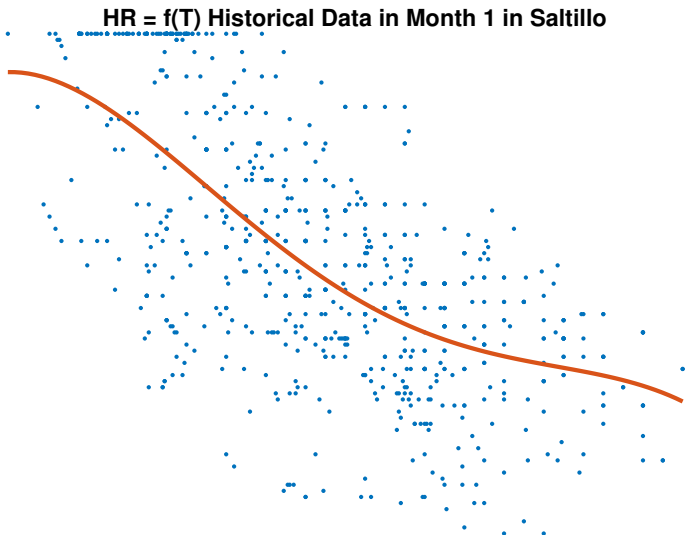


Figure 5.7: Scatter diagram and relative humidity adjustment curve as a function of temperature for January.

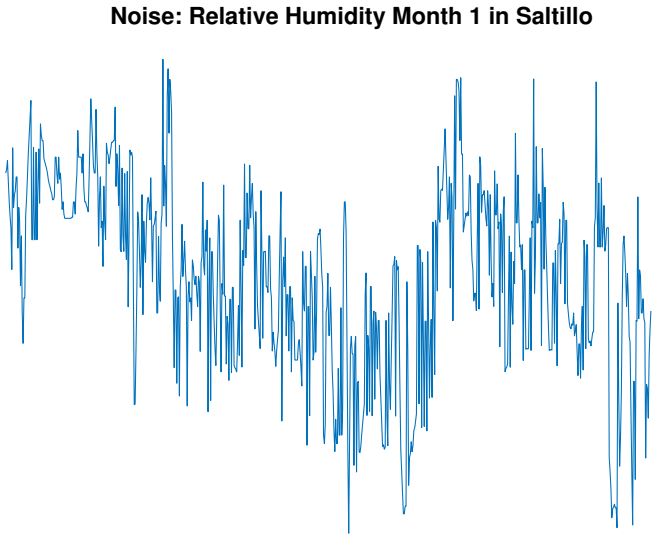


Figure 5.8: Noise diagram of relative humidity in January.

The programme also presents pairs of graphs for every month of the year.

2. Equations of least squares curves; relative humidity as a function of temperatures for each month.

$$HRT = \begin{bmatrix} -0.0002 & 0.0108 & -0.1323 & -2.1406 & 87.7813 \\ -0.0005 & 0.0321 & -0.6141 & 1.0502 & 96.4372 \\ 0.0005 & -0.0295 & 0.4966 & -2.1692 & 58.1605 \\ -0.0005 & 0.0420 & -1.3100 & 14.7756 & 14.8066 \\ -0.0003 & 0.0307 & -1.2587 & 19.1643 & -25.3882 \\ -0.0018 & 0.1706 & -5.7547 & 79.6454 & -297.5011 \\ 0.0001 & -0.0104 & 0.3101 & -6.9737 & 145.7270 \\ -0.0022 & 0.2041 & -6.9642 & 98.5296 & -404.1622 \\ -0.0008 & 0.0901 & -3.4534 & 52.3468 & -178.3008 \\ 0.0001 & 0.0080 & -0.6468 & 10.2899 & 38.2716 \\ -0.0007 & 0.0492 & -1.2639 & 11.2051 & 42.7231 \\ -0.0000 & 0.0053 & -0.1645 & -0.9869 & 86.1778 \end{bmatrix} \tag{5.9}$$

For example, for the month of June, row 6, the fit equation is

$$HR = -0.0018\,T^4 + 0.1706\,T^3 - 5.7547\,T^2 + 79.6454\,T - 297.5011.$$

In Figure 5.7, the coordinates of the points of the scatter diagram are abscissas: the first 744 temperatures of the month of January of the historical data, and ordinates: the first 744 historical relative humidities. It was experimented with these ordered pairs, (Table 5.5), subjecting them to a least squares fit, for polynomials of degrees 2, 3, 4 and 5. It was observed that the smallest sum of the squared or residual deviations occur with fourth degree equations.

As mentioned in page 139, relative humidity results from measurements in the field and as they are not available for the future, only a functional relationship between temperature and relative humidity is established here. Two of the pillars of comfort parameters are these, so it was decided to relate both factors. This decision was strengthened by the fact that the models discussed later are based exclusively on proposals for temperature values.

The noise graph in Figure 5.8 shows the differences between the relative humidities of the historical data and the values calculated with the fit curve.

The coding of this programme can be found in Appendix J on page 389.

5.4.7 Programme *TempHorizontes.m*

The programme runs like this:

```
>> [TC,TM,TL] = TempHorizontes;
```

It presents the following information:

1. Temperatures provided by the UNAM, contained in the work folder.

```
Monthly Near Horizon Temperatures  (2015-2039)
   minimum   medium    maximum
    5.2000   11.8000   20.0000
    6.0000   13.5000   20.9000
    8.5000   17.2000   26.0000
   12.9000   20.9000   30.5000
```

```
   15.8000   23.7000   33.1000
   17.0000   24.7000   34.6000
   17.1000   25.2000   34.4000
   16.5000   24.2000   33.9000
   15.1000   22.7000   31.6000
   12.3000   19.0000   28.3000
    8.9000   15.6000   24.4000
    6.5000   12.9000   20.1000

Monthly Medium Horizon Temperatures  (2045-2069)
   minimum   medium    maximum
    6.1000   13.0000   21.5000
    7.1000   14.3000   23.5000
    9.7000   17.9000   27.7000
   13.3000   21.7000   31.8000
   16.8000   24.8000   35.2000
   18.0000   25.8000   35.7000
   17.9000   25.8000   35.8000
   17.4000   25.2000   34.4000
   15.9000   23.4000   32.2000
   13.3000   19.9000   29.2000
    9.8000   15.9000   25.0000
    7.4000   14.1000   21.4000

Monthly Far Horizon Temperatures  (2075-2099)
   minimum   medium    maximum
    6.7000   12.8000   22.0000
    7.8000   15.3000   23.9000
   10.4000   18.9000   28.2000
   14.2000   22.7000   32.6000
   17.6000   25.3000   35.6000
   18.3000   25.7000   36.2000
   18.5000   26.8000   35.4000
   17.7000   26.2000   34.4000
   16.2000   23.7000   32.4000
```

```
13.8000   20.3000   29.0000
10.3000   16.5000   24.6000
 8.5000   13.9000   21.5000
```

2. The programme then presents these messages:

```
* With these temperatures of the horizons, their 4th Degree
equations are generated (least squares), they are shown below.

** These equations are used to evaluate the temperatures of the
horizons in each hour of the year.

*** With the temperatures of the horizons the relative humidity
in the horizons are evaluated.
```

The programme presents nine graphs of hours *versus* temperatures for Saltillo. For each of the three horizons, a graph is generated for minimum temperatures, another for average temperatures, and another for maximum temperatures, for each hour of the year. For illustrative purposes only the first three are included here. Figures 5.9 - 5.11.

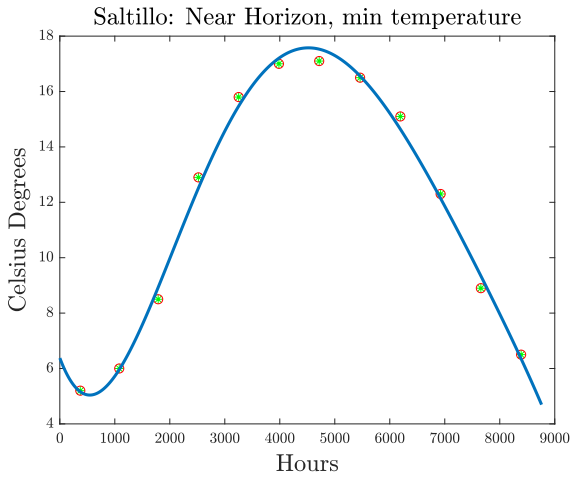


Figure 5.9: Saltillo: Near Horizon, Minimum Temperatures

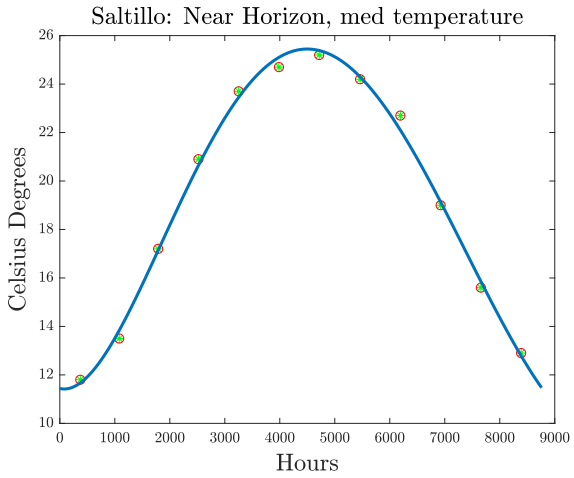


Figure 5.10: Saltillo: Near Horizon, Average Temperatures

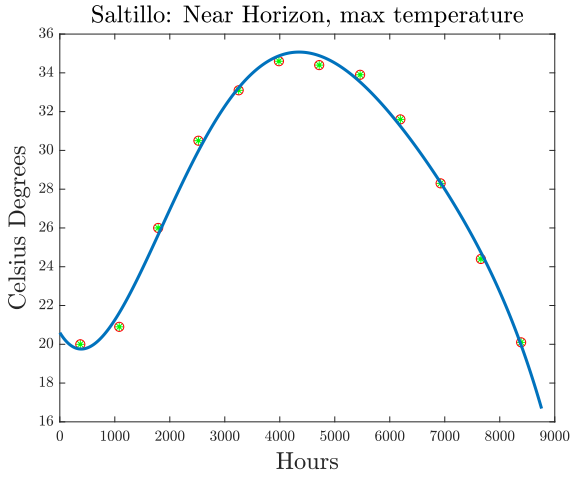


Figure 5.11: Saltillo: Near Horizon, Maximum Temperatures

3. Obtains as results the temperatures of the scenarios or horizons, calculated with least squares, in Saltillo, Coahuila, Table 5.8.

Table 5.8: Horizons Temperatures for Saltillo

Horizon	Variables	Matrix Order	Temperature Type
Near	TC	8760×3	Minimum, Average, Maximum
Medium	TM	8760×3	Minimum, Average, Maximum
Far	TL	8760×3	Minimum, Average, Maximum
	Total	78,840	

Each of the nine sets with 12 temperature data provided by the UNAM, fits to a fourth degree polynomial[6]. With this polynomial, the curve is graphed and the temperatures are evaluated for the 8760 hours per year.

This is, from the 108 temperature data provided by the UNAM, $78,840$ temperature values are estimated; calculated from the nine least square equations for each hour of the year.

The code for this programme is found in Appendix K on page 392.

5.4.8 Programme *HRh.m*

Taking the results of the previous programme as data, this programme calls:

```
>> [C1,C2,C3,M1,M2,M3,L1,L2,L3] = HRh (HRT,TC,TM,TL,hrMes);
```

The following lists appear in its development:

1. It presents the Table 5.9

[6]It was determined experimentally, (Table 5.5), that adjusting the data to a fourth degree polynomial the best results are obtained.

Table 5.9: Fourth degree equations to calculate the relative humidity by month

Month	Interval in hours	Equations to calculate the relative humidity of the horizons				
Jan	$1-744$	-0.00019387	0.010757	-0.13231	-2.1406	87.781
Feb	$745-1416$	-0.00052104	0.032122	-0.61408	1.0502	96.437
Mar	$1417-2160$	0.00046794	-0.029453	0.49664	-2.1692	58.161
Apr	$2161-2880$	-0.00047624	0.041999	-1.31	14.776	14.807
May	$2881-3624$	-0.00026592	0.030703	-1.2587	19.164	-25.388
Jun	$3625-4344$	-0.0018315	0.17065	-5.7547	79.645	-297.5
Jul	$4345-5088$	0.00013565	-0.010439	0.31009	-6.9737	145.73
Aug	$5089-5832$	-0.0021563	0.20411	-6.9642	98.53	-404.16
Sep	$5833-6552$	-0.00082221	0.090123	-3.4534	52.347	-178.3
Oct	$6553-7296$	$7.8535e-05$	0.0080059	-0.64685	10.29	38.272
Nov	$7297-8016$	-0.0006784	0.04919	-1.2639	11.205	42.723
Dec	$8017-8760$	$-1.4085e-05$	0.0053194	-0.16448	-0.98689	86.178

These are the intervals and coefficients of the equations (5.9).

2. The programme then presents these messages:

```
**** With the determination of the relative humidities for each
hour, the temperatures and relative humidities of the stations
are known for the three temperatures. OK

Dimensions of temperatures and relative humidities:
        8760           9        8760           9
```

3. Obtains as results:

```
C1, C2, C3  hourly pairs of temperature and relative humidity
            in the near horizon.
M1, M2, M3  hourly pairs of temperature and relative humidity
            in the medium horizon.
L1, L2, L3  hourly pairs of temperature and relative humidity
            in the far horizon.

            Subscript 1, 2 and 3, are minimum, average, and
            maximum temperatures correspondingly.
```

These results are presented in Appendix F for near, medium and far horizons, Tables F.2, F.3 and F.4, correspondingly. The summarised information with the obtained values appears like in Table 5.10.

Table 5.10: Temperatures and relative humidities for the near horizon, Saltillo

Month	Hour	Minimum		Average		Maximum	
i	j	$(T,$	$H)$	$(T,$	$H)$	$(T,$	$H)$
1	1	6.3759	71.222	11.439	58.765	20.599	46.664
	2	6.3706	71.236	11.438	58.766	20.594	46.667
	⋮	⋮	⋮	⋮	⋮	⋮	⋮
	744	5.1826	74.491	12.589	56.457	20.308	46.864
2	745	5.184	89.477	12.592	63.327	20.311	44.915
	746	5.1854	89.473	12.596	63.316	20.314	44.91
	⋮	⋮	⋮	⋮	⋮	⋮	⋮
	1416	7.2136	82.706	15.331	55.17	23.401	40.123
⋮	⋮	⋮	⋮	⋮	⋮	⋮	⋮
12	8017	7.8991	70.686	14.289	53.426	22.598	37.595
	8018	7.895	70.697	14.285	53.437	22.592	37.601
	⋮	⋮	⋮	⋮	⋮	⋮	⋮
	8760	4.6951	78.462	11.471	61	16.686	47.537

4. At the end, its suggested to back up the results in *.mat* files:

```
Near Horizon, minimum, average and maximum projections
>> save CerMinS.mat C1; save CerMedS.mat C2; save CerMaxS.mat C3;

Medium Horizon, minimum, average and maximum projections
>> save MedMinS.mat M1; save MedMedS.mat M2; save MedMaxS.mat M3;

Far Horizon, minimum, average and maximum projections
>> save LejMinS.mat L1; save LejMedS.mat L2; save LejMaxS.mat L3;
```

5.4.9 Master Programmes for Monclova y Torreón

The procedure that was carried out for the city of Saltillo was done in the same way for the cities of Monclova y Torreón as mentioned in Subsection 5.4.3. These developments are covered from Subsection 5.4.4 to Subsection 5.4.8.

The codes of these programmes can be consulted in the Appendix G.1.1 for Monclova, and in Appendix H.1.1 for Torreón.

The summarised information with the obtained values appears in Tables G.1, G.2 and G.3 for near, medium and far horizons for Monclova, and Tables H.1, H.2 and H.3 for Torreón.

5.5 Conclusions

At early stages of this research, the IPCC climate information for SRES scenarios was available for Coahuila.

In mid-2020, this information was updated with the RCP pathways for Mexico, and they were made available for consultation in the UNAM Climatic Atlas website. Because of this, it was chosen to use this updated information in the development of Algorithm DGG3.

Even so, the previous information generated by both Algorithm DGG1 and Algorithm DGG2, including the SRES and RCPs, can also be used to generate weather files with Algorithm DGG3.

Some characteristics of this algorithm are listed below.

1. This is an objective numerical method, which resorts to least squares approximations of polynomial functions.

2. The large amount of information involved in this algorithm is handled with MATLAB, which specialises in efficiently operating with arrays. For this and its graphic facilities it is widely used in universities and industry.

3. This algorithm is not a climate model. It uses historical numerical information from weather files and projected temperatures for future scenarios supplied by climate experts.

   (a) The columns of temperature and relative humidity are extracted from the historical weather file *.epw* for each city; this establishes a relationship of relative humidity as a function of temperature, for each hour of the year.

   (b) From the temperatures provided by the climate experts, equations are adjusted for each year, type, horizon and location.

   (c) The relative humidities that correspond to these temperatures are calculated with the formulas of point (b).

   (d) Of the 324 temperature data provided by the UNAM, a total of 473,040 pairs of temperature and relative humidity values were estimated with the algorithm. See total in (5.6), page 140.

4. The values obtained with Algorithm DGG3, from step 3, are introduced as new parameters in the temperature and relative humidity columns of the *.epw* weather files. This updated information is processed to obtain new weather files used in energy simulations.

5. Different scenarios and projections can be analysed (SRES, RCP,...), as the algorithm is not restrictive of the climate model used to gather these data.

6. Although this research was applied to regional data from Coahuila, it is possible to adapt it to anywhere in the country[7].

   It can even be used to generate files for other countries, if the following information is available: historical weather file, and at least one temperature per month for weather projections.

7. Generally, average temperatures are used for energy simulations. However, the algorithm also allows obtaining weather files of extreme maximum and minimum temperatures, in case it is wanted to study these two components.

[7] In any case, an adaptation of the programme shown in Appendix F can be used, replacing the information from Saltillo for the desired location; available in the UNAM Climatic Atlas website.

8. Unlike the common methods that handle information by cities, data interpolation is generated depending on the geographic coordinate, not on the city, so accuracy is higher in the generation of these weather files.

9. It is not computationally expensive; weather files are generated for the cases required instead of the use of a big database containing the *.epw* files.

10. The generality of the algorithm allows modifying hypothetical or real parameters; a basic research question can be formulated and studied with the use of the algorithm, and explore answers to questions like: 'What if...?'

11. The coding of the algorithm developed here is easily accessible, since MATLAB is a widely available software in the research environment.

The Algorithm DGG3 expands the possibilities of studying with greater precision the thermal behavior of buildings, and if desired, the energy savings. The possibility that it offers when generating the climate projections weather files for specific locations allows the study of the multiple differences that can be found even within the same city.

The files that were generated with this procedure were used for the simulations presented in Chapters 6 and 7 of this document.

Part III

Social Housing Climate Resilience

Chapter 6

Building Thermal Simulation

This part of the document focuses on social housing climate resilience, and defines the parameters used to study thermal comfort in the proposed study cases and the results obtained with dynamic thermal simulations; this is covered in this chapter and in Chapter 7 correspondingly. While in this chapter, the characteristics and parameters that were assigned to the dwellings to perform the dynamic simulations are explained and defined, in the following chapter the results of the simulations are presented.

The typical characteristics of social housing in Coahuila as documents by NAMA [121] were used to set the parameters for simulation. Thence, diverse modifications in the parameters composing the building were changed to analyse the most suitable for each location. This chapter details all the components that were chosen for the dynamic thermal simulations, as the reasoning and rationale behind these choices. A total of 984 simulations were performed, of which 246 were considering current weather, and 738 for climate change projections weather files. These simulations include three sets conformed by 41 cases with two different house orientations for each city. All the simulations displayed by case are shown in Appendix L.

Simulation cases and strategies were performed for Saltillo, Monclova, and Torreón in three future climate change horizons; the Near Horizon (NH) for years 2015-2039, the Medium Horizon (MH) for years 2045-2069 and the Far Horizon (FH) for years 2075-2099. Subsequently, a Base Case, and cases from 1 to 40 were evaluated. Synthesized information of this assignations appears in Figure 6.1, in where a diagram shows the

disposition of simulation cases and the definition of the parameters considered for the building thermal simulations. In addition to the presented diagram, in this chapter the software used to accomplish the needed by simulations is described, as the envelope elements detailed characteristics.

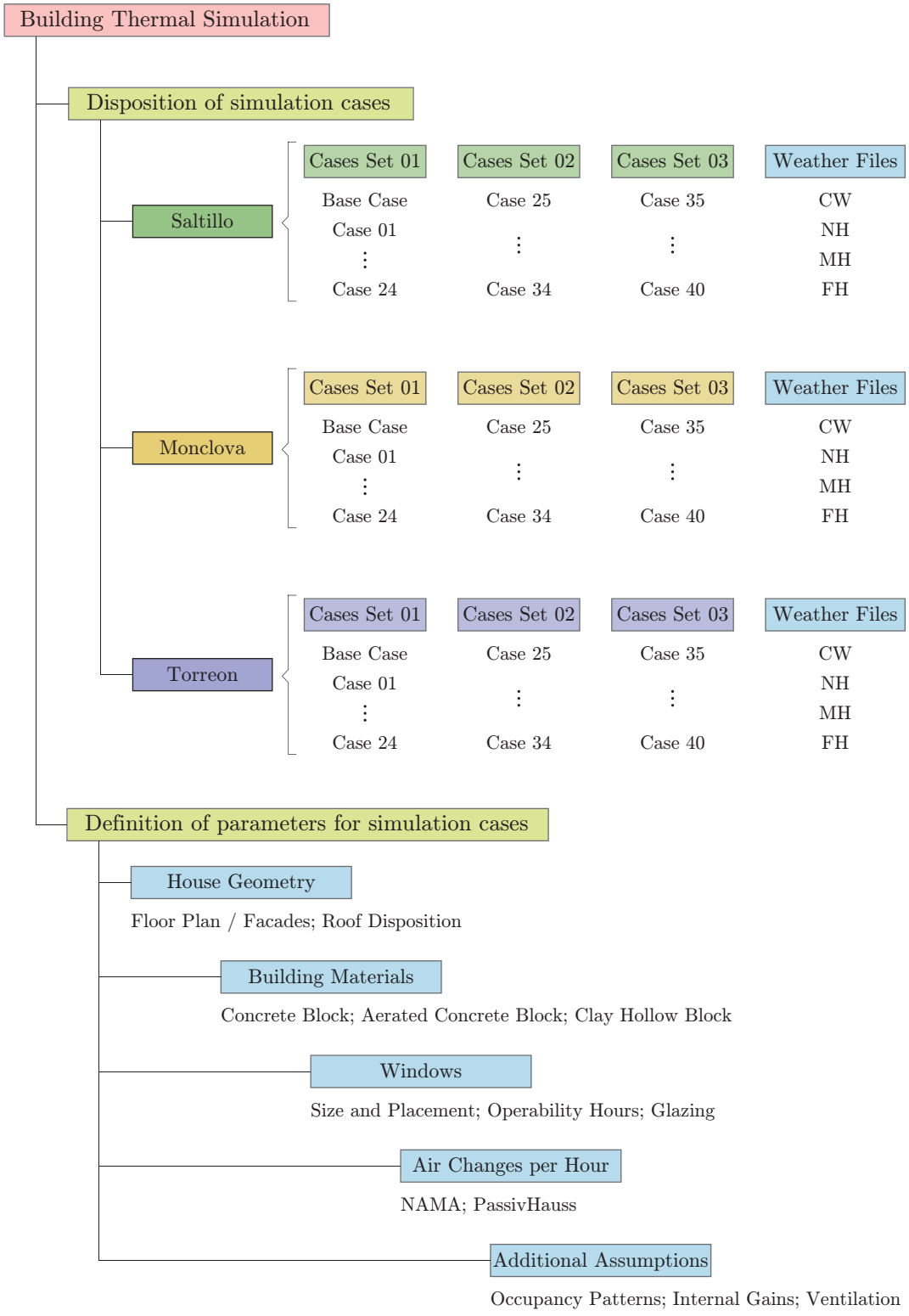


Figure 6.1: Building Thermal Simulation Diagram.

Dynamic simulations were performed in three parts or sets of simulations through a parametric study to analyse the most appropriate interaction between the envelope components. Each case was specified under certain building envelope characteristics that are explained in Section 6.1. In the mentioned section, three diagrams disclose in more detail the disposition of cases assigned to the three sets of dynamic simulations, with the envelope elements conforming them: house geometry and roof disposition, building materials, window size and placement, specifications of operable windows, glazing, and air changes per hour.

In Section 6.2, the study used a representative model of an affordable housing typology defined as a *Reference Dwelling*. Considering this dwelling, the physical characteristics along with the floor plan disposition and dimensions of the denominated *Base Case* and the *Compact Floor Plan* dwellings are described; these two comprise all the architectural floor plans of the simulations.

To perform dynamic simulations, many specifications of the architectural object must be covered, among which the physical characteristics and qualities of the building, as well as the activities and objects that operate within it, stand out. This is covered in Section 6.3, which specifies the software that was used for the investigation, assumptions for the dynamic simulation, and the meteorological files that were used to cover the study for the current and projections of climate, specified in the previous chapter.

Additional variations regarding the building envelope are described in Section 6.4 such as building materials and layers in walls, roofs, floors, windows and frames, as the slight geometry modifications in roofs.

6.1 Dynamic Simulation Scope

The research criteria was determined by indoor thermal comfort stated in annual percentages. For the research scope, results were compared in terms of comfort hours increment and resultant envelope performance of a typical social house and the proposed changes on it; this to find the best performing envelope combination among those proposed for the three cities.

The parametric study was accomplished through dynamic simulations; simulation sets were divided in three parts to analyse and define the most appropriate interaction between the building envelope components for the proposed locations.

The first set is conformed by the interaction of all elements comprising the envelope; this is the integration of every different material in walls, layers of glass in windows, and the use of overhangs in windows and roofs. For the second set, the best case of the first set was taken, and a new disposition of windows and roofs was evaluated. Finally, for the third set, a new compact geometry with gable roof was simulated to compare it with the base case geometry and the best case of the second set.

There is a big amount of parameters considered for the dynamic simulations, so in order to clarify the envelope components used for these, their key codes appear in Table 6.1. In this table, they are mentioned, and their interaction is shown in diagrams 6.2, 6.3, and 6.4. All of these envelope parameters and their characteristics are thoroughly explained from Subsections 6.4.1 to 6.4.5, starting from page 183.

Table 6.1: Key Codes for Envelope Components used in Dynamic Simulations.

Key Code	Acronym	Envelope Components
		(A) House Geometry and Roof Disposition
A1	BCG	Base Case Geometry with Flat Roof
A2	SRO	Sloped Roof with Overhang
A3	HOR	Horizontal Overhang in Roof, two extra stretcher courses of block in walls
A4	OR	Horizontal Over Roof, two extra stretcher courses of block in walls
A5	ORS	Over Roof Rotated South, two extra stretcher courses of block in walls
A6	ORN	Over Roof Rotated North, two extra stretcher courses of block in walls
A7	GR	Gable Roof
A8	GRC	Gable Roof and Ceiling
		(B) Building Materials
B1	CB	Concrete Block
B2	AACB	Autoclaved Aerated Concrete Block
B3	CHB	Clay Hollow Block
		(C) Window Size and Placement
C1	WBC	Window Base Case
C2	WM1	Window size and placement Modification for Base Case Geometry
C3	WM2	Window size and placement Modification for Compact Geometry
C4	WM3	Window size and placement Modification for Compact Geometry with additional windows
		(D) Operable Windows (months)
D1	OWBC	Operable Windows Base Case
D2	OW1	Operable Windows 1
D3	OW2	OW 2 with horizontal overhangs in (a) W, (b) SEW, and clerestory windows
D4	OW3	OW 3 with clerestory windows
D5	OW4	OW 4 with clerestory windows in added stretcher courses
D6	OW5	OW 5 for Compact Geometry
		(E) Glazing
E1	SG	Single Glazing
E2	DG	Double Glazing
		(F) Air Changes per Hour
F1	ACHBC	5.0 ACH @ 50 Pa, NAMA Base Case
F2	ACH1	0.6 ACH @ 50 Pa, *PassivHaus* Standard
F3	ACH2	0.3 ACH @ 50 Pa, *PassivHaus* Standard (lower target)

The interaction between the envelope components were used for simulations in the base case, and in cases from 1 to 24 for the three cities.

It was proposed to compare the typical housing made of concrete block with other two materials used in the state and had shown a good performance in previous studies: these are described in more detail in Section 6.4. These building materials were simulated along with the rest of the components of the envelope; the assumptions of the internal heat gains are shown in Section 6.2. Single and double glazing were also used to compare their thermal performance in conjunction with the other elements, and how they affect the standard comfort levels.

The first part of the simulations and its elements interaction is shown in Figure 6.2.

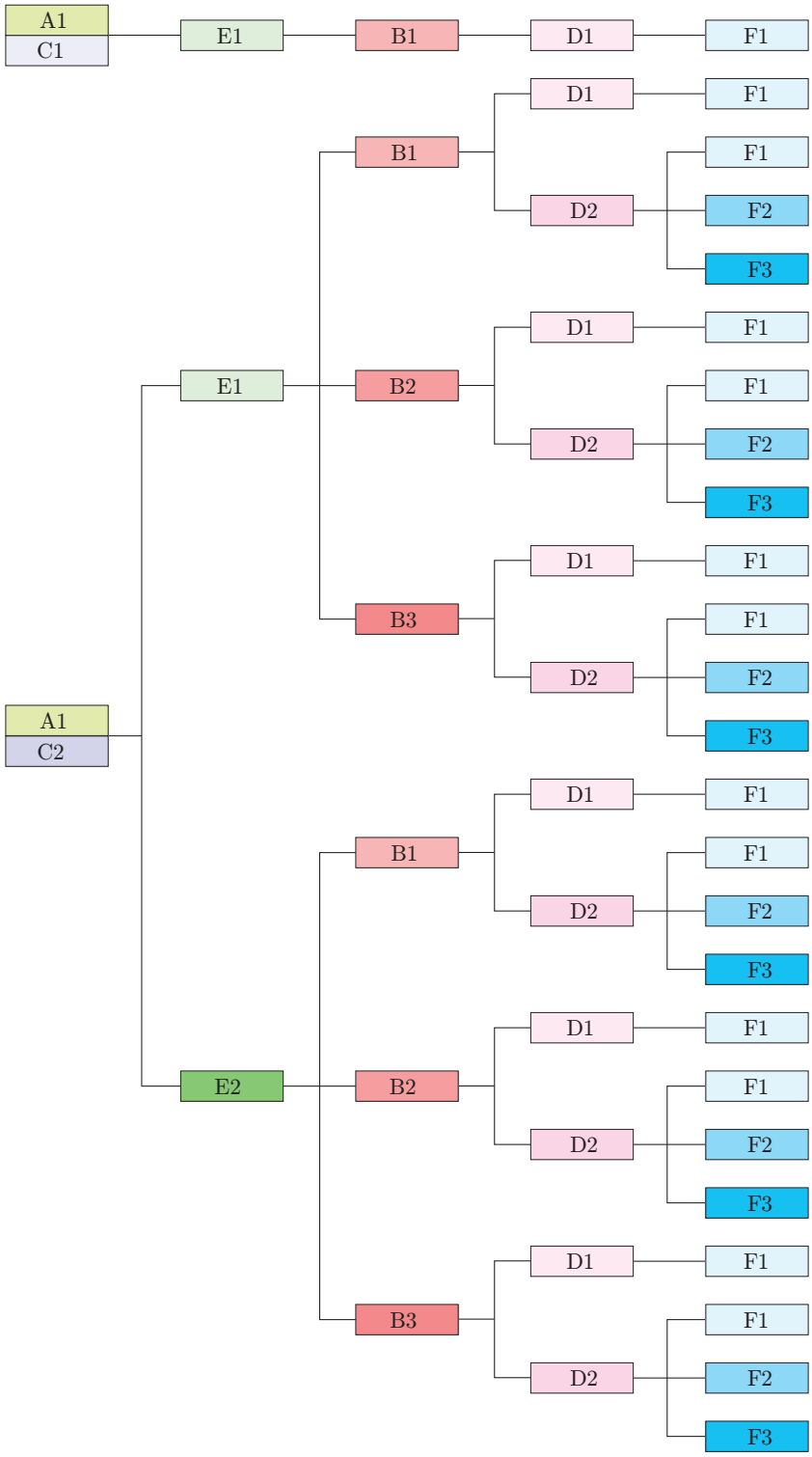


Figure 6.2: First Part of Dynamic Simulation Diagram.

The cases that shown the more annual hours of comfort were reevaluated to perform new simulations, these compose the part two. The new values on the parameters previously used where modified to find the fitter for each location. These correspond to

cases from 25 to 34; the interaction between these can be appreciated in Figure 6.3.

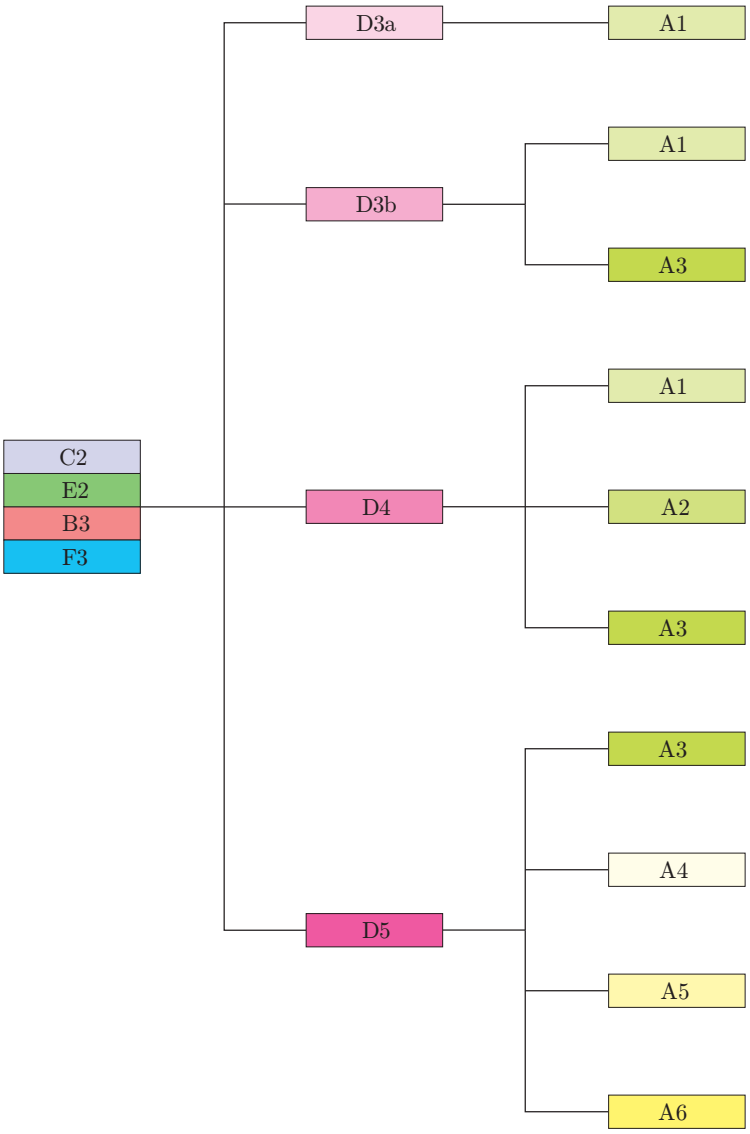


Figure 6.3: Second Part of Dynamic Simulation Diagram.

For the third part, a new geometry was considered, more compact in terms of form, and with gable roofs. Two envelope materials characteristics were applied to this new shape, those used for the base case in part one, and those used in the best case in part two. The intention behind this was to analyse how the form affected the thermal comfort under the same envelope characteristics.

The diagram of these is shown in Figure 6.4.

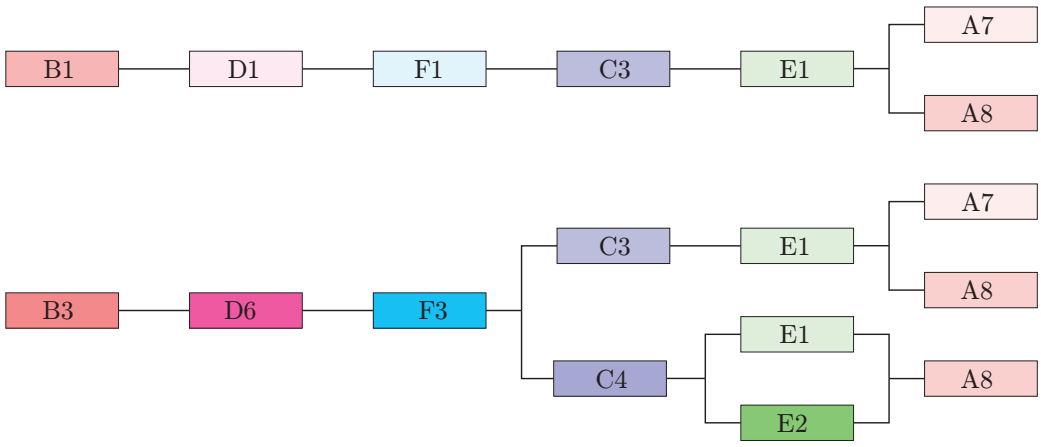


Figure 6.4: Third Part of Dynamic Simulation Diagram.

6.2 Disposition of the Dwelling

The most common distribution, areas and characteristics of dwellings for social housing in Mexico was explained in subsection 1.2.1. The typology *Popular Housing* from Table 1.3 was chosen for the simulations due to this, and because it was extensively explored in the NAMA documentation described in subsection 1.2.2, which consists of studies of sustainable housing in Mexico. The characteristics of this reference dwelling are described in subsection 6.2.1.

From the reference dwelling, a base case dwelling was generated and modeled for the simulations; its characteristics are specified in subsection 6.2.2, with its corresponding dimensions, plan and section. From this initial model, different attributes of the building envelope were further simulated, using the same floor plan.

A second distribution was considered for a different set of simulations, the compact floor plan dwelling, with equal amount of square meters as in the base case, the same spaces, and different volumes. A detailed description of the first of these cases appears on subsection 6.2.3, and further modifications were also performed for simulations using this floor plan.

6.2.1 Reference Dwelling

The floor plan, geometry and areas of the houses used for the simulations were considered taking into account the models used in the NAMA documentation [121]. As this is extensive and covers the main aspects on energy performance in social housing in Mexico, all specifications mentioned for the Base Case of this section were used to perform dynamic simulations and assumptions related with the operation of the houses.

The model considered was a real life social housing project provided by GOPA/GIZ, and based on a Campos project [7]. In Figure 6.5, it is shown the disposition and the 3D model developed for the named project. Plans and disposition were considered for its use as the Base Case for the simulations of this research.

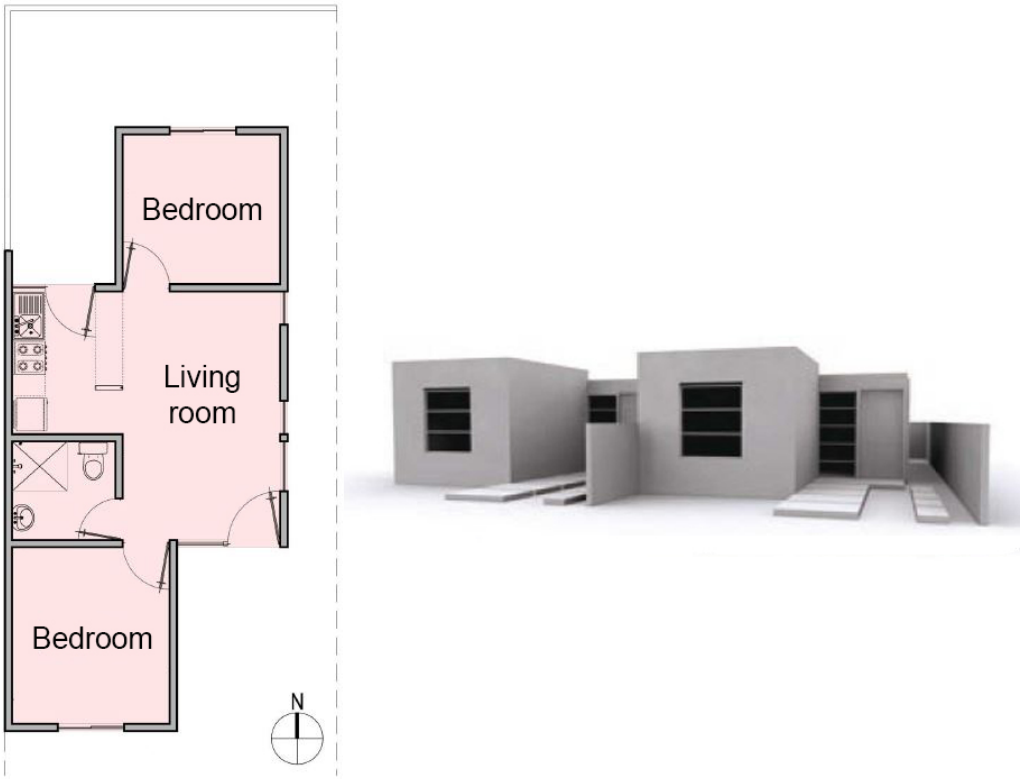


Figure 6.5: Detached House Typology. Floor Plan and 3D Model, not to scale. Source: Campos [7].

In the mentioned study, three typologies of houses were studied, the detached house, the semi-detached house, and the flat. These are representative of the most popular social housing building designs in Mexico. From the three models, the detached house was selected for its clarity with respect to the others and in order to appreciate the

envelope elements which perform better regarding thermal comfort.

It was found that in other typologies, like the duplex house, the highest energy demands were presented, so it requires a greater investment to reduce these demands. This demonstrate the importance of providing with designs and buildings specific characteristics depending on each climate region and typology, as well as the risks and costs involved in adopting the same construction and design systems without distinction.

Until 2016, only the 0.01% of the total housing in Coahuila were buildings of three or more levels that house at least three households. So vertical housing with flats are not a common typology of housing in this part of the country, this is why flats were not considered for this research. Attached and semi-detached housing are the predominant buildings used for this purpose, although there is a lack of information regarding in how many of each exist in Coahuila.

The detached house was selected because it allowed a better understanding of how each parameter behaved individually as a component of the building envelope without the action of external components. To perform these simulations, only one thermal zone was selected, this is why the semi-detached house was also discarded.

The aim of the research was to show how current and possible climate change scenarios impacted the thermal behavior of these houses adapting the weather files as shown in Chapters 3, 4 and 5, so it was a better choice to keep the models as simple as possible to see this impact.

6.2.2 Base Case Dwelling

Some minor modifications where made to fit the house to the common current conditions of social housing built in Mexico. The Base Case house was attached to the perimeter wall in such a way that it allows natural ventilation in the bathroom and kitchen, see Figure 6.6.

The area and dimensions were adequate to fit the regulations of this type of dwellings, the so called *Popular Housing*, with a floor area of 50 m^2. Its areas comprehend one bathroom, a kitchen, living room, dining room, two bedrooms and one parking spot.

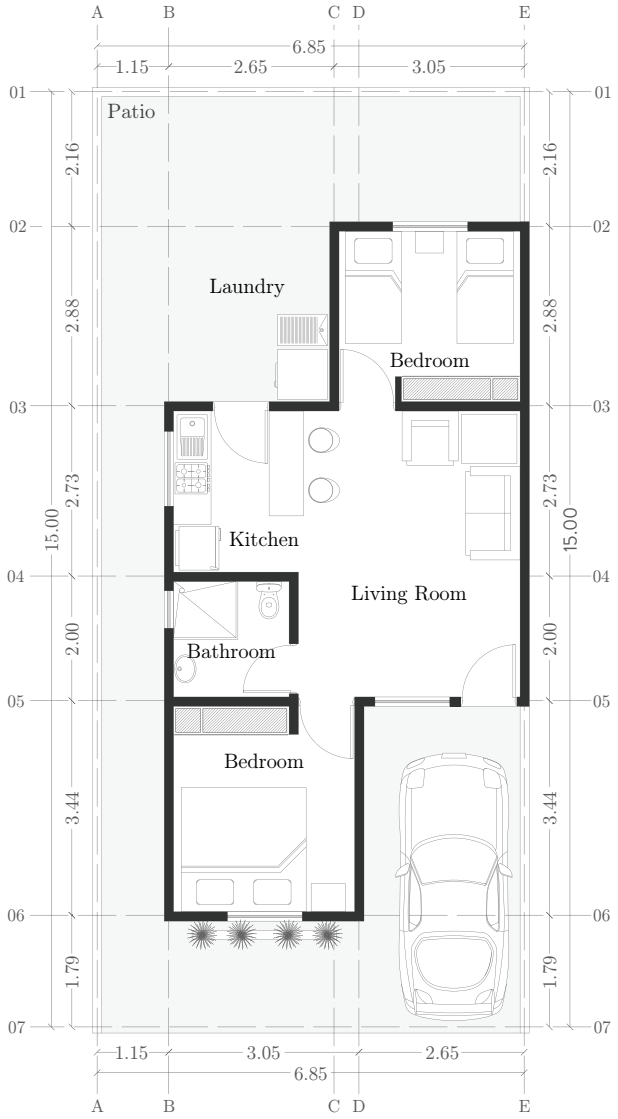


Figure 6.6: Base Case of Detached House Typology.

This house was used in the Base Case, and in cases from 1 to 34 considering two different orientations, north-south and east-west. This model was used to try the best combination of envelope components without modifying the floor plan in any of these cases. The Base Case Floor Plan appears in Figure 6.7; the two sections marked on this floor plan appear as Perspective Section A-A' in Figure 6.8 and Perspective Section B-B' in Figure 6.9.

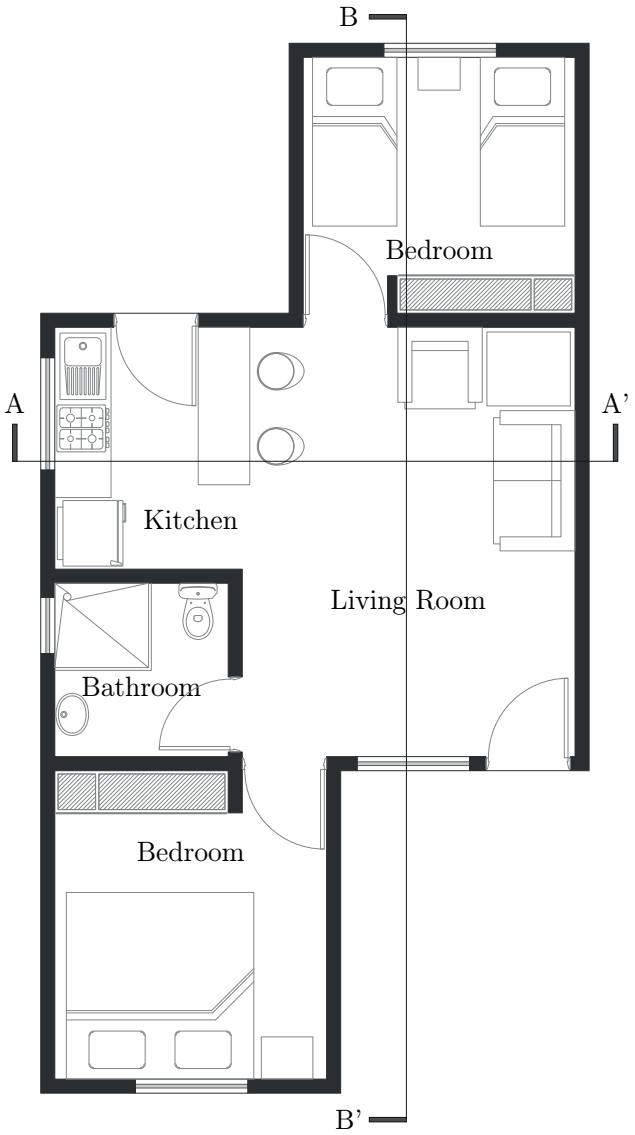


Figure 6.7: Base Case Floor Plan.

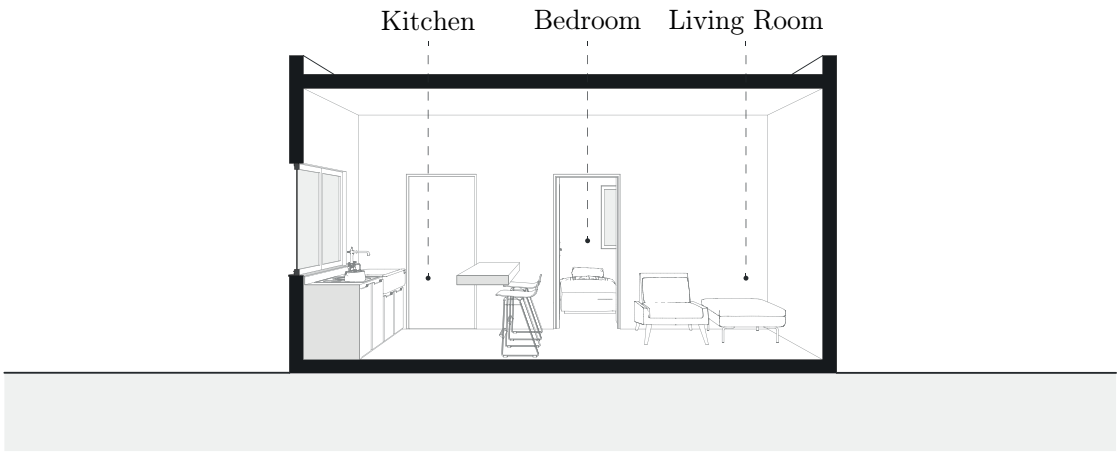


Figure 6.8: Base Case Perspective Section A-A'.

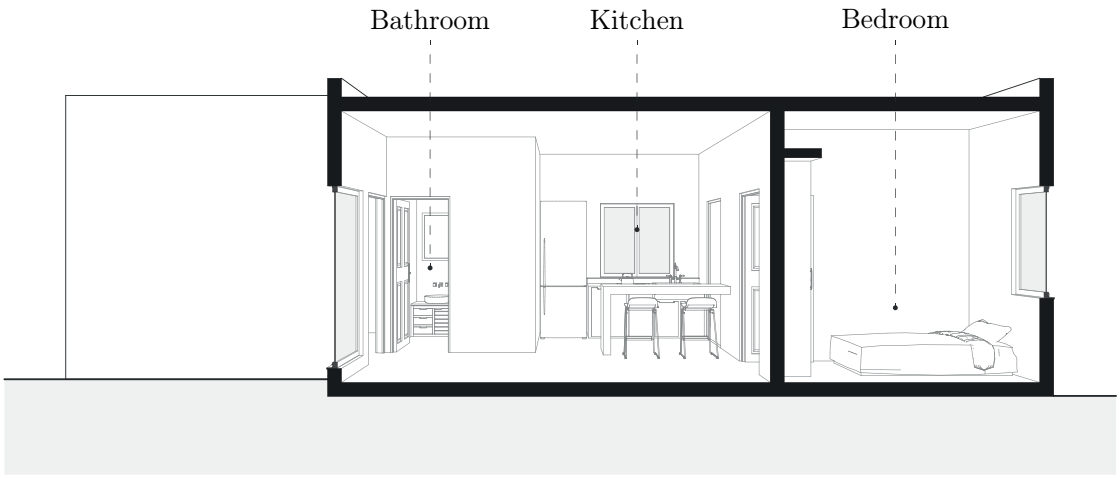


Figure 6.9: Base Case Perspective Section B-B'.

Regarding façades, the modifications were in terms of windows, their placing and dimensions depending on the case. Roofs were also modified so see its impact on the thermal performance and to favor ventilation with some strategies mentioned in Subsection 6.4.3.

6.2.3 Compact Floor Plan Dwelling

In previous stages of the research, it was considered to analyse exclusively the original disposition of the dwelling to study the best envelope for it. As the simulations progressed, it was established to analyse a different floor plan disposition to see the impact these had in the thermal performance of the houses, and to compare it with the original model. The floor area proposed is the same as in the Base Case, as are the spaces inside the house. Disposition of this option is rectangular and more compact, see Figure 6.10.

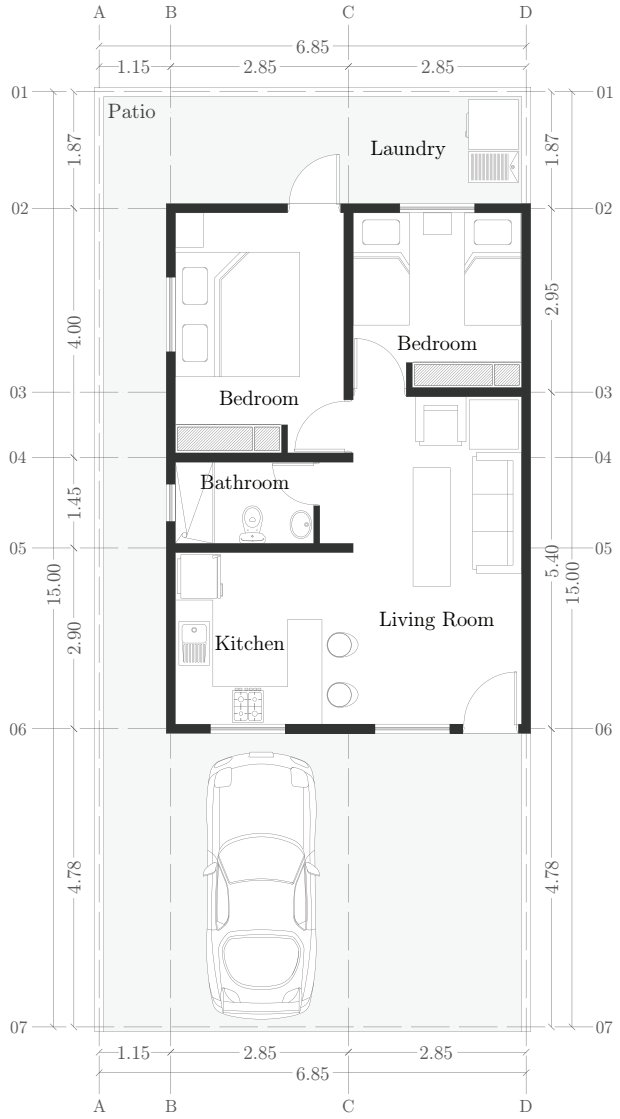


Figure 6.10: Detached House Typology. Case 36 Floor Plan with Site, not to scale.

The Compact Floor Plan appears in Figure 6.11; the two sections marked on this floor plan appear as Perspective Section A-A' in Figure 6.12 and Perspective Section B-B' in Figure 6.13.

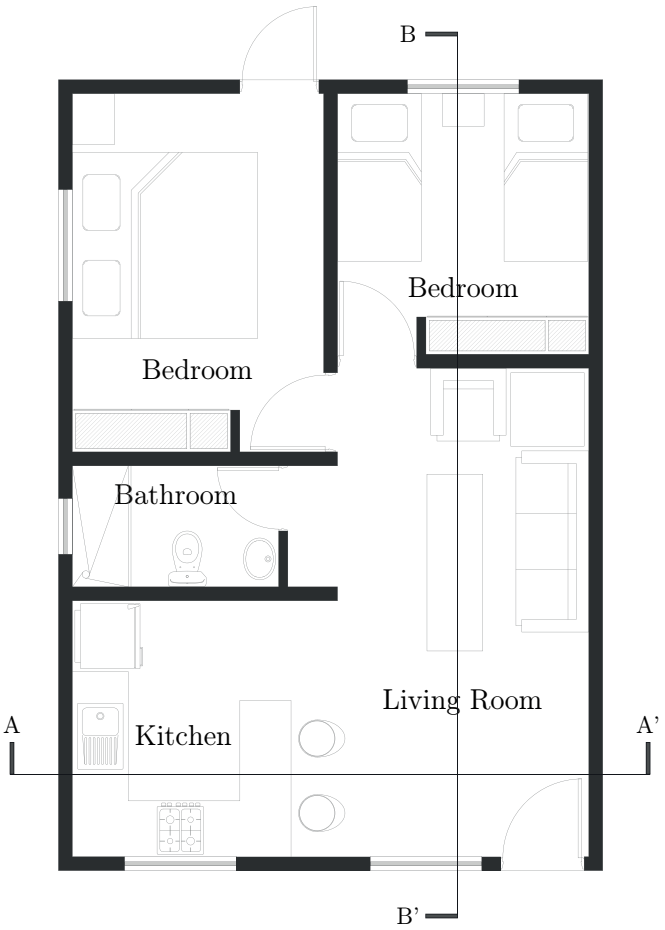


Figure 6.11: Compact Case Floor Plan.

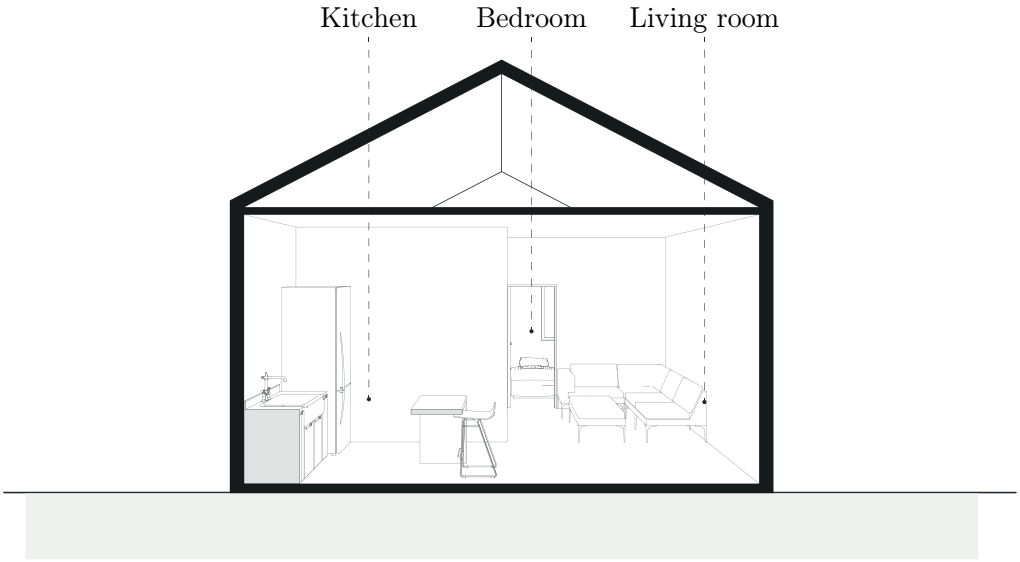


Figure 6.12: Compact Case Perspective Section A-A'.

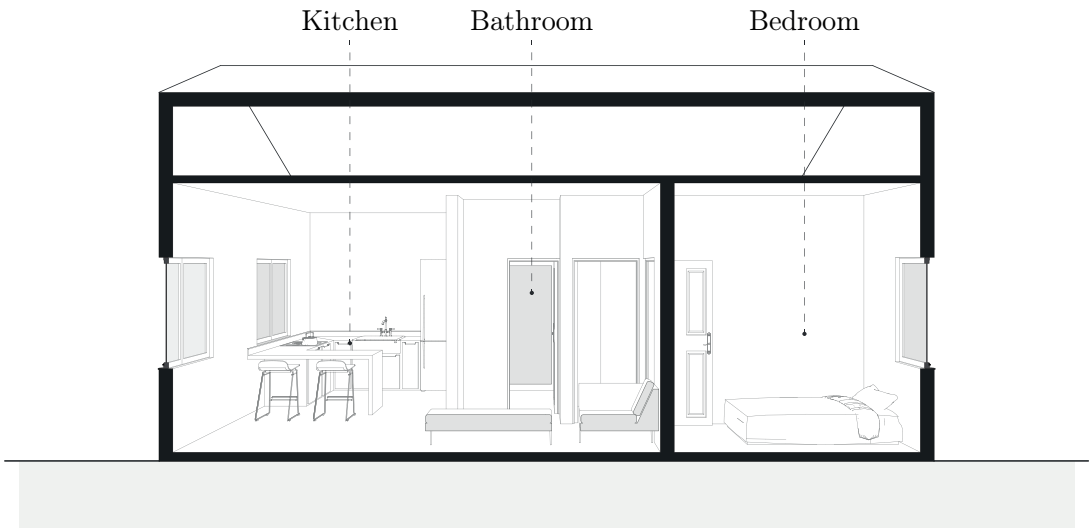


Figure 6.13: Compact Case Perspective Section B-B'.

6.3 Dynamic Thermal Simulation and Weather Files

Simulations to evaluate thermal performance, require to have a precise model with the most information available to reach a better accuracy. In this section, software used for all different stages of the making for these models is explained.

6.3.1 Software for Dynamic Thermal Simulations

For making the initial evaluation of dwellings thermal performance, the temperature variation was studied over time with dynamic simulations made with *EnergyPlusV8-7-0*. The importance of using a dynamic simulation relies in the tracing of hourly temperatures experienced inside the buildings, and in consequence, be able to analyse typical behaviour of temperatures to provide with better solutions depending on the location of the project. Simulations are performed considering one thermal zone for each case.

EnergyPlus was the energy simulation software used to analyse the thermal performance inside the houses because it is a free, open-source and cross-platform BEM[1] engine with useful features for the research. Among these, there are the calculation

[1]Building Energy Modeling

of heat balance-based solutions, radiant and convective effects that produce surface temperatures thermal comfort and condensation calculations through dynamic calculations. On it, the combination of heat and mass transfer is considered as air movement between zones.

To generate the 3-D Modeling needed by EnergyPlus, SketchUp software was used with *Euclid 0.9.3* plug-in, to allow interaction between SketchUp and EnergyPlus software. Euclid is also a free open-source tool in where geometry inputs for building energy models can be modified. EnergyPlus geometry has an IDF format, an editable format supported by Euclid. Geometric characteristics of the buildings to simulate were modified here; these include the change in size and placement of windows, overhangs, and cast shadows projected by building volumes and roofs.

6.3.2 Assumptions for Dynamic Simulations

In dynamic simulations, diverse assumptions have to be made in order to have higher accuracy on how houses behave in reality. With the dynamic thermal simulation, an attempt was made to reflect a realistic behavior of the house, however, when trying to simplify and assume parameters for its use, the conditions may differ from the real ones.

Envelope modifications were studied considering the big variation of day and night temperatures, as in seasonal and annual cycles. Campos [7] considered almost fundamental to pair architectural elements with thermal inertia and immediate gains affecting the appropriate energy regulation. This is why total thermal capacity and total heat absorbing surfaces must be directly related with the characteristics of the climates. Since dynamic aspects of thermal behaviour vary constantly over time, dynamic thermal simulations were carried out with Energy Plus.

The rest of the assumptions considered for the simulations are founded in previous studies from different authors performed for the country and are explained in the points below.

In dynamic simulations, fixed parameters must be considered across all cases to see the

elements that present the best qualities, and to establish homogeneous characteristics between the cases. Geometry, occupancy patterns, internal gains and air change rates were obtained from NAMA [121]. These and are detailed below along with the rest of the assumptions.

- Geometry, form, plan and orientation: Base Case and Cases from 1 to 24 were based in a Reference Home from the NAMA, which, in turn, was based on a real project of a social interest housing [7], in where the electrical appliances as they appear in INFONAVIT where considered. These current average appliances are used in social housing.

  The floor plan used for simulations from the Base Case to Case 34, was shown in Figure 6.7. Cases from 25 to 34 have a different disposition of roofs and windows with respect to the Base Case. Cases from 35 to 40 were modified in a more compact floor plan, Figure 6.11, with the same total area covering the site as the original model, this is, the same amount of square metres. Spaces, areas, size and place of windows are also the same, and all simulations were made in two different orientations, north-south, and east-west.

  Detached houses are conformed by two bedrooms, one bathroom, kitchen, living/dinning room and a service *patio*. To cover the characteristics of SISEVIVE, the detached house does not share walls or roofs. West wall has not solar protection, the main façade faces south, and the posterior one faces north. For thermal simulation, one zone was considered, including all areas.

- Weather data: in all cases, the hourly climate information was processed as a TMY. The weather data for each city was obtained from Climate One Building Repository [39], in where TMY files were downloaded for Saltillo, Monclova and Torreón in an EPW format. Weather files for near, medium and future horizons were created from these weather files using Algorithm DGG3, explained in Chapter 5.

- Comfort thresholds: thermal comfort is perceived differently depending on the source, the location and the building occupants perception. The Adaptive Comfort Model (ACM) is used for naturally ventilated buildings, so it was used for

simulations in this research and explained in p. 53.

Two comfort thresholds were analysed. For the narrow thermal comfort threshold the official standard ASHRAE 55-2010 was used. For a wider thermal comfort threshold, the research developed by Marincic et al. [103], explained in p. 55 was used. It was developed for housing with similar characteristics to the ones presented in this research, and it was adapted for hot dry climates in the north of Mexico.

- Occupancy patterns: the buildings were planned for a four inhabitants occupancy, but was set to two persons per building, as it was designed under the assumption that two persons would be the occupancy over a 30 year life cycle of the housing unit [121].

- Internal gains, domestic lighting and appliances: Lighting was considering using compact fluorescent light, as electrical domestic appliances were proposed for the common social housing market with information published by INFONAVIT and SENER; these are a refrigerator, a TV, an electric fan, a washing machine, and a microwave oven as shown in in Table 6.2. The total internal heat gains were calculated with PHPP, assuming $5.3W/m^2$.

Table 6.2: Reference House Domestic Lighting and Appliances Specifications [121].

Illumination type	Compact Fluorescent Lamps 20W
Electric Domestic Appliances	Refrigerator 2.68 kWh/d Television 0.19 kWh/d Electric Fan 100W Washing Machine 0.32 kWh/d Microwave Oven 0.17 kWh/d *Source: Infonavit 2011a, Infonavit 2011b, Luz y Fuerza n.d., SENER 2011.*
Water Heater	Tankless LP Gas Water Heater (e.g. CINSA CDP 06)
Cooking Stove	LP Gas Stove
Number of m^2 per person	20 m^2 per person
Internal Heat Gains	5.3 W/m^2
Air Exchange	5 h^{-1}

- Air Change Rate ACH @ 50Pa: These rates were compared by sets in simulations. The base one obtained from the NAMA [121] was of 5 air changes per hour. Another two were considered under the *Passivhaus* standard, 0.6 h^{-1} to meet the minimum required, and a lower target of 0.3 h^{-1}.

- Ventilation: natural ventilation was proposed for economic purposes and for being the regular type used in these houses. As simulations are performed in EnergyPlus, natural ventilation parameters that must be into consideration are the free opening area of the windows and their effective angle, and the wind-speed given by the climate data. Windows are assumed to be opened at all times, except when temperatures drop below $18^{\circ}C$, because this temperature was established as the lowest acceptable in the baseline cases of the NAMA. As no cooling system is considered, the set-point for maximum indoor temperatures

was established at $50^{\circ}\,C$.

- Heating and cooling: in previous studies for diverse Mexican regions, results showed that for the hot climate regions, the annual temperatures distribution inside the dwellings does not get into acceptable ranges of thermal comfort, which generally leads to the use of air conditioning equipment. Ideally users of these houses would not use an A/C system, so no active or hybrid systems were considered.

6.3.3 Solar Analysis

As well as to analyse the base cases, and to propose new solutions in the architectural design, an initial solar analysis was carried out. With this, the best geometry for the houses and the modifications that could be simulated afterwards were studied. It was sought to have the greatest amount of direct solar incidence in all the interior spaces in winter, and to avoid this in summer, for the warmer months.

To perform this solar analysis, *Heliodon 2.7-02* software was used, it is a free tool used for interactive design with solar radiation and natural light in architectural and urban projects [18]. The amount of sun hours entering the building through openings and affecting the envelope, were studied to propose suitable improvements to obtain a better thermal performance. After this analysis was made, new properties in the envelope were proposed to have more hours of comfort inside.

Firstly, a grid was placed to obtain results of the amount of direct sun hours for every point of the grid. The space between each point was of one metre and calculations were made every minute during the 24 hours, for a specific day for each month of the year. With this information it was established which points needed more sun protection. The simulations were made considering the envelope described for the base case, so the roof was included; the hours of sun projected on the floor correspond to the direct sunlight inside the house entering throughout the windows, see Appendix N.

Sunny periods inside and outside the house were obtained for every month, for the whole year, and for mean yearly hours. These hours of direct sun were obtained also for

the walls, windows and floors, for all seasons and for the whole year. The stereographic projections showing annual information was made for the north and south bedrooms, living room, bathroom and kitchen.

From this analysis, it was deduced that, for the city of Saltillo, there are more sun hours on the south bedroom from January to March (from 1.34 to 2.44 hrs), and more sun hours on the living room on January and February (from 1.11 to 2.01 hrs). Direct solar incidence was observed on the kitchen from January to March, and a bigger spectrum of it is shown in April. There is no direct sun incidence on both bedrooms from May to August. In September, there is a minimum direct sun incidence on the south bedroom (0.37 hrs) and its partially bigger from October to December (1.44 - 2.46 hrs).

There is no direct sun incidence on north bedroom and kitchen from September to December. There are less sun hours in September compared with the obtained from October to December. This is preferable except for results obtained for October, because September is still within the warmer months, and November and December, are within the colder ones.

For a more global appreciation of sun incidence, stereo-graphic projections were made for all the inner spaces in the house. The bathroom does not get any direct sunlight because of the size and placement of the window; kitchen receives direct sun light almost every month except for the cold ones; there is an obstruction in the living room, so more direct sun hours can be obtained with a different disposition of the window. The north bedroom does not receive any direct sunlight along the year; one window can be added on the west façade with sun protection in summer. The south bedroom receives two or more sun hours on cold months; if shape is modified, it can get more sun hours on winter, and avoid sun incidence in summer.

Derived from these results, a better placement and sizing of windows was proposed and used in new cases of study. For all simulations starting from Case 1, the best window disposition was used, this was, the one that allowed to have more sun incidence in winter, and less in summer. It was planned to keep the housing design the same as the base case with these minor modifications. Geometry of the building remained the same and only windows were modified.

6.3.4 Weather files and Locations per City

As discussed in Chapters 3, 4 and 5, weather files are generally provided by cities, and not for specific locations. Climate and micro-climates are different within cities; in Coahuila, altitudes fluctuate between 400 and 2000 metres, so it is desirable to have specific weather files for each location.

New weather files were generated for the three proposed set of years, so one specific location was chosen for each city; these sites are in neighborhoods with social housing. Altitudes, longitude and latitude coordinates can be seen in Table 6.3.

Table 6.3: Chosen Locations for Each City

City	Latitude	Longitude	Altitude
Saltillo	$25^\circ\,23'\,35''$ N	$100^\circ\,59'\,58''$ W	1719 m
Monclova	$26^\circ\,50'\,40''$ N	$101^\circ\,25'\,28''$ W	623 m
Torreón	$25^\circ\,32'\,24''$ N	$103^\circ\,19'\,58''$ W	1118 m

These are the three largest cities in Coahuila, and each of them has one of the three different climates of the state: Saltillo corresponds to the tempered sub-humid stripe, Torreón to the very dry, and Monclova to the dry. This is why they were chosen, to appreciate the differences in thermal performance of architectural designs, and to adapt the best fit for them depending on the climate. The location for each city is shown in Figure 6.14.

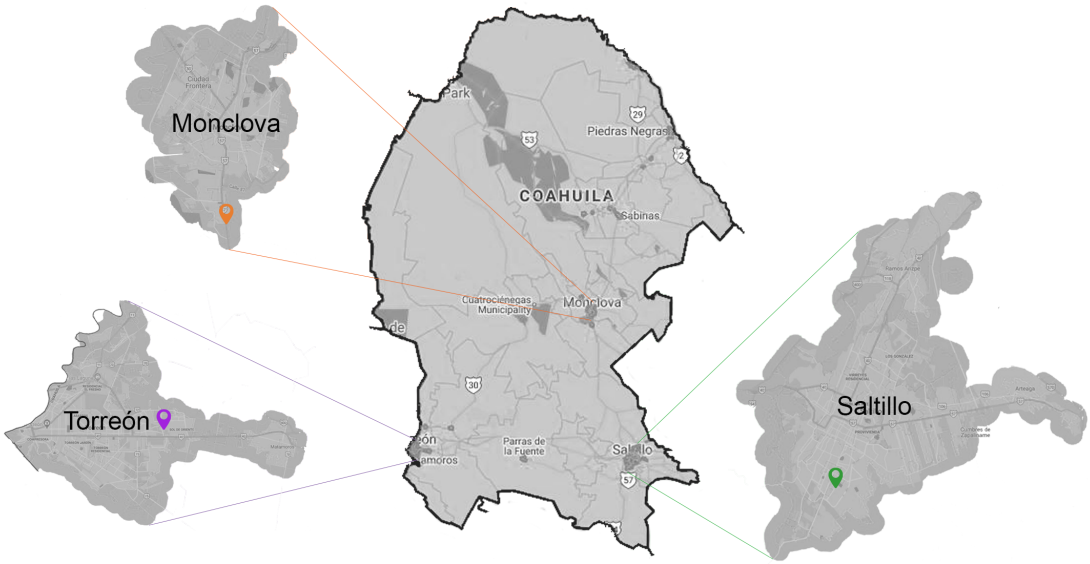
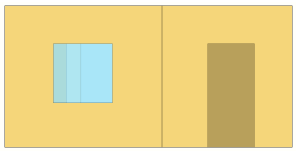


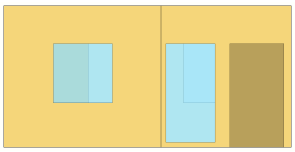
Figure 6.14: Projects Location.

6.4 Housing Envelope Simulation Parameters

In the Base Case floor plan, it is contemplated one bathroom, a kitchen, dining room and stay, two bedroom, a parking spot and a service patio. To perform the simulations, the 3D model had to be done in SketchUp with simplified forms as the ones shown in Figure 6.15. In here, a 3D view, and the four façades are presented.



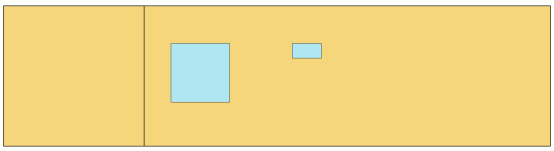
(a) Base Case North Façade



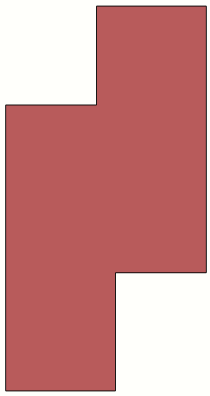
(b) Base Case South Façade



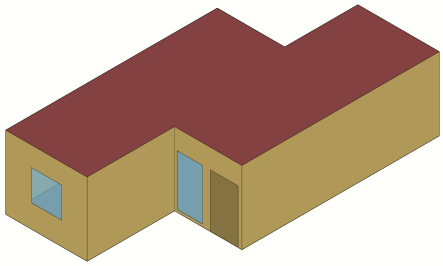
(c) Base Case East Façade



(d) Base Case West Façade



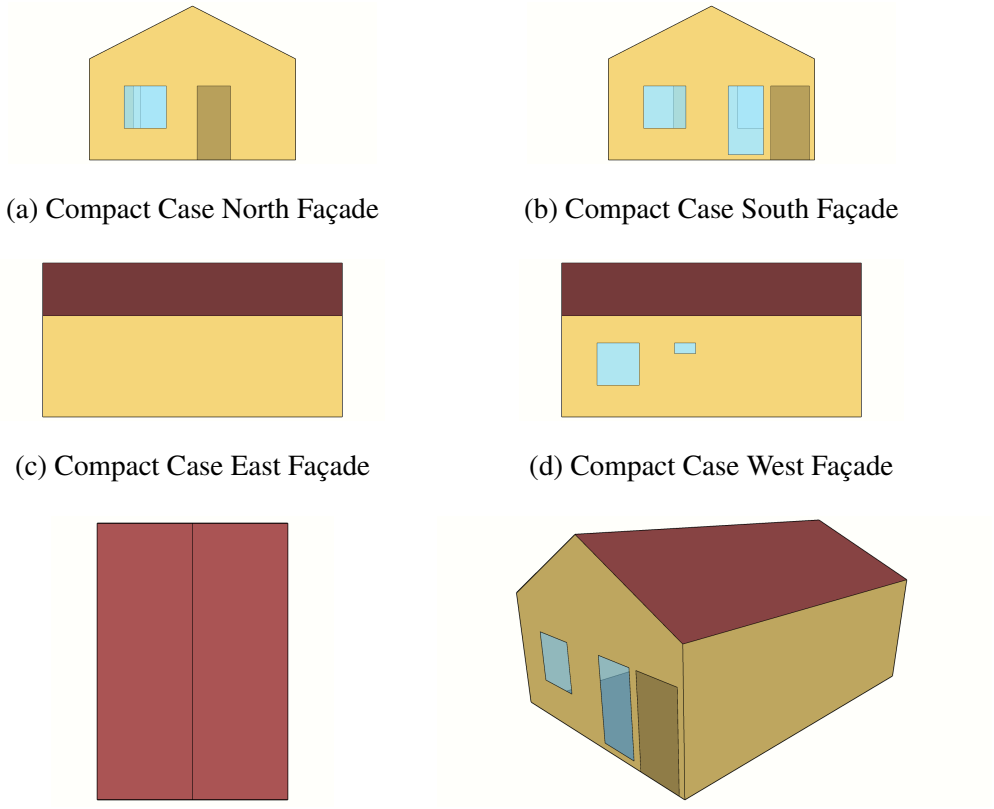
(e) Base Case Top View



(f) Base Case Isometric

Figure 6.15: Base Case Geometry. Simplified 3D model in SketchUp.

From the Base Case floor plan, simulations from cases 1 to 34 were performed. Variations in heights and roof dispositions were used in the second set, in cases from 28 to 34. In a third set of simulations, the compact geometry was simulated. The simplified geometry modeled in SketchUp with the engine Euclid to run simulations in EnergyPlus is shown in Figure 6.16.



(a) Compact Case North Façade

(b) Compact Case South Façade

(c) Compact Case East Façade

(d) Compact Case West Façade

(e) Compact Case Top View

(f) Compact Case Isometric

Figure 6.16: Compact Geometry. Simplified 3D model in SketchUp.

6.4.1 Envelope Materials

Three different envelope materials were simulated: Concrete Block (CB[2]), Autoclaved Aerated Concrete Block (AACB[3]) and Clay Hollow Block (CHB[4]) with their respective construction types unifying walls and roofs, and with a concrete floor slab. Details of these are shown with more depth starting from p. 185. The three envelope materials were simulated with both, single and double glazing, as with different overhanging and shading elements. Design strategies for its respective study cases are shown in Table 6.4.

[2]Concrete Block

[3]Autoclaved Aerated Concrete Block

[4]Clay Hollow Block

Table 6.4: Design Strategies.

Design Strategies Description	**Building Elements**
Shading and Sun Incidence	
Modifications derived from solar study, for lessen direct solar incidence in warm months, and increment it in cold months	Horizontal Overhangs Modification in sizing and placement of windows
Envelope Performance	
Simulation of different envelope materials to evaluate their combinations to propose the one with a better thermal performance	Concrete Block Autoclaved Aerated Concrete Block Clay Hollow Block Single Glazing in Windows Double Glazing in Windows
Ventilation	
Adjustment on windows to propitiate cross ventilation when necessary	Operable Windows Clerestory and Fold Up Windows

Further characteristics of each component of the envelope are shown in the following subsections. Thermal components for walls, roofs and ground floor are displayed respectively in Subsections 6.4.2, 6.4.3, and 6.4.5.

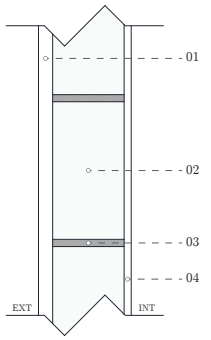
These strategies considered an online tool used to generate psychrometric charts to chose the possible design strategies that could be proposed [109] for the studied cases. These, for the three cities for current weather and future horizons, under two different comfort overlays. See Appendix M.

As the thermal simulations were performed in EnergyPlus, U-values are calculated using the thermal resistance values inputted for each material layer conforming the construction element. This within the surface's construction assembly, the inside and the outside film resistances. Characteristics of each material conforming these layers were added, including thickness (m), conductivity (W/mK), density (kg/m^3) and specific heat (J/kgK). As the U-value is not an input in EnergyPlus, the values stated in the subsequent subsections are the values given by the software after the simulations.

6.4.2 Walls

Diverse envelope materials were considered for the dynamic thermal simulations performed in EnergyPlus. In the reference house, the external wall build-up is $100\,mm$ thick concrete masonry units with an R-value of $0.37m^2K/W$, crestuco plaster on the exterior, and cement plaster in the interior, and a U-value of $2.68W/m^2K$ resulting from the simulation. The Base Case and first cases of each set, were proposed also with Concrete Block (CB), with a density of $\rho = 2300kg/m^3$ and a thermal conductivity of $\lambda = 2.3W/mK$.

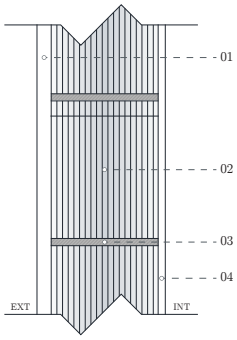
The sets of simulations were carried out with two other wall materials to compare their performance with the concrete block. Both of these are specified in regulation NOM-020-ENER-2011. The first one corresponds to the Autoclaved Aerated Concrete Block (AACB), with a thickness of 150 mm, a λ value of $0.19W/mK$, a density of $500kg/m^3$ and a U-value of $0.19W/m^2K$. The other material is the Clay Hollow Block (CHB), with a thickness of $120\,mm$, vertical hollow block units, $60-70\%$ solid, with a thermal conductivity of $\lambda = 0.998W/mK$, a density of $2050kg/m^3$ and a U-value of $1.00W/m^2K$. The thermal components for walls are described from the outside to the inside layer with their thickness in Figure 6.21.



(a) Concrete Block

1. 20 mm Crestuco plaster
2. 100 - 150 mm concrete block units (100 / 150 * 200 * 400 mm)
3. 10 mm sand lime mortar
4. 10 mm cement plaster

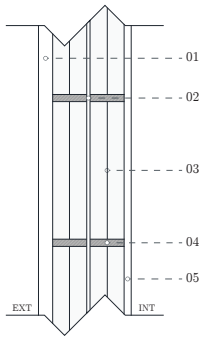
(b) Layers from outside to inside



(c) Clay Hollow Block

1. 20 mm lime cement plaster
2. 150 mm clay hollow block (150 * 200 * 400 mm)
3. 10 mm sand lime mortar
4. 10 mm cement plaster

(d) Layers from outside to inside



(e) Autoclaved Aerated Concrete Block

1. 20 mm lime cement plaster
2. steel bars reinforcement
3. 150 mm autoclaved aerated concrete block (150 * 200 * 610 mm)
4. 10 mm sand lime mortar
5. 10 mm cement plaster

(f) Layers from outside to inside

Figure 6.17: Details: Walls, not to scale.

6.4.3 Roofs

The first cases were analysed considering the roof as a reinforced concrete slab, $120\,mm$ thick, R-value of $0.30\,m^2K/W$, 2% slope, and white Plasticool layer as waterproofing; the thermal conductivity is $\lambda = 1.63\,W/mK$, and a density of $2400\,kg/m^3$. The U-values resulted from simulations are of $3.23W/m^2K$ for the Concrete Slab, of $0.90W/m^2K$ for the Autoclaved Aerated Concrete, and of of $1.05W/m^2K$ for the

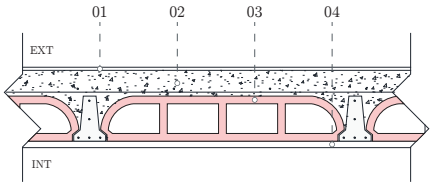
Clay Hollow Block system.

Having analysed the envelope with concrete slabs on the roofs, it was investigated the convenience of using a heat discharge system, or a flysheet with intermediate air, where the ventilation of the air between the slab and the highest layer was allowed externally. In various investigations such as those of Hernández and Morillón [64], these issues have been addressed, since this system was experimented with walls and depending on their location they were favorable at a thermal level.

As heat discharge systems require more material, and a more detailed knowledge of its elaboration, it was decided to use the second roof layer. This is placed independently of the structure that has been studied in the first cases, and a light roof is anchored in the upper part of the houses. Examples of this application can be found in the city of Monterrey, in the social interest housing project *Casa cubierta de comunidad Vivex*. The roof slab is made of lightweight concrete and the over roof is made of corrugated steel.

Three different materials in roofs were simulated with their corresponding materials in walls. In Figure 6.18 the thermal components are displayed, and the description of these with their thickness are further stated from the upper layer to the bottom one.

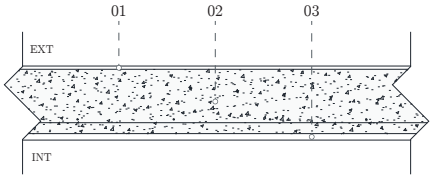
The Concrete Slab Roof construction detail and description by layer is specified in Figures 6.18a and 6.18b; for the Clay Hollow Block Roof they are displayed in Figures 6.18c and 6.18d; and for the Autoclaved Aerated Concrete Slab they are in Figures 6.18e and 6.18f.



(a) Concrete Slab

1. 10 mm Plasticool as white waterproofing
2. 120 mm reinforced concrete slab
3. 15 mm gypsum plaster

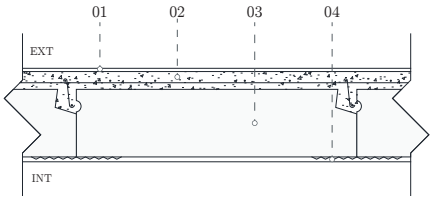
(b) Layers from outside to inside



(c) Clay Hollow Block

1. 10 mm waterproofing layer
2. 50 mm cast-in- place concrete slab
3. 130 mm hollow clay tiles
4. 15 mm gypsum plaster

(d) Layers from outside to inside



(e) Autoclaved Aerated Concrete

1. 10 mm waterproofing layer
2. 40 mm cast-in-place concrete slab
3. 125 mm autoclaved aerated concrete slab panels
4. 15 mm gypsum plaster

(f) Layers from outside to inside

Figure 6.18: Details: Roofs, not to scale.

These roof components were kept on rotated roofs to generate single sloped roofs. Below these, clerestory windows were placed to analyse if the thermal behavior of the houses improved by having extra ventilation elements and allowing the exit of hot air by stack effect. Different heights in rotation were considered, and none of them were better than the flat roof; therefore, these single sloped roofs were separated from the flat roof, as an over roof, in where the lowest separation was of $300\,mm$, and the highest, of $900\,mm$.

Over roofs with lighter materials like galvanised corrugated sheets, were also simu-

lated. A second layer over the roof was placed on the concrete slab to evaluate if there is an improvement in thermal insulation based on voids and natural air currents. The altitudes were studied individually to use the most appropriate separation between the roof and the over roof; the best suited separation was of $400\,mm$.

6.4.4 Windows and Frames

Values of glazing were proposed as in the Energy Efficiency Optimization Study in Social Housing (GIZ/INFONAVIT). Characteristics of single glazing were used for the base case, as double glazing was chosen for the optimal case in hot dry climates in the detached house. Windows were simulated with 1.5" aluminum frames.

For the reference case a clear single glazing of $3\,mm$ thick was used, with a Solar Heat Gain Coefficient (SHGC[5]) of 0.86 and a U-value of $5.75 W/m^2K$. For the cases using double glazing, it was simulated a low emissivity glass of $4\,mm$, $13\,mm$ of air, and an internal clear single glazing of $4\,mm$, with a SHGC value of 0.73 and a U-value of $2.72 W/m^2K$. EnergyPlus runs using the SHGC values of windows and not shading coefficients, so the rest of the glazing characteristics needed were obtained from the EnergyPlus DataSets of Windows Glass Materials, and adapted to the cases as shown in Figure 6.19.

Field	Units	Obj1	Obj2	Obj3
Name		CLEAR 3MM	CLEAR 4MM	LoE CLEAR 4MM
Optical Data Type		SpectralAverage	SpectralAverage	SpectralAverage
Window Glass Spectral Data Set Name				
Thickness	m	0.003	0.004	0.004
Solar Transmittance at Normal Incidence		0.837	0.775	0.6
Front Side Solar Reflectance at Normal Incidence		0.075	0.071	0.17
Back Side Solar Reflectance at Normal Incidence		0.075	0.071	0.22
Visible Transmittance at Normal Incidence		0.898	0.881	0.84
Front Side Visible Reflectance at Normal Incidence		0.081	0.08	0.055
Back Side Visible Reflectance at Normal Incidence		0.081	0.08	0.078
Infrared Transmittance at Normal Incidence		0	0	0
Front Side Infrared Hemispherical Emissivity		0.84	0.84	0.84
Back Side Infrared Hemispherical Emissivity		0.84	0.84	0.1
Conductivity	W/m-K	0.9	0.9	0.9

Figure 6.19: Window Glass Materials.

Both in Base Case and Compact geometries, windows used in kitchen and bedrooms

[5]Solar Heat Gain Coefficient

are bi-folding windows of $1.20\,m * 1.20\,m$. Awning windows of $0.60\,m * 0.40\,m$ were used in bathrooms.

Awning windows were used in clerestory windows of $2.00\,m * 0.40\,m$, and a $1.00\,m * 1.95\,m$ casement window with two hinged sashes was proposed in the main entrance of the Base Case geometry. To adapt the geometry and fit the clerestory windows, $0.40\,m$ were added in two masonry courses in all walls. The interaction between these is shown in Table 6.5. A zone summary of gross floor and wall area, glass area and zone volumes appear on Table 6.6.

For best cases, the U-value of the entire window must be $0.85W/m^2K$, and double glazing must be $0.6W/m^2K$.

Table 6.5: Window to Wall Ratio.

Wall/Window	**Total**	**North (315 - 45 °)**	**East (45 - 135 °)**	**South (135 - 225 °)**	**West (225 - 315 °)**
			Set 1: BC.		
Gross Wall Area [m^2]	97.87	16.79	32.14	16.79	32.14
Window Opening Area [m^2]	6.45	1.44	0.00	3.39	1.62
Gross Window-Wall Ratio [%]	6.59	8.58	0.00	20.19	5.04
			Set 1: C1-C24.		
Gross Wall Area [m^2]	97.87	16.79	32.14	16.79	32.14
Window Opening Area [m^2]	8.77	3.20	0.00	2.88	2.69
Gross Window-Wall Ratio [%]	8.96	19.06	0.00	17.15	8.37
			Set 2: C25-C27.		
Gross Wall Area [m^2]	97.87	16.79	32.14	16.79	32.14
Window Opening Area [m^2]	11.25	3.20	1.44	3.84	2.77
Gross Window-Wall Ratio [%]	11.50	19.06	4.48	22.87	8.62
			Set 2: C28.		
Gross Wall Area [m^2]	111.16	21.89	35.77	17.74	35.77
Window Opening Area [m^2]	13.53	4.73	1.80	4.09	2.91
Gross Window-Wall Ratio [%]	12.17	21.59	5.03	23.06	8.14
			Set 2: C29 - C34.		
Gross Wall Area [m^2]	111.51	19.13	36.62	19.13	36.62
Window Opening Area [m^2]	13.65	4.00	2.34	4.62	2.69
Gross Window-Wall Ratio [%]	12.24	20.91	6.38	24.18	7.35
			Set 3: C35 - C38.		
Gross Wall Area [m^2]	91.14	21.18	24.39	21.18	24.39
Window Opening Area [m^2]	6.45	1.44	0.00	3.39	1.62
Gross Window-Wall Ratio [%]	7.08	6.80	0.00	16.01	6.64
			Set 3: C39 - C40.		
Gross Wall Area [m^2]	91.14	21.18	24.39	21.18	24.39
Window Opening Area [m^2]	7.44	1.44	0.00	2.88	3.12
Gross Window-Wall Ratio [%]	8.16	6.80	0.00	13.60	12.79

Table 6.6: Zone Summary: Envelope Areas [m^2] and Volumes [m^3].

Case	**Total Gross Floor area** [m^2]	**Total Zone Volume** [m^3]	**Gross Wall Area** [m^2]	**Window Glass Area** [m^2]
BC	48.77	139.98	97.87	6.45
C1 - C27	48.77	144.42	97.87	8.77
C28	48.77	170.52	111.51	13.53
C29 - C34	48.77	230.81	111.51	13.65
C35, C38	49.73	144.20	91.14	6.45
C36, C37	49.73	180.50	91.14	6.45
C39, C40	49.73	144.20	91.14	7.44

6.4.5 Floors

The floor slab was contemplated the same regardless the materials in walls and roofs. The reference case uses only a $100\,mm$ reinforced concrete slab, but for these simulations the reinforced concrete slab has the characteristics described in the next paragraph; layers are disposed this way because they are more suitable to what is built in this type of house with the traditional building methods in Mexico. The U-value resulting from simulations are of $3.30 W/m^2K$

The Reinforced Concrete Slab has the following layers from top to bottom: 01) $10\,mm$ of Ceramic Tile; 02) $5\,mm$ of Adhesive Mortar; 03) a $150\,mm$ Reinforced Concrete Slab; and 04) $50\,mm$ of Stone Chipping above the ground, as can be appreciated in Figure 6.20.

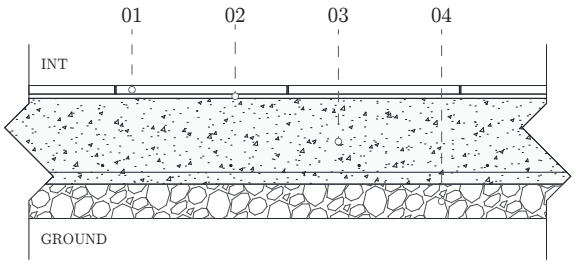


Figure 6.20: Floor Slab Construction Detail, not to scale.

6.4.6 Disposition of Simulation Cases

Once explained all components thermal and physical characteristics, it is shown a precise disposition of one set of cases. Each case was simulated for current weather, for near, medium and future horizons, for orientation north-south, and east-west, for each city.

Set 1

A Base Case was created considering the Reference House to represent the typical characteristics described in p. 166; it was first simulated considering the reference

house components with slight modifications made from the solar analysis; the rest of the cases were modified considering the most suited window sizes and placements. For these cases, the Base Case, from now on BC, was altered using different materials in walls, roofs, and diverse windows and frames characteristics, and simulations were made in sets of five. The cases are shown in Table 6.7.

Table 6.7: Envelope Elements used for Dynamic Simulations. Set 1, for Base Case and Cases from 1 to 24.

Case	Geometry	Windows	Glazing	Material	Operable Windows	ACH
BC	BCG	WBC	SG	CB	OWBC	ACHBC
1	BCG	WM1	SG	CB	OWBC	ACHBC
2	BCG	WM1	SG	AACB	OWBC	ACHBC
3	BCG	WM1	SG	CHB	OWBC	ACHBC
4	BCG	WM1	DG	CB	OWBC	ACHBC
5	BCG	WM1	DG	AACB	OWBC	ACHBC
6	BCG	WM1	DG	CHB	OWBC	ACHBC
7	BCG	WM1	SG	CB	OW1	ACHBC
8	BCG	WM1	SG	AACB	OW1	ACHBC
9	BCG	WM1	SG	CHB	OW1	ACHBC
10	BCG	WM1	DG	CB	OW1	ACHBC
11	BCG	WM1	DG	AACB	OW1	ACHBC
12	BCG	WM1	DG	CHB	OW1	ACHBC
13	BCG	WM1	SG	CB	OW1	ACH1
14	BCG	WM1	SG	AACB	OW1	ACH1
15	BCG	WM1	SG	CHB	OW1	ACH1
16	BCG	WM1	DG	CB	OW1	ACH1
17	BCG	WM1	DG	AACB	OW1	ACH1
18	BCG	WM1	DG	CHB	OW1	ACH1
19	BCG	WM1	SG	CB	OW1	ACH2
20	BCG	WM1	SG	AACB	OW1	ACH2
21	BCG	WM1	SG	CHB	OW1	ACH2
22	BCG	WM1	DG	CB	OW1	ACH2
23	BCG	WM1	DG	AACB	OW1	ACH2

continues on the next page . . .

Case	Geometry	Windows	Glazing	Material	Operable Windows	ACH
24	BCG	WM1	DG	CHB	OW1	ACH2

The first case was the BC, with concrete block; second case was considered using Autoclaved Aerated Concrete Block in the envelope components, and for the third case Clay Hollow Block was used, and these three materials were used along the rest of the simulations in that order, considering the use of single glazing. For these three cases concrete slabs in roof and floor were simulated. For Cases 4, 5, and 6, double glazing was used. This main characteristics in the first six simulations were used for the rest of the cases in that order, whit those components in envelopes and windows; this is how simulations of six different cases constitute a set.

In cases from 7 to 12, operable windows were used as specified in the assumptions. In the BC and cases from 1 to 12 the air changes per hour were considered as $5\,h^{-1}$; in cases from 13 to 18 a smaller rate was used, $0.6\,h^{-1}$, and from cases 19 to 24 a smaller rate was simulated, this was of $0.3\,h^{-1}$.

Set 2

From cases 25 to 34 different overhangs and clerestory windows were used to decrease the discomfort hours. Their interaction is show in Table 6.8.

Table 6.8: Envelope Elements used for Dynamic Simulations. Set 2, for Cases from 25 to 34.

Case	Geometry	Windows	Glazing	Material	Operable Windows	ACH
25	BCG	WM1	DG	CHB	OW2a	ACH2
26	BCG	WM1	DG	CHB	OW2b	ACH2
27	BCG	WM1	DG	CHB	OW3	ACH2
28	SRO	WM1	DG	CHB	OW3	ACH2
29	HOR	WM1	DG	CHB	OW2b	ACH2
30	HOR	WM1	DG	CHB	OW3	ACH2
31	HOR	WM1	DG	CHB	OW4	ACH2

continues on the next page ...

Case	Geometry	Windows	Glazing	Material	Operable Windows	ACH
32	OR	WM1	DG	CHB	OW4	ACH2
33	ORS	WM1	DG	CHB	OW4	ACH2
34	ORN	WM1	DG	CHB	OW4	ACH2

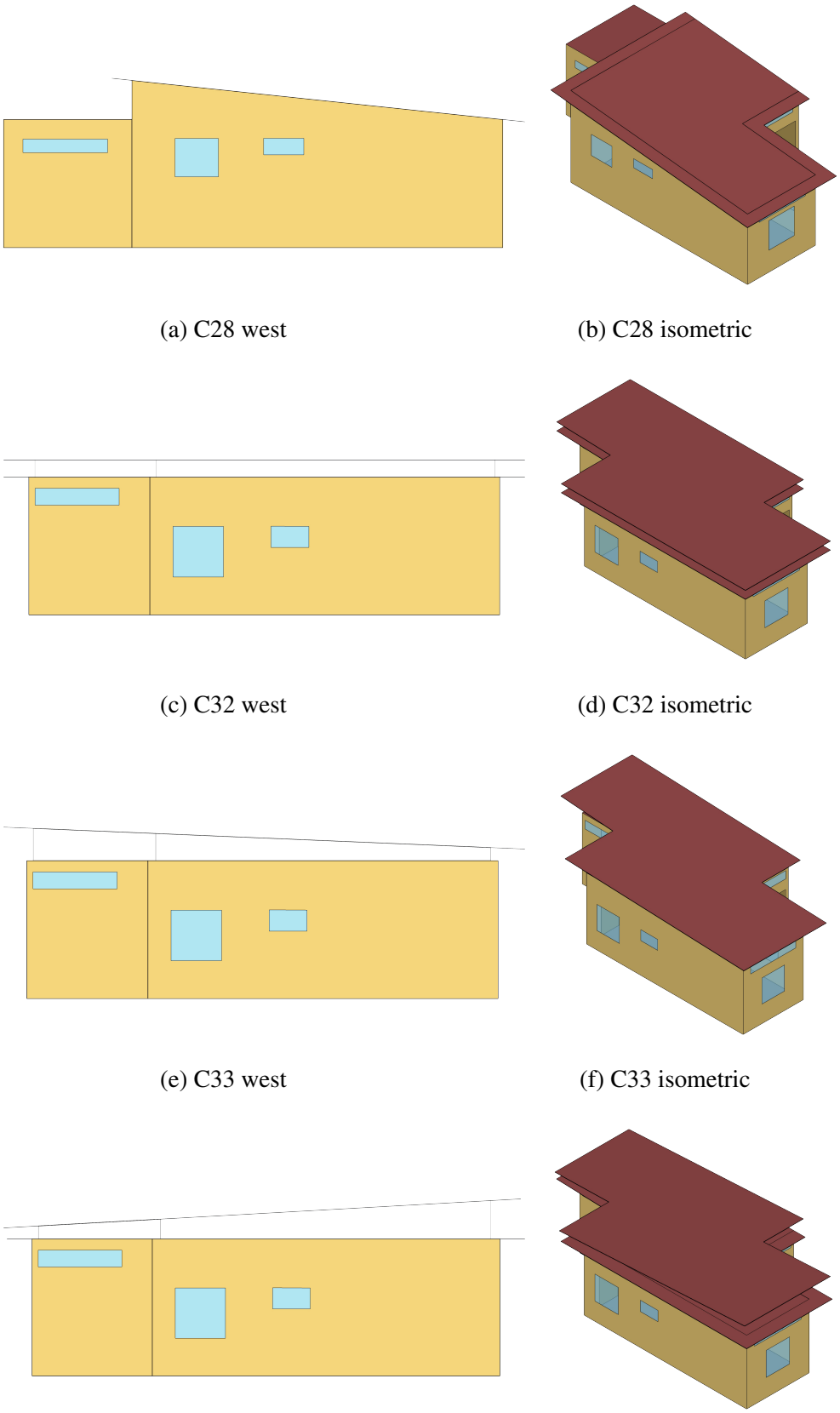
In these cases the use of the clay hollow block, with the use of double glazing in windows, and an ACH rate of $0.3\,h^{-1}$ was proposed in all cases, as they showed to work better in the first set of cases. The parameter modifications were in terms of the roof disposition, overhangs on top of the windows, the use of clerestory windows, and an increment in walls heights for some cases.

From case 25 to 27, the flat roof was simulated; the difference in parameters between these cases relies on the overhangs and the use of clerestory windows. In case 25, the overhangs above windows were placed in the west façade, and in case 26, on façades south, east, and west. In these last three façades, clerestory windows were used in cases 27, 28, and from 30 to 34. As the clerestory windows were proposed for this set, they were studied with the original geometry and height of the base case ($2.87\,m$), and also with this same floor plan but with the addition of two courses of block in walls, making them of $3.27\,m$.

An additional horizontal overhang in the roof was used for cases 29, 30 and 31. Prevailing winds move in a south-north direction, so diverse rotations in roofs were simulated to see which resulted in the most beneficial for the study.

For case 28 it was proposed to rotate the roof and have a sloped roof with an overhang in the common area and main bedroom (Fig. 6.21a - 6.21b). In case 32 a horizontal over roof was placed above the roof, allowing a flow of air between these two elements (Fig. 6.21c - 6.21d).

The over roof was rotated south and north in cases 33 and 34 respectively. This can be appreciated in west elevations and isometric figures in 6.21e, 6.21f, 6.21g, and 6.21h.



(a) C28 west

(b) C28 isometric

(c) C32 west

(d) C32 isometric

(e) C33 west

(f) C33 isometric

(g) C34 west

(h) C34 isometric

Figure 6.21: Geometry Modification.

Set 3

The third set of cases is composed by a new geometry with gable roofs. This was simulated with ceiling, in cases 35, 38-40, and without ceiling, in cases 36 and 37. The OW5 represents the opening windows preserved for this set, with similar characteristics to the sizes and placements of OW1. The characteristics of the envelope were used as in the base case for the first two simulations on cases 35 and 36. In cases from 37 to 40, an interaction between the best parameters resulted from simulations in Set 2 were used, as shown in Table 6.9.

Table 6.9: Envelope Elements used for Dynamic Simulations. Set 3, for Cases from 35 to 40.

Case	Geometry	Windows	Glazing	Material	Operable Windows	ACH
35	GRC	WM2	SG	CB	OWBC	ACHBC
36	GR	WM2	SG	CB	OWBC	ACHBC
37	GR	WM2	SG	CHB	OW5	ACH2
38	GRC	WM2	SG	CHB	OW5	ACH2
39	GRC	WM3	SG	CHB	OW5	ACH2
40	GRC	WM3	DG	CHB	OW5	ACH2

In cases 34, 35 and 36 a different floor plan was simulated, to study a different disposition and a more compact volumetry. In these cases, the best aspects from the previous cases were used.

6.5 Conclusions

The selection of simulation parameters was based on the elements that represent the greatest impact on the thermal behavior of the building. Most elements are based on literature from real social housing in Mexico, and the rest of them were assumed from similar projects performed in the country. The results they show, explained in next chapter, reflect how the chosen parameters impact the performance of the house, individually, and when they are interconnected.

The choice of these elements and the order of the simulations facilitated the understanding of the desirable characteristics for each modified parameter. Thus, with all the materials proposed in the opaque envelopes of houses, walls and ceilings, it could be evaluated which arrangement and type of window works best with each of them, as well as which solar protection is the most suitable.

In Appendix L, a simulation matrix with the cases can be consulted; it indicates the variety and breadth of simulations, considering that for each case, eight simulations were carried out; this is governed by the amount of weather files that was generated in previous chapters to obtain results for projections of possible weather scenarios in future years.

The eight simulations per case corresponds to the first four made for simulations with dwellings oriented north-south. The first one of these four, performed using the historical weather file; the second, third and fourth using the new generated weather files for the near, medium and far horizon for years 2015-2039, 2045-2069 and 2075-2099. The remaining four cases were performed using the mentioned weather files, this time for east-west oriented dwellings. These simulations were made for each case of every location chosen in the cities of Saltillo, Monclova and Torreón.

When making the selection for the envelope materials, concrete block was chosen for the base cases because it is the most common building material used in social housing in Mexico. It was considered important to bring the possibility to evaluate its performance compared with two other materials, that are more expensive, but allow the analysis intended for this research, the one of examine which one performs better thermally.

The Autoclaved Aerated Concrete Block has been used to evaluate its performance in the residential sector, and has been used in the country as an alternative considered more ecological, for reducing costs related to heating and cooling in buildings. Being a material that has benefits regarding these characteristics, it is considered by credit institutions as an ecological material that applies to obtain discounts when using it.

One of the materials that has been studied more widely today in the country, due to its thermal benefits, is the clay hollow block. Studies carried out for the country's

north-east region, place this material as one of the best for extreme climates, as it has considerable layers of air, and is less heated than traditional concrete blocks. The speed in the heat transmission is slower than with the concrete block, so having such extreme temperatures in this part of the country, it is a good alternative for both summer and winter seasons.

Open elements like windows, were reviewed with single glazing, as is the common approach to these buildings. The simulation of double glazing was proposed to compare the interaction of both with the walls of the three materials studied, to explore the possible increase or decrease in hours of comfort. Double glazing technical data state the thermal benefit obtained when using it on windows, so for this study it is proposed to see if it makes a difference with the common constructive systems in the three cities.

Flat slabs were considered in roofs, since they are commonly used in this region because there is little rainfall or other precipitations throughout the year. It was also considered to rotate the roofs to study the effect on single sloped roofs, and verify if there were thermal improvements by allowing the ventilation that is generated by placing clerestory windows under them. This was done by placing the highest height facing north, and later facing south, in the houses oriented north-south; the same was done in the east-west direction, placing the highest height in the east, and later in the west.

Over roofs with lighter materials were also proposed in simulations because similar projects worked well in cities with similar climatic conditions in the north-east of the country. These were proposed mimicking the flat roof, and also the single sloped roofs, to analyse the possibility of obtaining thermal improvements with the air voids and natural air currents possibly generated between the roof and the over roof.

The arrangement and size of windows was first evaluated by doing a solar analysis to have the lowest direct solar incidence income in summer, and the highest in winter. All this, considering the interior distribution of the house. Clerestory and mobile windows were used to allow their opening when appropriate. Different overhang placements and sizes were proposed on the roofs; smaller overhangs placed on top of the windows were also simulated to make a comparison of the most suitable for each case.

Infiltration is a complex and current issue that must be evaluated in detail. By means of the research, three air changes per hour were considered in simulations; the base case one obtained from a reference measurement from the NAMA documentation [121], and two others under the *Passivhaus* standard, for the possible obtaining of better results. These three rates were used in the simulations to evaluate how they performed with the constructive systems and materials proposed in the envelope, under the supposition that they can perform with those qualities of air tightness. The results may differ from those required in homes with such strict standardisation as the *Passivhaus*.

To see the impact in comfort, it was made a comparison between geometries; two different architectural floor plans were simulated, one more compact in form than the other, but with the similar amount of square meters. All these characteristics of envelope elements were intended to cover the modification of the most important parameters for the thermal performance of social housing in Coahuila. The components of the envelope interact with each other in the simulations to allow an analysis of what works best for each case.

Many more parameters can be integrated, and in greater detail and various modifications, especially if it was possible to compare the performance of these houses in the field, measuring them. However, it was considered that the parameters proposed for the dynamic simulations constitute the most important in terms of thermal behavior, and provide relevant information on the elements that have a better performance. Results of these simulations and the corresponding analysis are discussed in the next chapter.

Chapter 7

Simulation Cases and Resilience

This Chapter evaluates the best envelope characteristics for the locations chosen in Coahuila under the range of options specified in the previous chapter. The 41 cases per city were divided into three sets for the dynamic thermal simulations. The results obtained were compared in terms of annual comfort and temperatures inside the houses.

Saltillo was the city that was chosen as the pillar of the simulations since it is the capital of the state, with the largest population and the largest number of urban settlements of the social housing type. Once the first set of cases was analysed, the one with the best performance was chosen as the basis for the second set, in which modifications were made exclusively to the heights of the walls and the arrangement of roofs. In the third set, a different geometry was chosen, with gable roofs and a rectangular architectural floor plan; regarding the building envelope, the parameters used in the Base Case were simulated, as the ones used in the best case of the first two sets.

Once these first 40 cases were concluded together with the base case, giving a total of 328 simulations for Saltillo, another 82 cases were made for the two remaining locations. The cases evaluated for Saltillo, were simulated with exactly the same characteristics for the cities of Monclova and Torreón, resulting in 656 more simulations; the differences in results are due to the fact that the historical weather files were used initially, and then were compared with those weather files obtained with Algorithm DGG3 for the near, medium and far horizons.

It was chosen to carry out the analysis in this way to corroborate whether it was pertinent to consider improvements in the design for the state based on the modifications that can be made in a single location. In Figure 7.1 a diagram shows the arrangement of the results obtained from the dynamic thermal simulations. Results are described and explained in this chapter following this order.

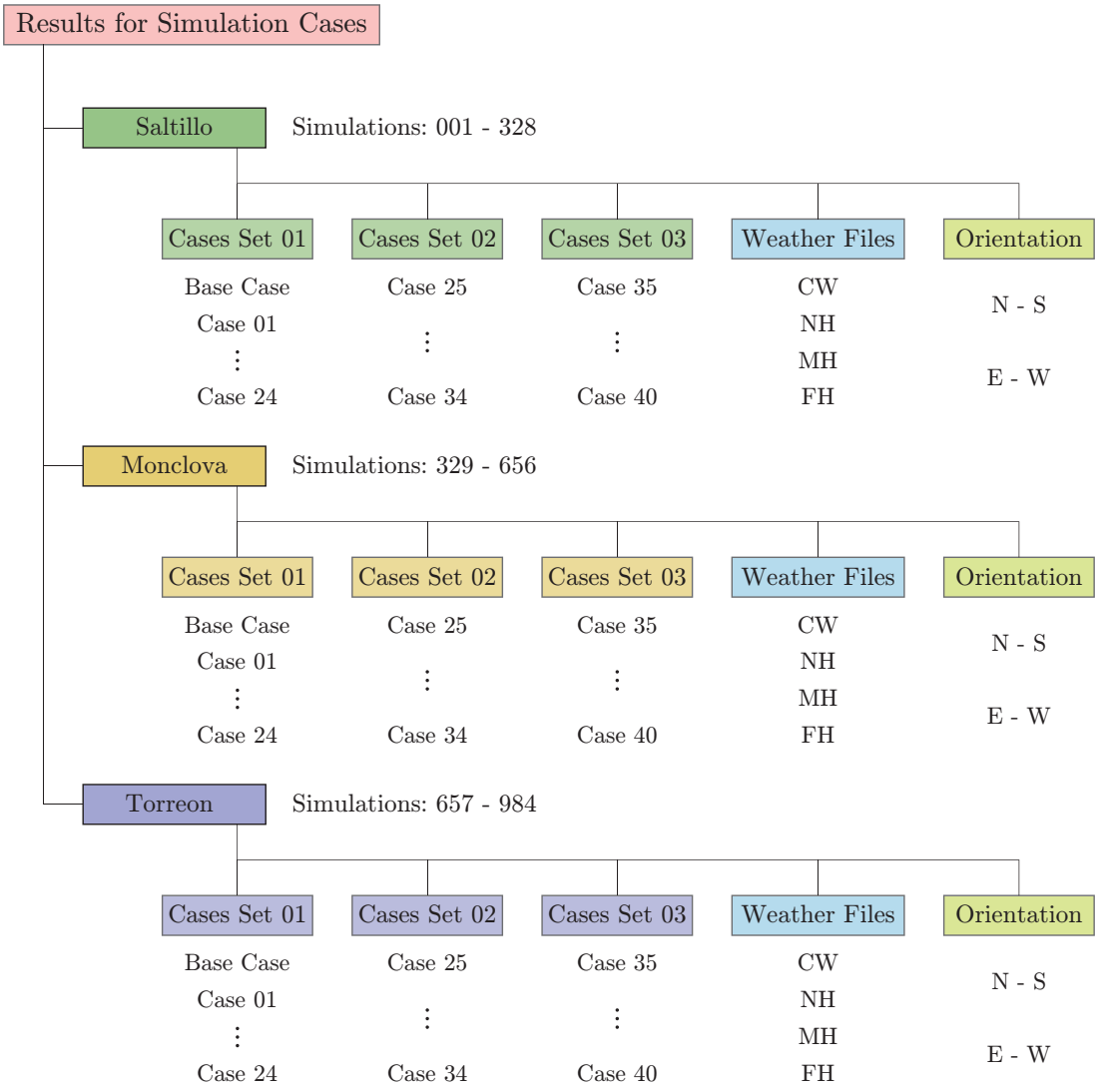


Figure 7.1: Diagram of Simulations Results Arrangement.

In the three cities for this study, there is a large day and night variation in temperatures, which are also seasonal. As micro climates can have big variations, even within the same city, this study focused on specific geographic coordinates, which were called by the name of the city, for practicality.

The chosen locations and their corresponding altitudes are $25^\circ\ 23'\ 35''$ N, $100^\circ\ 59'\ 58''$ W,

and 1719 m for Saltillo; $26^\circ\ 50'\ 40''$ N, $101^\circ\ 25'\ 28''$ W, and 623 m for Monclova; and $25^\circ\ 32'\ 24''$ N, $103^\circ\ 19'\ 58''$ W, and 1118 m for Torreón.

7.1 Simulation for Adapted Models, Saltillo

The weather characteristics of the city of Saltillo are specified in this section. Likewise, the results obtained from the simulations that were made for this city are shown in three sets of simulations, which include 24 cases and the base case containing 200 simulations for the first set, 10 cases with 80 simulations for the second, and six cases with 48 simulations for the third. The simulations contemplate two different orientations under weather files for historical weather, and three possible future horizons. The cases results of each set are analysed and the best characteristics of the envelope for each of them are explained.

7.1.1 Current and Future Weather

The weather data from the historical weather files for Saltillo consider a maximum and minimum temperatures of 38.00° C and -5.00° C respectively; the relative humidity fluctuates between 100% and 12% throughout the year.

The three horizons and temperatures according to the data obtained from the UNAM Climate Atlas website were gathered for the RCP4.5 of HadGEM2-ES model. The minimum, average and maximum temperatures for the Near Horizon (years 2015-2039), are 5.20° C, 19.28° C and 34.60° C correspondingly. For the Medium Horizon (2045-2069), same types of temperatures are 6.10° C, 20.15° C and 35.80° C, and for the Far Horizon (years 2075-2099), they are 6.70° C, 20.68° C and 36.20° C.

The data of minimum and maximum temperatures and relative humidity obtained from these projections, and interpolated using the Algoritmh DGG3 and appear in Table 7.1; these are displayed for the near, medium and far horizons.

Table 7.1: Minimum and Maximum Temperatures and Relative Humidity from *.epw* files used in Saltillo simulations for future horizons.

Weather File	**Max Temp [$^{\circ}C$]**	**Min Temp [$^{\circ}C$]**	**Max RH [%]**	**Min RH [%]**
Near Horizon	25.40	11.40	74.00	41.00
Medium Horizon	26.50	12.80	71.00	39.00
Far Horizon	26.90	11.40	69.00	38.00

7.1.2 Set 1

For this set, all simulation parameters were simulated making an interaction individually between each one of them. Results of Percentage of Annual Comfort (%) in Base Case and Cases from 1 to 24 are shown for current weather, near, medium, and far horizons in Table 7.2. These include both orientations, north-south, and east-west.

Table 7.2: Set 1 Saltillo, Percentage of Annual Comfort (%) in Base Case and Cases from 1 to 24 for current weather, near, medium, and far horizons, in north-south and east-west orientations.

Case	**C NS**	**NH NS**	**MH NS**	**FH NS**	**C EW**	**NH EW**	**MH EW**	**FH EW**
BC	22.72	27.53	27.91	28.36	22.91	28.16	28.46	29.00
1	25.27	29.43	29.51	29.71	25.61	30.35	30.49	30.72
2	26.19	29.50	28.58	29.51	26.44	29.89	29.21	30.09
3	31.33	29.02	28.40	29.48	31.80	29.90	28.86	30.26
4	25.44	29.37	29.44	29.63	25.70	30.29	30.38	30.63
5	26.24	29.38	28.43	29.37	26.50	29.82	28.99	29.95
6	31.10	28.94	28.18	29.42	31.56	29.89	28.84	30.13
7	25.88	32.33	32.09	31.43	25.93	33.32	33.16	32.57
8	28.40	34.07	33.67	34.03	28.89	34.75	34.33	34.96
9	33.73	34.23	33.70	34.77	34.48	35.62	35.11	36.28
10	26.04	32.34	32.10	31.45	26.15	33.30	33.08	32.44
11	28.38	33.96	33.59	33.94	28.93	34.80	34.40	34.68
12	32.49	33.01	32.17	33.37	33.09	34.47	33.40	34.62

continues on the next page ...

Case	C NS	NH NS	MH NS	FH NS	C EW	NH EW	MH EW	FH EW
13	26.42	33.35	33.08	32.29	26.59	34.31	34.27	33.47
14	29.13	35.37	35.14	35.49	29.73	36.34	36.36	36.32
15	34.58	35.56	34.77	35.78	35.31	37.01	36.28	37.05
16	26.58	33.39	33.09	32.34	26.76	34.42	34.31	33.51
17	29.22	35.31	35.09	35.39	29.75	36.17	36.21	36.25
18	34.97	36.16	35.64	36.57	35.74	37.90	37.00	37.97
19	26.52	33.26	32.93	32.16	26.63	34.22	34.12	33.36
20	29.27	35.34	34.99	35.35	29.81	36.16	36.23	35.83
21	34.88	35.87	35.54	36.36	**35.83**	37.72	37.01	37.58
22	26.64	33.31	32.95	32.16	26.80	34.35	34.17	33.35
23	29.36	35.27	34.91	35.25	29.89	36.14	36.03	36.13
24	**35.11**	**36.24**	**35.67**	**36.62**	35.47	**38.09**	**37.23**	**38.03**

In Figure 7.2 can be seen that the slight initial changes that were made to the design of the base case, resulted in a small increase in thermal comfort in all cases. The BC is shown in all the graphs to analyse the increase in comfort hours compared to the initial case. These cases were evaluated considering having the OWBC and 5 h^{-1} ACH. The material that performed the best with the historical weather file, which will be called Current Weather (CW) from now on, was the clay hollow block along with the use of single glazing, while for the climate files of the future horizons, the one that performed the best in all cases except in the near horizon with a north-south orientation, was the concrete block. This material was the one that had the worst performance in CW, while the CHB was the one that performed the worst in most future horizons, all of them with the use of double glazing.

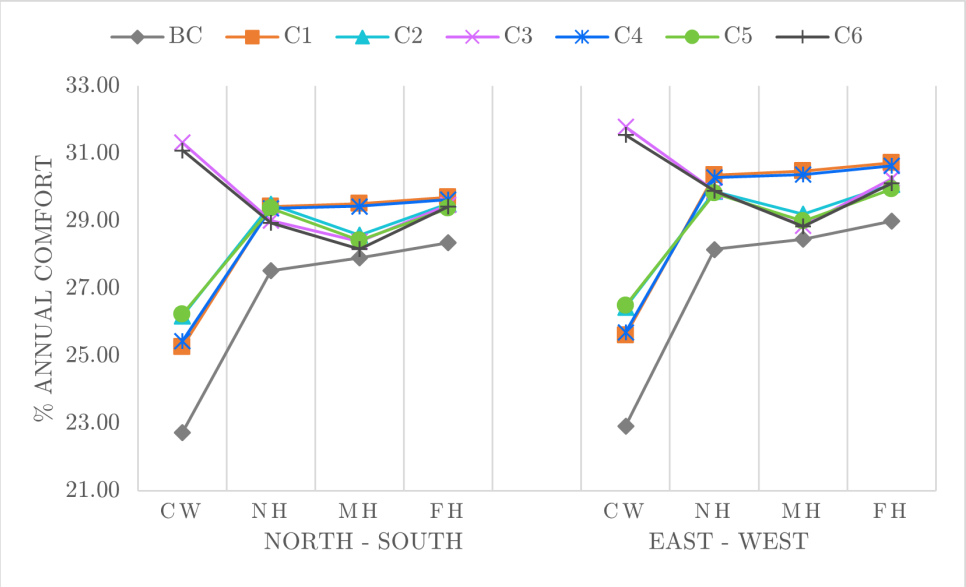


Figure 7.2: Saltillo Cases 1 to 6.

In the following cases it was used the OW1. For the cases shown in the Figure 7.3, it can be seen that in all the time periods studied and in all the configurations, the best case was C9, where single glazing and CHB are used. The worst case in the north-south orientation was the C7, where single glazing and concrete block are used in the envelope, as well as in the east-west orientation for the CW. For future horizons in this orientation, the worst case was C10, where double glazing with CHB in the envelope was proposed.

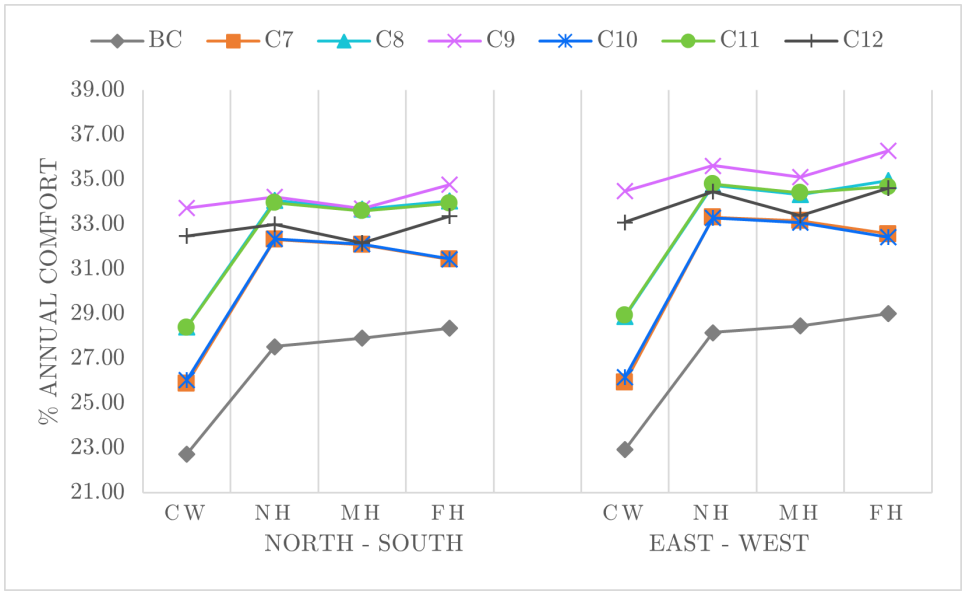


Figure 7.3: Saltillo Cases 7 to 12.

From case 13 to 18, Figure 7.4 a rate different from the one proposed in the previous cases was simulated. A 0.6 ACH rate was considered; this represented an increase in the hours of comfort in the house, with the best case being C18 for all horizons and both orientations. In this case double glazing was used in the CHB of the envelope. The worst case was also the same for all scenarios, Case 13, in which simple glazing in windows and concrete block in the envelope were used.

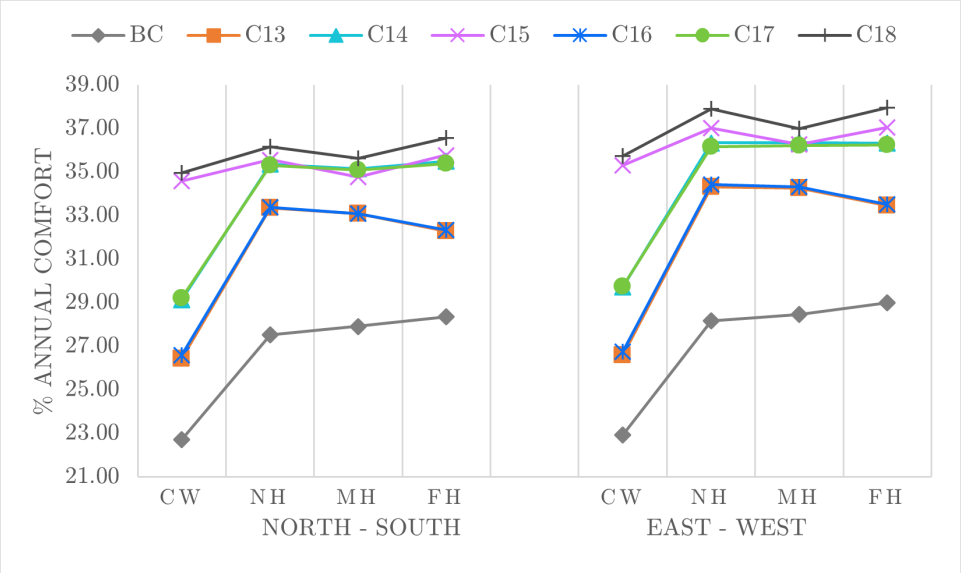


Figure 7.4: Saltillo Cases 13 to 18.

The attributes of the previous cases were preserved, except for ACH, which for the next six cases were used at a lower rate, 0.3 ACH. This was proposed considering the *PassivHaus* standards, to compare if this component respresented an increment in comfort hours even though the rest of the *PassivHaus* parameters are not strictly used in these simulations.

In Figure 7.5 it can be seen that changing this parameter did not always result in a better outcome. Even so, for case 24 it was favorable, and in all horizons for both orientations, it had the most hours of comfort, except for the CW in the east-west orientation. This case was considered the best of the first set, with double-glazed windows in a CHB surround.

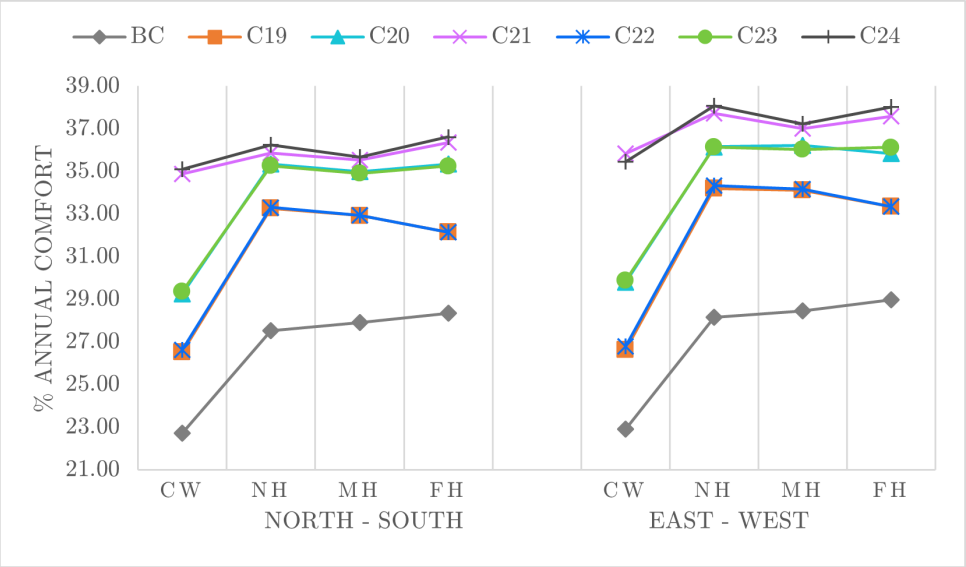


Figure 7.5: Saltillo Cases 19 to 24.

In general, the material with the best performance was the CHB, while the AACB was always intermediate between the values obtained between the CHB and the CB. The single glazing worked better in the first half of the cases, where an ACH of 5 h^{-1} was considered. By reducing this rate to 0.3 ACH, the double glaze worked better, as can be seen in the results corresponding to the second half of the cases in the set.

With the variation of these elements, the hours of comfort inside the house in the north-south orientation increased by 12.39% compared to the base case for the current weather; for the near horizon they increased by 8.71%, for the medium by 7.76%, and for the far horizon by 8.26%. The best case was 24 for all horizons and current weather.

For the east-west orientation, the comfort hours were higher in future horizons, and the percentage of benefit with respect to the base case were 9.93% for the near horizon, 8.77% for the medium, and 9.03% for the far horizon with the best case, wich was the same than in north-south orientation, Case 24. The best case was 21 for current weather, with a 12.92% improvement with respect to the base case.

7.1.3 Set 2

Considering the best case from the previous set, it was chosen the one with the best performance, and was modified in terms of heights and roof disposition for Set 2.

The use of clerestory windows was proposed in all cases of this set, to analyse if it resulted in a better envelope performance with the increase of openings that promoted different ventilation possibilities. Results are shown in Table 7.3.

Table 7.3: Set 2 Saltillo, Percentage of Annual Comfort (%) in Cases from 25 to 34 for current weather, near, medium, and far horizons, in north-south and east-west orientations.

Case	C NS	NH NS	MH NS	FH NS	C EW	NH EW	MH EW	FH EW
25	35.52	36.28	36.33	36.87	35.93	37.89	37.22	37.99
26	35.56	36.47	36.35	37.05	35.98	**38.22**	37.37	**38.09**
27	35.58	36.65	**36.62**	**37.11**	35.90	37.86	37.27	38.09
28	35.64	36.66	36.47	36.75	36.25	38.07	**37.55**	38.02
29	33.71	32.13	33.28	34.83	34.00	32.13	33.78	35.76
30	36.01	**36.97**	36.57	36.33	36.38	37.77	37.19	37.36
31	36.63	36.76	35.57	33.82	37.03	37.65	36.50	35.54
32	35.58	36.95	34.44	32.33	35.70	37.88	35.49	33.77
33	**36.72**	36.90	35.73	33.96	**37.10**	37.70	36.48	35.50
34	35.53	36.85	34.40	32.35	35.67	37.80	35.52	33.67

For cases 25, 26 and 27, the characteristics and geometry of the best case of Set 1 were preserved, which include double glazing in windows, the use of clay hollow block in the opaque envelope, and 0.3 ACH. The variable parameter in these cases was that in Case 25 horizontal overhangs were used on the top of the windows in the west, while in Case 26 these overhangs were simulated on the south, east and west façades.

In Case 28, openings were also proposed with overhangs on top of the windows placed in south, east, and west. It was proposed to use a sloped roof to assess whether a new roof arrangement would benefit from it. In evaluating which arrangement worked best, this one was chosen for this case. The common area with kitchen, bathroom,

and the master bedroom have this roof, while the remaining bedroom receives the benefits of the shade generated by it, and preserves the initial height. In the southern part, the sloped roof maintains its initial height, and in the highest part on the north façade, four courses of concrete block were added. On the north and south façades clerestory windows were arranged on all the walls. This was the best case of the set, see Figure 7.6.

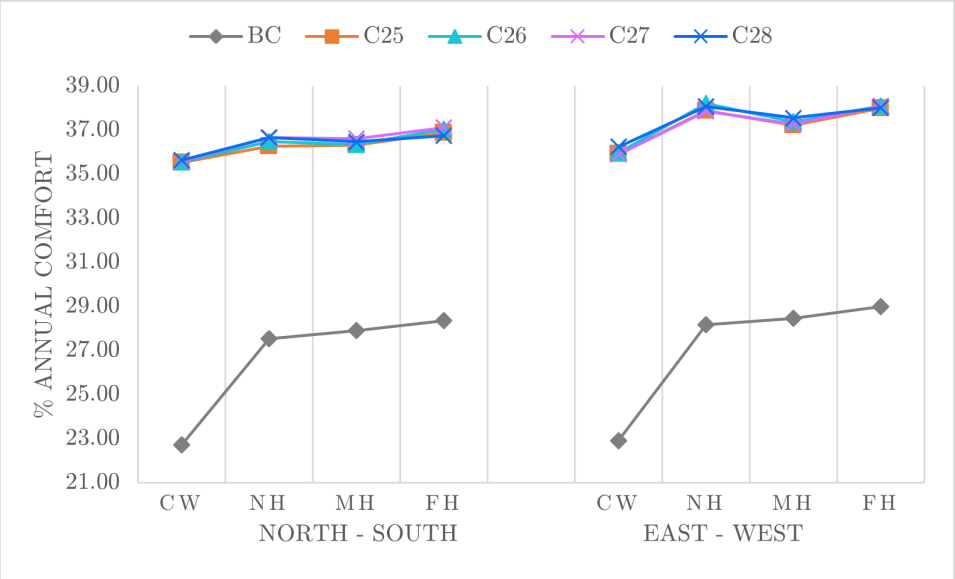


Figure 7.6: Saltillo Cases 25 to 28.

For the rest of the cases of this set, the heights on all the walls were increased, adding two courses of masonry block.

In cases 29-31, more pronounced overhangs of $0.60\,m$ were proposed on the façades that are not attached to the the site limit, which are the north, south and east, in the north-south orientation, and the east, west and north , in the east-west oriented house.

For cases 32-34, a corrugated sheet over roof separated from the ceiling at $0.40\,m$ was used for Case 32, with the horizontal over roof; for the other two cases, the shortest separation is $0.30\,m$, and the largest is $0.77\,m$; the shortest being on the south façade in Case 33, and the north in Case 34.

The corrugated over-roof was proposed in hand with these windows to apply Bernoulli's principle. With this, wind velocity increased, and therefore, the ventilation between the roof and the over-roof; most of the sun hitting the envelope heats the over-roof instead

of the roof this way.

In this set there was a variation of the best cases, while the worst was 29, in six of the eight simulation scenarios. The best case was 33 for both orientations with the CW, the over roof turned to the south works well, with which it can be confirmed that it is a good solution for the current weather; this can be seen in Figure 7.7. However, if we consider the climate scenario of this study, for the north-south orientation the best case for the near horizon is 30, where the steepest overhangs worked well, together with the increase in wall height. For the medium and future horizons, the best case was 27, where the geometry of the base case worked well, and the window opening hours were modified.

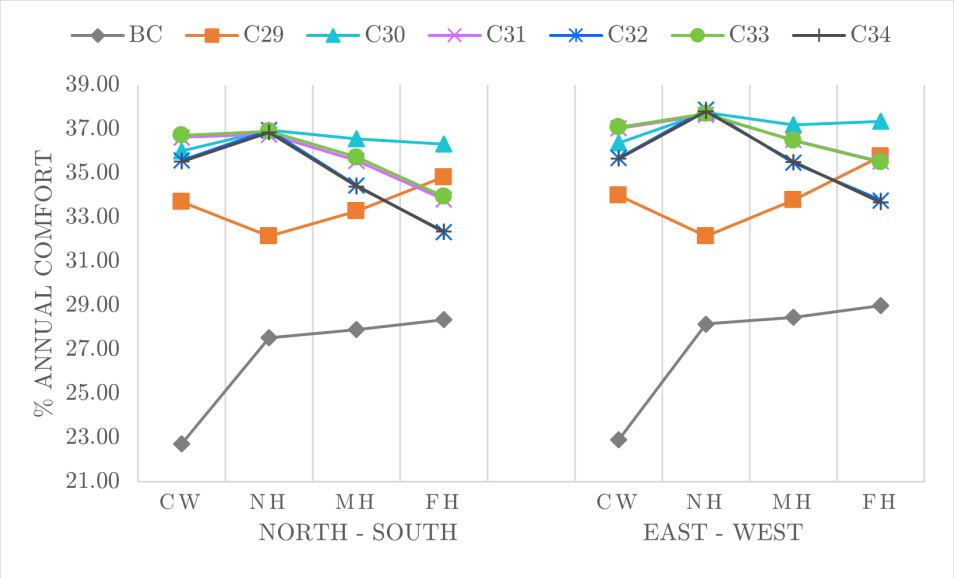


Figure 7.7: Saltillo Cases 29 to 34.

For the east-west orientation, Case 26 was the best for the near and far horizons, where the geometry of the base case and over hangs on top of the windows were used; for the medium horizon, Case 28 was the best, with the sloped roof arrangement. This case was the best in general, since a sum of comfort hours was made in simulations with the current climate, all horizons, and the two orientations, resulting in the best case. Under the assumption that only one design for housing in this area should be proposed, Case 28 would be the best. But if there were the possibility of proposing a design for the type of orientation, the best would still be this for the east-west orientation, while for the north-south orientation, the best proposal is that of Case 27.

The increase in comfort of best cases compared to the base case for north-south oriented housing, was 14% for CW, 9.44% for near horizon, 8.70% for medium, and 8.75% for the far. For east-west orientation was of 14.18% for CW, 10.06% for the near horizon, 9.09% for medium, and 9.10% for the far one.

7.1.4 Set 3

A different geometry was experimented with for Set 3. The use of gable roofs was proposed on the ceilings, and the geometry was also proposed in a more compact way, where the architectural plan is rectangular, but the measurements and orientations of the windows were preserved as in the base case. Results are shown in Table 7.4.

Table 7.4: Set 3 Saltillo, Percentage of Annual Comfort (%) in Cases from 35 to 40 for current weather, near, medium, and far horizons, in north-south and east-west orientations.

Case	C NS	NH NS	MH NS	FH NS	C EW	NH EW	MH EW	FH EW
35	22.23	27.06	27.42	27.78	22.18	26.77	27.15	27.54
36	22.77	27.70	28.22	28.82	22.72	27.45	27.81	28.43
37	34.79	**36.24**	34.99	**36.23**	34.97	36.14	35.13	36.40
38	35.25	35.93	34.90	35.66	35.32	35.79	34.92	35.61
39	35.52	35.64	**35.62**	36.14	35.99	**36.80**	**36.71**	**37.16**
40	**35.66**	35.68	35.55	36.04	**37.11**	36.76	36.61	37.11

The initial characteristics of the base case were simulated for the two initial cases, 35 and 36. With simple glazing in windows, and the opaque envelope of concrete block, and the original OWBC and air changes per hours as in base case. In C35 the volume was considered with ceiling, and in C36 without ceiling.

With these characteristics for the north-south orientation, the C36, where the ceiling was not considered, had improvements compared to the BC and the C35. With CW, near and far horizons, this case performed better than the base case, which only got better results at the medium horizon. For the east-west orientation, the base case had better results than the other two cases in all scenarios, so with these characteristics for

this orientation, the use of compact design is not convenient.

For cases 37-40 the best characteristics of Set 2 were used under this new geometry; the clay hollow block with operable windows with modified months of operation, and clerestory windows. Both single and double glazing, and gable roof with and without ceiling were simulated.

The best case for both orientations was the C40. For the north-south orientation, the best case for the near and far horizons was C37, while the best case for the middle horizon was C39. This was also the best case for the thee horizons in the east-west orientation, as shown in Figure 7.8.

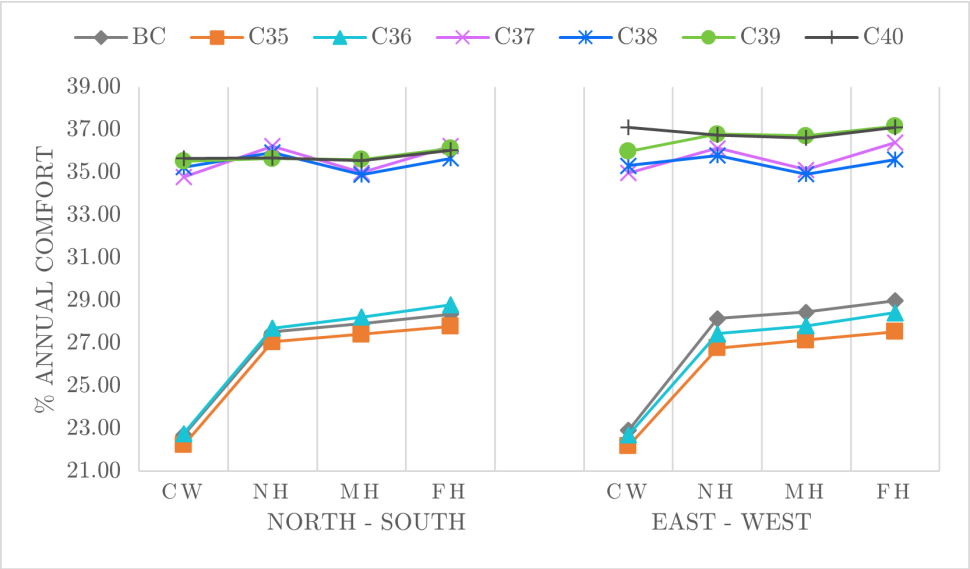


Figure 7.8: Saltillo Cases 35 to 40.

Making the sum of the greatest number of hours of comfort for both orientations, the best case was C40. Results of increase in comfort of best cases compared to the base case for north-south oriented housing, were of 12.94% for current weather, 8.70% for near horizon, 7.70% for medium, and 7.87% for the far. For east-west orientation, they were of 14.20% for CW, 8.64% for the near horizon, 8.25% for the medium, and 8.17% for the far horizon.

Comparing the best cases obtained with the three sets, the best one corresponds to Set 2, which has the bigger increments of thermal comfort hours regarding the base case. This performed better than the compact case in all scenarios except for the current

weather in east-west orientation, which had a slightly better performance. The worst design using the base case characteristics was the compact one, which in general behaved worst than the worst cases with the base case geometry. A table showing these results can be consulted in Table 7.4.

7.1.5 Results

Making a sum of the annual comfort hours evaluated for the current weather, it was possible to conclude that the best case in general for current weather was C33, with a south-rotated over roof, double glazing, an opaque clay hollow block envelope, 0.3 ACH, and OW4 window opening with clerestory windows, see Figure 7.9. For the north-south orientation this was also the best case, with 36.72% of annual comfort; while for the east-west it was C40, with 37.11%, figure slightly higher than the 37.10% obtained for this orientation in case C33.

On future horizons, the overall best case was the C28, with a south-rotated sloped roof, double glazing, an opaque clay hollow block envelope, 0.3 ACH, and OW3 window opening with clerestory windows.

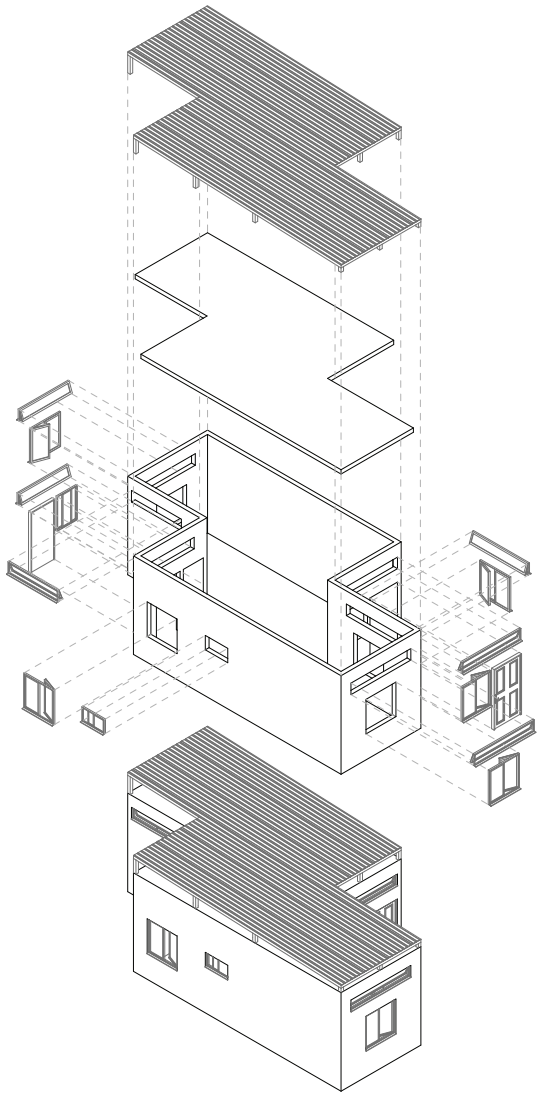


Figure 7.9: Saltillo Best Case for current weather, Case 33.

For all scenarios and simulations, the best case was C28. For the narrow thermal comfort threshold in north-south orientation for current weather, near, medium and far horizons correspondingly, annual comfort was of 35.64%, 36.66%, 36.47% and 36.75%; and for the east-west orientation was 36.25%, 38.07%, 37.55% and 38.02%.

For the wide thermal comfort threshold in north-south orientation the annual comfort was of 26.16%, 34.58%, 41.87% and 47.42%; and for the east-west orientation was 26.12%, 34.54%, 41.79% and 47.28%.

7.2 Simulation for Adapted Models, Monclova

In this section, the weather characteristics of the city of Monclova are specified. As analysed for Saltillo, the results obtained from the simulations that were made for Monclova are shown in three sets of simulations: the 24 cases and the base case containing 200 simulations for the first set, 10 cases with 80 simulations for the second, and six cases with 48 simulations for the third. Two different orientations under historical weather files and weather files for three possible future horizons were analysed. The results are explained and the best characteristics of the envelope for each of them are elucidated.

7.2.1 Current and Future Weather

The weather data from the historical weather files for Monclova consider a maximum and minimum temperatures of 43.60° C and 2.00° C respectively; the relative humidity fluctuates between 100% and 6% throughout the year.

The three horizons and temperatures according to the data obtained from the UNAM Climate Atlas website were gathered for the RCP4.5 of HadGEM2-ES model. The minimum, average and maximum temperatures for the Near Horizon (years 2015-2039), are 5.50° C, 22.18° C and 37.20° C correspondingly. For the Medium Horizon (2045-2069), same types of temperatures are 6.40° C, 22.98° C and 39.40° C, and for the Far Horizon (years 2075-2099), they are 7.10° C, 23.38° C and 38.70° C.

The data of minimum and maximum temperatures and relative humidity obtained from these projections, and interpolated using the Algoritmh DGG3 and appear in Table 7.5; these are displayed for the near, medium and far horizons.

Table 7.5: Minimum and Maximum Temperatures and Relative Humidity from *.epw* files used in Monclova simulations for future horizons.

Weather File	**Max Temp [$^\circ C$]**	**Min Temp [$^\circ C$]**	**Max RH [%]**	**Min RH [%]**
Near Horizon	29.47	12.13	78.20	47.99
Medium Horizon	30.47	14.22	76.97	44.69
Far Horizon	30.58	12.88	75.65	42.71

7.2.2 Set 1

In Table 7.6 the results obtained for the first set of simulations are shown; these are presented as percentages of annual comfort.

Table 7.6: Set 1 Monclova, Percentage of Annual Comfort (%) in Base Case and Cases from 1 to 24 for current weather, near, medium, and far horizons, in north-south and east-west orientations.

Case	**C NS**	**NH NS**	**MH NS**	**FH NS**	**C EW**	**NH EW**	**MH EW**	**FH EW**
BC	14.29	15.90	16.99	17.41	14.45	16.29	17.51	17.41
1	15.51	16.84	18.07	18.16	15.68	16.84	18.07	18.07
2	15.66	16.68	17.79	19.58	15.85	16.68	17.79	19.58
3	16.09	17.09	18.13	18.83	16.48	17.09	18.13	18.13
4	15.53	16.84	18.01	18.13	15.69	17.57	18.93	18.85
5	15.66	15.15	16.33	18.11	15.80	15.15	16.33	16.33
6	16.04	15.80	16.78	17.46	16.38	15.80	16.78	17.46
7	15.68	18.92	20.17	19.18	15.74	19.68	20.97	20.97
8	16.68	20.77	22.41	22.47	16.87	21.44	23.19	23.20
9	16.58	21.72	21.98	21.72	17.12	22.49	22.65	22.46
10	15.76	18.94	20.20	19.20	15.74	19.75	20.94	19.95
11	16.03	18.77	20.01	21.31	16.85	18.78	20.16	20.13
12	16.44	18.67	19.54	20.01	16.95	19.06	20.12	20.66
13	15.79	19.74	21.07	19.93	15.81	20.63	21.78	21.86
14	**16.99**	22.36	**23.62**	**23.61**	17.12	22.92	**24.62**	24.50

continues on the next page ...

Case	C NS	NH NS	MH NS	FH NS	C EW	NH EW	MH EW	FH EW
15	16.88	**23.17**	23.26	22.06	17.25	**23.64**	24.18	23.14
16	15.86	19.81	21.18	19.96	15.87	20.69	21.96	20.68
17	16.21	19.98	21.50	22.44	17.21	20.03	21.64	21.60
18	16.96	20.75	21.16	21.32	**17.37**	21.10	21.72	22.09
19	15.78	19.74	20.99	19.88	15.77	20.43	21.77	21.78
20	16.96	22.29	23.55	23.54	17.15	22.69	24.53	**24.54**
21	16.81	23.04	23.14	21.94	17.21	23.53	23.95	23.01
22	15.84	19.74	21.11	19.90	15.84	20.61	21.88	20.61
23	16.18	19.96	21.46	22.37	17.16	20.00	21.57	21.58
24	16.84	20.66	21.08	21.18	17.32	21.00	21.60	21.61

In Figure 7.10 it can be seen that considering the window openings of the base case, the best case for the current weather in both orientations was Case 3, with the use of single glazing and clay hollow block, while for the future horizon it was in both orientations the C2, with AACB in the opaque envelope. While the clay hollow block performed better in the near and middle horizons with single glazing in the north-south orientation, in the east-west the best cases showed that double glazing performed better with the concrete block envelope.

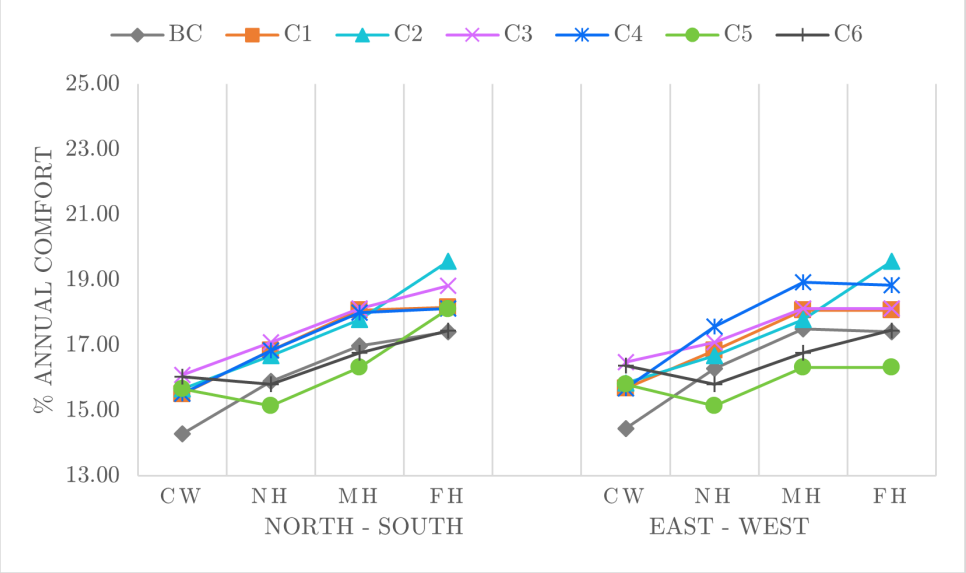


Figure 7.10: Monclova Cases 1 to 6.

By changing to OW1, between cases 7 and 12, it was observed that the best cases were between 8 and 9, where single glazing was used on windows. With the C8, the best results were for the current weather and the medium and far horizons in both orientations; an AACB envelope was used. The C9, where the use of clay hollow block was proposed, was the best case for the current weather of the east-west orientation, and the best for both orientations in the near horizon. See Figure 7.11.

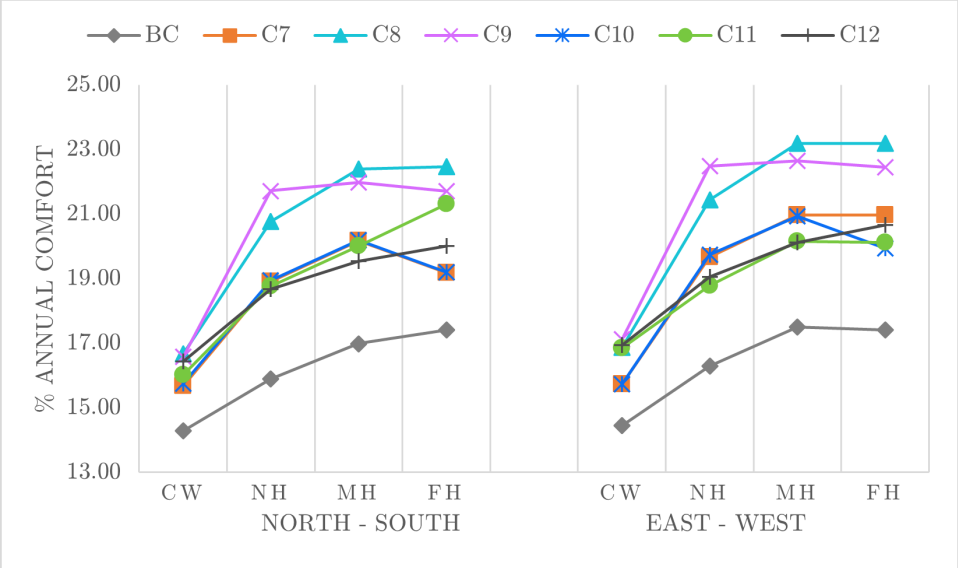


Figure 7.11: Monclova Cases 7 to 12.

With the change from ACH to 0.6 in cases 13-18, the best behavior was seen at C14 for the north-south orientation, and at C18 for the east-west orientation. For both orientations, the best case for the near horizon was C13, while the best case for the medium and far horizons was Case 14. The latter was the best case for the set, where AACB with single glazing is used, as appreciated in Figure 7.12.

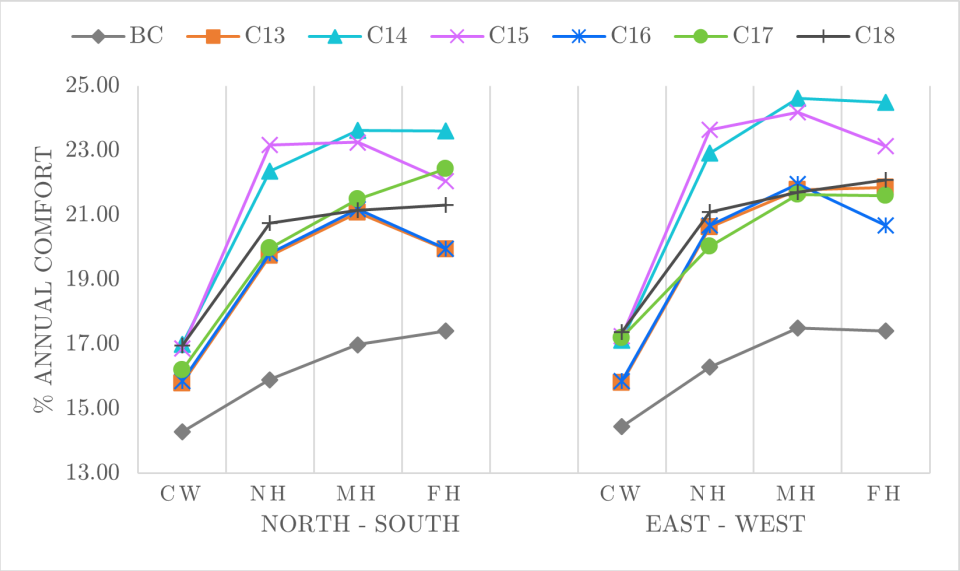


Figure 7.12: Monclova Cases 13 to 18.

In the last simulations of this set, a different ACH was used, 0.3. The behavior of the results for cases 19-24 were similar to those obtained in cases 11-15. The best cases were the same in both sets of simulations. However, the comfort hour values obtained were higher in the simulations of cases 11-15. Even the worst cases behaved in the same way in both sets, with cases 13 and 19 being the worst for both orientations in the current weather, as well as for the three horizons in the north-south orientation. This case was considered using concrete block with single glazing. See Figure 7.13.

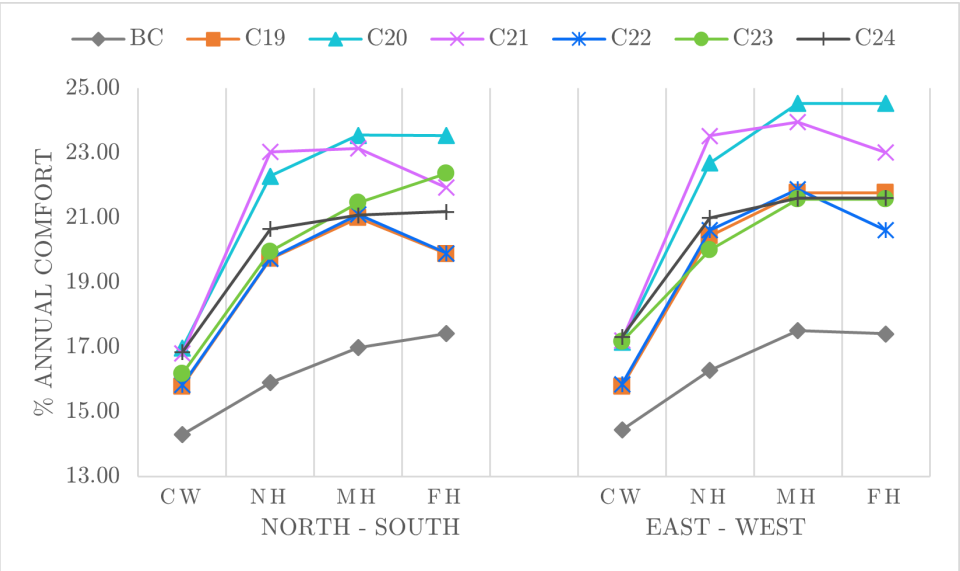


Figure 7.13: Monclova Cases 19 to 24.

7.2.3 Set 2

In Table 7.7 the results obtained for the second set of simulations performed for the chosen location in Monclova are presented.

Table 7.7: Set 2 Monclova, Percentage of Annual Comfort (%) in Cases from 25 to 34 for current weather, near, medium, and far horizons, in north-south and east-west orientations.

Case	C NS	NH NS	MH NS	FH NS	C EW	NH EW	MH EW	FH EW
25	16.93	23.14	23.47	22.08	17.22	23.55	24.10	24.10
26	17.09	**23.29**	23.55	22.32	17.37	**23.71**	24.24	24.24
27	16.92	23.27	**23.72**	22.32	17.15	23.50	24.13	24.12
28	16.80	23.12	23.40	21.74	17.15	23.57	24.25	24.28
29	18.46	21.93	23.16	23.38	18.76	22.33	23.92	23.76
30	16.55	22.61	22.83	21.00	16.87	23.45	23.45	23.45
31	15.29	17.85	18.87	18.69	15.59	18.34	19.25	19.25
32	19.00	22.38	23.52	24.01	19.41	22.77	24.12	24.24
33	**19.08**	22.39	23.58	**24.08**	**19.45**	22.79	**24.29**	**24.47**
34	18.44	21.92	23.17	23.36	18.77	21.92	23.17	23.17

The results of Set 2 are shown in the Figure 7.14, and Figure 7.15, considering that the building envelope characteristics were simulated for the best cases of Saltillo, results vary when the simulations are made for the city of Monclova. In this set, double glazing, clay hollow block, and the proposed window arrangement after the solar incidence analysis were considered. The case that overall had the worst performance was Case 31 for current weather in both orientations and all weather files, current and for the horizons.

The case that had the best results in both orientations for the current weather and far horizons was C33, as for the mid horizon in east-west, where the roof was disposed rotated to the south, this was also the best case of Set 2. For the near horizons the best was C26, and the medium horizon for north-south, was C27.

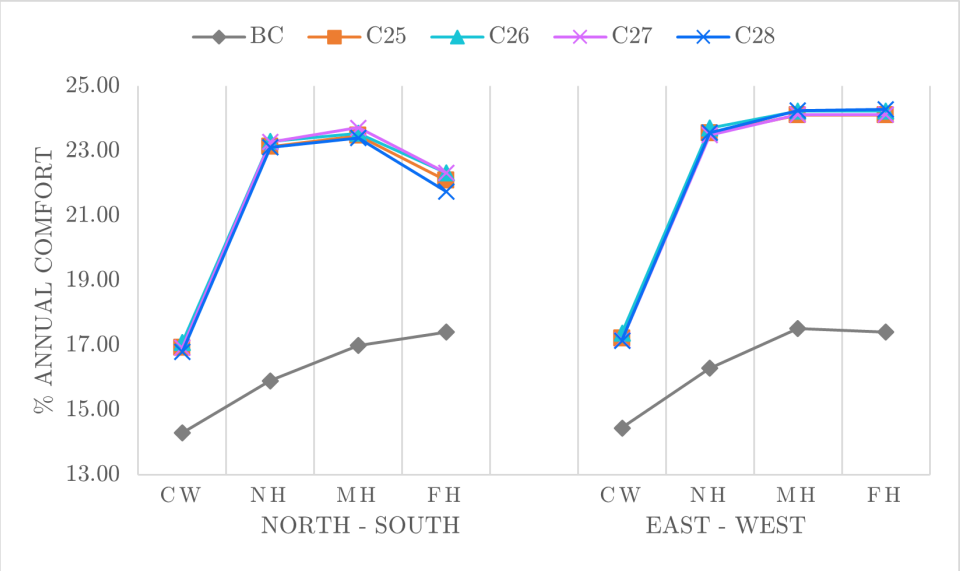


Figure 7.14: Monclova Cases 25 to 28.

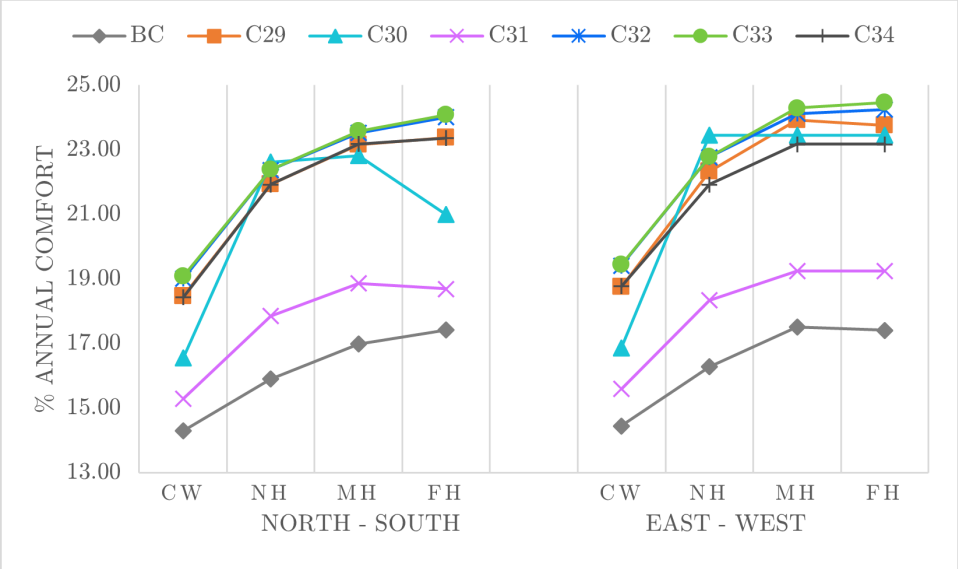


Figure 7.15: Monclova Cases 29 to 34.

7.2.4 Set 3

In Set 3, the simulation results were the same for both orientations (Table 7.8). The worst case was C35 for current weather and future horizons. In these simulations the characteristics of the base case with the geometry of the compact case were preserved.

Table 7.8: Set 3 Monclova, Percentage of Annual Comfort (%) in Cases from 35 to 40 for current weather, near, medium, and far horizons, in north-south and east-west orientations.

Case	C NS	NH NS	MH NS	FH NS	C EW	NH EW	MH EW	FH EW
35	14.15	15.80	16.77	17.07	14.09	15.64	16.56	16.56
36	14.36	16.02	17.09	17.64	14.26	15.81	16.83	16.83
37	**19.42**	22.52	**23.80**	**24.47**	**19.81**	22.52	**23.80**	**23.80**
38	16.65	22.74	22.79	21.77	16.53	17.81	18.78	18.78
39	16.60	22.86	23.10	21.66	16.94	17.92	18.95	18.95
40	16.57	**22.88**	23.05	21.68	16.91	**23.26**	23.57	23.57

The best case was C37 for current weather, mid and future horizons. Case 40 was the best for the near horizon. Case 37 was the best of the set, and uses the gable roof without ceiling, and single glazing used in windows of the WM2. See Figure 7.16.

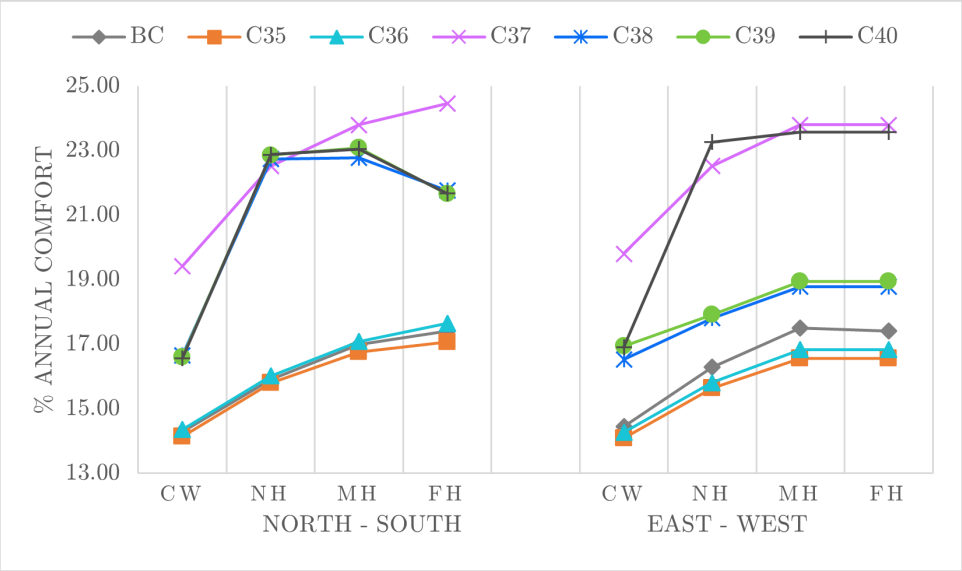


Figure 7.16: Monclova Cases 35 to 40.

7.2.5 Results

Monclova was, in general, the city with less annual comfort hours under all cases and simulations. The city is a valley surrounded by steel industries, so the lack of venti-

lation made difficult to propose useful design strategies considering the characteristics of the site.

Case 37 was the one that resulted in the best for current weather, mid and far horizons in both orientations, with an annual comfort of 19.42% in north-south orientation, and 19.81% in east-west orientation. This resulted in the more hours of thermal comfort along the time considered in all simulations for this location. The envelope material of this case is clay hollow block, 0.3 ACH, and a gable roof without ceiling; this increased the volume inside the house.

For future horizons in both orientations the fitter case was C16, Figure 7.17. Regular concrete block worked the best and geometry only suffered little modifications regarding the base case, with roof slab overhangs in the south façade. Higher values of annual comfort percentage for north-south and east-west orientations correspondingly are 4.63% and 5.23% for near horizon, 5.59% and 5.97% for medium horizon, and for the far horizon, 4.71% and 5.14%.

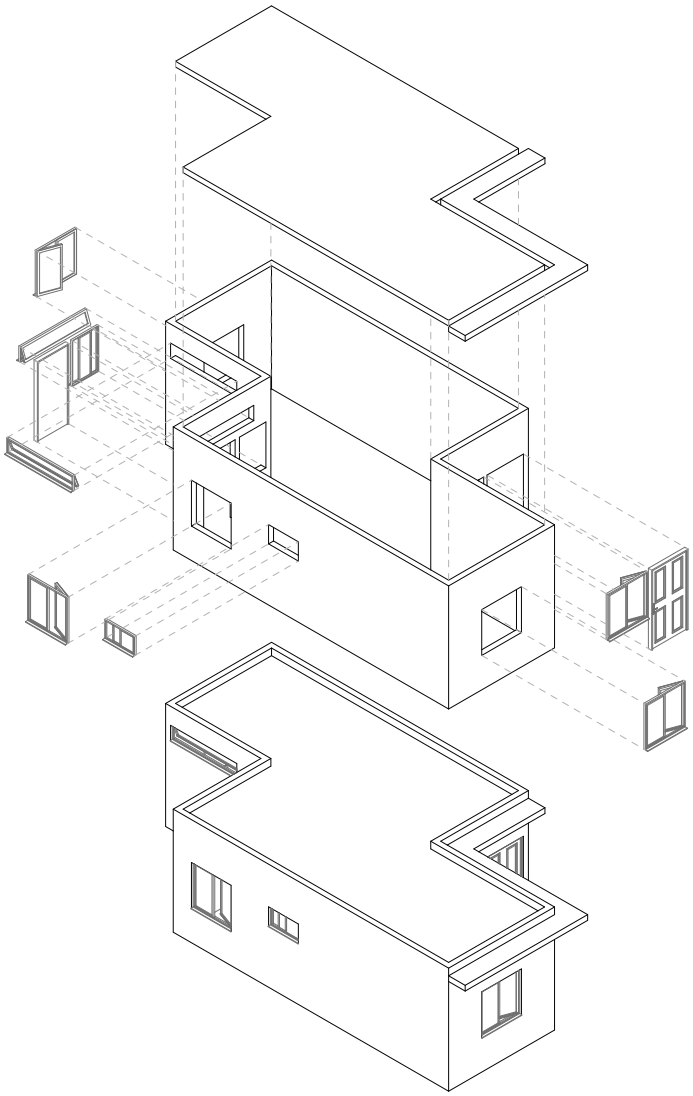


Figure 7.17: Monclova Best Case for future horizons, Case 16.

For all scenarios and simulations, the best case was C37. For the narrow thermal comfort threshold in north-south orientation for current weather, near, medium and far horizons correspondingly, annual comfort was of 19.42%, 22.52%, 23.80% and 24.47%; and for the east-west orientation was 19.81%, 22.52%, 23.80% and 23.80%.

For the wide thermal comfort threshold in north-south orientation the annual comfort was of 52.01%, 50.91%, 53.77% and 56.99%; and for the east-west orientation was 55.18%, 59.00%, 61.67% and 65.11%.

7.3 Simulation for Adapted Models, Torreón

As previously shown for Saltillo and Monclova, the weather characteristics of the city of Torreón are explained along with the analysis of the results obtained for the simulations of the three sets and the 328 simulations. The best characteristics of the envelope for each set is evaluated and described in this section.

7.3.1 Current and Future Weather

The weather data from the historical weather files for Torreón consider a maximum and minimum temperatures of 40.20° C and 2.00° C respectively; the relative humidity fluctuates between 100% and 4% throughout the year.

The three horizons and temperatures according to the data obtained from the UNAM Climate Atlas website were gathered for the RCP4.5 of HadGEM2-ES model. The minimum, average and maximum temperatures for the Near Horizon (years 2015-2039), are 5.60° C, 22.18° C and 38.60° C correspondingly. For the Medium Horizon (2045-2069), same types of temperatures are 6.60° C, 23.99° C and 39.60° C, and for the Far Horizon (years 2075-2099), they are 7.00° C, 24.46° C and 40.10° C.

The data of minimum and maximum temperatures and relative humidity obtained from these projections, and interpolated using the Algoritmh DGG3 and appear in Table 7.9; these are displayed for the near, medium and far horizons.

Table 7.9: Minimum and Maximum Temperatures and Relative Humidity from *.epw* files used in Torreón simulations for future horizons.

Weather File	**Max Temp [° *C*]**	**Min Temp [° *C*]**	**Max RH [%]**	**Min RH [%]**
Near Horizon	29.50	12.10	76.00	29.00
Medium Horizon	30.40	13.00	69.00	25.00
Far Horizon	30.80	14.10	68.00	23.00

7.3.2 Set 1

In Table 7.10 the results obtained for the first set of simulations are shown; these are presented as percentages of annual comfort.

Table 7.10: Set 1 Torreón, Percentage of Annual Comfort (%) in Base Case and Cases from 1 to 24 for current weather, near, medium, and far horizons, in north-south and east-west orientations.

Case	C NS	NH NS	MH NS	FH NS	C EW	NH EW	MH EW	FH EW
BC	21.03	20.21	23.76	24.13	20.89	20.73	24.15	24.41
1	21.90	22.81	25.26	25.32	21.91	23.80	25.63	25.60
2	23.56	19.83	23.89	24.69	23.74	20.49	24.85	25.55
3	25.16	21.37	23.26	25.00	25.69	22.13	24.65	26.12
4	21.97	22.75	25.22	25.33	22.01	23.70	25.74	25.65
5	23.60	19.51	23.77	24.52	23.79	20.01	24.55	25.40
6	24.87	20.71	22.78	24.04	25.44	21.47	23.82	25.33
7	22.12	24.36	25.02	24.87	22.17	25.07	25.32	25.03
8	25.02	23.76	26.32	26.57	25.00	24.57	26.73	27.03
9	25.95	24.99	26.52	27.19	26.75	25.98	28.55	28.14
10	22.19	24.38	25.05	24.95	22.23	25.01	25.34	25.05
11	25.09	23.52	26.33	26.66	25.10	24.12	26.99	27.07
12	25.74	23.97	25.13	25.78	26.42	24.85	26.97	27.29
13	22.53	25.68	25.41	25.25	22.46	26.37	25.61	25.30
14	26.06	25.83	27.58	26.06	25.95	26.72	28.17	28.25
15	**26.84**	**27.10**	**28.13**	**27.98**	27.41	**28.52**	**29.51**	29.03
16	22.58	25.78	25.48	25.31	22.65	26.44	25.82	25.43
17	26.18	25.64	27.79	27.82	26.16	26.34	28.37	28.37
18	26.68	26.11	27.43	27.37	**27.43**	27.55	29.11	28.60
19	22.43	25.53	25.37	25.22	22.43	26.21	25.63	25.32
20	25.86	25.59	27.48	27.58	25.77	26.12	27.91	28.15
21	26.67	26.87	28.01	26.67	27.26	28.12	29.37	**29.32**
22	22.48	25.62	25.43	25.29	22.58	26.29	22.58	25.42
23	26.00	25.41	27.69	27.71	25.97	26.08	28.31	28.28

continues on the next page ...

Case	C NS	NH NS	MH NS	FH NS	C EW	NH EW	MH EW	FH EW
24	26.48	25.95	27.33	27.30	27.29	27.38	29.04	28.62

The results obtained in the simulations with respect to the base case, showed that the best cases within 1 and 6 was C3 for the current weather in the two orientations; here the clay hollow block is used with single glazing on the windows. The worst cases in future horizons were mostly in Case 6, where this same material is used in the opaque envelope, but with double glazing. The best cases of the future horizons were the same for both orientations in the near horizon, C1, which retains the same characteristics of the base case, with a slight variation in the arrangement of the windows, derived from the solar analysis as it appears in Figure 7.18.

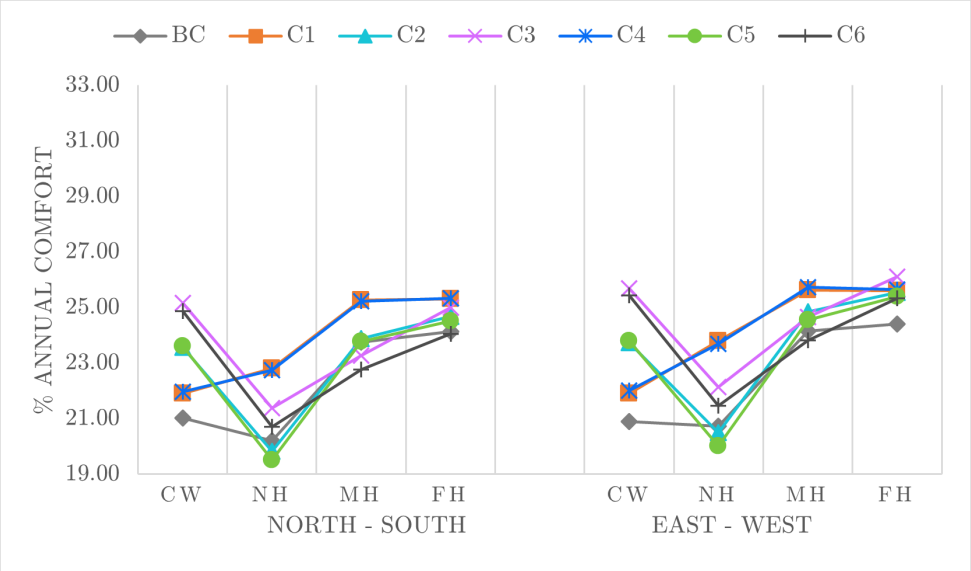


Figure 7.18: Torreón Cases 1 to 6.

In cases from 7 to 12, Figure 7.19, the worst case for both orientations simulated under current weather, and medium and far horizons was C7; while for the near horizon, was C11. The best case under simulations for all weather files and orientations was C12. In this, clay hollow block worked well with double glazing.

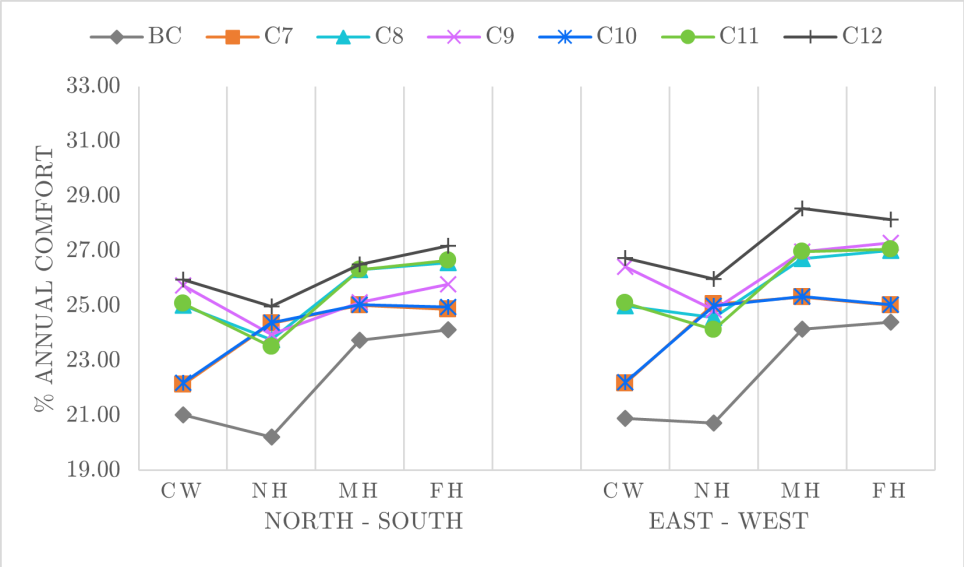


Figure 7.19: Torreón Cases 7 to 12.

The results obtained in cases 13-18 and 19-24 were very similar in terms of values, and more, in behavior. The worst cases in both orientations for the current weather and the far horizon were cases 13 and 19, where simple glazing is simulated with an opaque concrete block envelope.

The best cases were 18 and 24, Figure 7.20 and Figure 7.21, which share characteristics of the geometry of the base case, double glass in windows, a clay hollow block envelope, operable windows of the OW1 type and 0.3 ACH. These simulations yield results similar to those of Saltillo, so these characteristics of the envelope are beneficial for both locations. The best case for these simulations was case 18, with the highest values of annual comfort for current and future horizons in both orientations, except for the current weather.

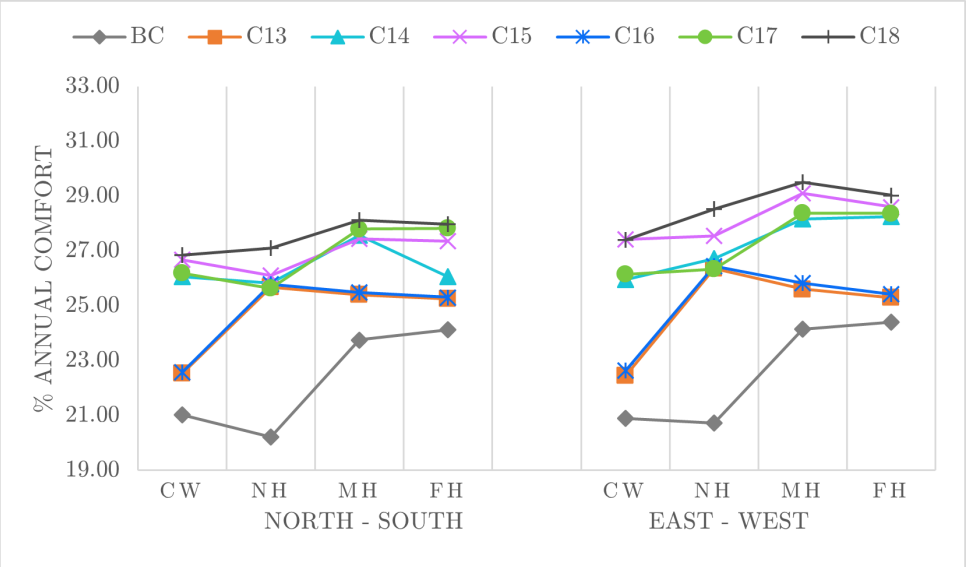


Figure 7.20: Torreón Cases 13 to 18.

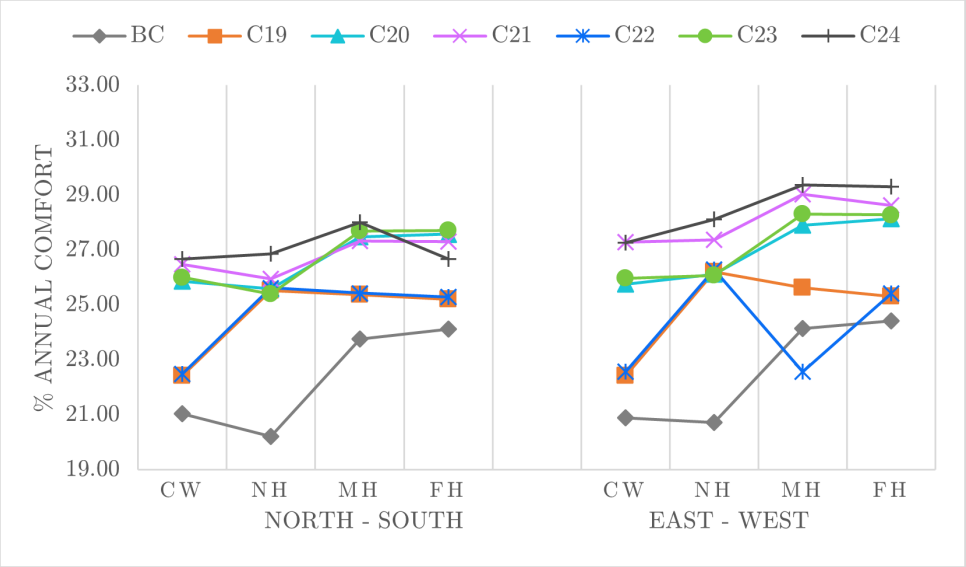


Figure 7.21: Torreón Cases 19 to 24.

7.3.3 Set 2

In Table 7.11 the results obtained for the second set of simulations in the chosen location in Torreón are presented.

Table 7.11: Set 2 Torreón, Percentage of Annual Comfort (%) in Cases from 25 to 34 for current weather, near, medium, and far horizons, in north-south and east-west orientations.

Case	C NS	NH NS	MH NS	FH NS	C EW	NH EW	MH EW	FH EW
25	26.74	27.41	28.43	28.56	27.13	28.43	29.16	29.34
26	26.98	27.43	28.72	28.74	27.47	28.48	29.52	29.62
27	26.61	27.89	28.64	28.54	26.82	28.30	28.99	29.27
28	26.58	27.95	28.14	28.25	26.91	**28.78**	28.86	29.28
29	**27.86**	26.52	**31.00**	**31.85**	**28.34**	27.52	**31.74**	**32.72**
30	26.29	**28.05**	27.42	27.89	26.63	28.49	27.95	28.49
31	24.49	27.89	30.57	31.30	27.87	27.98	31.08	31.96
32	24.39	23.25	25.91	26.15	24.63	24.11	26.42	26.89
33	24.54	23.90	26.16	27.35	24.82	24.26	26.51	27.84
34	24.40	23.22	25.92	26.15	24.63	24.13	26.39	26.89

In Figure 7.22 similar results can be seen between cases 25 and 28, and it is also shown that increases in thermal comfort are generated with respect to the base case.

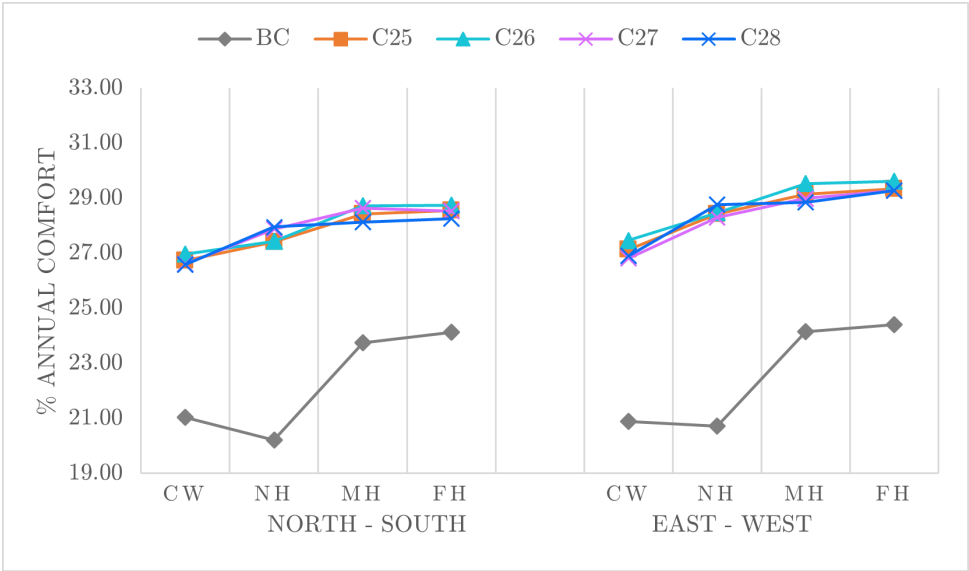


Figure 7.22: Torreón Cases 25 to 28.

However, in Set 2, the best results are mostly found in the C29 case, which was the best case of the set. See Figure 7.23. The results show the highest values for both orientations for the current climate and for the medium and far horizons. For the near horizon, the best cases were 30 and 28 for the north-south orientation, and east-west correspondingly.

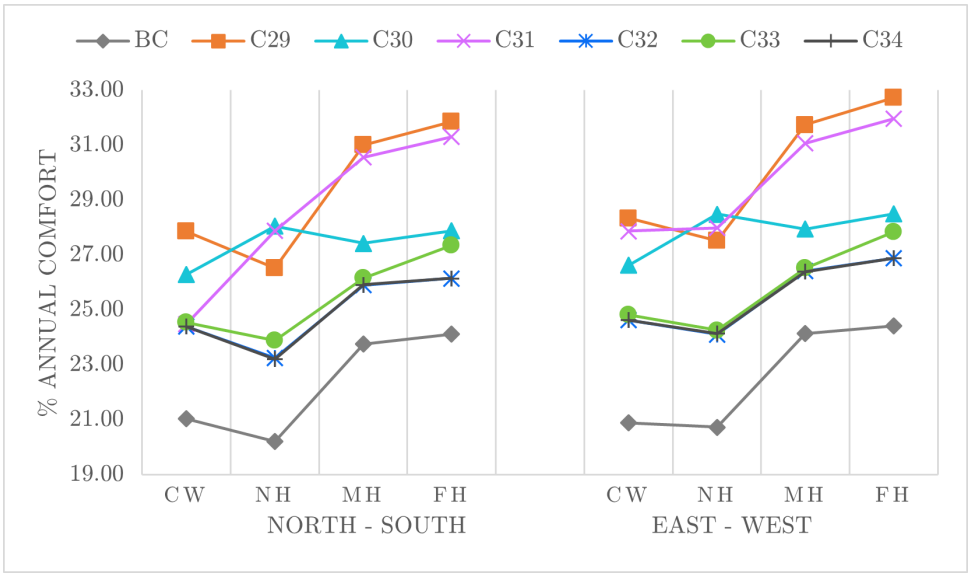


Figure 7.23: Torreón Cases 29 to 34.

In Case 29, it was contemplated to increase the height of the walls in two courses, to accommodate the clerestory windows under the roof slab, a double glazing in a clay

hollow block envelope, 0.3 ACH and an OW2b window opening , where overhangs were placed above the windows.

The worst cases of the set are observed in cases 32 and 34, where a horizontal over roof was proposed for the first, and one rotated to the north for the second.

7.3.4 Set 3

In Table 7.12 the results obtained for the third set of simulations are presented as percentages of annual comfort.

Table 7.12: Set 3 Torreón, Percentage of Annual Comfort (%) in Cases from 35 to 40 for current weather, near, medium, and far horizons, in north-south and east-west orientations.

Case	C NS	NH NS	MH NS	FH NS	C EW	NH EW	MH EW	FH EW
35	20.54	20.30	23.64	23.94	20.39	20.03	23.28	23.63
36	21.06	20.44	24.00	24.40	20.92	20.04	23.56	23.96
37	**27.12**	26.89	**28.34**	**28.04**	**27.11**	26.84	28.24	27.81
38	26.78	27.35	27.73	27.43	26.75	27.21	27.61	27.26
39	26.72	**27.54**	27.22	27.75	26.95	**28.35**	**28.30**	**28.60**
40	26.72	27.53	27.23	27.69	26.99	28.26	28.28	28.59

The case with the least amount of comfort hours for Set 3 was the C35, which retains the characteristics of the base case as well as the concrete block envelope, but with a compact geometry. The best case for both orientations simulating with the current weather file was the C37, with the gable roof, single glazing and the use of Clay Hollow Block. This case was also the one that obtained the best results for the north-south orientation in the middle and far horizons.

For the east-west orientation, the best case was C39, the same in which the characteristics of Case 37 are contemplated but with the use of a ceiling that serves as a barrier between the gable roof and the rest of the living space. See Figure 7.24.

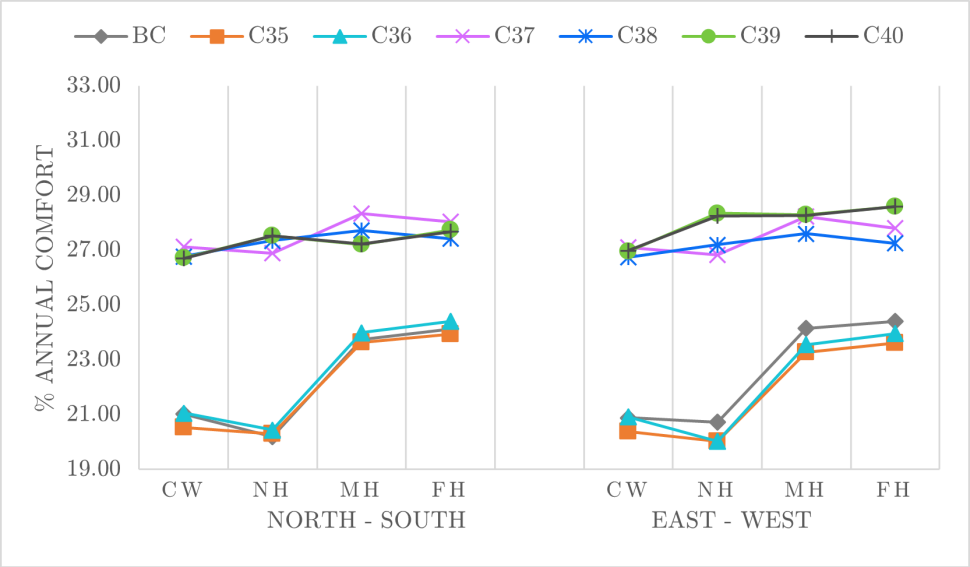


Figure 7.24: Torreón Cases 35 to 40.

7.3.5 Results

In Torreón the best case for current weather was Case 29 for both orientations with annual comfort of 27.86% for north-south, and 28.34% for east-west. This case considers the use of clay hollow block, 0.3 ACH, clerestory windows, a horizontal roof overhang on south façade, and horizontal overhangs on top of windows facing east, south and west. See Figure 7.25.

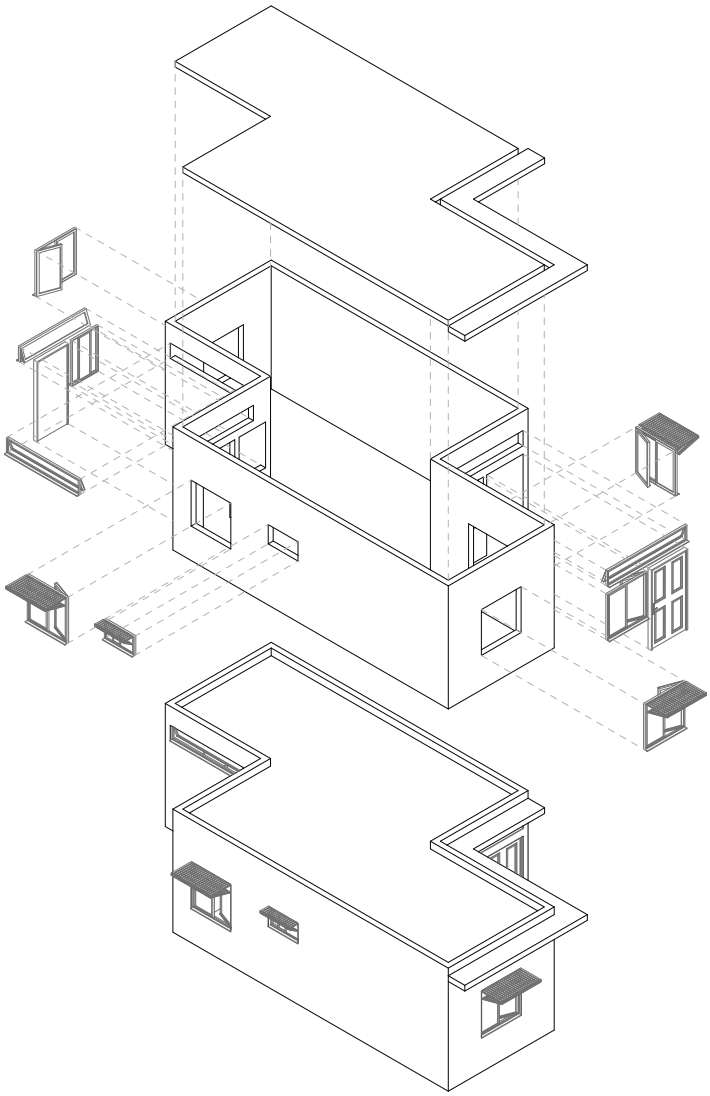


Figure 7.25: Torreón Best Case for current weather, Case 29.

For future horizons, the sum of comfort hours along the time resulted in Case 18 working the best for north-south and east-west orientations, with annual comfort between 27.10% and 29.51%.

For all scenarios and simulations, the best case was C29. For the narrow thermal comfort threshold in north-south orientation for current weather, near, medium and far horizons correspondingly, annual comfort was of 27.86%, 26.52%, 31.00% and 31.85%; and for the east-west orientation was 28.34%, 27.52%, 31.74% and 32.72%.

For the wide thermal comfort threshold in north-south orientation the annual comfort was of 57.88%, 54.57%, 67.04% and 70.34%; and for the east-west orientation was 58.15%, 54.62%, 67.43% and 70.76%.

7.4 Conclusions

Considering the possible changes for future horizons and temperatures projected for future years, it is necessary to provide designs of resilient buildings that can adapt to these changes. The importance of having buildings and the elasticity in designs these have, resides in having a more thought design of architectural projects, having into consideration the parameters that can be modified to provide with a better performance.

Since the parametric study performed in building simulations is used widely to identify the influence of input parameters in relation with each other, or in relation with the outputs, it has been established the use of this reasoning for making comparisons between elements that encompass the building thermal envelope.

As thermal analysis for housing in Mexico is under one national regulation based on a steady state heat transfer analysis, the thermal storage capacity in building envelope is not considered. This is relevant in climates with large external temperature variation and solar radiation as Coahuila, which was proved after analysing the results presented for this chapter.

In the dynamic simulations, the possibility of modifying the problematic elements in the cases to have a greater annual amount of comfort hours is clarified. Throughout the chapter, the results were analysed to select the optimal case between the given options. If it was intended to propose an exclusive design for the whole state, it would be extremely difficult to choose one, since the results show that the best cases vary from city to city, and even in the same location, as results vary depending on the house orientation, among other parameters.

These results were obtained without making big changes in the house reference, as it was intended to analyse if just by changing the envelope thermal components and adding shading elements represented an increase in thermal comfort. Although bigger percentages in annual thermal comfort were appreciated with these modifications in Saltillo and Torreón, it was not the case for Monclova, which was under the narrow thermal comfort threshold.

Opposed to this, Monclova and Torreón showed better results than Saltillo under the

wide thermal comfort interval. This is mainly because the research considered for this evaluation was made for a city with similar climate characteristics to the mentioned cities, with extreme dry weather, mainly warm along the year.

Although the weather files in all the cities were worked in the same way and did not offer drastic changes in the behavior of the temperatures and relative humidity in any of the cases, when applied in the simulations the results show the discrepancy in the behavior of temperatures inside the houses. For example, the solutions that were proposed for the city of Saltillo resulted in poor performance for the city of Monclova.

Apart from the adding of shading elements, one of the best strategies observed was the adjustment of sizing and disposition of the windows, as adding clerestory windows to favour the natural ventilation inside the houses. This did not make a big difference in Monclova because the wind speed and humidity are not enough to refresh the inner air temperatures.

Window opening was considered when temperatures were between 18° C and 50° C, but when outside temperatures are extreme, as is the case for the three cities, these strategies are not enough to have comfort most of the year.

Because of this, a new disposition in the floor plan was proposed and analysed with the three constructive systems used in the first 34 cases. Areas were considered as needed for the *Typical House* and total floor area was the same. A pitched roof was added, and a buffering zone was considered in the attic, to have an air zone between the ceiling and the pitched roof.

This is not a common design for social housing in Mexico, but it was proposed to study possible solutions regarding thermal comfort, and to see if there could be an increment in comfort hours with a different geometry, see Figure 7.26.

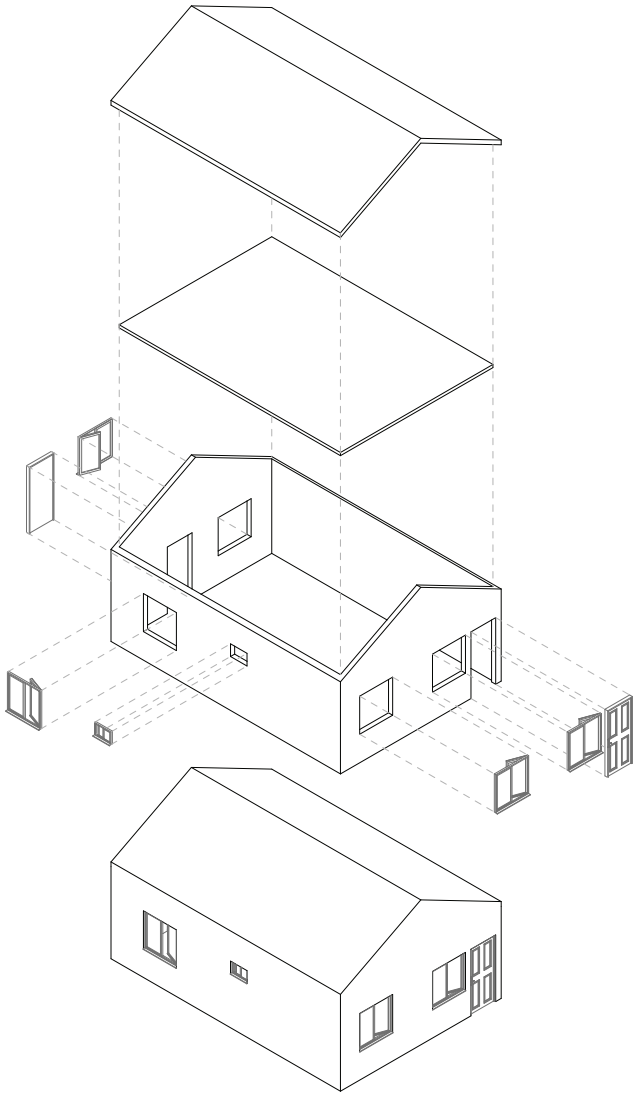


Figure 7.26: Compact model for Saltillo, Monclova and Torreón for current and future horizons.

This option worked better in Monclova, even by preserving the assumptions already mentioned for the simulations, so windows can still be opened. This increases the cost of the dwellings, so further investigation should be made, also because it must be considered than for a better functioning of this system, qualities inherent to *Passivhaus* design must be implemented and adapted.

A table with these results for the Base Case and the Compact Floor Plans can be seen in Tables 7.13 and 7.14 respectively.

Table 7.13: Higher Percentage of Annual Comfort for Base Case Floor Plan simulations. Set 1 and 2.

City	North - South Orientation				East - West Orientation			
	Current Weather	Near Horizon	Mid Horizon	Far Horizon	Current Weather	Near Horizon	Mid Horizon	Far Horizon
S	36.72	36.97	36.62	37.11	37.10	38.22	37.55	38.09
M	19.08	23.29	23.72	24.08	19.45	23.71	24.62	24.54
T	27.86	28.05	31.00	31.85	28.34	28.78	31.74	32.72

Table 7.14: Higher Percentage of Annual Comfort for Compact Floor Plan simulations. Set 3.

City	North - South Orientation				East - West Orientation			
	Current Weather	Near Horizon	Mid Horizon	Far Horizon	Current Weather	Near Horizon	Mid Horizon	Far Horizon
S	35.66	36.24	35.62	36.23	37.11	36.80	36.71	37.16
M	19.42	22.88	23.80	24.47	19.81	23.26	23.80	23.80
T	27.12	27.54	28.34	28.04	27.11	28.35	28.30	28.60

The initial intention to propose the best design of social housing for Coahuila matured showing that it is not appropriate to have one design for the entire state, since the variations that exist in each location are considerable and there is not a best case for the three cities. The best cases are shown in Table 7.15; in the last two columns there are shown the weather files in where results were better for the case (current weather (CW), near horizon (NH), medium horizon (MH), and far horizon (FH) weather files). For key codes of envelope components refer to Table 6.1 of Chapter 6.

Table 7.15: Final Best Cases.

Case	Geometry	Window Disp.	Glazing	Material	Op. Windows	ACH	N-S	E-W
				Saltillo				
C26	BCG	WM1	DG	CHB	OW2b	ACH2		NH/FH
C27	BCG	WM1	DG	CHB	OW3	ACH2	MH/FH	
C28	SRO	WM1	DG	CHB	OW3	ACH2		MH
C30	HOR	WM1	DG	CHB	OW3	ACH2	NH	
C33	ORS	WM1	DG	CHB	OW4	ACH2	CW	CW
C37	GR	WM2	SG	CHB	OW4	ACH2	NH/FH	
C39	GRC	WM3	SG	CHB	OW4	ACH2	NH	NH/MH/FH
C40	GRC	WM3	DG	CHB	OW4	ACH2	CW	CW
				Monclova				
C14	BCG	WM1	SG	AACB	OW1	ACH1		MH
C20	BCG	WM1	SG	AACB	OW1	ACH2		FH
C26	BCG	WM1	DG	CHB	OW2b	ACH2	NH	NH
C27	BCG	WM1	DG	CHB	OW3	ACH2	MH	
C33	ORS	WM1	DG	CHB	OW4	ACH2	CW/FH	CW
C37	GR	WM2	SG	CHB	OW4	ACH2	CWMH/FH	CW/MH/FH
C40	GRC	WM3	DG	CHB	OW4	ACH2	NH	NH
				Torreón				
C28	SRO	WM1	DG	CHB	OW3	ACH2		NH
C29	HOR	WM1	DG	CHB	OW2b	ACH2	CW/MH/FH	CW/MH/FH
C30	HOR	WM1	DG	CHB	OW3	ACH2	NH	
C37	GR	WM2	SG	CHB	OW4	ACH2	CW/MH/FH	CW
C39	GRC	WM3	SG	CHB	OW4	ACH2	NH	NH/MH/FH

In Saltillo there was the greatest variation of cases with better results depending on the used weather file and the orientation of the house. Nonetheless, the case that obtained the most hours of comfort in the sum of all, current and future scenarios on both orientations, was C28, with $25,878.30$ hours, that represent 36.93% of the year. In this design there is a sloping roof facing south, with clerestory windows in north and south façades, double glazing on windows and the use of clay hollow block in the opaque envelope. The windows operating hours were OW3 with an ACH of 0.3.

If the best case of these simulations had to be chosen for each city, it would be easier for the cities of Monclova and Torreón, since in both cities, the best cases behaved this way in most horizons.

For Monclova, the best case would be C37, since it has the best performance in current weather for both orientations, and in orientation north-south for future horizons; the results of the sum of hours of comfort over time is superior to that of the other cases. Along the time considered for all simulations, this case obtained the most hours of comfort, with $15,779.50$ hours, that represent 22.52% of the year. Only in this city was observed that the AACB performed better hand in hand with the single glazing, with variations in the windows operability schedules and in the air changes per hour of Set 1. In turn, it was the only city in which the best results were obtained with the gable roof geometry.

Although the city of Torreón showed similar behaviors to the city of Saltillo, here it was very clear that the best case was C29, which was the one with the best results for current weather in both orientations, along with the east-west orientation for future horizons. It was also the one that had the most hours of comfort over time, with $20,810.00$ hours, that represent 29.69% of the year. The opaque clay hollow block envelope obtained good results with double glazing in windows, with different hours of operation and an ACH of 0.3. Regarding the geometry, the best one was the base case geometry with two more courses in the walls, and overhangs in the horizontal roof slab.

Saltillo has in general the more hours of thermal comfort under the performed evaluation, and Monclova has the less. This is understandable due to the modifications made initially to improve thermal performance in the city of Saltillo. The comparison showed that the pertinent evaluations should be made for each city and location. Being projects that have many housing units, it is difficult to implement specific designs for each home. However, a design could be proposed for each project of housing complex, considering the main orientations of the units.

In the three climate regions studied, under historical and future projections in climates, the comfort hours resulted in higher values with architectural design modifications in geometry of the building, and envelope characteristic materials. When using the weather files with interpolated data for future horizons, the impact of weather on thermal comfort allowed to determine the best design cases for each city in possible future scenarios.

The strategies considered showed that an improvement in thermal comfort can be achieved by modifying the geometry and the envelope characteristics. However, to increase the percentage of annual thermal comfort, hybrid systems for air cooling and heating can be implemented. Because this solution has an installation cost and works with construction systems different to the ones used commonly in Mexico, it represents a change in the approach of design for these houses; it seems as a good idea only on a theoretical level at this moment.

Part IV

Conclusions and Discussion

Chapter 8

Conclusion and Discussion

The aim of this research was to develop a new methodology to generate the data needed to elaborate accurate weather files for possible future scenarios in order to apply them in dynamic simulations for specific locations. All this, to propose changes in the building envelope that resulted in better thermal performance that allowed users to experience more comfort hours inside the dwellings.

Both parts of the aim were achieved, as a new methodology was proposed and innovations developed from it. Firstly, in the way data interpolation is generated and allows the obtaining of missing information for the creation of accurate weather files using data from climate projections. Secondly, because by using these files, it was possible to identify which elements performed better for specific locations chosen in the cities of Saltillo, Monclova and Torreón, not only in the cities, but in the sites in where the study was placed. Results showed the most appropriate elements that could be used in order to have increments in the percentages of annual comfort.

The analysis was able to be carried out considering different climate scenarios and projections, for near, medium and far future horizons. Due to this, the elasticity, resilience and adaptation of the houses to these possibilities could be analysed, and assuredly, these dwellings designs can be further improved using the tools developed in this research.

The objectives mentioned in the introduction outlined the structure of the research, and are summarized as follows:

1. The literature review of this objective showed the most relevant literature and the gap in knowledge, that was in the way social housing is designed throughout the country without making considerations for the specificity of the location in where projects are placed. Thermal analysis for housing in Mexico is under one national regulation based on a steady state heat transfer analysis, so the thermal storage capacity in the building envelope is not considered. This is relevant in cities like Saltillo, Monclova and Torreón due to their big seasonal and day-night temperature variations.

2. Weather data gathering of GCMs and RCMs for the second objective made evident the need to generate a new methodology to manage these information. The scarce disposition of data resulted in a wide range of missing information needed for the dynamic simulations. Some methodologies of weather files generation were covered and were not applicable for the research, so it surged the need of creating a new one for the purposes of the investigation.

3. New procedures to use the gathered weather data and interpolate the missing information in the studied surfaces were developed. As data were provided from specific points in a rectangular grid (GCM), and in an irregular mesh (RCM) corresponding to the weather stations in Coahuila, two different approaches were covered, using mathematical concepts and procedures. Data response surfaces were generated to obtain interpolated data.

4. New weather files for future horizons and scenarios were adapted to the research proposed locations. Instead of the common approach of obtaining data from weather stations, the data interpolation facilitated the use of weather data for specific locations; this showed than even in the same city, weather characteristics perform differently because of the physiography, variations in altitude, humidity, among others. Weather files for future horizons are not available for all places in the country, and most of them are not of free access because are provided by commercial platforms. The ones that can be accessed for free are not updated;

both schemes still have the problem of the specificity of the location. The algorithms developed in this research for the creation of weather files covers these problems and can be adapted to new data.

5. The housing typology was defined from INEGI [85], as was needed for covering objective five. The typical parameters were analysed from previous studies [121] of social housing in Mexico, along with the most common building materials and envelope characteristics considered as sustainable in the country.

6. Dynamic simulations were performed, modifying individual parameters and a combination of them. The best interaction between these elements were found, and they were different depending on the city. All of them presented improvements in percentages of annual thermal comfort.

7. As stated in the last objective, objective seven, the best cases obtained from the dynamic simulations were assessed and their corresponding components were described.

In Section 8.1, the research impact and limitations are discussed; recommendations for further work are suggested in Section 8.2, and in Section 8.3, the conclusions and final comments of the research document are presented.

8.1 Research Impact, Limitations, and Discussion

The topics discussed in this section are about the research impact, its limitations, and a general discussion based on these topics. It is divided into three subsections to deal separately with the literature review, the innovative method surged from the investigation, and the dynamic simulations performed for the study cases.

8.1.1 Literature Review

When reviewing the relevant literature, the difficulty of addressing such complex issues as a constantly changing climate with such a large breadth of data became evident. There are countries in which information on weather files is available on the official pages of the governments in the form of *.epw* files used for climate simulations. This is not the case for Mexico for the purposes of this study, as the data that could be used for the elaboration of these weather files only included three temperature data per month for future years. The online platform is constantly updated, so obtaining this data is uncertain; this is due to the fact that it depends on public resources assigned for its operation, which are not always suited for this type of project.

The knowledge gap at the regional level originates from the management of information of this nature, which is not always available and is subject to the allocation of resources. The scarcity of resources means that many researchers do not have access to weather files to carry out studies of the climate's impact on buildings. Due to this, flexible tools are required that allow the management of results obtained by climate experts.

Adaptive comfort for the country is difficult to standardise, even by zones because of the big variations within them. In recent years, new research has focused on the study of thermal comfort related to climate change, considering the adjustments that could be implemented at local levels. There has been an increase in projects tackling this problem, although for Coahuila there is no study to date addressing it. Within the investigations carried out for the northern region of the country, there are several that mainly cover the western area, which has a dry arid climate. The cities of Torreón and Monclova fall into this category, but it is not the case for Saltillo, which has a portion of mountain climate and does not fall into the climate category of the mentioned studies.

At a global level, however, weather files use information from where measurements are made, that is, at meteorological stations. This works well for cities that have very similar weather characteristics, and have little variation in their elevations. However, in cities like Saltillo, where there is a great variation in temperatures throughout the city due to its morphological characteristics, these files are used despite the many variations

regarding the weather and characteristics of the site.

In recent years, new research has focused on the study of thermal comfort related to climate change, considering the adjustments that could be suffered at local levels. The research covering the adaptive thermal comfort in Mexico has been done for some cities, but in the northeast region only for one city that is not in Coahuila.

8.1.2 Algorithms

As it is impossible to have a meteorological station in all the places where a building is to be placed, it is feasible to use tools such as those developed for this research to interpolate missing information between the data of the weather stations. This is to have a response surface to collate all existing and missing information.

Three algorithms were created to use climate information and obtain new weather files for possible future climate scenarios. In many regions of the country and the state, climate variability is notable even within the same cities, so these files are generated for the study site, not just for the city. With this, the weather files can be entered into the energy simulation software, and later the most suitable solutions for the project to be studied can be compared; in this study, the results were evaluated in terms of percentages of annual thermal comfort.

Although in this research the methods were applied to regional data from Coahuila, data from anywhere in the country can be entered to generate climate files, and energy simulations can be run.

It was proposed to use a majority of free software for these ends, to allow researchers interested in these topics to access them more easily. Those that incur cost are generally accessible to the building industry and to universities.

It is a common practice in architecture to add temperatures in a linear way in weather files, considering that in general, temperatures will rise in future years. However, for this research it was proposed to make use of mathematical tools through the creations of algorithms to obtain the equations of the behavior of temperatures and relative humidity. In this way, data from future horizons is interpolated to obtain the necessary

information for the creation of weather files that consider these data.

Due to the great variability in the country, it is desirable to carry out studies of the type of this work with the procedures and tools that were generated in it. Some advantages are that it does not require specialised and expensive software or the use of machines with a huge memory arrangement. The methods that were developed here are absolutely general for numerically studying not only temperatures, but also atmospheric pressures, distribution of wind speeds, rainfall, etc.

8.1.3 Dynamic Simulation of Cases

Using weather files with historical data, and the new ones generated with the algorithms detailed in the previous part, dynamic simulations were carried out to evaluate the comfort hours per year in different cases for the three cities in Coahuila: Saltillo, Monclova, and Torreón. It was started from a base case, and 40 different cases for each city were studied using these weather files.

The clearest results of three sets of simulations were chosen as the best cases. These have the most appropriate architectural design solutions without using artificial systems for cooling or heating, such as air conditioning. Analysing the results obtained when using the different weather files, the variations in the design that the houses could suffer was observed. The best cases provide more hours of comfort to dwellers.

A parametric study was undertaken, in which the main elements of the thermal building envelope of the housing units were changed. With the use of the created weather files, differences in the design that are not generally considered in this type of study could be appreciated for the chosen location.

The results showed that a material that behaves well with the use of double glazing was Clay Hollow Block for the cities of Saltillo and Torreón. However, for Monclova this material was not the one that yielded the best results, rather Autoclaved Aerated Concrete Block with simple glazing for windows. This city was the only one that obtained benefits under the compact floor plan geometry.

All cases benefited from the use of clerestory windows. Saltillo benefited to a greater

extent from an increased window area. Monclova had better results from having smaller window areas. Torreón benefited from the use of overhangs that produced bigger cast shadows.

An interesting element analysed was the over roof, which had beneficial results under the current climate, but not so much for the future horizons. For Saltillo, the use of sloped roofs worked well, so it can be concluded that it is important to study thoroughly the interaction of the current and possible future weather with buildings to propose architectural improvements that enhance the thermal comfort of the users.

8.2 Recommendations for Further Work

Throughout the investigation, many possibilities were found to continue with the research proposed in this work, or even to delve into some parts of it. Most of these possibilities can be applied to the design of the built environment and to the analysis and changes of the methodology that contains the algorithms. This section divides these approaches more specifically into two parts, the one dealing with the algorithms developed for the innovative methodology, and the one of the simulations and new case studies.

8.2.1 For Algorithms

The application of Algorithms DGG1 and DGG2 can be used to study different phenomena. These are numerical procedures that offer the possibility of working with sets of data, and interpolate missing information. Diverse physical or theoretical situations can be analytically studied, assigning heights in the tri-dimensional space representing values of temperatures, atmospheric pressures, carbon dioxide emissions, etc.

The response surfaces obtained with these two algorithms are flexible, so that larger field or sites can be proposed for similar studies. They can be adapted to different scales, for example, different cities, states or areas of the country, since information is available from weather stations in the Meteorological National Service, as well as

projections of future horizons in the digital Climate Atlas.

Less extensive regions can also be studied, such as cities and neighborhoods within them. By having weather stations distributed in any of these scales, the effect of heat islands can be studied; on a smaller scale, sensors can be placed in parks or smaller areas. The data obtained can be used to generate the data response surface to interpolate missing data between the measured points.

Even if only a few sensors or thermometers were available, these could be arranged in a reticulated manner on walls or roofs to generate information for all of the surface to make design decisions of architectural elements or furniture placement, etc.

All three algorithms can also be used in other countries, as the historical weather information is available online; it is more complex to find these files in developing countries, so they can be generated with the methodology if the following information is available: historical weather file, and at least one temperature per month for weather projections. These climate files and possible future climate projections are required, even if the latest are scarce. The flexibility of these algorithms allows generation of the weather files needed for dynamic simulation once the mentioned data is available.

For the study of future climate scenarios, comparisons between different models of climate modeling systems can be analysed. Information from climate files can also be compared to information obtained through measurements, since the algorithms are applicable when conditions are not restricted, or when they are controlled, such as via laboratory or measurements. The stations can be in any arrangement.

With Algorithm DGG3, different columns can be extracted from those that constitute the weather file. For this research, two were studied: the temperature and the relative humidity columns; data for the rest of the columns can also be interpolated if the behaviour of the other components of the weather file would like to be studied numerically. As the input data of maximum and minimum extreme temperatures were obtained, a study of these can also be carried out.

The created weather files allow dynamic simulations to be run. For this research, the behaviour of temperatures inside buildings was studied, but the impact of climate change on energy consumption in the buildings can also be studied.

And finally, for a different discipline, algorithms can lead to the study of topographic surveys, where physical heights are measured at a more detailed level. The relief of the surface where the methods are applied does not matter, as is numerical and adapts to the values.

8.2.2 For Simulations and New Cases

The importance of having adequate climate files for each region was evident. With this, the thermal behavior of houses could be improved, although a more in-depth study with cost analysis and energy consumption could be developed to evaluate the relevance of making these changes.

At the same time, studies could be carried out on the implementation of hybrid systems to evaluate the energy savings they would represent, or the possibility of adapting systems that are not traditional in the country to evaluate their performance. This, coupled with studies of the perception of these construction systems to the occupants of these types of housing.

The use of active, passive or hybrid systems can be studied to evaluate and propose better practices in architectural design along with comparing energy savings and thermal comfort. Different construction systems, materials, or building geometry can be also correlated.

The results obtained with Algorithms DGG1 and DGG2 can be compared with measurements to evaluate their accuracy in the near future. New results provided by climate experts under new scenarios can be analysed. This type of information has been studied in this research for the last two reports of the IPCC; a new report is being produced, so when new values are assigned this can be worked with the algorithms and new updated weather files for the new projections can be obtained. It can be compared with the previous two to find affinities or differences between them.

8.3 Conclusions and Closing Comments

The three cities in the study are within the same state and showed significantly different behaviours. Because of this, it is important to consider that without making significant variations in the geometry of the houses, better results could be obtained if they were extensively studied.

This results favourable for social housing occupiers, because it is sometimes difficult to implement active systems, not only because of the economic expense they represent when acquiring them, but for their maintenance and energy consumption reflected on the bills.

Buildings more suitable to the site can be designed when analysing weather files, even considering the possible future horizons. With the novelty of the algorithms provided within this research, it is intended that there is a tool that allows designers to implement proposals that result in more comfortable places for users, where the use of active energies is reduced as much as possible, representing more hours of comfort, and less economic and environmental expenses.

The weather data is easy to input when using the algorithms, which provide better possibilities for a clear visualisation of the newly generated data, and it is easy to be analysed on a monthly basis. If an annual analysis had been carried out instead, the curve of fitting would flatten, so it would not mark the variability of existing parameters, thus, it would not be an accurate representation.

As this analysis parts from historical data, the more robust and up to date the TMY information is, the more accurate the results.

References

[1] A. A Abuelnuor, A. A. M. Omara, K. M. Saqr, and I. H. I. Elhag. Improving Indoor Thermal Comfort by Using Phase Change Materials: A review. *International Journal of Energy Research*, 42(6):2084–2103, January 2018. doi: 10.1002/er.4000.

[2] *ASHRAE Handbook, 1985 fundamentals*. American Society of Heating, Refrigerating and Air-conditioning Engineers, Atlanta, GA, 1985.

[3] *International Weather for Energy Calculations (IWEC Weather Files) Users Manual and CD-ROM*. American Society of Heating, Refrigerating and Air-conditioning Engineers, Atlanta, GA, 2001. ASHRAE 2001.

[4] *ASRAE55 Thermal Environmental Conditions for Human Occupancy, vol 27*. American Society of Heating, Refrigerating and Air-conditioning Engineers, Atlanta, GA, 2004. ASHRAE 2004.

[5] *ANSI/ASHRAE Standard 55-2010: Thermal Environmental Conditions for Human Occupancy*. American Society of Heating, Refrigerating and Air-conditioning Engineers, Atlanta, GA, 2010. ASHRAE 2010.

[6] Ahmad Sabry An-Naggar, Mohamed Aly Ibrahim, and Essam E. Khalil. Energy Performance Simulation in Residential Buildings. In Elsevier, editor, *Procedia Engineering*, number 205 in J. Proeng, pages 4187–4194, Jinan China, October 2017. doi: 10.1016/J.PROENG.2017.10.177. 10th International Symposium on Heating, Ventilation and Air Conditioning.

[7] Liliana Campos Arriaga. Estudio de optimización de la eficiencia energética en viviendas de interés social. Technical report, GIZ-Infonavit, 2011.

[8] Arup and Argos Analytics. Weathershift. URL `https://www.weathershift.com/`. Accessed: 2021-07-15.

[9] Fabrizio Ascione. Energy Conservation and Renewable Technologies for Buildings to Face the Impact of the Climate Change and Minimize the Use of Cooling. *Solar Energy*, 154:34–100, September 2017. doi: 10.1016/J.SOLENER.2017.01.022.

[10] Frank Ayres, Jr. *Theory and Problems of Differential and Integral Calculus*. Schaum Publishing, New York, second edition, 1964.

[11] G. Gómez Azpeitia. Caracterización Climática. Diagnóstico de confort. Facultad de Arquitectura y Diseño. Universidad de Colima, 2005. Spreadsheet.

[12] Walter William Rouse Ball and Harold Scott MacDonald Coxeter. *Mathematical Recreations and Essays*. Dover Publications, New York, thirteenth edition, 2010.

[13] Ronita Bardhan and Debnath Ramit. Evaluating Building Material Based Thermal Comfort of a Typical low-cost Modular House in India. In *Materials Today*, pages 311–317, February 2018. doi: 10.1016/J.MATPR.2017.11.087. Proceedings 5(1).

[14] G. Barrios, G. Huelsz, and J. Rojas. Ener-habitat: A Cloud Computing Numerical Tool to Evaluate the Thermal Performance of Walls/Roofs. In Elsevier, editor, *Energy Procedia*, number 57 in J. Egypro, pages 2042–2051, 2014. doi: 10. 1016/J.EGYPRO.2014.10.169.

[15] Guillermo Barrios, Pablo Elías Guadalupe, and Jorge Rojas. *Selección de los materiales de muros y techos para mejorar el confort térmico en edificaciones no climatizadas*, volume 3 of *Estudios sobre Arquitectura y Urbanismo del Desierto*, pages 69–84. Programa de Arquitectura de la Universidad de Sonora, October 2010. URL `http://www.arq.uson.mx/esaud/index.html`.

[16] V. R. Barros, C. B. Field, D. J. Dokken, M. D. Mastrandrea, K. J. Mach, T. E. Bilir, M. Chatterjee, K. L. Ebi, Y. O. Estrada, R. C. Genova, B. Girma, E. S. Kissel, A. N. Levy, S. MacCracken, P. R. Mastrandrea, and L. L. White, editors. *Climate Change 2014: Impacts, Adaptation, and Vulnerability. Part B: Regional Aspects. Contribution of Working Group II to the Fifth Assessment Report of the Intergovernmental Panel on Climate Change*. Cambridge University Press, Cambridge, United Kingdom and New York, NY, USA, 2014. IPCC, 688 pp.

[17] J. Kelly Beatty and Andrew Chaikin. *The New Solar System*. Sky Publishing Corporation, Cambridge Massachusetts, 1990.

[18] Benoit Beckers and Luc Masset. *Guía del Usuario Heliodon 2*. Liege, Compiegne and Barcelona, 2009.

[19] S. Belcher, J. Hacker, and D. Powell. Constructing design weather data for future climates. *Building Services Engineering Research and Technology*, 26 (1):49–61, 2005. doi: 10.1191/0143624405bt112oa.

[20] Bjørn Berge. *The Ecology of Building Materials*. Elsevier/Architectural Press, Oxford, second edition, 2009. Trad. Chris Butters and Filip Henle.

[21] Nadia Betancourt. Temperatura en Monclova alcanza los 46 grados centígrados. Vanguardia, 17 jun 2017. URL `www.vanguardia.com.mx`. Newspaper of Saltillo.

[22] F. Bre and V. D. Fachinotti. Generation of typical meteorological years for the Argentine Littoral Region. *Energy and Buildings*, 129:432–444, 2016. doi: 10.1016/J.ENBUILD.2016.08.006.

[23] F. Bre and V. D. Fachinotti. A computational multi-objective optimization method to improve energy efficiency and thermal comfort in dwellings. *Energy and Buildings*, 154:283–294, 2017. doi: 10.1016/J.ENBUILD.2017.08.002.

[24] F. Bre, A. S. Silva, E. Ghisi, and V. D. Fachinotti. Residential building design optimisation using sensitivity analysis and genetic algorithm. *Energy and Buildings*, 133:853–866, 2016. doi: 10.1016/J.ENBUILD.2016.10.025.

[25] Bruno Bueno, Aiko Nakano, Leslie Norford, and Christoph Reinhart. Urban weather generator - a novel workflow for integrating urban heat island effect within urban design process. In International Building Performance Simulation Association, editor, *Proceedings of the 14th Conference of International Building Performance Simulation Association, BS2015*, Massachusetts, USA, December 2015.

[26] V. L. Castaldo, A. L. Pisello, C. Piselli, C. Fabiani, F. Cotana, and M. Santamouris. How outdoor microclimate mitigation affects building thermal-energy performance: A new design-stage method for energy saving in residential near-zero energy settlements in italy. *Renewable Energy*, 127:920–935, 2018. doi: 10.1016/J.RENENE.2018.04.090.

[27] Cassandra L. Champagne and Can Baran Aktas. Assessing the Resilience of LEED Certified Green Buildings. In Elsevier, editor, *Procedia Engineering*, volume 145, pages 380–387, 2016. doi: 10.1016/j.proeng.2016.04.095.

[28] Arvind Chel and Geetanjali Kaushik. Renewable energy technologies for sustainable development of energy efficient building. In Elsevier, editor, *Alexandria Engineering Journal*, 2017. doi: 10.1016/J.AEJ.2017.02.027.

[29] B. Ciuffo, A. Miola, V. Punzo, and S. Sala. Dealing with uncertainty in sustainability assessment, 2011. https://doi.org/10.2788/5639.

[30] Silvia Coleman and John B. Robinson. Introducing the qualitative performance gap: stories about a sustainable building. *Building Research & Information*, 46 (5):485–500, 2018. doi: 10.1080/09613218.2017.1366138.

[31] Silvia Coleman and John. B. Robinson. Introducing the qualitative performance gap: stories about a sustainable building. *Building Research and Information*, 46(5):485–500, 2018. doi: 10.1080/09613218.2017.1366138.

[32] *Guía CONAFOVI de Uso eficiente de la energía en la vivienda*. Comisión Nacional de Fomento a la Vivienda, México, 2006. CONAFOVI: Pte. Mazaryk 214 Primer piso, Bosque de Chapultepec 11580.

[33] *Indoor environmental input parameters for design and assessment of energy performance of buildings addressing indoor air quality, thermal environment, lighting and acoustics*. Comité Européen de Normalisation (CEN) Standard EN 15251-2007, n. d. URL www.usgbc.org/resources/comite-européen-de-normalisation-cen-standard-en-15251â2007indoor-environmental-input-para. U. S. Green Building Council.

[34] SEDATU CONAVI. Mesa Transversal de Vivienda Sustentable. Updated Transversal Table of Sustainable Housing in Mexico, 2017. URL https://www.conavi.gob.mx/images/documentos/participacion_ciudadana/Sustentable/Ficha_enero_junio_2017_con_glosario.pdf.

[35] Javier Sánchez Corral. La vivienda social en México. Pasado-Presente-Futuro?, 2012. Sistema Nacional de Creadores de Arte Emisión 2008, México, DF.

[36] Richard Courant and Herbert Ellis Robbins. *What is Mathematics? An Elementary Approach to Ideas and Methods*. Oxford University Press, London, second edition, 1996. ISBN 0-19-510519-2. With additional material by Ian Stewart.

[37] Harold Scott MacDonald Coxeter. *Introduction to Geometry*. John Wiley and Sons, New York, second edition, 1969.

[38] Harold Scott MacDonald Coxeter and Samuel L. Greitzer. *Geometry Revisted*, volume 19 of *New Mathematical Library*. The Mathematical Association of America, Washington DC, 1967. ISBN 0-88385-619-0. Fifth printing.

[39] Dru Crawley and Linda Lawrie. Climate.onebuilding. Repository of free climate data for building performance simulation, 2014. URL http://climate.onebuilding.org/default.html.

[40] Secretaría de Desarrollo Agrario, Territorial y Urbano y Comisión Nacional de Vivienda. Gobierno de la República. Modelo Geoestadístico para la Actualización de los PCU, 2018. URL https://www.cmic.gob.mx. SEDATU: Statistical Model for the 2018 CPU Update.

[41] México: Plan Nacional de Desarrollo. Gobierno de la República. PND 2013-2018, 2013. URL https://www.snieg.mx/contenidos/espanol/normatividad/MarcoJuridico/PND_2013-2018.pdf. PND: Mexico: National Development Plan. National Government.

[42] México: Plan Nacional de Desarrollo. Gobierno de la República. PND 2019-2024, 2019. URL https://lopezobrador.org.mx/wp-content/uploads/2019/05/PLAN-NACIONAL-DE-DESARROLLO-2019-2024.pdf. PND: Mexico: National Development Plan. National Government.

[43] Instituto Nacional de Ecología y Cambio Climático. Mejoras metodológicas para los inventarios estatales de emisiones y absorciones del GEI por uso de suelo, la evaluación de utilidad y concordancia para el sistema de monitoreo, reporte y verificación (MRV) nacional y su contribución en los compromisos nacionalmente determinados, 2017. URL www.gob.mx/inecc/documentos/investigaciones-2018-2013-en-materia-de-mitigacion-del-cambio-climatico.

[44] Secretaría de Energía. Gobierno de la República. Balance Nacional de Energía 2002, pp. 184, 2003. URL https://www.gob.mx/. SENER: Deparment of Energy. National Energy Balance 2002.

[45] Secretaría de Energía. Gobierno de la República. Balance Nacional de Energía 2018, pp. 35, 2019. URL https://www.gob.mx/. SENER: Deparment of Energy. National Energy Balance 2018.

[46] Secretaría de Medio Ambiente (SEMA). Plan Estatal Contra Cambio Climático en Coahuila, 2013. URL www.gob.mx/cms/uploads/attachment/file/164919/2013_peacc_coah.pdf.

[47] Organismo Nacional de Normalización y Certificación de la Construcción y Edificación. Norma NMX460 Industria de la Construccion â Aislamiento Térmico â Valor R Para Las Envolventes En Vivienda Por Zona Térmica

Para La República Mexicana â Especificaciones y Verificación, 2009. URL www.onncce.org.mx/. ONNCCE: National Organization for Standarization and Certification of Construction and Building.

[48] Gobierno del Estado de Coahuila de Zaragoza. Programa Especial de Vivienda 2011–2017. Saltillo: Secretaría de Infraestructura, Desarrollo Urbano y Movilidad, 2012.

[49] Gobierno del Estado de Coahuila de Zaragoza. Programa Especial de Vivienda 2017–2023. Saltillo: Secretaría de Infraestructura, Desarrollo Urbano y Movilidad, 2018.

[50] *Manual de Organización de la Comisión Nacional Forestal*. Diario Oficial de la Federación, México, November 2016. URL www.dof.gob.mx/nota_detalle.php?codigo=5461274&fecha=16/11/2016.

[51] *Reglas de Operación del Programa de Vivienda Social*. Diario Oficial de la Federación, México, February 2020. URL https://www.dof.gob.mx/nota$_d$etalle.php?codigo $=$ $5595711 fecha = 26/06/2020$.

[52] M. Eames, T. Kershaw, and D. Coley. On the creation of future probabilistic design weather years from ukcp09. *Building Services Engineering Research and Technology*, 32(2):127–142, 2011. doi: 10.1177/0143624410379934.

[53] Agustín Fernández Eguiarte, Rosario Romero Centeno, and Jorge Zavala Hidalgo. Metodologías empleadas en el Atlas Climático Digital de México para la generación de mapas de alta resolución. *GEOACTA*, 39(1):165–173, 21 feb 2014. Asociación Argentina de Geofísicos y Geodestas.

[54] Agustín Fernández Eguiarte, Jorge Zavala Hidalgo, Rosario Romero Centeno, A. C. Conde Álvarez, and R. I. Trejo Vázquez. Actualización de los escenarios de cambio climático para estudios de impacto, vulnerabilidad y adaptación. Technical report, Centro de Ciencias de la Atmósfera, Universidad Nacional Autónoma de México, México, 2015. URL

atlasclimatico.unam.mx/AECC/servmapas/. Instituto Nacional de Ecología y Cambio Climático, Secretaría de Medio Ambiente y Recursos Naturales.

[55] Polv Ole Fanger. Calculation of Thermal Comfort: Introduction of a Basic Comfort Equation. ASHRE Trans., 1967. Vol.73, Pt 2.

[56] Polv Ole Fanger. Thermal Comfort-Analysis and Applications in Environmental Engineering. Danish Technical Press, 1970. Copenhagen, Denmark.

[57] Simone Fatichi, Valeriy Y. Ivanov, and Enrica Caporali. Simulation of future climate scenarios with a weather generator. *Advances in Water Resources*, 34 (4):448–467, 2011. doi: 10.1016/j.advwatres.2010.12.013.

[58] C. Filippín, F. Ricard, S. Flores Larsen, and M. Santamouris. Retrospective analysis of the energy consumption of single-family dwellings in central Argentina. retrofitting and adaptation to the climate change. *Renewable Energy*, 101:1226–1241, 2017. doi: 10.1016/j.renene.2016.09.064.

[59] A. P. Gagge, J. A. J. Stolwijk, and Ysaunobu Nishi. An Effective Temperature Scale Based on a Simple Model of Human Physiological Regulatory Response. ASHRAE Trans. Vol 70, Pt 1, 1970.

[60] R. Gagnon, L. Gosselin, and S. Decker. Sensitivity analysis of energy performance and thermal comfort throughout building design process. *Energy and Buildings*, 164:278–294, 2018. doi: 10.1016/J.ENBUILD.2017.12.066.

[61] Daniel Gómez García. *Raíces de Polinomios: Cálculo Numérico y Aplicaciones*. Universidad Autonóma de Coahuila, Saltillo Coahuila, 2009. ISBN 978-607-7584-44-5. Centro de Investigación en Matemáticas Aplicadas.

[62] E. García. *Modificaciones al Sistema de Clasificación Climática de Köpen*. Universidad Autónoma de México, México, 1973. Instituto de Geografía.

[63] Luis Eduardo Medrano Gómez and Azucena Escobedo Izquierdo. Social housing retrofit: Improving energy efficiency and thermal comfort for the housing stock recovery in Mexico. *Energy Procedia, Elsevier*, 121:41–48, 2017. doi: 10.1016/J.EGYPRO.2017.08.006.

[64] Victor Hugo Hernández Gómez and David Morillón Gálvez. Analytical model for double skin roofs. *Applied Thermal Engineering*, pages 218–224, October 2013. doi: 10.16/j.applthermaleng.2013.06.057.

[65] Danielle Griego, Moncef Krarti, and Abel Hernández Guerrero. *Optimization of energy efficiency and thermal comfort measures for residential buildings in Salamanca, México*, volume 54, pages 540–549. Energy and Buildings, Elsevier, November 2012. doi: 10.1016/J.ENBUILD.2012.02.019.

[66] M. Grudzińska and E. Jakusik. Energy performance of buildings in poland on the basis of different climatic data. *Indoor and Built Environment*, 26(4):551–566, 2017. doi: 10.1177/1420326X16631031.

[67] A. Gruner. Joint UN Environment â UNFCCC Workshop Mitigation in the Building Sector Lessons learned from Mexican Housing NAMA, jul 2017.

[68] Lance H. Gunderson, Craig R. Allen, and C. S. Holling. *Foundations of Ecological Resilience*. Island Press, 2009.

[69] Teresa Gutiérrez, Ramona Romero, and Cristina Sotelo. *Thermal Energy Impact of Bioclimatic Techniques Applied to low-income Housing in a Hot Dry Climate*, volume 57, pages 1743–1752. Energy procedia in Elsevier, November 2014. doi: 10.1016/J.EGYPRO.2014.10.163.

[70] Duane Hanselman and Bruce Littlefield. *Masternig Matlab 7*, pages 314–319. Pearson Education, New Jersey, 2005. ISBN 0-13-143018-1.

[71] P. Heiselberg, H. Brohus, A. Hesselholt, H. Rasmussen, E. Seinre, and S. Thomas. Application of sensitivity analysis in design of sustainable buildings. *Renewable Energy*, 34(9):2030–2036, 2009. doi: 10.1016/J.RENENE.2009.02.016.

[72] Juana María Mendoza Hernández. Climate Scenarios for Coahuila. Report, 2009. Universidad Autónoma Agraria Antonio Narro, in Saltillo Coahuila.

[73] Juana María Mendoza Hernández, Alejandro Zermeño González, Manuel Covarrubias Ramírez, and Jesús Cortés Bracho. Proyec-

ciones climáticas para el estado de Coahuila usando el modelo precis bajo dos escenarios de emisiones. *Agrociencia, Colegio de Postgraduados UAAAN*, 47(6):523–537, 2013. URL www.scielo.org.mx/scielo.php?script=sci_arttext&pid=S1405-31952_01300060000 1&lng=es&nrm=iso&tlng=es.

[74] M. Herrera, S. Natarajan, D. A. Coley, T. Kershaw, A. P. Ramallo GonzÃ¡lez, M. M. Eames, and M. Wood. A review of current and future weather data for building simulation. *Building Services Engineering Research and Technology*, 38(5):602–627, 2017. doi: 10.1177/0143624417705937.

[75] Manuel Herrera, Sukumar Natarajan, David A. Coley, Tristan Kershaw, Alfonso P. Ramallo González, Mathew Eames, Daniel Fosas, and Michael Wood. *A review of current and future weather data for building simulation*, volume 38 of *Building Services Engineering Research and Technology*, pages 602–627. SAGE PublicationsSage, London, England, April 2017. doi: 10.1177/0143624417705937.

[76] Crawford Stanley Holling. Resilience and stability of ecological systems. *Annual Review of Ecology and Systematics*, 4:1–23, 1973.

[77] J. Huang and K. R. Gurney. Impact of climate change on U.S. building energy demand: sensitivity to spatiotemporal scales, balance point temperature, and population distribution. *Climatic Change*, 137(1-2):171–185, 2016. doi: 10.1007/s10584-016-1681-6.

[78] Guadalupe Huelsz, Raúl Rechtman, and Jorge Rojas. Abc-050 altos valores de la resistencia térmica no aseguran un buen desempeño térmico de la envolvente de una edificación. In *Anes*, volume 176, pages 237–240, 2009.

[79] T. Huld, E. Paietta, P. Zangheri, and I. P. Pascua. Assembling typical meteorological year data sets for building energy performance using reanalysis and satellite-based data. *Atmosphere*, 9(2), 2018. doi: 10.3390/atmos9020053.

[80] Alejandra Martínez Ibarra and Jorge Ibarra Salazar. Los determinantes de la satisfacción residencial en México. *Estudios Demográficos y Urbanos, El Colegio de México, A. C.*, 32(2):283, 2017. doi: 10.24201/edu.v32i2.1635.

[81] Fundación IDEA. National Estrategy for Sustainable Housing. Environmental Components of Sustainability, 2013. URL http://fundacionidea.org/posts/52.

[82] Fundación IDEA. Energy and Environmental Efficiency in Housing. Survey of National and International Practices, (n.d). URL http://fundacionidea.org /posts/52.

[83] *Anuario Estadístico y Geográfico de Coahuila de Zaragoza 2015*. Instituto Nacional de Estadística y Geografía, 2015. URL www.inegi.org.mx/. INEGI: Statistical and Geographical Yearbook of Coahuila de Zaragoza.

[84] *Censo General de Población y Vivienda 2000. Marco Geoestadístico Municipal 2000*. Instituto Nacional de Estadística y Geografía, 2000. URL www.inegi.org.mx/. INEGI: Census 2000 of General Population and Housing. Municipal Geostatistical Framework.

[85] *Censo General de Población y Vivienda 2010 Estados Unidos Mexicanos. Resultados Definitivos por Entidad y Municipio*. Instituto Nacional de Estadística y Geografía, 2010. URL www.inegi.org.mx/. INEGI: Census 2010 of General Population and Housing United Mexican States. Definitive Results by Entity and Municipality.

[86] *Aspectos Normativos y Metodológicos. Clasificaciones y Catálogos. Clasificación para Actividades Económicas*. Instituto Nacional de Estadística y Geografía, 2012. URL http://www.inegi.org.mx/. INEGI: Regulatory and Methodological Aspects. Classifications and Catalogs. Classification for Economic Activities.

[87] *Conjunto Nacional de Uso Actual de Uso de Suelo y Vegetación a escala 1:250000*. Instituto Nacional de Estadística y Geografía, 2013. Serie V, INEGI, México.

[88] *Manual de Validación de Atributos del Sisevive. Sistema de Evaluación de la Vivienda Verde Sisevive-Ecocasa*. Instituto Nacional de Estadística y Geografía, 2020. URL https://

portalmx.infonavit.org.mx/wps/wcm/connect/820866d3-ca0d-4d7b-b17a-7345390505b1/4. +Manual_SISEVIVE.pdf?MOD=AJPERES&CONVERT_TO=url&CACHEID=ROOTWORKSPACE-820866d3-ca0d-4d7b-b17a-7345390505b1-mmCFAYf.

[89] *Making the energy sector more resilient to climate change*. International Energy Agency, Paris, 2015. URL www.iea.org/t&c/. IEA.

[90] *World Energy Outlook 2019*. International Energy Agency, Paris, 2019. URL https://www.iea.org/reports/world-energy-outlook-2019. IEA.

[91] *International Energy Agency World Energy Statistics, 1960-2018*. International Energy Agency, Paris, eighth edition, 2020. IEA: Data Collection (UK Data Service. SN: 6302).

[92] R. Jack, D. Loveday, D. Allinson, and K. Lomas. First evidence for the reliability of building co-heating tests. *Building Research and Information*, 46(4): 383–401, 2018. doi: 10.1080/09613218.2017.1299523.

[93] Mark F. Jentsch, AbuBakr S. Bahaj, and Patrick A. B. James. *Manual CCWorldWeatherGen Climate change world weather file generator*. Sustainable Energy Research Group, University of Southampton, UK, 2012. Highfield Southampton.

[94] Mark F. Jentsch, Patrick A. B. James, Leonidas Bourikas, and AbuBakr S. Bahaj. Transforming existing weather data for worldwide locations to enable energy and building performance simulation under future climates. *Renewable Energy*, 55:514–524, 2013. doi: 10.1016/j.renene.2012.12.049.

[95] Aiyin Jiang, Xudong Liu, Emily Czarnecki, and Chengyi Zhang. Hourly weather data projection due to climate change for impact assessment on building and infrastructure. *Sustainable Cities and Society*, 50, 2019. doi: 10.1016/j.scs.2019.101688.

[96] D. Johnston, D. Miles Shenton, and D. Farmer. Quantifying the domestic build-

ing fabric 'performance gap'. *Building Services Engineering Research and Technology*, 36(5):614–627, 2015. doi: 10.1177/0143624415570344.

[97] David Johnston, Dominic Miles Shenton, and David Farmer. Quantifying the domestic building fabric "performance gap". *Building Services Engineering Research and Technology. SAGE PublicationsSage UK, London, England*, 36 (5):614–627, sep 2015. doi: 10.1177/0143624415570344.

[98] N. Kampelis, K. Gobakis, V. Vagias, D. Kolokotsa, L. Standardi, D. Isidori, and M. Santamouris. Evaluation of the performance gap in industrial, residential and tertiary near zero energy buildings. *Energy and Buildings*, 148:58–73, 2017. doi: 10.1016/J.ENBUILD.2017.03.057.

[99] G. Kanellopoulos, V. G. Koutsomarkos, K. J. Kontoleon, and K. Georgiadis Filikas. Numerical analysis and modelling of heat transfer processes through perforated clay brick masonry walls. *Procedia Environmental Sciences*, 38: 492–499, 2017. doi: 10.1016/j.proenv.2017.03.112.

[100] Georgios Kontes, Georgios Giannakis, Philip Horn, Simone Steiger, and Dimitrios Rovas. Using thermostats for indoor climate control in office buildings: The effect on thermal comfort. *Energies, MDPI AG*, 10(9):1368, sep 2017. doi: 10.3390/en10091368.

[101] A. K. Kvellheim. The power of buildings in climate change mitigation: The case of Norway. *Energy Policy*, 110:653–661, 2017. doi: 10.1016/J.ENPOL.2017.08.0.

[102] J. H. Lim and G. Y. Yun. Cooling energy implications of occupant factor in buildings under climate change. *Sustainability (Switzerland)*, 9(11), 2017. doi: 10.3390/su9112039.

[103] Irene Marincic Lovriha, José Manuel Ochoa de la Torre, María Guadalupe Alpuche Cruz, and Luis Gabriel Gómez Azpeitia. Adaptive thermal comfort in warm dry climate: Economical dwellings in mexico. In Elsevier, editor, *PLEA 2009 Proceedings*, Code 87959, Quebec City, Canada, June 2009. 26th International Conference on Passive and Low Energy Architecture.

[104] Irene Marincic Lovriha, José Manuel Ochoa de la Torre, María Guadalupe Alpuche Cruz, and Luis Gabriel Gómez Azpeitia. Adaptive thermal comfort for occupants of low-cost dwellings in a hot dry climate. *Journal of Civil Engineering and Architecture.*, 6(3), 2012. doi: 10.17265/1934-7359/2012.03.009.

[105] Irene Marincic Lovriha, José Manuel Ochoa de la Torre, and María Guadalupe Alpuche Cruz. Passive house for a desert climate. *Eco-Architecture*, 142:13–24, 2014. doi: 10.2495/ARC140021.

[106] M. Lyu, X. Zhu, and Q. Yang. Connection stiffness identification of historic timber buildings using temperature-based sensitivity analysis. *Engineering Structures*, 131:180–191, 2017. doi: 10.1016/J.ENGSTRUCT.2016.11.012.

[107] Víctor Magaña, Cecilia Conde, Oscar Sánchez, and Carlos Gay. Evaluación de escenarios regionales de clima actual y de cambio climático futuro para méxico. In *México: Una Visión Hacia el Siglo XXI. El Cambio Climático en México*. Instituto Nacional de Ecología, Universidad Autónoma de México, U.S. Country Studies Program, México, 2000.

[108] T. A. Mara and S. Tarantola. Application of global sensitivity analysis of model output to building thermal simulations. *Building Simulation*, 1(4):290–302, 2008. doi: 10.1007/s12273-008-8129-5.

[109] Andrew Marsh. Psychrometric chart app. Bitbucket, 30 oct 2018. URL `https://drajmarsh.bitbucket.io/psychro-chart2d.html`. Accessed: 2021-07-04.

[110] Christian Martínez. Baja temperatura hasta -18° C en Arteaga. Vanguardia, 10 dec 2017. URL `www.vanguardia.com.mx`. Newspaper of Saltillo.

[111] Ann S. Masten, Karin M. Best, and Norman Garmezy. Resilience and development: Contributions from the study of children who overcome adversity. *Development and Psychopathology*, 2(4):425–444, oct 1990. doi: 10.1017/S0954579400005812.

[112] Thomas Richard McCalla. *Introduction to Numerical Methods and FORTRAN Programming*, pages 203–204. John Wiley, New York, 1967.

[113] E. McKenna and M. Thomson. High-resolution stochastic integrated thermal-electrical domestic demand model. *Applied Energy*, 165:445–461, 2016. doi: 10.1016/j.apenergy.2015.12.089.

[114] Randall McMullan. *Environmental Science in Buildings*. Basingstoke: Palgrave Macmillan, London, seventh edition, 2012. Ebook Library.

[115] Norma Mexicana. NMX–AA–164–SCFI–2013., Edificación Sustentable – Criterios y Requerimientos Ambientales Mínimos, 2013. URL `https://biblioteca.semarnat.gob.mx/janium/Documentos/Ciga/agenda/DOFsr/DO3156.pdf`. NOM: Mexican Standard, Sustainable Building – Criteria and Minimal Environmental Requirements.

[116] Norma Oficial Mexicana. NOM–008–ENER–2001., Eficiencia Energética en Edificaciones, Envolvente de Edificios no Residenciales, 2001. URL `www.gob.mx/cms/uploads/attachment/file/181648/NOM_008_ENER_2001.pdf`. NOM: Mexican Official Standard, Energy Efficiency in Buildings, Non-Residential Buildings Envelope.

[117] Norma Oficial Mexicana. NOM–018–ENER–2001., Aislantes Térmicos para Edificaciones. Características y Métodos de Prueba, 2011. URL `http://dof.gob.mx/normasOficiales/4576/sener/sener.htm`. NOM: Mexican Official Standard, Thermal Insulators for Buildings. Characteristics and Test Methods.

[118] Norma Oficial Mexicana. NOM–020–ENER–2011. Eficiencia Energética en Edificaciones, Envolvente de Edificios para Uso Habitacional, 2011. URL `www.gob.mx/cms/uploads/attachment/file/181660/NOM_020_ENER_2011.pdf`. NOM: Mexican Official Standard, Energy Efficiency in Buildings, Residential Buildings Envelope.

[119] Carl Dean Meyer. *Matrix Analysis and Applied Linear Algebra*, pages 223–224.

Society for Industrial and Applied Mathematics, Philadelphia, 2000. ISBN 0-89871-454-0.

[120] E. Moreles, G. Huelsz, and G. Barrios. Hysteresis effects on the thermal performance of building envelope PCM-walls. *Building Simulation*, 11(3):519–531, 2018. doi: 10.1007/s12273-017-0426-4.

[121] NAMA. Supported NAMA for Sustainable Housing in Mexico - Mitigation Actions and Financing Packages, 2012. URL `www.nama-database.org/index.php/Mexico`. Collaborative work CONAVI, SEMARNAT, INFONAVIT, GIZ.

[122] J. F. Nicol and M. A. Humphreys. Adaptive thermal comfort and sustainable thermal standards for buildings. *Energy and Buildings, Elsevier*, 34:563–572, 2002. doi: 10. 1016/S0378-7788(02)00006-3.

[123] Vahid M. Nik and Jesper Arfvidsson. Using typical and extreme weather files for impact assessment of climate change on buildings. *Energy Procedia, Elsevier*, 132:616–621, 2017. doi: 10.1016/J.EGYPRO.2017.09.686.

[124] Charles Stanley Ogilvy. *Excursions in Geometry*. Oxford University Press, New York, 1969. Reprinted by Dover, New York, 1990.

[125] Ivan Oropeza-Perez, Astrid Petzold-Rodriguez, and Claudia Bonilla-Lopez. Adaptive thermal comfort in the main mexican climate conditions with and without passive cooling. *Energy and Buildings, Elsevier*, 145:251–258, 2017. doi: 10.1016/j.enbuild.2017.04.031.

[126] Ken Parsons. *Human Thermal Environments: The Effects of Hot, Moderate, and Cold Environments on Human Health, Comfort, and Performance*. The Chemical Rubber, Cleveland, Ohio, third edition, 2014. doi: 10.1201/b16750.

[127] D. Peñaloza, M. Erlandsson, J. Berlin, M. Wålinder, and A. Falk. Future scenarios for climate mitigation of new construction in Sweden: Effects of different technological pathways. *Journal of Cleaner Production*, 187:1025–1035, 2018. doi: 10.1016/J.JCLEPRO.2018.03.285.

[128] Stuart L. Pimm. The complexity and stability of ecosystems. *Nature*, 307: 321–326, 1984. doi: 10.1038/307321a0.

[129] Lorenza Pistore, Giovanni Pernigotto, Francesca Cappelletti, Piercarlo Romagnoni, and Andrea Gasparella. International high performance buildings conference. In *4th International High Performance Buildings Conference at Purdue*, 2016. URL `http://docs.lib.purdue.edu/ihpbc/201`. Paper 201.

[130] Stamp S. Lowe R. and H. Altamirano Medina. *Assessing uncertainty in co-heating tests: Calibrating a whole building steady state heat loss measurement method*. PhD thesis, University College London, London, United Kingdmon, 2016.

[131] Sayanthan Ramakrishnan, Xiaoming Wang, Jay Sanjayan, and John Wilson. Thermal performance of buildings integrated with phase change materials to reduce heat stress risks during extreme heatwave events. *Applied Energy, Elsevier*, 194:410–421, may 2017. doi: 10.1016/J.APENERGY.2016.04.084.

[132] Justin Ritchie and Hadi Dowlatabadi. The 1000 gtc coal question: Are cases of vastly expanded future coal combustion still plausible? *Energy Economics, Elsevier B. V.*, 65:16–31, jun 2017. doi: 10.1016/j.eneco.2017.04.015.

[133] Anne Rooban and Anika Terton. *Safeguarding NDC Implementation: Building resilience into energy systems*. Brief by International Institute for Sustainable Development, IISD, sep 2018.

[134] D. G. Leo Samuel, K. Dharmasastha, S. M. Shiva Nagendra, and M. P. Maiya. Thermal comfort in traditional buildings composed of local and modern construction materials. *International Journal of Sustainable Built Environment*, 6 (2):463–475, 2017. doi: 10.1016/J.IJSBE.2017.08.001.

[135] D. García Sánchez, B. Lacarrière, M. Musy, and B. Bourges. Application of sensitivity analysis in building energy simulations: Combining first and second-order elementary effects methods. *Energy and Buildings*, 68:741–750, 2014. doi: 10.1016/J.ENBUILD.2012.08.048.

[136] V. Sánchez. Estudian desempeño térmico de materiales para construcción, 10 sep 2015. URL www.conacytprensa.mx/index.php/tecnologia/materiales/2806-estudian-desempeno-termico-de-materiales-para-construccion. Information Agency of *Comisión Nacional de Ciencia y Tecnología* (Conacyt), Mexico.

[137] C. Sandoval, S. Calderón, and J. L. Almazán. Experimental cyclic response assessment of partially grouted reinforced clay brick masonry walls. *Earthquake Engineering*, pages 1–26, 2018. doi: 10.1007/s10518-018-0308-x. Bulletin.

[138] P. Shen. Impacts of climate change on U.S. building energy use by using downscaled hourly future weather data. *Energy and Buildings*, 134:61–70, 2017. doi: 10.1016/J.ENBUILD.2016.09.028.

[139] George W. Snedecor and William Gemmell Cochran. *Statistical Methods*. The Iowa State University Press, Ames, Iowa, 1967.

[140] S. Solomon, D. Qin, M. Manning, Z. Chen, M. Marquis, K. B. Averyt, M. Tignor, and H. L. Miller, editors. *Climate Change 2007: The Physical Science Basis. Contribution of Working Group I to the Fourth Assessment Report of the Intergovernmental Panel on Climate Change*. Cambridge University Press, Cambridge, United Kingdom and New York, NY, USA, 2007. IPCC, 996 pp.

[141] X. Song and C. Ye. Climate change adaptation pathways for residential buildings in southern China. *Energy Procedia*, 105:3062–3067, 2017. doi: 10.1016/j.egypro.2017.03.635.

[142] Angus Stevenson. *Oxford Dictionary of English*. Oxford University Press, 2010. ISBN 9780191727665. doi: 10.1093/acref/9780199571123.001.0001. URL https://www.oxfordreference.com/view/10.1093/acref/9780199571123.001.0001/acref-9780199571123.

[143] James Stewart. *Calculus —Early Transcendentals*, pages 689–690. Brooks/Cole Publishing Company, Pacific Grove, California, 3rd edition, 1995.

[144] Sebastian Strunz. Is conceptual vagueness an asset? Arguments from philoso-

phy of science applied to the concept of resilience. *Ecological Economics*, 76: 112–118, apr 2012. doi: 10.1016/j.ecolecon.2012.02.012.

[145] Camara Tamba, Bernard Kamsu Foguem, Badié Diourte, Alhouseini Issa Maiga, and Abdallah Habbadi. *Management and assessment of performance risks for bioclimatic buildings*, pages 654–667. Number 147 in Journal of Cleaner Production. Elsevier, March 2017. doi: 10.1016/J.JCLEPRO.2017.01.063.

[146] Iris Tien. Resilient by design: the case for increasing resilience of buildings and their linked food-energy-water systems. *Elem Sci Anth.*, 6(18), 2018. doi: https://doi.org/10.1525/elementa.142.

[147] Nereyda Morgan Torres and Luis Gabriel Gómez Azpeitia. Development of a mexican standard of thermal comfort for naturally ventilated buildings. In *Proceedings of Windsor Conference, Rethinking comfort*, pages 596–608, Windsor, UK, 2018. NCEUB, Cumberland Lodge.

[148] A. W. M. van Schijndel (Jos). A simulation and mapping tool for the evaluation of building systems for future climate scenarios on european scale. *Energy Procedia*, 132:646–651, 2017. doi: /10.1016/J.EGYPRO.2017.09.705.

[149] Brian Walker, C. S. Holling, Stephen R. Carpenter, and Ann Kinzig. Resilience, adaptability and transformability in social-ecological systems. *Ecology and Society 9*, 2(5), 2004. URL `www.ecologyandsociety.org/vol9/iss2/art5/`.

[150] R. T. Watson and the Core Writing Team, editors. *TAR Climate Change 2001: Synthesis Report. Contribution of Working Groups I, II, and III to the Third Assessment Report of the Intergovernmental Panel on Climate Change*. Cambridge University Press, Cambridge, United Kingdom and New York, NY, USA, 2001. IPCC, 398 pp.

[151] Stephen Wilcox and William Marion. Users manual for tmy3 data sets. Technical Report NREL/TP-581-43156, TMY, 1994. URL `www.nrel.gov/docs/fy08osti/43156.pdf`. Revised May 2008.

[152] Peng Xu, Yu Joe Huang, Norman L Miller, and Nicole Jeanne Schlegel. Impacts of climate change on building heating and cooling energy patterns in California. *Energy, Pergamon*, 44(1):792–804, jun 2012. doi: 10.1016/J.ENERGY.2012.05.013.

Part V

Appendices

Appendix A

Code of Algorithm DGG1

The following code represents the Algorithm DGG1, consisting of the process to obtain a three-dimensional response surface and its projected contour lines from a $\mathbf{3} \times \mathbf{3}$ two-dimensional rectangular mesh of data.

A.1 3×3 Rectangular Mesh Code

```
1
2   function XYZ = grid9 (x,y,w,XY,fs,n,m,ex,ey,ez,v)
3   %
4   %         XYZ = grid9 (x,y,w,XY,fs,n,m,ex,ey,ez,v)
5   %
    ----------------------------------------------------------------
6   % On a 3x3 rectangular mesh of known coordinates and their
7   % corresponding heights, the program generates a response
8   % surface and its contour lines.
9   %
10  % The response surface has cantilevers that exceed the data.
11  %
12  % It is possible to interpolate the Z heights, given the
13  % coordinates of the points (X,Y) within the validity domain.
14  % It gets the coordinates (X,Y,Z) of the points on the
15  % response surface.
16  %
```

```
17  %
    ++++++++++++++++++++++++++++++++++++++++++++++++++++
18  % IMPORTANT NOTE  + Heights can be temperature measurements,
        +
19  % about the       + atmospheric pressure, carbon dioxide
    emissions, +
20  % heights         + etc.
        +
21  %
    ++++++++++++++++++++++++++++++++++++++++++++++++++++
22  %
23  %
    ---------------------------------------------------------------
24  %
25  % Data is required from a 3x3 point rectangular grid
26  %
27  %    y    ^
28  %         |
29  %    y=f  |    pf ->   1(a,f,w1)---------2(b,f,w2)---------3(c,f,
    w3)
30  %         |                |                |                |
31  %         |                |                |                |
32  %         |                |                |                |
33  %    y=e  |    pe ->   4(a,e,w4)---------5(b,e,w5)---------6(c,e,
    w6)
34  %         |                |                |                |
35  %         |                |                |                |
36  %         |                |                |                |
37  %    y=d  |    pd ->   7(a,d,w7)---------8(b,d,w8)---------9(c,d,
    w9)
38  %         |
39  %         |                ^                ^                ^
40  %         |                |                |                |
41  %         |               pa               pb               pc
42  %         |
43  %
    +----------------+----------------+----------------+---->
44  %                         x=a              x=b              x=c
       x
```

```
45  %
46  % Description:
47  % With three given points each of six parabolas are determined:
48  % pf, pe y pd, in a direction; and pa, pb y pc, in the other one
    .
49  % With these base parabolas, the equations of other intermediate
50  % parabolas are determined, supported in the previous ones, to
51  % evaluate the heights on a mesh of nxn.
52  %
53  % Finally, a 3D response surface and its corresponding m contour
54  % lines are obtained.
55  %
56  % The interpolation is carried out with parabolas belonging to
57  % the response surface.
58  %
59  % Data:
60  %       x    vector with the three x abscissas of the points.
61  %               Decimal format:     [x1 x2 x3].
62  %               Dms format:         [d1 m1 s1;d2 m2 s2;d3 m3 s3]
63  %       y    vector with the three y ordinates of the points
64  %               Idem
65  %       w    vector with the nine z heights of the points
66  %       ex   x-axis name between apostrophes
67  %       ey   y-axis name between apostrophes
68  %       ez   z-axis name between apostrophes
69  %       n    to size the mesh of order nxn
70  %       m    number of contour lines
71  %       XY   abscissas and ordinates (X,Y) where it is desired
    to
72  %               obtain the Z heights by interpolation.
73  %               Decimal format:
74  %               [x1 y1; x2 y2; ...; xk yk].
75  %               Dms format:
76  %               [dx1 mx1 sx1 dy1 my1 sy1; dx2 mx2 sx2 dy2 my2
    sy2;
77  %                ... ... ... ... ... ...; dxk mxk sxk dyk myk
    syk]
78  %            When XY = [], then the interpolation is performed
    on the
```

```
79  %               x abscissas, and the y ordinates and the nine
    data
80  %               belonging to the original rectangular grid 3x3
81  %       v    cantilevers in all four directions  v = [x1 x2 y1
    y2]
82  %               being x1, x2, y1, y3 positive, to expand   ac,
    df:
83  %               (a-x1) x (c+x2)   in the abscissas
84  %               (d-y1) x (f+y2)   in the ordinates.
85  %            Cantilevers are zero by default:  v = [0 0 0 0].
86  %
87  % Results;
88  %       XYZ  with the previous data XY the interpolation Z
    heights are
89  %               obtained, (points on the response surface)
90  %               XYZ = (X,Y,Z).
91  %
92  %       Required routines: cuadrxStr, cuadryStr, titxyz, dms.
93  %
94
95  warning off
96  clc
97  z = [];
98
99  % Variables according to the number of input arguments
100
101 if nargin >= 1
102     abc = dms(x);                                % abscissas data
103 end
104 if nargin >= 2
105     def = dms(y);                                % ordinates data
106 end
107 if nargin >= 4
108     XY = dms(XY);                                % interpolation
    (x,y)
109 end
110
111                                                  % Default Values
    :
```

```
112     if nargin == 0
113         abc = [-107.5 -102.5 -97.5];                % abscissas
114     end
115     if nargin <= 1
116         def = [22.5 27.5 32.5];                     % ordinates
117     end
118     if nargin <= 2
119        w = [30  27 30 34 30 29 30 24 23];           % heights
120     end
121     if nargin <= 3
122         XY = [];                                    % interpolation
    (x,y)
123     end
124     if nargin <= 4
125         fs = 18;                                    % fonstize
126     end
127     if nargin <= 5
128         n = 30;                                     % grid 30x30
129     end
130     if nargin <= 6
131         m = 12;                                     % 12 contour
    lines
132     end
133     if nargin <= 7
134         ex = 'Abscissas';                           % x axis sign
135     end
136     if nargin <= 8
137         ey = 'Ordinates';                           % y axis sign
138     end
139     if nargin <= 9
140         ez = 'Heights';                             % z axis sign
141     end
142     if nargin <= 10
143         v = [0 0 0 0];                              % null
    cantilevers
144     end
145
146     disp(' ')
147     disp('  With the following coordinates:')
```

```
148     disp(' ')
149     disp('  x = Abscissas')
150     disp(abc)
151     disp('  y = Ordinates')
152     disp(def)
153     disp('  w = heights of temperatures/atmospheric pressures, etc.'
    )
154     disp('      in normal writing order of the 9 given points, ')
155     disp('      from left to right and from top to bottom.')
156     disp(w)
157     disp('      A 3D response surface is generated')
158     disp(' ')
159     disp('      Press Enter to continue...')
160     pause
161     format shortg
162
163     % increments for text in z
164     dz = min(w(:))/20;
165     dZ = dz/2;
166
167     % components of abscissas in x
168     a = abc(1);
169     b = abc(2);
170     c = abc(3);
171
172     % components of ordinates in y
173     d = def(1);
174     e = def(2);
175     f = def(3);
176
177     % components (x,y,z) of w
178     xp = [abc abc abc];
179     yp = [f f f e e e d d d];
180     zp = w;
181
182     wm = min(w(:))/2;
183
184     % horizontal parabolas    (x,w)
185     pf = polyfit(abc,[w(1) w(2) w(3)],2);
```

```
186     pe = polyfit(abc,[w(4) w(5) w(6)],2);
187     pd = polyfit(abc,[w(7) w(8) w(9)],2);
188
189     % vertical parabolas      (y,w)
190     pa = polyfit(def,[w(7) w(4) w(1)],2);
191     pb = polyfit(def,[w(8) w(5) w(2)],2);
192     pc = polyfit(def,[w(9) w(6) w(3)],2);
193
194     % evaluation of horizontal parabolas
195     x13 = linspace(a,c);
196     y13 = linspace(f,f);
197     p13 = polyval(pf,x13);
198
199     x46 = x13;
200     y46 = linspace(e,e);
201     p46 = polyval(pe,x46);
202
203     x79 = x13;
204     y79 = linspace(d,d);
205     p79 = polyval(pd,x79);
206
207     % evaluation of vertical parabolas
208     x71 = linspace(a,a);
209     y71 = linspace(d,f);
210     p71 = polyval(pa,y71);
211
212     x82 = linspace(b,b);
213     y82 = y71;
214     p82 = polyval(pb,y82);
215
216     x93 = linspace(c,c);
217     y93 = y71;
218     p93 = polyval(pc,y82);
219
220     h = (c+v(2)-(a-v(1)))/(n-1);
221     x = linspace(a-v(1),c+v(2),n);
222     y = linspace(d-v(3),f+v(4),n);
223     [x,y] = meshgrid(x,y);
224
```

```
225     % Points for the contour lines
226     for i = 1:n
227        xx = a-v(1)+(i-1)*h;
228        zf = polyval(pf,xx,2);
229        ze = polyval(pe,xx,2);
230        zd = polyval(pd,xx,2);
231        p1 = polyfit([d e f],[zd ze zf],2);
232        p2 = polyval(p1,y(:,i),2);
233        z = [z p2];
234     end
235     clf
236
237     % Pole plots of the values of w
238     % Initial information of the 9 points
239     stem3 (xp,yp,zp,'w')
240     hold on
241     plot(xp,yp,'b.','markersize',12)
242     titxyz('Initial information on the $3\times 3$ mesh',ex,ey,ez,fs
    )
243     grid on
244     box on
245     shg
246     pause
247
248     for i = 1:9
249         stem3(xp(i),yp(i),zp(i),'b')
250         text(xp(i),yp(i),zp(i)+3*dz,sprintf('$w(%g)=%g$',i,w(i)),...
251             'interpreter','latex',...
252             'horizontalalignment','center',...
253             'backgroundcolor','white',...
254             'color','blue')
255         shg
256         pause
257     end
258     clf
259
260     % Graphs of the parabolas (x,w),  y = constant
261     stem3(xp,yp,zp,'w')
262     hold on
```

```
263     plot(xp,yp,'b.','markersize',12)
264     grid on
265     box on
266     titxyz('parabolas: $\quad z(x,w),\quad  y = $ constant',ex,ey,ez
        ,fs)
267
268     for i = 1:3
269         stem3(xp(i),yp(i),zp(i),'b')
270         text(xp(i),yp(i),wm,sprintf('$w(%g)=%g$',i,w(i)),...
271             'interpreter','latex',...
272             'horizontalalignment','center',...
273             'color','blue')
274     end
275     plot3(x13,y13,p13,'-r','linewidth',1.5)
276     text(b,f,zp(2)+2.7*dz,cuadrxStr(pf),...
277         'interpreter','latex',...
278         'HorizontalAlignment','center',...
279         'backgroundcolor','white',...
280         'color','red')
281     shg
282     pause
283
284     for i = 4:6
285         stem3(xp(i),yp(i),zp(i),'b')
286         text(xp(i),yp(i),wm,sprintf('$w(%g)=%g$',i,w(i)),...
287             'interpreter','latex',...
288             'horizontalalignment','center',...
289             'color','blue')
290     end
291     plot3(x46,y46,p46,'-r','linewidth',1.5)
292     text(b,e,zp(5)+2.7*dz,cuadrxStr(pe),...
293         'HorizontalAlignment','center',...
294         'backgroundcolor','white',...
295         'color','red')
296     shg
297     pause
298
299     for i = 7:9
300         stem3(xp(i),yp(i),zp(i),'b')
```

```
        text(xp(i),yp(i),wm,sprintf('$w(%g)=%g$',i,w(i)),...
            'interpreter','latex',...
            'horizontalalignment','center',...
            'color','blue')
    end
    plot3(x79,y79,p79,'r-','linewidth',1.5)
    text(b,d,zp(8)+2.7*dz,cuadrxStr(pd),...
        'interpreter','latex',...
        'HorizontalAlignment','center',...
        'backgroundcolor','white',...
        'color','red')
    shg
    pause
    clf

    % Graphs of the parabolas (y,w), x = constant
    stem3(xp,yp,zp,'w')
    hold on
    plot(xp,yp,'b.','markersize',12)
    grid on
    box on
    titxyz('parabolas:\quad $z(y,w),\quad  x = $ constant',ex,ey,ez,
    fs)

    for i = [7 4 1]
        stem3(xp(i),yp(i),zp(i),'b')
        text(xp(i),yp(i),wm,sprintf('$w(%g)=%g$',i,w(i)),...
            'interpreter','latex',...
            'horizontalalignment','center',...
            'color','blue')
    end
    plot3(x71,y71,p71,'k-','linewidth',1.5)
    text(a,e,zp(4)+2.7*dz,cuadryStr(pa),...
        'interpreter','latex',...
        'backgroundcolor','white',...
        'HorizontalAlignment','center')
    shg
    pause

```

```
    for i = [8 5 2]
        stem3(xp(i),yp(i),zp(i),'b')
        text(xp(i),yp(i),wm,sprintf('$w(%g)=%g$',i,w(i)),...
            'interpreter','latex',...
            'horizontalalignment','center',...
            'color','blue')
    end
    plot3(x82,y82,p82,'k-','linewidth',1.5)
    text(b,e,zp(5)+2.7*dz,cuadryStr(pb),...
        'interpreter','latex',...
        'backgroundcolor','white',...
        'HorizontalAlignment','center')
    shg
    pause

    for i = [9 6 3]
        stem3(xp(i),yp(i),zp(i),'b')
        text(xp(i),yp(i),wm,sprintf('$w(%g)=%g$',i,w(i)),...
            'interpreter','latex',...
            'horizontalalignment','center',...
            'color','blue')
    end
    plot3(x93,y93,p93,'k-','linewidth',1.5)
    text(c,e,zp(6)+2.7*dz,cuadryStr(pc),...
        'interpreter','latex',...
        'backgroundcolor','white',...
        'HorizontalAlignment','center')
    shg
    pause
    clf

    % Graphs of the 6 basic parabolas (with heights poles)
    % that will receive nxn parabolas
    grid on
    box on
    stem3 (xp,yp,zp,'b')
    hold on

    % 3 parabolas (y,w), x=constant
```

```
    plot3(x71,y71,p71,'k-','LineWidth',1.5)
    plot3(x82,y82,p82,'k-','LineWidth',1.5)
    plot3(x93,y93,p93,'k-','LineWidth',1.5)

    % 3 parabolas (x,w), y=constant
    plot3(x13,y13,p13,'r-','LineWidth',1.5)
    plot3(x46,y46,p46,'r-','LineWidth',1.5)
    plot3(x79,y79,p79,'r-','LineWidth',1.5)
    plot(xp,yp,'b.','markersize',12)

    for i = 1:9
        text(xp(i),yp(i),zp(i)+dz,num2str(w(i)),...
            'interpreter','latex',...
            'horizontalalignment','center',...
            'color','blue',...
            'fontsize',12)
    end
    ti = '$6$ parabolas to support $%g$ parabolas on each direction'
    ;
    ti = sprintf(ti,n-3);
    titxyz (ti,ex,ey,ez,fs)
    box on
    shg
    pause
    clf

    % Graphs of the 6 basic parabolas (without heights poles)
    % that will receive nxn parabolas
    grid on
    box on
    plot3(xp,yp,zp,'bo','markersize',8)
    hold on

    % 3 parabolas (y,w), x=constant
    plot3(x71,y71,p71,'k-','LineWidth',1.5)
    plot3(x82,y82,p82,'k-','LineWidth',1.5)
    plot3(x93,y93,p93,'k-','LineWidth',1.5)

    % 3 parabolas (x,w), y=constant
```

```
    plot3(x13,y13,p13,'r-','LineWidth',1.5)
    plot3(x46,y46,p46,'r-','LineWidth',1.5)
    plot3(x79,y79,p79,'r-','LineWidth',1.5)

    minp = min([p71 p82 p93 p13 p46 p79]);
    for i = 1:9
        plot3([xp(i) xp(i)],[yp(i) yp(i)],[minp zp(i)],'b.-')
    end
    for i = 1:9
        text(xp(i),yp(i),zp(i)+dz/2,num2str(w(i)),...
            'interpreter','latex',...
            'horizontalalignment','center',...
            'color','blue',...
            'fontsize',12)
    end
    grid on
    titxyz (ti,ex,ey,ez,fs)
    box on
    axis tight
    shg
    pause
    clf

    mesh(x,y,z)
    hidden off
    minz = min(min(z));
    hold on
    for i = 1:9
        plot3([xp(i) xp(i)],[yp(i) yp(i)],[minz zp(i)],'b.-')
    end
    plot3(xp,yp,zp,'bo','markersize',8)
    for i = 1:9
        plot3([xp(i) xp(i)],[yp(i) yp(i)],[minz zp(i)],'b.-')
    end
    t2 = sprintf('Transparent Response Mesh $%g \\times %g$',n,n);
    titxyz(t2,ex,ey,ez,fs)
    box on
    axis tight
    shg
```

```
455     pause
456     clf
457
458     mesh(x,y,z)
459     hold on
460     plot3 (xp,yp,zp,'r.','markersize',15)
461     t2 = sprintf('Response Mesh %$g \\times %g$',n,n);
462     titxyz (t2,ex,ey,ez,fs)
463     box on
464     axis tight
465     shg
466     pause
467     clf
468
469     mesh(x,y,z,'EdgeColor','black')
470     hold on
471     plot3 (xp,yp,zp,'r.','markersize',15)
472     t2 = sprintf('Black Response Mesh $%g \\times %g$',n,n);
473     titxyz (t2,ex,ey,ez,fs)
474     box on
475     axis tight
476     shg
477     pause
478     clf
479
480     meshc(x,y,z)
481     hold on
482     plot3 (xp,yp,zp,'r.','markersize',15)
483     t2 = sprintf('Response Mesh $%g \\times %g$',n,n);
484     t2 = [t2 ' and Contour Lines'];
485     titxyz (t2,ex,ey,ez,fs)
486     box on
487     axis tight
488     shg
489     pause
490     clf
491
492     meshz(x,y,z)
493     hold on
```

```
494     plot3 (xp,yp,zp,'r.','markersize',15)
495     t2 = sprintf('Response Mesh $%g \\times %g$',n,n);
496     t2 = [t2 ' and Lower Plane'];
497     titxyz (t2,ex,ey,ez,fs)
498     box on
499     axis tight
500     shg
501     pause
502     clf
503
504     surf(x,y,z)
505     hold on
506     plot3 (xp,yp,zp,'r.','markersize',15)
507     t2 = sprintf('Response Surface $%g \\times %g$',n,n);
508     titxyz (t2,ex,ey,ez,fs)
509     box on
510     axis tight
511     shg
512     pause
513     clf
514
515     surfl(x,y,z)
516     hold on
517     plot3 (xp,yp,zp,'r.','markersize',15)
518     t2 = sprintf(' Colored $%g \\times %g$',n,n);
519     t2 = ['Response Surface' t2];
520     titxyz (t2,ex,ey,ez,fs)
521     box on
522     axis tight
523     shg
524     pause
525     clf
526
527     surf(x,y,z); shading flat
528     hold on
529     plot3 (xp,yp,zp,'r.','markersize',15)
530     t2 = sprintf(' Without Lines $%g \\times %g$',n,n);
531     t2 = ['Response Surface' t2];
532     titxyz (t2,ex,ey,ez,fs)
```

```
533     box on
534     axis tight
535     shg
536     pause
537     clf
538
539     surf(x,y,z); shading interp
540     hold on
541     plot3 (xp,yp,zp,'r.','markersize',15)
542     t2 = sprintf(' Response Surface $%g \\times %g$',n,n);
543     t2 = ['Soft ' t2];
544     titxyz (t2,ex,ey,ez,fs)
545     box on
546     axis tight
547     shg
548     pause
549     clf
550
551     pcolor(x,y,z)
552     hold on
553     plot3 (xp,yp,zp,'r.','markersize',15)
554     t2 = sprintf('Plan View in Pseudocolor $%g \\times %g$',n,n);
555     titxyz (t2,ex,ey,ez,fs)
556     shg
557     axis tight
558     pause
559     clf
560
561     waterfall(x,y,z)
562     hold on
563     plot3 (xp,yp,zp,'r.','markersize',15)
564     t2 = 'Response Surface ';
565     t2 = [t2 sprintf('in Waterfall $%g \\times %g$',n,n)];
566     titxyz (t2,ex,ey,ez,fs)
567     box on
568     axis tight
569     shg
570     pause
571     clf
```

```
572
573     surfc(x,y,z)
574     hold on
575     plot3 (xp,yp,zp,'r.','markersize',15)
576     t2 = 'Response Surface ';
577     t2 = [t2 sprintf('$%g \\times %g$ and Contour Lines',n,n)];
578     titxyz (t2,ex,ey,ez,fs)
579     box on
580     axis tight
581     shg
582     pause
583     clf
584
585     % contour lines
586     [c1,h1] = contour(x,y,z,m,'linewidth',2);
587     clabel(c1,h1)
588     hold on
589
590     % marks of the 9 stations
591     for i = 1:3
592        for j = 1:3
593           plot(abc(i),def(j),'+r','markersize',20)
594           plot(abc(i),def(j),'or','markersize',20)
595        end
596     end
597     ti = sprintf('$%g$ Contour Lines',m);
598     titxyz (ti,ex,ey,ez,fs)
599     grid
600     shg
601     pause
602
603     % Interpolation at points (X,Y)
604
605     % When XY = [], then the interpolation is performed on the x
    abscissas,
606     % and the y ordinates and the nine data belonging to the
    original
607     % rectangular grid 3x3
608
```

```
609     % XY = (X,Y) is desired to obtain the Z heights by interpolation
610     if isempty(XY)
611         XY = [xp' yp'];                     % default interpolation
    points
612     end
613     minx = min(min(x));
614     maxx = max(max(x));
615     miny = min(min(y));
616     maxy = max(max(y));
617     xx = linspace(minx,maxx);
618     yy = linspace(miny,maxy);
619     xx = linspace(minx,maxx);
620     yy = linspace(miny,maxy);
621     z1 = polyval(pf,xx,2);
622     z2 = polyval(pe,xx,2);
623     z3 = polyval(pd,xx,2);
624     z4 = polyval(pa,yy,2);
625     z5 = polyval(pb,yy,2);
626     z6 = polyval(pc,yy,2);
627
628     L = [];
629     XYZ = [];
630     [m1,n1] = size(XY);
631     for i = 1:m1
632        xi = XY(i,1);                        % abscissas and
633        yi = XY(i,2);                        % ordinates to
    interpolate
634        zf = polyval(pf,xi,2);               % parabolas in
635        ze = polyval(pe,xi,2);               % the direction
636        zd = polyval(pd,xi,2);               % of x-axis
637        pi = polyfit([d e f],[zd ze zf],2);  % parabola in y
    direction
638        zi = polyval(pi,yi,2);               % parabolas with heights
     z
639        Zi = polyval(pi,yy);                 % interpolation's
    parabola
640
641        if i <= 4
642            clf
```

```
643             stem3(xp,yp,zp,'w')
644             hold on
645             grid on
646             box on
647             plot3(xx,linspace(f,f),z1,'r-','linewidth',1.5)
648             plot3(xx,linspace(e,e),z2,'r-','linewidth',1.5)
649             plot3(xx,linspace(d,d),z3,'r-','linewidth',1.5)
650             plot(xi,yi,'.b','markersize',15)
651             plot3([minx xi xi],[yi yi miny],[0 0 0],'b--','linewidth'
    ,1.5)
652             t = 'Use of scaffolding to interpolate in $(%g, %g)$';
653             ti = sprintf(t,xi,yi);
654             titxyz(ti,ex,ey,ez,fs)
655             shg
656             pause
657
658             plot3([minx xi],[yi yi],[0,0],'b--','linewidth',1.5)
659             stem3([xi xi xi],[f e d],[zf ze zd],'bo','markersize',12)
660             text(xi,f,wm,sprintf('$w=%g$',zf),...
661                 'interpreter','latex',...
662                 'horizontalalignment','center',...
663                 'color','blue')
664             text(xi,e,wm,sprintf('$w=%g$',ze),...
665                 'interpreter','latex',...
666                 'horizontalalignment','center',...
667                 'color','blue')
668             text(xi,d,wm,sprintf('$w=%g$',zd),...
669                 'interpreter','latex',...
670                 'horizontalalignment','center',...
671                 'color','blue')
672             ti = sprintf('3 points located in $ x=%g$',xi);
673             titxyz(ti,ex,ey,ez,fs)
674             shg
675             pause
676
677             plot3(linspace(xi,xi),yy,Zi,'b--','linewidth',1.5)
678             text(xi,f,wm,sprintf('$w=%g$',zf),...
679              'interpreter','latex',...
680              'horizontalalignment','center',...
```

```
681             'color','blue')
682
683         text(xi,e,ze+2.7*dz,cuadryStr(pi),...
684             'interpreter','latex',...
685             'HorizontalAlignment','center',...
686             'backgroundcolor','w',...
687             'color','blue')
688         ti = 'generate the interpolation parabola';
689         titxyz(ti,ex,ey,ez,fs)
690         shg
691         pause
692
693         plot3([xi xi],[yi yi],[0 zi],'b--','linewidth',1.5)
694         ti = sprintf('In $(%g, %g)$, height of the parabola = %g'
    ,...
695             xi,yi,zi);
696         titxyz(ti,ex,ey,ez,fs)
697         shg
698         pause
699
700         plot3(xi,yi,zi,'o',...
701             'markersize',12,...
702             'markeredgecolor','k',...
703             'markerfacecolor','c')
704         t = sprintf('The interpolation point is $(%g, %g, %g)$'
    ,...
705             xi,yi,zi);
706         titxyz(t,ex,ey,ez,fs)
707         shg
708         pause
709     end
710     L = [L; zi];                          % heights of
    interpolation
711                                           % points
712  end
713  XYZ = [XY L];                            % coordinates of
    interpolation
714                                           % located on the
    response
```

```
                                                % surface

 % interpolation points
 clf
 [mi,ni] = size(XYZ);
 mesh(x,y,z)
 hold on
 plot3(XYZ(:,1),XYZ(:,2),XYZ(:,3),'o',...
     'markersize',12,...
     'markeredgecolor','k',...
     'markerfacecolor','c')
 plot3 (xp,yp,zp,'r.','markersize',18)
 ti = sprintf('$%g$ Interpolation Values',mi);
 titxyz(ti,ex,ey,ez,fs)
 box on
 axis tight
 shg
 format
```

A.1.1 Subroutine for Writing Quadratic Equations on the x-axis

This subroutine belongs to the *grid9.m* code, and is used to write the quadratic equations along the X axis.

```
function cadx = cuadrxStr (p)
%
%
-------------------------------------------------------------------------

% Converts the three element numerical vector p to a string
variable of
% the corresponding quadratic equation in the variable x.
%
-------------------------------------------------------------------------

%        cadx = cuadrxStr (p)
%
% Data
```

```
% p: numerical vector [a b c]
%
% Results
% cadx: string with ax^2 + bx + c
%
%

format shortg
cadx = '';
a = p(1);
b = p(2);
c = p(3);

% ax^2
if abs(a) > eps
   s = sign(a);
   if abs(a) == 1
      if s == 1
         cadx = [cadx 'x^2'];
      elseif s == -1
         cadx = [cadx '-x^2'];
      end
   else
      cadx = [cadx num2str(a) 'x^2'];
   end
end

% ax^2+bx
if abs(b) > eps
   s = sign(b);
   if s == 1
      if abs(b) == 1
         cadx = [cadx ' + x'];
      else
         cadx = [cadx ' + ' num2str(abs(b)) 'x'];
      end
   elseif s == -1
      if abs(b) == 1
         cadx = [cadx ' - x'];
```

```
        else
            cadx = [cadx ' - ' num2str(abs(b)) 'x'];
        end
    end
end

% ax^2+bx+c
if abs(c) > eps
    s = sign(c);
    if s == 1
        cadx = [cadx ' + ' num2str(abs(c))];
    elseif s == -1
        cadx = [cadx ' - ' num2str(abs(c))];
    end
end
format
```

A.1.2 Subroutine for Writing Quadratic Equations on the y-axis

This subroutine belongs to the *grid9.m* code, and is used to write the quadratic equations along the Y axis.

```
function cady = cuadryStr (p)
%
%
-------------------------------------------------------------------------

% Converts the three element numerical vector p to a string
variable of
% the corresponding quadratic equation in the variable y.
%
-------------------------------------------------------------------------

%        cady = cuadryStr (p)
%
% Data
% p: numerical vector [a b c]
```

```
%
% Results
% cady: string with ay^2 + by + c
%
%

format shortg
cady = '';
a = p(1);
b = p(2);
c = p(3);

% ay^2
if abs(a) > eps
   s = sign(a);
   if abs(a) == 1
      if s == 1
         cady = [cady 'y^2'];
      elseif s == -1
         cady = [cady '-y^2'];
      end
   else
      cady = [cady num2str(a) 'y^2'];
   end
end

% ay^2+by
if abs(b) > eps
   s = sign(b);
   if s == 1
      if abs(b) == 1
         cady = [cady ' + y'];
      else
         cady = [cady ' + ' num2str(abs(b)) 'y'];
      end
   elseif s == -1
      if abs(b) == 1
         cady = [cady ' - y'];
      else
```

```
            cady = [cady ' - ' num2str(abs(b)) 'y'];
        end
    end
end

% ay^2+by+c
if abs(c) > eps
    s = sign(c);
    if s == 1
        cady = [cady ' + ' num2str(abs(c))];
    elseif s == -1
        cady = [cady ' - ' num2str(abs(c))];
    end
end
format
```

A.1.3 Subroutine to Generate Titles

Subroutine belonging to the *grid9.m* code to generate titles on the three axis.

```
function titxyz (t,x,y,z,fs)

title(t,...
    'interpreter','latex',...
    'Fontsize',fs)

xlabel(x,...
    'interpreter','latex',...
    'Fontsize',fs)

ylabel(y,...
    'interpreter','latex',...
    'Fontsize',fs)

zlabel(z,...
    'interpreter','latex',...
    'Fontsize',fs)
```

A.1.4 Subroutine to Convert Angles to Decimal Format

Subroutine belonging to the *grid9.m* code to convert angular values of the format degrees minutes and seconds to decimal degrees.

```
function  D = dms (ang3)
%
%         D = dms (ang3)
%
-------------------------------------------------------------------------

% Converts angle values from degrees minutes seconds to values
in
% decimal degrees, as required by the gridD program
%
-------------------------------------------------------------------------

%
% Data and results:
%
% 1)    ang3      [x1  x2  x3]
%
%       D         [x1  x2  x3]
%
%
-------------------------------------------------------------------
%
% 2)    ang3      [d1  m1  s1
%                  d2  m2  s2
%                  d3  m3  s3]
%
%       D         [D1  D2  D3]
%
%       Example
%           ang3 = [-100 59 58; -101 25 28; -103 19 46]
%           D    = [-100.9994   -101.4244   -103.3294]
%
%
-------------------------------------------------------------------
```

```
28  %
    ------------------------------------------------------------------
29  %
30  % 3)    ang3        [ x1   y1
31  %                     x2   y2
32  %                    ...  ...
33  %                     xk   yk]
34  %
35  %       D           [ X    Y ]
36  %
37  %
    ------------------------------------------------------------------
38  %
39  % 4)    ang3        [dx1  mx1  sx1   dy1  my1  sy1
40  %                    dx2  mx2  sx2   dy2  my2  sy2
41  %                         ...             ...
42  %                    dxk  mxk  sxk   dyk  myk  syk]
43  %
44  %       D           [      X              Y      ]
45  %
46  %       Example
47  %           ang3 = [-100 59 58  25 23 35; -101 25 28  25 50 40]
48  %           D     = [-100.9994   25.3931;  -101.4244   25.8444 ]
49  %
50  %
    ------------------------------------------------------------------------


51  %

52

53  format
54  D = [];

55

56  [m,n] = size(ang3);
57  if m == 1 & n == 3
58      D = ang3;
59  elseif m == 3 & n == 3
60      D = sign(ang3(:,1)).*(abs(ang3(:,1))+ang3(:,2)/60+ang3(:,3)
    /3600);
61      D = D';
```

```
62      elseif n == 2
63          D = ang3;
64      elseif n == 6
65          X = ang3(:,1:3);
66          X = sign(X(:,1)).*(abs(X(:,1))+X(:,2)/60+X(:,3)/3600);
67          Y = ang3(:,4:6);
68          Y = sign(Y(:,1)).*(abs(Y(:,1))+Y(:,2)/60+Y(:,3)/3600);
69          D = [X Y];
70      else
71          errordlg('Data Order Error',...
72              'Wrong Order','error')
73          disp(' ')
74          return
75      end
```

Appendix B

Figures from Algorithm DGG1

Coordinates of the nine points correspond to the global grid in where Coahuila is located. Heights for this case represent the temperatures obtained for those points, but the study variables can be chosen, hypothetical or measured.

Figures obtained with the programme for Algorithm DGG1, whose code is explained in Appendix A are shown below.

B.1 Figures Obtained with grid9.m

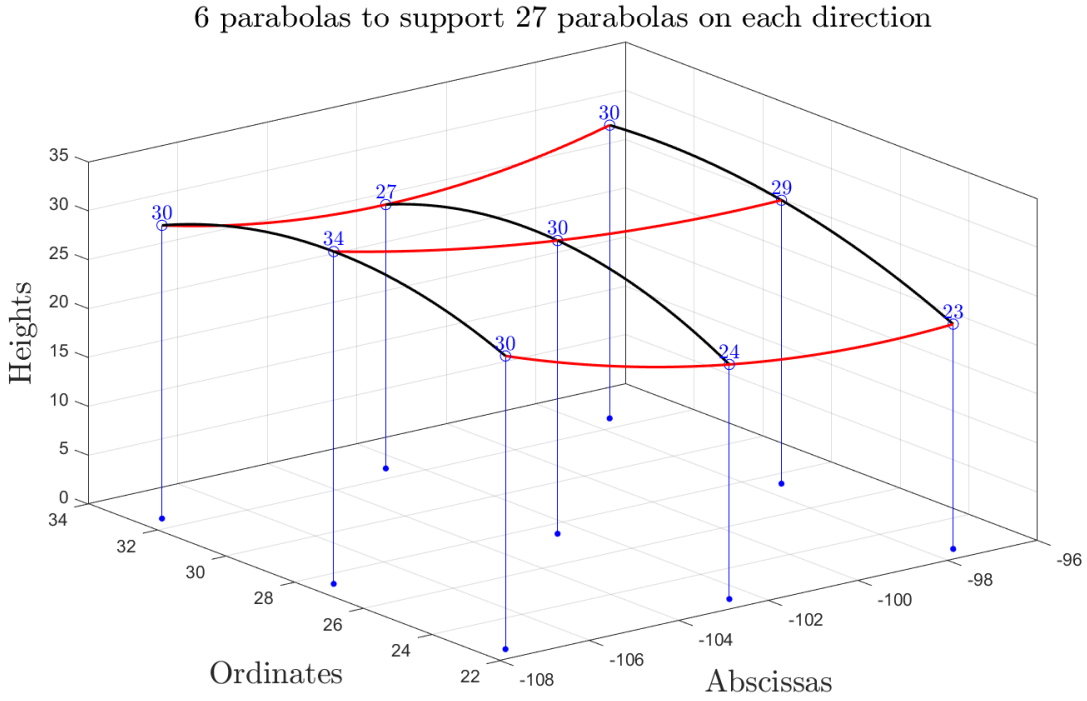


Figure B.1: Poles.

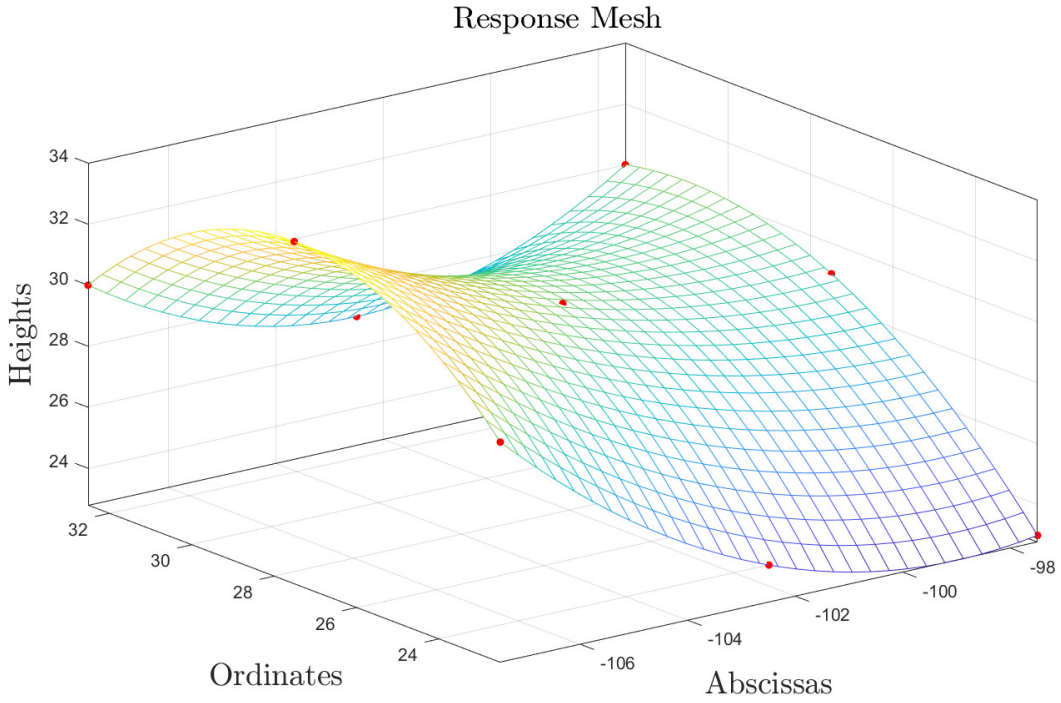


Figure B.2: Coloured Response Mesh.

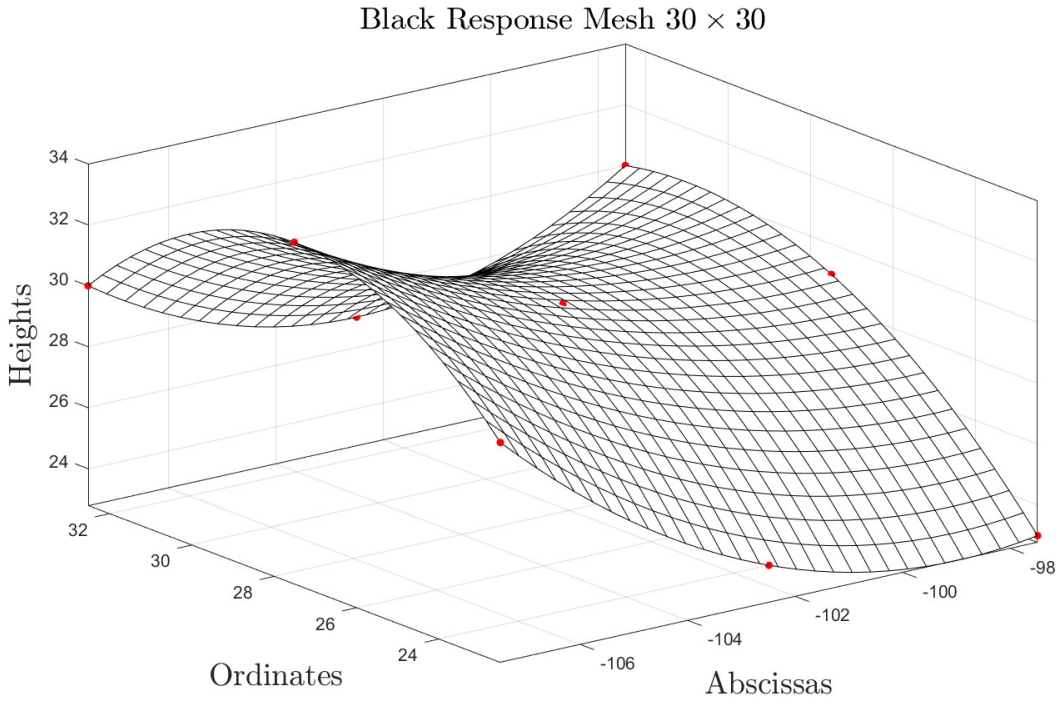


Figure B.3: Black Response Mesh.

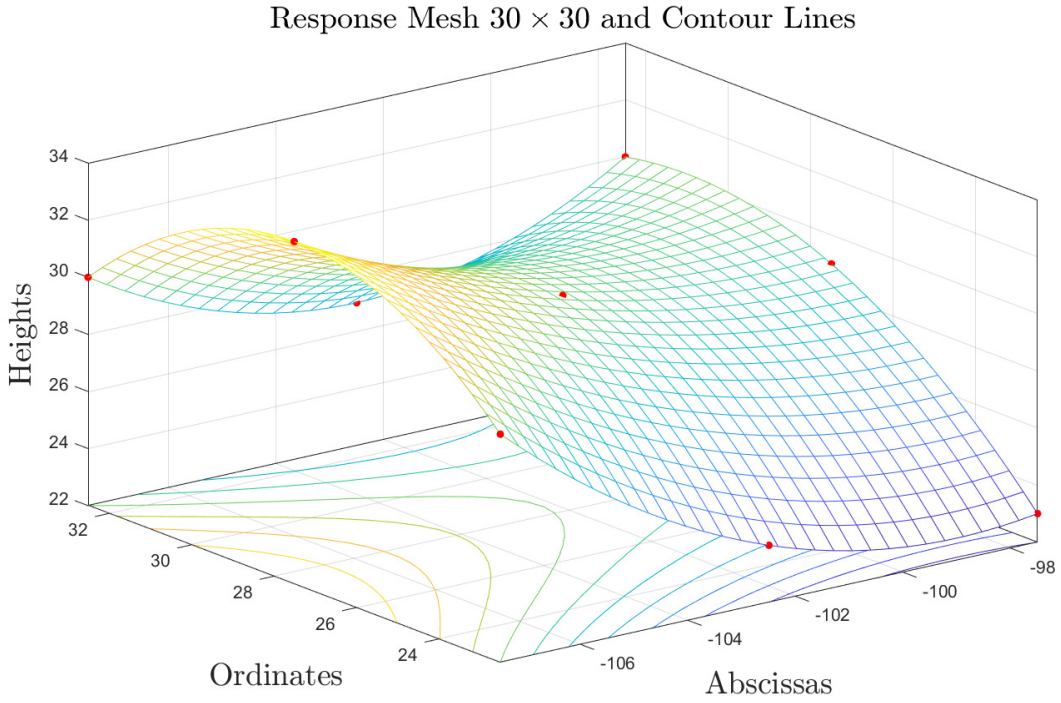


Figure B.4: Response Mesh and Projected Contour Lines.

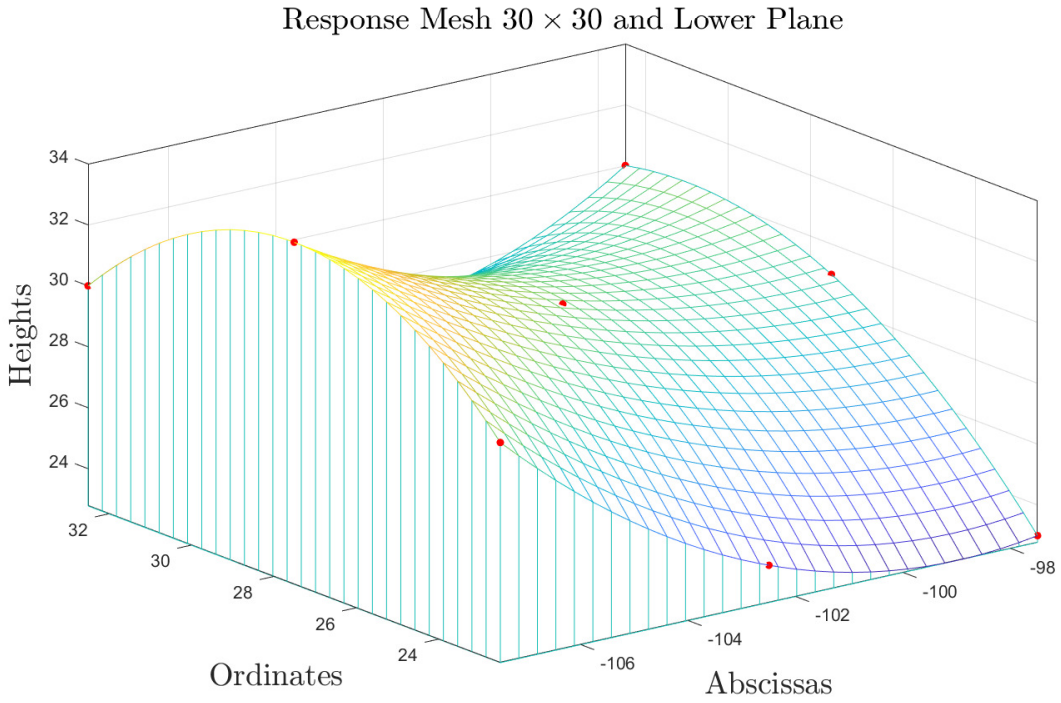


Figure B.5: Lower Plane.

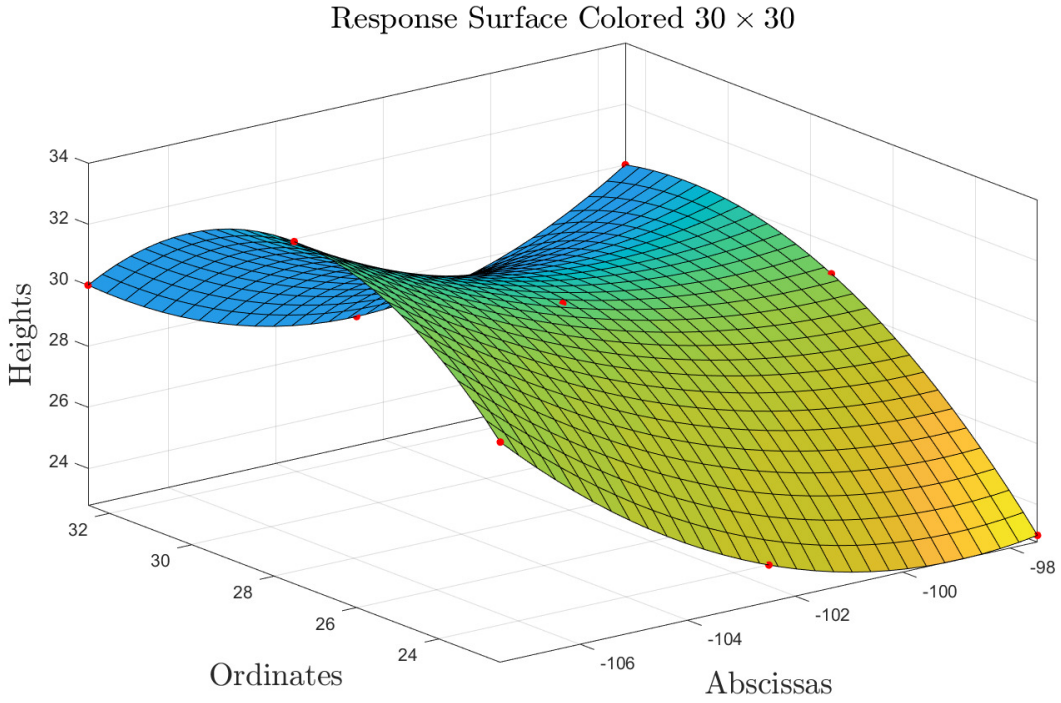


Figure B.6: Response Surface.

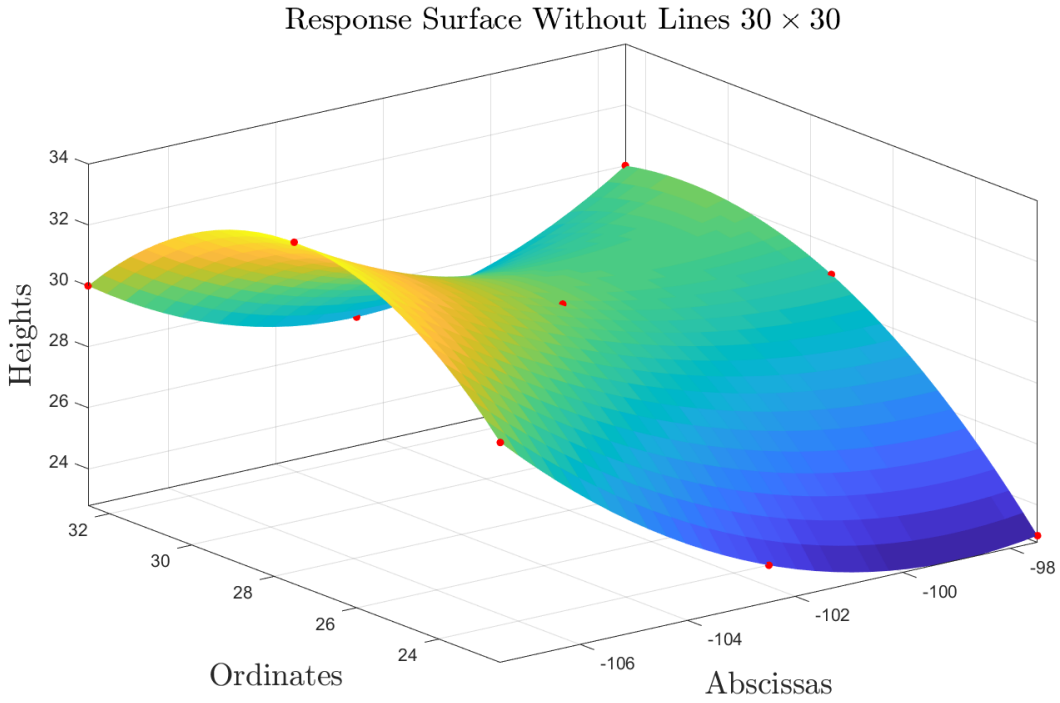


Figure B.7: Response Surface without Lines.

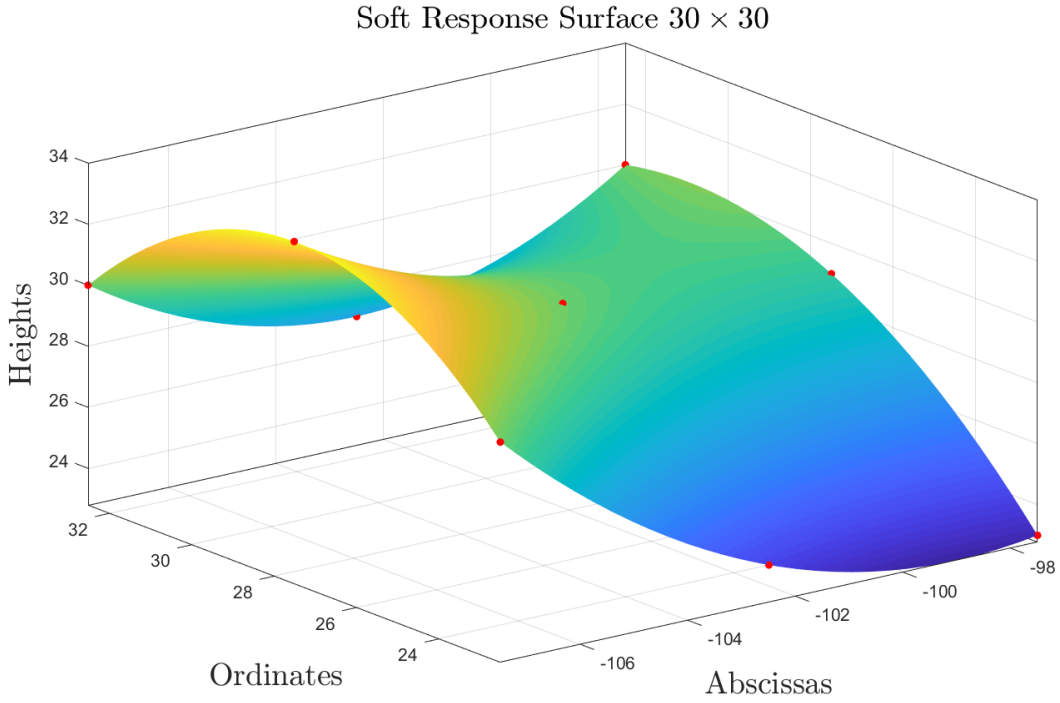


Figure B.8: Soft Response Surface.

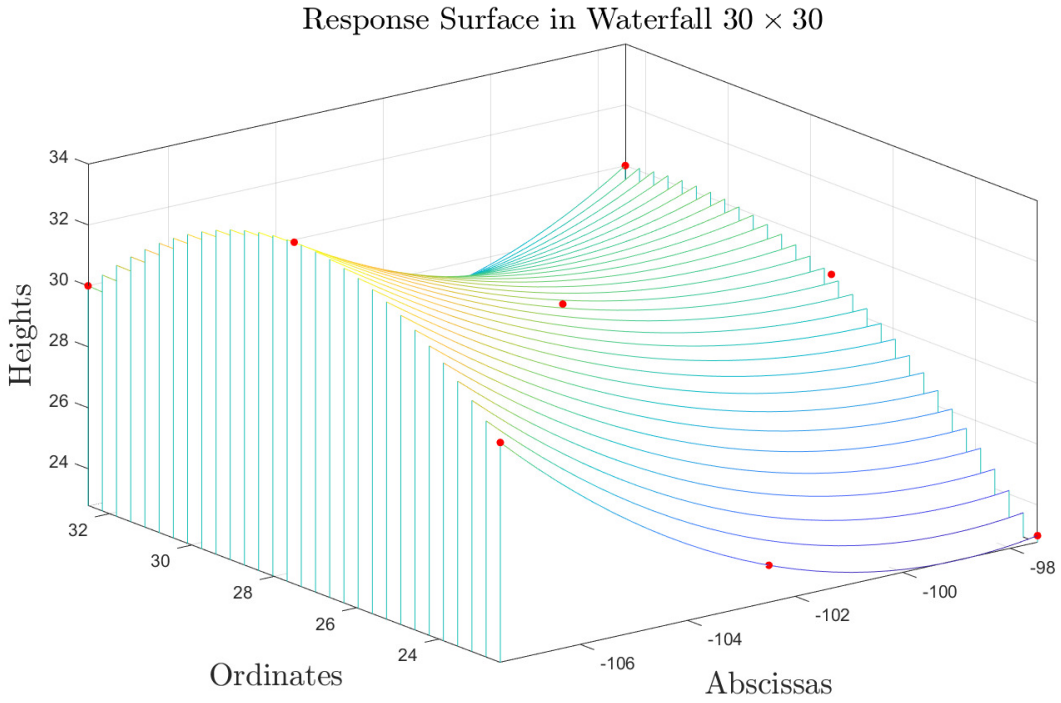


Figure B.9: Response Surface in Waterfall.

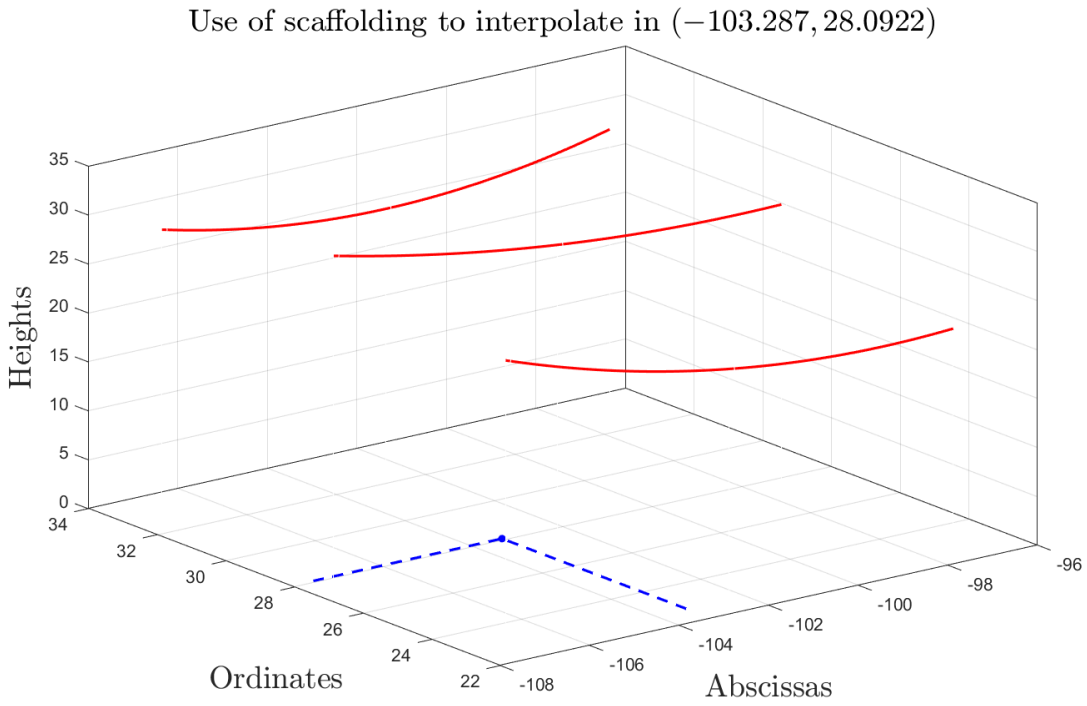


Figure B.10: Scaffolding to Interpolate One Point.

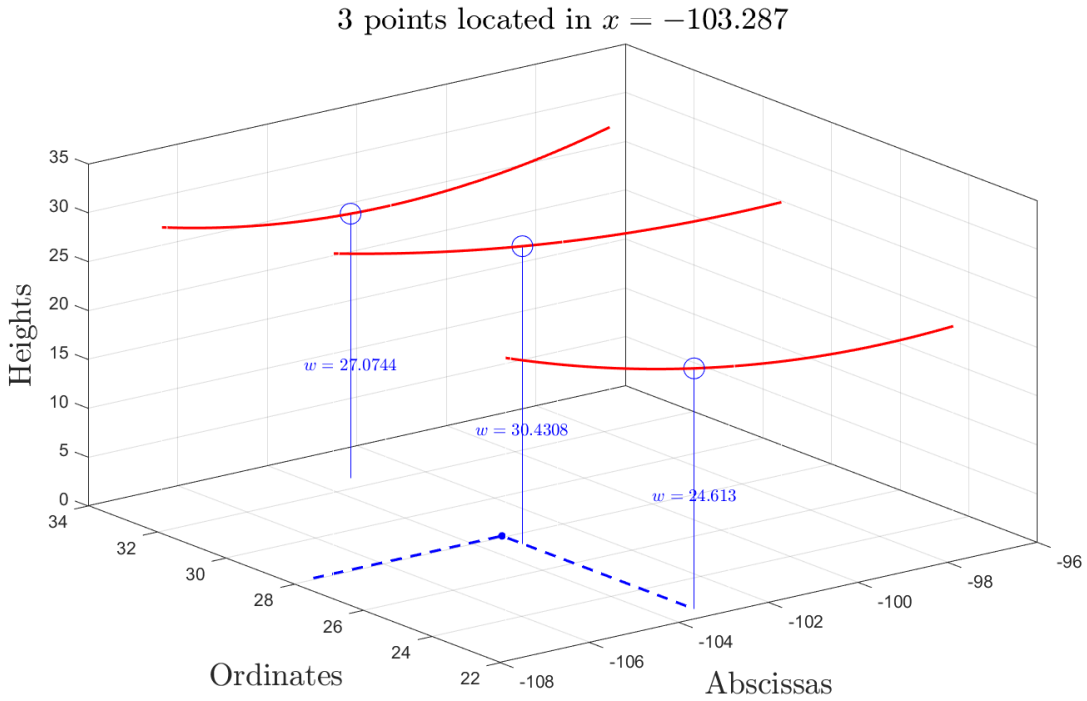


Figure B.11: 3 points in x.

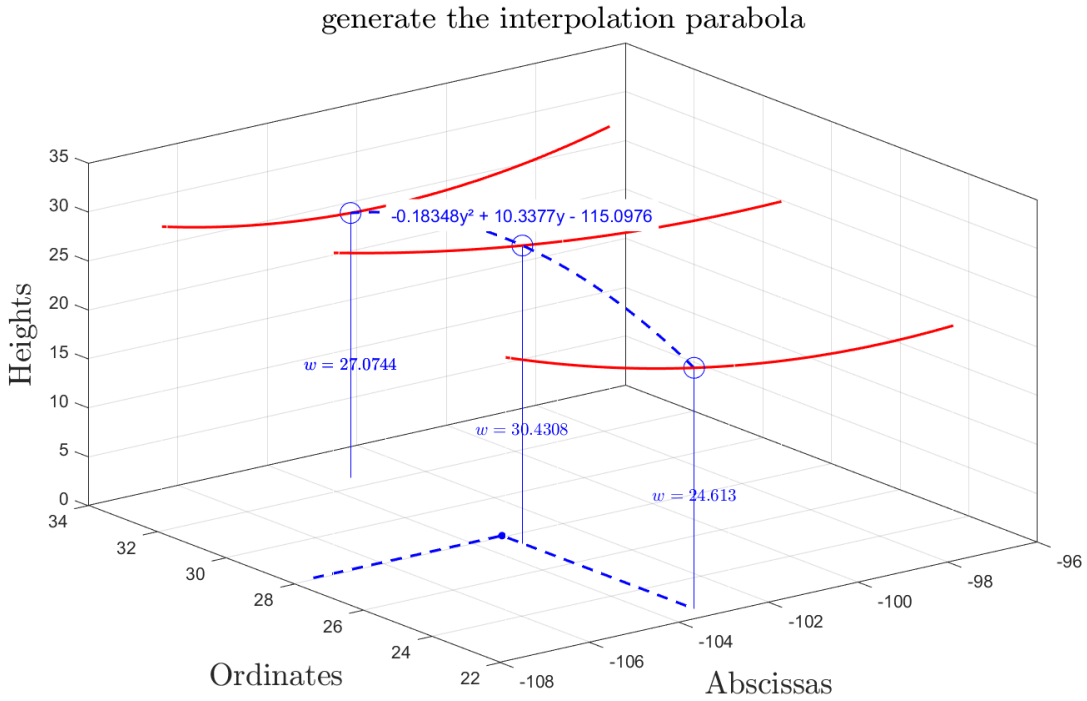


Figure B.12: Generation of Interpolation Parabola.

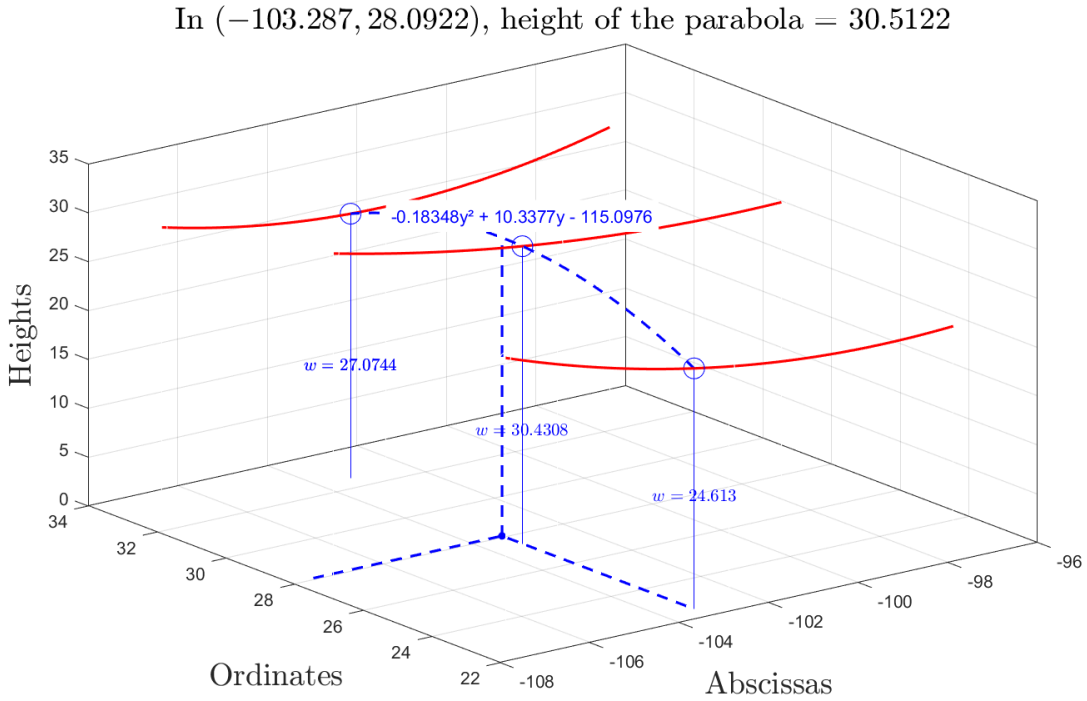


Figure B.13: Height of the Parabola.

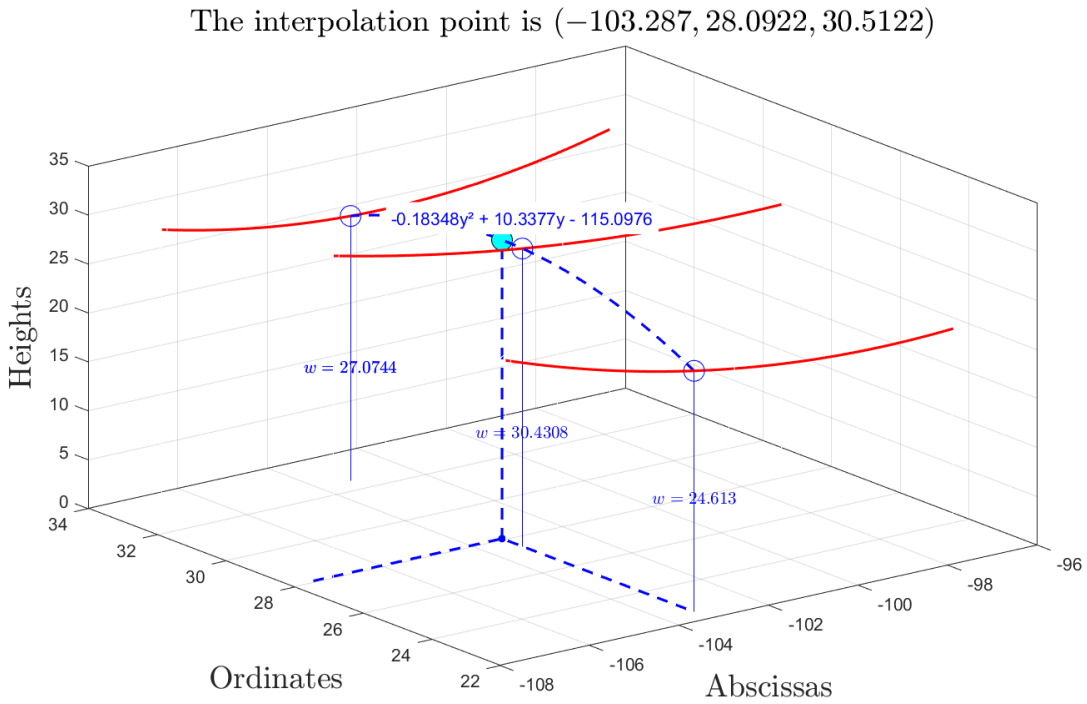


Figure B.14: Interpolation Point.

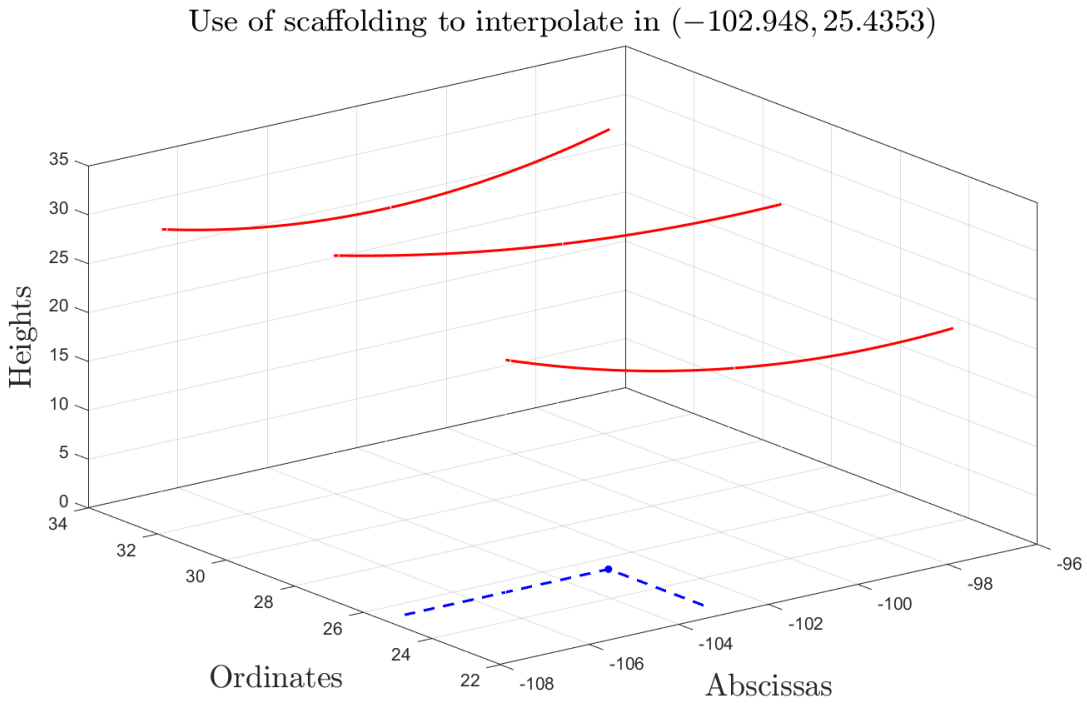


Figure B.15: Scaffolding to Interpolate One Point.

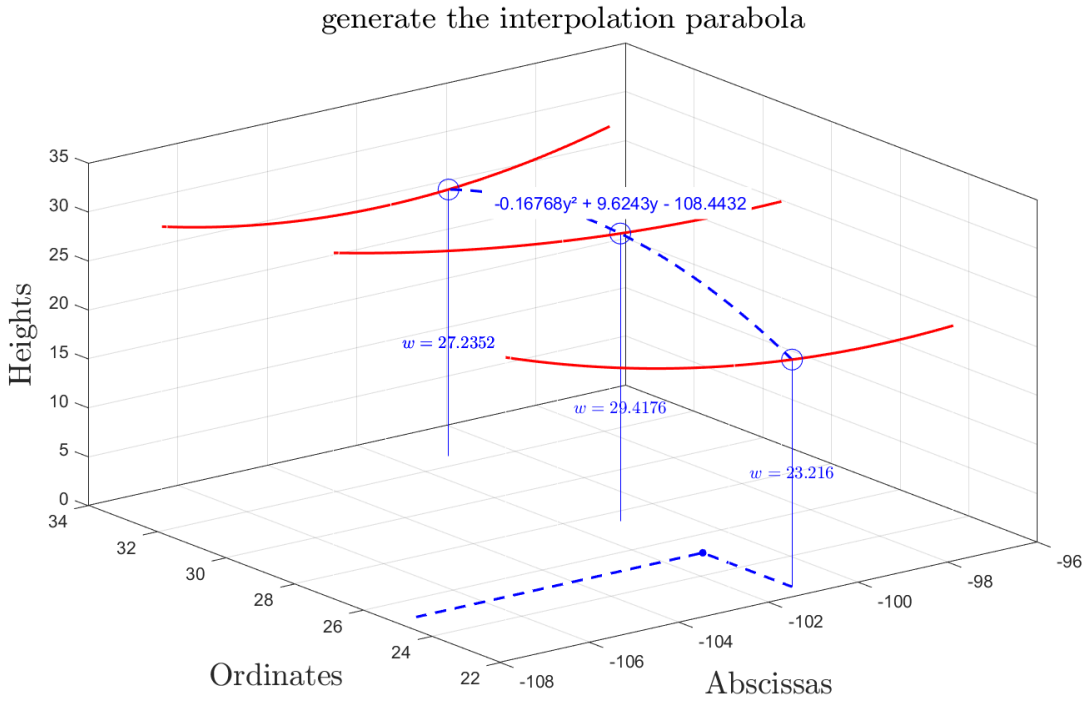


Figure B.16: Generation of Interpolation Parabola.

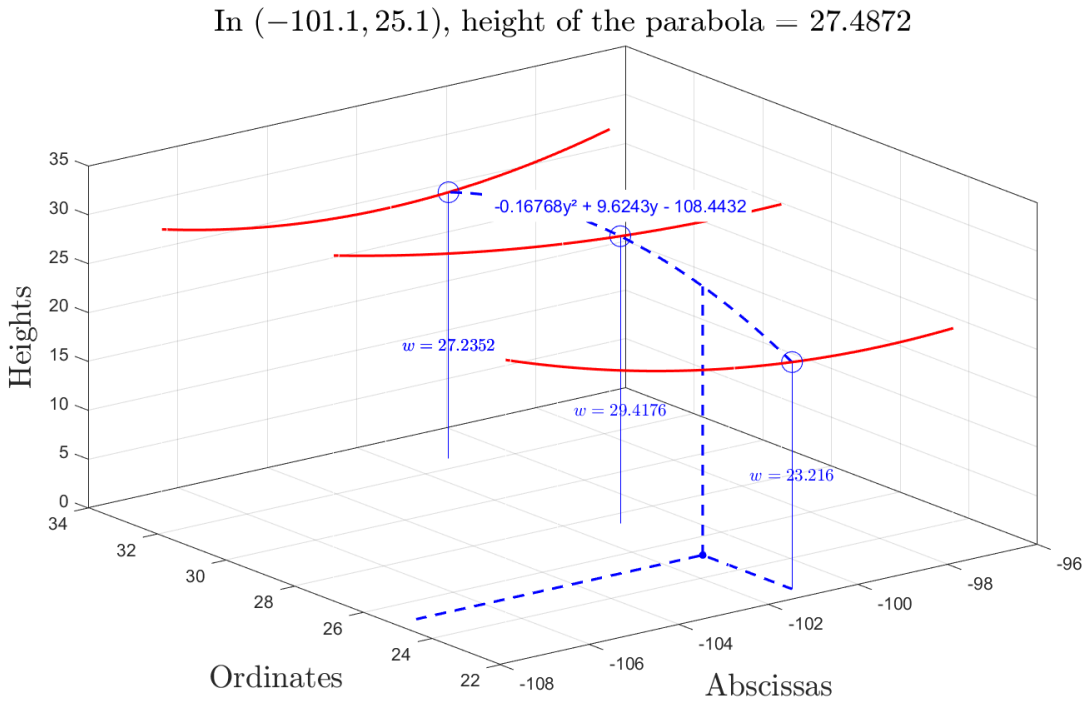


Figure B.17: Height of the Parabola.

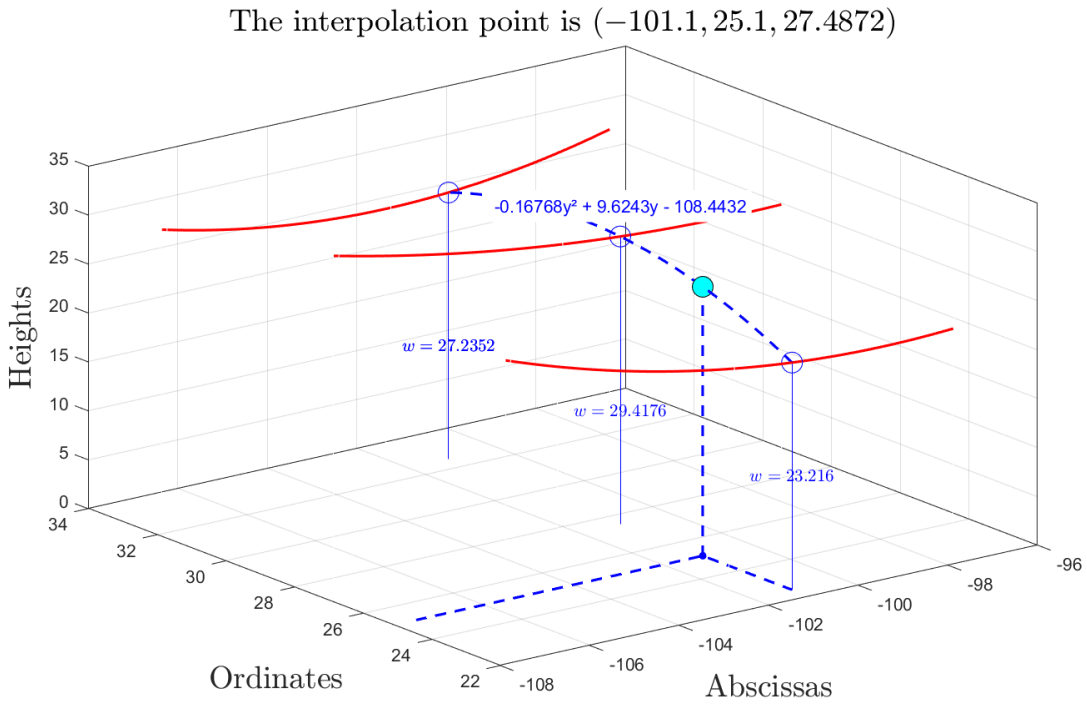


Figure B.18: Interpolation Point.

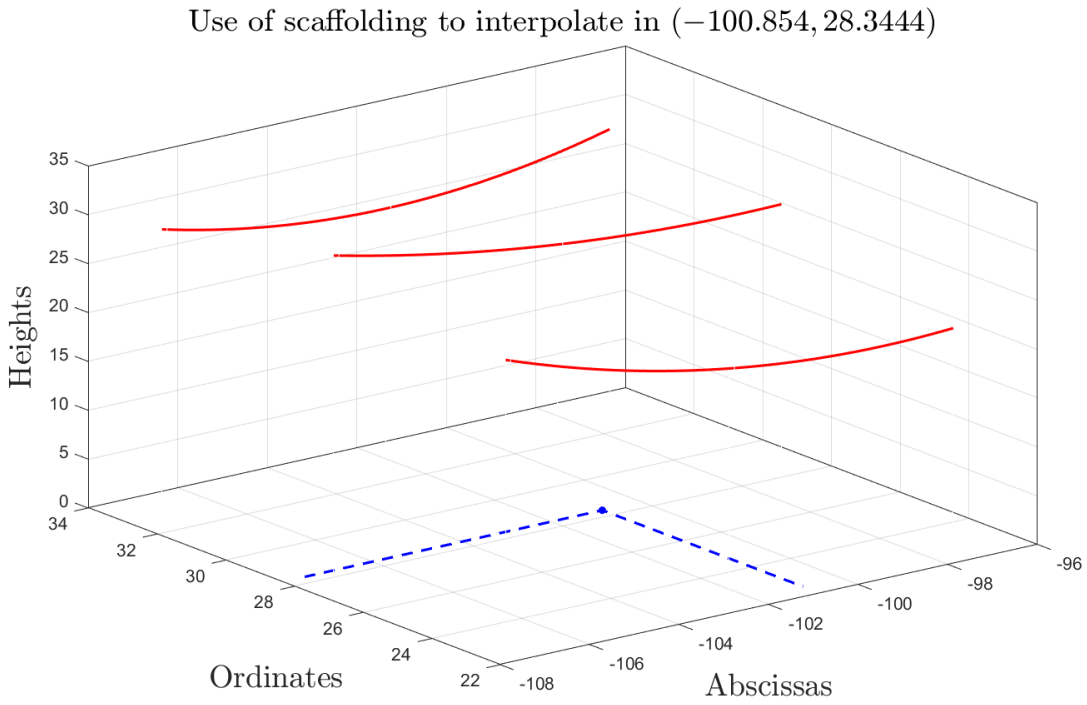


Figure B.19: Scaffolding to Interpolate One Point.

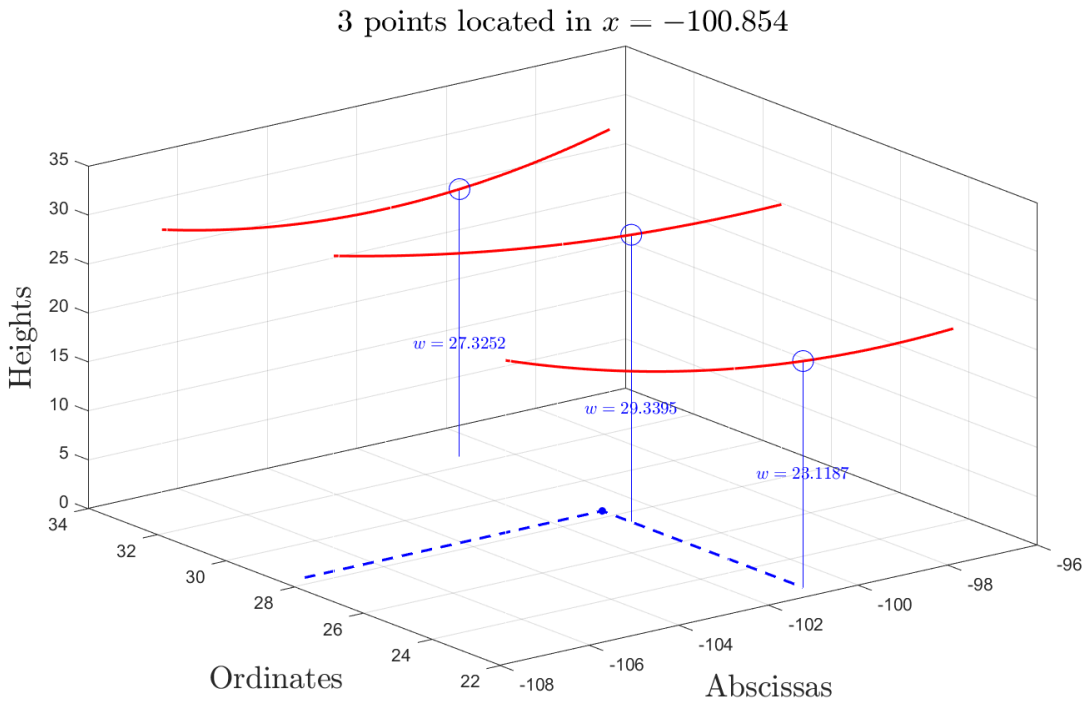


Figure B.20: 3 points in x.

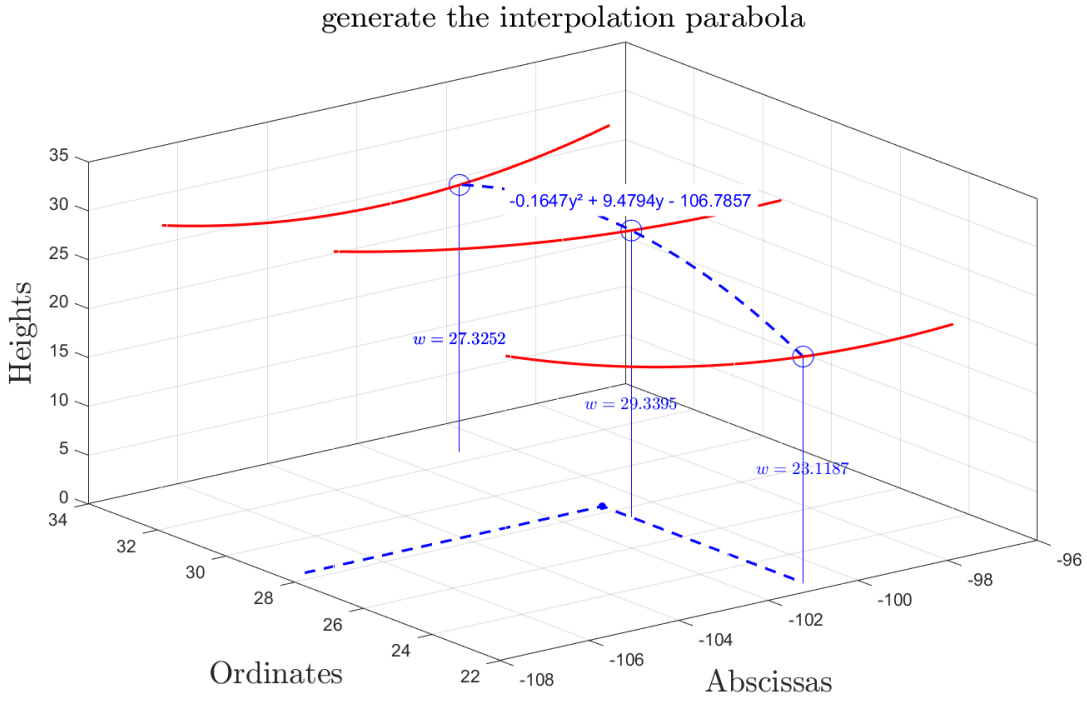


Figure B.21: Generation of Interpolation Parabola.

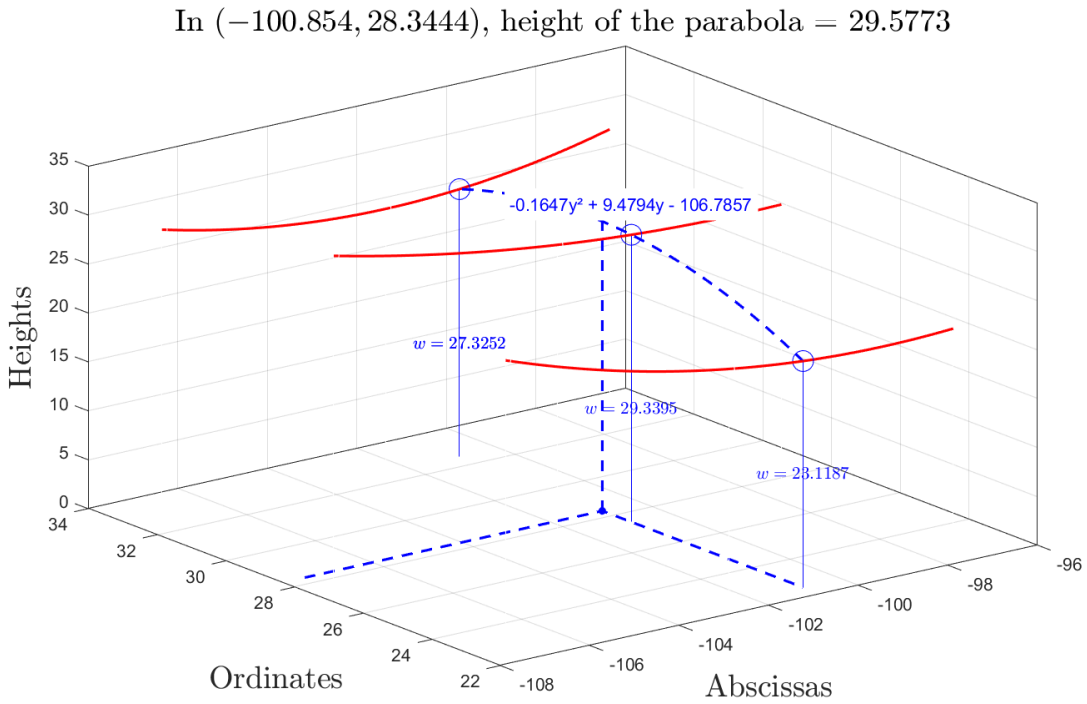


Figure B.22: Height of the Parabola.

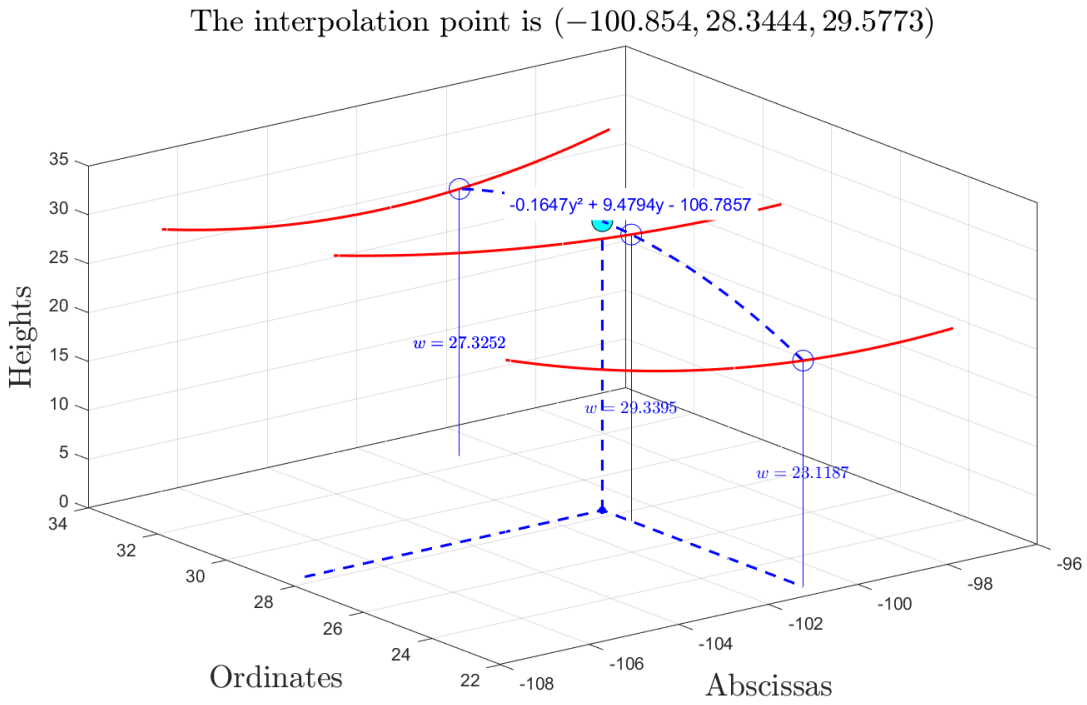


Figure B.23: Interpolation Point.

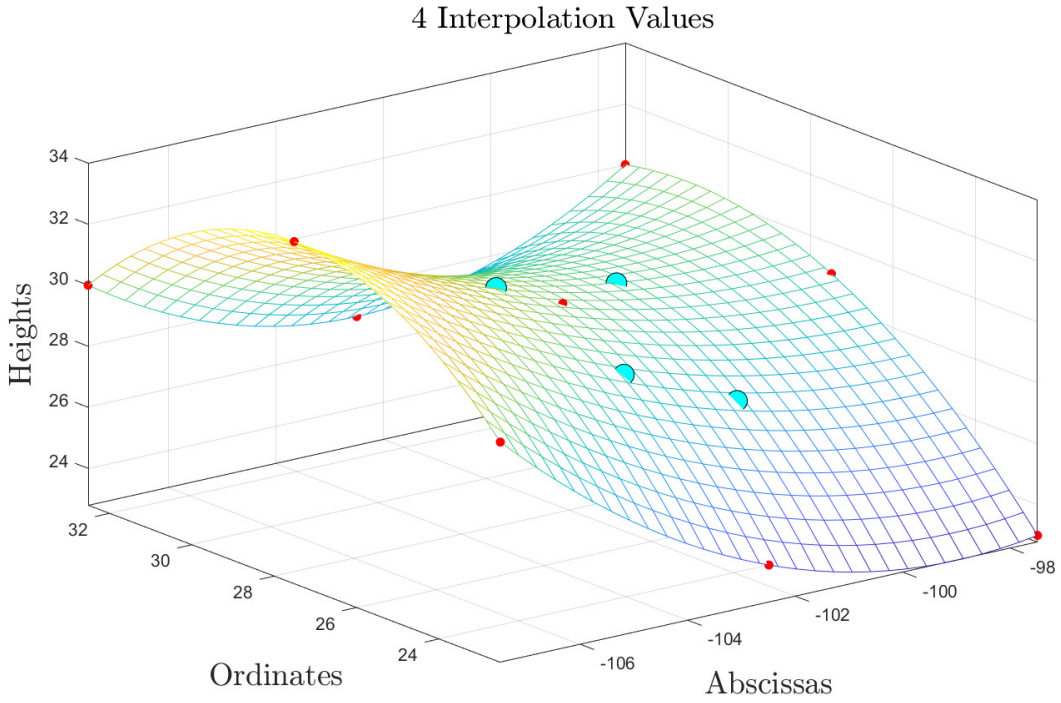


Figure B.24: 4 Interpolation Values.

Appendix C

Code of Algorithm DGG2

The programme obtains the heights corresponding to the temperature in the desired coordinate. In relation to the results for the research, these surfaces are obtained for the A2 and B2 SRES scenarios of the IPCC, for the years 2020, 2050 and 2080.

In the code are shown in greater detail the elements that are obtained with its application, vertices as a result of the triangulation of data, mesh composition, values obtained, interpolation, among others.

C.1 Code *methodB.m*

```
function [vert,XYZ,uvw] = methodB (x,y,z,cn,fs,u,v);
%
%        [vert,XYZ,uvw] = methodB (x,y,z,cn,fs,u,v);
%
-----------------------------------------------------------------------

% This program performs the calculations of the author's methodB.
% See the important notes at the end of these comments.
%
% Given the vectors of points (x,y,z) in the three-dimensional
space,
% with the abscissae (x), the ordinates (y), and the heights (z),
 which
```

```
10  % can be points in the three-dimensional space, from data
    obtained by
11  % experimentation or another form. The following data is also
    required:
12  % cn: number of contour lines.                      12 by default
13  % fs: number of fontsize.                           11 by default
14  %  u: abscissas of the points to be interpolated     x mean by
    default
15  %        column vectors with decimal angles
16  %        or matrices with 3 columns: degrees, minutes and seconds
17  %  v: ordinates of the points to be interpolated     y mean by
    default
18  %        column vectors with decimal angles
19  %        or matrices with 3 columns: degrees, minutes and seconds
20  %
21  %  uvw: to obtain the heights in the chosen coordinate
22  %
23  % The program obtains:
24  %
25  % a.- vert: number of vertices of the triangles in which the
    convex
26  %     polygon of the data (x,y) has been dissected.
27  %
28  % b.- XYZ = (X,Y,Z): response surface values on a mesh, from the
    data
29  %     (x,y,z).
30  %
31  % c.- It performs the interpolation in (u,v) to obtain w. Thus,
    the
32  %     points belonging to the response surface (u,v,w) are
    obtained,
33  %     in the uvw matrix form.
34  %
35  %     The program does the following:
36  %
37  % 1) Determines interior triangles of a convex polygonal in the
    plane.
38  %    It draws them and determines the indices of the coordinates
    (x,y)
```

```
39  %    of the data.
40  %
41  %    Assuming that triangle number 1 is formed with the vertices
42  %    (x5,y5), (x3,y3), (x2,y2), and the number 2 is formed with
    the
43  %    vertices (x1,y1), (x7,y7), (x4,y4), and so on, the indices
    of the
44  %    vertices, one line for each triangle, will be:
45  %    vert = [5 3 2;1 7 4];].
46  %
47  % 2) Colors the triangles of the previous convex polygonal.
48  %
49  % 3) Forms truncated triangular prisms by vertical projection,
    from the
50  %    convex polygonal, to the heights z5, z3, z2, z1, z7 z4 ...
51  %
52  % 4) Colors the upper triangles of the truncated triangular
    prisms.
53  %
54  % 5) Forms a response surface with coordinates (X,Y,Z). To do
    this, it
55  %    smoothes the roofs of the prisms (x,y,z) by iterpolation on
    a mesh
56  %    (X,Y), obtaining the interpolation heights Z.
57  %    Z = f(X,Y).
58  %
59  % 6) Presents relative errors of the response surface versus the
    values
60  %    estimatd by interpolation.
61  %
62  % 7) Draws the contour lines of the response surface.
63  %    Z = f(X,Y) = c, being c a constant. Contour lines cut Z in
64  %    horizontal planes of constant height c.
65  %
66  % 8) Interpolate to get the heights w = f(u,v).
67  %    If u and v are not given, x and y mean values are assigned.
68  %
69  %
```

```
70  %
71  %                                IMPORTANT
72  %
    ------------------------------------------------------------------------

73  %
74  % The program works independently, on the condition that the data
     is
75  % consistent.
76  %
    ------------------------------------------------------------------------

77  %
78  % IN THE AUTHOR'S RESEARCH, (methodB), THE DATA IS CONTAINED, FOR
79  % CONVENIENCE, IN THE FILE:  scenarios.mat.
80  %
81  % THEY ARE DOWNLOADED FROM THE MATLAB PROMPT:
82  %     >> load scenarios
83  %
    ------------------------------------------------------------------------

84  %
    ------------------------------------------------------------------------

85  %
86  % Required routine:      enLaMalla
87  %
88  % Ana Berenice Gomez de Leon.    28 de agosto de 2018.
89  %
90
91  warning off
92  set(groot,'defaultAxesTickLabelInterpreter','latex'); % ticks in
     latex
93  clf
94  vert = [];
95  XYZ  = [];
96  uvw  = [];
97
```

```
98  if nargin < 3
99      h = errordlg('Insufficient Data','Data Error','error');
100     disp(' ')
101     return
102 else
103     x = x(:);
104     y = y(:);
105     z = z(:);
106     if length(x) ~= length(y) | length(x) ~= length(z)
107         h = errordlg('They must be of the same order',...
108             'Data Error','error');
109     disp(' ')
110     return
111     end
112 end
113 dx = abs(max(x)-min(x))/20;
114 dy = abs(max(y)-min(y))/20;
115
116
117 if nargin <= 5
118     u = sum(x)/length(x);                % by default
119     v = sum(y)/length(y);                % by default
120 end
121 if nargin <= 4
122     fs = 11;                             % by default
123 end
124 if nargin == 3
125     cn = 12;                             % by default
126 end
127
128 %
    ------------------------------------------------------------------------

129 % 2D
130
131 % establishes the boundary of the data, considering a convex
    polygonal
132 [k,A] = convhull(x,y);                   % MATLAB instruction
133
```

```
134 % Three highly specialized instructions have been found
135
136 % shapes and draws the triangles
137 triang = delaunayTriangulation (x,y);     % MATLAB instruction
138 hold on
139 grid on
140
141 % graphs the triangles
142 triplot (triang)                          % MATLAB instruction
143
144 for i = 1:length(x)                       % enumeration of the
    points
145    text(x(i),y(i),int2str(i),...
146        'interpreter','latex',...
147        'HorizontalAlignment','center',...
148        'BackGroundColor','w')             % all at once
149 end
150 grid on
151 box on
152 xlabel('X-Axis',...
153     'interpreter','latex',...
154     'fontsize',fs)
155 ylabel('Y-Axis',...
156     'interpreter','latex',...
157     'fontsize',fs)
158 tt = sprintf('$%g$',length(x));
159 tt = ['Triangulation of ' tt ' Data in 2D'];
160 title(tt,...
161     'interpreter','latex',...
162     'fontsize',fs)
163 xlim([min(x)-dx max(x)+dx])
164 ylim([min(y)-dy max(y)+dy])
165 shg
166 pause
167
168 % downloads the vertices field of the variable triang
169 vert = triang.ConnectivityList;           % MATLAB instruction
170
171 % colors the triangles in 2D
```

```
172   [nv,mv] = size(vert);
173   con = vert;
174   tt = sprintf('$%g$',nv);
175   tt = ['Coloring of ' tt ' Triangles in 2D'];
176   title(tt,...
177       'interpreter','latex',...
178       'fontsize',fs)
179   j = 0;
180   for i = 1:nv
181      j = j+1;
182      i = con(i,:);
183      fill(x(i),y(i),rand)
184      text(sum(x(i))/3,sum(y(i))/3,int2str(j),...
185          'interpreter','latex',...
186          'HorizontalAlignment',...
187          'center',...
188          'fontsize',fs)
189   end
190   xlabel('X-Axis',...
191       'interpreter','latex',...
192       'fontsize',fs)
193   ylabel('Y-Axis',...
194       'interpreter','latex',...
195       'fontsize',fs)
196   box on
197   shg
198   pause
199
200   %
      ------------------------------------------------------------------------
201   % 3D
202
203   clf
204   plot3(x(1),y(1),z(i),'.')
205   hold on
206   plot(x(k),y(k),'k-','LineWidth',1.2)     % border at the base
207   plot3(x(k),y(k),z(k),'k-','LineWidth',1.2)% border on the roof
208   for i = 1:length(x)                       % vertical poles
```

```
209       plot3([x(i) x(i)],[y(i) y(i)],[0 z(i)],'r-')
210    end
211    for i = 1:nv                              % triangular roofs
212       i = con(i,:);
213       plot3 (x(i),y(i),z(i),'b-')
214       plot3 (x(i),y(i),[0 0 0],'b-')         % triangular bases
215    end
216    grid
217    xlabel('X-Axis',...
218        'interpreter','latex',...
219        'fontsize',fs)
220    ylabel('Y-Axis',...
221        'interpreter','latex',...
222        'fontsize',fs)
223    zlabel('Z-Axis',...
224        'interpreter','latex',...
225        'fontsize',fs)
226    box on
227    tt = sprintf('%g',nv);
228    tt = [tt ' Truncated Triangular Prisms in 3D'];
229    title(tt,...
230        'interpreter','latex',...
231        'fontsize',fs)
232    xlim([min(x)-dx max(x)+dx])
233    ylim([min(y)-dy max(y)+dy])
234    shg
235    pause
236
237    clf
238    plot(x(k),y(k),'k-','LineWidth',1.2)      % border at the base
239    for i = 1:length(x)                       % vertical poles
240       plot3([x(i) x(i)],[y(i) y(i)],[0 z(i)],'r-')
241       hold on
242    end
243    hold on
244    for i = 1:nv
245       i = con(i,:);
246       plot3(x(i),y(i),[0 0 0],'b-')          % triangular bases
247       fill3 (x(i),y(i),z(i),rand)            % roofs coloring
```

```
248                                                 % triangular
249     end
250     grid on
251     xlabel('X-Axis',...
252         'interpreter','latex',...
253         'fontsize',fs)
254     ylabel('Y-Axis',...
255         'interpreter','latex',...
256         'fontsize',fs)
257     zlabel('Z-Axis',...
258         'interpreter','latex',...
259         'fontsize',fs)
260     box on
261     tt = sprintf('%g',nv);
262     tt = ['Coloring of ' tt ' Upper Triangles in 3D'];
263     title(tt,...
264         'interpreter','latex',...
265         'fontsize',fs)
266     xlim([min(x)-dx max(x)+dx])
267     ylim([min(y)-dy max(y)+dy])
268
269     shg
270     pause
271
272     clf
273     xi = linspace(min(x),max(x),100);
274     yi = linspace(min(y),max(y),100);
275     [Xi,Yi] = meshgrid (xi,yi);
276     Zi = griddata (x,y,z,Xi,Yi,'cubic');      % available cubic and v4
277     [min(min(Zi)) max(max(Zi))];              % cubic realist, v4
        pretty
278     surfc(Xi,Yi,Zi); colorbar('AxisLocation','in')
279     inter = [min(min(Zi)) max(max(Zi))];
280     XYZ = [Xi Yi Zi];                         % interpolation values
281     TF = isnan(XYZ);
282     XYZ(TF) = 1;
283
284     box on
285     xlabel('X-Axis',...
```

```
286         'interpreter','latex',...
287         'fontsize',fs)
288     ylabel('Y-Axis',...
289         'interpreter','latex',...
290         'fontsize',fs)
291     zlabel('Z-Axis',...
292         'interpreter','latex',...
293         'fontsize',fs)
294     title('Response Surface',...
295         'interpreter','latex',...
296         'fontsize',fs)
297     shg
298     pause
299
300     % From the estimated points of the mesh (Xi,Yi,Zi)
301     % the height zz is interpolated at the points (x,y)
302     zz = interp2(Xi,Yi,Zi,x,y,'nearest');
303     nb = ~isnan(zz);
304     nm = isnan(zz);
305     tt = 1:length(x);
306     buenos = tt(nb);                          % good points
307     mal = tt(nm);                             % bad points
308     verticesmalos = vert(mal);
309     nOk = length(buenos);
310     nmal = length(mal);
311     zmal = zeros(length(mal),1);
312     nume = [x y z zz];
313     nume = nume(nb,:);
314     size(nume);
315
316     errorm = sum(abs((nume(:,3)-nume(:,4))./nume(:,3)))/nOk;
317
318     stem3(nume(:,1),nume(:,2),abs((nume(:,3)-nume(:,4)))/nume(:,3));
319     hold on
320     ta = sprintf(' = %g',errorm);
321     ta = ['Arithmetic Mean of Relative Errors ' ta];
322     title(ta,...
323         'interpreter','latex',...
324         'fontsize',fs)
```

```
325   t2 = sprintf('%g invalid values',nmal);
326   box on
327   xlim([min(x)-dx/10 max(x)+dx/10])
328   ylim([min(y)-dy/10 max(y)+dy/10])
329   xlabel('X-Axis',...
330       'interpreter','latex',...
331       'fontsize',fs)
332   ylabel('Y-Axis',...
333       'interpreter','latex',...
334       'fontsize',fs)
335   zlabel('Reltive Errors  $|(Z-Z_i)/Z|$',...
336       'interpreter','latex',...
337       'fontsize',fs)
338   shg
339   pause
340
341   clf
342   contour (Xi,Yi,Zi,cn,'showtext','on','LineWidth',1.2)
343   box on
344   grid on
345   xlabel('X-Axis',...
346       'interpreter','latex',...
347       'fontsize',fs)
348   ylabel('Y-Axis',...
349       'interpreter','latex',...
350       'fontsize',fs)
351   zlabel('Z-Axis',...
352       'interpreter','latex',...
353       'fontsize',fs)
354   tt = sprintf('%g',cn);
355   tt = [tt ' Contour Lines'];
356   title(tt,...
357       'interpreter','latex',...
358       'fontsize',fs)
359
360   uvw = enLaMalla (x,y,z,u,v);              % interpolation for (u,v
      )
```

C.1.1 Response Surface Interpolation

At the end of Algorithm DGG2 an interpolation is required to obtain the results. For this purpose, the following programme was developed. Performs the interpolation in the two dimensional space to obtain the heights of each point in the plane. Thus, the points belonging to the response surface are obtained.

The Algorithm DGG2 generates a 3D response surface. To quantify any point of it, interpolation must be used, which is achieved with the following code from the programme *enLaMalla.m*. This code is a subroutine required by the code *methodB.m*.

```
1  function uvw = enLaMalla (x,y,z,u,v)
2  %
3  %
   ------------------------------------------------------------------------

4  % For the data (x,y,z) it determines a mesh of order 100x100
5  % [Xi,Yi,Zi] to form a response surface.
6  %
7  % Performs the interpolation in (u,v) to obtain w. Thus the
   points
8  % belonging to the response surface (u,v,w) are obtained.
9  %
   ------------------------------------------------------------------------

10 %        uvw = enLaMalla (x,y,z,u,v)
11 %
12 %
   ________________________________________________________________________

13 %
14 % Downloading data from scenarios.mat, through
15 %    >> load scenarios
16 %    the following three vectors are obtained:
17 %
18 % x = [-100.8539 -101.9167 -100.7250 -101.9867 -101.4308
   -100.5939
19 %      -100.9872 -101.1239 -101.3731 -101.1239 -101.5194
```

```
    -103.2872
20  %       -102.9483 -102.3975 -103.7017 -103.4414 -103.2806
    -103.3819
21  %       -103.3158 -102.9667 -103.5678 -102.9483 -102.2019
    -102.2525
22  %       -102.7833 -101.0000 -100.6000 -100.9667 -101.4047
    -101.1000
23  %       -101.0000 -101.0667 -101.0000 -100.8667]
24  %
25  % y = [28.3444 28.4917 27.6139 29.1644 26.9047 27.4586 27.4283
26  %       27.8461 27.8869 27.8444 27.8692 28.0922 28.6367 27.3156
27  %       27.2864 25.5442 25.6353 25.5006 25.4169 25.7500 25.8833
28  %       25.4353 25.4586 25.6483 25.3375 25.4167 25.3500 25.5000
29  %       25.6983 25.1000 25.0000 26.1167 25.3833 25.6167]
30  %
31  % z = [28.9000 34.5000 31.4000 29.4000 30.2000 29.9000 30.3000
32  %       30.3000 28.8000 29.4000 24.6000 27.6000 29.7000 29.7000
33  %       26.4000 29.0000 29.3000 27.7000 28.0000 28.8000 27.9000
34  %       27.1000 27.4000 28.3000 28.5000 24.4000 26.2000 24.4000
35  %       25.5000 21.1000 23.3000 27.5000 22.9000 24.9000]
36  %
37  % From them, it is wanted to solve the following example:
38  %
39  % Eg. To obtain (u,v,w) from points
40  %                   (u,v):  (-102,27), (-102.5,27.5).
41  %
42  %                         Requires row or column vectors
43  %
44  %                         u = [-102 -102.5]
45  %
46  %                         v = [27 27.5]
47  %
48  % uvw = enLaMalla (x,y,z,u,v)
49  %
50  % produces    uvw =
51  %                 -102.0000   27.0000   29.9477
52  %                 -102.5000   27.5000   29.7099
53  %
54  % which is, (u,v,w):  (-102,27,29.9492), (-102.5,27.5,29.6958)
```

```
%
% The two values of w have been obtained by interpolation.
%
% NOTE
%
% u and v can be represented with respective matrices, with the 3
% columns of degrees, minutes and seconds. For example:
%
%          u = [-102 31 27
%               -101 26 32]
%
%          v = [27 10 15
%               28 18 44]
%
% These values are internally converted to decimal degrees.
%
```

```
%
% Although the previous example has been presented, the program
works
% for arbitrary data x, y, z, u, v, as long as they are
consistent.
%
% NOTE:  THIS PROGRAM CAN BE USED INDEPENDENTLY. HOWEVER, IT WAS
%        ESTABLISHED TO BE CALLED FROM:  methodB
%
```

```
%
% Ana Berenice Gomez de Leon.
%
% Nottingham, England.       Fecha:
%

warning off

uvw = [];

```

```
88  % column vectors
89  x = x(:);
90  y = y(:);
91  z = z(:);
92
93  % validacion de datos
94  if nargin > 5 | nargin < 5
95      msgbox('Must be 5 data','Data Error','error')
96      disp(' ')
97      return
98  end
99  [mu,nu] = size(u);
100 [mv,nv] = size(v);
101 if (mu ~= mv) | (nu ~= nv)
102     msgbox('u and v must be of the same order','Data Error',...
103         'error')
104     disp(' ')
105     return
106 end
107 if ~((nu == 1) | (nu == 3))
108     msgbox('Must be of 1 or 3 columns','Error in u and v',...
109         'error')
110     disp(' ')
111     return
112 end
113
114 % conversion of u and v (degree minutes seconds) to decimal
    format
115 if (nu+nv == 6)
116     u = sign(u(:,1)).*(abs(u(:,1))+u(:,2)/60+u(:,3)/3600);
117     v = sign(v(:,1)).*(abs(v(:,1))+v(:,2)/60+v(:,3)/3600);
118 end
119
120 % formation of triangles
121 triang = delaunayTriangulation (x,y);    % MATLAB instruction
122
123 % downloads the field of the vertices from the variable triang
124 vert3 = triang.ConnectivityList;         % MATLAB instruction
125
```

```
126   xi = linspace(min(x),max(x),100);
127   yi = linspace(min(y),max(y),100);
128   [Xi,Yi] = meshgrid (xi,yi);
129
130   % interpolation values
131   Zi = griddata (x,y,z,Xi,Yi,'cubic');      % available cubic and v4
      :
132                                             % cubic realistic,
133                                             % v4    pretty.
134
135   w = interp2(Xi,Yi,Zi,u,v,'nearest');      % interpolation
136
137   disp(' ')
138   l = [];                                   % detects out of range
139   l = find(isnan (w));
140   m = length(l);
141   if m == 1
142       disp(sprintf('   Data  %g  is out of range',l))
143   elseif m > 1
144       disp('   The data whose indices are out of range are:')
145       disp(l')
146   end
147
148   uvw = [u v w];                            % results
```

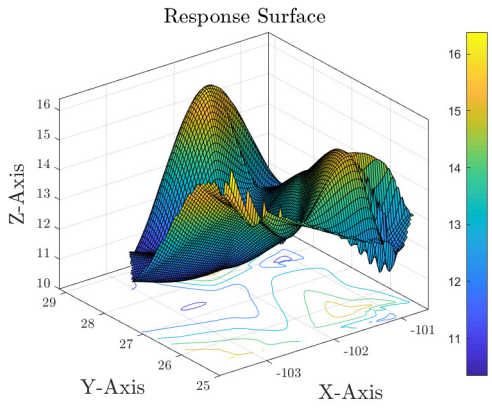
Appendix D

3D Figures from Algorithm DGG2

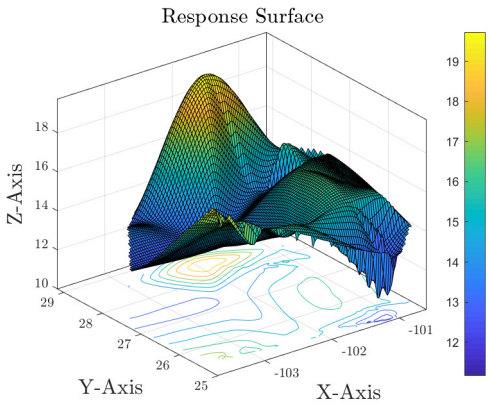
In relation to these graphical results:

1. Response Surfaces from Z1 to Z72: A2 and B2 Climate Change Scenarios; years 2020, 2050, 2080; from January to December.
2. The graphs shown in this Appendix, are the more explanatory of *Algorithm DGG2*, although with the algorithm, precise information for each point conforming them can be obtained, as the numerical information for each contour line.
3. From these figures, it can be appreciated that in zones with higher altitudes, mountains and higher altitudes vegetation, temperatures are lower than in zones with plains.
4. The graphs below clearly show the great diversity of temperature values in this region. And the same could be said of the great variability that exists in the rest of the country.

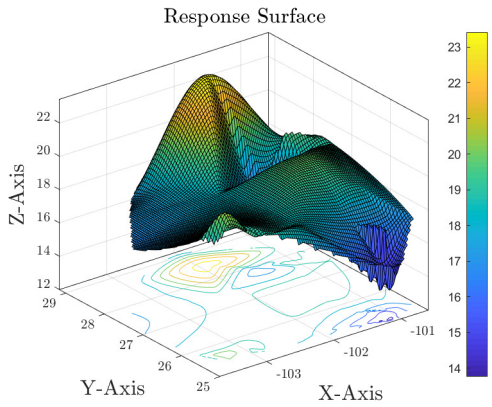
D.1 Response Surfaces obtained with Algorithm DGG2



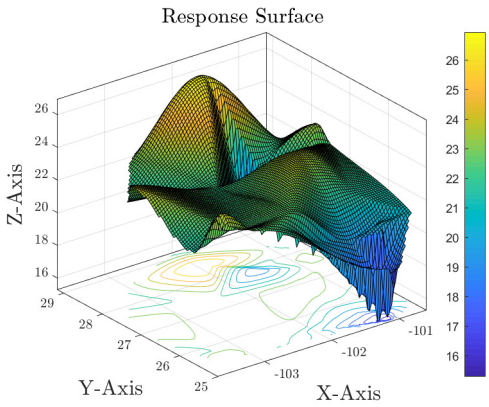
(a) Z1: A2 2020 January



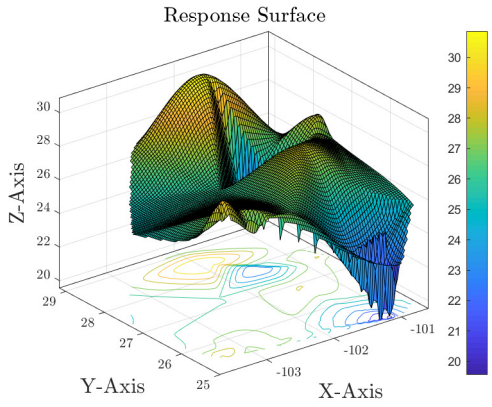
(b) Z2: A2 2020 February



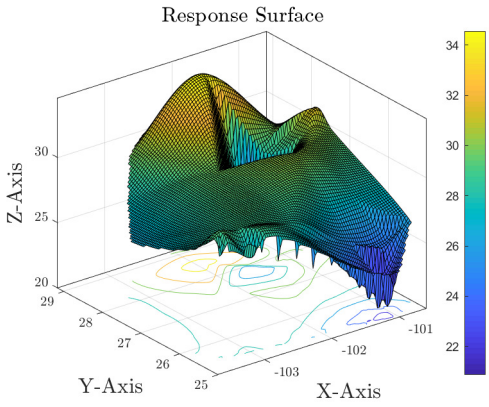
(c) Z3: A2 2020 March



(d) Z4: A2 2020 April

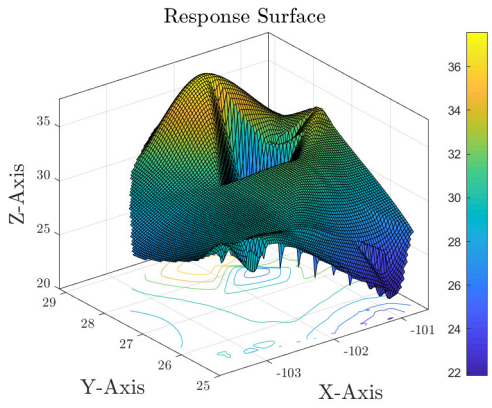


(e) Z5: A2 2020 May

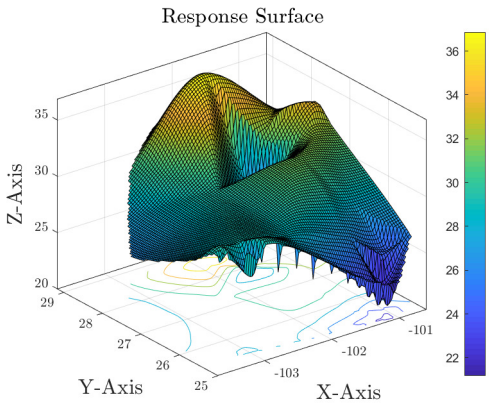


(f) Z6: A2 2020 June

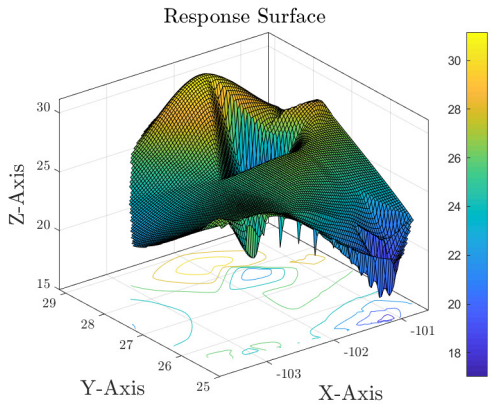
Figure D.1: Response Surfaces A2 Scenario, 2020, from January to June (Z1-Z6)



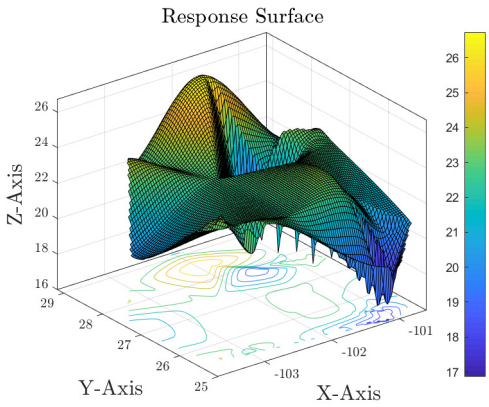
(a) Z7: A2 2020 July



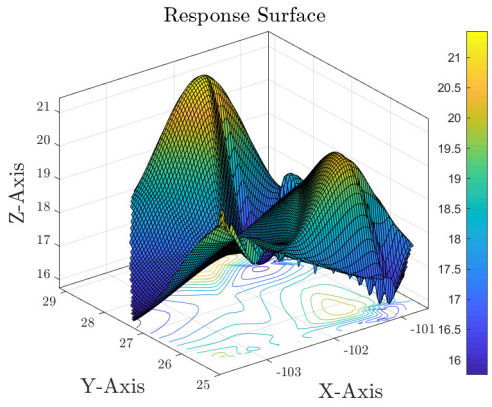
(b) Z8: A2 2020 August



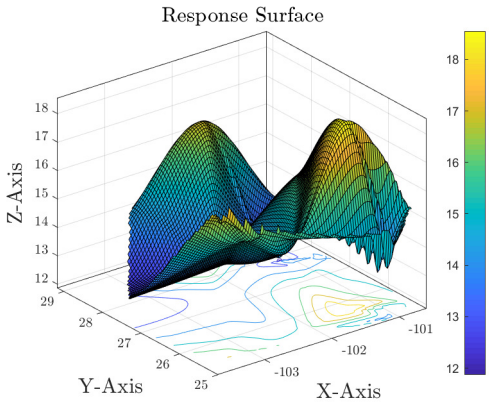
(c) Z9: A2 2020 September



(d) Z10: A2 2020 October

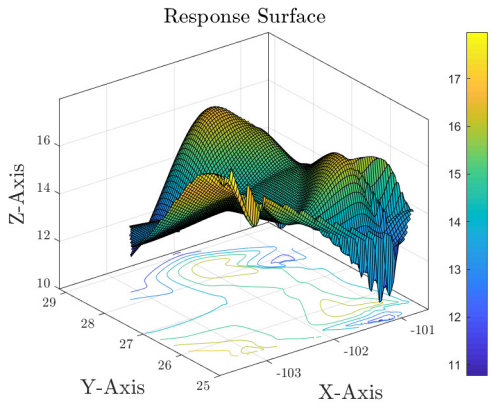


(e) Z11: A2 2020 November

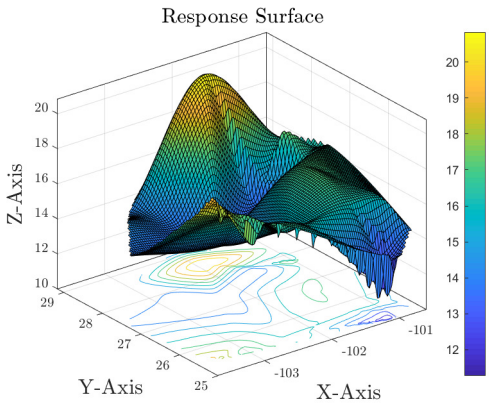


(f) Z12: A2 2020 December

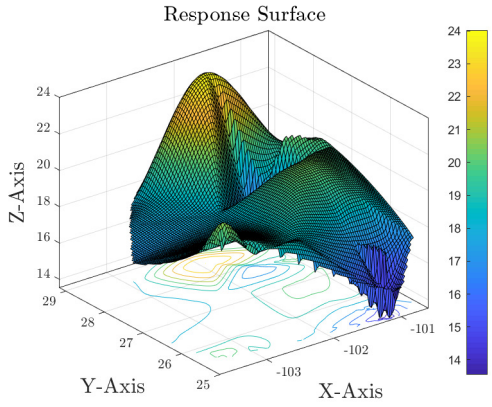
Figure D.2: Response Surfaces A2 Scenario, 2020, from July to December (Z7-Z12)



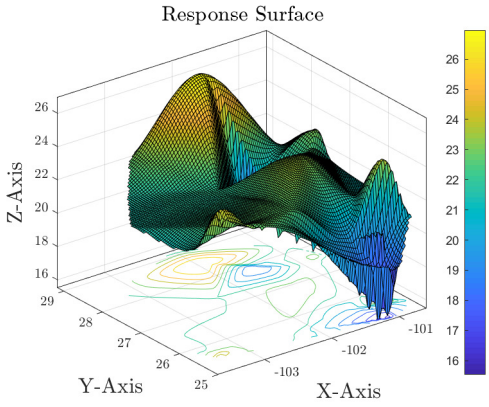
(a) Z13: A2 2050 January



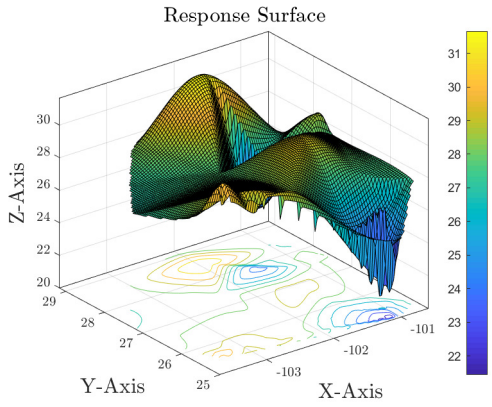
(b) Z14: A2 2050 February



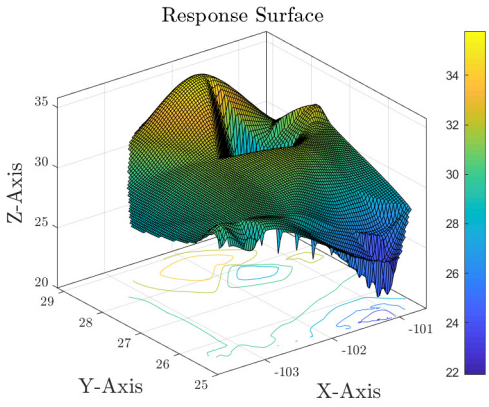
(c) Z15: A2 2050 March



(d) Z16: A2 2050 April

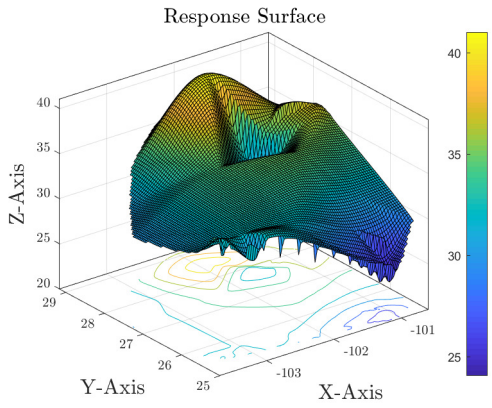


(e) Z17: A2 2050 May

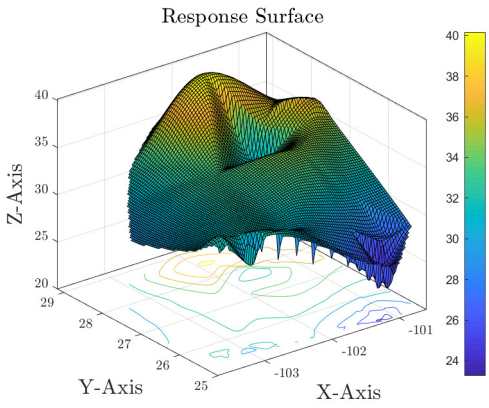


(f) Z18: A2 2050 June

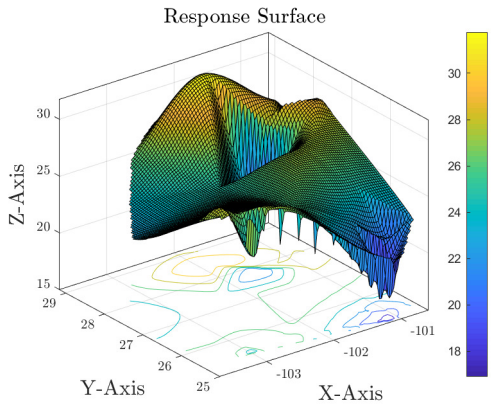
Figure D.3: Response Surfaces A2 Scenario, 2050, from January to June (Z13-Z18)



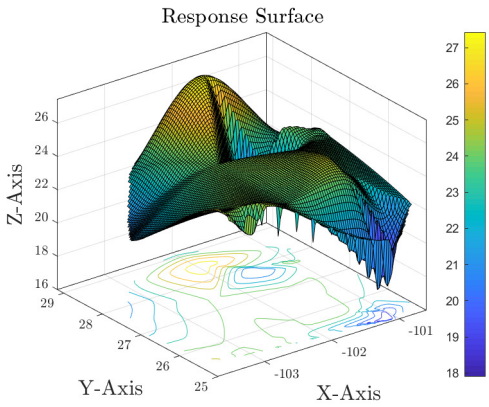
(a) Z19: A2 2050 July



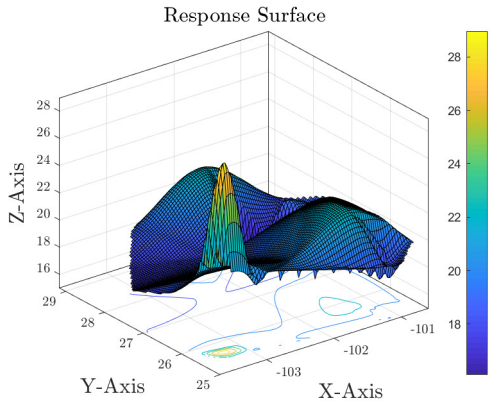
(b) Z20: A2 2050 August



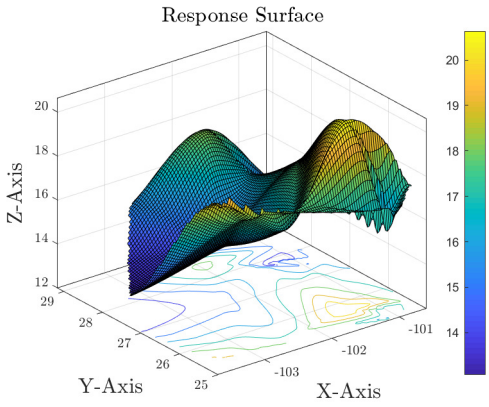
(c) Z21: A2 2050 September



(d) Z22: A2 2050 October

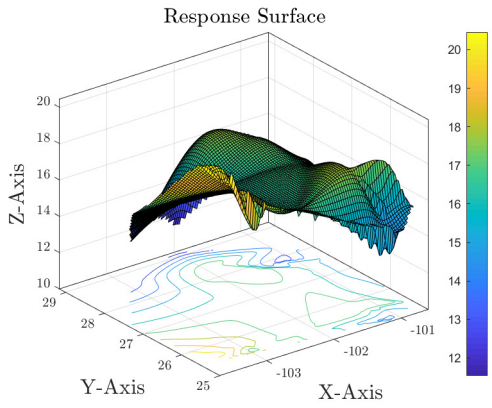


(e) Z23: A2 2050 November

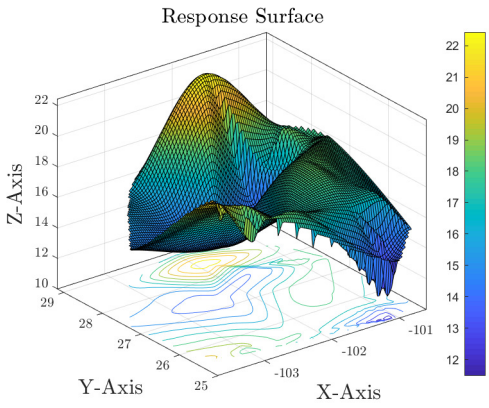


(f) Z24: A2 2050 December

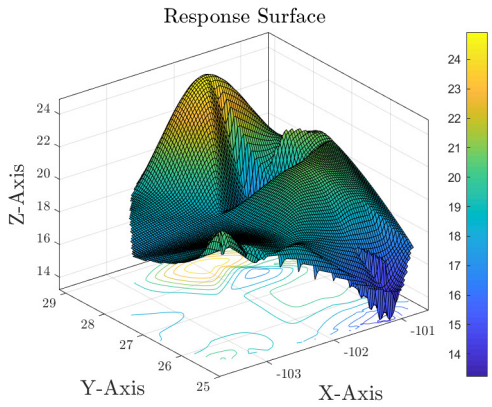
Figure D.4: Response Surfaces A2 Scenario, 2050, from July to December (Z19-Z24)



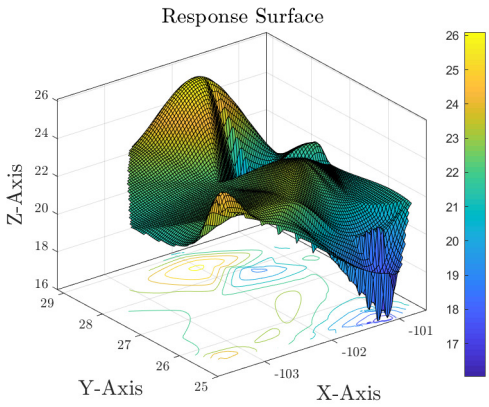
(a) Z25: A2 2080 January



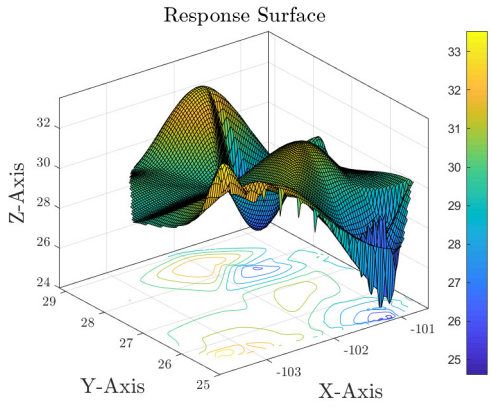
(b) Z26: A2 2080 February



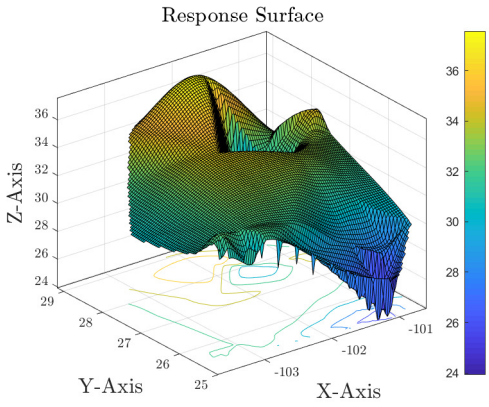
(c) Z27: A2 2080 March



(d) Z28: A2 2080 April

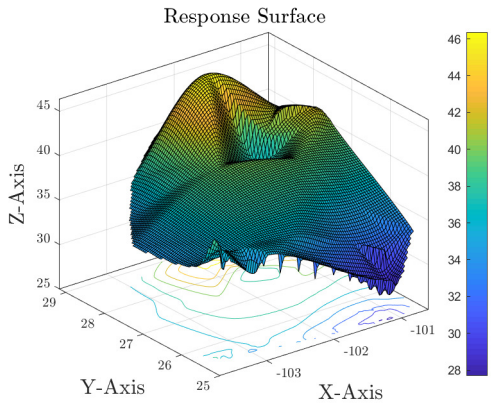


(e) Z29: A2 2080 May

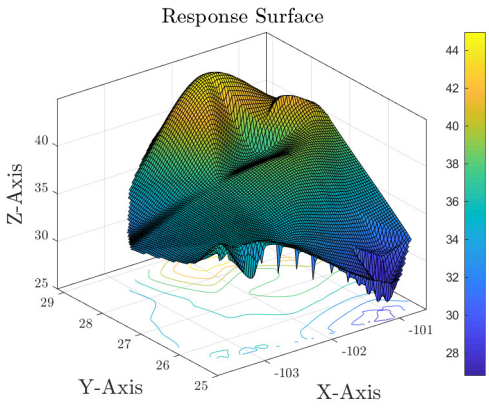


(f) Z30: A2 2080 June

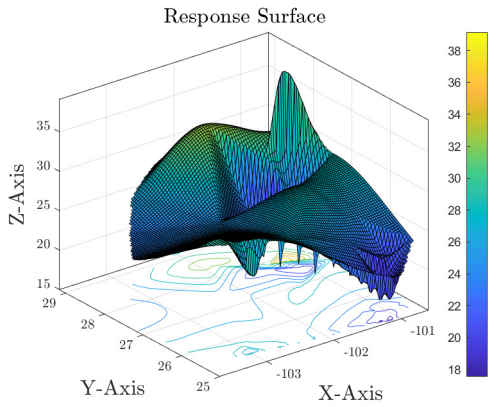
Figure D.5: Response Surfaces A2 Scenario, 2080, from January to June (Z25-Z30)



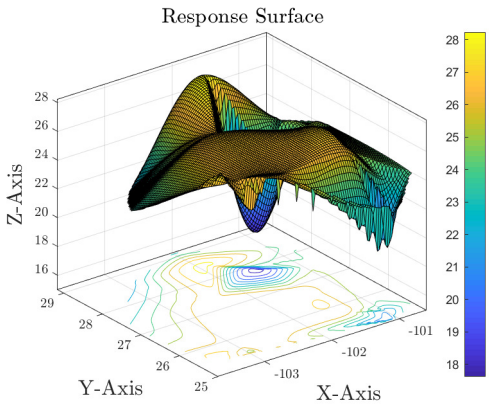
(a) Z31: A2 2080 July



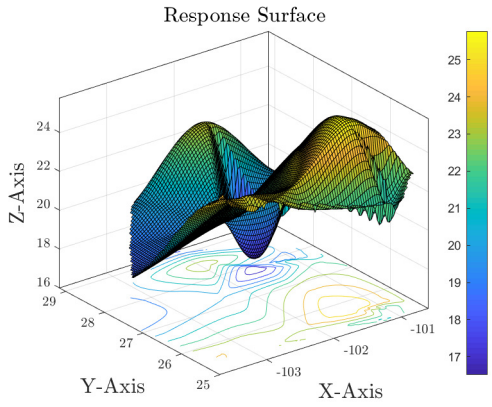
(b) Z32: A2 2080 August



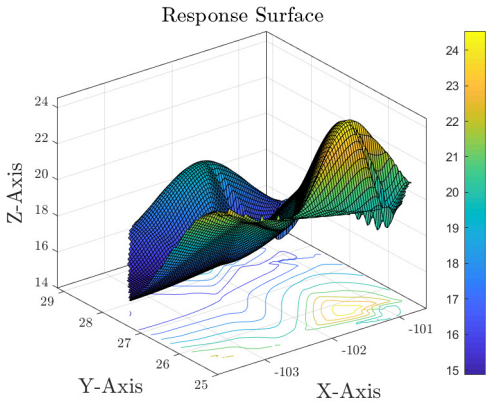
(c) Z33: A2 2080 September



(d) Z34: A2 2080 October

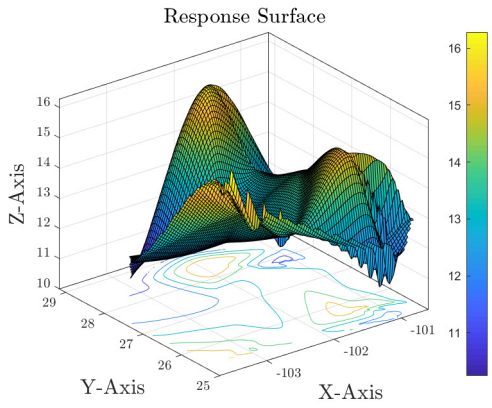


(e) Z35: A2 2080 November

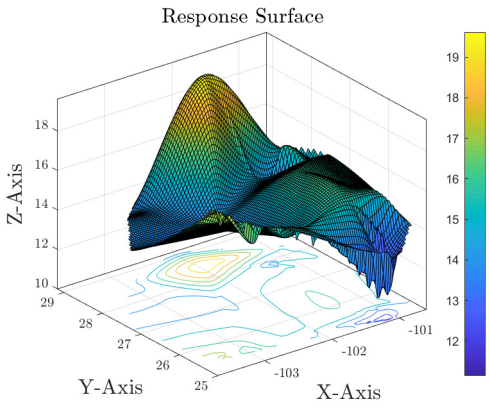


(f) Z36: A2 2080 December

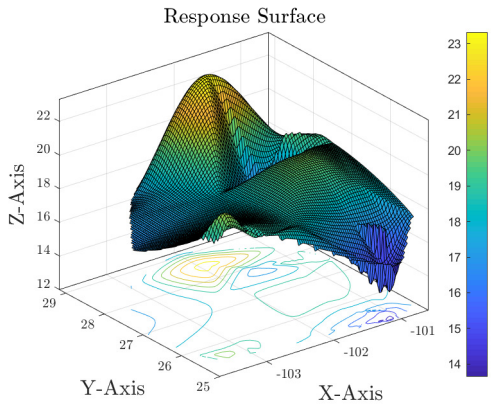
Figure D.6: Response Surfaces A2 Scenario, 2080, from July to December (Z31-Z36)



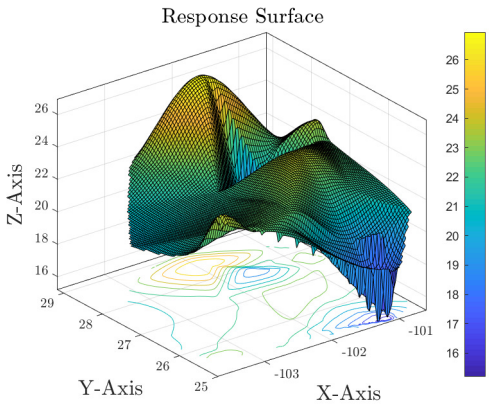
(a) Z37: B2 2020 January



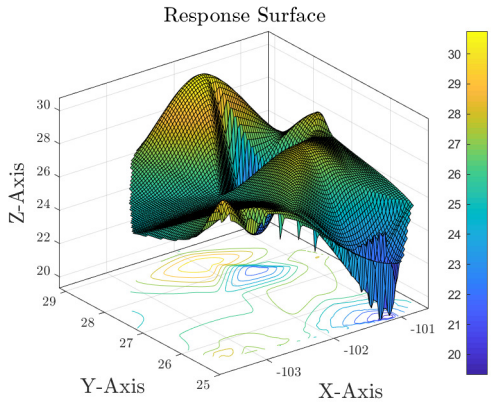
(b) Z38: B2 2020 February



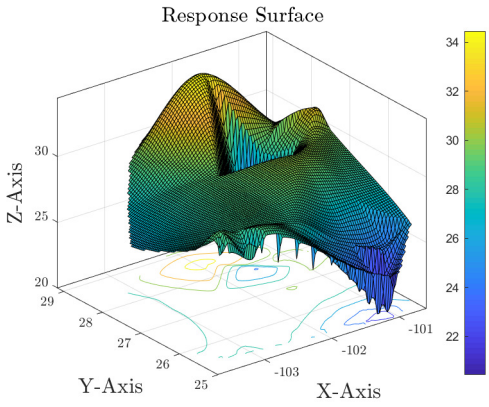
(c) Z39: B2 2020 March



(d) Z40: B2 2020 April

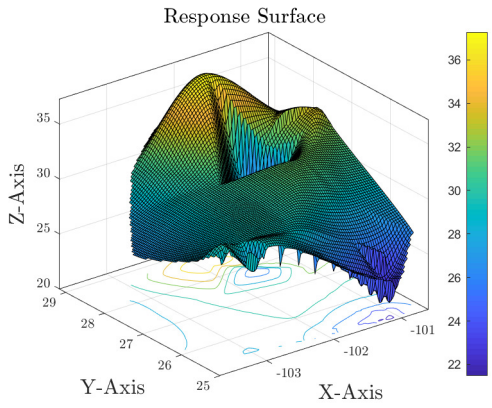


(e) Z41: B2 2020 May

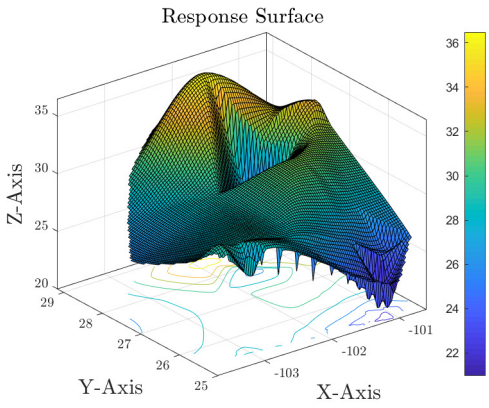


(f) Z42: B2 2020 June

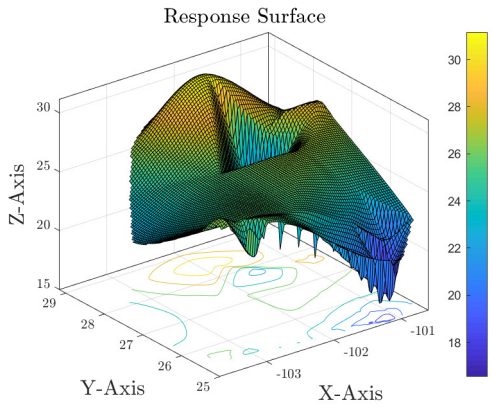
Figure D.7: Response Surfaces B2 Scenario, 2020, from January to June (Z37-Z42)



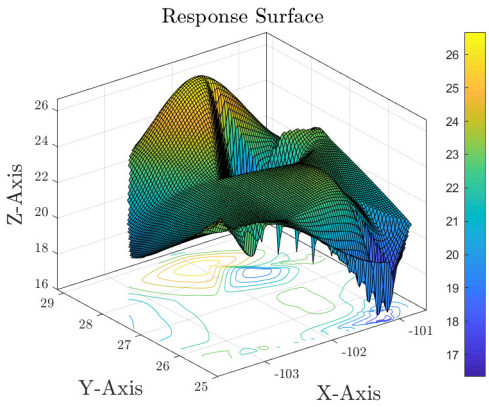
(a) Z43: B2 2020 July



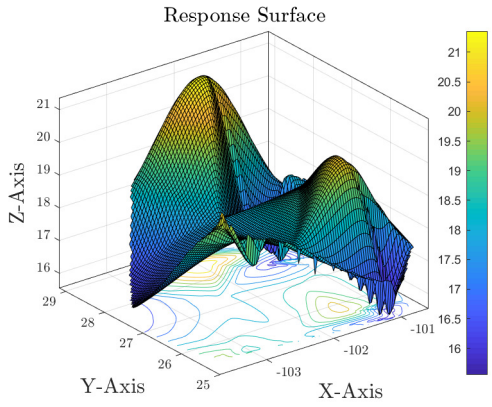
(b) Z44: B2 2020 August



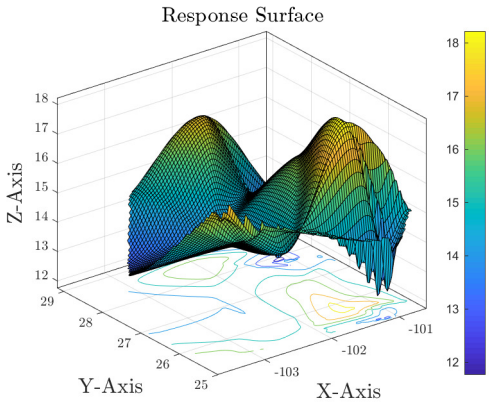
(c) Z45: B2 2020 September



(d) Z46: B2 2020 October

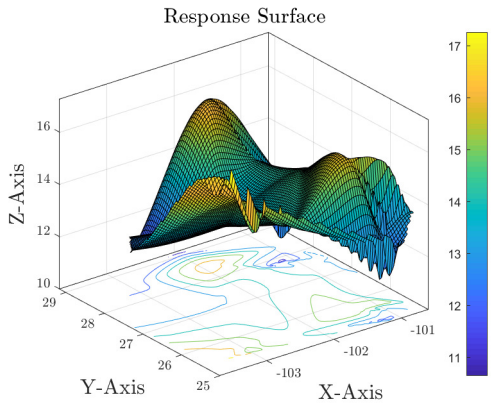


(e) Z47: B2 2020 November

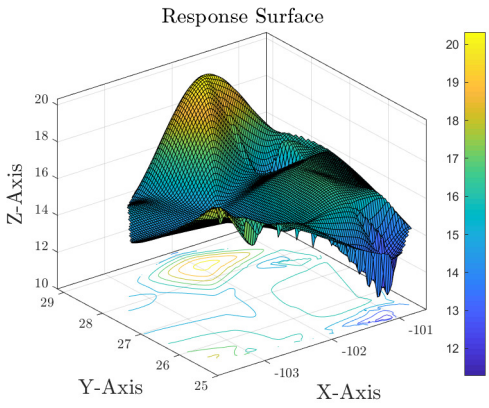


(f) Z48: B2 2020 December

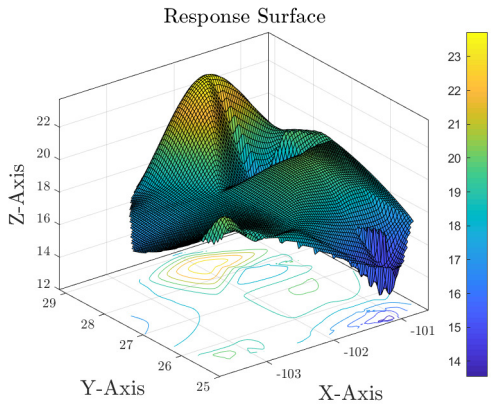
Figure D.8: Response Surfaces B2 Scenario, 2020, from July to December (Z43-Z48)



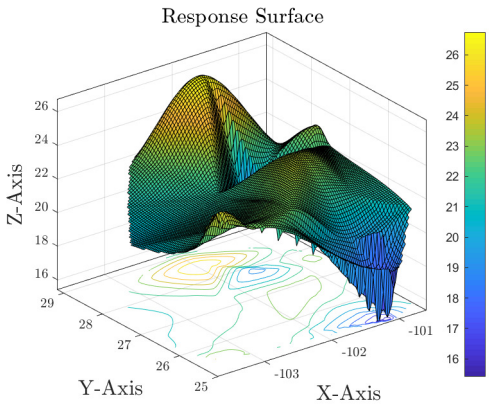
(a) Z49: B2 2050 January



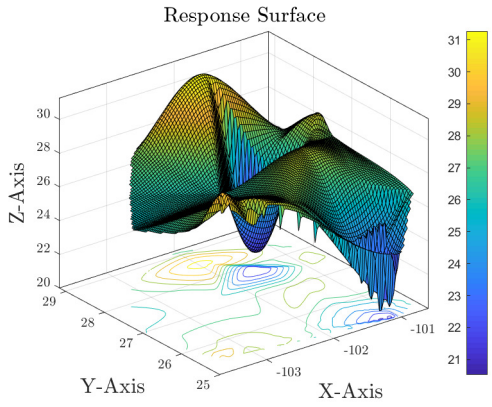
(b) Z50: B2 2050 February



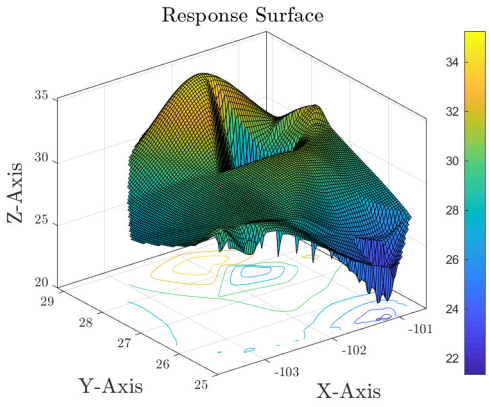
(c) Z51: B2 2050 March



(d) Z52: B2 2050 April

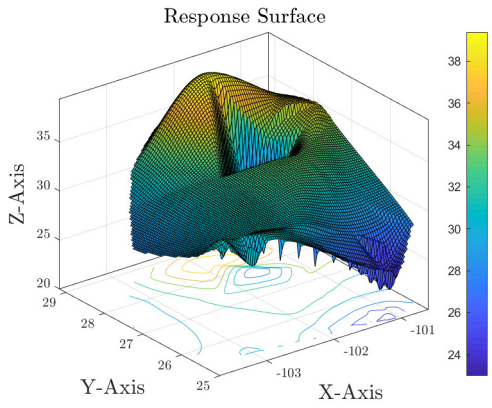


(e) Z53: B2 2050 May

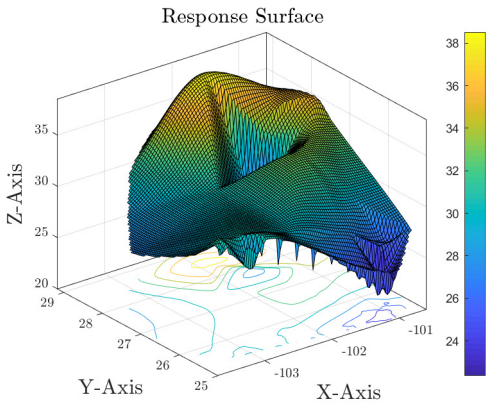


(f) Z54: B2 2050 June

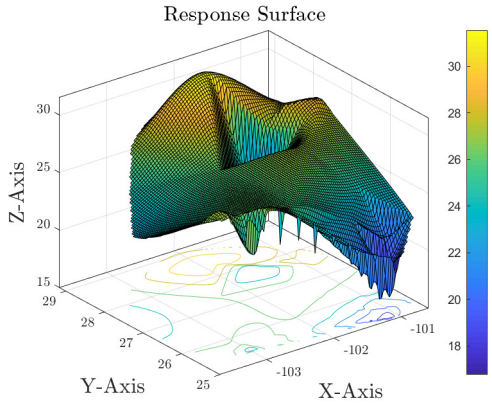
Figure D.9: Response Surfaces B2 Scenario, 2050, from January to June (Z49-Z54)



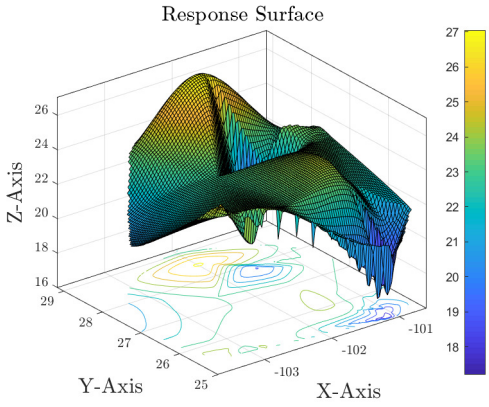
(a) Z55: B2 2050 July



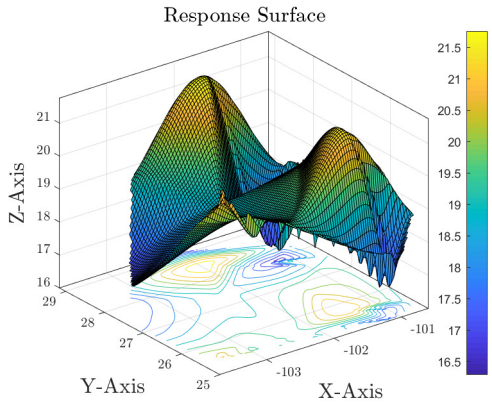
(b) Z56: B2 2050 August



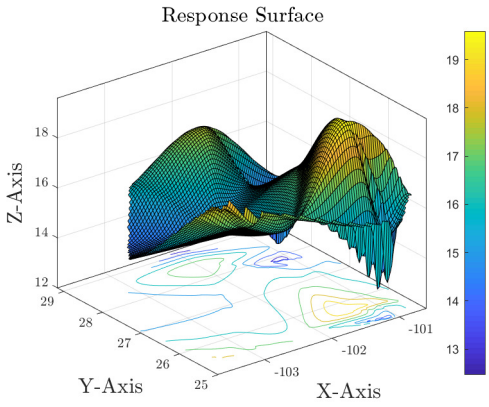
(c) Z57: B2 2050 September



(d) Z58: B2 2050 October

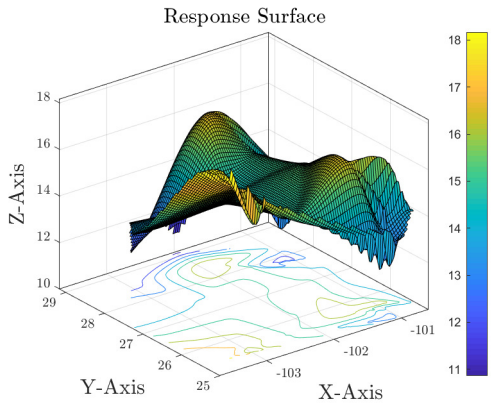


(e) Z59: B2 2050 November

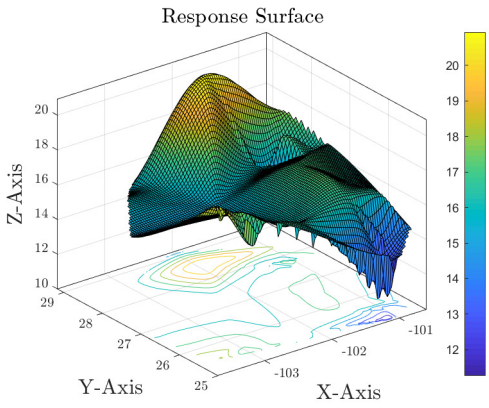


(f) Z60: B2 2050 December

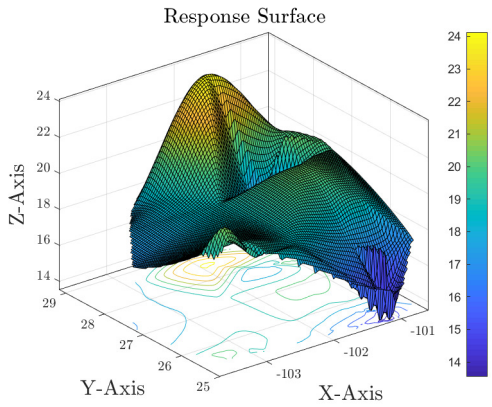
Figure D.10: Response Surfaces B2 Scenario, 2050, from July to December (Z55-Z60)



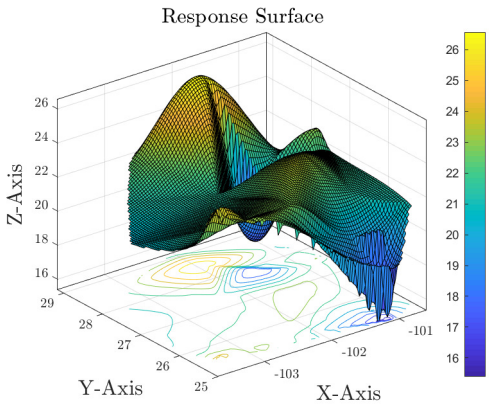
(a) Z61: B2 2080 January



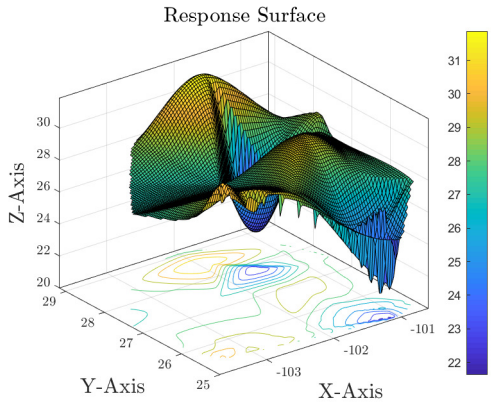
(b) Z62: B2 2080 February



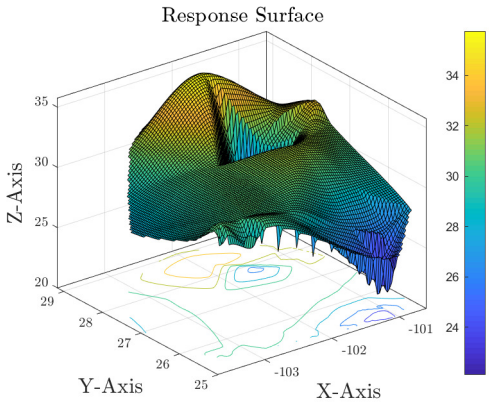
(c) Z63: B2 2080 March



(d) Z64: B2 2080 April

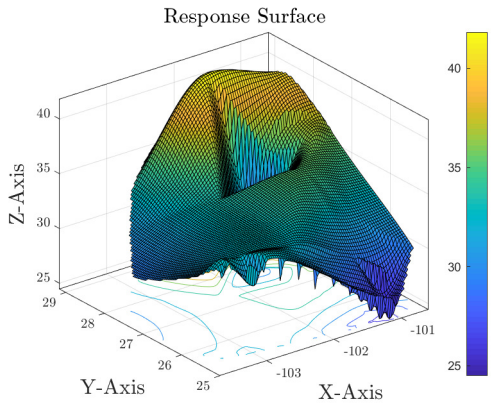


(e) Z65: B2 2080 May

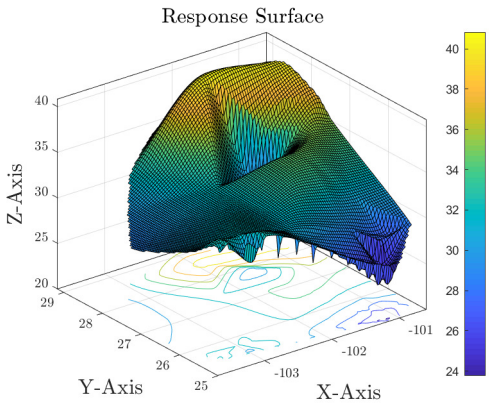


(f) Z66: B2 2080 June

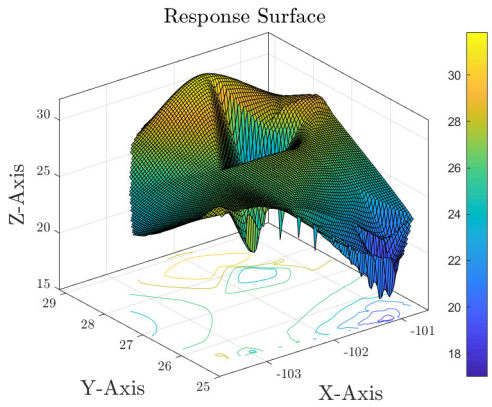
Figure D.11: Response Surfaces B2 Scenario, 2080, from January to June (Z61-Z66)



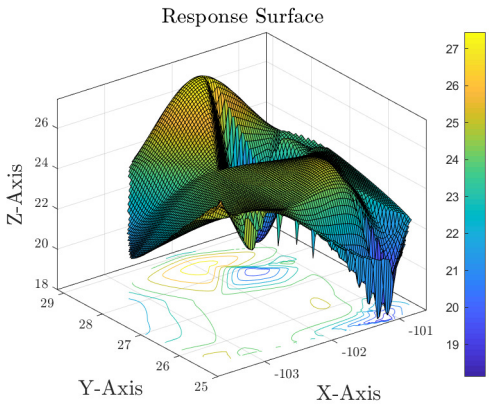
(a) Z67: B2 2080 July



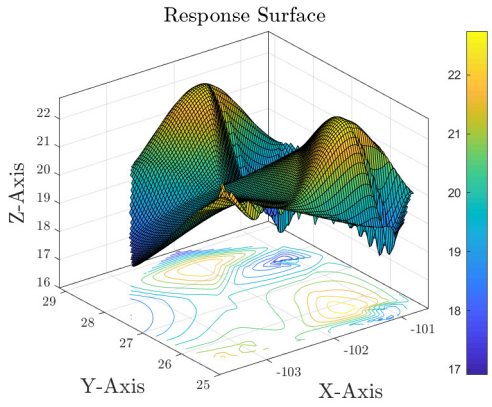
(b) Z68: B2 2080 August



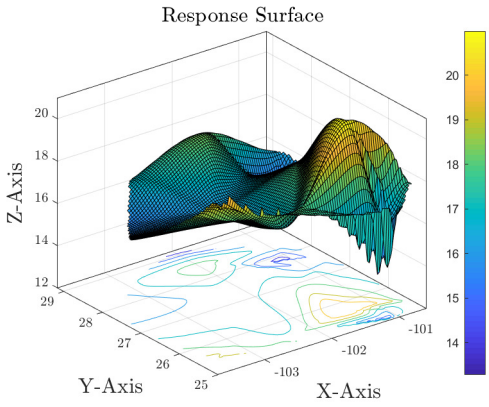
(c) Z69: B2 2080 September



(d) Z70: B2 2080 October



(e) Z71: B2 2080 November



(f) Z72: B2 2080 December

Figure D.12: Response Surfaces B2 Scenario, 2080, from July to December (Z67-Z72)

Appendix E

Fitting of Polynomials of Least Squares

Algorithm DGG3, see Section 5.3 starting in p. 126, requires adjusting polynomials using the least squares technique, and to facilitate its explanation the data was adjusted to obtain parabola equations. The following code makes this adjustment.

E.1 Code *parabol.m*, Least Squares

```
function parabol (x,y,tit)
%
%        parabol (x,y,tit)
% ------------------------------------------------------------
% parabol   Given points (x,y) in the form of two vectors: x y,
%           are graphed on the Cartesian plane.
% ------------------------------------------------------------
%
% Datos:
% x       abscissae vector    vectors of
% y       ordinates vector    the same order.
% tit     graph title         between apostrophes.
%
%

warning off
```

```
17  set(groot,'defaultAxesTickLabelInterpreter','latex'); % ticks in
     latex
18  clc
19  if nargin == 0
20     x = 1:5;
21     y = [2 3 5 8 17];
22     tit = ' ';
23     xlim([-1 6])
24     ylim([-2 19])
25  end
26  x = x(:);
27  y = y(:);
28  f = polyfit(x,y,2);
29  t = linspace(0.5,5.1,1000);
30  ft = polyval(f,t);
31
32  disp(' ')
33  disp('     (x   ,   y)')
34  disp(' ')
35  disp([x y]);
36  u = x;
37  v = y;
38  n = length(x);
39  disp('   Press Enter to see the Scatter Diagram...')
40  disp(' ')
41  pause;
42
43  % No Axis
44  minx = min(u);
45  maxx = max(u);
46  miny = min(v);
47  maxy = max(v);
48  dx = (maxx-minx)/15;
49  dy = (maxy-miny)/15;
50  izq = minx-dx;
51  der = maxx+dx;
52  aba = miny-dy;
53  arr = maxy+dy;
54
```

```
clf
plot([izq der],[aba arr],'w.')
hold on
plot(u,v,'g*',u,v,'ro')
grid on
title(tit)
xlabel('x')
ylabel('y')
shg
pause

grid off
pause
grid on
pause

% With Axis
minx = min(u);
minx = min(minx,0);
maxx = max(u);
maxx = max(maxx,0);
dx = (maxx-minx)/15;
miny = min(v);
miny = min(miny,0);
maxy = max(v);
maxy = max(maxy,0);
dy = (maxy-miny)/15;
if dx > dy
   dd = dx;
else
   dd = dy;
end
izq = minx-dd;
der = maxx+dd;
aba = miny-dd;
arr = maxy+dd;
iz = izq+dd/2;
de = der-dd/2;
ab = aba+dd/2;
```

```
  ar = arr-dd/2;

  clf
%  plot([left right],[aba arr],'w.')
%  hold on
  plot(u,v,'g*',u,v,'ro')
  hold on
  plot([iz de],[0 0],'b-')
  plot(de,0,'b>')
  plot([0 0],[ab ar],'b-')
  plot(0,ar,'b^')
  plot(t,ft)
  grid on
  title(tit)
  xlabel(' ')
  ylabel(' ')
  shg
  pause

  %grid off
```

Appendix F

Temperature and Relative Humidity Estimates for Horizons in Saltillo from Algorithm DGG3

For the three horizons of Saltillo: near, medium, far, with minimum, average and maximum temperatures, in each of them, temperature and relative humidity pairs are estimated.

The total size of the results ascends to $157,680$ real values: 8760 hours $\times$ 3 horizons $\times$ 3 temperature types $\times$ 2 columns (one of temperature, and one of relative humidity).

The obtained columns are ready to be entered in the horizons weather files for Saltillo.

The following code performs the calculations mentioned above.

F.1 Code *SaltilloHorizontes.m*

```
function [C1,C2,C3,M1,M2,M3,L1,L2,L3] = SaltilloHorizontes
%
%        [C1,C2,C3,M1,M2,M3,L1,L2,L3] = SaltilloHorizontes;
% ------------------------------------------------------------
% For the three horizons of Saltillo: near, medium and far,
% with minimum, average and maximum temperatures, in each of
```

```
% them, temperature and relative humidity pairs are estimated.
%
% For each horizon and temperature, pairs are estimated for
% each horizon hour.
%
% Total size of the results: 157 680 real values.
% 8760 hours * 3 horizons * 3 locations
% * 2 columns of temperature and HR
% ------------------------------------------------------------
%
% Data:
% IMPORTANT NOTE
%  To use this program the following must be available:
%  Tc.mat,  Tm.mat,  Tl.mat monthly data of horizon temperatures:
%                           minimum, average and maximum.
%  SaltilloWD.mat           data with historical information.
%                           Previously this information had Excel
%                           and .epw EnergyPlus formats.
%
% Results:
%  C1, C2, C3  hourly pairs of temperature and relative humidity
%              in the near horizon.
%  M1, M2, M3  hourly pairs of temperature and relative humidity
%              in the medium horizon.
%  L1, L2, L3  hourly pairs of temperature and relative humidity
%              in the far horizon.
%
%              Subscript 1, 2 and 3, are minimum, average, and
%              maximum temperatures correspondingly.
%
% At the end, results must be backed up in .mat files:
%
% Near Horizon, minimum, average and maximum projections
% >> save CerMinS.mat C1; save CerMedS.mat C2; save CerMaxS.mat C3
 ;
%
% Medium Horizon, minimum, average and maximum projections
% >> save MedMinS.mat M1; save MedMedS.mat M2; save MedMaxS.mat M3
 ;
```

```
%
% Far Horizon, minimum, average and maximum projections
% >> save LejMinS.mat L1; save LejMedS.mat L2; save LejMaxS.mat L3
 ;
%
% 1) Apply this program
%       [C1 C2 C3,M1 M2 M3,L1,L2 L3] = SaltilloHorizontes;
% 2) At the end, users can save generated .mat files to preserve
 the
%       results.
%
% Routines used               THR, HR_T, TempHorizontes, HRh.
%
% 6 January 2020.
%

warning off
set(groot,'defaultAxesTickLabelInterpreter','latex'); % ticks in
 latex
clc
format
[T,HR,hrMes] = THR; % historic temperatures T and relative
                    % humidities HR

% cuadratic ecuations HR f(T) to be applied each month
HRT = HR_T (T,HR,hrMes);
format shortg
disp(HRT)
disp('  Monthly relative humidity equations, as a function of')
disp('  temperature, obtained from historical records.')
pause

% equations for the three times of each horizon
[TC,TM,TL] = TempHorizontes;
T = [TC TM TL];

[C1,C2,C3,M1,M2,M3,L1,L2,L3] = HRh (HRT,TC,TM,TL,hrMes);

disp ('  At the end, results must be backed up in .mat files:')
```

```
disp(' ')
disp(' Near Horizon, minimum, average and maximum projections')
t = '  >> save CerMinS.mat C1;    save CerMedS.mat C2;    ';
disp([t  'save CerMaxS.mat C3;'])
disp(' ')
disp(' Medium Horizon, minimum, average and maximum projections')
t = '  >> save MedMinS.mat M1;    save MedMedS.mat M2;    ';
disp([t  'save MedMaxS.mat M3;'])
disp(' ')
disp(' Far Horizon, minimum, average and maximum projections')
t = '  >> save LejMinS.mat L1;    save LejMedS.mat L2;    ';
disp([t  'save LejMaxS.mat L3;'])
disp(' ')
pause
```

F.1.1 Hourly Temperatures and Relative Humidity for Saltillo

The programme calculates the relative humidity for each hour in Saltillo, it produces hourly temperature and relative humidity pairs for the horizons. This code is a subroutine required by the *SaltilloHorizontes* code. The required data and the results obtained are shown below.

Data:

HRT	relative humidity formulas as a function of temperature
TC	hourly temperatures in the near horizon
TM	hourly temperatures in the medium horizon
TL	hourly temperatures in the far horizon
$hrMes$	interval in hours of each month

Results:

C_1,	C_2,	C_3,	hourly pairs of temperature and relative humidity in the near horizon
M_1,	M_2,	M_3	hourly pairs of temperature and relative humidity in the medium horizon
L_1,	L_2,	L_3	hourly pairs of temperature and relative humidity in the far horizon

Subscript 1, 2 and 3, are minimum, average and maximum temperatures correspondingly.

Code *HRh.m* for Saltillo

Table F.1: Hourly Temperatures and Relative Humidity

Data

i	j	F				
1	1 : 744	−0.00019387	0.010757	−0.13231	−2.1406	87.781
2	745 : 1416	−0.00052104	0.032122	−0.61408	1.0502	96.437
3	1417 : 2160	0.00046794	−0.029453	0.49664	−2.1692	58.161
4	2161 : 2880	−0.00047624	0.041999	−1.31	14.776	14.807
5	2881 : 3624	−0.00026592	0.030703	−1.2587	19.164	−25.388
6	3625 : 4344	−0.0018315	0.17065	−5.7547	79.645	−297.5
7	4345 : 5088	0.00013565	−0.010439	0.31009	−6.9737	145.73
8	5089 : 5832	−0.0021563	0.20411	−6.9642	98.53	−404.16
9	5833 : 6552	−0.00082221	0.090123	−3.4534	52.347	−178.3
10	6553 : 7296	$7.8535e-05$	0.0080059	−0.64685	10.29	38.272
11	7297 : 8016	−0.0006784	0.04919	−1.2639	11.205	42.723
12	8017 : 8760	$-1.4085e-05$	0.0053194	−0.16448	−0.98689	86.178
Temperatures:		$TC\ (8760 \times 3)$,		$TM\ (8760 \times 3)$,		$TL\ (8760 \times 3)$

Relative Humidity Calculation

for $i = 1$ to 12

$$HC_j = F_i\,(TC_j)$$
$$HM_j = F_i\,(TM_j)$$
$$HL_j = F_i\,(TL_j)$$

end

Obtained Temperatures and Relative Humidities

$$k = 1,\ 2,\ 3 \begin{cases} C_k = [TC_k \quad HC_k] \\ M_k = [TM_k \quad HM_k] \\ L_k = [TL_k \quad HL_k] \end{cases}$$

```
function [C1,C2,C3,M1,M2,M3,L1,L2,L3] = HRh (HRT,TC,TM,TL,hrMes)
%
%        [C1,C2,C3,M1,M2,M3,L1,L2,L3] = HRh (HRT,TC,TM,TL,hrMes)
% ------------------------------------------------------------------
% Calculate the relative humidity, every hour, in Saltillo,
% Coahuila.
% ------------------------------------------------------------------
%
% Data:
%  HRT  relative humidity formulas as a function of temperature.
%  TC   hourly temperatures in the near horizon.
%  TM   hourly temperatures in the medium horizon.
%  TL   hourly temperatures in the far horizon.
%  hrMes interval in hours of each month.
%
% Results:
%  C1, C2, C3  hourly pairs of temperature and relative humidity
%              in the near horizon.
%  M1, M2, M3  hourly pairs of temperature and relative humidity
%              in the medium horizon.
%  L1, L2, L3  hourly pairs of temperature and relative humidity
%              in the far horizon.
%
%              Subscript 1, 2 and 3, are minimum, average, and
%              maximum temperatures correspondingly.
%
% At the end, results must be backed up in .mat files:
%
% Near Horizon, minimum, average and maximum projections
% >> save CerMinS.mat C1; save CerMedS.mat C2; save CerMaxS.mat C3
 ;
%
% Medium Horizon, minimum, average and maximum projections
% >> save MedMinS.mat M1; save MedMedS.mat M2; save MedMaxS.mat M3
 ;
%
% Far Horizon, minimum, average and maximum projections
% >> save LejMinS.mat L1; save LejMedS.mat L2; save LejMaxS.mat L3
 ;
```

```
%
% 23 December 2019.
%

warning off
set(groot,'defaultAxesTickLabelInterpreter','latex'); % ticks in
 latex
disp(' ')
HRC = [];
HRM = [];
HRL = [];
lt = '        Interval in hours. Equations to calculate the ';
disp([lt  'relative humidity of the horizons'])
lt = '        ___________________________________________________';
disp([lt '_____________________________'])
disp(' ')
for i = 1:12
   a = hrMes(i,1);
   b = hrMes(i,2);
   f = HRT(i,:);
   disp([a b f])
   pause
   tc = TC(a:b,:);
   tm = TM(a:b,:);
   tl = TL(a:b,:);
   hrc = polyval(f,tc);
   hrm = polyval(f,tm);
   hrl = polyval(f,tl);
   HRC = [HRC;hrc];
   HRM = [HRM;hrm];
   HRL = [HRL;hrl];
end
k = find(HRC < 0);
if k
   HRC(k) = 0;
end
k = find(HRC > 100);
if k
   HRC(k) = 100;
```

```
  end
  k = find(HRM < 0);
  if k
     HRM(k) = 0;
  end
  k = find(HRM > 100);
  if k
     HRM(k) = 100;
  end
  k = find(HRL < 0);
  if k
     HRL(k) = 0;
  end
  k = find(HRL > 100);
  if k
     HRL(k) = 100;
  end

C1=[TC(:,1) HRC(:,1)];C2=[TC(:,2) HRC(:,2)];C3=[TC(:,3) HRC(:,3)];
M1=[TM(:,1) HRM(:,1)];M2=[TM(:,2) HRM(:,2)];M3=[TM(:,3) HRM(:,3)];
L1=[TL(:,1) HRL(:,1)];L2=[TL(:,2) HRL(:,2)];L3=[TL(:,3) HRL(:,3)];
T = [TC TM TL];
H = [HRC HRM HRL];

  disp(' ')
  lt = ' ****With the determination of the relative humidities ';
  disp([lt  'for each hour, the temperatures'])
  disp(' ')
  lt = '        and relative humidities of the stations ';
  disp([lt  'are known for the three temperatures. OK'])
  lt = '        ____________________________________________________';
  disp([lt '_____________________________'])
  pause

  disp(' ')
  disp('        Subtraction Verifications of Null Results:')
  disp(' ')
  pause
  TC - [C1(:,1) C2(:,1) C3(:,1)]
```

```
114 pause
115 clc
116 TM = [M1(:,1) M2(:,1) M3(:,1)]
117 pause
118 clc
119 TL = [L1(:,1) L2(:,1) L3(:,1)]
120 pause
121 clc
122 HRC = [C1(:,2) C2(:,2) C3(:,2)]
123 pause
124 clc
125 HRM = [M1(:,2) M2(:,2) M3(:,2)]
126 pause
127 clc
128 HRL = [L1(:,2) L2(:,2) L3(:,2)]
129 pause
130 clc
131 disp(' ')
132 disp('  Dimensions of temperatures and relative humidities:')
133 disp([size(T) size(H)])
134 disp(' ')
135 pause
136 disp ('  At the end, results must be backed up in .mat files:')
137 disp(' ')
138 disp(' Near Horizon, minimum, average and maximum projections')
139 t = '  >> save CerMinS.mat C1;    save CerMedS.mat C2;    ';
140 disp([t  'save CerMaxS.mat C3;'])
141 disp(' ')
142 disp(' Medium Horizon, minimum, average and maximum projections')
143 t = '  >> save MedMinS.mat M1;    save MedMedS.mat M2;    ';
144 disp([t  'save MedMaxS.mat M3;'])
145 disp(' ')
146 disp(' Far Horizon, minimum, average and maximum projections')
147 t = '  >> save LejMinS.mat L1;    save LejMedS.mat L2;    ';
148 disp([t  'save LejMaxS.mat L3;'])
149 disp(' ')
150 pause
```

F.1.2 Other Subroutines

The code *SaltilloHorizontes* requires the routines of the appendices I, J, and K.

F.1.3 Summarized Results

The values of the results generated with the programme appear summarized in the following tables.

Table F.2: Temperatures and relative humidities for the near horizon, Saltillo

Month	Hour	Minimum		Average		Maximum	
i	j	$(T,$	$H)$	$(T,$	$H)$	$(T,$	$H)$
1	1	6.3759	71.222	11.439	58.765	20.599	46.664
	2	6.3706	71.236	11.438	58.766	20.594	46.667
	⋮	⋮	⋮	⋮	⋮	⋮	⋮
	744	5.1826	74.491	12.589	56.457	20.308	46.864
2	745	5.184	89.477	12.592	63.327	20.311	44.915
	746	5.1854	89.473	12.596	63.316	20.314	44.91
	⋮	⋮	⋮	⋮	⋮	⋮	⋮
	1416	7.2136	82.706	15.331	55.17	23.401	40.123
3	1417	7.2178	58.571	15.335	61.348	23.406	42.234
	1418	7.222	58.576	15.34	61.344	23.412	42.215
	⋮	⋮	⋮	⋮	⋮	⋮	⋮
	2160	10.767	61.904	18.959	55.291	27.917	28.062
4	2161	10.772	68.046	18.963	48.735	27.923	30.848
	2162	10.777	68.04	18.968	48.723	27.929	30.839
	⋮	⋮	⋮	⋮	⋮	⋮	⋮
	2880	14.094	61.626	22.143	41.166	31.757	23.624
5	2881	14.098	70.155	22.147	51.24	31.762	26.726
	2882	14.102	70.151	22.151	51.228	31.766	26.717

Continues on next page ...

Month	Hour	Minimum		Average		Maximum	
i	j	$(T,$	$H)$	$(T,$	$H)$	$(T,$	$H)$
	⋮	⋮	⋮	⋮	⋮	⋮	⋮
	3624	16.525	66.316	24.454	44.482	34.279	22.122
6	3625	16.527	80.65	24.456	49.357	34.281	15.371
	3626	16.53	80.641	24.458	49.351	34.283	15.353
	⋮	⋮	⋮	⋮	⋮	⋮	⋮
	4344	17.537	76.554	25.415	46.846	35.071	7.9776
7	4345	17.537	75.324	25.415	54.011	35.071	37.469
	4346	17.538	75.322	25.415	54.01	35.071	37.469
	⋮	⋮	⋮	⋮	⋮	⋮	⋮
	5088	17.191	76.294	25.006	55.055	34.355	37.817
8	5089	17.19	80.172	25.004	53.358	34.353	33.722
	5090	17.189	80.177	25.003	53.361	34.351	33.735
	⋮	⋮	⋮	⋮	⋮	⋮	⋮
	5832	15.682	85.063	23.303	57.102	32.465	43.254
9	5833	15.679	91.162	23.3	64.207	32.462	51.695
	5834	15.676	91.168	23.297	64.217	32.459	51.694
	⋮	⋮	⋮	⋮	⋮	⋮	⋮
	6552	13.464	93.406	20.712	73.872	29.887	51.376
10	6553	13.46	81.683	20.708	59.508	29.883	44.403
	6554	13.457	81.69	20.704	59.522	29.879	44.397
	⋮	⋮	⋮	⋮	⋮	⋮	⋮
	7296	10.744	85.134	17.48	70.587	26.614	44.281
11	7297	10.741	69.187	17.475	51.797	26.61	32.63
	7298	10.737	69.195	17.471	51.808	26.605	32.643
	⋮	⋮	⋮	⋮	⋮	⋮	⋮
	8016	7.9032	73.97	14.293	59.99	22.605	41.222
12	8017	7.8991	70.686	14.289	53.426	22.598	37.595

Continues on next page ...

Month	Hour	Minimum		Average		Maximum	
i	j	$(T,$	$H)$	$(T,$	$H)$	$(T,$	$H)$
	8018	7.895	70.697	14.285	53.437	22.592	37.601
	⋮	⋮	⋮	⋮	⋮	⋮	⋮
	8760	4.6951	78.462	11.471	61	16.686	47.537

Table F.3: Temperatures and relative humidities for the medium horizon, Saltillo

Month	Hour	Minimum		Average		Maximum	
i	j	T	H	T	H	T	H
1	1	7.0986	69.274	12.944	55.793	21.673	45.976
	2	7.0941	69.287	12.942	55.796	21.67	45.978
	⋮	⋮	⋮	⋮	⋮	⋮	⋮
	744	6.2167	71.655	13.544	54.721	22.278	45.612
2	745	6.2183	86.168	13.547	60.28	22.282	41.877
	746	6.2198	86.162	13.55	60.272	22.285	41.871
	⋮	⋮	⋮	⋮	⋮	⋮	⋮
	1416	8.2484	78.935	16.096	53.225	25.504	36.222
⋮	⋮	⋮	⋮	⋮	⋮	⋮	⋮
12	8017	8.7768	68.359	15.085	51.392	23.5	36.891
	8018	8.7728	68.369	15.082	51.401	23.494	36.895
	⋮	⋮	⋮	⋮	⋮	⋮	⋮
	8760	5.7264	76.117	13.068	56.652	18.651	43.364

Table F.4: Temperatures and relative humidities for the far horizon, Saltillo

Month	Hour	Minimum		Average		Maximum	
i	j	T	H	T	H	T	H
1	1	7.5755	68.01	11.416	58.813	22.055	45.745
	2	7.5713	68.021	11.419	58.807	22.053	45.746
	⋮	⋮	⋮	⋮	⋮	⋮	⋮
	744	6.8822	69.854	14.145	53.714	22.769	45.323
2	745	6.8839	83.875	14.149	58.467	22.772	41.121
	746	6.8856	83.869	14.153	58.455	22.776	41.116
	⋮	⋮	⋮	⋮	⋮	⋮	⋮
	1416	9.0095	76.112	17.199	50.683	26.063	34.949
⋮	⋮	⋮	⋮	⋮	⋮	⋮	⋮
12	8017	9.5857	66.171	15.152	51.225	23.414	36.947
	8018	9.5823	66.18	15.148	51.236	23.408	36.951
	⋮	⋮	⋮	⋮	⋮	⋮	⋮
	8760	7.1161	72.707	12.905	57.09	18.774	43.126

Appendix G

Temperature and Relative Humidity Estimates for Horizons in Monclova from Algorithm DGG3

For the three horizons of Monclova: near, medium, far, with minimum, average and maximum temperatures, in each of them, temperature and relative humidity pairs are estimated.

The total size of the results ascends to $157,680$ real values: 8760 hours $\times$ 3 horizons $\times$ 3 temperature types $\times$ 2 columns (one of temperature, and one of relative humidity).

The obtained columns are ready to be entered in the horizons weather files for Monclova.

The following code performs the calculations mentioned above.

G.1 Code *MonclovaHorizontes.m*

```
function [C1,C2,C3,M1,M2,M3,L1,L2,L3] = MonclovaHorizontes
%
%        [C1,C2,C3,M1,M2,M3,L1,L2,L3] = MonclovaHorizontes;
% ------------------------------------------------------------------
% For the three horizons of Monclova: near, medium and far,
```

```
% with minimum, average and maximum temperatures, in each of
% them, temperature and relative humidity pairs are estimated.
%
% For each horizon and temperature, pairs are estimated for
% each horizon hour.
%
% Total size of the results: 157 680 real values.
% 8760 hours * 3 horizons * 3 locations
% * 2 columns of temperature and HR
% ------------------------------------------------------------
%
% Data:
% IMPORTANT NOTE
%  To use this program the following must be available:
%  Tc.mat,  Tm.mat,  Tl.mat monthly data of horizon temperatures:
%                           minimum, average and maximum.
%  MonclovaWD.mat           data with historical information.
%                           Previously this information had Excel
%                           and .epw EnergyPlus formats.
%
% Results:
%  C1, C2, C3  hourly pairs of temperature and relative humidity
%              in the near horizon.
%  M1, M2, M3  hourly pairs of temperature and relative humidity
%              in the medium horizon.
%  L1, L2, L3  hourly pairs of temperature and relative humidity
%              in the far horizon.
%
%              Subscript 1, 2 and 3, are minimum, average, and
%              maximum temperatures correspondingly.
%
% At the end, results must be backed up in .mat files:
%
% Near Horizon, minimum, average and maximum projections
% >> save CerMinM.mat C1; save CerMedM.mat C2; save CerMaxM.mat C3
 ;
%
% Medium Horizon, minimum, average and maximum projections
% >> save MedMinM.mat M1; save MedMedM.mat M2; save MedMaxM.mat M3
```

```
 ;
%
% Far Horizon, minimum, average and maximum projections
% >> save LejMinM.mat L1; save LejMedM.mat L2; save LejMaxM.mat L3
 ;
%
% 1) Apply this program
%       [C1 C2 C3,M1 M2 M3,L1,L2 L3] = MonclovaHorizontes;
% 2) At the end, users can save generated .mat files to preserve
 the
%       results.
%
% Routines used               THR, HR_T, TempHorizontes, HRh.
%
% 6 January 2020.
%

warning off
set(groot,'defaultAxesTickLabelInterpreter', 'latex'); % ticks in
 latex
clc
format

% historic temperatures T and relative humidities HR
[T,HR,hrMes] = THR;

% quartic equations HR = f(T) to be applied each month
HRT = HR_T (T,HR,hrMes);
format shortg
disp(HRT)
disp('  Monthly relative humidity equations, as a function of')
disp('  temperature, obtained from historical records.')
pause

% equations for the three times of each horizon
[TC,TM,TL] = TempHorizontes;
T = [TC TM TL];

% results
```

```
79  [C1,C2,C3,M1,M2,M3,L1,L2,L3] = HRh (HRT,TC,TM,TL,hrMes);
80
81  disp ('  At the end, results must be backed up in .mat files:')
82  disp(' ')
83  disp('  Near horizon, minimum, average and maximum projections')
84  t = '    >> save CerMinM.mat C1;     save CerMedM.mat C2;     ';
85  disp([t  'save CerMaxM.mat C3;'])
86  disp(' ')
87  disp('  Medium Horizon, minimum, average and maximum projections')
88  t = '    >> save MedMinM.mat M1;     save MedMedM.mat M2;     ';
89  disp([t  'save MedMaxM.mat M3;'])
90  disp(' ')
91  disp('  Far Horizon, minimum, average and maximum projections')
92  t = '    >> save LejMinM.mat L1;     save LejMedM.mat L2;     ';
93  disp([t  'save LejMaxM.mat L3;'])
94  disp(' ')
95  pause
```

G.1.1 Hourly Temperatures and Relative Humidity for Monclova

The programme calculates the relative humidity for each hour in Monclova, it produces hourly temperature and relative humidity pairs for the horizons. This code is a subroutine required by the *MonclovaHorizontes* code. The required data and the results obtained are shown below.

Data:

HRT	relative humidity formulas as a function of temperature
TC	hourly temperatures in the near horizon
TM	hourly temperatures in the medium horizon
TL	hourly temperatures in the far horizon
$hrMes$	interval in hours of each month

Results:

C_1,	C_2,	C_3,	hourly pairs of temperature and relative humidity in the near horizon
M_1,	M_2,	M_3	hourly pairs of temperature and relative humidity in the medium horizon
L_1,	L_2,	L_3	hourly pairs of temperature and relative humidity in the far horizon

Subscript 1, 2 and 3, are minimum, average and maximum temperatures correspondingly.

Code *HRh.m* for Monclova

```
function [C1,C2,C3,M1,M2,M3,L1,L2,L3] = HRh (HRT,TC,TM,TL,hrMes)
%
%        [C1,C2,C3,M1,M2,M3,L1,L2,L3] = HRh (HRT,TC,TM,TL,hrMes)
% ------------------------------------------------------------------
% Calculate the relative humidity, every hour, in Monclova,
% Coahuila.
% ------------------------------------------------------------------
%
% Data:
%  HRT  relative humidity formulas as a function of temperature.
%  TC   hourly temperatures in the near horizon.
%  TM   hourly temperatures in the medium horizon.
%  TL   hourly temperatures in the far horizon.
%  hrMes interval in hours of each month.
%
% Results:
%  C1, C2, C3  hourly pairs of temperature and relative humidity
%              in the near horizon.
%  M1, M2, M3  hourly pairs of temperature and relative humidity
%              in the medium horizon.
%  L1, L2, L3  hourly pairs of temperature and relative humidity
%              in the far horizon.
%
%              Subscript 1, 2 and 3, are minimum, average, and
%              maximum temperatures correspondingly.
%
% At the end, results must be backed up in .mat files:
```

```
%
% Near Horizon, minimum, average and maximum projections
% >> save CerMinS.mat C1; save CerMedS.mat C2; save CerMaxS.mat C3;
%
% Medium Horizon, minimum, average and maximum projections
% >> save MedMinS.mat M1; save MedMedS.mat M2; save MedMaxS.mat M3;
%
% Far Horizon, minimum, average and maximum projections
% >> save LejMinS.mat L1; save LejMedS.mat L2; save LejMaxS.mat L3;
%

warning off
set(groot,'defaultAxesTickLabelInterpreter','latex'); % ticks in latex
disp(' ')
HRC = [];
HRM = [];
HRL = [];
lt = '        Interval in hours. Equations to calculate the ';
disp([lt  'relative humidity of the horizons'])
lt = '        ____________________________________________________';
disp([lt '_____________________________'])
disp(' ')
for i = 1:12
   a = hrMes(i,1);
   b = hrMes(i,2);
   f = HRT(i,:);
   disp([a b f])
   pause
   tc = TC(a:b,:);
   tm = TM(a:b,:);
   tl = TL(a:b,:);
   hrc = polyval(f,tc);
   hrm = polyval(f,tm);
   hrl = polyval(f,tl);
   HRC = [HRC;hrc];
```

```
63      HRM = [HRM;hrm];
64      HRL = [HRL;hrl];
65    end
66    k = find(HRC < 0);
67    if k
68      HRC(k) = 0;
69    end
70    k = find(HRC > 100);
71    if k
72      HRC(k) = 100;
73    end
74    k = find(HRM < 0);
75    if k
76      HRM(k) = 0;
77    end
78    k = find(HRM > 100);
79    if k
80      HRM(k) = 100;
81    end
82    k = find(HRL < 0);
83    if k
84      HRL(k) = 0;
85    end
86    k = find(HRL > 100);
87    if k
88      HRL(k) = 100;
89    end
90
91  C1=[TC(:,1) HRC(:,1)];C2=[TC(:,2) HRC(:,2)];C3=[TC(:,3) HRC(:,3)];
92  M1=[TM(:,1) HRM(:,1)];M2=[TM(:,2) HRM(:,2)];M3=[TM(:,3) HRM(:,3)];
93  L1=[TL(:,1) HRL(:,1)];L2=[TL(:,2) HRL(:,2)];L3=[TL(:,3) HRL(:,3)];
94  T = [TC TM TL];
95  H = [HRC HRM HRL];
96
97    disp(' ')
98    lt = ' ****With the determination of the relative humidities ';
99    disp([lt  'for each hour, the temperatures'])
100   disp(' ')
101   lt = '         and relative humidities of the stations ';
```

```
102 disp([lt  'are known for the three temperatures. OK'])
103 lt = '        ____________________________________________________';
104 disp([lt '_____________________________'])
105 pause
106
107 disp(' ')
108 disp('        Subtraction Verifications of Null Results:')
109 disp(' ')
110 pause
111 TC - [C1(:,1) C2(:,1) C3(:,1)]
112 pause
113 clc
114 TM - [M1(:,1) M2(:,1) M3(:,1)]
115 pause
116 clc
117 TL - [L1(:,1) L2(:,1) L3(:,1)]
118 pause
119 clc
120 HRC - [C1(:,2) C2(:,2) C3(:,2)]
121 pause
122 clc
123 HRM - [M1(:,2) M2(:,2) M3(:,2)]
124 pause
125 clc
126 HRL - [L1(:,2) L2(:,2) L3(:,2)]
127 pause
128 clc
129 disp(' ')
130 disp('  Dimensions of temperatures and relative humidities:')
131 disp([size(T) size(H)])
132 disp(' ')
133 pause
134 disp ('  At the end, results must be backed up in .mat files:')
135 disp(' ')
136 disp(' Near Horizon, minimum, average and maximum projections')
137 t = '  >> save CerMinS.mat C1;    save CerMedS.mat C2;    ';
138 disp([t  'save CerMaxS.mat C3;'])
139 disp(' ')
140 disp(' Medium Horizon, minimum, average and maximum projections')
```

```
141  t = '  >> save MedMinS.mat M1;    save MedMedS.mat M2;    ';
142  disp([t  'save MedMaxS.mat M3;'])
143  disp(' ')
144  disp(' Far Horizon, minimum, average and maximum projections')
145  t = '  >> save LejMinS.mat L1;    save LejMedS.mat L2;    ';
146  disp([t  'save LejMaxS.mat L3;'])
147  disp(' ')
148  pause
```

G.1.2 Other Subroutines

The code *MonclovaHorizontes* requires the routines of the appendices I, J, and K.

G.1.3 Summarized Results

The values of the results generated with the programme appear summarized in the following tables.

Table G.1: Temperatures and relative humidities for the near horizon, Monclova

Month	Hour	Minimum		Average		Maximum	
i	j	T	H	T	H	T	H
1	1	6.3759	71.222	11.439	58.765	20.599	46.664
	2	6.3706	71.236	11.438	58.766	20.594	46.667
	⋮	⋮	⋮	⋮	⋮	⋮	⋮
	744	5.1826	74.491	12.589	56.457	20.308	46.864
2	745	5.184	89.477	12.592	63.327	20.311	44.915
	746	5.1854	89.473	12.596	63.316	20.314	44.91
	⋮	⋮	⋮	⋮	⋮	⋮	⋮
	1416	7.2136	82.706	15.331	55.17	23.401	40.123
⋮	⋮	⋮	⋮	⋮	⋮	⋮	⋮
12	8017	7.8991	70.686	14.289	53.426	22.598	37.595
	8018	7.895	70.697	14.285	53.437	22.592	37.601
	⋮	⋮	⋮	⋮	⋮	⋮	⋮
	8760	4.6951	78.462	11.471	61	16.686	47.537

Table G.2: Temperatures and relative humidities for the medium horizon, Monclova

Month	Hour	Minimum		Average		Maximum	
i	j	T	H	T	H	T	H
1	1	7.0986	69.274	12.944	55.793	21.673	45.976
	2	7.0941	69.287	12.942	55.796	21.67	45.978
	⋮	⋮	⋮	⋮	⋮	⋮	⋮
	744	6.2167	71.655	13.544	54.721	22.278	45.612
2	745	6.2183	86.168	13.547	60.28	22.282	41.877
	746	6.2198	86.162	13.55	60.272	22.285	41.871
	⋮	⋮	⋮	⋮	⋮	⋮	⋮
	1416	8.2484	78.935	16.096	53.225	25.504	36.222
⋮	⋮	⋮	⋮	⋮	⋮	⋮	⋮
12	8017	8.7768	68.359	15.085	51.392	23.5	36.891
	8018	8.7728	68.369	15.082	51.401	23.494	36.895
	⋮	⋮	⋮	⋮	⋮	⋮	⋮
	8760	5.7264	76.117	13.068	56.652	18.651	43.364

Table G.3: Temperatures and relative humidities for the far horizon, Monclova

Month	Hour	Minimum		Average		Maximum	
i	j	T	H	T	H	T	H
1	1	7.5755	68.01	11.416	58.813	22.055	45.745
	2	7.5713	68.021	11.419	58.807	22.053	45.746
	⋮	⋮	⋮	⋮	⋮	⋮	⋮
	744	6.8822	69.854	14.145	53.714	22.769	45.323
2	745	6.8839	83.875	14.149	58.467	22.772	41.121
	746	6.8856	83.869	14.153	58.455	22.776	41.116
	⋮	⋮	⋮	⋮	⋮	⋮	⋮
	1416	9.0095	76.112	17.199	50.683	26.063	34.949
⋮	⋮	⋮	⋮	⋮	⋮	⋮	⋮
12	8017	9.5857	66.171	15.152	51.225	23.414	36.947
	8018	9.5823	66.18	15.148	51.236	23.408	36.951
	⋮	⋮	⋮	⋮	⋮	⋮	⋮
	8760	7.1161	72.707	12.905	57.09	18.774	43.126

Appendix H

Temperature and Relative Humidity Estimates for Horizons in Torreón from Algorithm DGG3

For the three horizons of Torreón: near, medium, far, with minimum, average and maximum temperatures, in each of them, temperature and relative humidity pairs are estimated.

The total size of the results ascends to $157,680$ real values: 8760 hours $\times$ 3 horizons $\times$ 3 temperature types $\times$ 2 columns (one of temperature, and one of relative humidity).

The obtained columns are ready to be entered in the horizons weather files for Torreón.

The following code performs the calculations mentioned above.

H.1 Code *TorreonHorizontes.m*

```
function [C1,C2,C3,M1,M2,M3,L1,L2,L3] = TorreonHorizontes
%
%         [C1,C2,C3,M1,M2,M3,L1,L2,L3] = TorreonHorizontes
%
  ------------------------------------------------------------------------
```

```
% For the three horizons of Torreon: near, medium and far,
% with minimum, average and maximum temperaatures, in each of
% them, temperaature and relative humidity pairs are estimated.
%
% For each horizon and temperature, pairs are stimated for
% each horizon hour.
%
% Total size of the results: 157 680 real values.
% 8 760 hours * 3 horizons * 3 locations
% * 2 columns of  temperature and HR
%
 ------------------------------------------------------------------------

%
% Data:
% IMPORTANT NOTE
%  To use this program the following must be available:
%  Tc.mat, Tm.mat, Tl.mat monthly data of horizons temperatures:
%                         minimum, average and maximum.
%
%  TorreonWD.mat          data with historical information.
%                         previously this information.
%                         and .epw Energy plus formats.
%
% Results:
%  Ci, C2, C3  hourly pairs of temperature and relative humidity
%              in the near horizon.
%  M1, M2, M3  hourly pairs of temperature and relative himidity
%              in the medium horizon.
%  L1, L2, L3  hourly pairs of temperature and relative humidity
%              in the far horizon.
%
%              Subscript 1, 2 and 3, are minimimu, average, and
%              maximum temperature correspondingly.
%
% At the  ende, results must be backed up in .mat files:
%
% Near horizon, minimum, average and maximum projections
% >> save CerMinT.mat C1; save CerMedT.mat C2; save CerMaxT.mat C3
```

```
  :
%
% Medium horizon, minimum, average and maximum projections
% >> save MedMinT.mat M1; save MedMedT.mat M2; save MedMaxT.mat M3
  ;
%
% Far horizon, minimum, average and maximum projections
% >> save LejMinT.mat L1; save LejMedT.mat L2; save LejMaxT.mat L3
  ;
%
% 1) Apply this program
%       [C1,C2,C3,M1 M2 M3,L1 L2 L3] = TorreonHorizontes;
% 2) At the end, users can save generated .mat files to preserve
  the
%       results.
%
% Routines used               THR,  HR_T,  tempHorizonte,  HRh.
%
% January 2020.
%

warning off
set(groot,'defaultAxesTickLabelInterpreter','latex'); % ticks in
  latex
clc
format

% historic temperatures T and relative himiditiesT HR
[T,HR,hrMes] = THR;

% quartic equation  Hr = f(T)  to be applied each month
HRT = HR_T (T,HR,hrMes);
format shortg
disp(HRT)
disp('  Monthly relative humidity equations, as a function of')
disp('  temperature, obtained from historical records.'
pause

% equations for the three times of each horizon
```

```
[TC,TM,TL] = TempHorizontes;
T = [TC TM TL];

% results
[C1,C2,C3,M1,M2,M3,L1,L2,L3] = HRh (HRT,TC,TM,TL,hrMes);

disp(' ')
disp ('  At the end, results must be backed up in .mat files:')
disp(' ')
disp('  Near horizons, minimum, average and maximum projections')
t = '    >> save CerMinT.mat C1;    save CerMedT.mat C2;    ';
disp([t  'save CerMaxT.mat C3;'])
disp(' ')
disp('  Medium horizon, minimum, average and maximum projections')
t = '    >> save MedMinT.mat M1;    save MedMedT.mat M2;    ';
disp([t  'save MedMaxT.mat M3;'])
disp(' ')
disp('  Far Horizon, minimum, average and maximum projections')
t = '    >> save LejMinT.mat L1;    save LejMedT.mat L2;    ';
disp([t  'save LejMaxT.mat L3;'])
disp(' ')
pause
```

H.1.1 Hourly Temperatures and Relative Humidity for Torreón

The programme calculates the relative humidity for each hour in Torreón, it produces hourly temperature and relative humidity pairs for the horizons. This code is a sub-routine required by the *TorreonHorizontes* code. The required data and the results obtained are shown below.

Data:

HRT	relative humidity formulas as a function of temperature
TC	hourly temperatures in the near horizon
TM	hourly temperatures in the medium horizon
TL	hourly temperatures in the far horizon
$hrMes$	interval in hours of each month

Results:

C_1,	C_2,	C_3,	hourly pairs of temperature and relative humidity in the near horizon
M_1,	M_2,	M_3	hourly pairs of temperature and relative humidity in the medium horizon
L_1,	L_2,	L_3	hourly pairs of temperature and relative humidity in the far horizon

Subscript 1, 2 and 3, are minimum, average and maximum temperatures correspondingly.

Code *HRh.m* for Torreón

```
function [C1,C2,C3,M1,M2,M3,L1,L2,L3] = HRh (HRT,TC,TM,TL,hrMes)
%
%        [C1,C2,C3,M1,M2,M3,L1,L2,L3] = HRh (HRT,TC,TM,TL,hrMes)
% ------------------------------------------------------------------
% Calculate the relative humidity, every hour, in Torreon,
% Coahuila.
% ------------------------------------------------------------------
%
% Data:
%  HRT  relative humidity formulas as a function of temperature.
%  TC   hourly temperatures in the near horizon.
%  TM   hourly temperatures in the medium horizon.
%  TL   hourly temperatures in the far horizon.
%  hrMes interval in hours of each month.
%
% Results:
%  C1, C2, C3  hourly pairs of temperature and relative humidity
%              in the near horizon.
%  M1, M2, M3  hourly pairs of temperature and relative humidity
%              in the medium horizon.
%  L1, L2, L3  hourly pairs of temperature and relative humidity
%              in the far horizon.
%
%              Subscript 1, 2 and 3, are minimum, average, and
%              maximum temperatures correspondingly.
%
% At the end, results must be backed up in .mat files:
```

```
28 %
29 % Near Horizon, minimum, average and maximum projections
30 % >> save CerMinS.mat C1; save CerMedS.mat C2; save CerMaxS.mat C3
    ;
31 %
32 % Medium Horizon, minimum, average and maximum projections
33 % >> save MedMinS.mat M1; save MedMedS.mat M2; save MedMaxS.mat M3
    ;
34 %
35 % Far Horizon, minimum, average and maximum projections
36 % >> save LejMinS.mat L1; save LejMedS.mat L2; save LejMaxS.mat L3
    ;
37 %
38
39 warning off
40 set(groot,'defaultAxesTickLabelInterpreter','latex'); % ticks in
    latex
41 disp(' ')
42 HRC = [];
43 HRM = [];
44 HRL = [];
45 lt = '        Interval in hours. Equations to calculate the ';
46 disp([lt  'relative humidity of the horizons'])
47 lt = '        ___________________________________________________';
48 disp([lt '_____________________________'])
49 disp(' ')
50 for i = 1:12
51    a = hrMes(i,1);
52    b = hrMes(i,2);
53    f = HRT(i,:);
54    disp([a b f])
55    pause
56    tc = TC(a:b,:);
57    tm = TM(a:b,:);
58    tl = TL(a:b,:);
59    hrc = polyval(f,tc);
60    hrm = polyval(f,tm);
61    hrl = polyval(f,tl);
62    HRC = [HRC;hrc];
```

```
63      HRM = [HRM;hrm];
64      HRL = [HRL;hrl];
65    end
66    k = find(HRC < 0);
67    if k
68      HRC(k) = 0;
69    end
70    k = find(HRC > 100);
71    if k
72      HRC(k) = 100;
73    end
74    k = find(HRM < 0);
75    if k
76      HRM(k) = 0;
77    end
78    k = find(HRM > 100);
79    if k
80      HRM(k) = 100;
81    end
82    k = find(HRL < 0);
83    if k
84      HRL(k) = 0;
85    end
86    k = find(HRL > 100);
87    if k
88      HRL(k) = 100;
89    end
90
91  C1=[TC(:,1) HRC(:,1)];C2=[TC(:,2) HRC(:,2)];C3=[TC(:,3) HRC(:,3)];
92  M1=[TM(:,1) HRM(:,1)];M2=[TM(:,2) HRM(:,2)];M3=[TM(:,3) HRM(:,3)];
93  L1=[TL(:,1) HRL(:,1)];L2=[TL(:,2) HRL(:,2)];L3=[TL(:,3) HRL(:,3)];
94  T = [TC TM TL];
95  H = [HRC HRM HRL];
96
97    disp(' ')
98    lt = ' ****With the determination of the relative humidities ';
99    disp([lt  'for each hour, the temperatures'])
100   disp(' ')
101   lt = '         and relative humidities of the stations ';
```

```
disp([lt  'are known for the three temperatures. OK'])
lt = '        ____________________________________________________';
disp([lt '_____________________________'])
pause

disp(' ')
disp('        Subtraction Verifications of Null Results:')
disp(' ')
pause
TC - [C1(:,1) C2(:,1) C3(:,1)]
pause
clc
TM - [M1(:,1) M2(:,1) M3(:,1)]
pause
clc
TL - [L1(:,1) L2(:,1) L3(:,1)]
pause
clc
HRC - [C1(:,2) C2(:,2) C3(:,2)]
pause
clc
HRM - [M1(:,2) M2(:,2) M3(:,2)]
pause
clc
HRL - [L1(:,2) L2(:,2) L3(:,2)]
pause
clc
disp(' ')
disp('  Dimensions of temperatures and relative humidities:')
disp([size(T) size(H)])
disp(' ')
pause
disp ('  At the end, results must be backed up in .mat files:')
disp(' ')
disp(' Near Horizon, minimum, average and maximum projections')
t = '  >> save CerMinS.mat C1;    save CerMedS.mat C2;    ';
disp([t  'save CerMaxS.mat C3;'])
disp(' ')
disp(' Medium Horizon, minimum, average and maximum projections')
```

```
141  t = '  >> save MedMinS.mat M1;    save MedMedS.mat M2;    ';
142  disp([t  'save MedMaxS.mat M3;'])
143  disp(' ')
144  disp(' Far Horizon, minimum, average and maximum projections')
145  t = '  >> save LejMinS.mat L1;    save LejMedS.mat L2;    ';
146  disp([t  'save LejMaxS.mat L3;'])
147  disp(' ')
148  pause
```

H.1.2 Other Subroutines

The code *TorreonHorizontes* requires the routines of the appendices I, J, and K.

H.1.3 Summarized Results

The values of the results generated with the programme appear summarized in the following tables.

Table H.1: Temperatures and relative humidities for the near horizon, Torreón

Month	Hour	Minimum		Average		Maximum	
i	j	T	H	T	H	T	H
1	1	6.3759	71.222	11.439	58.765	20.599	46.664
	2	6.3706	71.236	11.438	58.766	20.594	46.667
	⋮	⋮	⋮	⋮	⋮	⋮	⋮
	744	5.1826	74.491	12.589	56.457	20.308	46.864
2	745	5.184	89.477	12.592	63.327	20.311	44.915
	746	5.1854	89.473	12.596	63.316	20.314	44.91
	⋮	⋮	⋮	⋮	⋮	⋮	⋮
	1416	7.2136	82.706	15.331	55.17	23.401	40.123
⋮	⋮	⋮	⋮	⋮	⋮	⋮	⋮
12	8017	7.8991	70.686	14.289	53.426	22.598	37.595
	8018	7.895	70.697	14.285	53.437	22.592	37.601
	⋮	⋮	⋮	⋮	⋮	⋮	⋮
	8760	4.6951	78.462	11.471	61	16.686	47.537

Table H.2: Temperatures and relative humidities for the medium horizon, Torreón

Month	Hour	Minimum		Average		Maximum	
i	j	T	H	T	H	T	H
1	1	7.0986	69.274	12.944	55.793	21.673	45.976
	2	7.0941	69.287	12.942	55.796	21.67	45.978
	⋮	⋮	⋮	⋮	⋮	⋮	⋮
	744	6.2167	71.655	13.544	54.721	22.278	45.612
2	745	6.2183	86.168	13.547	60.28	22.282	41.877
	746	6.2198	86.162	13.55	60.272	22.285	41.871
	⋮	⋮	⋮	⋮	⋮	⋮	⋮
	1416	8.2484	78.935	16.096	53.225	25.504	36.222
⋮	⋮	⋮	⋮	⋮	⋮	⋮	⋮
12	8017	8.7768	68.359	15.085	51.392	23.5	36.891
	8018	8.7728	68.369	15.082	51.401	23.494	36.895
	8760	5.7264	76.117	13.068	56.652	18.651	43.364

Table H.3: Temperatures and relative humidities for the far horizon, Torreón

Month	Hour	Minimum		Average		Maximum	
i	j	T	H	T	H	T	H
1	1	7.5755	68.01	11.416	58.813	22.055	45.745
	2	7.5713	68.021	11.419	58.807	22.053	45.746
	⋮	⋮	⋮	⋮	⋮	⋮	⋮
	744	6.8822	69.854	14.145	53.714	22.769	45.323
2	745	6.8839	83.875	14.149	58.467	22.772	41.121
	746	6.8856	83.869	14.153	58.455	22.776	41.116
	⋮	⋮	⋮	⋮	⋮	⋮	⋮
	1416	9.0095	76.112	17.199	50.683	26.063	34.949
⋮	⋮	⋮	⋮	⋮	⋮	⋮	⋮
12	8017	9.5857	66.171	15.152	51.225	23.414	36.947
	8018	9.5823	66.18	15.148	51.236	23.408	36.951
	⋮	⋮	⋮	⋮	⋮	⋮	⋮
	8760	7.1161	72.707	12.905	57.09	18.774	43.126

Appendix I

Extraction of Temperature and Relative Humidity Columns from Historical Weather Files

Algorithm DGG3 operates with information pertaining to the historical data.

This programme extracts the fields corresponding to temperature and relative humidity from the historical weather files. This must be done for each city; in particular here it is exemplified for the city of Saltillo. This was also done for the cities of Monclova and Torreón.

Originally, the two columns corresponding to the Dry Bulb Temperature and Relative Humidity from the TMY file with historical weather data of the city of Saltillo, must be ready and displayed in the Excel file: SaltilloWD.xls.

This file is transferred to MATLAB to create a table with a compatible .mat format file: SaltilloWD.mat. The code is shown below.

This code is used as a subroutine of *SaltilloHorizontes*, *MonclovaHorizontes* and *TorreonHorizontes* of the appendices F, G, and H.

I.1 Code *THR.m* for Algorithm DGG3

```
function [T,HR,hrMes] = THR
%
%        [T,HR,hrMes] = THR
% ------------------------------------------------------------------
% This program extracts the fields corresponding to temperature
% and relative humidity.
%
% Originally, the two columns corresponding to Dry Bulb
% Temperature and Relative Humidity from the historical data
% of the city of Saltillo, Coahuila, are in the Excel file:
% SaltilloWD.xls.
%
% This file is transfered to Matlab to create a table with a
% compatible .mat format file: SaltilloWD.mat.
% ------------------------------------------------------------------
%
% Data:
% SaltilloWD   It is downloaded into the program on line 32 from
%              the SaltilloWD.mat data.
%
% Results for the original data in Saltillo, Coahuila:
% T            average temperature
% HR           relative humidity
% hrMes        interval of each month in hours
%
% 5 January 2020.
%

warning off
set(groot,'defaultAxesTickLabelInterpreter','latex'); % ticks in
 latex
clc
load SaltilloWD;                                % data download
T  = SaltilloWD{:,'DryBulbTemperatureC'};       % temperature
HR = SaltilloWD{:,'RelativeHumidity'};          % relative humidity
disp(' ')
disp('  Annual Minimum, Average and Maximum Values in Saltillo')
```

```
37  disp(' ')
38  disp('  Temperature in Celsius Degrees')
39  disp([min(T) sum(T)/8760 max(T)])
40  disp('  Percentage of Relative Humidity in Saltillo')
41  disp([min(HR) sum(HR)/8760 max(HR)])
42  pause
43
44  % interval in hours for each month, from January to December
45  hrMes = [1          744;                        % January
46         745         1416;                        % February
47        1417         2160;                        % March
48        2161         2880;                        % April
49        2881         3624;                        % May
50        3625         4344;                        % June
51        4345         5088;                        % July
52        5089         5832;                        % August
53        5833         6552;                        % September
54        6553         7296;                        % October
55        7297         8016;                        % November
56        8017         8760];                       % December
```

Appendix J

Relative Humidity as a Function of Temperature

With the data obtained as described in Appendix I, equations of least squares of relative humidity were obtained as a function of temperatures. Although a single equation can be obtained for the entire year, it was preferred to find an equation for each month, which is more representative.

Graphical representations of the minimum squares fits are obtained: thus, scatter diagrams are obtained with the temperatures on the abscissae axis, and the relative humidity on the ordinate axis.

It was determined that the polynomials that best represented the information were fourth degree equations of least squares. (See Table 5.5, p. 135).

The following code applies to the city of Saltillo, and the same was done for the other two cities.

This code is used as a subroutine of *SaltilloHorizontes*, *MonclovaHorizontes* and *TorreonHorizontes* of the appendices F, G, and H.

J.1 Code *HR_T.m* for Algorithm DGG3

```
function HRT = HR_T (T,HR,hrMes)
```

```
%
%        HRT = HR_T (T,HR,hrMes)
% ------------------------------------------------------------------
% Obtains the least squares equations: relative humidity as a
% function of temperature, for each month of the year, according
% to the historical data in Saltillo Coahuila,
% (SaltilloWD.mat table).
% ------------------------------------------------------------------
%
% Data:
% T       temperature.
% HR      relative humidity.
% hrMes   each month interval, in hours
%
% Results:
% HRT     least squares equations.
%
% 23 December 2019.
%

warning off
set(groot,'defaultAxesTickLabelInterpreter','latex'); % ticks in
 latex
clc
HRT = [];
disp(' ')
disp(' The graphs show the scatter diagrams and the')
disp(' corresponding fourth degree polynomials (least squares).')
disp(' ')
pause

for i = 1:12
   a = hrMes(i,1);
   b = hrMes(i,2);
   T_  = T(a:b);              % temperature
   HR_ = HR(a:b);             % relative humidity
   minHR_ = min(HR_);
   ti1 = 'HR = f(T) Historical Data in Month %g in Saltillo';
   ti1 = sprintf(ti1,i);
```

```
    ti2 = sprintf('Noise: Relative Humidity Month %g Saltillo',i);
    HRT_ = polyfit(T_,HR_,4);  % least squares equation
    HRT = [HRT;HRT_];
    t = linspace(min(T_),max(T_));
    hrt = polyval(HRT_,t);
    hrT = polyval(HRT_,T_);
    k = find(hrT > 100);
    if k
       hrT(k) = 100;
    end
    k = find(hrT < minHR_);
    if k
       hrT(k) = minHR_;
    end

    clf
    plot(T_,HR_,'.')          % scatter diagram
    hold on
    plot(t,hrt,'linewidth',2)% quartic of least squares
    title(ti1)
    axis off
    shg
    pause

    clf
    plot(HR_-hrT)             % HR differences, data and calculated
    title(ti2)
    axis off
    shg
    pause
end
clf
```

Appendix K

Hourly Horizons Temperatures

For each city:

The UNAM Climate Atlas provides data on the minimum, average and maximum temperature for each month on each horizon. (Total data = 108).

An hourly evaluation of the temperatures for each horizon and their corresponding minimum, average and maximum temperatures is required. (Estimated values = 78,840).

Which were obtained with least square polynomials. (Total equations = 108).

For the three cities the total is: 324 data available for future horizons; a total of 236,520 estimated values with the programme, obtained with 324 least squares equations.

This information is broken down in Chapter 5, p. 146. The following code shows what was done for Saltillo. It was run the same for Monclova and Torreón.

This code is used as a subroutine of *SaltilloHorizontes*, *MonclovaHorizontes* and *TorreonHorizontes* of the appendices F, G, and H.

K.1 Coding of *TempHorizontes.m* for Algorithm DGG3

```
1  function [TC,TM,TL] = TempHorizontes
```

```
%
%        [TC,TM,TL] = TempHorizontes
% ------------------------------------------------------------------
% Obtains the temperatures of the scenarios or horizons,
% calculated with least squares, in Saltillo, Coahuila.
% ------------------------------------------------------------------
%
% Results
% TC      near horizon temperature   (2015-2039)
% TM      medium horizon temperature (2045-2069)
% TL      far horizon temperature    (2075-2099)
%
% 5 December 2019
%

warning off
set(groot,'defaultAxesTickLabelInterpreter','latex'); % ticks in
 latex
clc
t = (1:8760);                                        % hours of the
 year
% hours of middays
hora = [372 1080 1788 2520 3252 3984 4716 5460 6192 6924 7656
 8388];
hora = hora'+0.5;
%  Tc = [136 151 197 239 273 286 291 282 263 221 179 143]'/10;
%  Tm = [148 157 206 243 281 297 299 291 270 229 181 156]'/10;
%  Tl = [144 168 216 256 281 296 304 296 272 232 187 154]'/10;
lt = '   minimum   medium    maximum';

load Tc
disp(' ')
disp('  Monthly Near Horizon Temperatures  (2015-2039)')
disp(lt)
disp(Tc)
pause

load Tm
disp('  Monthly Medium Horizon Temperatures  (2045-2069)')
```

```
disp(lt)
disp(Tm)
pause

load Tl
disp('  Monthly Far Horizon Temperatures  (2075-2099)')
disp(lt)
disp(Tl)
pause
lt = '  *With these temperatures of the horizons, their ';
disp([lt  '5th Degree equations'])
disp(' ')
lt = '   are generated (least squares), they are shown';
disp([lt  ' below.'])
disp(' ')
pause
titlei = ['min temperature';'med temperature';'max temperature'];
yaxis = 'Celsius Degrees';

% TC
TC = [];
for i = 1:3
   polTCi = polyfit(hora,Tc(:,i),5); % with 12 temperatures/year
   TCi = polyval(polTCi,t);          % for 8760 hours/year
   TCi = TCi(:);
   clf
   plot(hora,Tc(:,i),'*g',hora,Tc(:,i),'ro',hora,Tc(:,i),'.g')
   hold on
   plot(t,TCi,'linewidth',2)
   title(['Saltillo: Near Horizon, ' titlei(i,:)],...
       'interpreter','latex',...
       'fontsize',16)
   xlabel('Hours',...
       'interpreter','latex',...
       'fontsize',16)
   ylabel(yaxis,...
       'interpreter','latex',...
       'fontsize',16)
   shg
```

```
77      TC = [TC TCi];                      % at the end: 8760x3
78      pause
79  end
80
81  % TM
82  TM = [];
83  for i =1:3
84      polTMi = polyfit(hora,Tm(:,i),5); % with 12 temperatures/year
85      TMi = polyval(polTMi,t);          % for 8760 hours/year
86      TMi = TMi(:);
87      clf
88      plot(hora,Tm(:,i),'*g',hora,Tm(:,i),'ro',hora,Tm(:,i),'.g')
89      hold on
90      plot(t,TMi,'linewidth',2)
91      title(['Saltillo: Medium Horizon, ' titlei(i,:)],...
92          'interpreter','latex',...
93          'fontsize',16)
94      xlabel('Hours',...
95          'interpreter','latex',...
96          'fontsize',16)
97      ylabel(yaxis,...
98          'interpreter','latex',...
99          'fontsize',16)
100     shg
101     TM = [TM TMi];                      % at the end: 8760x3
102     pause
103 end
104
105 % TL
106 TL = [];
107 for i = 1:3
108     polTLi = polyfit(hora,Tl(:,i),5); % with 12 temperatures/year
109     TLi = polyval(polTLi,t);          % for 8760 hours/year
110     TLi = TLi(:);
111     clf
112     plot(hora,Tl(:,i),'*g',hora,Tl(:,i),'ro',hora,Tl(:,i),'.g')
113     hold on
114     plot(t,TLi,'linewidth',2)
115     title(['Saltillo: Far Horizon, ' titlei(i,:)],...
```

```
116         'interpreter','latex',...
117         'fontsize',16)
118     xlabel('Hours',...
119         'interpreter','latex',...
120         'fontsize',16)
121     ylabel(yaxis,...
122         'interpreter','latex',...
123         'fontsize',16)
124     shg
125     TL = [TL TLi];                    % at the end: 8760x3
126     pause
127 end
128
129 lt = '**These equations are used to evaluate the temperatures ';
130 disp([lt  'of the horizons in each hour of the year.'])
131 disp(' ')
132 pause
133 lt = '***With the temperatures of the horizons the relative ';
134 disp([lt  'humidities in the horizons are evaluated.'])
135 pause
```

Appendix L

Matrix of Simulation Cases

In the development of the research it was decided to perform 984 simulations. These were for current weather (CW), the near horizon (NH), medium horizon (MH) and far horizon (FH) for the cities of Saltillo (S), Monclova (M) and Torreón (T). Simulations were performed considering two orientations, north-south and east-west. Next they are identified with the number of simulations (Sim.) in cases from Base Case (BC), and cases from 1 to 40 on each set (C1-C40).

L.1 Simulation Cases Saltillo, Monclova and Torreón

Cases Saltillo

Table L.1: Simulation Cases Saltillo North-South

Sim.	Case CW	Sim.	Case NH	Sim.	Case MH	Sim.	Case FH
1	S BC CW	42	S BC NH	83	S BC MH	124	S BC FH
2	S C1 CW	43	S C1 NH	84	S C1 MH	125	S C1 FH
3	S C2 CW	44	S C2 NH	85	S C2 MH	126	S C2 FH
4	S C3 CW	45	S C3 NH	86	S C3 MH	127	S C3 FH
5	S C4 CW	46	S C4 NH	87	S C4 MH	128	S C4 FH
6	S C5 CW	47	S C5 NH	88	S C5 MH	129	S C5 FH

continues on the next page ...

Sim.	Case CW	Sim.	Case NH	Sim.	Case MH	Sim.	Case FH
7	S C6 CW	48	S C6 NH	89	S C6 MH	130	S C6 FH
8	S C7 CW	49	S C7 NH	90	S C7 MH	131	S C7 FH
9	S C8 CW	50	S C8 NH	91	S C8 MH	132	S C8 FH
10	S C9 CW	51	S C9 NH	92	S C9 MH	133	S C9 FH
11	S C10 CW	52	S C10 NH	93	S C10 MH	134	S C10 FH
12	S C11 CW	53	S C11 NH	94	S C11 MH	135	S C11 FH
13	S C12 CW	54	S C12 NH	95	S C12 MH	136	S C12 FH
14	S C13 CW	55	S C13 NH	96	S C13 MH	137	S C13 FH
15	S C14 CW	56	S C14 NH	97	S C14 MH	138	S C14 FH
16	S C15 CW	57	S C15 NH	98	S C15 MH	139	S C15 FH
17	S C16 CW	58	S C16 NH	99	S C16 MH	140	S C16 FH
18	S C17 CW	59	S C17 NH	100	S C17 MH	141	S C17 FH
19	S C18 CW	60	S C18 NH	101	S C18 MH	142	S C18 FH
20	S C19 CW	61	S C19 NH	102	S C19 MH	143	S C19 FH
21	S C20 CW	62	S C20 NH	103	S C20 MH	144	S C20 FH
22	S C21 CW	63	S C21 NH	104	S C21 MH	145	S C21 FH
23	S C22 CW	64	S C22 NH	105	S C22 MH	146	S C22 FH
24	S C23 CW	65	S C23 NH	106	S C23 MH	147	S C23 FH
25	S C24 CW	66	S C24 NH	107	S C24 MH	148	S C24 FH
26	S C25 CW	67	S C25 NH	108	S C25 MH	149	S C25 FH
27	S C26 CW	68	S C26 NH	109	S C26 MH	150	S C26 FH
28	S C27 CW	69	S C27 NH	110	S C27 MH	151	S C27 FH
29	S C28 CW	70	S C28 NH	111	S C28 MH	152	S C28 FH
30	S C29 CW	71	S C29 NH	112	S C29 MH	153	S C29 FH
31	S C30 CW	72	S C30 NH	113	S C30 MH	154	S C30 FH
32	S C31 CW	73	S C31 NH	114	S C31 MH	155	S C31 FH
33	S C32 CW	74	S C32 NH	115	S C32 MH	156	S C32 FH
34	S C33 CW	75	S C33 NH	116	S C33 MH	157	S C33 FH
35	S C34 CW	76	S C34 NH	117	S C34 MH	158	S C34 FH
36	S C35 CW	77	S C35 NH	118	S C35 MH	159	S C35 FH
37	S C36 CW	78	S C36 NH	119	S C36 MH	160	S C36 FH
38	S C37 CW	79	S C37 NH	120	S C37 MH	161	S C37 FH

continues on the next page ...

Sim.	Case CW	Sim.	Case NH	Sim.	Case MH	Sim.	Case FH
39	S C38 CW	80	S C38 NH	121	S C38 MH	162	S C38 FH
40	S C39 CW	81	S C39 NH	122	S C39 MH	163	S C39 FH
41	S C40 CW	82	S C40 NH	123	S C40 MH	164	S C40 FH

Table L.2: Simulation Cases Saltillo East-West

Sim.	Case CW	Sim.	Case NH	Sim.	Case MH	Sim.	Case FH
165	S BC CW	206	S BC NH	247	S BC MH	288	S BC FH
166	S C1 CW	207	S C1 NH	248	S C1 MH	289	S C1 FH
167	S C2 CW	208	S C2 NH	249	S C2 MH	290	S C2 FH
168	S C3 CW	209	S C3 NH	250	S C3 MH	291	S C3 FH
169	S C4 CW	210	S C4 NH	251	S C4 MH	292	S C4 FH
170	S C5 CW	211	S C5 NH	252	S C5 MH	293	S C5 FH
171	S C6 CW	212	S C6 NH	253	S C6 MH	294	S C6 FH
172	S C7 CW	213	S C7 NH	254	S C7 MH	295	S C7 FH
173	S C8 CW	214	S C8 NH	255	S C8 MH	296	S C8 FH
174	S C9 CW	215	S C9 NH	256	S C9 MH	297	S C9 FH
175	S C10 CW	216	S C10 NH	257	S C10 MH	298	S C10 FH
176	S C11 CW	217	S C11 NH	258	S C11 MH	299	S C11 FH
177	S C12 CW	218	S C12 NH	259	S C12 MH	300	S C12 FH
178	S C13 CW	219	S C13 NH	260	S C13 MH	301	S C13 FH
179	S C14 CW	220	S C14 NH	261	S C14 MH	302	S C14 FH
180	S C15 CW	221	S C15 NH	262	S C15 MH	303	S C15 FH
181	S C16 CW	222	S C16 NH	263	S C16 MH	304	S C16 FH
182	S C17 CW	223	S C17 NH	264	S C17 MH	305	S C17 FH
183	S C18 CW	224	S C18 NH	265	S C18 MH	306	S C18 FH
184	S C19 CW	225	S C19 NH	266	S C19 MH	307	S C19 FH
185	S C20 CW	226	S C20 NH	267	S C20 MH	308	S C20 FH
186	S C21 CW	227	S C21 NH	268	S C21 MH	309	S C21 FH
187	S C22 CW	228	S C22 NH	269	S C22 MH	310	S C22 FH
188	S C23 CW	229	S C23 NH	270	S C23 MH	311	S C23 FH
189	S C24 CW	230	S C24 NH	270	S C24 MH	312	S C24 FH

continues on the next page ...

Sim.	Case CW	Sim.	Case NH	Sim.	Case MH	Sim.	Case FH
190	S C25 CW	231	S C25 NH	272	S C25 MH	313	S C25 FH
191	S C26 CW	232	S C26 NH	273	S C26 MH	314	S C26 FH
192	S C27 CW	233	S C27 NH	274	S C27 MH	315	S C27 FH
193	S C28 CW	234	S C28 NH	275	S C28 MH	316	S C28 FH
194	S C29 CW	235	S C29 NH	276	S C29 MH	317	S C29 FH
195	S C30 CW	236	S C30 NH	277	S C30 MH	318	S C30 FH
196	S C31 CW	237	S C31 NH	278	S C31 MH	319	S C31 FH
197	S C32 CW	238	S C32 NH	279	S C32 MH	320	S C32 FH
198	S C33 CW	239	S C33 NH	280	S C33 MH	321	S C33 FH
199	S C34 CW	240	S C34 NH	281	S C34 MH	322	S C34 FH
200	S C35 CW	241	S C35 NH	282	S C35 MH	323	S C35 FH
201	S C36 CW	242	S C36 NH	283	S C36 MH	324	S C36 FH
202	S C37 CW	243	S C37 NH	284	S C37 MH	325	S C37 FH
203	S C38 CW	244	S C38 NH	285	S C38 MH	326	S C38 FH
204	S C39 CW	245	S C39 NH	286	S C39 MH	327	S C39 FH
205	S C40 CW	246	S C40 NH	287	S C40 MH	328	S C40 FH

Cases Monclova

Table L.3: Simulation Cases Monclova North-South

Sim.	Case CW	Sim.	Case NH	Sim.	Case MH	Sim.	Case FH
329	M BC CW	370	M BC NH	411	M BC MH	452	M BC FH
330	M C1 CW	371	M C1 NH	412	M C1 MH	453	M C1 FH
331	M C2 CW	372	M C2 NH	413	M C2 MH	454	M C2 FH
332	M C3 CW	373	M C3 NH	414	M C3 MH	455	M C3 FH
333	M C4 CW	374	M C4 NH	415	M C4 MH	456	M C4 FH
334	M C5 CW	375	M C5 NH	416	M C5 MH	457	M C5 FH
335	M C6 CW	376	M C6 NH	417	M C6 MH	458	M C6 FH
336	M C7 CW	377	M C7 NH	418	M C7 MH	459	M C7 FH
337	M C8 CW	378	M C8 NH	419	M C8 MH	460	M C8 FH

continues on the next page ...

Sim.	Case CW	Sim.	Case NH	Sim.	Case MH	Sim.	Case FH
338	M C9 CW	379	M C9 NH	420	M C9 MH	461	M C9 FH
339	M C10 CW	380	M C10 NH	421	M C10 MH	462	M C10 FH
340	M C11 CW	381	M C11 NH	422	M C11 MH	463	M C11 FH
341	M C12 CW	382	M C12 NH	423	M C12 MH	464	M C12 FH
342	M C13 CW	383	M C13 NH	424	M C13 MH	465	M C13 FH
343	M C14 CW	384	M C14 NH	425	M C14 MH	466	M C14 FH
344	M C15 CW	385	M C15 NH	426	M C15 MH	467	M C15 FH
345	M C16 CW	386	M C16 NH	427	M C16 MH	468	M C16 FH
346	M C17 CW	387	M C17 NH	428	M C17 MH	469	M C17 FH
347	M C18 CW	388	M C18 NH	429	M C18 MH	470	M C18 FH
348	M C19 CW	389	M C19 NH	430	M C19 MH	471	M C19 FH
349	M C20 CW	390	M C20 NH	431	M C20 MH	472	M C20 FH
350	M C21 CW	391	M C21 NH	432	M C21 MH	473	M C21 FH
351	M C22 CW	392	M C22 NH	433	M C22 MH	474	M C22 FH
352	M C23 CW	393	M C23 NH	434	M C23 MH	475	M C23 FH
353	M C24 CW	394	M C24 NH	435	M C24 MH	476	M C24 FH
354	M C25 CW	395	M C25 NH	436	M C25 MH	477	M C25 FH
355	M C26 CW	396	M C26 NH	437	M C26 MH	478	M C26 FH
356	M C27 CW	397	M C27 NH	438	M C27 MH	479	M C27 FH
357	M C28 CW	398	M C28 NH	439	M C28 MH	480	M C28 FH
358	M C29 CW	399	M C29 NH	440	M C29 MH	481	M C29 FH
359	M C30 CW	400	M C30 NH	441	M C30 MH	482	M C30 FH
360	M C31 CW	401	M C31 NH	442	M C31 MH	483	M C31 FH
361	M C32 CW	402	M C32 NH	443	M C32 MH	484	M C32 FH
362	M C33 CW	403	M C33 NH	444	M C33 MH	485	M C33 FH
363	M C34 CW	404	M C34 NH	445	M C34 MH	486	M C34 FH
364	M C35 CW	405	M C35 NH	446	M C35 MH	487	M C35 FH
365	M C36 CW	406	M C36 NH	447	M C36 MH	488	M C36 FH
366	M C37 CW	407	M C37 NH	448	M C37 MH	489	M C37 FH
367	M C38 CW	408	M C38 NH	449	M C38 MH	490	M C38 FH
368	M C39 CW	409	M C39 NH	450	M C39 MH	491	M C39 FH

continues on the next page ...

Sim.	Case CW	Sim.	Case NH	Sim.	Case MH	Sim.	Case FH
369	M C40 CW	410	M C40 NH	451	M C40 MH	492	M C40 FH

Table L.4: Simulation Cases Monclova East-West

Sim.	Case CW	Sim.	Case NH	Sim.	Case MH	Sim.	Case FH
493	M BC CW	534	M BC NH	575	M BC MH	616	M BC FH
494	M C1 CW	535	M C1 NH	576	M C1 MH	617	M C1 FH
495	M C2 CW	536	M C2 NH	577	M C2 MH	618	M C2 FH
496	M C3 CW	537	M C3 NH	578	M C3 MH	619	M C3 FH
497	M C4 CW	538	M C4 NH	579	M C4 MH	620	M C4 FH
498	M C5 CW	539	M C5 NH	580	M C5 MH	621	M C5 FH
499	M C6 CW	540	M C6 NH	581	M C6 MH	622	M C6 FH
500	M C7 CW	541	M C7 NH	582	M C7 MH	623	M C7 FH
501	M C8 CW	542	M C8 NH	583	M C8 MH	624	M C8 FH
502	M C9 CW	543	M C9 NH	584	M C9 MH	625	M C9 FH
503	M C10 CW	544	M C10 NH	585	M C10 MH	626	M C10 FH
504	M C11 CW	545	M C11 NH	586	M C11 MH	627	M C11 FH
505	M C12 CW	546	M C12 NH	587	M C12 MH	628	M C12 FH
506	M C13 CW	547	M C13 NH	588	M C13 MH	629	M C13 FH
507	M C14 CW	548	M C14 NH	589	M C14 MH	630	M C14 FH
508	M C15 CW	549	M C15 NH	590	M C15 MH	631	M C15 FH
509	M C16 CW	550	M C16 NH	591	M C16 MH	632	M C16 FH
510	M C17 CW	551	M C17 NH	592	M C17 MH	633	M C17 FH
511	M C18 CW	552	M C18 NH	593	M C18 MH	634	M C18 FH
512	M C19 CW	553	M C19 NH	594	M C19 MH	635	M C19 FH
513	M C20 CW	554	M C20 NH	595	M C20 MH	636	M C20 FH
514	M C21 CW	555	M C21 NH	596	M C21 MH	637	M C21 FH
515	M C22 CW	556	M C22 NH	597	M C22 MH	638	M C22 FH
516	M C23 CW	557	M C23 NH	598	M C23 MH	639	M C23 FH
517	M C24 CW	558	M C24 NH	599	M C24 MH	640	M C24 FH
518	M C25 CW	559	M C25 NH	600	M C25 MH	641	M C25 FH
519	M C26 CW	560	M C26 NH	601	M C26 MH	642	M C26 FH

continues on the next page ...

Sim.	Case CW	Sim.	Case NH	Sim.	Case MH	Sim.	Case FH
520	M C27 CW	561	M C27 NH	602	M C27 MH	643	M C27 FH
521	M C28 CW	562	M C28 NH	603	M C28 MH	644	M C28 FH
522	M C29 CW	563	M C29 NH	604	M C29 MH	645	M C29 FH
523	M C30 CW	564	M C30 NH	605	M C30 MH	646	M C30 FH
524	M C31 CW	565	M C31 NH	606	M C31 MH	647	M C31 FH
525	M C32 CW	566	M C32 NH	607	M C32 MH	648	M C32 FH
526	M C33 CW	567	M C33 NH	608	M C33 MH	649	M C33 FH
527	M C34 CW	568	M C34 NH	609	M C34 MH	650	M C34 FH
528	M C35 CW	569	M C35 NH	610	M C35 MH	651	M C35 FH
529	M C36 CW	570	M C36 NH	611	M C36 MH	652	M C36 FH
530	M C37 CW	571	M C37 NH	612	M C37 MH	653	M C37 FH
531	M C38 CW	572	M C38 NH	613	M C38 MH	654	M C38 FH
532	M C39 CW	573	M C39 NH	614	M C39 MH	655	M C39 FH
533	M C40 CW	574	M C40 NH	615	M C40 MH	656	M C40 FH

Cases Torreón

Table L.5: Simulation Cases Torreón North-South

Sim.	Case CW	Sim.	Case NH	Sim.	Case MH	Sim.	Case FH
657	T BC CW	698	T BC NH	739	T BC MH	780	T BC FH
658	T C1 CW	699	T C1 NH	740	T C1 MH	781	T C1 FH
659	T C2 CW	700	T C2 NH	741	T C2 MH	782	T C2 FH
660	T C3 CW	701	T C3 NH	742	T C3 MH	783	T C3 FH
661	T C4 CW	702	T C4 NH	743	T C4 MH	784	T C4 FH
662	T C5 CW	703	T C5 NH	744	T C5 MH	785	T C5 FH
663	T C6 CW	704	T C6 NH	745	T C6 MH	786	T C6 FH
664	T C7 CW	705	T C7 NH	746	T C7 MH	787	T C7 FH
665	T C8 CW	706	T C8 NH	747	T C8 MH	788	T C8 FH
666	T C9 CW	707	T C9 NH	748	T C9 MH	789	T C9 FH
667	T C10 CW	708	T C10 NH	749	T C10 MH	790	T C10 FH

continues on the next page ...

Sim.	Case CW	Sim.	Case NH	Sim.	Case MH	Sim.	Case FH
668	T C11 CW	709	T C11 NH	750	T C11 MH	791	T C11 FH
669	T C12 CW	710	T C12 NH	751	T C12 MH	792	T C12 FH
670	T C13 CW	711	T C13 NH	752	T C13 MH	793	T C13 FH
671	T C14 CW	712	T C14 NH	753	T C14 MH	794	T C14 FH
672	T C15 CW	713	T C15 NH	754	T C15 MH	795	T C15 FH
673	T C16 CW	714	T C16 NH	755	T C16 MH	796	T C16 FH
674	T C17 CW	715	T C17 NH	756	T C17 MH	797	T C17 FH
675	T C18 CW	716	T C18 NH	757	T C18 MH	798	T C18 FH
676	T C19 CW	717	T C19 NH	758	T C19 MH	799	T C19 FH
677	T C20 CW	718	T C20 NH	759	T C20 MH	800	T C20 FH
678	T C21 CW	719	T C21 NH	760	T C21 MH	801	T C21 FH
679	T C22 CW	720	T C22 NH	761	T C22 MH	802	T C22 FH
680	T C23 CW	721	T C23 NH	762	T C23 MH	803	T C23 FH
681	T C24 CW	722	T C24 NH	763	T C24 MH	804	T C24 FH
682	T C25 CW	723	T C25 NH	764	T C25 MH	805	T C25 FH
683	T C26 CW	724	T C26 NH	765	T C26 MH	806	T C26 FH
684	T C27 CW	725	T C27 NH	766	T C27 MH	807	T C27 FH
685	T C28 CW	726	T C28 NH	767	T C28 MH	808	T C28 FH
686	T C29 CW	727	T C29 NH	768	T C29 MH	809	T C29 FH
687	T C30 CW	728	T C30 NH	769	T C30 MH	810	T C30 FH
688	T C31 CW	729	T C31 NH	770	T C31 MH	811	T C31 FH
689	T C32 CW	730	T C32 NH	771	T C32 MH	812	T C32 FH
690	T C33 CW	731	T C33 NH	772	T C33 MH	813	T C33 FH
691	T C34 CW	732	T C34 NH	773	T C34 MH	814	T C34 FH
692	T C35 CW	733	T C35 NH	774	T C35 MH	815	T C35 FH
693	T C36 CW	734	T C36 NH	775	T C36 MH	816	T C36 FH
694	T C37 CW	735	T C37 NH	776	T C37 MH	817	T C37 FH
695	T C38 CW	736	T C38 NH	777	T C38 MH	818	T C38 FH
696	T C39 CW	737	T C39 NH	778	T C39 MH	819	T C39 FH
697	T C40 CW	738	T C40 NH	779	T C40 MH	820	T C40 FH

Table L.6: Simulation Cases Torreón East-West

Sim.	Case CW	Sim.	Case NH	Sim.	Case MH	Sim.	Case FH
821	T BC CW	862	T BC NH	903	T BC MH	944	T BC FH
822	T C1 CW	863	T C1 NH	904	T C1 MH	945	T C1 FH
823	T C2 CW	864	T C2 NH	905	T C2 MH	946	T C2 FH
824	T C3 CW	865	T C3 NH	906	T C3 MH	947	T C3 FH
825	T C4 CW	866	T C4 NH	907	T C4 MH	948	T C4 FH
826	T C5 CW	867	T C5 NH	908	T C5 MH	949	T C5 FH
827	T C6 CW	868	T C6 NH	909	T C6 MH	950	T C6 FH
828	T C7 CW	869	T C7 NH	910	T C7 MH	951	T C7 FH
829	T C8 CW	870	T C8 NH	911	T C8 MH	952	T C8 FH
830	T C9 CW	871	T C9 NH	912	T C9 MH	953	T C9 FH
831	T C10 CW	872	T C10 NH	913	T C10 MH	954	T C10 FH
832	T C11 CW	873	T C11 NH	914	T C11 MH	955	T C11 FH
833	T C12 CW	874	T C12 NH	915	T C12 MH	956	T C12 FH
834	T C13 CW	875	T C13 NH	916	T C13 MH	957	T C13 FH
835	T C14 CW	876	T C14 NH	917	T C14 MH	958	T C14 FH
836	T C15 CW	877	T C15 NH	918	T C15 MH	959	T C15 FH
837	T C16 CW	878	T C16 NH	919	T C16 MH	960	T C16 FH
838	T C17 CW	879	T C17 NH	920	T C17 MH	961	T C17 FH
839	T C18 CW	880	T C18 NH	921	T C18 MH	962	T C18 FH
840	T C19 CW	881	T C19 NH	922	T C19 MH	963	T C19 FH
841	T C20 CW	882	T C20 NH	923	T C20 MH	964	T C20 FH
842	T C21 CW	883	T C21 NH	924	T C21 MH	965	T C21 FH
843	T C22 CW	884	T C22 NH	925	T C22 MH	966	T C22 FH
844	T C23 CW	885	T C23 NH	926	T C23 MH	967	T C23 FH
845	T C24 CW	886	T C24 NH	927	T C24 MH	968	T C24 FH
846	T C25 CW	887	T C25 NH	928	T C25 MH	969	T C25 FH
847	T C26 CW	888	T C26 NH	929	T C26 MH	970	T C26 FH
848	T C27 CW	889	T C27 NH	930	T C27 MH	971	T C27 FH
849	T C28 CW	890	T C28 NH	931	T C28 MH	972	T C28 FH
850	T C29 CW	891	T C29 NH	932	T C29 MH	973	T C29 FH

continues on the next page ...

Sim.	Case CW	Sim.	Case NH	Sim.	Case MH	Sim.	Case FH
851	T C30 CW	892	T C30 NH	933	T C30 MH	974	T C30 FH
852	T C31 CW	893	T C31 NH	934	T C31 MH	975	T C31 FH
853	T C32 CW	894	T C32 NH	935	T C32 MH	976	T C32 FH
854	T C33 CW	895	T C33 NH	936	T C33 MH	977	T C33 FH
855	T C34 CW	896	T C34 NH	937	T C34 MH	978	T C34 FH
856	T C35 CW	897	T C35 NH	938	T C35 MH	979	T C35 FH
857	T C36 CW	898	T C36 NH	939	T C36 MH	980	T C36 FH
858	T C37 CW	899	T C37 NH	940	T C37 MH	981	T C37 FH
859	T C38 CW	900	T C38 NH	941	T C38 MH	982	T C38 FH
860	T C39 CW	901	T C39 NH	942	T C39 MH	983	T C39 FH
861	T C40 CW	902	T C40 NH	943	T C40 MH	984	T C40 FH

Appendix M

Psychrometric Charts

Psychrometric Charts for Saltillo, Monclova and Torreón with comfort overlays for ASHRAE 55-2017 and Givoni Bioclimatic Chart for current and future horizons weather files.

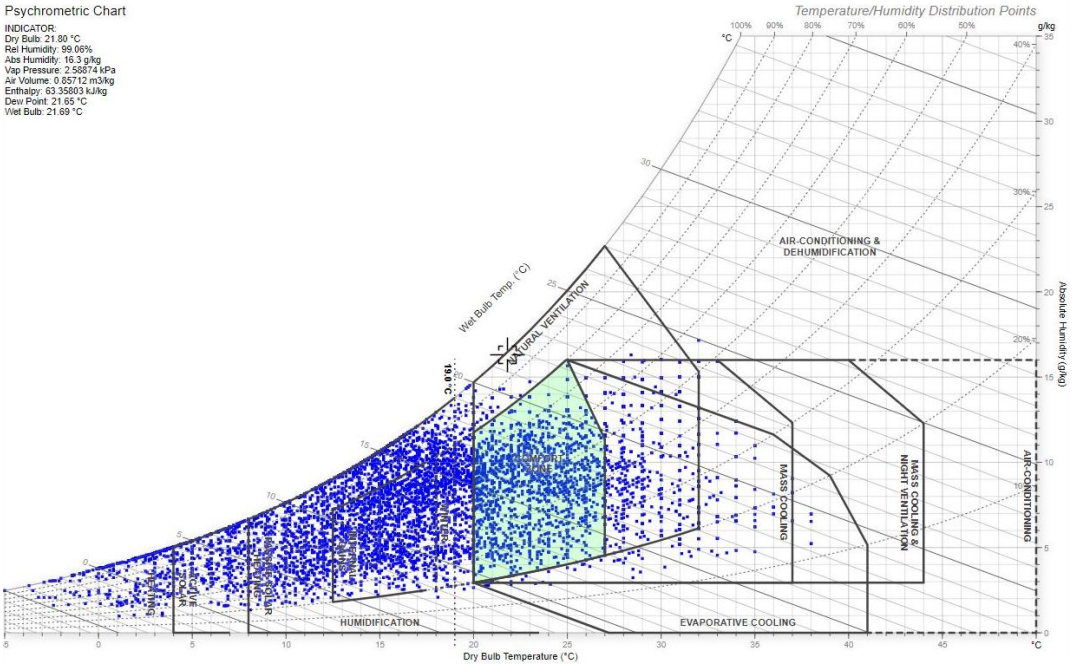


Figure M.1: Saltillo, Givoni Bioclimatic Chart for Current Weather.

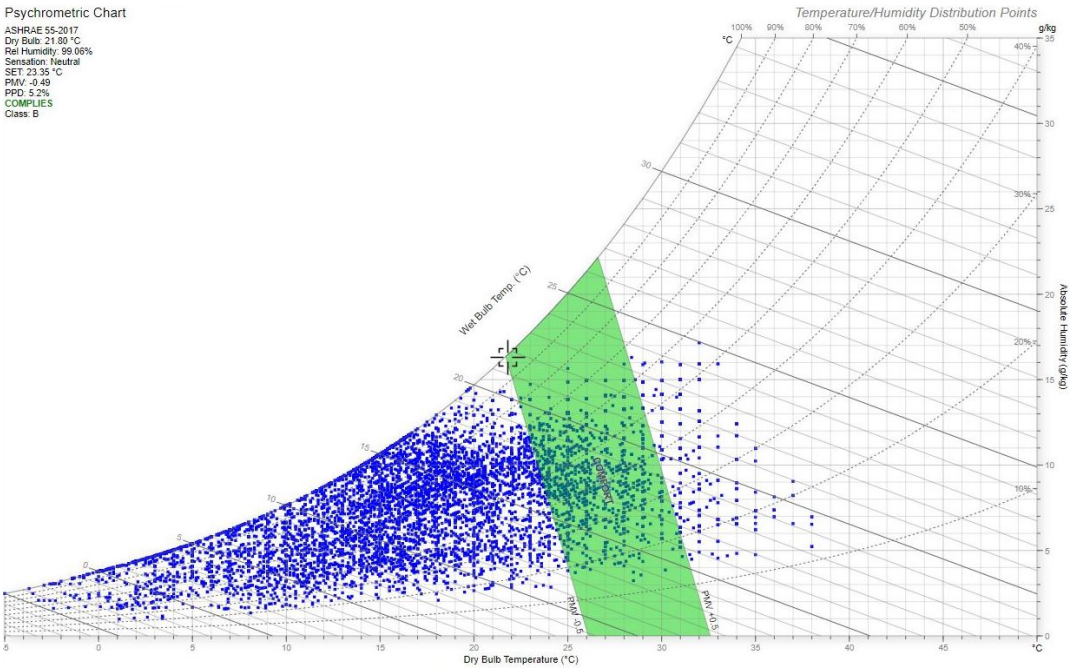


Figure M.2: Saltillo, ASHRAE 55-2017 for Current Weather.

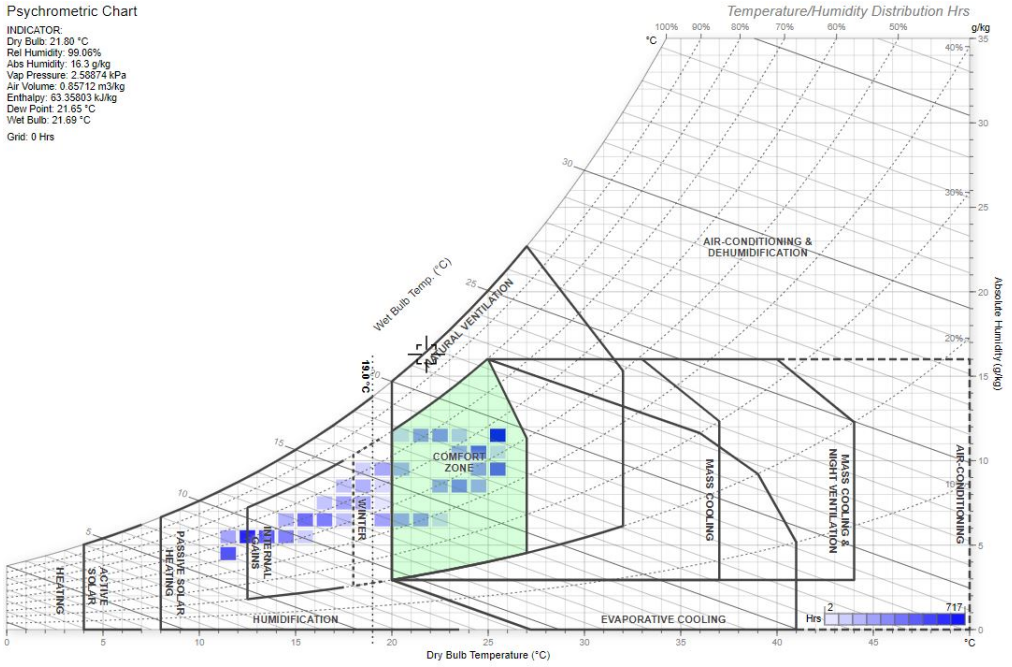


Figure M.3: Saltillo, Givoni Bioclimatic Chart for Near Horizon.

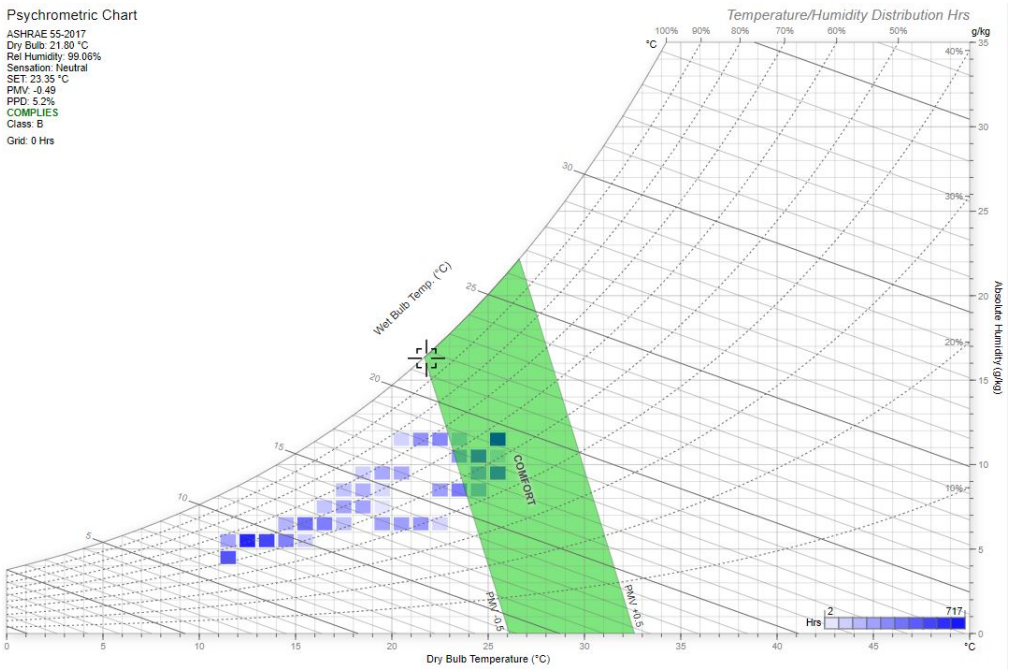


Figure M.4: Saltillo, ASHRAE 55-2017 for Near Horizon.

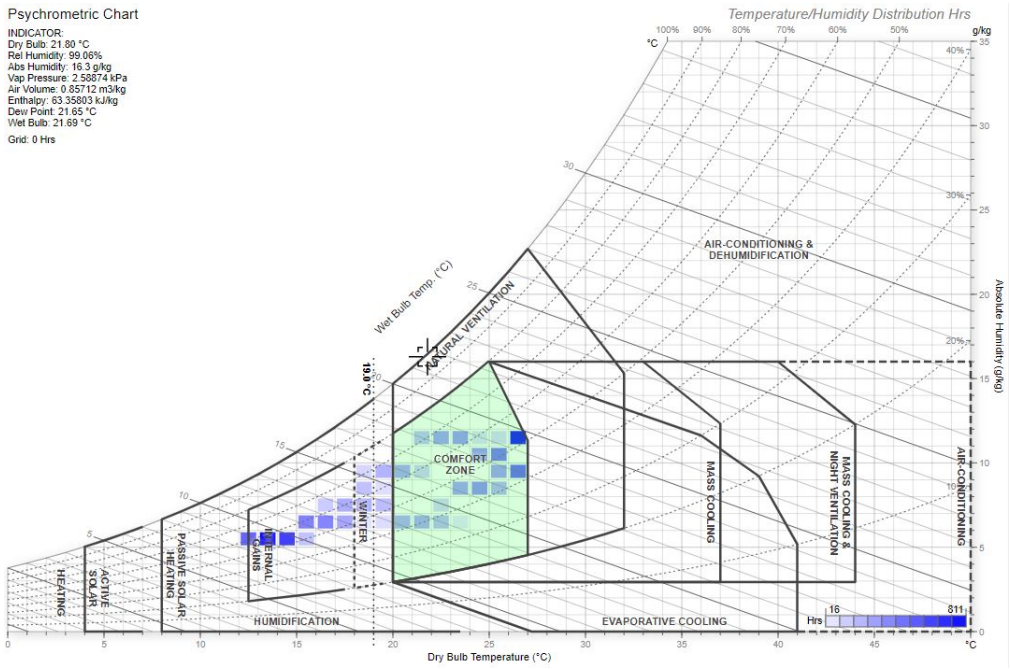


Figure M.5: Saltillo, Givoni Bioclimatic Chart for Medium Horizon.

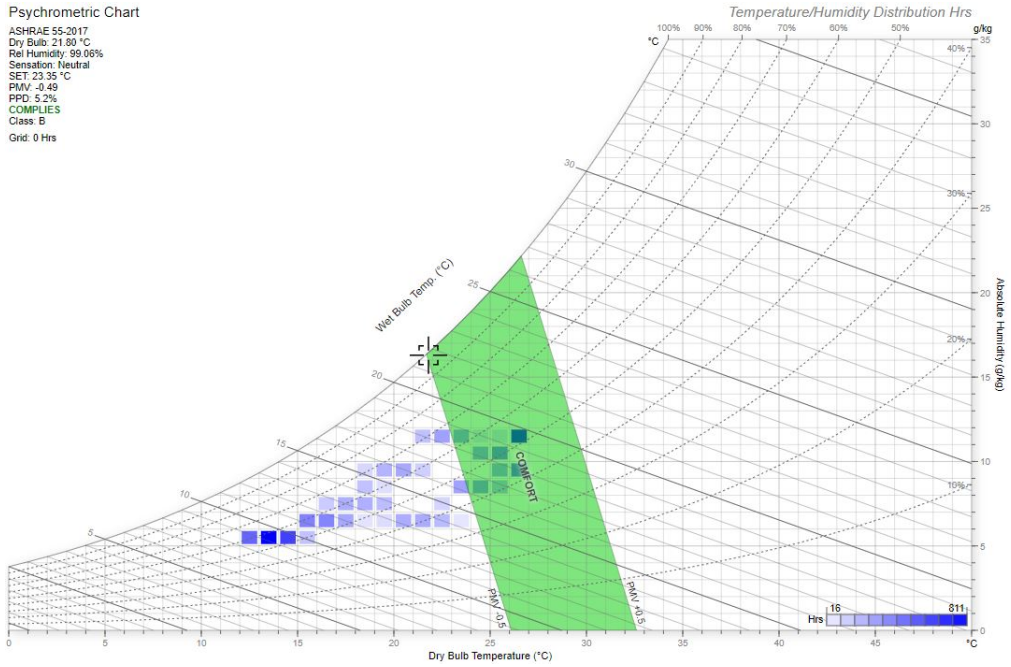


Figure M.6: Saltillo, ASHRAE 55-2017 for Medium Horizon.

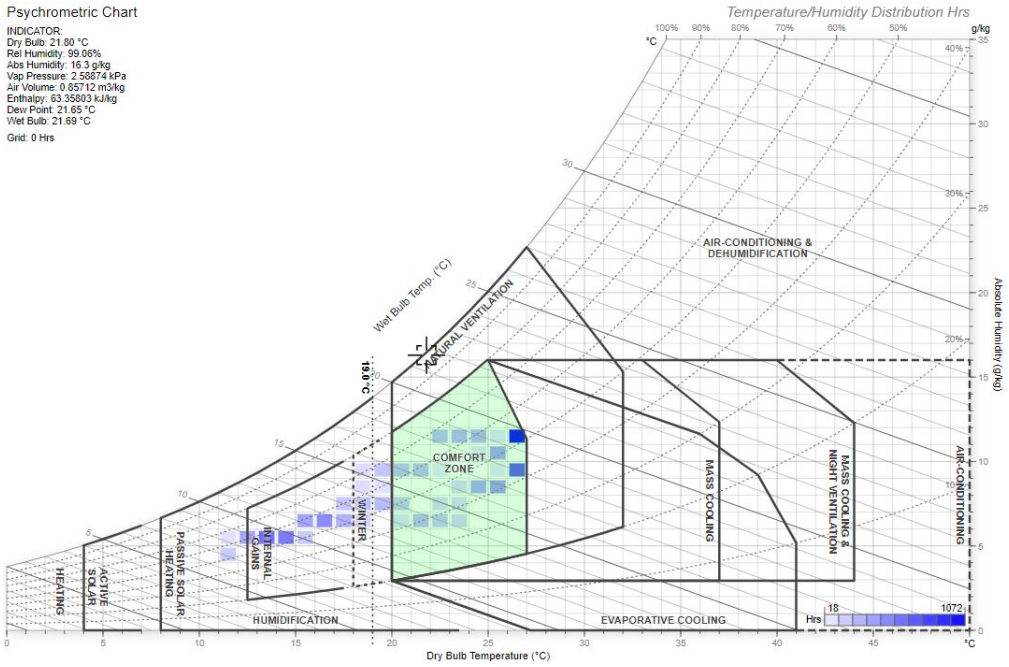


Figure M.7: Saltillo, Givoni Bioclimatic Chart for Far Horizon.

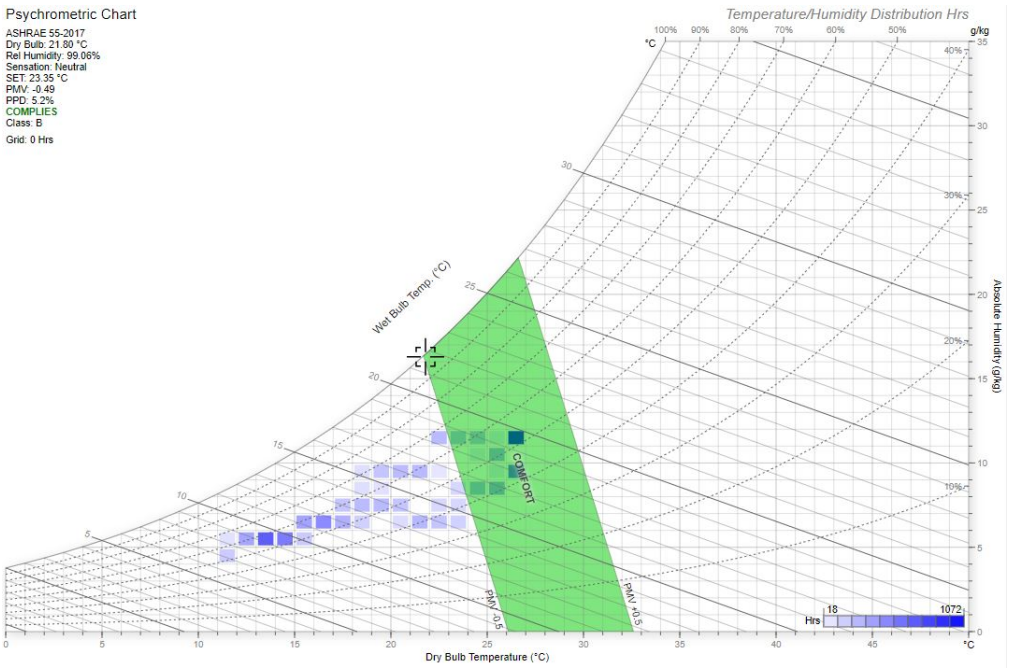


Figure M.8: Saltillo, ASHRAE 55-2017 for Far Horizon.

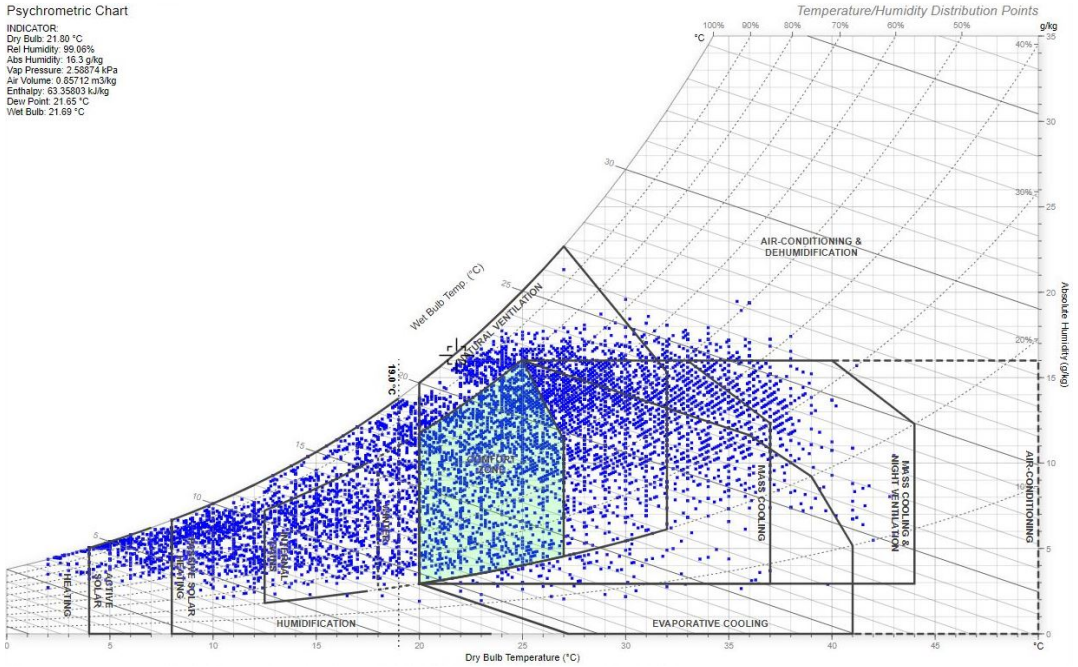


Figure M.9: Monclova, Givoni Bioclimatic Chart for Current Weather.

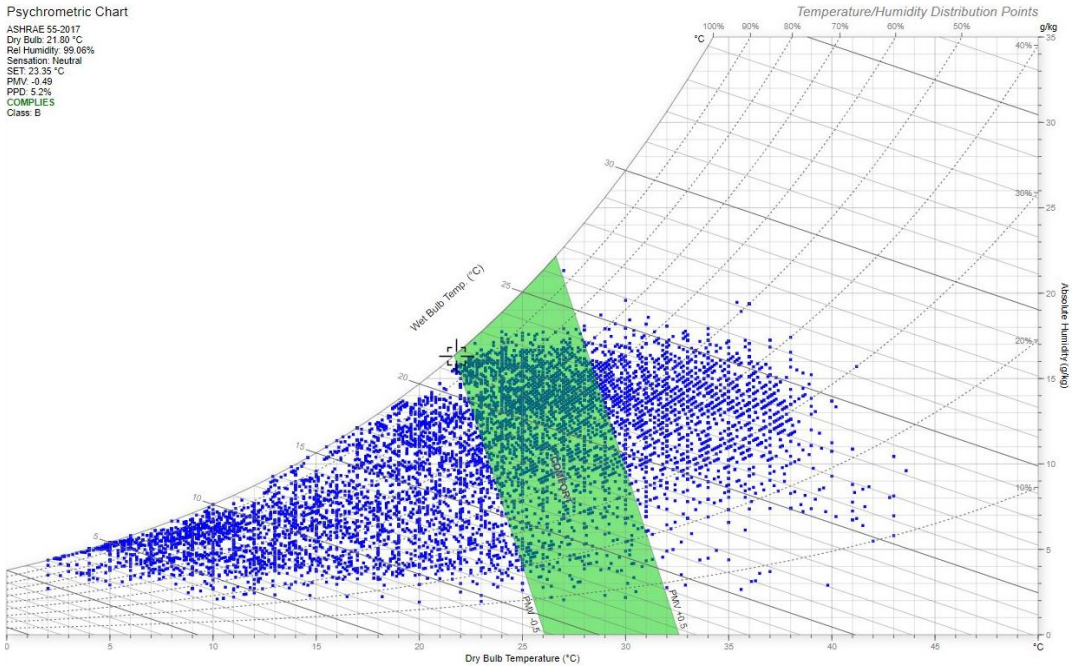


Figure M.10: Monclova, ASHRAE 55-2017 for Current Weather.

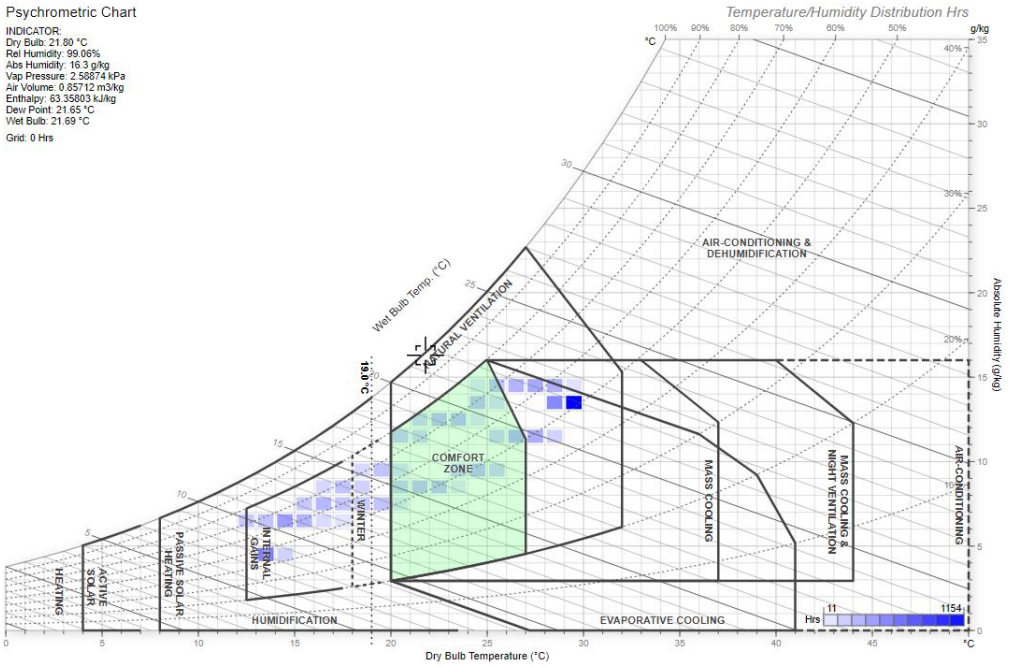


Figure M.11: Monclova, Givoni Bioclimatic Chart for Near Horizon.

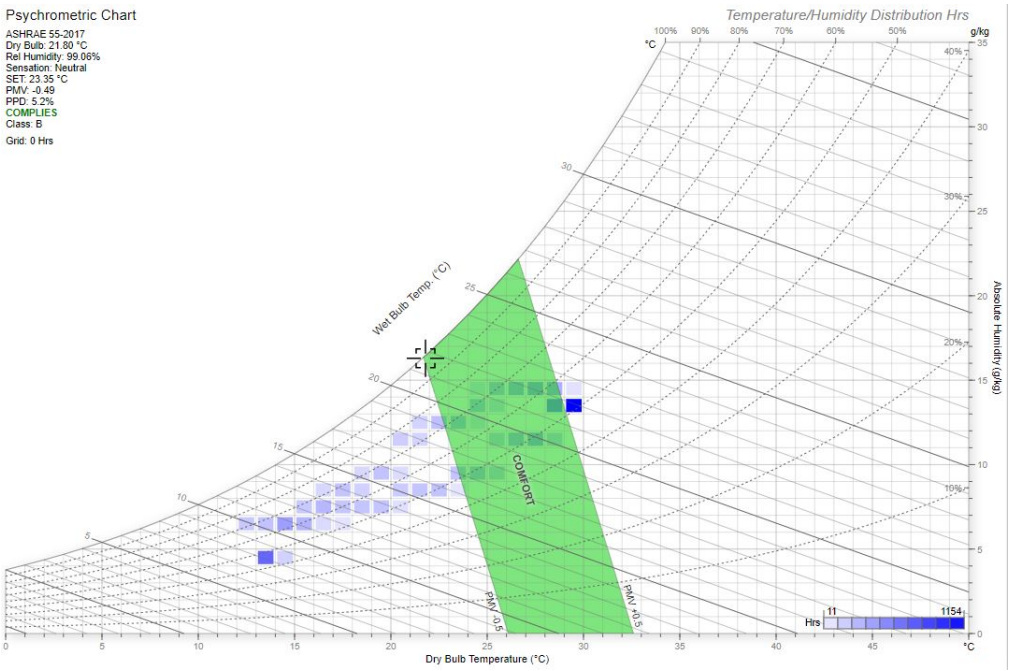


Figure M.12: Monclova, ASHRAE 55-2017 for Near Horizon.

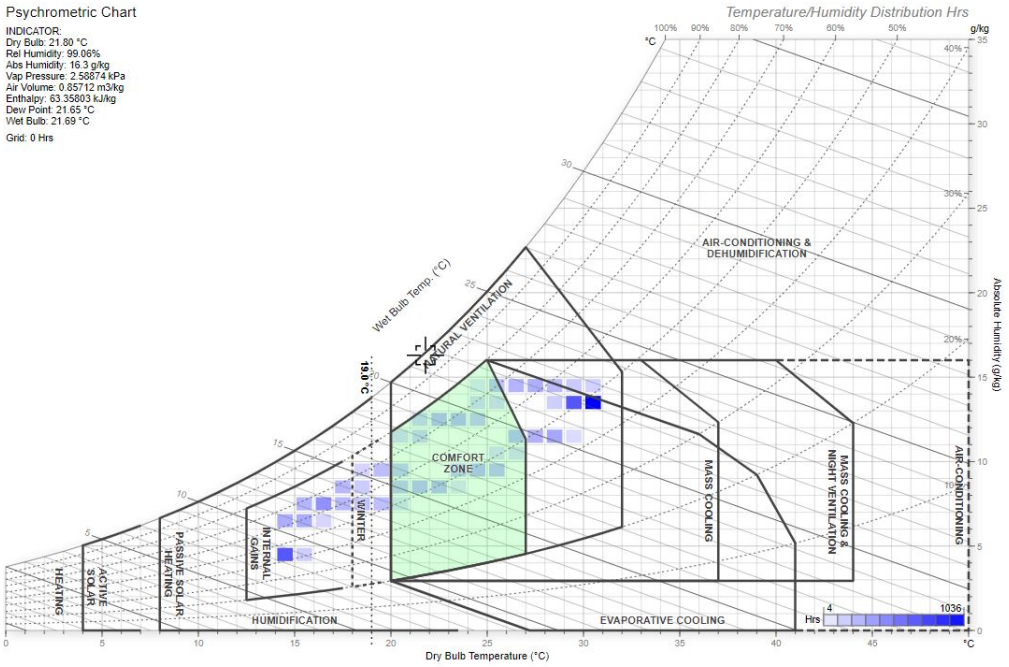


Figure M.13: Monclova, Givoni Bioclimatic Chart for Medium Horizon.

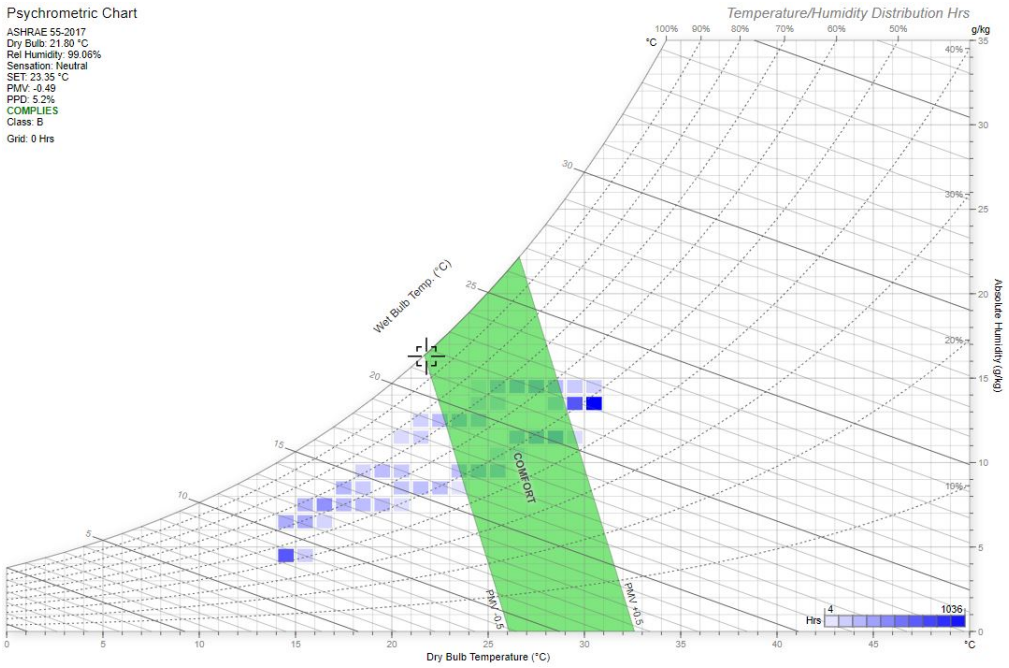


Figure M.14: Monclova, ASHRAE 55-2017 for Medium Horizon.

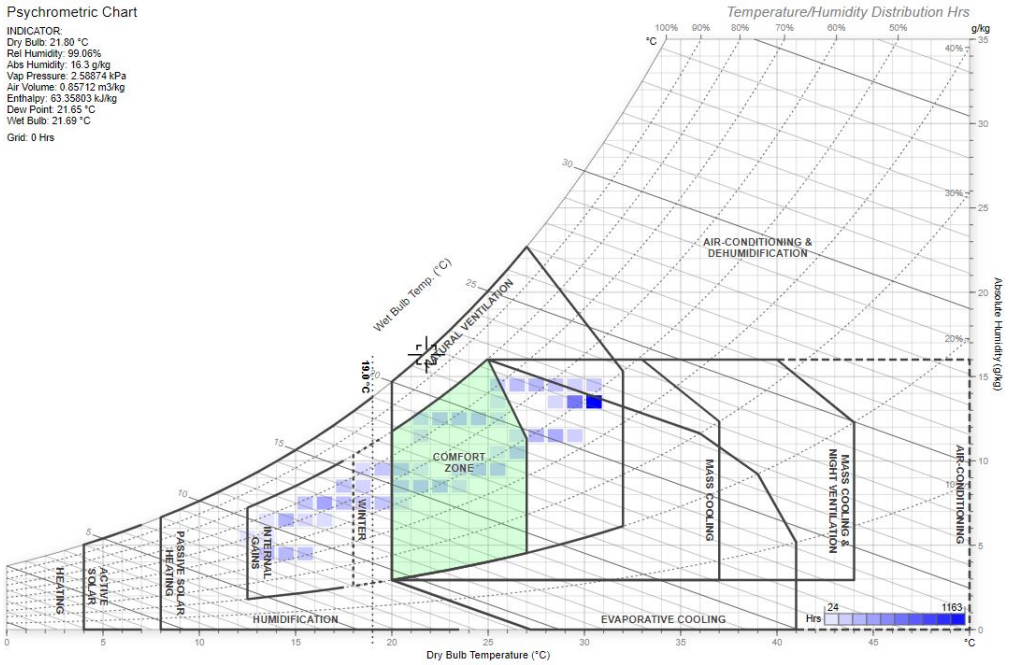


Figure M.15: Monclova, Givoni Bioclimatic Chart for Far Horizon.

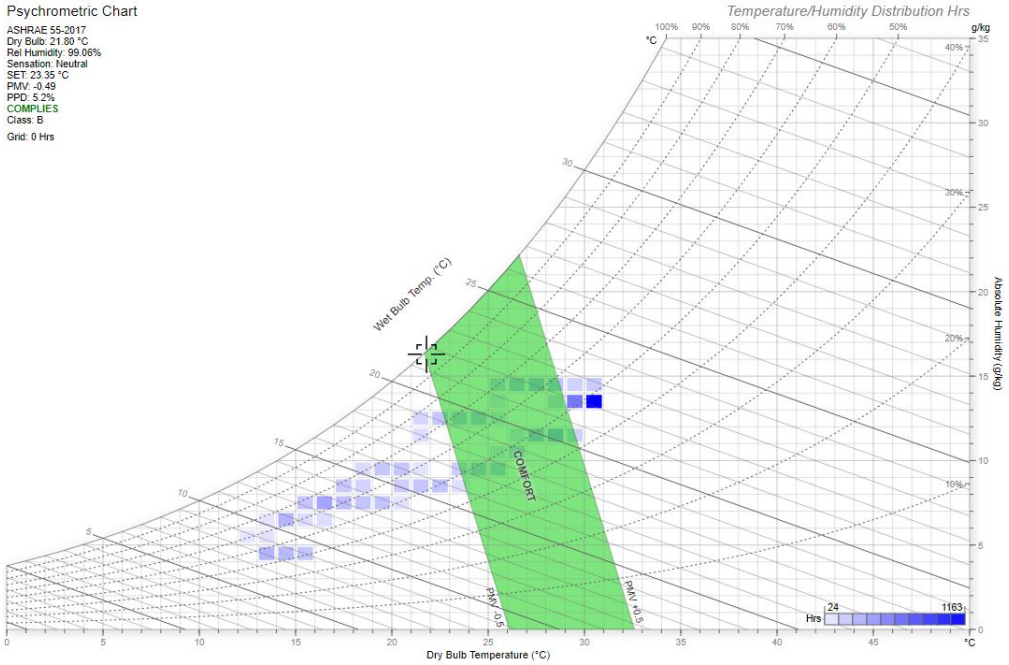


Figure M.16: Monclova, ASHRAE 55-2017 for Far Horizon.

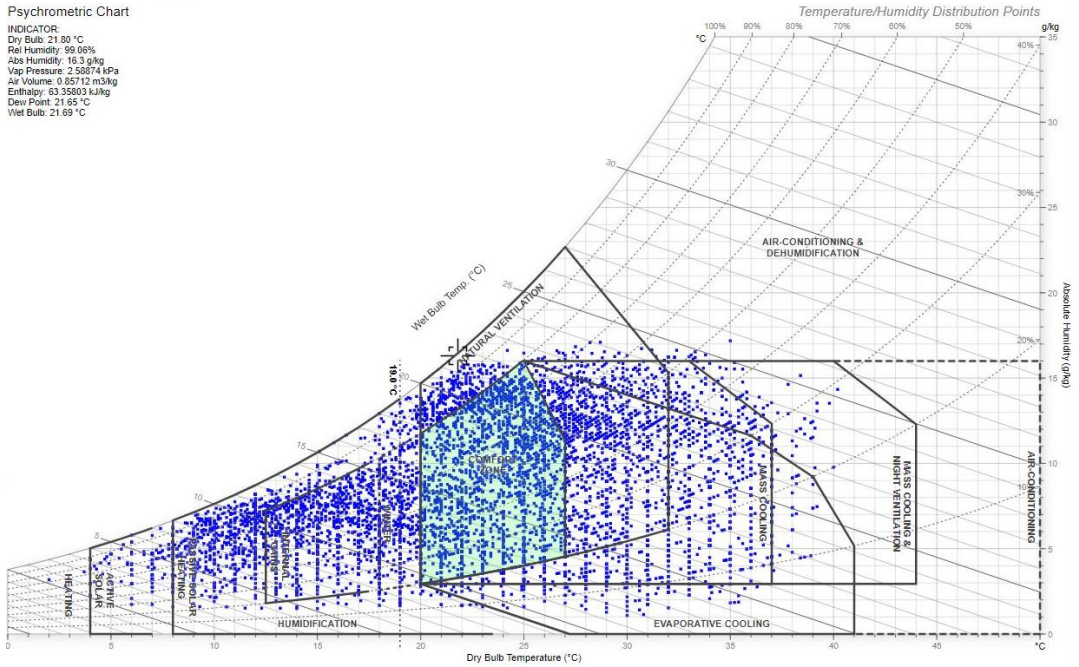


Figure M.17: Torreón, Givoni Bioclimatic Chart for Current Weather.

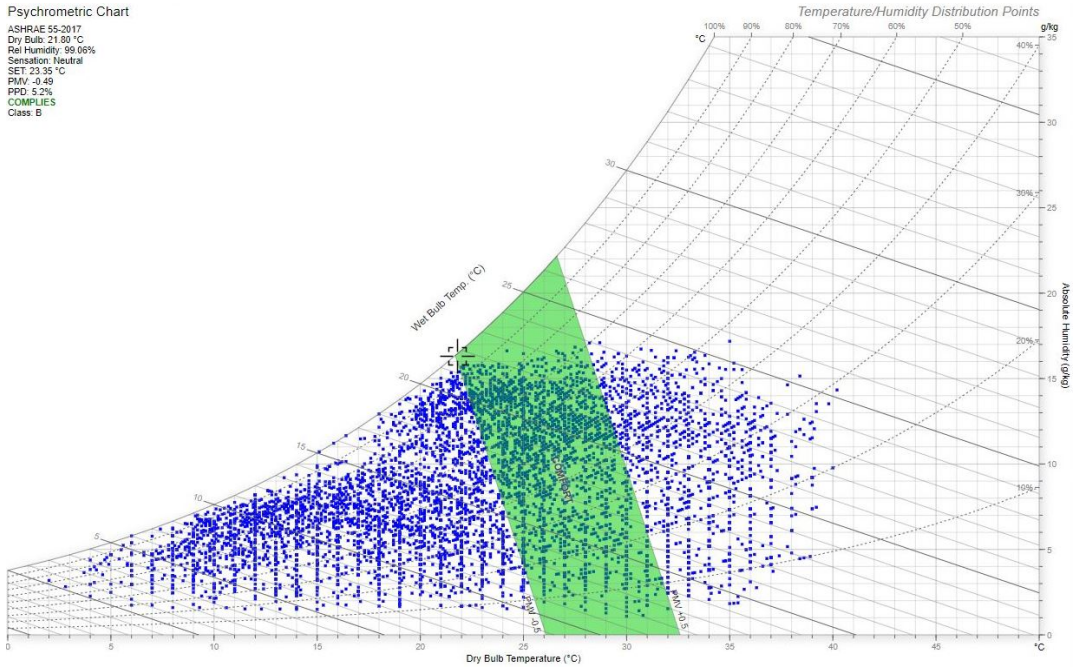


Figure M.18: Torreón, ASHRAE 55-2017 for Current Weather.

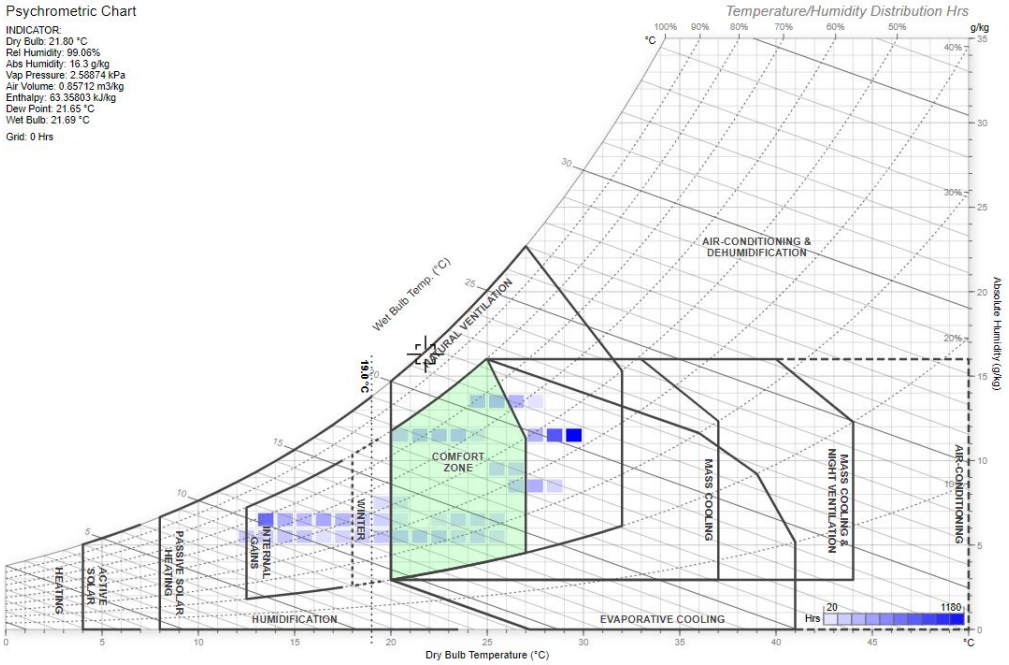


Figure M.19: Torreón, Givoni Bioclimatic Chart for Near Horizon.

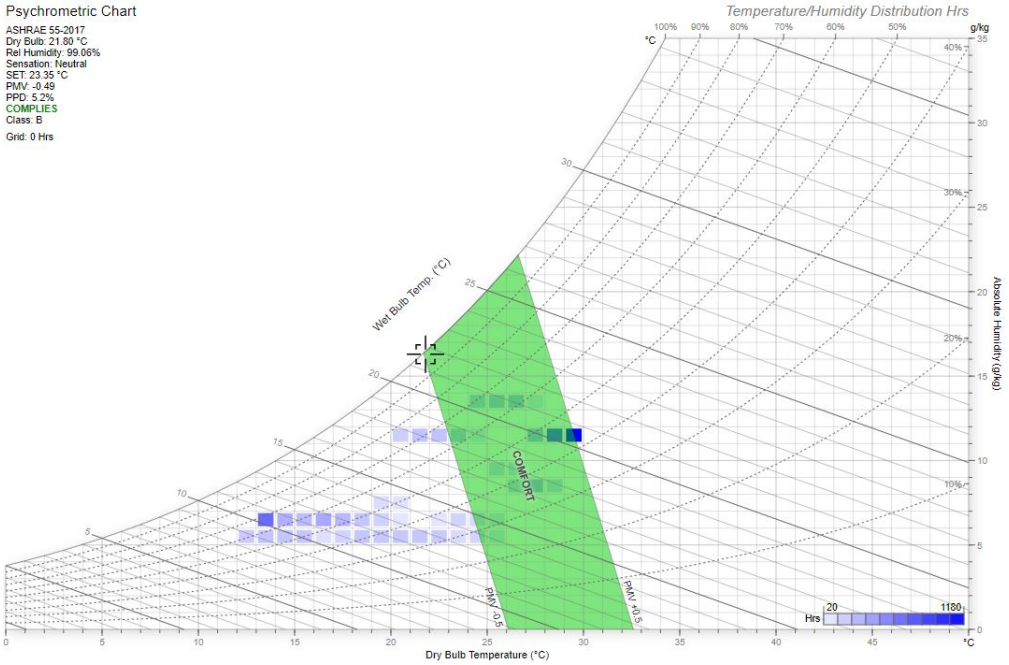


Figure M.20: Torreón, ASHRAE 55-2017 for Near Horizon.

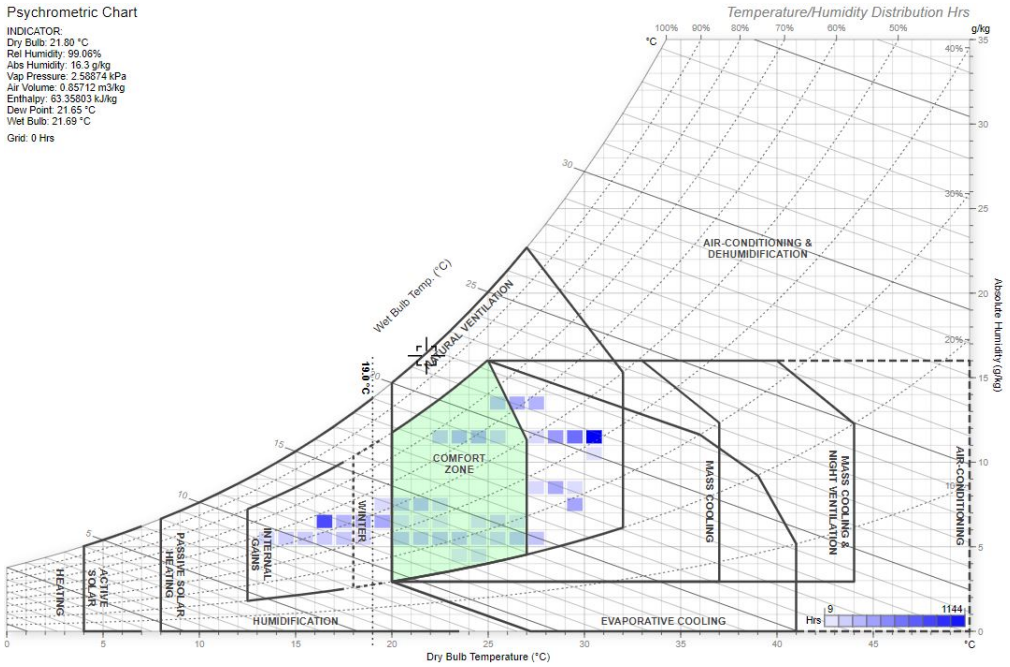


Figure M.21: Torreón, Givoni Bioclimatic Chart for Medium Horizon.

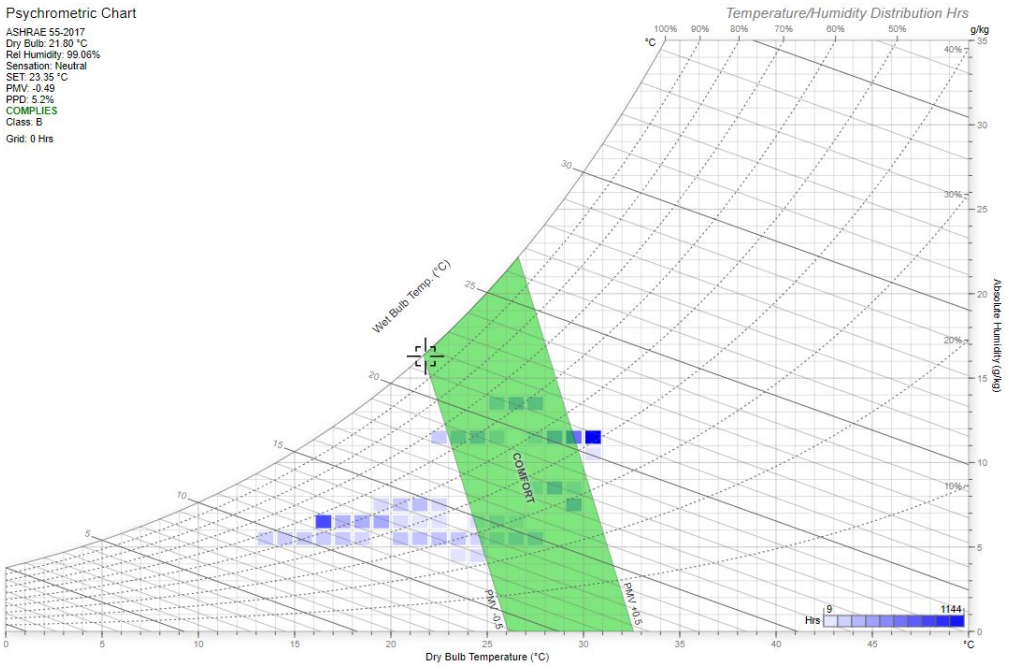


Figure M.22: Torreón, ASHRAE 55-2017 for Medium Horizon.

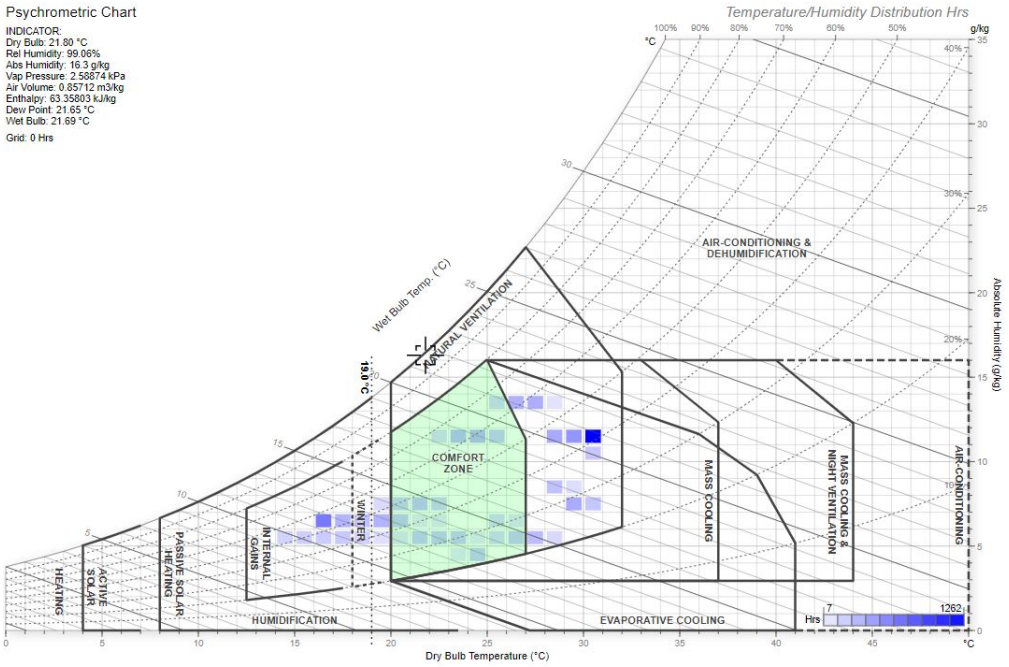


Figure M.23: Torreón, Givoni Bioclimatic Chart for Far Horizon.

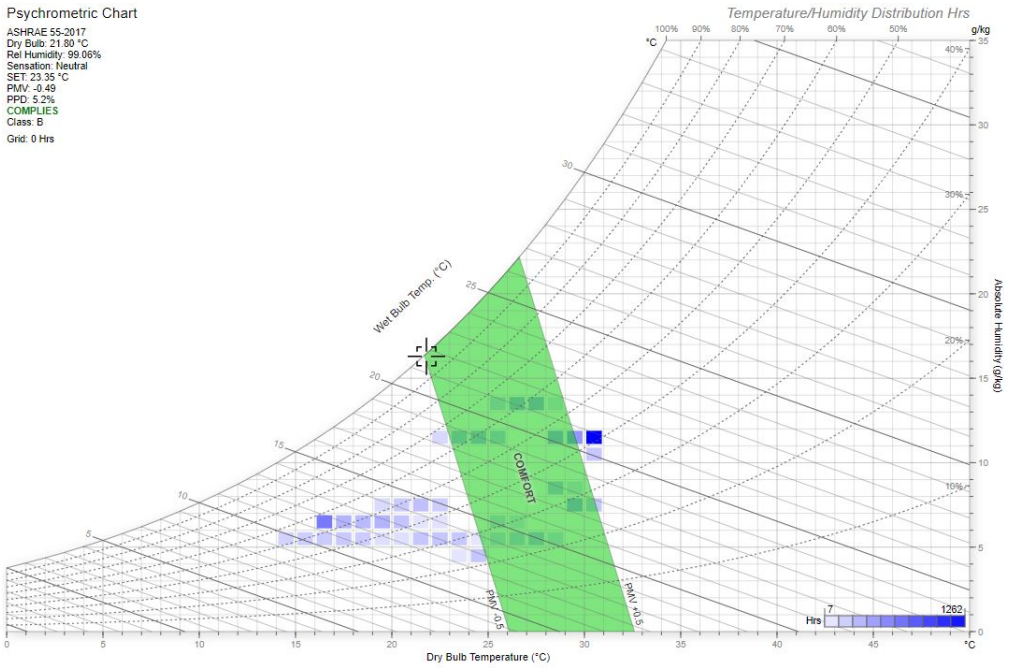


Figure M.24: Torreón, ASHRAE 55-2017 for Far Horizon.

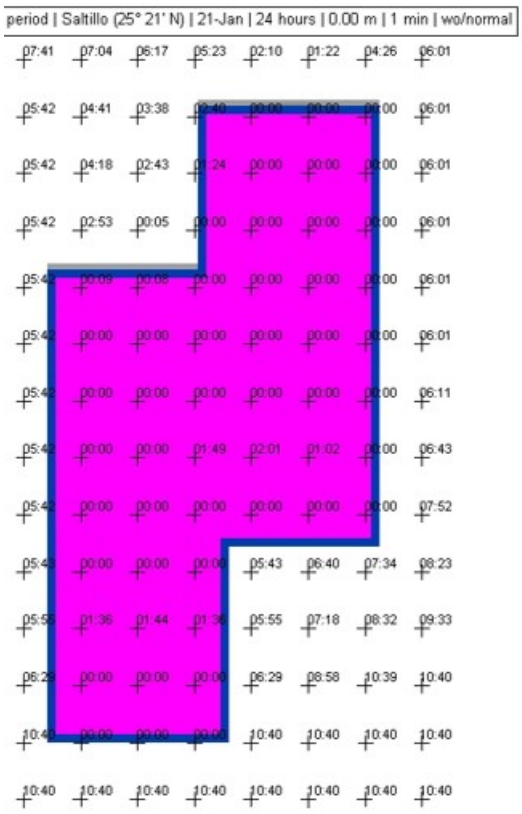
Appendix N

Solar Analysis

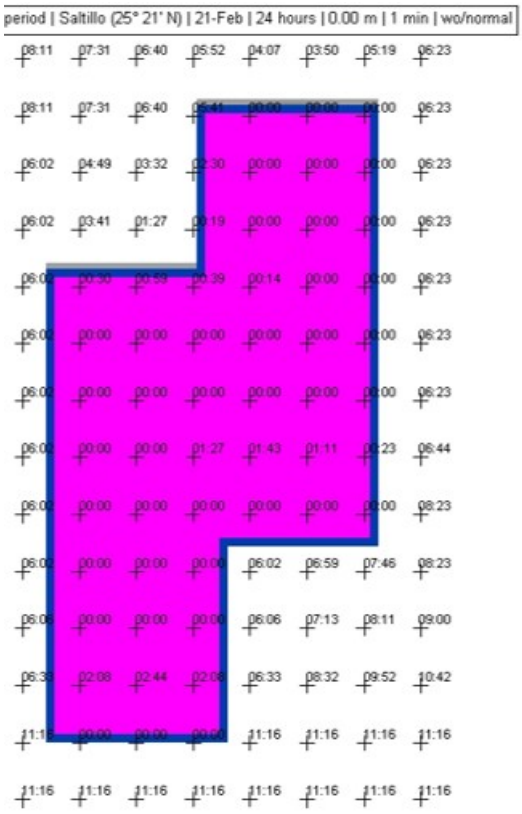
These graphical results show the solar analysis performed for the chosen location in Saltillo evaluated every minute, to assign appropriate design strategies and modifications in the base case:

1. Sunny Periods Inside and Outside the house: from January to December, annual, and annual mean. Grid showing
2. Sunny Periods Floors: winter, summer, spring / autumn, and all year.
3. Sunny Periods Windows: winter, summer, spring, autumn, and all year.
4. Sunny Periods Walls: winter, summer, spring, autumn, and all year.
5. Stereographic Projections: north and south bedrooms, living room, bathroom and kitchen.

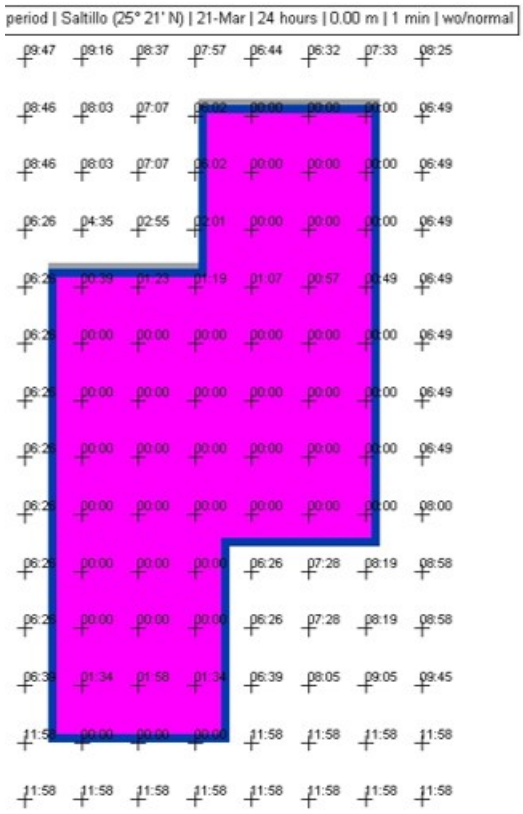
N.1 Sunny Periods



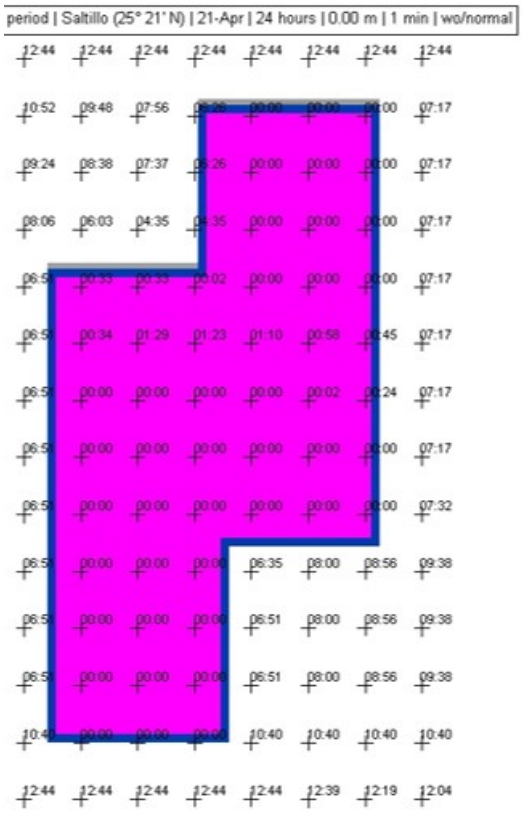
(a) January



(b) February

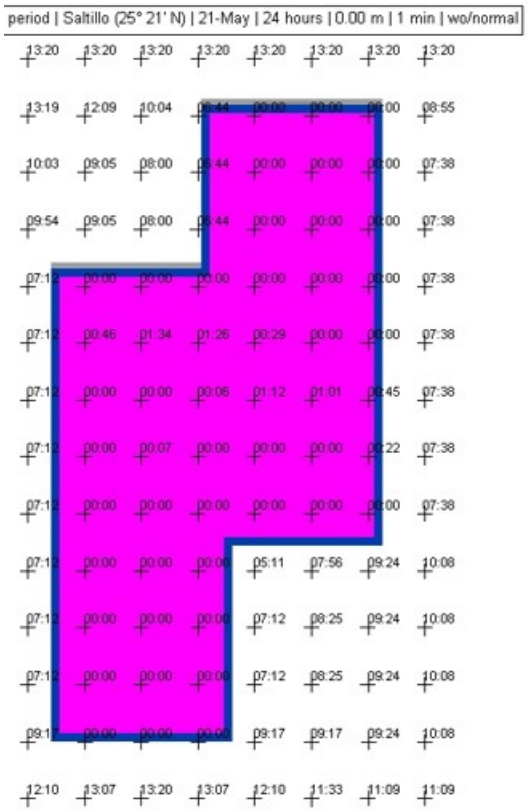


(c) March

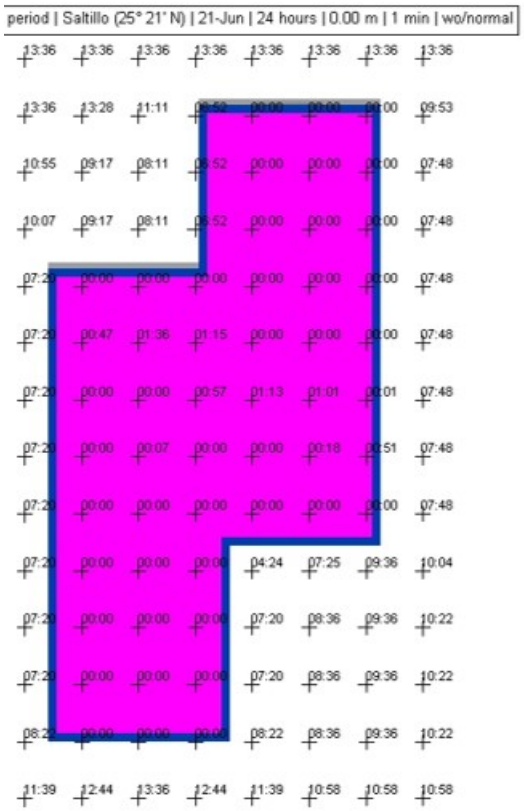


(d) April

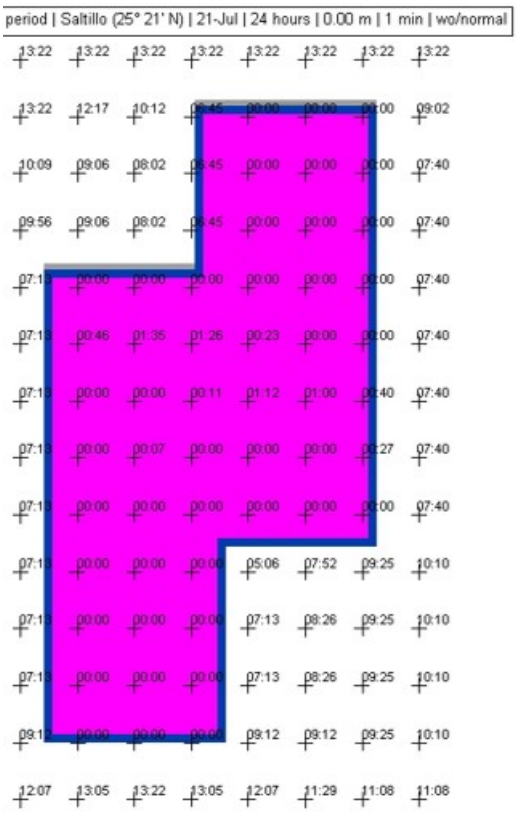
Figure N.1: Sunny Periods from January to April



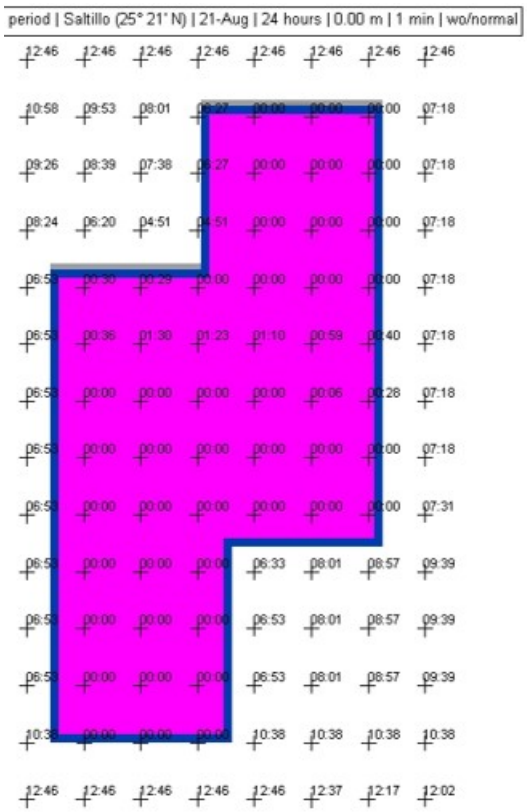
(a) May



(b) June

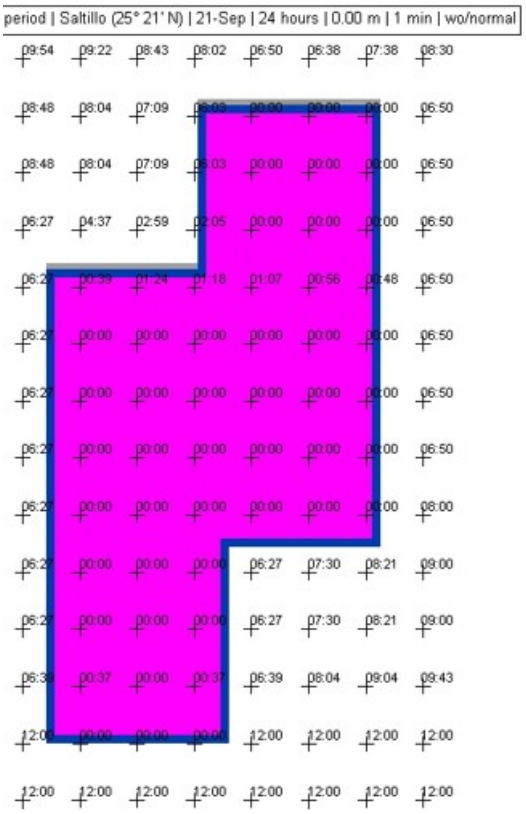


(c) July

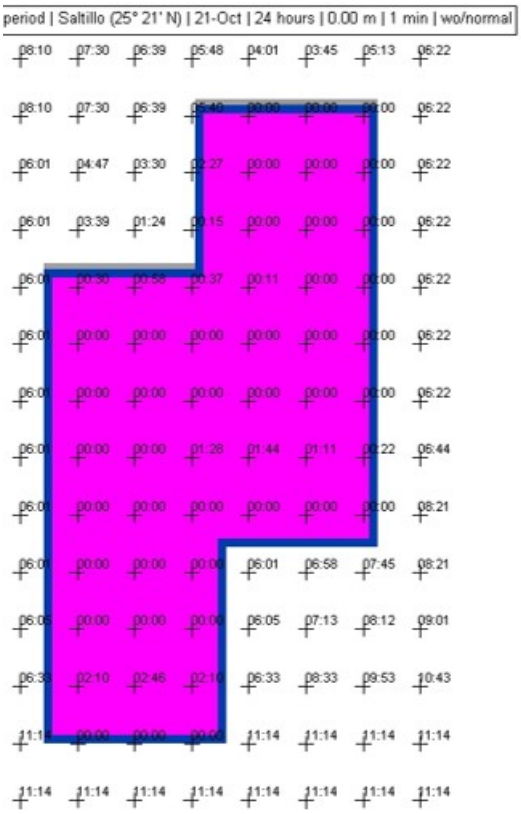


(d) August

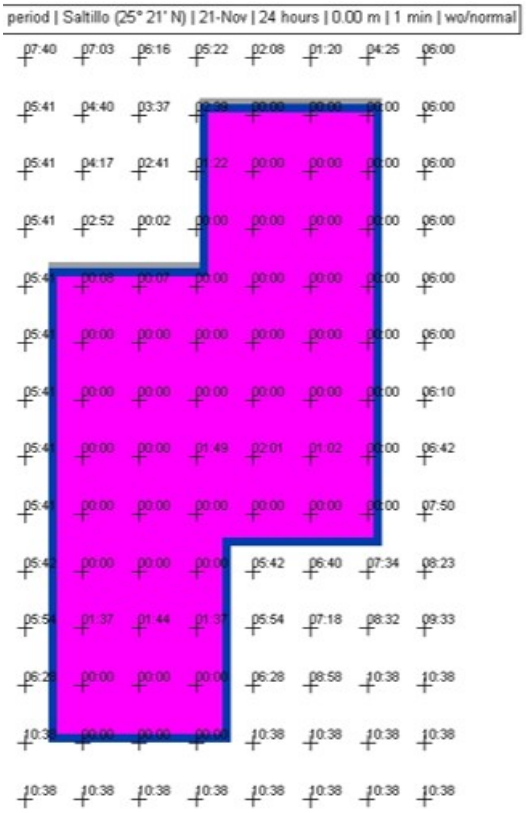
Figure N.2: Sunny Periods from May to August



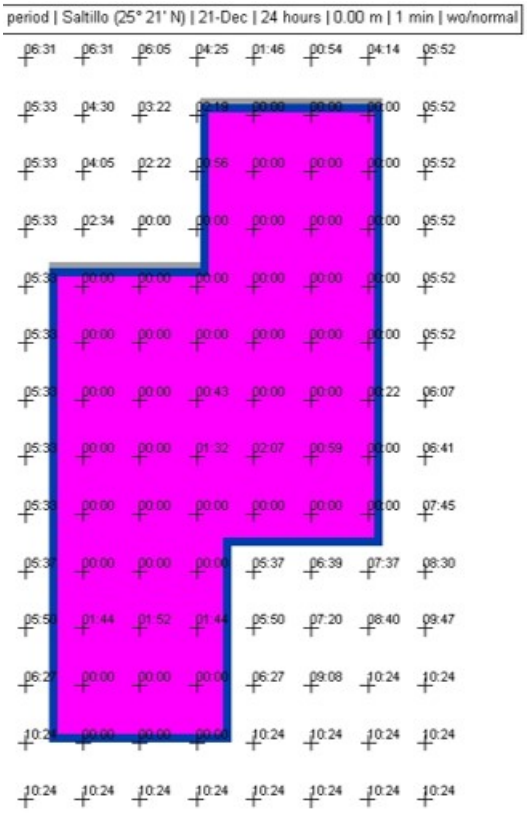
(a) September



(b) October

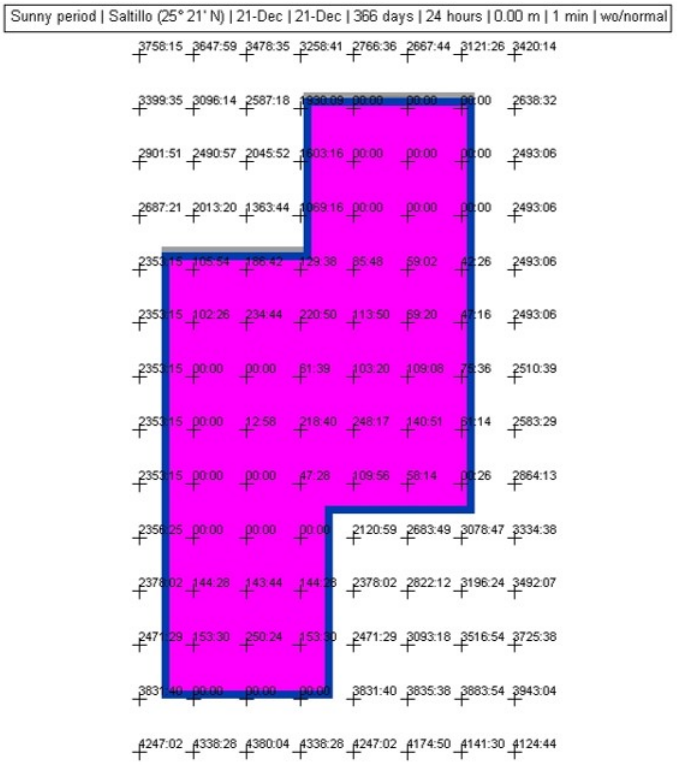


(c) November

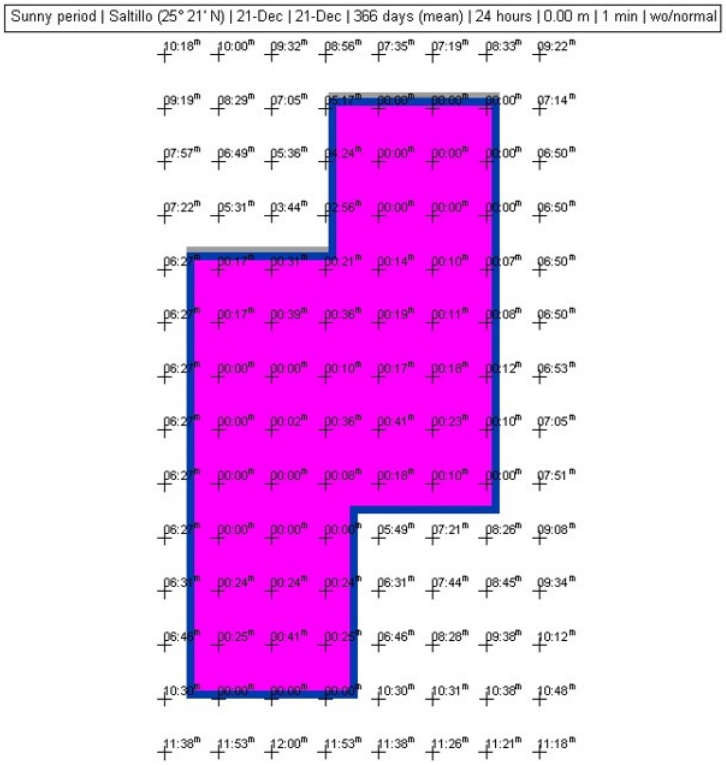


(d) December

Figure N.3: Sunny Periods from September to December

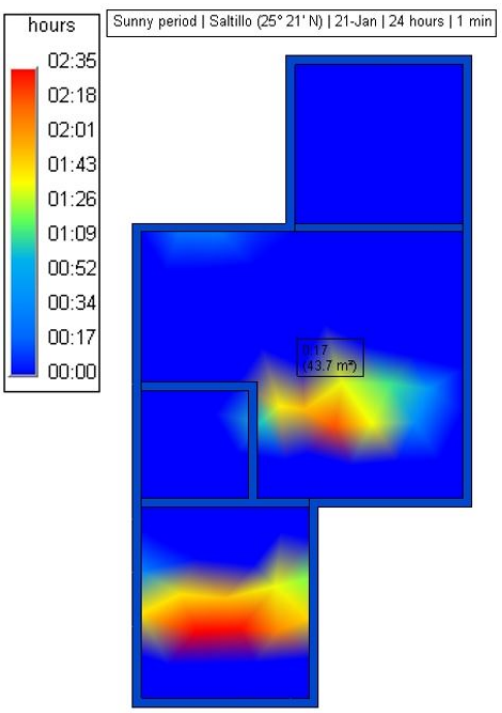


(a) Annual

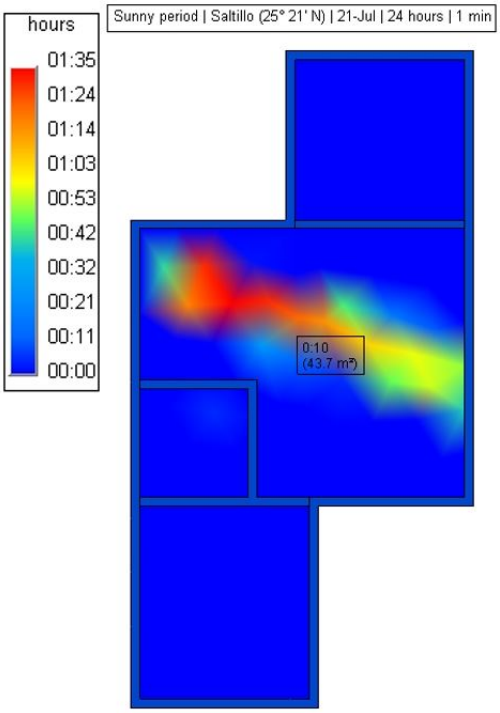


(b) Annual Mean

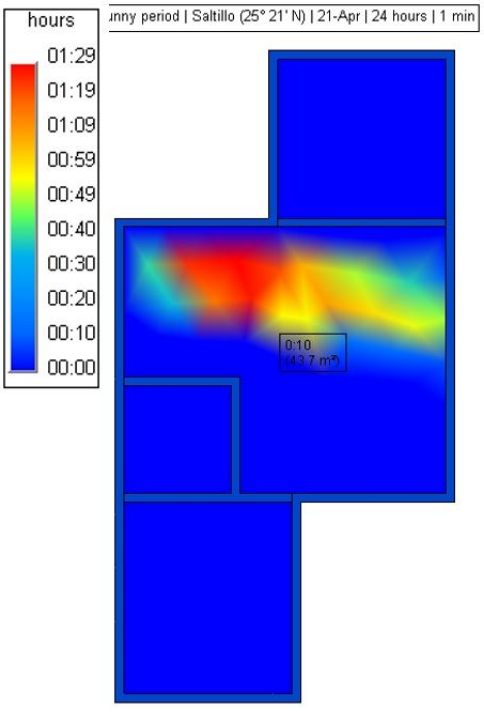
Figure N.4: Sunny Periods Annual and Annual Mean



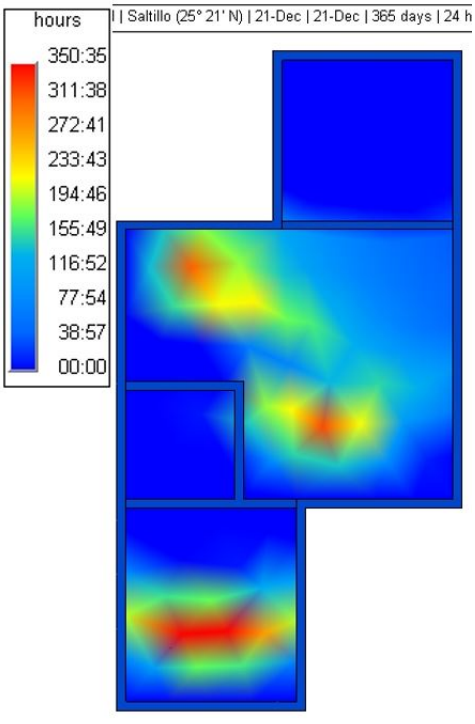
(a) Winter



(b) Summer

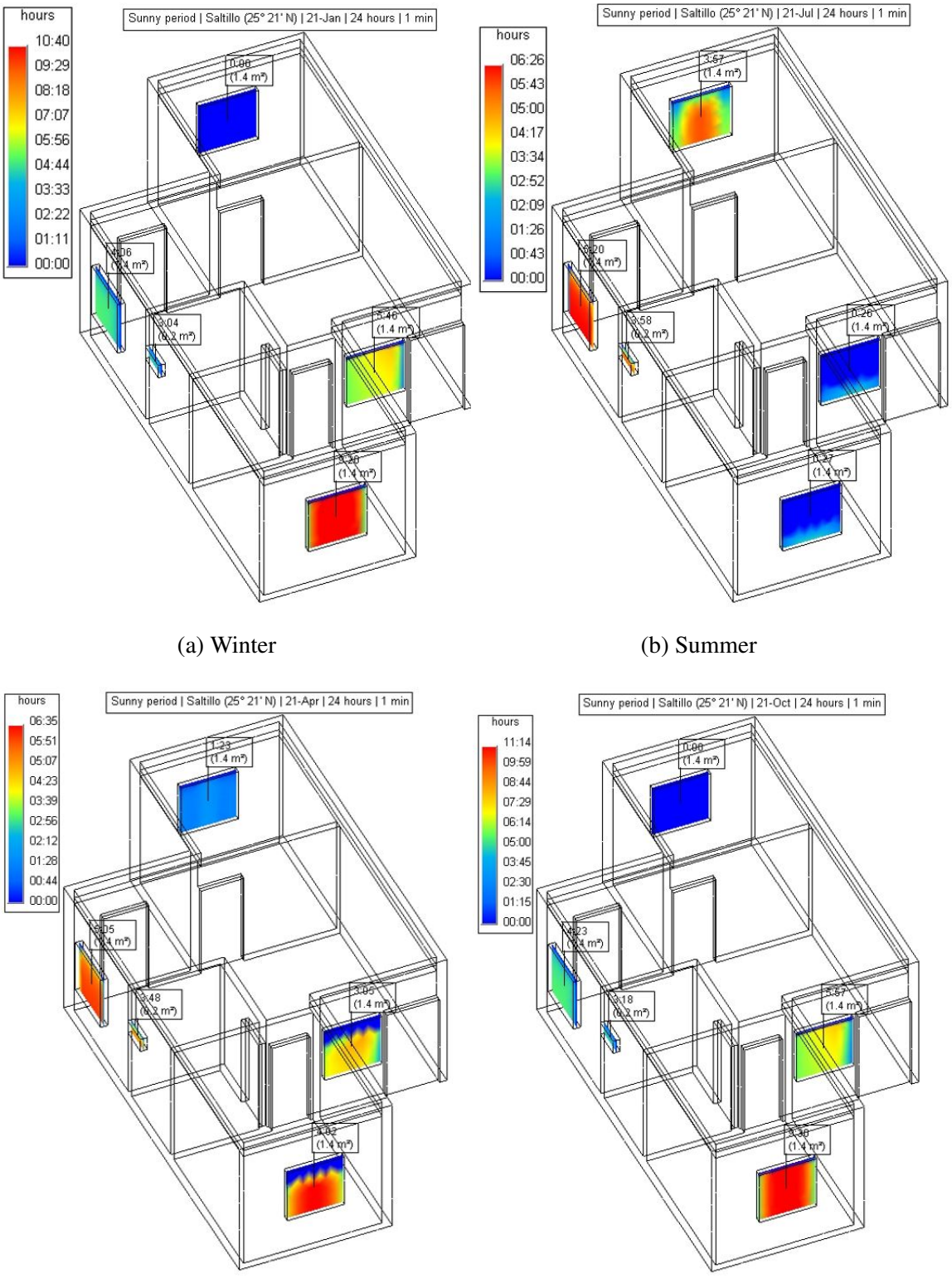


(c) Spring / Autumn



(d) Annual

Figure N.5: Sunny Periods Floors, winter, summer, spring / autumn, annual



(a) Winter

(b) Summer

(c) Spring

(d) Autumn

Figure N.6: Sunny Periods Windows, winter, summer, spring, autumn

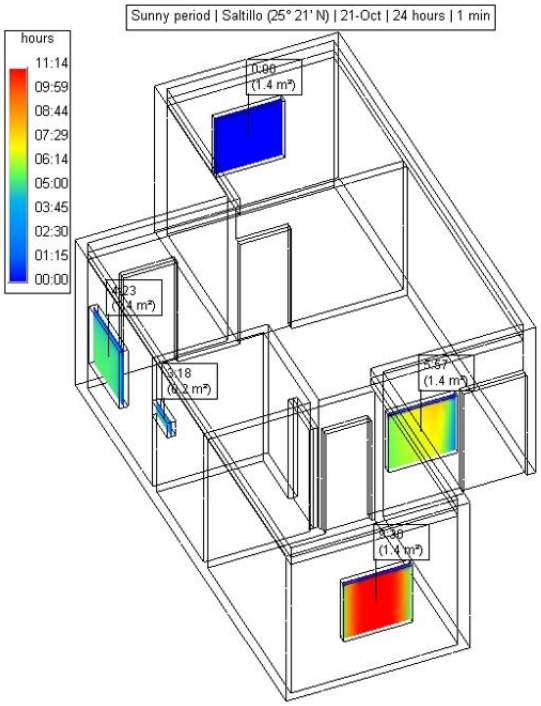


Figure N.7: Sunny Periods Windows, annual

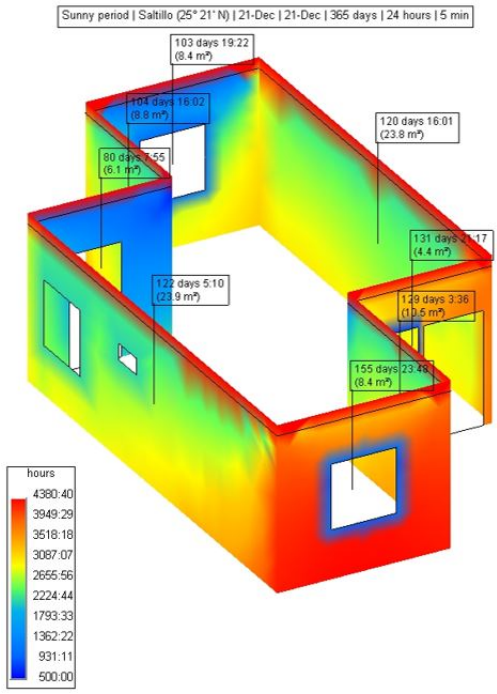
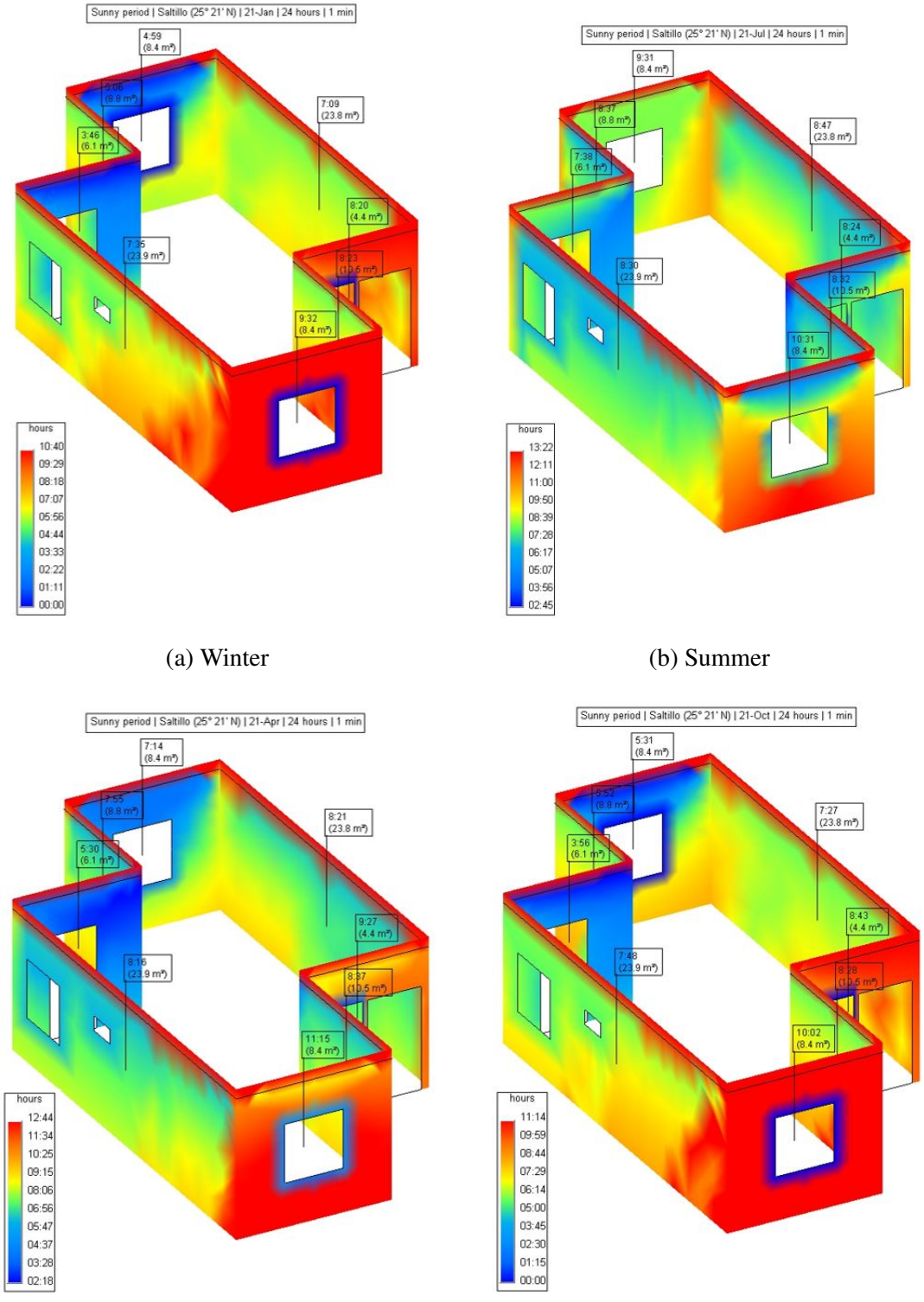


Figure N.8: Sunny Periods Walls, annual



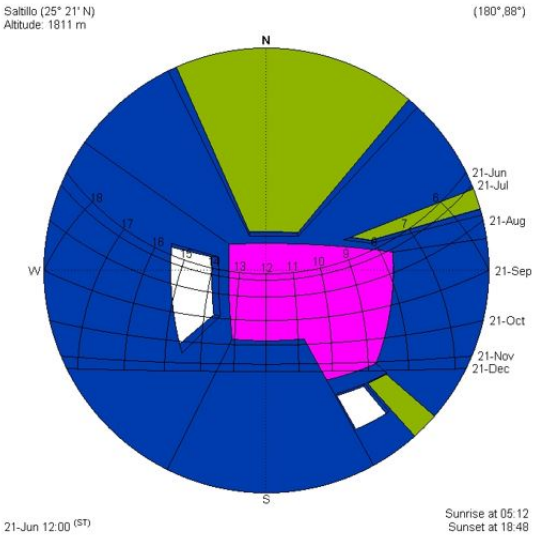
(a) Winter

(b) Summer

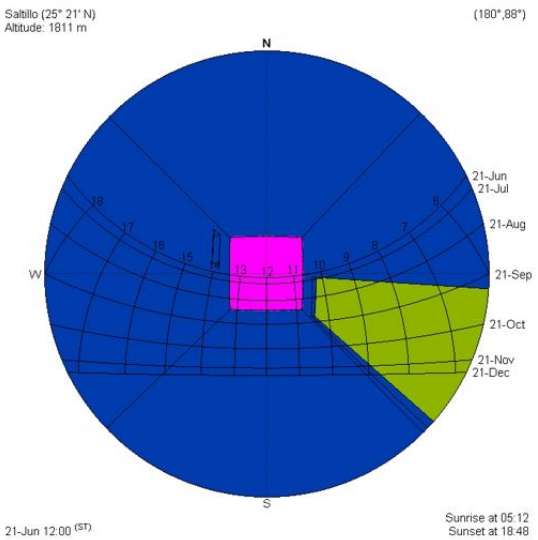
(c) Spring

(d) Autumn

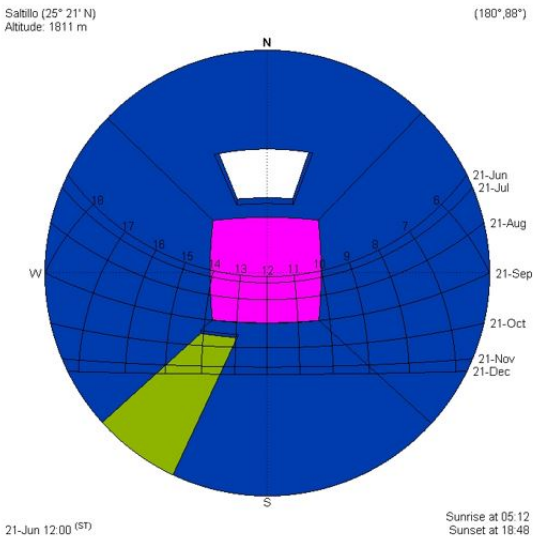
Figure N.9: Sunny Periods Walls, winter, summer, spring, autumn



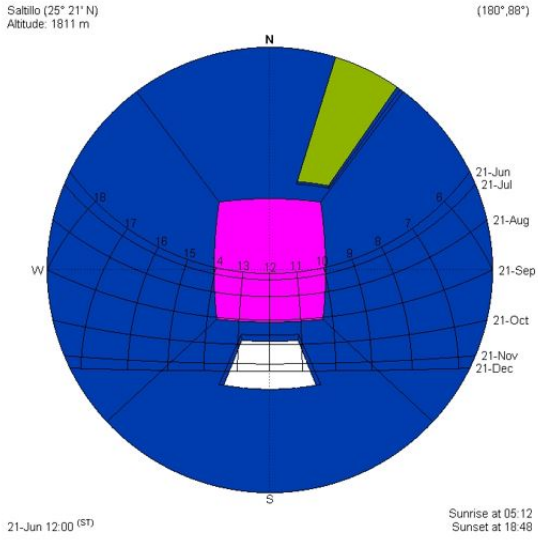
(a) Kitchen



(b) Bathroom



(c) North Bedroom



(d) South Bedroom

Figure N.10: Stereographic Projections kitchen, bathroom, north and south bedrooms

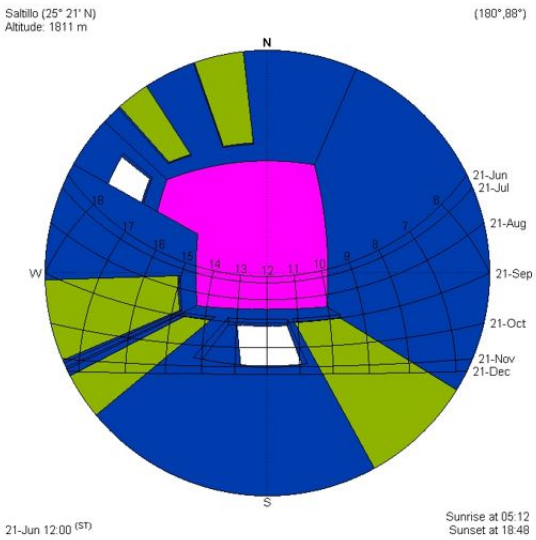


Figure N.11: Stereographic Projections living room